NASA TECHNICAL TRANSLATION

NASA TT F-531

C. 1

NASA TT F-531

TECH LIBRARY KAFB, NM
0068962

LOAN COPY: RETURN TO
AFWL (WLOL)
KIRTLAND AFB, N MEX

COURSE IN THEORETICAL ASTROPHYSICS

by V. V. Sobolev

"Nauka" Press, Moscow, 1967

NATIONAL AERONAUTICS AND SPACE ADMINISTRATION • WASHINGTON, D. C. • DECEMBER 1969

TECH LIBRARY KAFB, NM

0068962

NASA TT F-531

COURSE IN THEORETICAL ASTROPHYSICS

By V. V. Sobolev

Translation of "Kurs teoreticheskoy astrofiziki"
"Nauka" Press, Moscow, 1967

NATIONAL AERONAUTICS AND SPACE ADMINISTRATION

For sale by the Clearinghouse for Federal Scientific and Technical Information
Springfield, Virginia 22151 – Price $3.00

EDITOR'S NOTE

With the exception of certain trigonometric and hyperbolic functions, Soviet mathematical symbols are the same as those encountered in the American literature. For the reader's convenience a list of such exceptions and their American equivalents is given below.

Soviet Usage	American equivalent
Arch	$\cosh^{-1}$
Arcth	$\coth^{-1}$ (ctnh^{-1})
Arsh	$\sinh^{-1}$
Arth	$\tanh^{-1}$
arccos	$\cos^{-1}$ (arc cos)
arcctg	$\cot^{-1}$ (arc cot)
arcsin	$\sin^{-1}$ (arc sin)
arctg	$\tan^{-1}$ (arc tan)
ch	cosh
cosec	csc
ctg	cot (ctn)
cth	coth (ctnh)
lg	log
rot	curl
sch	sech
sh	sinh
tg	tan
th	tanh

FOREWORD

This book has been written on the basis of lectures delivered by the author at Leningrad University during the past twenty years.

Theoretical astrophysics has undergone significant changes over the years. First of all the scope of observational data, which theoretical astrophysics must interpret, has been extremely broadened. To an appreciable extent this is related to the birth and rapid growth of radio astronomy and beyond-the-atmosphere astrophysics. On the other hand, in theoretical astrophysics itself several new, important concepts have emerged: the vast role of nuclear reactions in stellar energy and evolution, the large influence of electromagnetic forces on the state of stellar atmospheres and interstellar space, etc. At the same time, powerful new methods (in particular, in radiative transfer theory) have been developed in this science, and old methods have been refined for the purpose of utilizing the possibilities presented by computers. The content of the lectures, of course, has varied, following the changes in theoretical astrophysics. During the writing of this book the author once more critically reviewed the lectures of past years and reworked them considerably, keeping in mind the long-term development of astrophysics.

This book comprises eight chapters. The problems of the formation of the continuous and line spectra of stars are considered in the first two chapters. The stellar layers, in which these spectra originate, are commonly called the "photosphere" and "atmosphere", respectively. Of course there is no sharp boundary between these layers; however, these are very convenient designations (if only because it is simpler to speak of the "theory of photospheres" than the "theory of the formation of the continuous spectra of stars"). In the chapters mentioned, the radiant energy absorption and emission processes, occurring in a volume element, are examined in detail, along with the processes of radiative energy transfer through the surface layers of a star. Here it is shown how the physical conditions in the surface layers of stars and their chemical compositions are determined from the observed stellar spectrum.

Chapter III is specifically devoted to the solar atmosphere. Our proximity to the sun permits studying the details of its disk, as well as the outer layers—chromosphere and corona—of the solar atmosphere. The results of solar radio emission observations are used in discussing these layers. Chapter IV discusses planetary atmospheres which are luminous because of their scattering of sunlight. The theory of light scattering in planetary atmospheres is set forth in this chapter, and their optical properties are determined. Atmospheric structure is discussed in the less detail since one can expect great discoveries in this area very soon in conjunction with the development of astronautics.

In Chapter V the physics of gaseous nebulae, being relatively simple and a very well developed portion of astrophysics, is discussed. Here, much space is allotted to the problems of atomic ionization and excitation, the formation of the emission spectra, etc. Results, obtained through a study of gaseous nebulae,

are then employed in discussing variable stars (in Chapter VI) and interstellar space (in Chapter VII). In these chapters the theory of nonthermal radiation of space objects is discussed along with the theory of their thermal radiation (in particular, in examining supernovae and cosmic radio emission outbursts). The book concludes with a chapter devoted to the theory of internal stellar structure.

In writing this book, the author has not attempted to cover the problems in all aspects of theoretical astrophysics with equal thoroughness. To do other than this, the book, for a given size, would consist of sections distantly related to each other and it would be impossible to take them into consideration. The main problems, associated with the radiation fields of space objects and with the formation of their spectra in different frequency regions, are discussed in this book. Other theoretical problems are considered in less detail. A theorectical astrophysics course of this nature should be considered perfectly reasonable since the study of the spectra of space objects constitutes the foundation of this science.

Many problems, treated briefly in this book, are usually discussed in greater detail in universities in other specialized courses (for example, in radio astronomy and cosmogony courses). The recently published book, "Course in General Astrophysics", by D. Ya. Martynov, can be recommended for a preliminary acquaintance with the various problems of theoretical astrophysics.

The manuscript of this book was read by V. V. Ivanov and I. N. Minin, associates in the astrophysics department of Leningrad University, who offered many valuable comments. S. A. Kaplan made several important suggestions directed toward improving the book. The author is sincerely grateful to them.

V. V. Sobolev

TABLE OF CONTENTS

EDITOR'S NOTE i

FOREWORD ii

CHAPTER I. STELLAR PHOTOSPHERES

1. Radiation Equilibrium of the Stellar Photosphere 1
   1. Radiation Field 1
   2. Radiative Transfer Equation 4
   3. Radiation Equilibrium Equation 6
   4. Geometrical Model of Photosphere 8
2. Theory of Photospheres with a Frequency-Independent Absorption Constant 9
   1. Basic Equations 9
   2. Approximate Solution of the Equations 11
   3. Application of Quadrature Formulas 15
   4. Milne's Integral Equation 16
   5. Brightness Distribution over the Stellar Disk 19
3. Exact Solution of the Basic Equations 20
   1. Equation for the Resolvent 20
   2. Auxiliary Equations 22
   3. Determination of the Function $\Phi(\tau)$ 24
   4. Solution of the Homogeneous Equation 25
   5. Intensity of the Emergent Radiation 26
   6. Application to Stellar Photospheres 29
4. Local Thermodynamic Equilibrium 32
   1. Radiation Field in Presence of Thermodynamic Equilibrium 32
   2. Assumption of Local Thermodynamic Equilibrium of the Stellar Photosphere 34
   3. Radiation Coming from Photosphere 36
   4. Dependence of Temperature and Density on Depth 40
   5. Radiation Pressure in the Photosphere 42
5. Frequency Dependence of the Absorption Coefficient 45
   1. Continuous Emission and Absorption Spectra 45
   2. Absorption by Hydrogen Atoms 47
   3. Absorption by Negative Hydrogen Ions 50
   4. Light Scattering by Free Electrons 51
   5. Mean Absorption Coefficient 52
6. Theory of Photospheres with a Frequency-Dependent Absorption Coefficient 57
   1. Approximate Theory 57
   2. Case of Absorption by Atoms of One Kind 59
   3. Photosphere Models 63

4. Hot Stars 65
5. Cold Stars 66
6. White Dwarfs 67
7. Special Problems of Photosphere Theory 69
1. Extended Photospheres 69
2. Blanketing Effect 71
3. Effect of Reflection in Close Pairs 72
4. Polarization of the Radiation of Hot Stars 75

CHAPTER II. STELLAR ATMOSPHERES 79

8. Spectral Line Absorption Coefficient 80
1. Einstein Transition Coefficients 80
2. Absorption Coefficient Caused by Radiation Damping and Thermal Motion of Atoms 83
3. Pressure Effects 88
4. Stark Effect 91
9. Absorption Lines in Presence of Local Thermodynamic Equilibrium 95
1. Basic Formulas 95
2. Determination of Line Profiles 98
3. Weak Lines and Wings of Strong Lines 100
4. Deviations from Thermodynamic Equilibrium 103
10. Absorption Lines in Presence of Coherent Scattering 104
1. Schwarzschild-Schuster Model 104
2. Eddington Method 109
3. Fluorescence in Stellar Atmospheres 112
4. Exact Solution of the Problem 116
11. Absorption Lines in Presence of Noncoherent Scattering 120
1. Frequency Redistribution Within the Line 120
2. Radiative Transfer Equation and Its Solution 123
3. Central Intensities of Absorption Lines 126
4. Variation of Line Profiles over the Solar Disk 129
12. Chemical Composition of Stellar Atmospheres 130
1. Equivalent Line Widths 130
2. Curve of Growth for Schwarzschild-Schuster Model 132
3. Curve of Growth for Eddington Model 135
4. Plotting of Curves of Growth from Observational Data 137
5. Amounts of Different Atoms in the Atmospheres 138
13. Physical Conditions in Atmospheres 141
1. Atom Excitation and Ionization 141
2. Density of Free Electrons 144
3. Turbulence in Atmospheres 146
4. Rotation of Stars 147
5. Magnetic Fields of Stars 151
14. Stars of Different Spectral Classes 152
1. Temperature Dependence of the Spectrum 152
2. Effect of Gravitational Acceleration on the Spectrum 155
3. Stars of Different Spectral Classes 156
4. Stars of Late Spectral Classes 159

5. White Dwarfs 160

CHAPTER III. THE SOLAR ATMOSPHERE 165

15. General Information 166
1. Solar Photosphere 166
2. Convection and Granulation 168
3. Sunspots 171
4. Solar Activity 172
16. Chromosphere 174
1. Line Intensities 174
2. Self-Absorption in Lines 175
3. Distribution of Atoms with Height 179
4. Excitation of Atoms in the Chromosphere 181
5. Ultraviolet Solar Spectrum 182
6. L_α -Line in the Solar Spectrum 184
17. Corona 186
1. Radiation of the Corona 186
2. Origin of the Continuous Spectrum 187
3. Electron Density 190
4. Coronal Lines 193
5. Corona Temperature 195
6. Atom Ionization and Excitation 198
7. Ultraviolet and X-Radiations 201
18. Solar Radio Emission 202
1. Results of Observations 202
2. Radio Emission of Quiet Sun 204
3. Distribution of Radio Emission over the Disk 207
4. Radio Wave Propagation in the Corona 210
5. Sporadic Radio Emission 212
6. Supercorona of the Sun 213

CHAPTER IV. PLANETARY ATMOSPHERES 216

19. Light Scattering in Planetary Atmospheres 216
1. Basic Equations 216
2. Semi-Infinite Atmosphere 219
3. Atmosphere of Finite Optical Thickness 221
4. Light Reflection by the Planet's Surface 225
5. Planet Albedo 228
20. Optical Properties of Planetary Atmospheres 231
1. The Venusian Atmosphere 231
2. The Martian Atmosphere 236
3. The Earth's Atmosphere 238
4. Interpretation of Planet Spectra 241
21. Structure of Planetary Atmospheres 245
1. Planetary Temperatures 245
2. Planetary Radio Emission 247
3. Planetary Atmosphere Models 249
4. Upper Layers of the Atmosphere 252

CHAPTER V. GASEOUS NEBULAE 256

22. Emission Mechanism of Nebulae 257
1. Observational Data 257
2. Cause of Nebular Emission 258
3. Rosseland Theorem 260
4. Determination of Stellar Temperatures from the Hydrogen Lines 262
5. Stellar Radiation in the Ultraviolet Region of the Spectrum 266
6. Determination of Stellar Temperatures from the "Nebular" Lines 268
23. Ionization of Atoms 270
1. Number of Recombinations 270
2. Degree of Ionization in a Nebula 273
3. Ionization in a Nebula of Large Optical Thickness 274
4. Energy Balance of Free Electrons 277
24. Excitation of Atoms 283
1. Excitation through Photoionizations and Recombinations 283
2. Intensities of Emission Lines 286
3. Role of Collisions 288
4. Masses and Densities of Nebulae 289
25. Forbidden Lines 292
1. Necessary Conditions for the Appearance of Forbidden Lines 292
2. Collision Probabilities 295
3. Intensities of Forbidden Lines 297
4. Electron Temperatures and Densities 300
5. Chemical Composition of Nebulae 302
26. Continuous Spectrum 304
1. Recombinations and Free-Free Transitions 304
2. Two-Photon Emission 308
3. Effect of Collisions 311
4. Comparison of Theory with Observations 313
27. Radiation Diffusion in Nebulae 315
1. L_c Radiation Field 315
2. $L\alpha$ Radiation Field in a Stationary Nebula 321
3. $L\alpha$ Radiation Field in an Expanding Nebula 327
4. Radiation Pressure in Nebulae 332

CHAPTER VI. VARIABLE STARS 338

28. Stars with Bright Spectral Lines 339
1. Early Class Stars with Bright Lines 339
2. Emission Line Profiles 341
3. Emission Line Intensities 345
4. Type Be Stars 349
5. Wolf-Rayet Type Stars 352
6. Late Class Stars with Bright Lines 356

29. Novae 359
1. Observational Data 359
2. Explanation of Outburst 362
3. First Period of Outburst 365
4. Nebular Phase 368
5. Hercules Nova of 1934 371
6. Novae Many Years After Outburst 376
30. Motion and Luminosity of Envelopes 377
1. Energy Released During Outburst 377
2. Interpretation of Light Curve 381
3. Ejection of Stellar Matter 385
4. Envelope Motion in Interstellar Space 387
31. Supernovae 389
1. Results of Observations 389
2. Synchrotron Radiation 391
3. Crab Nebula 394
4. Supernovae and Cosmic Rays 397

CHAPTER VII. INTERSTELLAR SPACE 399

32. Interstellar Dust 400
1. Relation Between Stars and Nebulae 400
2. Fluctuations of the Milky Way Brightness 402
3. Emission of Dust Nebulae 406
4. Nature of Dust Particles 412
5. Polarization of Starlight 414
33. Interstellar Gas 415
1. Ionization of Interstellar Hydrogen 415
2. Ionization of Other Atoms 418
3. Interstellar Absorption Lines 422
4. Physical State of Interstellar Gas 426
5. Motion of Interstellar Gas 427
34. Space Radio Emission 429
1. Emission of the H II Zone 429
2. Nonthermal Emission 431
3. Monochromatic Radio Emission 433
4. Absorption Lines at Radio Frequencies 436
5. Metagalactic Radio Emission 437

CHAPTER VIII. INTERNAL STRUCTURE OF STARS 441

35. Equations of Equilibrium of Stars 442
1. Equation of Mechanical Equilibrium 442
2. Density, Pressure, and Temperature Inside a Star 444
3. Gravitational Energy of a Star 447
4. Equation of Energy Equilibrium 449
5. Standard Stellar Model 450
36. Physical Processes Inside Stars 453
1. Equation of State of Stellar Matter 453
2. Gas Degeneracy 455

3. Energy Transfer Inside a Star 459
4. Nuclear Reactions as a Source of Stellar Energy 462
37. Structure and Evolution of Stars 464
1. Basic Equations 464
2. Structure of Main Sequence Stars 466
3. Structure of White Dwarfs 469
4. Problem of Stellar Evolution 474

TABLES OF FUNDAMENTAL PHYSICAL AND ASTRONOMICAL CONSTANTS 479

SUBJECT INDEX 480

CHAPTER I

STELLAR PHOTOSPHERES

The layer from which the continuous spectrum radiation comes to the observer is called the stellar photosphere. The stellar atmosphere, yielding a line spectrum, is located above the photosphere. There is, of course, no sharp boundary between the photosphere and atmosphere; but, nevertheless, spectral lines originate, on the average in higher layers than the continuous spectrum. The stellar interiors, inaccessible to observers, are below the photosphere. Later on we will see that for the overwhelming majority of stars the photosphere is relatively thin, i.e., the photosphere thickness is much less than the star radius. /9

The photosphere radiation determines the brightness of the star (this is the origin of the name "photosphere"—sphere of light). However, no energy is produced in the photosphere itself. The energy sources lie at the deeper layers of the star, and energy is only transferred outward through the photosphere.

It was established, even in the first studies of photosphere theory, that energy transfer in the photosphere is accomplished primarily by radiation. Energy transfer by thermal conduction plays no significant role because of the smallness of the thermal conductivity coefficient of gases. Energy transfer by convection can be important only for discrete points within the photosphere.

The study of the transfer of radiant energy through the photosphere is the fundamental problem of photosphere theory. The solution of this problem is related to a determination of the structure of the photosphere, i.e., to a determination of the dependence of the density, temperature and other physical quantities on depth.

One of the most important results of photosphere theory must be a derivation of the energy distribution in the continuous stellar spectrum. By comparing the theoretical and observed energy distribution in a stellar spectrum one can test the validity of the assumptions serving as the basis of photosphere theory.

1. Radiation Equilibrium of the Stellar Photosphere /10

1. Radiation field. Since our immediate problem consists of analyzing the radiation field in the photosphere, we then must first of all introduce the quantities that characterize the radiation field.

---

*Numbers in the margin indicate pagination in the foreign text.

The radiation intensity is the first of these quantities. This quantity is defined as follows. Let us imagine an area element, perpendicular to the radiation direction, at a given point in space. If the size of the area is $d\sigma$, and the radiation in the frequency interval from ν to $\nu + d\nu$ is incident within the solid angle $d\omega$ during time dt, then the amount of radiant energy dE_ν, striking the area, will be proportional to $d\sigma d\nu d\omega dt$, i.e., it will be equal to

$$dE_\nu = I_\nu d\sigma\, d\nu\, d\omega\, dt. \tag{1.1}$$

The proportionality constant, entering into this equation, is called the radiation intensity. One can say that the radiation intensity is the amount of radiant energy, within a unit interval of frequency, incident within a unit solid angle during unit time on a unit area, perpendicular to the radiation direction. Generally speaking, the radiation intensity depends on the coordinates of the given point, on the radiation direction and on the frequency ν. If the radiation intensity is given, then the other quantities, characterizing the radiation field, can easily be determined. One of these is the radiation density ρ_ν, which is the amount of radiant energy within a unit interval of frequency per unit volume.

In order to express ρ_ν in terms of I_ν let us proceed in the following manner. First of all let us assume that radiation of intensity I_ν is normally incident on an area $d\sigma$ in the frequency interval from ν to $\nu + d\nu$ during time dt within a small solid angle $\Delta\omega$. Then the amount of radiant energy, striking the area, will be equal to $I_\nu\, d\sigma\, d\nu\, dt\, \Delta\omega$. It is obvious that this energy occupies a volume $d\sigma\, cdt$, where c is the velocity of light. Therefore the amount of radiant energy per unit volume will be equal to $I_\nu\, d\nu\, \Delta\omega/c$. On the other hand, by definition this quantity is equal to $\rho_\nu\, d\nu$. Consequently, in the case being considered

$$\rho_\nu = I_\nu \frac{\Delta\omega}{c}. \tag{1.2}$$

In the general case, however, when the radiation is incident from all sides on the volume, the radiation density ρ_ν is expressed by the equation

$$\rho_\nu = \frac{1}{c}\int I_\nu\, d\omega, \tag{1.3}$$

where the integration is performed over the entire solid angle.

It is also easy to express the radiation flux H_ν, which represents the /11
amount of radiant energy passing in all directions through a unit area in a unit interval of frequency per unit time, in terms of the radiation intensity. In order to do this, let us first consider the radiation passing through the area $d\sigma$ in a direction including an angle ϑ with its outward normal (Fig. 1). In this case the area of the area element that is perpendicular to the radiation direction is equal to $d\sigma\cos\vartheta$. Therefore the amount of radiant energy, passing through the

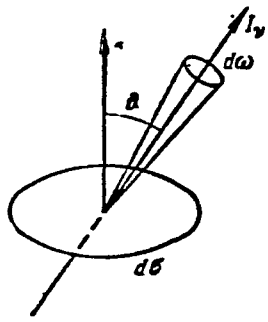

Figure 1.

area $d\sigma$ at an angle of ϑ to the normal within the solid angle $d\omega$ during time dt in the frequency interval from ν to $\nu + d\nu$, will be equal to $I_\nu\, d\sigma \cos\vartheta\, d\nu\, dt\, d\omega$. If we integrate this expression over all directions, then we obtain a quantity which, by definition, is equal to $H_\nu\, d\rho\, dt d\nu$. Consequently,

$$H_\nu = \int I_\nu \cos\vartheta\, d\omega. \tag{1.4}$$

In a spherical coordinate system with the polar axis directed along the outward normal to the surface $d\sigma$, the solid angle element is equal to $d\omega = \sin\vartheta\, d\vartheta\, d\varphi$, where φ is the azimuth of the radiation direction. Therefore the expression for the radiation flux can be rewritten in the form

$$H_\nu = \int_0^{2\pi} d\varphi \int_0^{\pi} I_\nu \cos\vartheta \sin\vartheta\, d\vartheta. \tag{1.5}$$

Since $\cos\vartheta < 0$ for $\vartheta > \pi/2$, then it follows from Eq. (1.5) that the radiation flux H_ν is the difference between two positive quantities:

$$H_\nu = \mathscr{E}_\nu - \mathscr{E}_\nu', \tag{1.6}$$

where

$$\mathscr{E}_\nu = \int_0^{2\pi} d\varphi \int_0^{\frac{\pi}{2}} I_\nu \cos\vartheta \sin\vartheta\, d\vartheta \tag{1.7}$$

and

$$\mathscr{E}_\nu' = -\int_0^{2\pi} d\varphi \int_{\frac{\pi}{2}}^{\pi} I_\nu \cos\vartheta \sin\vartheta\, d\vartheta. \tag{1.8}$$

The quantity $\mathscr{E}_\nu$ is the irradiance of the surface from one side, and the quantity $\mathscr{E}'_\nu$—the irradiance of the surface from the other side. Thus, the radiation flux /12 through any surface is the difference in the irradiances of this surface.

Let us mention an important property of the radiation intensity: in free space (i.e., when there is no absorption and emission of radiant energy in it) the radiation intensity does not change along the radiation direction.

To demonstrate this property, let us imagine two area elements in the beam, situated perpendicular to the beam and separated from each other by a

distance s. Let $d\sigma$ and $d\sigma'$ be the areas of these surfaces, and $d\omega$ and $d\omega'$—the solid angles which each surface subtends at the other. Considering the radiant energy, passing through both surfaces, we can write: $I_\nu \, d\sigma \, d\omega = I'_\nu \, d\sigma' \, d\omega'$, where I_ν and I'_ν are the radiation intensity incident on one and the other surface, respectively. But $d\omega = s^2 d\sigma'$ and $d\omega' = s^2 d\sigma$. Therefore we have $I_\nu = I'_\nu$, as was stated.

From what has been said it follows, in particular, that the solar radiation intensity at the distance from Sun to Earth is the same as when it left the Sun. It is obvious, however, that the radiation density and flux decrease with distance from the Sun.

2. Radiative transfer equation. It has already been stated above that in free space the radiation intensity does not change along the path of the radiation. Now let us assume that the space is filled by a medium capable of absorbing and emitting radiative energy. In such a case the radiation intensity will change along the radiation path, and we will now derive an equation describing this change. Beforehand, however, let us introduce into the consideration quantities characterizing the absorptivity and emissivity of the medium.

Let a radiation intensity I_ν within a solid angle $d\omega$ in the frequency interval from ν to $\nu + d\nu$ be incident on a surface $d\sigma$, perpendicular to the radiation direction, within the time dt. The amount of energy, striking the surface, will be equal to $I_\nu \, d\sigma \, d\omega \, d\nu \, dt$. If the medium is able to absorb the radiation, then along the path length ds some fraction, proportional to ds, of this amount of energy will be absorbed. We will designate this fraction $\alpha_\nu ds$. Thus, the amount of absorbed energy along the path length ds will be equal to

$$\alpha_\nu \, ds \, I_\nu \, d\sigma \, d\omega \, d\nu \, dt. \tag{1.9}$$

The quantity α_ν is called the absorption coefficient. Since the absorbed energy fraction $\alpha_\nu ds$ is a dimensionless quantity, then the absorption coefficient α_ν has the dimensions of reciprocal length. Let us mention that the absorption coefficient depends on the frequency of the radiation and on the coordinates of the given point, but is independent of the radiation direction (in an isotropic medium).

If the medium is also able to emit energy, then the amount of energy, emitted by a volume dV within a solid angle $d\omega$ in the frequency interval from ν to $\nu + d\nu$ in a time dt, will be proportional to $dV \, d\omega \, d\nu \, dt$. We will designate this energy quantity by /13

$$\varepsilon_\nu dV \, d\omega \, d\nu \, dt \tag{1.10}$$

and will call the quantity ε_ν the emission coefficient. Consequently, the emission coefficient is the amount of energy emitted by a unit volume into unit solid

angle within unit frequency interval in unit time. The emission coefficient depends on the frequency ν, on the coordinates of the given point and, in general, on the direction of emission.

Considering the quantities α_ν and ε_ν to be given, let us determine how the radiation intensity changes along the radiation path. We will assume that the radiation field is stationary, i.e., it does not change with time.

Let us imagine a cylinder element whose axis is directed along the given radiation path. Let the area of the base of the cylinder be equal to $d\sigma$, and the altitude—ds (the altitude is small compared with the linear dimensions of the base). Let us examine the radiation entering the cylinder and leaving it within the solid angle $d\omega$ in the frequency interval from ν to $\nu + d\nu$ during the time dt. If the intensity of the radiation, entering the cylinder, is I_ν, then the amount of energy entering the cylinder will be equal to

$$I_\nu \, d\sigma \, d\omega \, d\nu \, dt.$$

We will designate the intensity of the radiation leaving the cylinder by $I_\nu + dI_\nu$. Then the amount of energy leaving the cylinder will be equal to

$$(I_\nu + dI_\nu) \, d\sigma \, d\omega \, d\nu \, dt.$$

The difference between these energy quantities arises both because of energy absorption in the cylinder and because of energy emission by the cylinder. The amount of energy absorbed in the cylinder is determined by Eq. (1.9). Insofar as the energy emitted by the cylinder is concerned, it will be given in Eq. (1.10) if in it we set $dV = d\sigma \, ds$. Thus, we obtain

$$\begin{aligned}(I_\nu + dI_\nu) \, d\sigma \, d\omega \, d\nu \, dt &= \\ &= I_\nu \, d\sigma \, d\omega \, d\nu \, dt - \alpha_\nu \, ds \, I_\nu \, d\sigma \, d\omega \, d\nu \, dt + \varepsilon_\nu \, d\sigma \, ds \, d\omega \, d\nu \, dt,\end{aligned}$$

or, after the necessary cancellations,

$$\frac{dI_\nu}{ds} = -\alpha_\nu I_\nu + \varepsilon_\nu. \tag{1.11}$$

This is the desired equation, defining the variation of the intensity of the radiation as it passes through an absorbing and emitting medium. It is called the radiative transfer equation. /14

In the special case when absorption of radiant energy occurs in the medium, but not emission (i.e., $\alpha_\nu \neq 0$, and $\varepsilon_\nu = 0$), instead of Eq. (1.11) we have

$$\frac{dI_\nu}{ds} = -\alpha_\nu I_\nu. \tag{1.12}$$

Integration of this equation yields

$$I_\nu(s) = I_\nu(0)\, e^{-\int_0^s \alpha_\nu(s')\, ds'}, \tag{1.13}$$

where $I_\nu(0)$ is the radiation intensity for s = 0 (for example, the intensity of the radiation entering the medium).

The dimensionless quantity

$$\int_0^s \alpha_\nu(s')\, ds'$$

is called the optical distance between two points. The radiation intensity is reduced by a factor of e when it passes through a unit optical distance.

In the general case (i.e., when $\alpha_\nu \neq 0$ and $\varepsilon_\nu \neq 0$), by solving Eq. (1.11) with respect to I_ν, we obtain

$$I_\nu(s) = I_\nu(0)\, e^{-\int_0^s \alpha_\nu(s')\, ds'} + \int_0^s \varepsilon_\nu(s')\, e^{-\int_{s'}^s \alpha_\nu(s'')\, ds''}\, ds'. \tag{1.14}$$

The relation (1.14) can be called the radiative transfer equation in integral form.

We see that in the general case the radiation intensity consists of two parts. The first part represents the intensity of the original radiation (at the point s = 0), reduced because of absorption along the path from 0 to s. The second part is the radiation intensity produced by the emission of radiant energy along the path from 0 to s and by its corresponding attenuation because of absorption along the path from the point of emission s' to the point being considered s.

3. Radiation equilibrium equation. The radiation transfer Eq. (1.11) derived above enables one to find the radiation intensity I_ν if the emission coefficient ε_ν and absorption coefficient α_ν are known. Usually, however, in radiation transfer problems the emission coefficient ε_ν is not specified, and depends on the amount of radiant energy absorbed in the volume element, i.e., on the /15 quantities α_ν and I_ν. In order to determine this dependence, it is necessary to examine the energy processes occurring in a volume element of the given medium.

These processes are specified for each problem. We will now consider the energy processes occurring in a volume element of a stellar photosphere.

As already stated in the introduction to this chapter, there are no energy sources in the photosphere and the energy produced within the star is transferred radiatively through the photosphere. Therefore the radiation of each volume element of the photosphere occurs because of the radiant energy absorbed in it. Assuming the photosphere to be stationary, we can say that each volume element of the photosphere emits as much energy as it absorbs. This condition of the photosphere is termed the radiation equilibrium condition.

Of course, only the photospheres of those stars which do not undergo rapid changes with time are in the state of radiation equilibrium. As is known, they constitute the vast majority of the stars. It is these stars that will be the subject of this chapter. Stars with rapidly changing brightness and spectrum (for examples, novae) will be discussed later (see Chapter VI).

We will give a mathematical formulation of the radiation equilibrium condition. For this we will determine the amount of radiant energy absorbed by a volume element and the amount of energy emitted by this element.

Let us imagine a volume element with a base area $d\sigma$ and altitude dr. Let radiation of intensity I_ν be incident on this volume within a solid angle $d\omega$ in a direction forming an angle ϑ with the normal to the base. The amount of energy, striking the volume in the frequency interval from ν to $\nu + d\nu$ during time dt, will be equal to $I_\nu \, d\sigma \cos\vartheta \, d\omega \, d\nu \, dt$. Since the length of the path, traversed by the radiation in the volume, is equal to $dr \sec\vartheta$, then a fraction $\alpha_\nu \, dr \sec\vartheta$, of the total amount of energy striking the volume will be absorbed. Consequently, the amount of absorbed energy will be equal to

$$d\sigma \, dr \, dt \alpha_\nu I_\nu \, d\nu \, d\omega.$$

In order to determine the total amount of energy absorbed by tne volume, it is necessary to integrate this expression over all frequencies and over all directions. As a result, we find that the total amount of energy absorbed by the volume is given by the expression

$$d\sigma \, dr \, dt \int_0^\infty \alpha_\nu \, d\nu \int I_\nu \, d\omega. \tag{1.15}$$

On the basis of (1.10) the amount of energy, radiated by the volume $d\sigma \, dr$ /16
within the solid angle $d\omega$ in the frequency interval from ν to $\nu + d\nu$ during time dt, will be equal to

$$\varepsilon_\nu \, d\sigma \, dr \, d\omega \, d\nu \, dt.$$

Since the energy in the continuous spectrum is emitted by the volume element with the same probability in all directions, then for the total amount of energy, emitted by this volume, we obtain the expression

$$4\pi \, d\sigma \, dr \, dt \int_0^\infty \varepsilon_\nu \, d\nu. \tag{1.16}$$

Equating Eqs. (1.15) and (1.16), we find

$$4\pi \int_0^\infty \varepsilon_\nu \, d\nu = \int_0^\infty \alpha_\nu \, d\nu \int I_\nu \, d\omega. \tag{1.17}$$

Equation (1.17) is called the radiation equilibrium equation.

The radiation transfer Eq. (1.11) and the radiation equilibrium Eq. (1.17) are among the fundamental equations of stellar photosphere theory.

4. Geometrical model of photosphere. Equation (1.11) is the completely general form of the radiation transfer equation. In specific cases the form of the radiation transfer equation is determined by the coordinate system adopted, and also on what arguments the radiation intensity depends.

We can assume that a star has spherical symmetry. In this case the radiation intensity I_ν depends on two arguments: the distance r from the center of the star and the angle ϑ between the radiation direction and the radius vector. In the given case we have

$$\frac{dI_\nu}{ds} = \frac{\partial I_\nu}{\partial r}\frac{dr}{ds} + \frac{\partial I_\nu}{\partial \vartheta}\frac{d\vartheta}{ds} \tag{1.18}$$

and

$$\frac{dr}{ds} = \cos\vartheta, \qquad \frac{d\vartheta}{ds} = -\frac{\sin\vartheta}{r}. \tag{1.19}$$

Therefore the radiation transfer equation in the case of a spherically symmetric photosphere assumes the form

$$\cos\vartheta \frac{\partial I_\nu}{\partial r} - \frac{\sin\vartheta}{r}\frac{\partial I_\nu}{\partial \vartheta} = -\alpha_\nu I_\nu + \varepsilon_\nu. \tag{1.20}$$

In the case being considered, the radiation equilibrium Eq. (1.17) can be replaced by another, simpler equation having the same physical meaning. After /17 integrating Eq. (1.20) over all frequencies and over all directions, we obtain

$$\frac{1}{r^2}\frac{d}{dr}\left(r^2 \int_0^\infty H_\nu \, d\nu\right) = -\int_0^\infty \alpha_\nu \, d\nu \int I_\nu \, d\omega + 4\pi \int_0^\infty \varepsilon_\nu \, d\nu. \tag{1.21}$$

From (1.21) it is seen that if Eq. (1.17) is satisfied, then the equation

$$\frac{d}{dr}\left(r^2 \int_0^\infty H_\nu \, d\nu\right) = 0. \tag{1.22}$$

must also be satisfied. From (1.22) it follows that

$$\int_0^\infty H_\nu \, d\nu = \frac{C}{r^2}, \tag{1.23}$$

where C is some constant, determined by the energy sources of the star.

Thus, the total radiation flux (i.e., the radiation flux integrated over the entire spectrum) in a spherically symmetric photosphere is inversely proportional to the square of the distance from the center of the star. Relation (1.23), just as Eq. (1.17), is the consequence of no energy sources or sinks in the photosphere.

As already stated, nearly all stars have photospheres whose thickness is very small compared with the star radius. For these stars Eqs. (1.20) and (1.23) can be greatly simplified. This simplification is not possible for special types of stars (for example, Wolf-Rayet type stars).

If the photosphere thickness is much less than the star radius, then the photosphere layers can be considered to be plane-parallel rather than spherical (Fig. 2). In this case the angle ϑ does not change along the radiation path and instead of Eq. (1.20) we obtain

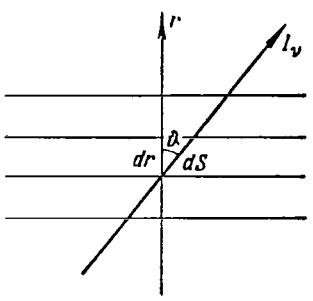

Figure 2.

$$\cos\vartheta \frac{dI_\nu}{dr} = -\alpha_\nu I_\nu + \varepsilon_\nu. \tag{1.24}$$

Since the distance r from the center of the star varies within very narrow limits in the photosphere, then instead of Eq. (1.22) we have

$$\int_0^\infty H_\nu \, d\nu = \text{const}. \tag{1.25}$$

Thus, Eqs. (1.24) and (1.17) or Eqs. (1.24) and (1.25) should be used when the radiation field in the photospheres of "conventional" stars is being considered.

2. Theory of Photospheres with a Frequency-Independent Absorption Constant

1. Basic equations. In photosphere theory the absorption coefficient was initially assumed to be independent of the frequency, leading to considerable simplification of the theory. Subsequently, however, it was established that this assumption is very crude. Nevertheless a photosphere theory with an absorption coefficient, independent of frequency, continues to have value since it can be considered as a first approximation to a more rigorous theory.

Assuming that the absorption coefficient does not depend on the frequency (i.e., $\alpha_\nu = \alpha$), instead of the radiative transfer Eq. (1.24) and the radiation equilibrium Eq. (1.17) we obtain

$$\cos\vartheta \frac{dI_\nu}{dr} = -\alpha I_\nu + \varepsilon_\nu, \tag{2.1}$$

$$4\pi \int_0^\infty \varepsilon_\nu \, d\nu = \alpha \int d\omega \int_0^\infty I_\nu \, d\nu. \tag{2.2}$$

Let us introduce the quantities

$$\int_0^\infty I_\nu \, d\nu = I, \qquad \int_0^\infty \varepsilon_\nu \, d\nu = \varepsilon. \tag{2.3}$$

The quantity I can be designated as the total radiation intensity, and the quantity ε—as the total emission coefficient.

After integrating Eq. (2.1) over all frequencies, we find

$$\cos\vartheta \frac{dI}{dr} = -\alpha I + \varepsilon, \tag{2.4}$$

and Eq. (2.2) is rewritten in the form

$$4\pi\varepsilon = \alpha \int I \, d\omega. \tag{2.5}$$

In a study of radiative transfer in any medium it is expedient to change over from geometrical distances to optical distances. In the given case it is convenient to introduce the optical depth τ, defined by the formula /19

$$\tau = \int_r^\infty \alpha \, dr. \tag{2.6}$$

Let us also set

$$\varepsilon = \alpha S. \tag{2.7}$$

Then Eqs. (2.4) and (2.5) assume the form

$$\left.\begin{aligned} \cos\vartheta \frac{dI}{d\tau} &= I - S, \\ S &= \int I \frac{d\omega}{4\pi}. \end{aligned}\right\} \tag{2.8}$$

Thus, we have derived two equations for determining the two unknowns I and S.

In the system of Eqs. (2.8) the quantity I is a function of τ and ϑ, and the quantity S is a function of τ. Taking into account that $d\omega = \sin\vartheta\, d\vartheta\, d\varphi$ and integrating with respect to φ over the limits from 0 to 2π, instead of (2.8) we obtain

$$\left.\begin{aligned} \cos\vartheta \frac{dI(\tau, \vartheta)}{d\tau} &= I(\tau, \vartheta) - S(\tau), \\ S(\tau) &= \frac{1}{2}\int_0^{\pi} I(\tau\ \vartheta)\sin\vartheta\, d\vartheta. \end{aligned}\right\} \tag{2.9}$$

It is still necessary to add a boundary condition to the system of Eqs. (2.9). It expresses the fact that there is no radiation incident on the star from the outside, i.e.,

$$I(0, \vartheta) = 0 \quad \text{when} \quad \vartheta > \frac{\pi}{2}. \tag{2.10}$$

Moreover, to obtain a completely defined solution of the system of Eqs. (2.9) under the boundary condition (2.10) the total radiation flux in the photosphere, equal to

$$H = \frac{L}{4\pi R^2}, \tag{2.11}$$

must still be specified, where L is the luminosity of the star (i.e., the total amount of energy emitted by the star in 1 second) and R is the star radius.

Systems of equations such as (2.9) are encountered very often in astrophysics. These same equations occur in geophysics (in the study of light scattering in the earth's atmosphere and in water tanks). Certain physics problems /20
(for example, the problem of neutron diffusion) also lead to similar equations. Therefore systems of equations such as (2.9) have been the subject of numerous studies and several methods have been proposed for their solution. Some of these methods, which are of greatest interest for astrophysics, are described below.

2. Approximate solution of the equations. Approximate methods, based on an averaging of the radiation intensity over directions, have been proposed for solving the system of Eqs. (2.9). The first of these methods is that of Schwarzschild [1] and Schuster [2], the second—that of Eddington [3]. We will now solve the system of Eqs, (2.9) by means of each of these methods.

Schwarzschild-Schuster method. Let us represent the average intensity of the upward radiation by $I_1(\tau)$, and the average intensity of the downward radiation—by $I_2(\tau)$. These quantities are equal to

$$I_1(\tau) = \int_0^{\frac{\pi}{2}} I(\tau, \vartheta)\sin\vartheta\, d\vartheta, \quad I_2(\tau) = \int_{\frac{\pi}{2}}^{\pi} I(\tau, \vartheta)\sin\vartheta\, d\vartheta. \tag{2.12}$$

Multiplying the first of Eqs. (2.9) by $\sin\vartheta\, d\vartheta$ and integrating over the limits from 0 to $\pi/2$, we obtain

$$\frac{d}{d\tau}\int_0^{\frac{\pi}{2}} I(\tau, \vartheta)\cos\vartheta\sin\vartheta\, d\vartheta = I_1(\tau) - S(\tau). \tag{2.13}$$

The integral on the left side of this equation will be approximated in the form

$$\int_0^{\frac{\pi}{2}} I(\tau, \vartheta)\cos\vartheta\sin\vartheta\, d\vartheta = \frac{1}{2} I_1(\tau), \tag{2.14}$$

i.e., let us take the average value of $\cos\vartheta$ in the upper hemisphere, equal to 1/2, outside the integral sign. Then instead of (2.13) we will have

$$\frac{1}{2}\frac{dI_1(\tau)}{d\tau} = I_1(\tau) - S(\tau). \tag{2.15}$$

Similarly, multiplying the first of Eqs. (2.9) by $\sin\vartheta\, d\vartheta$ and integrating over the limits from $\pi/2$ to π, we find

$$-\frac{1}{2}\frac{dI_2(\tau)}{d\tau} = I_2(\tau) - S(\tau). \tag{2.16}$$

With the aid of the quantities $I_1(\tau)$ and $I_2(\tau)$ the second of Eqs. (2.9) is rewritten thus:

$$S(\tau) = \frac{1}{2}[I_1(\tau) + I_2(\tau)]. \tag{2.17}$$

Thus, we have proceeded from the set of Eqs. (2.9) to the set (2.15)-(2.17), which is very simply solved.

Adding Eqs. (2.15) and (2.16) term by term and making use of (2.17), we find

$$I_1(\tau) - I_2(\tau) = F, \tag{2.18}$$

where F is an arbitrary constant. Substracting (2.16) from (2.15) and taking (2.18) into account, we obtain

$$I_1(\tau) + I_2(\tau) = 2F\tau + C, \tag{2.19}$$

where C is a new constant.

To determine the constants F and C let us first of all turn to the boundary condition (2.10). In the given case it means that $I_2(0) = 0$. Determining the value of $I_2(0)$ from (2.18) and (2.19) and making use of this condition, we have

$$C = F. \tag{2.20}$$

Insofar as the constant F is concerned, it is expressed in terms of the total radiation flux H, which is constant in the photosphere and is given by Eq. (2.11). By definition, the total radiation flux is equa to

$$H = 2\pi \int_0^{\pi} I(\tau, \vartheta) \cos\vartheta \sin\vartheta \, d\vartheta. \tag{2.21}$$

In the approximation assumed

$$H = 2\pi \left[\frac{1}{2} \int_0^{\frac{\pi}{2}} I(\tau, \vartheta) \sin\vartheta \, d\vartheta - \frac{1}{2} \int_{\frac{\pi}{2}}^{\pi} I(\tau, \vartheta) \sin\vartheta \, d\vartheta \right] = \pi [I_1(\tau) - I_2(\tau)]. \tag{2.22}$$

Comparing (2.22) with (2.18), we obtain /22

$$H = \pi F. \tag{2.23}$$

Substitution of (2.19) and (2.20) into (2.17) yields one of the desired functions:

$$S(\tau) = F\left(\tau + \frac{1}{2}\right) \tag{2.24}$$

The other desired function $I(\tau, \vartheta)$ is easily expressed in terms of $S(\tau)$ with the help of the first of Eqs. (2.9).

Eddington method. We will multiply the first of Eqs. (2.9) by $2\pi \cos\vartheta \sin\vartheta \, d\vartheta$ and integrate from 0 to π. Using Eq. (2.21), we obtain

$$2\pi \frac{d}{d\tau} \int_0^{\pi} I(\tau, \vartheta) \cos^2\vartheta \sin\vartheta \, d\vartheta = H. \tag{2.25}$$

Let us take the average value of $\cos^2\vartheta$ over a sphere, equal to 1/3, outside the integral, i.e., let us make the approximation

$$\int_0^{\pi} I(\tau, \vartheta) \cos^2\vartheta \sin\vartheta \, d\vartheta = \frac{1}{3} \int_0^{\pi} I(\tau, \vartheta) \sin\vartheta \, d\vartheta. \tag{2.26}$$

Then, when the second of Eqs. (2.9) is taken into consideration, we find

$$\frac{4\pi}{3}\frac{dS(\tau)}{d\tau}=H. \tag{2.27}$$

instead of (2.25).

Since the total radiation flux is constant in the photosphere, then from (2.27) it follows that

$$S(\tau)=\frac{3}{4\pi}H\tau+C, \tag{2.28}$$

where C is an arbitrary constant.

To determine C let us write the expression for the quantities $S(\tau)$ and H for $\tau = 0$. Taking the boundary condition (2.10) into account, we find

$$S(0)=\frac{1}{2}\int_{0}^{\frac{\pi}{2}} I(0,\vartheta)\sin\vartheta\, d\vartheta, \tag{2.29}$$

and also approximately /23

$$H=\pi\int_{0}^{\frac{\pi}{2}} I(0,\vartheta)\sin\vartheta\, d\vartheta. \tag{2.30}$$

Therefore we have

$$S(0)=\frac{H}{2\pi}. \tag{2.31}$$

In light of the condition (2.31), for the constant C we obtain

$$C=\frac{H}{2\pi}. \tag{2.32}$$

Substitution of (2.32) into (2.28) gives

$$S(\tau)=F\left(\frac{3}{4}\tau+\frac{1}{2}\right), \tag{2.33}$$

where, just as before, the relationship (2.23) is used.

We see that Eq. (2.33) for the function $S(\tau)$ is not very different from Eq. (2.24), derived by the previous method.

3. Application of quadrature formulas. The approximation methods discussed above have found rather wide application in astrophysics. However, accuracy of the results, obtained by these methods, is comparatively poor. Recently, therefore, another approximation method, based on the replacement of the integral term of the radiant equilibrium equation by the Gaussian sum for numerical quadratures, has come into widespread use. The radiative transfer equation in this case is written for those values of $\cos\vartheta$ which are interval division points in the quadrature formula. This permits one to reduce the problem to a system of linear differential equations with constant coefficients.

The advantage of this method is the fact that one can improve the accuracy of the results by increasing the number of terms of the quadrature formula. Even with a small number of terms in this formula, however, satisfactory results are obtained because of the high accuracy of the integral replacement by the Gaussian sum.

This method has been worked out in detail by Chandrasekhar [4]. Let us now apply this method to the solution of the system of Eqs. (2.9).

Let us begin by rewriting this system in the form of one equation:

$$\mu \frac{dI(\tau, \mu)}{d\tau} = I(\tau, \mu) - \frac{1}{2}\int_{-1}^{+1} I(\tau, \mu')\,d\mu', \tag{2.34}$$

where $\mu = \cos\vartheta$.

Let us represent the integral term of Eq. (2.34) in the form of a summation in accordance with the Gaussian quadrature formula: /24

$$\int_{-1}^{+1} I(\tau, \mu)\,d\mu = \sum_{j=-n}^{n} a_j I(\tau, \mu_j). \tag{2.35}$$

Here $\mu_{-n}, \ldots, \mu_{-1}, \mu_1, ---, \mu_n$ are the roots of the Legendre polynomial $P_{2n}(\mu)$ and a_j are some weighting factors ($a_{-j} = a_j$). The larger n, the more accurate the representation (2.35).

In the n-th approximation Eq. (2.34) is replaced by a system of linear differential equations of order 2n:

$$\mu_i \frac{dI_i}{d\tau} = I_i - \frac{1}{2}\sum_j a_j I_j \qquad (i = \pm 1, \pm 2, \ldots, \pm n), \tag{2.36}$$

where, for brevity, $I(\tau, \mu_i)$ is written as I_i.

The arbitrary constants, entering into the general solution of this system, are determined from the following conditions: 1) no external radiation is incident on the photosphere, i.e., $I_{-i} = 0$ for $\tau = 0$ ($i = 1, 2, \ldots, n$), 2) there can be no terms increasing exponentially with τ, 3) the radiation flux is given by $H = \pi F$.

After the determination of the quantities I_i from Eqs. (2.36), the desired fundamental function $s(\tau)$ is defined by the formula

$$S(\tau) = \frac{1}{2} \sum a_i I_i \tag{2.37}$$

By way of an example, let us find the function $S(\tau)$ in the first approximation. In the given case $\mu_1 = -\mu_{-1} = 1/\sqrt{3}$, $a_1 = -a_{-1} = 1$. Therefore instead of (2.36) we obtain

$$\left.\begin{aligned} \frac{1}{\sqrt{3}} \frac{dI_1}{d\tau} &= I_1 - \frac{1}{2}(I_1 + I_{-1}), \\ -\frac{1}{\sqrt{3}} \frac{dI_{-1}}{d\tau} &= I_{-1} - \frac{1}{2}(I_1 + I_{-1}). \end{aligned}\right\} \tag{2.38}$$

The system of Eqs. (2.38) must be solved under the conditions that $I_{-1} = 0$ when $\tau = 0$ and

$$\frac{2}{\sqrt{3}}(I_1 - I_{-1}) = F. \tag{2.39}$$

Determining I_1 and I_{-1} from (2.38) under the stated conditions, for the desired function $S(\tau)$ we obtain /25

$$S(\tau) = \frac{3}{4} F \left(\tau + \frac{1}{\sqrt{3}}\right). \tag{2.40}$$

As we will see later, Eq. (2.40) for the function $S(\tau)$ is more accurate than the Eqs. (2.24) and (2.33) derived previously. After increasing the number of terms in the quadrature formula (2.35), one can obtain still more accurate expressions for $S(\tau)$.

4. Milne's integral equation. From the system of Eqs. (2.9) one can derive one integral equation for determining the function $S(\tau)$. To do this it is necessary to solve the first of Eqs. (2.9) in terms of $I(\tau, \theta)$ and to substitute the resulting expression for $I(\tau, \theta)$ as a function of $S(\tau)$ into the second of these equations. This method of solving the problem is the most reasonable since we obtain one equation for determining the function, depending on only one argument.

The general solution of the first of Eqs. (2.9) has the form

$$I(\tau, \vartheta) = I(\tau_*, \vartheta) e^{-(\tau_* - \tau)\sec\vartheta} + \int^{\tau_*} e^{-(\tau' - \tau)\sec\vartheta} S(\tau') \sec\vartheta \, d\tau'. \tag{2.41}$$

It is the radiative transfer equation in integral form (compare with Eq. (1.14).

Equation (2.41) must be examined separately for two cases: for upward radiation and for downward radiation.

In the first case, assuming $\tau_* = \infty$ and that the radiation intensity does not increase exponentially with an increase in τ, we obtain

$$I(\tau, \vartheta) = \int_\tau^\infty e^{-(\tau' - \tau)\sec\vartheta} S(\tau') \sec\vartheta \, d\tau' \quad \left(\vartheta < \frac{\pi}{2}\right). \tag{2.42}$$

In the second case, assuming $\tau_* = 0$ and keeping in mind the boundary condition (2.10), we find

$$I(\tau, \vartheta) = -\int_0^\tau e^{-(\tau' - \tau)\sec\vartheta} S(\tau') \sec\vartheta \, d\tau' \quad \left(\vartheta > \frac{\pi}{2}\right) \tag{2.43}$$

Now we must substitute Eqs. (2.42) and (2.43) into the second of Eqs. (2.9). Making this substitution and changing the order of integration, we have /26

$$S(\tau) = \frac{1}{2}\int_\tau^\infty S(\tau') d\tau' \int_0^{\frac{\pi}{2}} e^{-(\tau' - \tau)\sec\vartheta} \sec\vartheta \sin\vartheta \, d\vartheta - \\ - \frac{1}{2}\int_0^\tau S(\tau') d\tau' \int_{\frac{\pi}{2}}^{\pi} e^{-(\tau' - \tau)\sec\vartheta} \sec\vartheta \sin\vartheta \, d\vartheta. \tag{2.44}$$

Let us set $\sec\vartheta = x$ in the first integral and $-\sec\vartheta = x$ in the second. Realizing that $\sec\vartheta \sin\vartheta \, d\vartheta = dx/x$, instead of the foregoing equation we obtain

$$S(\tau) = \frac{1}{2}\int_\tau^\infty S(\tau') d\tau' \int_1^\infty e^{-(\tau' - \tau)x} \frac{dx}{x} + \frac{1}{2}\int_0^\tau S(\tau') d\tau' \int_1^\infty e^{-(\tau - \tau')x} \frac{dx}{x}. \tag{2.45}$$

Since the exponent in both exponential terms can be represented in the form $-|\tau - \tau'|x$, then (2.45) can be abbreviated thus:

$$S(\tau) = \frac{1}{2}\int_0^\infty S(\tau') d\tau' \int_1^\infty e^{-|\tau - \tau'|x} \frac{dx}{x}. \tag{2.46}$$

The kernel of the integral function (2.46) is an integral exponential function, defined by the equality

$$\mathrm{Ei}\,\tau = \int_1^\infty e^{-\tau x}\frac{dx}{x}. \tag{2.47}$$

Let us note that the function Eiτ has a logarithmic character when $\tau = 0$, and as $\tau \to \infty$ it approaches zero as $e^{-\tau}/\tau$.

With the aid of (2.47) the integral equation for determining $S(\tau)$ is finally written in the form

$$S(\tau) = \frac{1}{2}\int_0^\infty \mathrm{Ei}\,|\tau - \tau'|\,S(\tau')\,d\tau'. \tag{2.48}$$

This integral equation is called Milne's equation [5].

Equation (2.48) defines the function $S(\tau)$ with an accuracy to within an arbitrary factor, which is determined from the condition that the radiation flux is given by $H = \pi F$.

We will express the radiation flux in terms of the function $S(\tau)$. To do this it is necessary to substitute Eqs. (2.41) and (2.42) into Eq. (2.21). Carrying out the same transformation as in the derivation of Eq. (2.48), we find /27

$$F = 2\int_\tau^\infty S(\tau')\,\mathrm{E}_2(\tau' - \tau)\,d\tau' - 2\int_0^\tau S(\tau')\,\mathrm{E}_2(\tau - \tau')\,d\tau', \tag{2.49}$$

where $\mathrm{E}_2\tau$ is the second of the integral exponential functions, defined by the equation

$$E_n\tau = \int_1^\infty e^{-\tau x}\frac{dx}{x^n}. \tag{2.50}$$

The function Eiτ introduced above is often written as $\mathrm{E}_1\tau$.

Milne's integral equation has been discussed by many authors. The most thorough analysis is that of Hopf [6], who has determined that the exact solution of this equation has the form

$$S(\tau) = \frac{3}{4}F[\tau + q(\tau)], \tag{2.51}$$

where $q(\tau)$ is a function that varies monotonically within narrow limits between

$$q(0)=\frac{1}{\sqrt{3}}=0.58 \quad \text{and} \quad q(\infty)=0.71.$$

It is interesting to compare the approximate expressions for $S(\tau)$, derived above with the Schwarzschild-Schuster, Eddington and Chandrasekhar (in the first approximation) methods, with the precise formula (2.51). These approximate expressions yield the formulas (2.24), (2.33) and (2.40) respectively. We see that Eq. (2.40) is the most accurate. The values of the function $S(\tau)$, determined with this formula for $\tau = 0$ and for large τ, namely

$$S(0)=\frac{\sqrt{3}}{4}F \tag{2.52}$$

and

$$S(\tau)=\frac{3}{4}F\tau \quad \text{for} \quad \tau \gg 1, \tag{2.53}$$

are identical to the exact values of $S(\tau)$. Formula (2.33) gives precise values of the function $S(\tau)$ only for $\tau \gg 1$. The values of $S(\tau)$, obtained from Eq. (2.24), differ from the exact values both for $\tau = 0$ and for $\tau \gg 1$.

5. Brightness distribution over the stellar disk. Knowing the function $S(\tau)$ makes it possible to determine the radiation intensity at any optical depth. In particular, we can find the intensity of the radiation emanating from the star, /28
i.e., the quantity $I(0, \vartheta)$. It is obvious that the intensity of the radiation, emanating from the photosphere at an angle ϑ to the normal, is the brightness of the stellar disk at an angular distance ϑ from the center of the disk (Fig. 3). Therefore the stellar disk is given by the quantity $I(0, \vartheta)$.

In order to find the quantity $I(0, \vartheta)$, it is necessary to set $\tau = 0$ in Eq. (2.42), giving the upward radiation intensity (i.e., for $\vartheta < \pi/2$), Doing this and replacing the integration variable τ' by τ, we find

$$I(0, \vartheta)=\int_0^\infty S(\tau)e^{-\tau \sec\vartheta}\sec\vartheta\, d\tau. \tag{2.54}$$

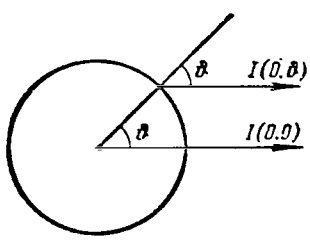

Figure 3.

Various approximate formulas have been derived above for the function $S(\tau)$. Let us see to what distribution of brightness over the stellar disk each of these formulas leads.

Using formulas (2.24), (2.33) and (2.40), derived in the Schwarzschild-Schuster and Eddington

approximations and in the first Chandrasekhar approximation respectively, for the function $S(\tau)$, we find

$$I(0,\vartheta)=F\left(\frac{1}{2}+\cos\vartheta\right), \tag{2.55}$$

$$I(0,\vartheta)=F\left(\frac{1}{2}+\frac{3}{4}\cos\vartheta\right) \tag{2.56}$$

and

$$I(0,\vartheta)=F\left(\frac{\sqrt{3}}{4}+\frac{3}{4}\cos\vartheta\right). \tag{2.57}$$

For the ratio of the brightness at the center of the disk to the brightness at the edge, i.e., for the quantity $I(0, 0)/I(0, \pi)$, these formulas give 3, 2.5 and 2.7, respectively. As we will see below, the precise value of this quantity is equal to 2.9.

Thus, the brightness at the center of the disk is considerably greater than the brightness at the edge. This is explained by the fact that at the center of the disk the radiation emanates, on the average, from deeper layers than at the edge.

The theoretical expression presented above for the brightness distribution over the stellar disk is confirmed, in general, by observational data. These data are obtained primarily with solar radiation since we do not see the disks /29 of other stars. An analysis of the luminosity variation curves of eclipsing variables also provides some information on the darkening of the stellar disk from the center to the edge. In this case one star periodically blocks the other and one can judge the brightness distribution over the disk from the radiation of the portion of the disk that remains uneclipsed.

Let us emphasize that the topic of discussion in this section has been total brightnesses (i.e., integrated over the entire spectrum). Observations, however, yield not only the distribution of the total brightness over the stellar disk, but also the brightness distribution at various wavelengths. The question of the rule for the darkening of the stellar disk from center to edge at various wavelengths will be considered below.

3. Exact Solution of the Basic Equations

1. Equation for the resolvent. Milne's integral equation, presented above, represents a special case of equations that are frequently encountered in astrophysics. All these equations have a kernel which depends on the absolute value of the difference of two arguments. A relatively simple method, which we will now discuss, has been proposed for solving such equations (see [7]). Then this method will be used to obtain an exact solution of the problem of radiation transfer through the stellar photosphere. Later, other astrophysical problems

(concerning the formation of absorption lines in stellar spectra, light scattering in planetary atmospheres, etc.) will be solved by the same method.

Let us examine the integral equation

$$S(\tau)=\int_0^\infty K(|\tau-\tau'|)S(\tau')d\tau'+g(\tau), \tag{3.1}$$

defining the function $S(\tau)$ (not identical, generally speaking, with the previously introduced function $S(\tau)$, but having an analogous physical meaning). Here $K(|\tau-\tau'|)$ is the kernel of the equation and $g(\tau)$ is a function characterizing the distribution of radiation sources in the medium. The functions $K(\tau)$ and $g(\tau)$ are specified differently for different problems (we will become acquainted with examples later).

The solution of Eq. (3.1) can be represented in the form

$$S(\tau)=g(\tau)+\int_0^\infty \Gamma(\tau,\tau')g(\tau')d\tau', \tag{3.2}$$

where $\Gamma(\tau, \tau')$ is the resolvent, satisfying, as is known, the equation /30

$$\Gamma(\tau,\tau')=K(|\tau-\tau'|)+\int_0^\infty K(|\tau-\tau''|)\Gamma(\tau'',\tau')d\tau''. \tag{3.3}$$

Here, $\Gamma(\tau, \tau')$ is a symmetrical function of τ and τ', i.e., $\Gamma(\tau, \tau') = \Gamma(\tau', \tau)$.

By using Eq. (3.3), we can derive a new equation for the resolvent. To do this let us rewrite (3.3) in the form

$$\Gamma(\tau,\tau')=K(|\tau-\tau'|)+\int_0^\tau K(a)\Gamma(\tau-a,\tau')da+\int_0^\infty K(a)\Gamma(\tau+a,\tau')da. \tag{3.4}$$

Differentiating (3.4) first with respect to τ, then with respect to τ' and adding the resulting equations term by term, we find

$$\frac{\partial\Gamma}{\partial\tau}+\frac{\partial\Gamma}{\partial\tau'}=K(\tau)\Gamma(0,\tau')+\int_0^\infty K(|\tau-\tau''|)\left(\frac{\partial\Gamma}{\partial\tau}+\frac{\partial\Gamma}{\partial\tau'}\right)d\tau''. \tag{3.5}$$

On the other hand, from Eq. (3.3) we have

$$\Gamma(0,\tau)=K(\tau)+\int_0^\infty K(|\tau-\tau''|)\Gamma(\tau'',0)d\tau''. \tag{3.6}$$

A comparison of (3.5) and (3.6) yields

$$\frac{\partial \Gamma}{\partial \tau} + \frac{\partial \Gamma}{\partial \tau'} = \Phi(\tau)\Phi(\tau'), \tag{3.7}$$

where

$$\Gamma(0, \tau) = \Phi(\tau). \tag{3.8}$$

From (3.7) it follows (for $\tau' > \tau$) that

$$\Gamma(\tau, \tau') = \Phi(\tau' - \tau) + \int_0^{\tau} \Phi(a)\Phi(a + \tau' - \tau)\,da. \tag{3.9}$$

Thus, the resolvent $\Gamma(\tau, \tau')$ is expressed in terms of the function $\Phi(\tau)$, depending only on one argument.

The equation

$$\Phi(\tau) = K(\tau) + \int_0^{\infty} K(|\tau - \tau'|)\Phi(\tau')\,d\tau', \tag{3.10}$$

which is Eq. (3.6) with (3.8) taken into consideration, can be used for determining the function $\Phi(\tau)$. Another equation for determining $\Phi(\tau)$ will be derived below. /31

2. Auxiliary equations. The solution of Eq. (3.1) for any function $g(\tau)$ is expressed in terms of the function $\Phi(\tau)$. Therefore the function $\Phi(\tau)$ must play a fundamental role in the theory of the equations under consideration. For the purpose of determining this function we will now derive some auxiliary equations. Moreover, as we shall see later, these equations are of interest in themselves.

Let us consider the equation

$$S(\tau, x) = \int_0^{\infty} K(|\tau - \tau'|)S(\tau', x)\,d\tau' + e^{-x\tau}, \tag{3.11}$$

which is a special case of Eq. (3.1). On the basis of Eq. (3.2) we have

$$S(\tau, x) = e^{-x\tau} + \int_0^{\infty} \Gamma(\tau', \tau)e^{-x\tau'}\,d\tau'. \tag{3.12}$$

Multiplying (3.7) by $e^{-x\tau'}$, integrating with respect to τ' over the limits from 0 to ∞ and taking (3.12) into consideration, we obtain

$$\frac{\partial S(\tau, x)}{\partial \tau} = -xS(\tau, x) + \Phi(\tau)\left[1 + \int_0^{\infty} \Phi(\tau')e^{-x\tau'}d\tau'\right]. \tag{3.13}$$

But from (3.12) it follows that

$$S(0,x)=1+\int_0 \Phi(\tau)e^{-x\tau}d\tau. \tag{3.14}$$

Therefore we find

$$\frac{\partial S(\tau,x)}{\partial\tau}=-xS(\tau,x)+S(0,x)\Phi(\tau). \tag{3.15}$$

Integration of Eq. (3.15) gives

$$S(\tau,x)=S(0,x)\left[e^{-x\tau}+\int_0^\tau e^{-x(\tau-\tau')}\Phi(\tau')d\tau'\right]. \tag{3.16}$$

In most radiative transfer problems the kernel of the integral equation (3.1) is represented in the form

$$K(\tau)=\int_a^b A(y)e^{-y\tau}dy, \tag{3.17}$$

where A(y) is an arbitrary function, a and b are some numbers. In this case relatively simple equations are obtained for determining the function S(0, x). In turn, the desired function $\Phi(\tau)$ is expressed in terms of the function S(0, x). /32

If $K(\tau)$ is given by Eq. (3.17), then from Eq. (3.11) it follows that

$$S(0,x)=1+\int_a^b A(y)dy\int_0^\infty S(\tau,x)e^{-y\tau}d\tau. \tag{3.18}$$

Multiplying (3.15) by $e^{-y\tau}$, integrating with respect to τ over the limits from 0 to ∞ and bearing in mind (3.14), we find

$$\int_0^\infty S(\tau,x)e^{-y\tau}d\tau=\frac{S(0,x)S(0,y)}{x+y}. \tag{3.19}$$

Substitution of (3.19) into (3.18) yields

$$S(0,x)=1+S(0,x)\int_a^b A(y)\frac{S(0,y)}{x+y}dy. \tag{3.20}$$

We have derived a nonlinear integral equation for determining S(0, x), which can be readily solved numerically.

From Eq. (3.20) one can also derive a linear integral equation for determining S(0, x). Multiplying (3.20) by A(x)/(x-z) and integrating with respect to x over the limits from a to b, we find, after some manipulations,

$$S(0,z)\left[1-2\int_a^b A(x)\frac{x\,dx}{x^2-z^2}\right]=1-\int_a^b A(x)\frac{S(0,x)}{x-z}\,dx. \tag{3.21}$$

The solution of this equation can be derived in explicit form.

3. Determination of the function $\Phi(\tau)$. Comparing Eqs. (3.10) and (3.11) with each other, we see that the free term of Eq. (3.10) is a superposition of the free terms of Eq. (3.11). Therefore we have

$$\Phi(\tau)=\int_a^b A(x)S(\tau,x)\,dx. \tag{3.22}$$

Multiplying (3.16) by A(x) and integrating with respect to x over the limits from a to b, we find /33

$$\Phi(\tau)=L(\tau)+\int_0^\tau L(\tau-\tau')\Phi(\tau')\,d\tau', \tag{3.23}$$

where

$$L(\tau)=\int_a^b A(x)S(0,x)e^{-x\tau}\,dx. \tag{3.24}$$

Equation (3.23) is the desired equation for defining the function $\Phi(\tau)$. Applying the Laplace transformation to it, we obtain

$$\int_0^\infty \Phi(\tau)e^{-s\tau}\,d\tau=\frac{1}{1-\int_a^b A(x)S(0,x)\frac{dx}{x+s}}-1. \tag{3.25}$$

Thus, the determination of the resolvent of Eq. (3.1) reduces to finding the function S(0, x) from Eq. (3.20) [or (3.21)] and to the subsequent determination of the function $\Phi(\tau)$ from (3.25) by means of the inverse Laplace transformation. The latter operation is easily done by the contour integration method through the utilization of the relation (3.21).

If the function $\Phi(\tau)$ is known, then with the aid of Eqs. (3.2) and (3.9) the function $S(\tau)$ can be found for any radiation sources. In some cases the function $S(\tau)$ is very simply expressed in terms of $\Phi(\tau)$. The case when the radiation sources are exponentially distributed in the medium can serve as an example. As already shown above, when $g(\tau)=e^{-x\tau}$, the function $S(\tau)$, which we have designated by $S(\tau, x)$, is given by Eq. (3.16).

An especially simple expression for the function $S(\tau)$ is obtained for a uniform distribution of radiation sources in the medium, i. e., for $g(\tau) = 1$. Assuming $x = 0$ in Eq. (3.16), we find

$$S(\tau, 0) = S(0, 0)\left[1 + \int_0^{\tau} \Phi(\tau')\,d\tau'\right]. \tag{3.26}$$

The quantity $S(0, 0)$ entering into Eq. (3.26), is directly expressed in terms of the function $A(x)$. Let us set $x = 0$ in (3.20) and $z = 0$ in (3.21). Then from the resulting equations it follows that

$$S^2(0, 0)\left[1 - 2\int_a^b A(x)\frac{dx}{x}\right] = 1. \tag{3.27}$$

Simple formulas for the function $S(\tau)$ can also be derived when $g(\tau) = \tau^n$, where n is a whole number. /34

4. Solution of the homogeneous equation. It has been shown above that the solution of the nonhomogeneous Eq. (3.1) for any function $g(\tau)$ is expressed in terms of the function $\Phi(\tau)$. Now let us show that the solution of the homogeneous equation

$$S(\tau) = \int_0^{\infty} K(|\tau - \tau'|)S(\tau')\,d\tau'. \tag{3.28}$$

is expressed in terms of the same function $\Phi(\tau)$. From the physical point of view this equation corresponds to the case when the energy sources are located at an infinitely great depth.

Assuming that a solution of Eq. (3.28) exists, let us differentiate it with respect to τ. As a result we find

$$S'(\tau) = \int_0^{\infty} K(|\tau - \tau'|)S'(\tau')\,d\tau' + S(0)K(\tau). \tag{3.29}$$

Comparing Eqs. (3.29) and (3.10) with each other, we see that

$$S'(\tau) = kS(\tau) + S(0)\Phi(\tau), \tag{3.30}$$

where k is some constant. From (3.30) it follows that

$$S(\tau) = S(0)\left[e^{k\tau} + \int_0^{\tau} e^{k(\tau-\tau')}\Phi(\tau')\,d\tau'\right]. \tag{3.31}$$

To determine the constant k, let us consider Eq. (3.28) for $\tau = 0$. Taking (3.17) into consideration, we have

$$S(0)=\int_a^b A(x)\,dx\int_0^\infty S(\tau)e^{-x\tau}\,d\tau. \tag{3.32}$$

Multiplying (3.30) by $e^{-x\tau}$, integrating with respect to τ over the limits from 0 to ∞ and taking (3.14) into consideration, we find

$$\int_0^\infty S(\tau)e^{-x\tau}\,d\tau = S(0)\frac{S(0,x)}{x-k}. \tag{3.33}$$

Substitution of (3.33) into (3.32) yields

$$\int_a^b A(x)\frac{S(0,x)}{x-k}\,dx = 1, \tag{3.34}$$

or, when (3.21) is taken into consideration, /35

$$2\int_a^b A(x)\frac{x\,dx}{x^2-k^2} = 1. \tag{3.35}$$

Thus, the solution of the homogeneous Eq. (3.28) is expressed in terms of the function $\Phi(\tau)$ by Eq. (3.31), in which the constant k is defined by Eq. (3.35).

It should be noted that the various mathematical problems, associated with the analysis of the integral equations of radiative transfer theory (both homogeneous as well as nonhomogeneous), are considered in detail in the book of Busbridge [8]. There the solutions of some of these equations are given in explicit form, expressed in terms of the function $\Phi(\tau)$.

5. Intensity of the emergent radiation. The auxiliary function $\Phi(\tau)$ is of interest not only because the resolvent of the integral Eq. (3.1) is expressed in terms of it. No less significant is the fact that the intensity of radiation, emerging from the medium, is in many cases directly expressed in terms of the same function.

We will now examine some of these cases; however we will first derive an important general formula for the intensity of the radiation emanating from the medium.

Let us consider the radiation emanating from a semi-infinite medium at an angle ϑ to the normal. Denoting $\cos\vartheta$ by μ, we have

$$I(0,\mu)=\int_0^\infty S(\tau)e^{-\frac{\tau}{\mu}}\frac{d\tau}{\mu}. \tag{3.36}$$

for the intensity of this radiation. Here, $S(\tau)$ is understood to be the solution of the integral Eq. (3.1) for any function $g(\tau)$, i.e., for any radiation sources.

The function $S(\tau)$ is expressed in terms of $g(\tau)$ and of the resolvent $\Gamma(\tau, \tau')$ by means of Eq. (3.2). Substituting (3.2) into (3.36), we obtain

$$I(0,\mu)=\int_0^\infty g(\tau)\frac{d\tau}{\mu}\left[e^{-\frac{\tau}{\mu}}+\int_0^\infty \Gamma(\tau,\tau')e^{-\frac{\tau'}{\mu}}d\tau'\right]. \tag{3.37}$$

From this, on the basis of (3.12), it follows that

$$I(0,\mu)=\int_0^\infty g(\tau)S\left(\tau,\frac{1}{\mu}\right)\frac{d\tau}{\mu}. \tag{3.38}$$

This is the desired formula for the radiation intensity. Thus, to determine the function $I(0, \mu)$ for any radiation sources it is sufficient to know only the function $S(\tau, x)$, defined by Eq. (3.11). /36

However, as already stated, in many special cases we need only know the function $S(0, x)$ to determine the radiation intensity. Since, however, this function is determined from Eq. (3.20) or (3.21), then in these cases it is not required that the function $\Phi(\tau)$ be known to determine $I(0, \mu)$.

Let us consider the following special cases of radiation source distributions:

1. Let the function $g(\tau)$ decrease exponentially with the optical depth, i.e.,

$$g(\tau) = e^{-m\tau}. \tag{3.39}$$

In the given case, by using Eq. (3.19) we find

$$I(0,\mu)=\frac{S(0,m)S\left(0,\frac{1}{\mu}\right)}{1+m\mu}. \tag{3.40}$$

2. Let us assume that the radiation sources are uniformly distributed in the medium, i.e., $g(\tau) = 1$. In this case, assuming $m = 0$ in (3.40), we obtain

$$I(0,\mu)=S(0,0)S\left(0,\frac{1}{\mu}\right). \tag{3.41}$$

Substitution of $S(0, 0)$ from (3.37) into (3.41) yields

$$I(0,\mu)=S\left(0,\frac{1}{\mu}\right)\left[1-2\int_a^b A(x)\frac{dx}{x}\right]^{-1/2}. \tag{3.42}$$

3. Let us assume that $g(\tau) = \tau$. On the basis of Eq. (3.38) we have

$$I(0,\mu)=\int_0^\infty \tau S\left(\tau,\frac{1}{\mu}\right)\frac{d\tau}{\mu}. \tag{3.43}$$

We will use Eq. (3.15) to determine the integral of (3.43). Multiplying the former by τ and integrating with respect to τ from 0 to ∞, we obtain

$$x\int_0^\infty S(\tau,x)\tau\,d\tau=\int_0^\infty S(\tau,x)\,d\tau+S(0,x)\int_0^\infty \Phi(\tau)\tau\,d\tau. \tag{3.44}$$

But from Eqs. (3.38) and (3.41) it follows that /37

$$x\int_0^\infty S(\tau,x)\,d\tau=S(0,0)S(0,x). \tag{3.45}$$

Therefore instead of (3.44) we find

$$x\int_0^\infty S(\tau,x)\tau\,d\tau=S(0,x)\left[\frac{1}{x}S(0,0)+\int_0^\infty \Phi(\tau)\tau\,d\tau\right]. \tag{3.46}$$

To determine the integral on the right side of Eq. (3.46) we will multiply this relation by $A(x)dx/x$ and integrate from a to b. Making use of Eq. (3.22) and Eq. (3.20), for $x = 0$ we obtain

$$\int_0^\infty \Phi(\tau)\tau\,d\tau=S^2(0,0)\int_a^b A(x)S(0,x)\frac{dx}{x^2}. \tag{3.47}$$

Replacing x in (3.46) by $1/\mu$ and substituting (3.47) into it, we finally find

$$I(0,\mu)=S(0,0)S\left(0,\frac{1}{\mu}\right)\left[\mu+S(0,0)\int_a^b A(x)S(0,x)\frac{dx}{x^2}\right]. \tag{3.48}$$

Similarly, making use of Eq. (3.38) and (3.15), one can find the radiation intensity $I(0, \mu)$ in the case when $g(\tau) = \tau^n$ for any whole number n.

4. Let us assume that the radiation sources are located at an infinitely great depth. In this case the function $S(\tau)$, defined by the homogeneous Eq. (3.28), is related to the function $\Phi(\tau)$ by the expression (3.20). Multiplying this expression by $e^{-\tau/\mu}$ and integrating with respect to τ from 0 to ∞, we find

$$I(0,\mu)(1-k\mu)=S(0)\left[1+\int_0^\infty \Phi(\tau)e^{-\frac{\tau}{\mu}}d\tau\right]. \tag{3.49}$$

From this, with the use of Eq. (3.14), it follows that

$$I(0,\mu)=S(0)\frac{S\left(0,\frac{1}{\mu}\right)}{1-k\mu}. \tag{3.50}$$

We see that in all the cases considered the radiation intensity $I(0, \mu)$ is expressed in terms of the function $S(0, x)$ by very simple formulas. Later these formulas will be used repeatedly.

6. Application to stellar photospheres. We will apply the method discussed above to the solution of the problem of radiative transfer through the stellar photosphere. As we know, under the assumption of the frequency-independence of the absorption coefficient this problem reduces to the Milne integral equation /38

$$S(\tau)=\frac{1}{2}\int_0^\infty \mathrm{Ei}|\tau-\tau'|S(\tau')d\tau'. \tag{3.51}$$

We see that this equation is a special case of the homogeneous Eq. (3.28) for

$$K(\tau)=\frac{1}{2}\mathrm{Ei}\,\tau=\frac{1}{2}\int_1^\infty e^{-\tau x}\frac{dx}{x}, \tag{3.52}$$

i.e., for $A(x) = 1/2x$, $a = 1$ and $b = \infty$.

The application of the method discussed must begin with the formulation of an equation for determining the function $S(0, x)$. To simplify the notation we will designate x by $1/\mu$ and $S(0, x)$ by $\varphi(\mu)$. Then Eq. (3.20) for the given case assumes the form

$$\varphi(\mu)=1+\frac{\mu}{2}\varphi(\mu)\int_0^1\frac{\varphi(\mu')}{\mu+\mu'}d\mu'. \tag{3.53}$$

Equation (3.53) was first derived by V.A. Ambartsumyan [9] by another method. Detailed tables of the function $\varphi(\mu)$ have been compiled by solving this equation numerically. This function increases monotonically from the value $\varphi(0) = 1$ to the value $\varphi(1) = 2.9$. An expression for $\varphi(\mu)$ has also been derived in explicit form*.

*See Chapter IV for a more detailed discussion of equations of the type (3.53).

If the function $\varphi(\mu)$ is known, then the function $\Phi(\tau)$ can be found. For its definition we have the equation

$$\int_0^\infty \Phi(\tau) e^{-s\tau} d\tau = \frac{1}{1 - \frac{1}{2}\int_0^1 \varphi(\mu) \frac{d\mu}{1+s\mu}} - 1, \tag{3.54}$$

resulting from (3.25). Performing a Laplace transformation yields

$$\Phi(\tau) = \sqrt{3} + 2\int_0^1 \frac{e^{-\frac{\tau}{\mu}} d\mu}{\left[(\pi\mu)^2 + \left(2 + \mu \ln\frac{1-\mu}{1+\mu}\right)^2\right]\mu\varphi(\mu)}. \tag{3.55}$$

Equation (3.55) was derived by this means in I. N. Minin's paper [10]. A table of values of the function $\Phi(\tau)$ is given there. /39

Knowing the function $\Phi(\tau)$ allows one to obtain the solution of the homogeneous Eq. (3.51) as well as the solution of the corresponding nonhomogeneous equation. Now, however, we are only interested in the solution of Eq. (3.51). This solution is determined by Eq. (3.31).

From Eq. (3.35) it follows that in the given case k = 0. Therefore we have

$$S(\tau) = S(0)\left[1 + \int_0^\tau \Phi(\tau')d\tau'\right]. \tag{3.56}$$

The desired exact solution of Milne's integral equation is given by Eq. (3.56).

We can also derive an exact relation for the brightness distribution over the stellar disk. The brightness at an angular distance of ϑ from the center of the disk is given by Eq. (2.53). Assuming $\cos\vartheta = \mu$ in it, we pass over to Eq. (3.36). It has been shown above that the radiation intensity $I(0, \mu)$ for sources at infinity is determined by Eq. (3.50). But in the given case k = 0 and $S(0, 1/\mu) = \varphi(\mu)$. Therefore the brightness at an angular distance of arccos μ from the center of the disk will be equal to

$$I(0, \mu) = S(0)\varphi(\mu). \tag{3.57}$$

For the ratio of the brightness at the center of the disk to the brightness at the edge we find the value $\varphi(1)/\varphi(0) = 2.9$, already mentioned in previous section.

The quantity S(0) entering into Eqs. (3.56) and (3.57) can be expressed in terms of the radiation flux πF in the photosphere. We have

$$F = 2\int_0^1 I(0, \mu)\mu\, d\mu = 2S(0)a_1 \tag{3.58}$$

where the notation

$$\alpha_n = \int_0^1 \varphi(\mu)\mu^n d\mu. \tag{3.59}$$

is used.

The quantities α_n, representing the moments of the function $\varphi(\mu)$, can be found from Eq. (3.53). Integrating this equation with respect to μ over the limits from 0 to 1, we obtain /40

$$\alpha_0 = 1 + \frac{1}{2}\int_0^1\int_0^1 \varphi(\mu)\varphi(\mu')\frac{\mu}{\mu+\mu'}d\mu\, d\mu' = 1 + \frac{1}{2}\alpha_0^2 -$$

$$-\frac{1}{2}\int_0^1\int_0^1 \varphi(\mu)\varphi(\mu')\frac{\mu'}{\mu+\mu'}d\mu\, d\mu' = 2 + \frac{1}{2}\alpha_0^2 - \alpha_0, \tag{3.60}$$

from which it follows that

$$\alpha_0 = 2. \tag{3.61}$$

Multiplying (3.53) by $\mu^2 d\mu$ and integrating over the limits from 0 to 1, we similarly find

$$\alpha_1 = \frac{2}{\sqrt{3}}. \tag{3.62}$$

Substitution of (3.62) into (3.58) yields

$$F = \frac{4}{\sqrt{3}} S(0). \tag{3.63}$$

This formula, expressing the exact relationship between the quantities F and S(0), has already been presented in a previous section.

Substituting (3.63) into (3.56), we find

$$S(\tau) = \frac{\sqrt{3}}{4} F\left[1 + \int_0^\tau \Phi(\tau')d\tau'\right]. \tag{3.64}$$

A comparison of (3.64) with (2.50) yields

$$q(\tau) = \frac{1}{\sqrt{3}}\left[1 + \int_0^\tau \Phi(\tau')d\tau'\right] - \tau. \tag{3.65}$$

If we substitute Eq. (3.55) into (3.65), then we arrive at the formula for $q(\tau)$ first derived in Mark's work by another method.

4. Local Thermodynamic Equilibrium

1. Radiation field in presence of thermodynamic equilibrium. As we will see later, formulas describing the state of thermodynamic equilibrium are widely used in photosphere theory. Therefore we should cite some of these equations. The problem of the radiation field in the presence of thermodynamic equilibrium is of special interest to us.

Thermodynamic equilibrium, as is known, is established in a cavity whose walls are heated to some constant temperature T. The state of thermodynamic equilibrium is characterized by the fact that each process is in equilibrium with its opposing process (this constitutes the "principle of detailed equilibrium"). From this, in particular, it follows that the radiation intensity in the presence of thermodynamic equilibrium is independent of position and direction. If this were not so, then there would be a transfer of energy from one point to another in certain directions. /41

It is also obvious that the radiation intensity in the presence of thermodynamic equilibrium does not depend on the individual properties of the cavity. To clarify this it is sufficient to assume that there are two cavities with identical temperatures, but with different intensity values of radiation of frequency ν. Then when these cavities are connected, there would be a transfer of energy from one cavity to the other, in violation of the second law of thermodynamics.

Thus, the radiation intensity in the presence of thermodynamic equilibrium depends only on the frequency and temperature. We will denote this intensity by $B_\nu(T)$.

We will apply the radiative transfer Eq. (1.11) to the case under consideration. Since $dI_\nu/ds = 0$ in the given case, then from (1.11) it follows that

$$\frac{\varepsilon_\nu}{\alpha_\nu} = B_\nu(T). \tag{4.1}$$

Kirchhoff's law is expressed by Eq. (4.1): in the presence of thermodynamic equilibrium the ratio of the emission coefficient to the absorption coefficient is equal to the radiation intensity, being a universal function of frequency and temperature.

An expression for the radiation intensity under thermodynamic equilibrium was first determined by Planck. Planck's formula has the form

$$B_\nu(T) = \frac{2h\nu^3}{c^2}\frac{1}{e^{\frac{h\nu}{kT}}-1}, \tag{4.2}$$

where h is Planck's constant and k is Boltzmann's constant.

As already stated, the radiation intensity in the presence of thermodynamic equilibrium does not depend on direction, i.e., the radiation is isotropic. In this case, as follows from Eq. (1.3), the radiation density is equal to

$$\rho_\nu(T) = \frac{4\pi}{c} B_\nu(T). \tag{4.3}$$

Therefore in the presence of thermodynamic equilibrium we obtain /42

$$\rho_\nu(T) = \frac{8\pi h\nu^3}{c^3} \frac{1}{e^{\frac{h\nu}{kT}} - 1}. \tag{4.4}$$

for the radiation intensity $\rho_\nu(T)$.

The radiation flux in the presence of thermodynamic equilibrium is obviously equal to zero. However, the radiation flux emanating through a small opening from the cavity mentioned differs from zero. To determine this flux it is necessary to utilize Eq. (1.4) and to bear in mind that the intensity of the radiation emanating from the cavity is independent of direction, and there is no radiation entering the cavity. As a result, for the radiation flux $H_\nu(T)$ in this case we obtain

$$H_\nu(T) = \pi B_\nu(T). \tag{4.5}$$

Let us mention that if radiation enters the cavity through a small opening, then it is practically completely absorbed in it. One can say that in this case we are dealing with an absolutely black body. Therefore the quantity $B_\nu(T)$ is often called the radiation intensity of an absolute black body.

After integrating Eq. (4.4) over all frequencies, we obtain the total radiation density in the presence of thermodynamic equilibrium:

$$\rho(T) = \int_0^\infty \rho_\nu(T)\, d\nu = \frac{8\pi h}{c^3} \int_0^\infty \frac{\nu^3 d\nu}{e^{\frac{h\nu}{kT}} - 1}, \tag{4.6}$$

or

$$\rho(T) = aT^4, \tag{4.7}$$

where

$$a = \frac{8\pi^5 k^4}{15 c^3 h^3}. \tag{4.8}$$

Equation (4.7) expresses the Stefan-Boltzmann law. The quantity a is Stefan's constant.

Integrating Eq. (4.2) over all frequencies, we find the total radiation intensity of an absolute black body

$$B(T) = \frac{ac}{4} T^4. \tag{4.9}$$

From (4.5) and (4.9) it follows that the total radiation flux, emanating from an absolute black body, is equal to

$$H(T) = \sigma T^4, \tag{4.10}$$

where /43

$$\sigma = \frac{ac}{4}. \tag{4.11}$$

2. Assumption of local thermodynamic equilibrium of the stellar photosphere. The radiation field in the photosphere differs drastically from the radiation field in the presence of thermodynamic equilibrium. This has already been seen from the fact that the radiation intensity in the photosphere depends on the depth and on the direction. Therefore nothing can be said concerning the presence of thermodynamic equilibrium in the photosphere on the whole.

Even the conditions in a volume element of the photosphere are far removed from the conditions of thermodynamic equilibrium (if only because of the anisotropy of the radiation incident on the volume). However, the radiation absorbed by the volume element is reprocessed to a considerable degree of it. As known from thermodynamics, this reprocessing is in the direction of establishing thermodynamic equilibrium. Therefore one can assume that at each point of the photosphere the emission coefficient ε_ν is related to the absorption coefficient α_ν by the same relation as in the presence of thermodynamic equilibrium with some temperature T characteristic of a given point. In this situation the temperature is determined from the condition that the total amount of energy, emitted by the volume element, is equal to the total amount of energy absorbed by this volume, i.e., from the radiant equilibrium condition.

This assumption is called the assumption of local thermodynamic equilibrium of the stellar photosphere. There is no doubt that it is satisfied with high accuracy in the deep layers of the photosphere. The question of to what extent this assumption is satisfied in the surface layers of stars is rather difficult to analyze theoretically. Some conclusions on this question can be drawn by comparing theory with observations (see Section 6).

The assumption of local thermodynamic equilibrium means that in the stellar photosphere the ratio of the emission coefficient to the absorption coefficient is given by Eqs. (4.1) and (4.2), i.e.,

$$\frac{\varepsilon_\nu}{\alpha_\nu} = \frac{2h\nu^3}{c^2} \frac{1}{e^{\frac{h\nu}{kT}} - 1}. \tag{4.12}$$

Equation (4.12) is one of a number of the fundamental relations of photosphere theory (together with the radiative transfer equation and the radiant equilibrium equation).

The adoption of the assumption of local thermodynamic equilibrium greatly simplifies photosphere theory. Without such an assumption the calculation of the radiation field in the photosphere for different frequencies would be extremely difficult. /44

Just as before, we will now assume that the absorption coefficient is frequency independent. In this case the dependence of the temperature on the optical thickness is obtained in explicit form and it is quite easy to calculate the radiation field in the photosphere for different frequencies.

If the absorption coefficient does not depend on the frequency, then Eq. (4.12) assumes the form

$$\varepsilon_\nu = \alpha \frac{2h\nu^3}{c^2} \frac{1}{e^{\frac{h\nu}{kT}} - 1}. \tag{4.13}$$

Integrating (4.13) over all frequencies, we obtain

$$\varepsilon = \alpha \frac{ac}{4\pi} T^4, \tag{4.14}$$

where (4.9) has been taken into consideration. Just as in Section 2, we will define $\varepsilon = \alpha S$. The quantity S was determined in the theory of radiant equilibrium as a function of the optical depth τ. Therefore we have

$$S(\tau) = \frac{ac}{4\pi} T^4. \tag{4.15}$$

The relationship between temperature and optical depth is also given by this formula.

If the quantity $S(\tau)$ is found in the Eddington approximation, then it is defined by Eq. (2.33). In this case we obtain

$$\frac{ac}{4} T^4 = \pi F \left(\frac{1}{2} + \frac{3}{4} \tau \right). \tag{4.16}$$

After taking for $S(\tau)$ the exact expression given by Eq. (2.50), we find

$$\frac{ac}{4} T^4 = \pi F \frac{3}{4} [\tau + q(\tau)]. \tag{4.17}$$

The quantity πF entering into Eqs. (4.16) and (4.17) is the total radiation flux in the photosphere. It is convenient to represent it as the total radiation flux of an absolute black body at some temperature T_e, i.e., based on Eq. (4.10), to set

$$\pi F = \sigma T_e^4, \tag{4.18}$$

where $\sigma = ac/4$. The temperature T_e is called the effective stellar temperature. It is related to the stellar luminosity L and stellar radius R by the expression /45

$$L = 4\pi R^2 \sigma T_e^4. \tag{4.19}$$

Substitution of (4.18) into Eqs. (4.16) and (4.17) yields

$$T^4 = T_e^4 \left(\frac{1}{2} + \frac{3}{4}\tau\right), \tag{4.20}$$

$$T^4 = T_e^4 \frac{3}{4}[\tau + q(\tau)]. \tag{4.21}$$

Assuming $\tau = 0$ in the formulas that have been derived, we can define the surface temperature T_0. In the Eddington approximation we find

$$T_0 = \frac{1}{\sqrt[4]{2}} T_e = 0.841\, T_e. \tag{4.22}$$

The exact relationship between T_0 and T_e is

$$T_0 = \left(\frac{\sqrt{3}}{4}\right)^{1/4} T_e = 0.811\, T_e. \tag{4.23}$$

After setting $T = T_e$ in these same formulas, we find the optical depth corresponding to the effective stellar temperature. It is found to be equal to $\tau = 2/3$ from Eq. (4.20) and $\tau = 0.64$ from Eq. (4.21).

3. Radiation coming from the photosphere. In order to determine the radiation field in the photosphere for different frequencies, we must make use of the radiation transfer equation

$$\cos\vartheta \frac{dI_\nu}{dr} = -\alpha_\nu I_\nu + \varepsilon_\nu. \tag{4.24}$$

Assuming here

$$\frac{\varepsilon_\nu}{\alpha_\nu} = S_\nu \tag{4.25}$$

and introducing the optical depth in the photosphere at frequency ν

$$\tau_\nu = \int_r^\infty \alpha_\nu \, dr, \tag{4.26}$$

instead of (4.24) we obtain /46

$$\cos\vartheta \frac{dI_\nu(\tau_\nu, \vartheta)}{d\tau_\nu} = I_\nu(\tau_\nu, \vartheta) - S_\nu(\tau_\nu). \tag{4.27}$$

Integrating Eq. (4.27), one can determine the radiation intensity at different optical depths. Of most interest to us is the intensity of the radiation coming from the star, i.e., the quantity $I_\nu(0, \vartheta)$. The quantity is equal to

$$I_\nu(0, \vartheta) = \int_0^\infty S_\nu(\tau_\nu) e^{-\tau_\nu \sec\vartheta} \sec\vartheta \, d\tau_\nu. \tag{4.28}$$

Equation (4.28) is a simple consequence of the radiation transfer equation. Let us now make use of the assumption of local thermodynamic equilibrium. Comparing Eqs. (4.25) and (4.1) with each other, we see that with this assumption

$$S_\nu(\tau_\nu) = B_\nu(T), \tag{4.29}$$

where $B_\nu(T)$ is the intensity of the radiation of an absolute black body, given by Eq. (4.2). Therefore in the case of local thermodynamic equilibrium, instead of (4.28) we obtain

$$I_\nu(0, \vartheta) = \int_0^\infty B_\nu(T) e^{-\tau_\nu \sec\vartheta} \sec\vartheta \, d\tau_\nu, \tag{4.30}$$

or

$$I_\nu(0, \vartheta) = \frac{2h\nu^3}{c^2} \int_0^\infty \frac{e^{-\tau_\nu \sec\vartheta} \sec\vartheta \, d\tau_\nu}{e^{\frac{h\nu}{kT}} - 1}. \tag{4.31}$$

Equation (4.31) gives the intensity of radiation of frequency ν, emanating from the star at an angle of ϑ with respect to the radius vector. At the same time it gives the brightness of the stellar disk at frequency ν at an angular distance of ϑ from the center of the disk (see Section 2).

The quantity $I_\nu(0, \vartheta)$ can be determined from observations of the Sun and of eclipsing variables. From observations of other stars only a quantity, proportional to the radiation flux H_ν from the stellar surface, is obtained. More precisely, these observations give the stellar illuminance, equal to

$$\mathscr{E}_\nu = \frac{L_\nu}{4\pi r^2}, \tag{4.32}$$

where L_ν is the stellar luminosity at the frequency ν and r is the distance from the star to the observer. But /47

$$L_\nu = 4\pi R^2 H_\nu, \tag{4.33}$$

where R is the star radius. Therefore we have

$$\mathscr{E}_\nu = \left(\frac{R}{r}\right)^2 H_\nu. \tag{4.34}$$

Thus, the radiation flux H_ν characterizes the relative distribution of energy in the stellar spectrum.

The radiation flux H_ν is defined by the formula

$$H_\nu = 2\pi \int_0^{\frac{\pi}{2}} I_\nu(0, \vartheta) \cos\vartheta \sin\vartheta \, d\vartheta, \tag{4.35}$$

resulting from (1.5). Substituting Eq. (4.28) into (4.35) and changing the order of integration, we find

$$H_\nu = 2\pi \int_0^\infty S_\nu(\tau_\nu) E_2 \tau_\nu \, d\tau_\nu, \tag{4.36}$$

where $E_2 \tau_\nu$ is the second integral exponential function [compare with Eq. (2.48)].

With the assumption of local thermodynamic equilibrium in the photosphere, from (4.36) it follows that

$$H_\nu = 2\pi \int_0^\infty B_\nu(T) E_2 \tau_\nu \, d\tau_\nu, \tag{4.37}$$

or

$$H_\nu = \frac{4\pi h\nu^3}{c^2}\int_0^\infty \frac{E_2\tau_\nu d\tau_\nu}{e^{\frac{h\nu}{kT}}-1}. \tag{4.38}$$

Equations (4.31) and (4.38) are valid for any frequency dependence of the absorption coefficient. However, in order to make use of these formulas, it is necessary to know the relationship between the quantities T and τ_ν. Later we will undertake to establish this relationship for an arbitrary absorption coefficient α_ν. Now, just as before, we will, however, assume that the absorption coefficient is independent of the frequency. In this case $\tau_\nu = \tau$, and the relationship between T and τ is given by Eq. (4.21) [or by the approximate Eq. (4.20)].

Instead of Eqs. (4.31) and (4.38), in the case cited we obtain /48

$$I_\nu(0, \vartheta) = \frac{2h\nu^3}{c^2}\int_0^\infty \frac{e^{-\tau\sec\vartheta}\sec\vartheta\, d\tau}{e^{\frac{h\nu}{kT_e}\left(\frac{1}{2}+\frac{3}{4}\tau\right)^{-\frac{1}{4}}}-1} \tag{4.39}$$

and

$$H_\nu = \frac{4\pi h\nu^3}{c^2}\int_0^\infty \frac{E_2\tau d\tau}{e^{\frac{h\nu}{kT_e}\left(\frac{1}{2}+\frac{3}{4}\tau\right)^{-\frac{1}{4}}}-1}, \tag{4.30}$$

where Eq. (4.20) has been used.

Calculations show that the energy distribution in the continuous spectrum of a star, given by Eq. (4.40), does not differ greatly from the Planckian distribution at a temperature equal to the effective stellar temperature, i.e.,

$$H_\nu \simeq \pi\frac{2h\nu^3}{c^2}\frac{1}{e^{\frac{h\nu}{kT_e}}-1}. \tag{4.41}$$

Only in the far ultraviolet portion of the spectrum is there an appreciable excess of radiation compared with the Planckian case, with it increasing with an increase in the frequency ν.

However, the observed energy distribution in stellar spectra does not agree with the theoretical distribution given by Eq. (4.40). The discrepancies between observations and theory are different for stares of different spectral classes. For example, the discrepancies are not very large for the visible portion of the spectra of A and B class stars. It is explained by the fact that Eq. (4.40) has been written under the assumption that the absorption coefficient is independent of the frequency. It is obvous that the effect of a frequency

dependence of the absorption coefficient on the energy distribution in the stellar spectrum must be significant.

The question of the frequency dependence of the absorption coefficient and the effect of this dependence on the form of the stellar spectrum will be examined in detail in the next two sections. Now, however, let us attempt to determine some of the characteristics of the stellar photosphere, retaining the assumption of a frequency independent absorption coefficient. The results derived below can be used as a first approximation to real photospheres if some average absorption coefficient is used (i.e., an absorption coefficient, averaged over all frequencies).

4. Dependence of temperature and density on depth. The dependence of the temperature on the optical depth in the photosphere was determined earlier. In this, assumptions were made concerning radiative equilibrium and local thermodynamic equilibrium. Now let us determine the dependence of the temperature and density on the geometrical depth in the photosphere. For this we must make one more assumption—concerning the mechanical equilbrium at the photosphere. It is obvious that there is no doubt about the validity of this assumption for the overwhelming majority of stars (except for Wolf-Rayet type stars, novae and stars similar to these, which we will not consider now). /49

We will assume that each volume element in the photosphere is in equilibrium under the influence of two forces: gravitational force and gas pressure force (we will disregard radiation pressure for the present). Equating these forces to each other, we obtain the equation of hydrostatic equilibrium

$$dp = -g\rho\, dr, \tag{4.42}$$

where p is the pressure, ρ is the density and g is the acceleration of gravity in the photosphere.

It is obvious that the gas in the photosphere can be considered to be ideal. Therefore to Eq. (4.42) we will add the equation of state of an ideal gas:

$$p = \frac{R^*}{\mu}\rho T, \tag{4.43}$$

where μ is the average molecular weight and R* is the gas constant.

Assuming that μ does not change in the photosphere, from (4.42) and (4.43) we find

$$\frac{R^*}{\mu} d(\rho T) = -g\rho\, dr. \tag{4.44}$$

Let us also utilize the relationship, derived above, between the temperature T and the optical depth τ. An approximate relationship between these quan-

tities is given by Eq. (4.20), from which it follows that

$$dT^4 = -\frac{3}{4} T_e^4 \alpha \, dr. \tag{4.45}$$

Here, as already stated, α can be understood to be the average absorption coefficient.

From the last two equations one can determine ρ and T in the form of functions of r. But to do this it is necessary to specify the dependence of α on ρ and T. Let us set $\alpha = \varkappa\rho$ and initially we will assume $\varkappa$ = const. Then from Eqs. (4.44) and (4.45) we obtain /50

$$d(\rho T) = \frac{4}{3} \frac{g\mu}{\varkappa R^*} \frac{dT^4}{T_e^4}, \tag{4.46}$$

or, after integration

$$\rho = \frac{4}{3} \frac{g\mu}{\varkappa R^*} \frac{T^4 - T_0^4}{T_e^4 T}, \tag{4.47}$$

where T_0 is the stellar surface temperature.

In the deep photosphere layers, where $T^4 \gg T_0^4$, the density is related to the temperature by the expression

$$\rho = \frac{4}{3} \frac{g\mu T^3}{\varkappa R^* T_e^4}. \tag{4.48}$$

Substituting (4.48) into (4.44), we arrive at the following formula for the temperature gradient:

$$\frac{dT}{dr} = -\frac{g\mu}{4R^*}. \tag{4.49}$$

Equations (4.44) and (4.45) can easily be solved even for the more general assumptions concerning α. Let us assume, for example, that

$$\alpha \sim \frac{\rho^2}{T^s}, \tag{4.50}$$

where s is some parameter (this formula for α, as we shall see in Section 5, actually occurs). Then instead of (4.48) and (4.49) we obtain

$$\rho \sim T^{\frac{s+3}{2}} \tag{4.51}$$

and

$$\frac{dT}{dr} = -\frac{2}{s+5}\frac{g\mu}{R^*}. \tag{4.52}$$

Let us apply the formulas derived above to the Sun's photosphere. Assuming in Eq. (4.49) $g = 2.7 \cdot 10^4$, $\mu = 1$, $R^* = 8.3 \cdot 10^7$, we find: $dT/dr = -10^{-4}$ deg/cm. Consequently, the temperature increases by 10 degrees over a depth of 1 kilometer into the photosphere.

From the formulas derived one can also determine the quantity $|dr/d\tau|$, i.e., the geometrical thickness of a layer of unit optical thickness. Substituting Eq. (4.48) into the formula $d\tau = -\varkappa\rho dr$, we find /51

$$\frac{dr}{d\tau} = -\frac{3}{4}\frac{R^* T_e^4}{g\mu T^3}. \tag{4.53}$$

Here if we set $T = T_e$, then the quantity $|dr/d\tau|$ will characterize the photosphere thickness. In the case of the Sun, the photosphere thickness is of the order of 100 km. Since the Sun's radius is equal to 700,000 km, then we verify that the photosphere thickness is much less than the radius. We have already used this result earlier in considering the photosphere layers to be plane-parallel.

5. Radiation pressure in the photosphere. In the discussion of the mechanical equilibrium of the photosphere we ignored the radiation pressure. We will now evaluate the role of radiation pressure in the photosphere, determining the ratio of radiation to gas pressure. To do this we will first derive general formulas defining the intensity of the radiation pressure. Later these formulas are necessary for application not only to the photosphere, but also to other objects.

As is known, each photon possesses a momentum equal to $h\nu/c$. If the photon is absorbed by an atom, then the atom acquires a momentum $h\nu/c$ in the direction of motion of the photon. This gives rise to the radiation pressure on an atom.

Let us imagine a volume element with a base area $d\sigma$ and thickness dr. We will assume that radiation strikes the volume from all sides, and we will find the intensity of the radiation pressure acting on the volume in a direction normal to the base. We will first consider the radiation striking the volume at an angle ϑ to the normal within a solid angle $d\omega$ in the frequency interval from ν to $\nu + d\nu$ within a time interval dt. If the radiation intensity is I_ν, then the amount of energy striking the volume will be equal to $I_\nu d\sigma \cos\vartheta\, d\omega d\nu\, dt$. However, not all of this energy produces a pressure on the volume, but only that fraction of it absorbed by the volume. Since the path length of the photons in the volume is equal to $dr \sec\vartheta$, the amount of energy absorbed by the volume

is equal to $\alpha_\nu I_\nu \, d\sigma \, dr \, d\omega \, d\nu \, dt$. In order to determine the momentum acquired by the volume in the direction normal to the base, it is necessary to mulitply this energy by $\cos\vartheta/c$. Consequently, this momentum will be equal to

$$\frac{\cos\vartheta}{c} \alpha_\nu I_\nu \, d\sigma \, dr \, d\omega \, d\nu \, dt.$$

Integrating this expression over all frequencies anc over all directions, we obtain the total momentum acquired by the volume during time dt. It is equal to /52

$$\frac{1}{c} d\sigma \, dr \, dt \int \alpha_\nu \, d\nu \int I_\nu \cos\vartheta \, d\omega,$$

or

$$\frac{1}{c} d\sigma \, dr \, dt \int \alpha_\nu H_\nu \, d\nu. \tag{4.54}$$

Let us designate by

$$f_r d\sigma \, dr \, dt \tag{4.55}$$

the impulse of the radiation pressure intensity acting on the volume $d\sigma \, dr$ during time dt. From a basic law of mechanics it follows that the last two expressions must be equal to each other. Therefore we obtain

$$f_r = \frac{1}{c} \int \alpha_\nu H_\nu \, d\nu. \tag{4.56}$$

The intensity of the radiation pressure, acting on a unit volume, is given by this formula.

The force, acting on a volume element, can also be represented as the difference in the pressures on the base of the volume. Denoting the radiation pressure by p_r, we can write this force in the form

$$-dp_r d\sigma \, dt. \tag{4.57}$$

Equating expressions (4.54) and (4.57), we find

$$\frac{dp_r}{dr} = -\frac{1}{c} \int \alpha_\nu H_\nu \, d\nu. \tag{4.58}$$

We will apply the latter formula to the stellar photosphere. Assuming, as before, that the absorption coefficient does not depend on the frequency,

instead of (4.58) we obtain

$$dp_r = -\frac{1}{c} H\alpha\, dr, \tag{4.59}$$

or, using (4.18),

$$dp_r = -\frac{a}{4} T_e^4 \alpha\, dr. \tag{4.60}$$

A comparison of (4.60) with (4.45) gives

$$p_r = \frac{1}{3} aT^4. \tag{4.61}$$

Thus, in the case under consideration the same expression is obtained for the radiation pressure as in the presence of thermodynamic equilibrium.

Above we assumed that the photosphere exists in equilibrium under the influence of gravity and gas pressure, and therefore in Eq. (4.42) p was understood to be the gas pressure only. Let us now understand p to be the sum of the gas pressure p_g and the radiation pressure p_r. Then Eq. (4.42) is written in the form /53

$$d(p_g + p_r) = -g\rho\, dr. \tag{4.62}$$

Using Eqs. (4.62) and (4.45), as well as Eq. (4.43) for the gas pressure and Eq. (4.61) for the radiation pressure, one can derive, as before, the temperature and density distribution in the photosphere. However, we will not do that, and we will find only the ratio of the radiation pressure p_r to the total pressure $p = p_g + p_r$. After dividing (4.59) by (4.62) and setting $\alpha = \varkappa\rho$, we obtain

$$\frac{dp_r}{d(p_g + p_r)} = \frac{\varkappa H}{gc}. \tag{4.63}$$

The total radiation flux H is constant in the photosphere. Let us note that $\varkappa =$ = const. In this case, integration yields

$$p_r - p_r^0 = \frac{\varkappa H}{cg}(p_g + p_r - p_r^0), \tag{4.64}$$

where p_r^0 is the radiation pressure on the stellar surface. Whence for the deep photosphere layers it follows that

$$\frac{p_r}{p} = \frac{\varkappa H}{gc}. \tag{4.65}$$

For calculations with Eq. (4.65) it is necessary to know the quantity $\varkappa$ (i.e., the average absorption coefficient calculated per unit mass). The formulas presented in the following section can be used for this. Calculations show that for stars like the Sun the quantity p_r/p is of the order of a few thousandths, and for stars of later spectral classes of the main sequence it is still smaller. Consequently, for these stars one can disregard radiation pressure in comparison with the gas pressure. However, the role of radiation pressure increases with an increase in the effective stellar temperature, and for hot supergiants the ratio of the radiation to gas pressure is about unity.

5. Frequency Dependence of the Absorption Coefficient

1. Continuous emission and absorption spectra. Thus far we have not touched on the question of what physical processes are associated with energy emission and absorption in a continuous spectrum. Passing now to an examination of this question, let us consider the energy level diagram of an atom (Fig. 4).

As is known, each atom can exist in several stable states with certain discrete energy values: $E_1, E_2, \ldots, E_i, \ldots$ These energy values are negative ($E_i < 0$). In the corresponding states the outer electron is bound to the atom, or, as is sometimes said, it exists in an elliptical orbit. During the transitions of an atom between these states, the emission and absorption of quanta in spectral lines occur. /54

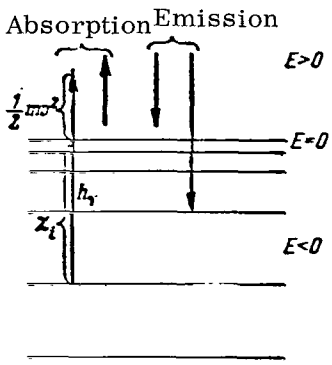

Figure 4.

At the same time the atom can also exist in states with a positive energy ($E > 0$). In these states the electron is not bound to the atom, i.e., it is in a hyperbolic orbit. The positive energy levels of an atom are a continuum.

The transition of an atom from a state with negative energy into a state with positive energy (i.e., the transition of an electron from a bound to a free state) is called ionization of the atom. Ionization can occur due to the effect of radiation; in this case it is called photoionization.

The absorption of a light quantum occurs during photoionization. In this situation the energy of the quantum is partially expended in detaching the electron from the atom, and partially in imparting a kinetic energy to the liberated electron. In other words, in this case the relationship

$$h\nu = \chi_i + \frac{1}{2} m v^2, \tag{5.1}$$

exists, where $\chi_i = -E_i$. The quantity χ_i is the energy for atom ionization of the i-th state. The relation (5.1) was first derived by Einstein during an investigation of the photoelectric effect.

During photoionization from the i-th level, any quantum whose energy is greater or equal to the ionization energy, i.e., $h\nu \geq \chi_i$, can be absorbed. Consequently, energy absorption in a continuous spectrum occurs during photoionization.

The process that is the opposite of ionization, i.e., the capture of a free electron by an ionized atom, is called recombination. The emission of energy in a continuous spectrum occurs during recombination. If an electron with velocity v is captured in the i-th level; then a quantum of frequency ν, determined /55
by the same relation (5.1), is emitted.

Besides photoionization and recombination, transitions of atoms between states with positive energy, i.e., electron transitions from free states to free states, also lead to the absorption and emission of energy in a continuous spectrum. It is obvious that quanta of any frequency can be absorbed and emitted during such transitions.

The probabilities of all these transitions are characterized by the corresponding absorption and emission coefficients. We will denote the absorption coefficient of quanta of frequency ν, calculated for one atom in the i-th state, by $k_{i\nu}$. Then the volume absorption coefficient of quanta of frequency ν by atoms in the i-th state will be equal to $\alpha_{i\nu} = n_i k_{i\nu}$, where n_i is the number of atoms in the i-th state in a unit volume. And the volume absorption coefficient produced, by all photoionizations, will be equal to

$$\alpha_\nu' = \sum_{i=i_0}^{\infty} n_i k_{i\nu}, \tag{5.2}$$

where i_0 is determined for each frequency from the condition that the inequality $h\nu \geq \chi_i$ is satisfied when $i \geq i_0$.

The volume absorption coefficient, caused by free-free transitions, will be denoted by α_ν''. Obviously it is proportional to the number of free electrons and the number of ionized atoms in a unit volume (since the free-free transitions occur in the field of an ion).

The total volume absorption constant α_ν (appearing in the previous section) is the sum:

$$\alpha_\nu = \alpha_\nu' + \alpha_\nu''. \tag{5.3}$$

We see that the absorption coefficient α_ν is inherently dependent on the state distribution of the atoms. As already stated, in photosphere theory the assumption of local thermodynamic equilibrium is made. Therefore let us imagine the state distribution of the atoms to be the same as in the case of thermodynamic equilibrium.

As is known, in this case the distribution of atoms in terms of discrete energy levels is given by the Boltzmann formula:

$$\frac{n_i}{n_1} = \frac{g_i}{g_1} e^{-\frac{\chi_1 - \chi_i}{kT}}, \tag{5.4}$$

where g_i is the statistical weight of the i-th level. The quantity $\chi_1 - \chi_i$ represents the excitation energy of the i-th level.

Generalizing (5.4) to an atomic state with positive energy, one can obtain the ratio of the number of ionized atoms to the number of neutral atoms. This ratio is given by the formula

$$n_e \frac{n^+}{n_1} = 2 \frac{g^+}{g_1} \frac{(2\pi mkT)^{3/2}}{h^3} e^{-\frac{\chi_1}{kT}}, \tag{5.5}$$

which is called the ionization formula or Saha formula. Here n_e is the number of free electrons and n^+ is the number of ions in the ground state in 1 cm^3, g^+ is the statistical weight of the ground state of the ion.

Later we will present expressions for the absorption coefficients k_{ir} and α_ν'' for certain atoms and, utilizing Eqs. (5.2)—(5.5), we will formulate an expression for the volume absorption coefficient α_ν. Formulas for the emission coefficients corresponding to the different types of transitions, are not required by us in photosphere theory since in the presence of thermodynamic equilibrium the volume emission coefficient ε_ν required by us is expressed in terms of the volume absorption coefficient α_ν by means of the Kirchhoff-Planck law.

2. Absorption by hydrogen atoms. To calculate the absorption coefficients in the continuous spectrum it is necessary to know the atom wave functions both for states with negative energy as well as for states with positive energy. Calculation of the wave functions is, as is known, a very difficult problem. It is more or less satisfactorily resolved only for the simplest cases.

We will now present the results of a determination of the absorption coefficients for the hydrogen atom. The absorption coefficient $k_{i\nu}$, calculated for

one hydrogen atom in the i-th state, is equal to

$$k_{i\nu} = \frac{2^6\pi^4}{3\sqrt{3}} \frac{me^{10}}{ch^6 i^5 \nu^3} g_{i\nu}, \tag{5.6}$$

where m and e are the electron mass and charge, respectively; $g_{i\nu}$ is some correction factor close to unity (the so-called Gaunt factor). Equation (5.6) is valid only for frequencies satisfying the inequality $\nu \geq \nu_i = \chi_i/h$, i.e., beyond the i-th series. We see that beyond the series the absorption coefficient $k_{i\nu}$ decreases in inverse proportion to the cube of the frequency. The values of the absorption coefficient immediately beyond the first series are of the order of 10^{-17} cm^2 ($0.63 \cdot 10^{-17}$ cm^2 immediately beyond the Lyman series, $1.4 \cdot 10^{-17}$ cm^2 immediately beyond the Balmer series, etc.).

In order to find the volume absorption coefficient α'_ν it is necessary to substitute Eq. (5.6) into Eq. (5.2). At the same time we assume that the state distribution of the atoms is given by Eqs. (5.4) and (5.5). From the last two formulas we obtain /57

$$n_i = n_e n^+ \frac{g_i}{g^+} \frac{h^3}{2(2\pi mkT)^{3/2}} e^{\frac{\chi_i}{kT}}. \tag{5.7}$$

Substituting (5.6) and (5.7) into Eq. (5.2), we find

$$\alpha_\nu' = n_e n^+ \frac{2^5\pi^2 e^6}{3\sqrt{3}\, ch} \frac{\chi_1}{(2\pi mkT)^{3/2}} \cdot \frac{1}{\nu^3} \sum_{i=i_0}^{\infty} \frac{g_{i\nu}}{i^3} e^{\frac{\chi_i}{kT}}, \tag{5.8}$$

where the quantity χ_1, just as before, is the ionization energy of the first state, equal to

$$\chi_1 = \frac{2\pi^2 me^4}{h^2}. \tag{5.9}$$

For frequencies beyond the Lyman series $i_0 = 1$ in Eq. (5.8); for frequencies from the edge of the Balmer series to the edge of the Lyman series $i_0 = 2$, etc.

For the absorption coefficient α''_ν, caused by free-free transitions of an electron in the field of a proton, quantum mechanics yields

$$\alpha_\nu'' = n_e n^+ \frac{2^4\pi^2 e^6 kT}{3\sqrt{3}\, ch(2\pi mkT)^{3/2}} \frac{1}{\nu^3} g_\nu, \tag{5.10}$$

where n_e and n^+ are the number of free electrons and the number of protons in 1 cm^3, respectively; g_ν is the Gaunt correction factor, approximately equal to unity. In the derivation of Eq. (5.10) it is assumed that the velocity distribution of the free electrons is given by the Maxwell equation with temperature T. The absorption coefficient α''_ν, just like $k_{i\nu}$, is inversely proportional to the cube of the frequency. However, Eq. (5.10), in contrast to Eq. (5.6), is valid for all frequencies.

However, Eqs. (5.8) and (5.10) are not completely exact since the so-called negative absorption is disregarded. The negative absorption will be discussed in detail in Section 8. For the present, however, let us note that in the presence of thermodynamic equilibrium (more precisely, when the Maxwell, Boltzmann and Saha formulas are satisfied) the expression presented above for the absorption coefficient should be multiplied by the quantity $(1-e^{-h\nu/kT})$ to take account of the negative absorption.

Substituting (5.8) and (5.10) into Eq. (5.3) and taking negative absorption into account, we obtain the following expression for the volume absorption coefficient produced by hydrogen atoms: /58

$$\alpha_\nu = n_e n^+ \frac{2^4 \pi^2 e^6 kT}{3\sqrt{3}\, ch\,(2\pi mkT)^{3/2}} \left[2\frac{\chi_1}{kT}\sum_{i=i_0}^{\infty}\frac{g_{i\nu}}{i^3}e^{\frac{\chi_i}{kT}} + g_\nu\right]\frac{1}{\nu^3}\left(1-e^{-\frac{h\nu}{kT}}\right). \qquad (5.11)$$

The frequency dependence of the absorption coefficient, given by Eq. (5.11), is represented schematically in Fig. 5. We see that this function is very complex. There are conspicuous discontinuities in the absorption coefficient at the series limits.

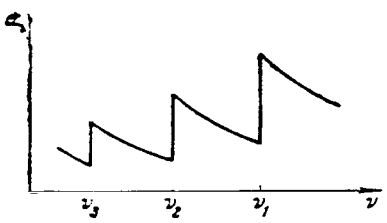

Figure 5.

The frequency dependence of the absorption coefficient for hydrogen-like ions (He^+, Li^{++}, etc.) has a similar character. In this case the absorption coefficients are determined by the formulas presented above, slightly modified. For an ion with atomic number Z, a factor Z^4 must be inserted into the right side of Eq. (5.6), and a factor Z^2—into the right side of Eqs. (5.10) and (5.11). In this case, χ_1 in Eq. (5.11) should be understood to be the ionization energy of the ground state of the ion being considered.

The formulas that have been presented can also be used for an approximate calculation of the absorption coefficients of non-hydrogen-like atoms. This can be done in those cases when the absorption is associated with the transitions of electrons from high energy levels. Generally, however, the absorption coefficients

of different atoms must be determined by specific calculations or experimentally. It turns out that the frequency dependence of the absorption coefficient is very different for different atoms. For example, the absorption coefficient of the ground state of neutral helium is inversely proportional to the square of the frequency; the absorption coefficient of the ground state of neutral oxygen increases at first with an increase in frequency, and then decreases; etc.

Among all non-hydrogen-like atoms, the negative hydrogen ion plays the major role in photospheres. Therefore we must consider the question of absorption by negative hydrogen ions in more detail.

3. Absorption by negative hydrogen ions. The negative hydrogen ion (denoted by H^-) is a system consisting of a netural hydrogen atom with an electron attached to it. Such a system has only one stable state with a very low ionization energy equal to $\chi_1 = 0.75$ eV. For comparison let us note that the ionization energy of the ground state of hydrogen is equal to 13.6 eV, and the energy of quanta in the visible portion of the spectrum is equal to 2-3 eV. Consequently the ionization frequency of the negative hydrogen ion, $\nu_1 = \chi_1/h$, lies in the far infrared region of the spectrum. In the photoionization of the negative hydrogen ion all quanta with frequencies $\nu \geq \nu_1$, in particular quanta in the visible region of the spectrum, can be absorbed. /59

The determination of the absorption coefficient of the H^- ion has been the subject of many studies. The absorption coefficient k_ν, calculated for one negative hydrogen ion, is shown in Fig. 6 as a function of the frequency. This relationship was derived in Chandrasekhar's paper [11] (subsequent studies have changed it little). From Fig. 6 it is seen that in the visible region of the spectrum the absorption coefficient of the H^- ion varies smoothly and within relatively narrow limits.

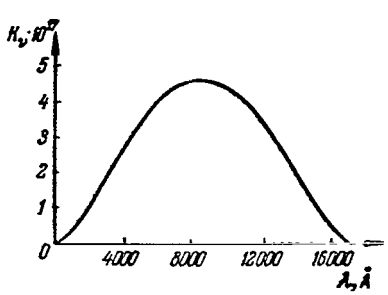

Figure 6.

The volume absorption coefficient, caused by the negative hydrogen ion, is equal to $\alpha'_\nu = n^- k_\nu$, where n^- is the number of H^- ions in 1 cm^3. In order to obtain the total volume absorption coefficient of the H^- ion, it is necessary to add to this expression the volume absorption coefficient α''_ν, caused by free-free transitions of an electron in the field of a neutral hydrogen atom (which plays the role of an ionized atom for the H^- ion). It is obvious that the absorption coefficient α''_ν is proportional to the number of neutral hydrogen atoms and the number of free electrons in 1cm^3. Therefore, we can represent it in the form $\alpha''_\nu = n_1 p_e \alpha_\nu$, where $p_e = n_e kT$ is the electron pressure.

Thus, the total volume absorption coefficient of the H^- ion is equal to

$$\alpha_\nu = (n^- k_\nu + n_1 p_e a_\nu)\left(1 - e^{-\frac{h\nu}{kT}}\right), \tag{5.12}$$

where the factor $(1-e^{-h\nu/kT})$, as before, takes account of the negative absorption. /60

To compute the absorption coefficient α_ν from Eq. (5.12) it is necessary to find the number of H^- ions in 1 cm^3. This can be done with the help of the ionization formula (5.5), which in the given case assumes the form

$$n_e \frac{n_1}{n^-} = \frac{g_1}{g^-} \frac{2(2\pi mkT)^{3/2}}{h^3} e^{-\frac{\chi_1}{kT}}, \tag{5.13}$$

where g_1 and g^- are the statistical weights of the ground state of the neutral hydrogen atom and of the negative hydrogen ion, respectively ($g_1 = 2$, $g^- = 1$), χ_1 is the ionization energy of the H^- ion.

Substituting n^- from (5.13) into (5.12), we obtain

$$\alpha_\nu = n_1 p_e \left[k_\nu \frac{h^3}{4(2\pi m)^{3/2}(kT)^{5/2}} e^{\frac{\chi_1}{kT}} + a_\nu\right]\left(1 - e^{-\frac{h\nu}{kT}}\right). \tag{5.14}$$

The calculation of the absorption coefficient α_ν from Eq. (5.14) was done in the work of Chandrasekhar and Breene (see [4]). Their results are presented on a graph giving the absorption coefficient α_ν, referenced to one neutral hydrogen atom and to units of electron pressure, as a function of the wavelength for different temperatures (Fig. 7). From the calculations in particular, it follows that the absorption produced by free-free transitions plays a significant role only for long wavelengths (approximately for values of $\lambda > 12000$ Å).

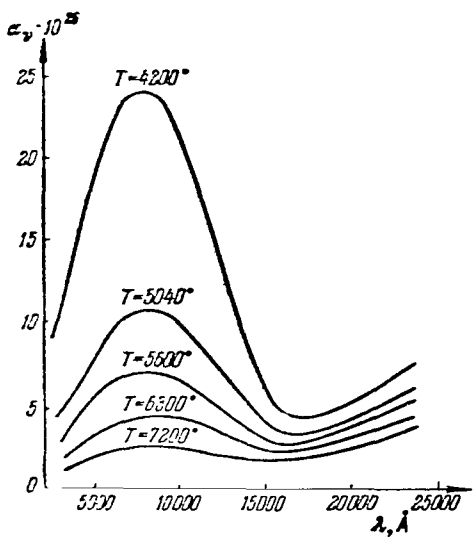

Figure 7.

4. Light scattering by free electrons. In addition to light absorption by atoms, radiation scattering—by free electrons, atoms and molecules—also plays some role in radiation transfer through the photosphere. Of the scattering processes, the most important is scattering by free electrons. /61

The scattering coefficient, calculated for one free electron, is given by the Thomson formula:

$$\sigma_0 = \frac{8\pi}{3}\left(\frac{e^2}{mc^2}\right)^2, \tag{5.15}$$

where m and e are the electron mass and charge, respectively, c is the velocity of light. The numerical value of this coefficient is equal to $\sigma_0 = 6.65 \cdot 10^{-25}$ cm^2.

The volume coefficient of scattering by free electrons is equal to

$$\sigma_e = n_e \sigma_0, \tag{5.16}$$

where n_e is the number of free electrons in 1 cm^3. Obviously one does not need to introduce a factor, taking account of negative absorption, into Eq. (5.16).

By using Eqs. (5.16) and (5.11) one can compare the role of electron scattering and the role of absorption by hydrogen atoms. Finding, with the aid of these formulas, the ratio σ_e/α_ν, we see that it is larger, the lower the density and the higher the temperature. Therefore the role of electron scattering is especially significant in the photospheres of the hot supergiants.

If light absorption and light scattering by free electrons occur in a volume element of the photosphere, then the volume emission coefficient is equal to

$$\varepsilon_\nu = \alpha_\nu \frac{2h\nu^3}{c^2} \frac{1}{e^{\frac{h\nu}{kT}} - 1} + \sigma_e \int I_\nu \frac{d\omega}{4\pi}, \tag{5.17}$$

where α_ν is the volume absorption coefficient and I_ν is the intensity of the radiation incident on the volume. The difference between radiation absorption and scattering is clearly evident from Eq. (5.17): only the absorbed energy is converted in the volume element and reradiated by it in accordance with the Kirchhoff-Planck law (if local thermodynamic equilibrium exists).

However, electron scattering does, nevertheless, contribute to the reconversion of the radiation since it is by virtue of the electron scattering that the photon path length in the medium is increased and this means an increase in the absorption probability.

In Eq. (5.17) the approximation is made that light scattering by free electrons is isotropic. In reality the intensity of the radiation, scattered by the volume element, depends on the angle γ between the directions of the incident and scattered radiation (namely, it is proportional to $1 + \cos^2\gamma$). Let us note /62
that the radiation, scattered by free electrons, is polarized.

5. Mean absorption coefficient. The results of a determination of the absorption coefficients for some atoms have been presented above. In each volume element of the photosphere there exists, in reality, a mixture of atoms of various chemical elements. Therefore the volume absorption coefficient depends not only on the physical conditions at a certain point (i.e., on the temperature and density), but also on the chemical composition. Because of this, the frequency dependence of the volume absorption coefficient is even more complicated.

Meanwhile, in the photosphere theory discussed in previous sections the assumption was made concerning the frequency independence of the absorption coefficient. With the rejection of this assumption, photosphere theory becomes much more complicated. Therefore a problem arises as to whether it is impossible to make use of the results of the discussed photosphere theory even for the case when the absorption coefficient depends on the frequency, at least as a first approximation. To this end the mean absorption coefficient (i.e., the absorption coefficient averaged over the frequency) is introduced into the photosphere theory. An attempt has to be made to define it such that the previously derived dependence of the temperature on optical depth can be retained.

Let us take the radiative transfer equation

$$\cos\vartheta \frac{dI_\nu}{dr} = -\alpha_\nu I_\nu + \varepsilon_\nu. \tag{5.18}$$

Multiplying this equation by $\cos\vartheta$, integrating over all directions and removing the average value of $\cos^2\vartheta$, equal to 1/3, outside the integral, we obtain

$$\frac{4\pi}{3}\frac{d\bar{I}_\nu}{dr} = -\alpha_\nu H_\nu, \tag{5.19}$$

where H_ν is the radiation flux and $\bar{I}_\nu$ is the mean radiation intensity, equal to

$$\bar{I}_\nu = \int I_\nu \frac{d\omega}{4\pi}. \tag{5.20}$$

Integrating (5.19) over all frequencies and introducing the notation

$$\alpha = \frac{\int \alpha_\nu H_\nu d\nu}{H}, \tag{5.21}$$

we find /63

$$\frac{4\pi}{3}\frac{d\bar{I}}{dr} = -\bar{\alpha}H, \tag{5.22}$$

where H is the total radiation flux in the photosphere and $\bar{I}$ is the mean total radiation intensity.

The quantity $\bar{\alpha}$, defined by Eq. (5.21), is the mean absorption coefficient. Introducing the corresponding optical depth τ from the formula

$$\tau = \int_r^\infty \bar{\alpha}\, dr, \tag{5.23}$$

instead of (5.21) we have

$$\frac{4\pi}{3}\frac{d\bar{I}}{d\tau}=H. \tag{5.24}$$

Since the radiation flux H is constant in the photosphere, then integration of (5.24) yields

$$\bar{I}=\frac{H}{2\pi}\left(1+\frac{3}{2}\tau\right). \tag{5.25}$$

Here we have made use of the boundary condition: $2\pi\bar{I} = H$ for $\tau = 0$.

Considering that the quantity $\bar{I}$ is equal to the total radiation intensity in the case of thermodynamic equilibrium, i.e., $\bar{I} = \sigma T^4/\pi$, and expressing the total radiation flux in terms of the effective temperature T_e through the formula $H = \sigma T_e^4$, instead of (5.25) we obtain

$$T^4=T_e^4\left(\frac{1}{2}+\frac{3}{4}\tau\right), \tag{5.26}$$

i.e., the previously derived Eq. (4.20).

Thus, by defining the mean absorption coefficient $\bar{\alpha}$ by Eq. (5.21) and making use of the Eddington approximation, we arrive at the same relationship between temperature and optical depth as in the case when the absorption coefficient is independent of the frequency. However, we cannot calculate the quantity $\bar{\alpha}$ precisely since the radiation flux H_ν in a real photosphere, in which the absorption coefficient depends on the frequency, enters into Eq. (5.21). Therefore the mean absorption coefficient $\bar{\alpha}$ must be computed approximately.

The following procedures have been proposed for the approximate computation of the quantity $\bar{\alpha}$.

1. We will assume that the radiation flux H_ν is equal to the radiation flux /64
of an absolute black body, i.e., $H_\nu = \pi B_\nu(T)$, where $B_\nu(T)$ is the Planckian intensity of temperature T. Then

$$\bar{\alpha}=\frac{\int \alpha_\nu B_\nu(T)\,d\nu}{\int B_\nu(T)\,d\nu}. \tag{5.27}$$

2. We will take the expression for H_ν given by Eq. (5.19). Replacing $\bar{I}_\nu$ in it by the Planckian intensity $B_\nu(T)$. we obtain

$$H_\nu = -\frac{4\pi}{3}\frac{1}{\alpha_\nu}\frac{dB_\nu(T)}{dT}\frac{dT}{dr}. \tag{5.28}$$

Substitution of (5.28) into (5.21) yields

$$\bar{\alpha} = \frac{\int \frac{dB_\nu(T)}{dT}d\nu}{\int \frac{1}{\alpha_\nu}\frac{dB_\nu(T)}{dT}d\nu}. \tag{5.29}$$

Equation (5.29) has been suggested by Rosseland [12].

3. For H_ν we will use the expression which is obtained in the case when the absorption coefficient does not depend on frequency. Denoting the radiation flux for this case by $H_\nu^0(\tau)$, we obtain

$$\bar{\alpha} = \int \alpha_\nu \frac{H_\nu^0(\tau)}{H}d\nu. \tag{5.30}$$

Equation (5.30) was proposed by Chandrasekhar [4], who also tabulated the quantity $H_\nu^0(\tau)/H$.

We will not make a comparison between the different methods of calculating the quantity $\bar{\alpha}$. Let us only note that calculations with Eqs. (5.27) and (5.30) are simpler than with Eq. (5.29). This is especially noteworthy in the case of a complex chemical composition since the terms corresponding to different atoms enter additively in Eqs. (5.27) and (5.30). Equation (5.29), however, is obviously more precise.

As an example let us find the mean absorption coefficient from Eq. (5.27) in the case when absorption is caused by hydrogen atoms.

Using Eq. (5.11) for α_ν and Eq. (4.2) for $B_\nu(T)$, we obtain /65

$$\int_0^\infty \alpha_\nu B_\nu(T)\,d\nu = n_e n^+ \frac{2^4\pi^2\epsilon^6 kT}{3\sqrt{3}\,ch(2\pi mkT)^{3/2}} \times$$

$$\times \frac{2h}{c^2}\int_0^\infty \left[1 + 2\frac{\chi_1}{kT}\sum_{i=i_0}^{\infty}\frac{1}{i^3}e^{\frac{\chi_1}{kT}}\right]e^{-\frac{h\nu}{kT}}d\nu. \tag{5.31}$$

Here, for simplicity, we have set $g_{i\nu} = 1$ and $g_\nu = 1$. Changing the order of integration and summation and integrating, we obtain

$$\int_0^\infty \alpha_\nu B_\nu(T)\,d\nu = n_e n^+ \frac{2^4\pi^2 e^6 kT}{3\sqrt{3}\,ch(2\pi mkT)^{3/2}c^2}\frac{2h}{h}\frac{kT}{h}\left[1+2{,}4\frac{\chi_1}{kT}\right]. \tag{5.32}$$

Moreover, we have

$$\int_0^\infty B_\nu(T)\,d\nu = \frac{2h}{c^2}\left(\frac{kT}{h}\right)^4\int_0^\infty \frac{x^3dx}{e^x-1} = \frac{2h}{c^2}\left(\frac{kT}{h}\right)^4\frac{\pi^4}{15}. \tag{5.33}$$

Substitution of (5.32) and (5.33) into Eq. (5.27), with relation (5.10) used, yields

$$\bar{\alpha} = \frac{40}{\pi^4\sqrt{3}}\frac{e^6h^4}{mc(2\pi m)^{3/2}}\chi_1\left[1+2{,}4\frac{\chi_1}{kT}\right]\frac{n_e n^+}{(kT)^{7/2}}. \tag{5.34}$$

We derived Eq. (5.34) for a hydrogen atom, but it is valid without change for hydrogen-like ions (since the atomic number Z enters in χ_1). Equation (5.34) is approximately valid for other atoms.

Let us recall that the first term within the square brackets of Eq. (5.34) corresponds to free-free transitions, and the second term—to bound-free transitions. In the case of radiation absorption by hydrogen atoms the first term predominates at temperatures above 400,000°, and the second term—at temperatures below 400,000° (since for hydrogen $\chi_1/k = 157{,}200$).

Assuming that the hydrogen atoms are completely ionized (this means $n_e = n^+ \sim \rho$, in both of the cases cited we obtain /66

$$\bar{\alpha} \sim \frac{\rho^2}{T^{7/2}} \tag{5.35}$$

from Eq. (5.34) (for relatively high temperatures) and

$$\bar{\alpha} \sim \frac{\rho^2}{T^{3/2}} \tag{5.36}$$

(for relatively low temperatures). Equations (5.35) and (5.36) are used quite often in astrophysics.

6. Theory of Photospheres With a Frequency-Dependent Absorption Coefficient

1. Approximate theory. The simplest way to construct an approximate theory for photospheres, when the absorption coefficient depends on frequency, consists of using the results of the photosphere theory discussed above when it was assumed that the absorption coefficient was independent of frequency. It was for this reason that the mean absorption coefficient $\bar{\alpha}$ is introduced into the photosphere theory. As shown in the preceding section, it can be defined such that the dependence of the temperature T on the optical depth τ remains the same as in the case when the absorption coefficient is independent of frequency. Therefore the conclusions previously derived concerning stellar photosphere structure, i.e., concerning variations in its density and temperature with geometrical depth, are retained (it is only necessary to replace α by $\bar{\alpha}$ in the appropriate formulas of Section 4).

However, to determine the radiation field in the photosphere for different frequencies it is necessary that the absorption coefficient α_ν or the corresponding optical depth τ_ν appear in the theory. Of special interest to us is the intensity of the radiation coming from a star. As shown previously, it is determined by Eq. (4.30), which is valid for any dependence of τ_ν on ν. We will assume that the temperature T entering into this formula is expressed by means of Eq. (5.26) in terms of the optical depth τ corresponding to the mean absorption coefficient. Therefore, for a calculation with Eq. (4.30), τ_ν must be expressed in terms of τ. We will make the approximation that α_ν/α does not change in the photosphere. Then we obtain

$$\tau_\nu = \int_\tau^\infty \alpha_\nu \, dr = \frac{\alpha_\nu}{\bar{\alpha}} \int_\tau^\infty \bar{\alpha} \, dr = \frac{\alpha_\nu}{\bar{\alpha}} \tau. \tag{6.1}$$

In reality, the quantity $\alpha_\nu/\bar{\alpha}$ depends on the depth in the photosphere. It is obvious that in order to calculate the radiation intensity coming from a star, it is necessary that the value in the surface layers of the photosphere be taken for the quantity $\alpha_\nu/\bar{\alpha}$ (more precisely, in those layers in which the continuous spectrum originates on the average). /67

Substituting (6.1) into (4.30), we obtain

$$I_\nu(0, \vartheta) = \int_0^\infty B_\nu(T) e^{-\frac{\alpha_\nu}{\bar{\alpha}} \tau \sec \vartheta} \sec \vartheta \frac{\alpha_\nu}{\bar{\alpha}} d\tau, \tag{6.2}$$

for the intensity of the radiation coming from a star at an angle ϑ to the radius vector at a frequency ν, where $B_\nu(T)$ is the Planckian intensity at temperature T.

Taking (4.2) and (5.26) into consideration, instead of (6.2) we obtain

$$I_\nu(0, \vartheta) = \frac{2h\nu^3}{c^2}\int_0^\infty \frac{e^{-\frac{\alpha_\nu}{\bar{\alpha}}\tau\sec\vartheta}}{e^{\frac{h\nu}{kT_e}\left(\frac{1}{2}+\frac{3}{4}\tau\right)^{-\frac{1}{4}}}-1}\sec\vartheta\,\frac{\alpha_\nu}{\bar{\alpha}}\,d\tau. \tag{6.3}$$

In the same approximation (i.e., for $\alpha/\bar{\alpha}$ = const.) we have

$$H_\nu = \frac{4\pi h\nu^3}{c^2}\int_0^\infty \frac{E_2\left(\frac{\alpha_\nu}{\bar{\alpha}}\tau\right)\frac{\alpha_\nu}{\bar{\alpha}}d\tau}{e^{\frac{h\nu}{kT_e}\left(\frac{1}{2}+\frac{3}{4}\tau\right)^{-\frac{1}{4}}}-1}. \tag{6.4}$$

for the radiation flux at frequency ν at the surface of the star.

The previously derived Eqs. (4.39) and (4.40) are special cases of Eq. (6.3) and (6.4) (for $\tau_\nu = \tau$).

Sometimes in the calculation of the quantity $I_\nu(0, \vartheta)$ from Eq. (6.2) the function $B_\nu(T)$ is represented in the form of a power series in τ:

$$B_\nu(\tau) = B_\nu(T_0)(1 + \beta_\nu\tau + \ldots), \tag{6.5}$$

in which only the first two terms are retained. We have

$$\beta_\nu = \frac{1}{B_\nu(T_0)}\left[\frac{dB_\nu}{dT}\frac{dT}{d\tau}\right]_{\tau=0} \tag{6.6}$$

or, on the basis of Eqs. (4.2) and (5.26),

$$\beta_\nu = \frac{3}{8}\frac{h\nu}{kT_0}\frac{1}{1-e^{-\frac{h\nu}{kT_0}}}. \tag{6.7}$$

For the quantity $I_\nu(0, \vartheta)$ we obtain the approximation /68

$$I_\nu(0, \vartheta) = B_\nu(T_0)\int_0^\infty (1+\beta_\nu\tau)e^{-\frac{\alpha_\nu}{\bar{\alpha}}\tau\sec\vartheta}\frac{\alpha_\nu}{\bar{\alpha}}\sec\vartheta\,d\tau, \tag{6.8}$$

or, after integration,

$$I_\nu(0, \vartheta) = B_\nu(T_0)\left(1+\frac{\bar{\alpha}}{\alpha_\nu}\beta_\nu\cos\vartheta\right). \tag{6.9}$$

Substituting (6.9) into (4.35), we obtain

$$H_\nu = \pi B_\nu(T_0)\left(1 + \frac{2}{3}\frac{\bar{\alpha}}{\alpha_\nu}\beta_\nu\right). \tag{6.10}$$

for the radiation flux.

Equations (6.9) and (6.10) are quite crude approximations; however, it is clearly evident from them how the ratio α_ν/α affects the quantities $I_\nu(0,\vartheta)$ and H_ν.

As is known, the brightness distribution over the stellar disk is given by the quantity $I_\nu(0, \vartheta)$. From Eq. (6.9) it follows that at frequencies for which the absorption coefficient α_ν is very large, the disk brightness is approximately the same everywhere; at frequencies, however, for which the absorption coefficient is very small, the brightness falls off drastically from center to edge. As an example, let us consider stars in the photospheres of which the absorption is caused primarily by hydrogen atoms (i.e., A and B class stars, as we will see below). From Eq. (5.11) it is seen that the absorption coefficient α_ν immediately beyond the Balmer series limit is several times greater than below the limit (since $i_0 = 2$ beyond the limit and $i_0 = 3$ below the limit). Therefore the brightness distribution over the stellar disk at frequencies beyond the Balmer limit must be markedly different from the disk brightness distribution at frequencies below the Balmer limit. This conclusion can be compared with the results of observations of eclipsing class A and B variable stars.

The quantity H_ν characterizes the relative energy distribution in the continuous stellar spectrum. The intensity discontinuities at series limits, caused by absorption coefficient discontinuities, are an important feature of the stars of some classes. In particular, there should be discontinuities at the Balmer series limit in the spectra of class A and B stars (the intensity below the limit is greater than the intensity beyond the limit). The Balmer discontinuity can be determined approximately from Eq. (6.10). More precise data on the Balmer discontinuities in stellar spectra will be presented below.

By using Eq. (6.10) and the observational data on the energy distribution /69
in the continuous spectrum of a star, one can determine approximately the frequency dependence of the absorption coefficient in the photosphere (more precisely, the frequency dependence of the quantity $\alpha_\nu/\bar{\alpha}$). Such a determination has been made for the Sun even though the problem concerning what atoms are the primary cause of absorption in the solar photosphere has not been solved. This analysis has greatly facilitated the solution of this problem.

2. Case of absorption by atoms of one kind. The approximate theory discussed above yields results which can be used only for crude estimates. Passing over, now, to a more rigorous photosphere theory, let us first consider one special case in which this theory is relatively simple. That is to say, let us

assume that the absorption in the photosphere is caused primarily by atoms of one kind, i.e., by atoms of one element in a specific ionization state. In this case the volume absorption coefficient can be represented in the form of the product of two functions, one of which depends only on the frequency and temperature, and the other—only on the temperature and density, i.e.,

$$\alpha_\nu = \Phi(\nu, T)\Psi(T, \rho). \tag{6.11}$$

The possibility of such a representation is seen, for example, from Eq. (5.11), which defines the absorption coefficient α_ν for hydrogen.

If α_ν is given by Eq. (6.11), then the radiative transfer equation can be written thus:

$$\cos\vartheta \frac{dI_\nu}{d\zeta} = \Phi(\nu, T)[I_\nu - B_\nu(T)], \tag{6.12}$$

where $B_\nu(T)$ is the intensity of an absolute black body at temperature T and

$$\zeta = \int_r^\infty \Psi(T, \rho)\, dr. \tag{6.13}$$

The radiation equilibrium Eq. (1.17) in this case assumes the form

$$\int_0^\infty \Phi(\nu, T) B_\nu(T)\, d\nu = \int_0^\infty \Phi(\nu, T)\, d\nu \int I_\nu \frac{d\omega}{4\pi}. \tag{6.14}$$

From Eqs. (6.12) and (6.14) one integral equation can be derived for determining the temperature T in the form of a function of ζ. If this function is determined, then from Eq. (6.12) one can determine the radiation intensity /70
$I_\nu(\zeta, \vartheta)$ and, in particular, the radiation intensity at the boundary of the star, i.e., the quantity $I_\nu(0, \vartheta)$.

Introduction of the independent variable ζ makes it possible to avoid finding the density distribution in the photosphere in the determination of the stellar spectrum. If, however, we are interested not only in the stellar spectrum but also the quantities T and ρ as a function of r, then, knowing the function $T(\zeta)$, these can easily be determined from Eq. (6.13) and the mechanical equilibrium equation (4.52).

Since the most prevalent element in the surface layers of stars is hydrogen, then one could suppose that radiation absorption in the photospheres of all stars is caused primarily by hydrogen atoms. In reality, this is not the case. In the photospheres of stars of the later classes, the hydrogen atoms are almost entirely in the first state, so that they absorb radiation only, for the most part, beyond the Lyman series limit. Meanwhile, at low temperatures the distribution

curve of energy vs. frequency has a maximum in the infrared region of the spectrum. Consequently, in the photospheres of stars of the later classes, radiation absorption by hydrogen atoms cannot play a significant role.

With an increase in temperature, however, the number of hydrogen atoms in excited states increases. At the same time, a shift of the maximum of the energy vs. frequency distribution curve toward higher frequencies occurs. Therefore, with an increase in temperature the role of hydrogen atoms in absorption increases. Calculations show that in the photospheres of class A and B stars (more precisely, in stars with effective temperatures of the order of 10,000-20,000°) the absorption is produced primarily by hydrogen atoms. In the photospheres of the hotter stars, helium atoms also play a significant role in absorption.

Thus, for stars with $T_e \simeq 10,000-20,000°$ the absorption coefficient is caused primarily by hydrogen and can be represented in the form of (6.11). The theory of the photospheres of these stars was developed by E.R. Mustel' [13]. Instead of considering the integral equation for the function $T(\zeta)$ referenced above, he proposed to determine it by successive approximations from the equation

$$\frac{dT}{d\zeta} = \frac{H}{4\pi \int_0^\infty \frac{1}{\Phi(\nu, T)} \frac{dK_\nu}{dT} d\nu}, \tag{6.15}$$

where

$$K_\nu = \int I_\nu \cos^2 \vartheta \frac{d\omega}{4\pi}. \tag{6.16}$$

Equation (6.15) is derived from (6.12) by multiplying the latter by $\cos\vartheta/\Phi(\nu, T)$ and integrating over all frequencies and directions. The quantity H is the total radiation flux in the photosphere. As we know, H = const, which is the result of Eq. (6.14). As a solution of Eq. (6.15), one can assume $K_\nu = B_\nu(T)$ as a first approximation. /71

E.R. Mustel' calculated the energy distribution in the continuous spectrum of stars with effective temperatures of 10,500°, 15,000 and 20,000°. A portion of the results obtained by him is shown in Fig. 8 and Table 1.

The theoretical energy distribution curve in the spectrum of a class B5 star ($T_e = 15,000°$) is presented in Fig. 8 as an example. Also plotted here is the Planckian curve corresponding to the same temperature T_e (the areas under the curves are identical and equal to $\sigma T_e^4/\pi$). We see that the actual energy distribution curve in the stellar spectrum is very drastically different from the Planckian curve. The large discontinuities at the series limits should be

TABLE 1. SPECTROPHOTOMETRIC TEMPERATURES AND BALMER DISCONTINUITIES OF STARS OF VARIOUS SPECTRAL CLASSES

Spectral class		A0	B5	B2
T_e		10 500°	15 000°	20 000°
T'_s	theor.	19 000	21 000	23 000
	obs.	16 500	23 000	26 500
T''_s	theor.	10 500	15 000	19 000
	obs.	11 000	16 000	19 000
D	theor.	0.49	0.22	0.10
	obs.	0.47	0.24	0.11

especially noted. The energy distribution curves in the spectra of stars of the types considered, obtained from observations, exhibit the same character.

Listed in Table 1 are the theoretical and observed values of the spectrophotometric temperature T_s and of the Balmer discontinuity D. Here T'_s and T''_s represent the values of T_s below the Balmer limit (i.e., for $\nu < \nu_2$) and beyond it, respectively.

Let us recall that the slope of the energy distribution curve at a given point in the spectrum is characterized by the spectrophotometric temperature. More precisely, it is defined from the condition that the derivative of the logarithm of the spectral intensity is equal to the derivative of the logarithm of the Planckian intensity at the temperature T_s, i.e., /72

$$\frac{d}{d\nu}\lg H_\nu = \frac{d}{d\nu}\lg B_\nu(T_s). \tag{6.17}$$

Substituting here the expression for $B_\nu(T)$, we obtain the following equation for determining T_s:

$$\frac{d}{d\nu}\lg H_\nu = \frac{3}{\nu} - \frac{h}{kT_s}\frac{1}{1-e^{-\frac{h\nu}{kT_s}}}. \tag{6.18}$$

Insofar as the Balmer discontinuity is concerned, it is then defined by the formula

$$D = \log_{10}\frac{H_{\nu<\nu_2}}{H_{\nu>\nu_2}}. \tag{6.19}$$

From Table 1 it is seen that the theory is in good agreement with observations. This says, first of all, that in the photospheres of the stars being considered the major role in radiation absorption actually belongs to hydrogen atoms.

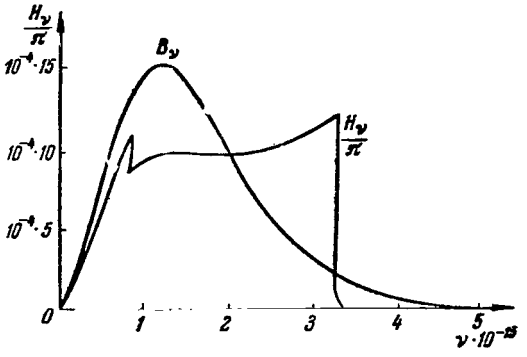

Figure 8.

3. Photosphere models. As explained above, in the case when the absorption coefficient α_ν is represented in the form of (6.11), photosphere theory is greatly simplfied. In this case one can first calculate the radiation field in the photosphere and then determine the photosphere structure. Usually, however, α_ν is not represented in the form of (6.11) (since the absorption is caused by different atoms), so that both of the problems mentioned must be solved concurrently. To do /73 this, several of the equations already derived above must be solved together. We will now present these equations, which are the basic equations of photosphere theory.

1) The radiative transfer equation:

$$\cos\vartheta \frac{dI_\nu}{dr} = -\alpha_\nu I_\nu + \varepsilon_\nu. \tag{6.20}$$

2) The condition that the total radiation flux is a constant (equivalent to the radiation equilibrium condition):

$$2\pi \int_0^\infty d\nu \int_0^\pi I_\nu \cos\vartheta \sin\vartheta \, d\vartheta = \sigma T_e^4. \tag{6.21}$$

3) The Kirchhoff-Planck law, expressing the assumption of local thermodynamic equilibrium:

$$\varepsilon_\nu = \alpha_\nu \frac{2h\nu^3}{c^2} \frac{1}{e^{\frac{h\nu}{kT}} - 1}. \tag{6.22}$$

4) The equation of photosphere mechanical equilibrium:

$$d(p_g + p_r) = -g\rho \, dr, \tag{6.23}$$

where

$$p_g = \frac{R_*}{\mu}\rho T, \qquad p_r = \frac{1}{3}aT^4. \tag{6.24}$$

In these equations the given quantities are the effective stellar temperature T_e, the acceleration of gravity g at the surface of the star and the chemical composition of the photosphere. Moreover, the expression for the absorption coefficient α_ν, which depends on the chemical composition and on the physical conditions in the photosphere (i.e., on T and ρ), must be assumed to be given.

The solution of these equations results in a photosphere model, i.e., the dependence of the temperature T and density ρ on depth, as well as the radiation field in the photosphere. In particular, the theoretical stellar spectrum, which can be compared with the observed spectrum, is defined.

The basic equations of photosphere theory are usually solved by the method of successive approximations. In formulating the first approximation, the mean absorption coefficient $\bar{\alpha}$ and its corresponding optical depth τ are used and it is assumed that the temperature T is related to τ in the same manner as in the case /74 when the absorption coefficient is independent of the frequency. In other words, it is assumed that

$$T^4 = T_e^4 \frac{3}{4}[\tau + q(\tau)], \tag{6.25}$$

where

$$d\tau = -\bar{\alpha}\, dr = -\bar{\varkappa}\rho\, dr. \tag{6.26}$$

From relations (6.23) and (6.26) we also have

$$\frac{dp}{d\tau} = \frac{g}{\bar{\varkappa}}, \tag{6.27}$$

where p = pg = pr. Since the quantity $\bar{\varkappa}$ can be expressed in terms of T and ρ, and the temperature T is expressed in terms of τ by Eq. (6.25), then integration of Eq. (6.27) allows one to obtain p as a function of τ. Knowing the dependence of T and p on τ, we can, with the aid of Eq. (6.26), convert from optical depth τ to geometrical depth $z = r_0 - r$, where r_0 is an arbitrary distance from the center of the star, adopted as the zero point for measuring depth.

The calculation of photosphere models is very often concluded at the first approximation. Sometimes, however, subsequent approximations are carried out; several procedures have been proposed for accomplishing these (see [13]

and [14]). A particularly convenient procedure has recently been developed by Averett and Krook [15]. Tables of values of the absorption coefficient α_ν and the mean absorption coefficient $\bar{\alpha}$ as a function of chemical composition, density and temperature have been compiled to facilitate the calculations (see, for example, [16]. Computers have recently begun to be used for photosphere model calculations.

The results of a calculation of photosphere models for stars of various spectral classes are presented below in the form of examples.

4. Hot stars. In the photospheres of hot stars, radiation absorption is caused primarily by hydrogen and helium. As already established above, in the photospheres of stars with effective temperatures of 10,000-20,000° the major role in absorption belongs to hydrogen. With an increase in temperature, however, the role of helium in the absorption increases. As we will see below, the number of helium atoms in photospheres is only about one order of magnitude less than the number of hydrogen atoms. In the photospheres of cold stars, however, the role of helium in the absorption is negligible. This is explained in the same way as the weak absorption by hydrogen atoms at low temperatures. The only difference lies in the fact that the excitation energy of helium is even /75 higher than the excitation energy of hydrogen. Therefore absorption by helium atoms sets in at even higher temperatures. With a further increase in temperature the absorption by ionized helium becomes significant.

At the same time, light scattering by free electrons plays an important role in radiation transfer in the photospheres of hot stars. This is related with the intense ionization of hydrogen and helium atoms at high temperatures.

Photosphere models of hot stars have been computed by many authors. The results of Traving, who computed the photosphere model of the 10 Lacerta star (spectral class 09V, $T_e = 37,450°$, $\lg g = 4.45$), are presented in Table 2. The columns of the table, in sequence, list the optical depth τ, the temperature T, the logarithm of the gas pressure p_g, the logarithm of the electron pressure p_e and the geomtrical depth z in kilometers. The energy distribution in the continuous stellar spectrum, found on the basis of this model, agreed well with the observed distribution (for example, the calculated Balmer discontinuity is equal to D = 0.044, and the observed value is D = 0.047).

The results of hot star photosphere model calculations, carried out by Underhill, Hunger and other authors, also corroborate observational data on the energy distribution in the visible portion of the spectrum. In particular, for many class B stars the computed and observed continuous spectra agree satisfactorily with each other throughout the entire interval from 3400 to 8000 Å.

In recent years spectrograms of class B stars in the far ultraviolet region have been obtained with the aid of rockets. A study of these has led to the conclusion that there are significant differences between theory and observations since the values found for the radiative flux have turned out to be several times /76

less than the theoretical values (by about a factor of three for a wavelength of 1314 Å). A number of hypotheses have been advanced to explain this difference. Without dwelling on these, let us note that agreement between observations and theory will apparently be achieved after various errors in the observations are corrected, after some refinement of the photosphere models (in particular, by taking account of line absorption) and after an adequately precise determination of the magnitude of interstellar light absorption. A detailed comparison of the observed and calculated continuous spectra of class B stars has been made by Stromgren [17].

TABLE 2. PHOTOSPHERE MODEL OF 10 LACERTA

τ	T	$\lg p_g$	$\lg p_e$	z in km	τ	T	$\lg p_g$	$\lg p_e$	z in km
0	27 700	—	—	—	0,20	36 100	3,87	3,58	3520
0,01	29 000	2,78	2,48	0	0,40	38 700	4,09	3,81	4420
0,02	29 700	3,06	2,76	850	0,60	40 800	4,22	3,94	4970
0,04	30 800	3,31	3,01	1640	0,80	42 300	4,31	4,03	5390
0,06	31 900	3,46	3,16	2090	1,00	43 500	4,37	4,10	5730
0,08	32 800	3,56	3,26	2420	2,00	47 800	4,57	4,30	6840
0,10	33 500	3,64	3,34	2680	3,00	50 900	4,68	4,41	7580

NOTE: Commas represent decimal points.

5. Cold stars. As an example of a cold star, we will first consider the Sun. The Balmer discontinuity is not observed in the continuous solar spectrum. One thing this implies is that the prime role in absorption in the solar photosphere does not belong to hydrogen atoms. The determination of the sources of absorption in the solar photosphere has been an important problem—long before the advent of astrophysics. The frequency dependence of the absorption coefficient was found from observations with the aid of the approximate photosphere theory; however, no known atoms possessed such an absorptive character. Finally, in 1939 Wild expressed the correct concept: the negative hydrogen ion is the primary source of absorption in the solar photosphere.

A quantum mechanical calculation of the negative hydrogen ion involves considerable difficulties; however, they have been surmounted by Chandrasekhar (see Section 5). Calculations have shown that the absorption coefficient of the H^- ion has approximately the same frequency dependence as the absorption coefficient in the solar photosphere, determined by the method mentioned above. In particular, the absence of discontinuities in the visible portion of the solar spectrum is explained by the absence of discontinuities in the absorption coefficient of the H^- ion.

It has already been noted that the photosphere theory, when the absorption coefficient does not depend on frequency, yields fair results when applied to the Sun. This is associated with the fact that the absorption coefficient of the H^- ion changes relatively slightly in that region of the spectrum in which the solar radiation is most intense. Making use of this last fact, Chandrasekhar developed

a special photosphere theory, for application to the Sun, with an absorption coefficient differing little from the mean value. On the basis of this theory some corrections were obtained for the temperature values previously determined for the case when the absorption coefficient does not depend on frequency (see [4]). A calculation of the solar photosphere model, using this theory, was performed by Munch. A portion of his results is given at the start of Chapter III, devoted to the Sun.

The negative hydrogen ion, of course, plays a primary role in absorption /77 not only in the solar photosphere, but also in the photospheres of other stars, resembling the Sun. In general the H^- ion plays the principal role in the formation of the continuous spectrum of all cold stars (with effective temperatures somewhat less than 8000°). A higher temperatures, hydrogen atoms produce very intense absorption and it predominates over the absorption by the H^- ion. Moreover, at very high temperatures these ions are small since the neutral hydrogen atoms, which form H^- ions upon meeting free electrons, are small. On the other hand, at low temperatures the hydrogen atoms absorb weakly and their role in absorption is much smaller than the role of H^- ions. Negative hydrogen ions are quite abundant in the photospheres of cold stars since nearly all the hydrogen atoms exist in the neutral state and free electrons appear through the ionization of metals.

Along with the H^- ion, metal atoms play some role in absorption in the photospheres of cold stars. Absorption in the photospheres of the coldest stars is also caused by molecules.

Photosphere models of cold stars have been developed in a number of papers. In particular, V. G. Buslavskiy [18] developed a photosphere model for a class MO star (with a surface temperature of 3000°C) under the assumption that absorption is caused by negative hydrogen ions and by metals. The energy distribution in the continuous stellar spectrum was determined on the basis of the model. The calculated color temperatures were found to be in satisfactory agreement with observations.

6. White dwarfs. White dwarfs—stars with much lower luminosity than stars of the main sequence of the same spectral class—occupy a special place among stars. The radii of white dwarfs are very small—about 0.01 of the radius of the Sun—but their masses are of the order of the Sun's mass. Therefore the gravitational acceleration at the surface of white dwarfs is very high—in some cases it amounts to 10^{10} cm/sec^2. Such high g values lead to a number of special characteristics both in the structure of the photospheres of white dwarfs and in the energy distribution in their spectra.

As an example of calculations of white dwarf photosphere models, we will present the results of A. K. Kolesov [18]. Observations show only hydrogen lines are present in the spectra of some white dwarfs (the majority of them), while in the spectra of the others—only helium lines. According, purely hydrogen and purely helium photospheres have been considered separately in the analyses. The calculations were carried out for surface temperatures T_0 equal to 12,000, 15,000 and 20,000° (and at T_0 = 30,000° for purely helium photospheres), and

for gravitational acceleration values g equal to 10^6, 10^8 and 10^{10} cm/sec^2. The results of a calculation for the case of a purely hydrogen photosphere for T_0 = = 15,000° and g = 10^8 cm/sec^2 are compiled in Table 3.

TABLE 3. PHOTOSPHERE MODEL OF WHITE DWARF

τ	T	$p \cdot 10^{-5}$ dynes/ /cm^2	$n_e \cdot 10^{-17}$ см$^{-3}$	$\rho \cdot 10^7$ g/cm^3	z, km
0,1	15 900	0,92	0,200	0,364	0
0,2	16 500	1,41	0,296	0,536	0,110
0,4	17 500	2,24	0,448	0,799	0,229
0,6	18 300	3,00	0,577	1,02	0,323
0,8	19 000	3,72	0,694	1,21	0,378
1,0	19 600	4,43	0,802	1,39	0,433
2,0	22 100	7,86	1,28	2,18	0,621
3,0	23 900	11,2	1,68	2,86	0,753
4,0	25 400	14,4	2,04	3,45	0,855
5,0	26 600	17,5	2,37	4,00	0,938

NOTE: Commas represent decimal points.

The geometrical depth, in kilometers, is listed in the last column of Table 3. We see that unit optical depth corresponds to a geometrical depth of about 0.4 km. In other words, the "photosphere thickness" of white dwarfs is of this order, i.e., it is extremely small. The photosphere thickness is much greater for other stars. For example, as seen in Table 2, it is about 6000 km for the star 10 Lacerta. This difference is explained by the enormously high gravitational acceleration at the surface of a white dwarf, as a result of which a large pressure gradient is required in order to counterbalance gravity.

The high pressures in the photospheres of white dwarfs are reflected in their spectra. At high pressures the high discrete atomic levels do not occur because of the effect of the electric field of the ions and free electrons (see Section 8 for more details on this effect). Therefore the frequency of each series limit is lowered and ionization from the occurring low levels can be produced by low frequency radiation. The role of this effect is obviously different at different points of the photosphere (namely, it increases with depth because of the pressure increase). Because of this the intensity discontinuities at the series limits should wash out in the formation of the stellar spectrum. In particular, the Balmer discontinuity, lying in the visible region of the spectrum, should vanish.

The theoretical spectrum of a star with a surface temperature of 15,000° /79
near the Balmer series limit is shown in Fig. 9, taken from Kolesov's paper. From the figure it is seen how the washing out of the discontinuity increases with an increase in the gravitational acceleration in the photosphere. At high

values of g the discontinuities are practically absent. The observed spectra of white dwarfs exhibit precisely this behavior.

7. Special Problems of Photosphere Theory

1. Extended photospheres. The assumption made above concerning the fact that the photosphere thickness is much less than the star radius cannot be applied to certain special stars (for example, to the Wolf-Rayet type stars). This is the situation, then, when the density in the photosphere decreases relatively slowly with an increase in distance from the center of the star. In such photospheres the layers of isodensity should not be considered as plane-parallel, but spherical.

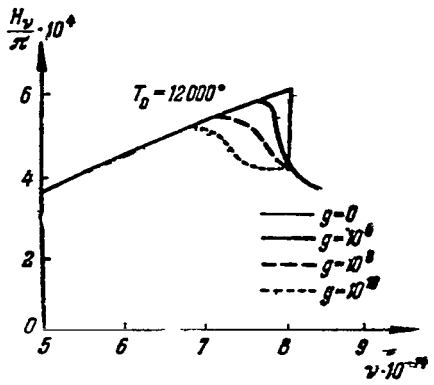

Figure 9.

Let us find the dependence of the temperature on the optical depth in the case given. To do this, we must make use of the radiative transfer equation in the form of (1.20). After integrating this equation over all frequencies, we obtain

$$\cos\vartheta\frac{\partial I}{\partial r}-\frac{\sin\vartheta}{r}\frac{\partial I}{\partial\vartheta}=-\bar{\alpha}I+\varepsilon, \tag{7.1}$$

where $\bar{\alpha}$ is the mean absorption coefficient. Denoting, as usual, $\varepsilon=\bar{\alpha}S$, we have

$$S=\int I\frac{d\omega}{4\pi}. \tag{7.2}$$

as the radiative equilibrium condition. Integration of (7.1) over all directions, with (7.2) taken into consideration, leads to the formula

$$H=\frac{C}{r^2}, \tag{7.3}$$

where C is some constant. (It is obvious that $4\pi C$ is the stellar luminosity.) /80

Multiplying (7.1) by $\cos\vartheta$ and integrating over all directions, in the Eddington approximation we obtain

$$\frac{4\pi}{3}\frac{dS}{dr}=-\bar{\alpha}H, \tag{7.4}$$

or, on the basis of (4.15),

$$\frac{ac}{3}\frac{dT^4}{dr} = -\bar{\alpha}H. \tag{7.5}$$

For the absorption coefficient $\bar{\alpha}$ we will take the expression

$$\bar{\alpha} \sim \frac{\rho^2}{T^s} \tag{7.6}$$

[compare with Eqs. (5.35) and (5.36)] and we will assume that the density in the photosphere is inversely proportional to some power of the distance from the center of the star, i.e.,

$$\rho \sim \frac{1}{r^n}. \tag{7.7}$$

Substituting (7.3), (7.6) and (7.7) into Eq. (7.5) and integrating the latter, we obtain

$$T = T_1\left(\frac{r_1}{r}\right)^{\frac{2n+1}{4+s}}, \tag{7.8}$$

where T_1 is the temperature at the distance r_1.

By using Eqs. (7.7) and (7.8), one can also easily derive the dependence of the optical depth τ on the distance r. Substitution of these formulas into the relation $d\tau = -\bar{\alpha}\, dr$ and integration yield

$$\tau = \left(\frac{r_1}{r}\right)^{2\frac{4n-s-2}{4+s}}, \tag{7.9}$$

where, now, r_1 represents the distance from the center of the star for $\tau = 1$.

From (7.8) and (7.9) we obtain the desired dependence of T on τ:

$$T = T_1\tau^{\frac{2n+1}{2(4n-s-2)}}. \tag{7.10}$$

Let us take, for example, n = 2 and s = 4. Then we have /81

$$T = T_1\tau^{3/4}. \tag{7.11}$$

Thus, in an extended photosphere the temperature increases much more rapidly with the optical depth than in a photosphere consisting of plane-parallel layers.

Knowledge of the dependence of T on τ makes it possible to calculate the energy distribution in the continuous stellar spectrum. To do this, it is necessary to make use of the radiative transfer Eq. (1.20), after setting $\varepsilon_\nu = \alpha_\nu B_\nu(T)$ on the basis of the hypothesis of local thermodynamic equilibrium. In the theory of extended photospheres, it was initially assumed [19] that the absorption coefficient does not depend on the frequency. In this case a curve of the energy distribution in the continuous stellar spectrum was obtained which differs very markedly from the Planckian curve—with a large excess of radiation in the ultraviolet portion of the spectrum. When, however, the frequency dependence of the absorption coefficient is taken into account, this radiation excess is not obtained because of the heavy absorption beyond the limits of the principal atomic series. It should also be borne in mind that very large divergences from local thermodynamic equilibrium are possible in extended photospheres.

2. Blanketing effect. The continuous spectrum radiation of a star, passing through the surface layers of a star, undergoes partial absorption in spectral lines. The energy, absorbed in lines, returns to the photosphere. As a result, the radiation density in the photosphere is increased and, consequently, also its temperature. This phenomenon is called the blanketing effect.

We will designate by A the energy fraction absorbed in the spectral lines. This quantity can be found directly from observations. For example, for the Sun it is equal to approximately 10%.

Energy absorption in lines occurs in a surface layer with an optical depth of the order of several tenths in the continuous spectrum. For simplicity, however, we will now assume that energy is absorbed in lines at the boundary of the star (at $\tau = 0$). Then, under the assumption that the absorption coefficient in the continuous spectrum does not depend on frequency (or using the mean absorption coefficient) the blanketing effect can be taken into precise consideration.

In formulating the radiative equilibrium equation for the problem at hand, one must keep in mind that both diffuse radiation, coming from all sides, as well as radiation reflected from the boundary and attenuated along its path, strike each volume element in the photosphere. We will denote the intensity of the diffuse radiation by $I(\tau, \mu)$ and the intensity of the radiation reflected from the boundary—by I_*. Then we obtain /82

$$S(\tau) = \frac{1}{2}\int_{-1}^{+1} I(\tau, \mu)\, d\mu + \frac{1}{2} I_* \int_0^1 e^{-\frac{\tau}{\mu}}\, d\mu. \tag{7.12}$$

as the radiative equilibrium equation.

Substituting into (7.12) the expression for $I(\tau, \mu)$ in terms of $S(\tau)$ obtained from the radiative transfer equation (i.e., proceeding in the same manner as in the derivation of Milne's equation), we find

$$S(\tau) = \frac{1}{2}\int_0^\infty \mathrm{Ei}|\tau - \tau'| S(\tau')\, d\tau' + \frac{1}{2} I_* \mathrm{E}_2\tau. \tag{7.13}$$

To determine the quantity I_* we must make use of the relation

$$I_* = 2A \int_0^1 I(0, \mu) \mu \, d\mu, \tag{7.14}$$

which expresses the fact that a fraction A, of the energy incident on the boundary, is reflected. In the given case, obviously, the radiative flux must be the same as in the absence of the blanketing effect (i.e., equal to πF). Therefore we have

$$2(1-A) \int_0^1 I(0, \mu) \mu \, d\mu = F. \tag{7.15}$$

From (7.14) and (7.15) it follows that

$$I_* = \frac{A}{1-A} F. \tag{7.16}$$

Substituting (7.16) into (7.13), we obtain

$$S(\tau) = \frac{1}{2} \int_0^\infty \mathrm{Ei} |\tau - \tau'| S(\tau') d\tau' + \frac{AF}{2(1-A)} \mathrm{E}_2 \tau. \tag{7.17}$$

When A = 0, Eq. (7.17) passes over to Milne's equation.

It is easily verified that the solution of Eq. (7.17) has the form

$$S(\tau) = \frac{A}{1-A} F + \frac{3}{4} F [\tau + q(\tau)], \tag{7.18}$$

where $q(\tau)$ is the Hopf function [see Eq. (2.50)].

Using the known relations $S(\tau) = \sigma T^4/\pi$ and $F = \sigma T_e^4/\pi$, instead of (7.18) we obtain /83

$$T^4 = T_e^4 \left\{ \frac{A}{1-A} + \frac{3}{4} [\tau + q(\tau)] \right\}. \tag{7.19}$$

From Eq. (7.19) it is seen how the blanketing effect influences the temperature in the photosphere. This formula, however, cannot be used with very small τ values (because of the assumption made above concerning the fact that radiation is reflected from the star boundary itself).

3. Effect of reflection in close pairs. If two stars are in close proximity, then in studying their luminosity it is necessary to take into consideration the interchange of radiative energy between them. In this case the radiation reflected

from each star is added to the intrinsic radiation. In reality, of course, the reflection process is very complicated: a temperature increase occurs in each star because of the effect of the radiation of the neighboring star, so that the amount of energy radiated by the star increases.

Let us write the radiative equilibrium equation for this situation. We will assume that at the boundary of the star A radiation from star B is incident within the solid angle Ω (Fig. 10). For simplicity we will assume the angle Ω is small. The mean intensity of the radiation, incident within the solid angle Ω, we will denote by I_0, and the mean angle between the direction of this radiation and the normal to the photosphere layers—by ϑ_0. Then the radiative equilibrium equation will have the form

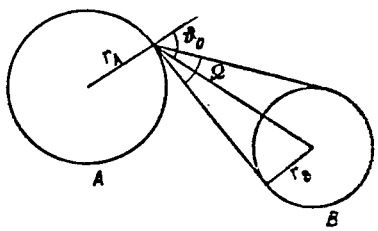

Figure 10.

$$S(\tau, \mu_0) = \frac{1}{2}\int_{-1}^{+1} I(\tau, \mu', \mu_0)\, d\mu' + \frac{I_0\Omega}{4\pi} e^{-\frac{\tau}{\mu_0}}, \quad (7.20)$$

where $I(\tau, \mu', \mu_0)$ is the intensity of the diffuse radiation in the photosphere ($\mu' = \cos\vartheta'$, $\mu_0 = \cos\vartheta_0$).

Using Eq. (7.20) and the radiative transfer equation, just as in the derivation of Eq. (2.45), we obtain

$$S(\tau, \mu_0) = \frac{1}{2}\int_0^\infty \mathrm{Ei}|\tau - \tau'| S(\tau', \mu_0)\, d\tau' + \frac{I_0\Omega}{4\pi} e^{-\frac{\tau}{\mu_0}}. \quad (7.21)$$

/84

Equation (7.21) belongs to the type of equations discussed in detail in Section 3. The solution of this equation will consist of two terms: the first term is determined by the energy sources existing within the star (at an infinitely great depth), and the second—by the energy entering the photosphere of star A from star B. On the basis of Eqs. (3.16) and (3.64) we obtain

$$S(\tau, \mu_0) = \frac{\sqrt{3}}{4} F\left[1 + \int_0^\tau \Phi(\tau')\, d\tau'\right] + \frac{I_0\Omega}{4\pi}\varphi(\mu_0)\left[e^{-\frac{\tau}{\mu_0}} + \int_0^\tau e^{-\frac{\tau-\tau'}{\mu_0}} \Phi(\tau')\, d\tau'\right], \quad (7.22)$$

where $\varphi(\mu_0)$ and $\Phi(\tau)$ are functions defined by Eqs. (3.53) and (3.55), respectively.

When $\tau = 0$, the following simple equation is obtained from (7.22):

$$S(0, \mu_0) = \frac{\sqrt{3}}{4} F + \frac{I_0\Omega}{4\pi}\varphi(\mu_0). \quad (7.23)$$

Since the quantity $S(\tau, \mu_0)$ is proportional to T^4, then with the aid of Eq. (7.22) the temperature T at any optical depth and for an arbitrary position of the neighboring star with respect to a given point in the photosphere can be calculated. Equation (7.23) allows one to determine the value of the surface temperature T_0.

If the temperature in the photosphere is known, then by using Eq. (6.3), one can find the intensity of the radiation emanating from a given point of the stellar surface at any frequency ν.

It is obvious that the temperature does not need to be known to determine the total radiation intensity. We will denote the reflection angle, i.e., the angle between the direction of the radiation leaving the star and the direction of the radius vector, by ϑ ($\cos\vartheta = \mu$). Then the radiation intensity $I(0, \mu, \mu_0)$ will be determined by the formula

$$I(0, \mu, \mu_0) = \int_0^\infty S(\tau, \mu_0) e^{-\frac{\tau}{\mu}} \frac{d\tau}{\mu}, \tag{7.24}$$

into which Eq. (7.22) must be substituted. This substitution has already been done in Section 3. On the basis of Eq. (3.40) (in which $m = 1/\mu_0$) and of Eqs. (3.57) and (3.63), we find

$$I(0, \mu, \mu_0) = \frac{\sqrt{3}}{4} F\varphi(\mu) + \frac{I_0\Omega}{4\pi} \frac{\varphi(\mu)\varphi(\mu_0)}{\mu + \mu_0} \mu_0. \tag{7.25}$$

From the formulas derived it is seen that the reflection effect is greater, the larger the ratio $I_0\Omega/\pi F$. This ratio can be represented in a more convenient form. If the solid angle Ω is small, then we obtain /85

$$I_0\Omega = \frac{L_B}{4\pi r^2}, \tag{7.26}$$

where L_B is the luminosity of star B and r is the distance between stars A and B. On the other hand we have

$$\pi F = \frac{L_A}{4\pi r_A^2}, \tag{7.27}$$

where L_A and r_A are the liminosity and radius of star A, respectively. From (7.26) and (7.27) it follows that:

$$\frac{I_0\Omega}{\pi F} = \frac{L_B}{L_A}\left(\frac{r_A}{r}\right)^2. \tag{7.28}$$

Calculations with these formulas show that the role of the reflection effect can be appreciable. It depends, of course, on the location of star B with respect to the point of interest in the photosphere of star A (it is greater, the smaller the angle ϑ). The reflection effect affects the curves of brightness variation of eclipsing variables.

4. Polarization of the radiation of hot stars. Light scattering by free electrons plays a large role in radiation transfer in the photosphere of hot stars. In this case the light, scattered by a volume element, is polarized. Therefore the transfer of polarized radiation must be considered in studying the photospheres of hot stars. With the radiation polarization taken into account we should obtain more precise values of the total radiation intensity and also determine the state of the radiation polarization (i.e., the degree of polarization and the location of the polarization plane).

Light scattering by free electrons obeys a law which can be formulated in the following manner. Let $I_{\parallel}$ and $I_{\perp}$ be the intensities of linearly polarized radiation with the electric vector respectively parallel and perpendicular to the scattering plane (i.e., the plane in which the incident and scattered rays lie). If the radiation strikes the volume element within a solid angle $d\omega$, then the amount of energy, scattered by this volume in a direction making an angle γ with the direction of the incident radiation, in a unit solid angle is equal to $\frac{3}{2}\sigma_e I_{\parallel}\cos^2\gamma\, d\omega/4\pi$ and $\frac{3}{2}\sigma_e I_{\perp} d\omega/4\pi$ respectively, with the scattered radiation having its electric vector in the same direction as the incident radiation. Here σ_e is the volume coefficient of scattering by free electrons, defined by Eq. (5.16).

As we know, the radiation field in the photosphere possesses axial symmetry: the radiation intensity depends only on τ and the angle ϑ but is independent of the azimuth. In a given case, therefore, it is sufficient to specify only two quantities (and not four, as in the general case) to characterize the polarized radiation. As these quantities we can take the radiative intensities I_l and I_r with oscillations in the plane passing through the ray and the normal to the photosphere layer and the plane perpendicular to this, respectively. Instead of the intensities I_l and I_r, one can also take the intensities I and K, equal to

$$I = I_r + I_l, \qquad K = I_r - I_l. \tag{7.29}$$

The quantity I is the total radiation intensity, and the quantity $p = K/I$ is the degree of radiation polarization.

For determining the quantities I and K we have the usual radiative transfer equations·

$$\left.\begin{aligned} \cos\vartheta\frac{dI}{d\tau} &= I - S, \\ \cos\vartheta\frac{dK}{d\tau} &= K - R, \end{aligned}\right\} \tag{7.30}$$

where $d\tau = -\sigma_e dr$.

On the basis of the law for scattering of light by free electrons one can determine that the quantities S and R entering into these equations are related to the radiation intensities I and K by the following radiative equilibrium equations:

$$S(\tau, \mu) = \frac{1}{2} \int_{-1}^{+1} I(\tau, \mu') \left[1 + \frac{1}{2} P_2(\mu) P_2(\mu')\right] d\mu' + \\ + \frac{3}{8} P_2(\mu) \int_{-1}^{+1} K(\tau, \mu')(1 - \mu'^2) d\mu', \tag{7.31}$$

$$R(\tau, \mu) = \frac{3}{8}(1 - \mu^2) \int_{-1}^{+1} I(\tau, \mu') P_2(\mu') d\mu' + \\ + \frac{9}{16}(1 - \mu^2) \int_{-1}^{+1} K(\tau, \mu')(1 - \mu'^2) d\mu', \tag{7.32}$$

where $P_2(\mu) = 1/2(3\mu^2 - 1)$ is the second Legendre polynomial. In the derivation of Eqs. (7.31) and (7.32) it is assumed that we are dealing with a purely electronic photosphere. /87

We will not dwell on the derivation of the equations presented and their solution, and we will only give the results of the solution (see [4] and [20]). Values of the quantities I and K and the degree of polarization p for the radiation leaving the star are listed in Table 4.

TABLE 4. THE RADIATION OF A STAR WITH PURELY ELECTRONIC PHOTOSPHERE

μ	0	0,1	0,2	0,3	0,4	0,5	0,6	0,7	0,8	0,9	1,0
$I(0, \mu)$	1,00	1,24	1,46	1,67	1,87	2,07	2,27	2,46	2,66	2,85	3,04
$10K(0, \mu)$	1,25	1,00	0,84	0,70	0,58	0,47	0,37	0,27	0,18	0,09	0
$p(\mu)$ in %	12,5	8,0	5,8	4,2	3,1	2,3	1,6	1,1	0,7	0,3	0

NOTE: Commas represent decimal points.

From the table it is seen that the brightness distribution over the disk of a star with a purely electronic photosphere does not differ greatly from the brightness distribution over the disk of a normal star (the ratio of the brightness at the center of the disk to the brightness at the edge is equal to 3.04 instead of 2.91). Insofar as the degree of polarization is concerned, it is equal to zero at the center of the disk and increases to 12.5% at the edge.

For real stars, however, the degree of polarization is less than listed in Table 4 since in photospheres energy absorption and emission by the atoms occur along with light scattering by free electrons.

It is obvious that the radiation, coming from the entire disk of a spherically symmetric star, will be unpolarized. Therefore this starlight polarization effect can be detected only through observations of eclipsing variables, one component of which is a hot star while the other is cold. In such a case the radiation of the system will be slightly polarized when the hot star is eclipsed by its cold satellite. This effect, predicted by the theory, was then actually detected through observations.

Of special interest is the fact that a new phenomenon—light polarization of uneclipsed stars and even light polarization of isolated stars—was discovered during these observations. Basically, this phenomenon is explained by the polarization of the radiation during its passage through interstellar space (which we will discuss in detail in Section 32). In some cases, however, this phenomenon can also be caused by light scattering by free electrons. The polarization of the radiation of an uneclipsed binary system can be the result of the scattering of the light of one star at the free electrons in the photosphere of the other /88
star or in the gaseous streams which are sometimes observed in binary systems. The radiation of an isolated star can be polarized because of light scattering at free electrons with a deviation from sphericity.

REFERENCES

1. Schwarzschild, K.: On the equilibrium of the solar atmosphere, Über das Gleichgewicht der Sonnenatmosphäre, Cöttinger Nachr. 41, 1906.
2. Schuster, A.: Radiation through a Foggy atmosphere, A. J. 21. 1, 1905.
3. Eddington, A. S.: Internal consistution of the stars, 1926.
4. Chandrasekhar, S.: Radiative Transfer, 1950 (Russ. translation: S. Chandrasekhar, Radiative transfer, Izd-vo inostr. lit. 1953).
5. Milne, E. A.: Radiative equilibrium in the outer layers of a star, MN 81, 361, 1921.
6. Hopf, E.: Mathematical Problems of Radiative Equilibrium, Cambridge Tracts 31, 1934.
7. Sobolev, V. V.: Theory of radiative diffusion in stellar atmospheres, Astron, Zh. 36, No. 4, 1959.
8. Busbridge, I. W.: The mathematics of radiative transfer, Cambridge, 1960.
9. Ambartsumyan, V. A.: Light scattering by planet atmospheres, Astron. Zh. 19, No. 5, 1942.
10. Minin, I. N.: Theory of radiative diffusion in a semi-infinite medium, Doklady AN SSSR 120, 63, 1958.
11. Chandrasekhar, S.: On the continuous absorption coefficient of the negative hydrogen ion, Astrophys. J. 102, 223, 395, 1945.
12. Rosseland, S.: Astrophysics on the basis of atomic theory, 1931 (Russ. translation: S. Rosseland, Astrophysics on the basis of atomic theory, 1936).
13. Mustel', E. R.: Stellar atmospheres, Fizmatgiz, 1960.
14. Kourganoff, V.: Basic methods in transfer problems, 1952.

15. Avrett, E. H and Max Krook: The temperature distribution in a stellar atmosphere, Astrophys. J. 137, 874, 1963.
16. Ueno, S., S. Saito and J. Jugaku: Continuous Absorption Coefficients of the Model Stellar Atmosphere, Contr. Inst. of Astrophys. Kyoto 42-43, 1954.
17. Stromgren, B.: Comparison of observed and theoretically calculated intensities in the continuous spectra of main-sequence B stars, Rev. Mod. Physics 36, N 2, 1964.
*18. Compilation "Theory of stellar spectra," Izd-vo "Nauka," 1966.
19. Kosirev, N. A.: Radiative equilibrium of the extended photosphere, MN 94, 430, 1934.
20. Sobolev, V. V.: Polarization of scattered light, Uchen. zap. LGU, No. 116, 1949.

Translator's Note:

* The entire book has been translated into English and is available as NASA TTF-457.

CHAPTER II

STELLAR ATMOSPHERES

We will understand stellar atmosphere to mean the layer in which the stellar line spectrum forms. On the average the atmosphere is above the photosphere, which gives rise to the continuous spectrum. This is explained by the fact that the line absorption coefficient is much greater than the continuous spectrum absorption coefficient. Therefore in the outermost portions of a star the continuous spectrum absorption no longer plays any appreciable role, but the line absorption remains significant. /89

In the early days of astrophysics it was even assumed that there is a sharp boundary between the photosphere and atmosphere. In other words, it was assumed that a continuous radiation spectrum with no lines comes from the photosphere, and absorption lines appear as it passes through the atmosphere (or, as it was called then, through the reversing layer). Nowadays this assumption is usually not made, i.e., both line and continuous spectrum absorption are considered to occur in every volume element. Even in this case, however, photosphere theories, i.e., problems concerned with the formation of the continuous stellar spectrum, are studied first, and then atmosphere theories, i.e., problems concerned with the formation of absorption lines. In this situation the effect of lines is usually ignored in photosphere theories, and in atmosphere theories the solution of the problem of continuous spectrum formation is assumed to be known.

In this chapter the problem of the spectral line absorption coefficient is considered first, then the problem of the formation of stellar line spectra is solved and, finally, the various characteristics of stellar atmospheres are determined by comparing the theory with observations. It should be emphasized that most of our information about the stars is obtained on the basis of the radiation from their line spectra. Information on the chemical composition of stellar atmospheres, on motions in the atmospheres, on the rotation of stars, on the magnetic fields of stars, etc., is obtained from the line spectra. Therefore the theory of the formation of absorption lines in stellar spectra occupies an exceptionally important place in theoretical astrophysics.

8. The Spectral Line Absorption Coefficient /90

1. Einstein transition coefficients. Spectral line emission and absorption are associated with the transitions of an atom from one discrete state to another. If an atom is in an excited state, then it can spontaneously jump into any state with a lower energy. When an atom makes a spontaneous transition from the k-th state into the i-th, a photon with energy

$$h\nu_{ik} = E_k - E_i, \tag{8.1}$$

is emitted, where E_k and E_i are the initial and final energy states, respectively. The reverse transition, whereby a photon is absorbed, can occur through the action of radiation of frequency ν_{ik} can also produce an atom transition from the k-th to the i-th state, accompanied by the emission of a photon. This process is called stimulated emission or negative absorption.

The probabilities of these processes are characterized by certain coefficients, introduced by Einstein. Let n_k be the number of atoms in the k-th state in 1 cm^3. Obviously the number of spontaneous transitions from the k-th to the i-th state, occuring in 1 cm^3 during a time dt, is proportional to the number n_k and the time dt, i.e., it is equal to $n_k A_{ki} dt$. The quantity A_{ki} is called the Einstein coefficient of spontaneous transition. The number of transitions from the i-th to the k-th state, associated with the absorption of photons, in 1 cm^3 during time dt is equal to $n_i B_{ik} \rho_{ik} dt$, where n_i is the number of atoms in the i-th state in 1 cm^3 and ρ_{ik} is the density of radiation with frequency ν_{ik}. The quantity B_{ik} is the Einstein absorption coefficient. The number of transitions from the k-th to the i-th state, caused by radiation, in 1 cm^3 during time dt can be written in the form

$$n_k B_{ki} \rho_{ik} dt,$$

where B_{ki} is the Einstein negative absorption coefficient.

The Einstein transition coefficients are not independent, but are interrlated by two expressions. To derive these relations we will examine the thermodynamic equilibrium condition. In this case detailed balance occurs in which any process is compensated by reverse process. In particular, the number of transitions from the k-th to the i-th state is equal to the number of transitions from the i-th to the k-th state, i.e.,

$$n_k A_{ki} + n_k B_{ki} \rho_{ik} = n_i B_{ik} \rho_{ik}. \tag{8.2}$$

On the other hand, in the presence of thermodynamic equilibrium the atomic state distribution is given by Boltzmann's formula /91

$$\frac{n_k}{n_i} = \frac{g_k}{g_i} e^{-\frac{h\nu_{ik}}{kT}}, \tag{8.3}$$

where g_i and g_k are the statistical weights of the states. From (8.2), with the aid of (8.3), we obtain

$$\rho_{ik} = \frac{A_{ki}}{B_{ki}} \frac{1}{\frac{g_i}{g_k}\frac{B_{ik}}{B_{ki}} e^{\frac{h\nu_{ik}}{kT}} - 1}. \tag{8.4}$$

Comparing (8.4) with Planck's formula (4.4), also applicable in the presence of thermodynamic equilibrium, we find

$$A_{ki} = \frac{8\pi h\nu_{ik}^3}{c^3} B_{ki}, \quad B_{ki} = \frac{g_i}{g_k} B_{ik}. \tag{8.5}$$

Thus, if one of the Einstein coefficients is known, then the other two are determined with the aid of the relations (8.5). Let us note that although these relations are derived under the assumption of thermodynamic equilibrium, they are always valid since the Einstein transition coefficients characterize the properties of an atom and photon and are independent of what the atomic states are and what the photon frequency distributions are.

A vast difference between spontaneous and stimulated radiation must be emphasized. During spontaneous transitions the photons are emitted in all directions. In stimulated transitions the photons are emitted in the same direction in which the photons, stimulating these transitions, are moving. Therefore the intensity of the radiation beam striking the atom decreases because of absorption, but increases because of the stimulated transitions. This explains why stimulated radiation is also called negative absorption.

From what has been said it follows that the total number of photons, absorbed in the line being considered in 1 cm^3 during 1 second, is equal to

$$n_i B_{ik}\rho_{ik} - n_k B_{ki}\rho_{ik} = n_i B_{ik}\rho_{ik}\left(1 - \frac{n_k B_{ki}}{n_i B_{ik}}\right).$$

On the basis of the second of relations (8.5), this expression can be rewritten in the form

$$n_i B_{ik}\rho_{ik}\left(1 - \frac{g_i n_k}{g_k n_i}\right).$$

Thus, to take negative absorption into account the number of photons undergoing normal absorption must be multiplied by the quantity $1-g_i n_k/g_k n_i$*. /92

If the distribution of atomic levels is given by Boltzmann's formula (particularly in the presence of thermodynamic equilibrium), then instead of the last expression we have

$$n_i B_{ik} \rho_{ik} \left(1 - e^{-\frac{h\nu_{ik}}{kT}}\right).$$

Consequently, in this case the factor that takes account of negative absorption is equal to $1-e^{-h\nu_{ik}/kT}$. We have already made use of this result in discussing continuous spectrum absorption (Section 5).

Knowing the Einstein spontaneous transition coefficients makes it possible to determine the average lifetime of atoms in the excited states. Let $n_k(0)$ be the number of atoms in the k-th state at time $t = 0$. Decay, because of spontaneous transitions into all the lower lying levels. follows the law

$$dn_k = -n_k \sum_{i=1}^{k-1} A_{ki}\, dt, \tag{8.6}$$

or, after integration,

$$n_k(t) = n_k(0)\, e^{-\gamma_k t}, \tag{8.7}$$

where

$$\gamma_k = \sum_{i=1}^{k-1} A_{ki}. \tag{8.8}$$

From this we obtain

$$\bar{t}_k = \int_0^\infty t e^{-\gamma_k t} \gamma_k\, dt = \frac{1}{\gamma_k}. \tag{8.9}$$

for the average lifetime of an atom in the k-th state.

---

*It is interesting to note that this quantity can become negative when the population of the upper level is large. In such a case the radiation intensity will increase as it passes through the medium. This is the principle on which lasers are based.

For allowed transitions the values of A_{ki} are of the order of 10^7 sec^{-1}. Therefore the average lifetime of an atom in an excited state is approximately 10^{-7} sec. Metastable states, from which all transitions to lower lying levels are forbidden, constitute an exception. The values of A_{ki} are much smaller for /93 forbidden transitions than for allowed transitions. Therefore the average lifetime of an atom in a metastable state is very long (sometimes amounting to several hours).

The atomic wave functions must be known in order to calculate the Einstein transition coefficients. Since a determination of the wave functions is a very complex problem, the Einstein transition coefficients have been calculated for the simplest cases only.

Values of the quantities A_{ki} for the hydrogen atom are given in Table 5. Here, i and k represent the principal quantum numbers, and the quantities A_{ki} have the following significance. If n_k is the number of atoms in all states with principal quantum number k, then the total number of transitions into the state with principal quantum number i, occurring in 1 sec, is equal to $n_k A_{ki}$. Here it is assumed that the distribution of atomic states with different azimuthal quantum numbers is proportional to the statistical weights of these states.

The Einstein transition coefficients A_{ki}; B_{ik} and B_{ki} are simply expressed in terms of the so-called oscillator strength f_{ik}. For example, the spontaneous transition Einstein coefficient is equal to

$$A_{ki} = \frac{8\pi^2 e^2 \nu_{ik}^2}{mc^3} \frac{g_k}{g_i} f_{ik}, \tag{8.10}$$

where m is the electron mass and e is its charge. The quantity f_{ik} is dimensionless and represents the number of classical oscillators which replace one atom /94 in the absorption effect.

2. Absorption coefficient caused by radiation damping and thermal motion of atoms. Spectral lines are not strictly monochromatic. Photons of different frequencies, close to the central line frequency ν_0, can be absorbed at each line. The absorption probability of photons of frequency ν within a line is determined by many factors. Just as before (see Section 1) we will characterize this probability by the volume absorption coefficient, which we will denote by σ_ν. The physical significance of this quantity, as we recall, is that the absorption probability of a photon of frequency ν along a path length ds is equal to $\sigma_\nu ds$. Let us also note that the amount of energy of frequency ν, absorbed in a unit volume in 1 sec, is equal to $\sigma_\nu \int I_\nu d\omega$ where I_ν is the radiation intensity and the integration is done over all directions.

TABLE 5. A_{ki} VALUES FOR THE HYDROGEN ATOM

k \ i	1	2	3	4	5	6	7
2	$4,67\cdot10^8$	—	—	—	—	—	—
3	$5,54\cdot10^7$	$4,39\cdot10^7$	—	—	—	—	—
4	$1,27\cdot10^7$	$8,37\cdot10^6$	$8,94\cdot10^6$	—	—	—	—
5	$4,10\cdot10^6$	$2,52\cdot10^6$	$2,19\cdot10^6$	$2,68\cdot10^6$	—	—	—
6	$1,64\cdot10^6$	$9,68\cdot10^5$	$7,74\cdot10^5$	$7,67\cdot10^5$	$1,02\cdot10^6$	—	—
7	$7,53\cdot10^5$	$4,37\cdot10^5$	$3,34\cdot10^5$	$3,03\cdot10^5$	$3,24\cdot10^5$	$4,50\cdot10^5$	—
8	$3,85\cdot10^5$	$2,20\cdot10^5$	$1,64\cdot10^5$	$1,42\cdot10^5$	$1,38\cdot10^5$	$1,55\cdot10^5$	$2,26\cdot10^5$

Commas represent decimal points.

Let the line being considered arise through the transition of an atom from the i-th state into the k-th and let n_i be the number of atoms per cm^3 in the i-th state. We can represent the quantity σ_ν in the form $\sigma_\nu = n_i k_\nu$, where k_ν is the absorption coefficient, calculated for one atom. It is obvious that the quantities σ_ν and k_ν depend on the indices i and k, but for simplicity of notation we will omit these indices.

The absorption coefficient k_ν is related in a simple fashion to the Einstein absorption coefficient B_{ik}. In order to determine this relationship, let us write the expression for the number of transitions from the i-th level to the k-th, occurring in 1 cm^3 in 1 sec, first with the aid of B_{ik}, and then with the aid of k_ν. In the former case, the number of transitions is equal to $n_i B_{ik} \rho_{ik}$. In the latter case, the same number of transitions can be represented in the form $n_i \int k_\nu d\nu / / h\nu \int I_\nu d\omega$. Equating these two expressions and taking into account that $\int I_\nu d\omega = c\rho_\nu$, where ρ_ν is the radiation density, we find

$$c \int k_\nu \frac{\rho_\nu}{h\nu} d\nu = B_{ik} \rho_{ik}. \tag{8.11}$$

Since the absorption coefficient k_ν has a sharp maximum at the center frequency ν_0, the average value of the quantity $\rho_\nu / h\nu$ can be taken outside the integral sign. Then, instead of (8.11) we obtain

$$\int k_\nu d\nu = \frac{h\nu_0}{c} B_{ik}. \tag{8.12}$$

The relation (8.12) is applicable in all cases, independently of what factors cause the shape of the function k_ν. In particular, from this relation it follows that the wider the frequency interval within which the quantity k_ν does not differ drastically from its value at the center of the line, the smaller the average value of the coefficient k_ν in this interval. /95

The frequency dependence of the absorption coefficient k_ν, as already stated, depends on a number of factors. Among these, the principal ones are the following: 1) radiation damping (in terms of the classical electron theory) or the spreading of the atomic energy levels (in terms of quantum mechanics), 2) Doppler effect, occurring due to the thermal motion of the atoms.

Let us first assume that the absorption coefficient is determined by radiation damping only. In this case, according to quantum radiation theory (see, for example, [1]), we have

$$k_\nu = \frac{c^2}{32\pi^3\nu_0^2}\frac{g_k}{g_i}\frac{A_{ki}\Gamma_{ik}}{(\nu-\nu_0)^2+\left(\frac{\Gamma_{ik}}{4\pi}\right)^2}, \tag{8.13}$$

where $\Gamma_{ik} = \gamma_i + \gamma_k$, and the quantity γ_k is given by Eq. (8.8). Let us denote the distance from the center of the line at which the value of k_ν amounts to one-half the maximum value $k_{\nu 0}$ by $\Delta\nu_E$. Obviously, $\Delta\nu_E = \Gamma_{ik}/4\pi$. The quantity $2\Delta\nu_E$ is called the natural spectral line width. From the width, expressed in frequencies, we can convert to width, expressed in wavelengths, by using the formula $\Delta\lambda_E = \lambda_0\Delta\nu_E/\nu_0$. The natural line width, expressed in wavelength, is of the order of 0.001 Å.

We will now consider that the frequency dependence of k_ν is determined only by the thermal motion of the atoms. In this case the expression for k_ν can be derived very easily. If a stationary atom absorbs photons with frequency ν_0, then a moving atom absorbs photons with frequency $\nu = \nu_0 + \nu_0 v_x/c$, where v_x is the atom velocity projected along the radiation direction (x-axis). We will assume tnat the velocity distribution of the atoms is given by Maxwell's equation, i.e., the number of atoms with velocities from v_x to $v_x + dv_x$ is equal to

$$dn \sim e^{-\frac{Mv_x^2}{2kT}}dv_x, \tag{8.14}$$

where M is the atomic mass. Obviously the probability of absorption of photons with frequencies from ν to $\nu + d\nu$ is proportional to the number of atoms with

velocities from v_x to $v_x + dv_x$. Therefore, for the absorption coefficient we have /96

$$k_\nu = k_0 e^{-\frac{M}{2kT}\left(\frac{\nu-\nu_0}{\nu_0}c\right)^2}, \tag{8.15}$$

where k_0 is the value of k_ν at the center of the line.

We do not yet know the value of k_0; however, in all cases, when the line absorption coefficient is known to within a constant factor, this factor can be found with the aid of Eq. (8.12). Substituting (8.15) into (8.12), we obtain

$$k_0 = \frac{c^3}{8\pi^{3/2}\nu_0^3 v}\frac{g_k}{g_i}A_{ki}. \tag{8.16}$$

Equation (8.15) can be rewritten in the form

$$k_\nu = k_0 e^{-\left(\frac{\nu-\nu_0}{\Delta\nu_D}\right)^2}, \tag{8.17}$$

where $\Delta\nu_D = \nu_0 v/c$ and v is the average thermal velocity of an atom, equal to $v = \sqrt{2kT/M}$. The quantity $2\Delta\nu_D$ is called the Doppler spectral line width. The Doppler width, expressed in wavelength, is of the order of 0.1 Å (for an average atom velocity of about 1 km/sec). Consequently, the Doppler width is much greater than the natural width.

It is easy to derive that the absorption coefficient, when radiation damping and Doppler effect are acting concurrently, is equal to

$$k_\nu = k_0\frac{a}{\pi}\int_{-\infty}^{+\infty}\frac{e^{-y^2}dy}{(u+y)^2+a^2}, \tag{8.18}$$

where

$$u = \frac{\nu-\nu_0}{\Delta\nu_D}, \quad a = \frac{\Delta\nu_E}{\Delta\nu_D} \tag{8.19}$$

and k_0 is given by Eq. (8.16).

Introducing the notation $k_\nu/k_0 = H(u, a)$, we have

$$H(u, a) = \frac{a}{\pi}\int_{-\infty}^{+\infty}\frac{e^{-y^2}dy}{(u+y)^2+a^2}. \tag{8.20}$$

The function H(u, a) plays a very important role in the theory of stellar line spectra and, therefore, it has been investigated and tabulated.

Because the quantity a is usually very small, it is convenient to expand the function H(u, a) in a power series of a, i.e., to represent it in the form /97

$$H(u, a) = H_0(u) + aH_1(u) + a^2H_2(u) + \ldots \tag{8.21}$$

It turns out that

$$H_0(u) = e^{-u^2}, \tag{8.22}$$

$$H_1(u) = -\frac{2}{\sqrt{\pi}}\left[1 - 2ue^{-u^2}\int_0^u e^{t^2}\,dt\right] \tag{8.23}$$

and so forth. Values of the functions $H_0(u)$, $H_1(u)$ and $H_2(u)$ are listed in Table 6 for some values of u. Detailed tables of the functions $H_i(u)$ have been given by Garrison [2].

TABLE 6. VALUES OF THE FUNCTIONS $H_0(u)$, $H_1(u)$ AND $H_2(u)$

u	$H_0(u)$	$H_1(u)$	$H_2(u)$	u	$H_0(u)$	$H_1(u)$	$H_2(u)$
0	1,0000	−1,1284	+1,0000	1,6	0,0773	+0,3157	−0,3185
0,2	0,9608	−1,0405	+0,8839	1,8	0,0392	+0,2803	−0,2146
0,4	0,2521	−0,8035	+0,5795	2,0	0,0183	+0,2317	−0,1232
0,6	0,6977	−0,4855	+0,1953	2,2	0,0079	+0,1849	−0,0636
0,8	0,5273	−0,1672	−0,1476	2,4	0,0032	+0,1461	−0,0[illegible]2
1,0	0,3679	+0,0859	−0,3679	2,6	0,0012	+0,1165	−0,0[illegible]45
1,2	0,2369	+0,2454	−0,4454	2,8	0,0004	+0,0947	−0,0058
1,4	0,1409	+0,3139	−0,4113	3,0	0,0001	+0,0786	−0,0021

Commas represent decimal points.

With the approximation that $a \ll 1$ in the central portions of the line, the absorption coefficient is equal to

$$k_\nu = k_0 e^{-u^2}. \tag{8.24}$$

For regions far from the center of the line, from Eq. (8.18) we obtain

$$k_\nu = k_0 \frac{a}{\sqrt{\pi}} \frac{1}{u^2}. \tag{8.25}$$

The transition region between the regions where Eqs. (8.24) and (8.25) are applicable is found from the condition that the values of k_ν, given by these formulas, are of the same order in it.

It is easy to see that Eq. (8.24) is identical to (8.17) and Eq. (8.25)—to (8.13) (if, in the latter, $\Gamma_{ik}/4\pi$ is neglected in comparison with $|\nu-\nu_0|$). Consequently, near the center of the line the absorption coefficient is determined by the Doppler effect, and far from it—by radiation damping. /98

3. Pressure effects. In the derivation of Eq. (8.18) only the natural spreading of atomic energy levels and the thermal motion of the atom were taken into consideration. However, the presence of foreign particles also exerts considerable influence on the form of the k_ν function. We will call this influence pressure effects (since this effect is greater, the higher the pressure).

The simplest aspect of pressure effects is the collision of an atom with a foreign particle, whereby the excitation energy of the atom is transferred to the particle (collision of the second kind). Because of such collisions the average lifetime of an atom in an excited state will be less than that determined from Eq. (8.9), and the energy level spreading—correspondingly greater. The latter comes about because of the Heisenberg uncertainty principle, according to which $\Delta E \Delta t \simeq h$. With collisions taken into consideration, the average lifetime of an atom in an excited state is now given by

$$\bar{t}_k = \frac{1}{\gamma_k + \gamma_c}, \tag{8.26}$$

instead of by Eq. (8.9), where γ_c is the number of collisions in 1 sec, computed for one excited atom.

With collisions taken into consideration, the absorption coefficient will again be determined by Eq. (8.18) in which a will become the quantity

$$a = \frac{\Delta\nu_E + \Delta\nu_c}{\Delta\nu_D}, \tag{8.27}$$

where $\Delta\nu_c$ is the half-width due to collisions (i.e., corresponding to the quantity γ_c).

However, it is not just collisions of the second kind that influence the absorption coefficient. The passage of foreign particles near the atom produces a much greater effect on it. Under such conditions the high field near the atom is altered, leading to a displacement of the energy levels. It is obvious that this displacement of the levels of a given atom changes with time, and for a specific instant of time the levels of the various atoms are displaced a different amount. Therefore this effect gives rise to a broadening of the spectral lines.

The problem of determining the absorption coefficient is very complex when the passage of foreign particles near the atom is taken into consideration (see [3]). To solve it, one must take into consideration both the different types of atoms (neutral and ionized) as well as different types of foreign particles (free /99
electrons, ions, neutral atoms, molecules). It is usually assumed that if the

foreign particle is at a distance r from the atom, then the frequency is shifted by an amount

$$\Delta\nu = \frac{C_k}{r^k}, \tag{8.28}$$

where k and C_k are some constants, different for different cases. When a charged particle passes near the atom, k = 2 or K = 4 (linear and quadratic Stark effect, respectively). If the atoms being considered encounter atoms that are similar to them, then k = 3 (intrinsic pressure effect). For encounters of atoms with atoms of other elements or with molecules, k = 6 (van der Waals force effect). The constant C_k for each case is determined from theoretical considerations or experimentally.

Two methods have been developed for determining the absorption coefficient for a specified interaction law between the atoms and the foreign particles. The first of these consists of treating the encounter of the atoms with the particles on an individual basis, and then summing the results of the encounters (discrete encounter method). The second method is based on a determination of the field intensity probability for a random distribution of perturbing particles, which are considered to be at rest (statistical theory).

When the first method is used, the atom is usually replaced by a classical oscillator and it is assumed that each encounter of an atom with a particle leads to a change in the oscillation phase. The computation of the phase change is done for encounters with arbitrary impact parameters with Eq. (8.28) taken into consideration. A Fourier series expansion of the oscillation with a rapidly changing phase leads to an expression for the absorption coefficient, analogous to Eq. (8.13). When the thermal motion of the atoms is also taken into account, Eq. (8.18), in which the quantity a is given by Eq. (8.27) and $\Delta\nu_c = \gamma_c/4\pi$, is obtained for the absorption coefficient. A calculation of the quantity γ_c by the method given led to the following results for the different cases:

$$\gamma_c = 4\pi^3 C_3 n \qquad (\text{for } k = 3), \tag{8.29}$$

$$\gamma_c = 38.8 C_4^{2/3} v^{1/3} n \quad (\text{for } k = 4), \tag{8.30}$$

$$\gamma_c = 17.0 C_6^{2/5} v^{3/5} n \qquad (\text{for } k = 6). \tag{8.31}$$

In these formulas v is the average relative velocity of the atom and perturbing particle, and n is the number of particles in 1 cm^3.

Thus, in the approximate theory that has been assumed, the close approach of perturbing particles to an atom affects the absorption coefficient in the same manner as collisions of the second kind. Moreover, this effect is similar to the radiation damping effect. Therefore the quantity γ_c is usually called the damping constant due to collisions. /100

The statistical theory is very simple, if it is assumed that only particles very close to the atom cause a perturbation. Such an approximation can be made because the perturbations of remote particles compensate each other to some extent. Let us denote the probability that a particle is at a distance from r to r + + dr from the atom by $W_1(r)dr$. As it is easy to show,

$$W_1(r)\,dr = e^{-(r/r_0)^3}\,d\left(\frac{r}{r_0}\right)^3, \tag{8.32}$$

where r_0 is the average distance between particles, defined by the relation

$$\frac{4}{3}\pi r_0^3 n = 1. \tag{8.33}$$

From the probability $W_1(r)dr$ we can, with the aid of Eq. (8.28), go over to the probability of different frequency shifts. Since the absorption coefficient k_ν is proportional to this probability, we obtain

$$k_\nu \sim \frac{C_k^{3/k} n}{(\Delta\nu)^{\frac{3+k}{k}}}\, e^{-\frac{4}{3}\pi n\left(\frac{C_k}{\Delta\nu}\right)^{3/k}}. \tag{8.34}$$

Equation (8.34) obviously cannot be considered valid for small values of $\Delta\nu$ since small perturbations are caused primarily by remote particles. Large perturbations, however, are caused by the near particles. Therefore Eq. (8.34) can be used for large values of $\Delta\nu$. In the given case, by replacing the exponential factor in Eq. (8.34) by unity (this is possible when $r \ll r_0$), we find

$$k_\nu \sim \frac{C_k^{3/k} n}{(\nu - \nu_0)^{\frac{3+k}{k}}}. \tag{8.35}$$

Equation (8.35) gives an asymptotic expression for the absorption coefficient in the line wings.

Of course, both theories considered would give indentical results if they were precise. In both theories, however, simplifying assumptions are made so that each of them has a region of applicability. A study of this problem has shown that the discrete encounter method gives valid results for the central portions of the line, and the statistical method—for the outer portions. In other words, in the central portions of the line the absorption coefficient is determined by Eq. (8.18) with appropriate values of a and γ_c, and in the outer portions of the line—by Eq. (8.35) (which, as already stated, is valid for only these portions). /101

The boundary between the regions of applicability of the expressions for k_ν presented above depends both on the type of interaction between the atoms and

perturbing particles, and on the physical conditions in the stellar atmosphere (it turns out that this boundary is farther from the line center, the greater the concentration of perturbing particles and the lower the average relative velocity of the particle and atom).

In stellar atmospheres different types of perturbing particles are present, and they all exert some influence on the absorption coefficient in a given line. Usually one kind of particle causes the major effect in the central portions of the line; in the outer portions—it is another kind. However, with a change in depth in the atmosphere the relative role of the different particles is altered. Of course, a change also occurs in the relative role of the particles when other lines and other types of atmospheres are considered. Therefore it is a rather difficult task to take proper account of the effect of foreign particles (i.e., of pressure effects) on the spectral line absorption coefficient.

4. Stark effect. The presence of charged particles (ions and free electrons) near the absorbing atoms exerts an especially large influence on the absorption coefficient. In the electric field, created by these particles, a shift occurs in the atomic energy levels, i.e., the Stark effect occurs. It is obvious that the level shift in different atoms at a given instant of time is different so that the spectral line is broadened. As is known, the linear and quadratic Stark effects are different. In the first case the level shift is proportional to the first power of the field intensity, in the second—to its square. Corresponding to these two cases, in Eq. (8.28), defining the level displacement, $k = 2$ and $k = 4$ (since the field intensity is proportional to r^{-2}.

Let us now consider (in more detail than before) the linear Stark effect, which occurs in hydrogen levels and the upper helium levels. First of all, we will assume that the perturbing particles are ions. Since the thermal velocities /102 of ions are relatively low, then in this case one can use the statistical (or, as it is sometimes called, the static) theory.

Above, an expression was derived for k_ν under the assumption that perturbation is produced only by particles near the atom. Now let us take into consideration all particles, which we will assume to be randomly distributed in space.

Let F be the intensity of the field created by a particle at a distance r from the atom, i.e.,

$$F = \frac{e}{r^2}, \tag{8.36}$$

and F_0 be the "average" field intensity, corresponding to the value r_0, defined by Eq. (8.33), i.e.,

$$F_0 = \frac{e}{r_0^2} = \left(\frac{4\pi}{3}\right)^{2/3} e n^{2/3} = 2.60 e n^{2/3}. \tag{8.37}$$

We will denote by β the quantity F/F_0, and by $W(\beta)d\beta$—the probability that this quantity lies within the interval from β to $\beta + d\beta$.

The function $W(\beta)$, when the effect of all particles is taken into consideration, was first determined by Holtsmark [4]. It is given by the formula

$$W(\beta) = \frac{2}{\pi\beta}\int_0^\infty x \sin x e^{-\left(\frac{x}{\beta}\right)^{3/2}} dx. \tag{8.38}$$

When $\beta \gg 1$, from (8.38) we obtain

$$W(\beta) = 1{,}496\beta^{-5/2}(1 + 5.106\beta^{-3/2} + 14{,}43\beta^{-3} + \ldots), \tag{8.39}$$

and when $\beta \ll 1$:

$$W(\beta) = \frac{4}{3\pi}\beta^2(1 - 0.4628\beta^2 + 0.1227\beta^4 + \ldots). \tag{8.40}$$

Values of the Holtsmark function are given in Table 7.

TABLE 7. THE HOLTSMARK FUNCTION

β	$W(\beta)$	β	$W(\beta)$	β	$W(\beta)$	β	$W(\beta)$	β	$W(\beta)$	β	$W(\beta)$
0	0	1,6	0,367	3,0	0,176	4,6	0,0573	6,0	0,0242	8,5	0,0087
0,2	0,017	1,8	0,360	3,2	0,150	4,8	0,0494	6,2	0,0219	9,0	0,0075
0,4	0,063	2,0	0,339	3,4	0,128	5,0	0,0431	6,4	0,0199	10,0	0,0056
0,6	0,130	2,2	0,310	3,6	0,111	5,2	0,0379	6,6	0,0181	15,0	0,00188
0,8	0,203	2,4	0,275	3,8	0,098	5,4	0,0336	6,8	0,0166	20,0	0,00089
1,0	0,271	2,6	0,238	4,0	0,086	5,6	0,0299	7,0	0,0153	25,0	0,00050
1,2	0,324	2,8	0,206	4,2	0,075	5,8	0,0268	7,5	0,0125	30,0	0,00031
1,4	0,356			4,4	0,065			8,0	0,0104		

Commas represent decimal points.

If we were to consider only the effect of the nearest particles, then, using Eq. (8.32) and the fact that $\beta = (r_0/r)^2$, we would obtain

$$W(\beta) = \frac{3}{2} e^{-\beta^{-3/2}} \beta^{-5/2}. \tag{8.41}$$

When $\beta \gg 1$, Eq. (8.41) gives almost the same $W(\beta)$ values as Eq. (8.38). This is explained by the fact that the higher field intensities are caused primarily by the nearest particles.

After determination of the $W(\beta)$ function, the absorption coefficient k_ν can be found without difficulty. The quantity β can obviously be represented in the form $\beta = (\nu-\nu_0)/(\Delta\nu)_0$, where $(\Delta\nu)_0$ is the line displacement for the field intensity F_0. Therefore the probability of absorption of photons with frequencies from ν to $\nu + d\nu$ will be equal to $W[(\nu-\nu_0)/\Delta\nu)_0]\,[d\nu/(\Delta\nu)_0]$. In actuality, however, a line in an electric field is split into several components. Let us denote by I_j the relative strength of the j-th component and by b_j—the displacement of this component for a unit field intensity (consequently, $(\Delta\nu)_0 = b_j F_0$). Then for the absorption coefficient we obtain /103

$$k_\nu \sim \sum \frac{I_j}{b_j F_0} W\left(\frac{\nu-\nu_0}{b_j F_0}\right). \tag{8.42}$$

As is known (see, for example, [3]),

$$b_j = \frac{3h}{8\pi^2 me} n_j, \tag{8.43}$$

where m and e are the electron mass and charge, n_j is a whole number, depending on the initial and final levels.

In order to completely determine k_ν, we use, as is usually done in such cases, Eq. (8.11). As a result we find

$$k_\nu = \frac{h\nu_0}{c} B_{ik} \sum \frac{I_j}{b_j F_0} W\left(\frac{\nu-\nu_0}{b_j F_0}\right). \tag{8.44}$$

The behavior of the absorption coefficient in portions of the line far from the center is of most interest. In this case, taking for $W(\beta)$ only the first term in Eq. (8.39), we have /104

$$k_\nu = \frac{h\nu_0}{c} B_{ik} \frac{1.496 F_0^{3/2}}{(\nu-\nu_0)^{3/2}} \sum I_j b_j^{3/2}. \tag{8.45}$$

This formula, as it should, exactly corresponds to Eq. (8.35) for k = 2.

Let us convert from frequency ν to wavelength λ in Eq. (8.45) and write it in the form

$$k_\lambda = C \frac{F_0^{3/2}}{(\lambda-\lambda_0)^{3/2}}, \tag{8.46}$$

where C is a constant that is different for different lines. For the Balmer lines, computations gave $C = 3.13 \cdot 10^{-16}$ for H_α, $0.885 \cdot 10^{-16}$ for H_β, $0.442 \cdot 10^{-16}$ for H_γ and $0.309 \cdot 10^{-16}$ for H_δ, with $\lambda - \lambda_0$ being expressed in angstroms.

It should be emphasized that the quantity F_0 entering into Eq. (8.46) represents the "average" intensity of the field caused by the ions. Substituting (8.37) into (8.46), we obtain

$$k_\lambda = \frac{4\pi}{3} C \frac{e^{3/2} n}{(\lambda - \lambda_0)^{5/2}}, \tag{8.47}$$

where n is the number of ions in 1 cm^3. We see that in the wings of the hydrogen lines the absorption coefficient is greater, the higher the ion concentration. Therefore one can expect broad hydrogen absorption lines in the spectra of stars with high densities in their atmospheres (especially in the spectra of white dwarfs).

From Eq. (8.47) it is also seen that in the outer portions of the lines the absorption coefficient, caused by the Stark effect, decreases as $(\lambda - \lambda_0)^{-5/2}$. In this it differs significantly from the absorption coefficient, caused by damping, which decreases as $(\lambda - \lambda_0)^{-2}$.

Let us now consider the question of what influence the Stark effect, produced by free electrons, has on the absorption coefficient. In this case the method of discrete encounters can be used because of the high velocities of the free electrons. It leads to the absorption coefficient, given by Eq. (8.18) with the appropriate collisional damping constant. It turns out that this expression for k_λ is valid out to a very great distance from the line center. Let us denote this limiting distance by $\Delta\lambda_g$. Values of the quantity $\Delta\lambda_g$ (expressed in angstroms), taken from Unsold's paper [2], are given in Table 8 for some of the Balmer lines. Values of $\Delta\lambda_g$ for the proton-caused Stark effect are given in the same table for comparison. We see that in the latter case the $\Delta\lambda_g$ values are very small. For $\lambda - \lambda_0$ values exceeding $\Delta\lambda_g$, the expression for K_λ, given by the statistical theory, should be used. /105

Calculations, made by the method discussed, led to the conclusion that the absorption coefficient, caused by electrons, is considerably smaller than the absorption coefficient caused by protons. Therefore, the effect of electrons on the absorption coefficient was disregarded. Subsequently, however, it was established that experiment does not corroborate the theory based only on the effect of protons being considered. In view of this, a number of investigations have recently been performed in which the simultaneous effect of protons and electrons on a hydrogen atom has been examined. Moreover, the nonadiabatic effects, involved in in transitions between the components into which the energy level is split in an electric field, were taken into consideration (this had not been done previously).

TABLE 8. VALUES OF THE QUANTITY $\Delta\lambda_g$ FOR THE BALMER LINES

T		25 000°	10 000°	5000°	3000°
H_α	electrons	250	230	110	70
	protons	0,63	0,25	0,12	0,08
H_β	electrons	120	48	24	14
	protons	0,13	0,05	0,03	0,02
H_γ	electrons	48	19	9	6
	protons	0,05	0,02	0,01	0,006
H_δ	electrons	32	13	6	4
	protons	0,03	0,01	0,007	0,004

Commas represent decimal points.

As a result it was shown that the effect of electrons on the absorption coefficient is significant (see, for example, [5]).

According to the results obtained, the absorption coefficient in the wings of the hydrogen lines is represented in the form

$$k_\lambda = C \frac{F_0^{3/2}}{(\lambda - \lambda_0)^{5/2}} [1 + R(n_e, T)(\lambda - \lambda_0)^{1/2}], \tag{8.48}$$

where the factor in front of the square brackets is the absorption coefficient caused by protons, and the second term in the brackets takes account of the effect of electrons. Values of the quantity $R(n_e, T)$ for three Balmer lines are given in Table 9 for different values of the electron density n_e and temperature T (it is assumed that $\lambda - \lambda_0$ is expressed in angstroms). /106

It should be noted that these theoretical results agree well with experimental data.

9. Absorption Lines in Presence of Local Thermodynamic Equilibrium

1. Basic formulas. After the determination of the spectral line absorption coefficient, let us pass on to the problem of the formation of absorption lines in the stellar spectrum. We will consider the line arising from a transition from the i-th state into the k-th of a given atom. We will denote, as before, the line absorption coefficient by σ_ν, and the emission coefficient—by ε_ν. These quantities depend on the indices i and k, but for simplicity of notation we will omit them. Let us denote the continuous spectrum absorption and emission coefficients by α_ν and ε_ν^0, respectively. These quantities are caused by all the atoms in a given volume

TABLE 9. VALUES OF THE QUANTITY $R(n_e, T)$

$\lg n_e$ \ T	H_α			H_β			H_γ		
	10^4	$2\cdot10^4$	$4\cdot10^4$	10^4	$2\cdot10^4$	$4\cdot10^4$	10^4	$2\cdot10^4$	$4\cdot10^4$
10	1,05	0,79	0,59	1,05	0,80	0,60	1,37	1,04	0,78
12	0,82	0,63	0,48	0,81	0,62	0,48	1,03	0,80	0,62
14	0,59	0,46	0,36	0,56	0,45	0,35	0,70	0,56	0,45
15	0,47	0,38	0,30	0,45	0,35	0,28	0,53	0,44	0,35
16	0,35	0,30	0,25	0,33	0,26	0,22	0,37	0,31	0,26
17	0,24	0,22	0,19	0,21	0,17	0,15	0,21	0,19	0,17
18	0,12	0,14	0,13	0,09	0,09	0,08	0,09	0,09	0,09

Commas represent decimal points.

element. Within the line limits the coefficients α_ν and ε_ν^0 are very slightly dependent on the frequency.

Assuming that the atmosphere consists of plane-parallel layers, we obtain the following equation of radiation transfer in a spectral line:

$$\cos\vartheta \frac{dI_\nu}{dr} = -(\sigma_\nu + \alpha_\nu) I_\nu + \varepsilon_\nu + \varepsilon_\nu^0. \tag{9.1}$$

Here, just as before, ϑ is the angle between the radiation direction and the outward normal to the atmosphere layers, and the radiation intensity I_ν depends on r and ϑ. /107

In the discussion of the continuous spectrum of stars we made an assumption concerning local thermodynamic equilibrium. In this case we have

$$\varepsilon_\nu^0 = \alpha_\nu B_\nu(T), \tag{9.2}$$

where $B_\nu(T)$ is the Planckian radiation intensity for the given line frequencies.

First of all, let us make a similar assumption in considering the formation of the spectral lines, i.e., we will assume

$$\varepsilon_\nu = \sigma_\nu B_\nu(T). \tag{9.3}$$

It is obvious that Eq. (9.3) must be applicable on a broader basis then Eq. (9.2) since, on the average, lines appear in star layers that are nearer the surface than for the continuous spectrum.

With the aid of (9.2) and (9.3), instead of Eq. (9.1) we find

$$\cos\vartheta \frac{dI_\nu}{dr} = -(\sigma_\nu + \alpha_\nu)(I_\nu - B_\nu). \tag{9.4}$$

Let t_ν be the optical depth in the atmosphere at the frequency within the line, i.e.,

$$t_\nu = \int_r^\infty (\sigma_\nu + \alpha_\nu)\, dr. \tag{9.5}$$

Then Eq. (9.4) assumes the form

$$\cos\vartheta \frac{dI_\nu(t_\nu, \vartheta)}{dt_\nu} = I_\nu(t_\nu, \vartheta) - B_\nu(T). \tag{9.6}$$

Of greatest interest to us is the intensity of the line emission emanating from the atmosphere. From Eq. (9.6) we obtain

$$I_\nu(0, \vartheta) = \int_0^\infty B_\nu(T)\, e^{-t_\nu \sec\vartheta} \sec\vartheta\, dt_\nu. \tag{9.7}$$

ıor this quantity.

The intensity of the radiation, leaving the atmosphere in the continuous spectrum in the neighborhood of the line, will be denoted by $I_\nu^0(0, \vartheta)$. This quantity is equal to /10

$$I_\nu^0(0, \vartheta) = \int_0^\infty B_\nu(T)\, e^{-\tau_\nu \sec\vartheta} \sec\vartheta\, d\tau_\nu, \tag{9.8}$$

where τ_ν is the optical depth in the atmosphere in the continuous spectrum in the neighborhood of the line, i.e.,

$$\tau_\nu = \int_r^\infty \alpha_\nu\, dr. \tag{9.9}$$

The ratio

$$r_\nu(\vartheta) = \frac{I_\nu(0, \vartheta)}{I_\nu^0(0, \vartheta)} \tag{9.10}$$

characterizes the absorption line profile at an angular distance of ϑ from the center of the stellar disk. The quantity $r_\nu(\vartheta)$ can obviously be found from observations for the Sun only (and in principle—for eclipsing variables). For conventional stars, however, only the absorption line profile in the spectrum of the entire disk is determined from observations. This profile is characterized by

the ratio

$$r_\nu = \frac{H_\nu}{H_\nu^0}, \tag{9.11}$$

where H_ν is the radiant flux emanating from the star at the frequency ν within the line and H_ν^0 is the radiant flux emanating from the star in the continuous spectrum in the neighborhood of the line. The quantity H_ν is determined by the formula

$$H_\nu = 2\pi \int_0^\infty B_\nu(T)\, E_2 t_\nu \, dt_\nu, \tag{9.12}$$

where $E_2 t_\nu$ is the second integral exponential function. The quantity H_ν^0 is determined by a similar formula (with t_ν replaced by τ_ν) (see Section 4).

If the quantity r_ν is known, then the so-called equivalent absorption line width can easily be found. The latter represents the width of the adjacent portion of the continuous spectrum whose energy is equal to the energy absorbed in the line (Fig. 11). Denoting the equivalent line width by W, on the basis of the definition we have

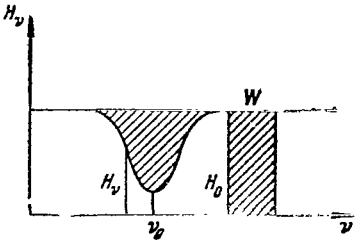

Figure 11.

$$H_\nu^0 W = \int (H_\nu^0 - H_\nu)\, d\nu, \tag{9.13}$$

or, with (9.11) used, /109

$$W = \int (1 - r_\nu)\, d\nu. \tag{9.14}$$

Below, we will make frequent use of these formulas defining the line profiles and equivalent widths.

2. Determination of line profiles. To compute the absorption line profiles we must know the relationship between the temperature T and the optical depth t_ν. The exact relationship between these quantities can be found only on the basis of a stellar photosphere model calculation. There is, however, some interest in the approximate relationship between T and t_ν, which we are now going to use.

The following approximate formula, interrelating the temperature T and the continuous spectrum optical depth τ_ν, results from Eqs. (7.1) and (7.4):

$$B_\nu(T) = B_\nu(T_0)\left(1 + \beta_\nu \frac{\bar{a}}{a_\nu}\tau_\nu\right). \tag{9.15}$$

In the derivation of this formula it was assumed that the ratio of the continuous spectrum absorption coefficient α_ν to the mean absorption coefficient $\bar{\alpha}$ does not depend on depth. Now we will assume that the ratio of the line absorption coefficient to the continuous spectrum absorption coefficient, i.e., the quantity σ_ν/α_ν, also does not depend on depth. Then, on the basis of Eqs. (9.5) and (9.9), we have

$$t_\nu = \left(\frac{\sigma_\nu}{\alpha_\nu} + 1\right)\tau_\nu. \tag{9.16}$$

Substitution of (9.16) into (9.15) yields

$$B_\nu(T) = B_\nu(T_0)\left(1 + \beta_\nu \frac{\bar{\alpha}}{\sigma_\nu + \alpha_\nu} t_\nu\right). \tag{9.17}$$

To find the quantity $r_\nu(\vartheta)$, defined by Eq. (9.10), we must substitute (9.17) /110
into (9.7) and (9.15) into (9.8). Doing this, we obtain

$$r_\nu(\vartheta) = \frac{1 + \beta_\nu \dfrac{\bar{\alpha}}{\sigma_\nu + \alpha_\nu}\cos\vartheta}{1 + \beta_\nu \dfrac{\bar{\alpha}}{\alpha_\nu}\cos\vartheta}. \tag{9.18}$$

Equation (9.18) defines the line profile at an angular distance of ϑ from the center of the disk. An expression for the quantity r_ν, characterizing the line profile in the total stellar spectrum, is obtained in a similar fashion:

$$r_\nu = \frac{1 + \dfrac{2}{3}\beta_\nu \dfrac{\bar{\alpha}}{\sigma_\nu + \alpha_\nu}}{1 + \dfrac{2}{3}\beta_\nu \dfrac{\bar{\alpha}}{\alpha_\nu}} \tag{9.19}$$

It should, however, be remembered that the approximate formulas (9.18) and (9.19) can, in some cases, be very inexact since the quantities σ_ν/α_ν and α_ν/α, which we have assumed to be constant, can vary appreciably with depth in real atmospheres.

As already stated, preliminary stellar photosphere model calculations are necessary to obtain accurate line profiles. These calculations give the temperature and density distribution in the surface layers of the star, in which the absorption lines appear. Using such data, one can compute the absorption coefficients σ_ν and α_ν at different depths, and therefore the optical depths t_ν and τ_ν, in the form of functions of the geometrical depth.

As an example of the construction of photosphere stellar models and the subsequent computation of continuous and line spectra of stars, one can cite the important work of de Jager and Neven [6]. These authors constructed 50 photosphere models with surface temperatures T_0 from 4000 to 25,000° and with lg g values from 1 to 5. For each model the continuous spectrum energy distribution was determined, and the profiles and equivalent widths of many lines (hydrogen, helium, carbon, nitrogen and other atoms) were determined. A portion of the results, referring to the H_γ line, is given in Table 10. This table, compiled for the case $T_0 = 14,000°$, contains values of the quantity r_ν at different distances from the line center (expressed in angstroms) and for different lg g values. Values of the equivalent width W, in angstroms, are given in the last column of the table. /111

TABLE 10. THE QUANTITIES r_ν AND W FOR THE H_γ LINE FOR DIFFERENT GRAVITATIONAL FORCES IN A STELLAR ATMOSPHERE

lg g \ Δλ	0	0,5	1	2	4	8	16	32	W
1	0,70	0,74	0,92	0,97	1,00				0,60
2	0,72	0,76	0,84	0,92	0,99	1,00			0,90
3	0,74	0,78	0,81	0,86	0,91	0,96	1,00		2,05
4	0,75	0,76	0,77	0,80	0,86	0,93	0,98	1,00	3,50
5	0,78	0,79	0,81	0,83	0,86	0,90	0,95	1,00	4,20

Commas represent decimal points.

In calculating the H_γ line profile, the absorption coefficient expression, taking the Stark effect into consideration, was chosen. As is known, this effect is greater, the greater the density; and the density in the atmosphere is greater, the greater the gravitational force. This is demonstarted by the fact that the equivalent line width W increases with an increase in g.

3. Weak lines and wings of strong lines. The formulas given above, which determine the absorption line profiles, are greatly simplified in the case of weak lines, i.e., those for which $\sigma_\nu \ll \alpha_\nu$. This inequality is obviously also valid for the outer portions of strong lines (which are usually called the line wings). Therefore the simplification of the formula for r_ν will also apply to them.

Let us consider any line in the total stellar spectrum. When the condition $\sigma_\nu \ll \alpha_\nu$ is satisfied, Eq. (9.19) can be rewritten in the form

$$1 - r_\nu = \frac{\beta_\nu}{\frac{3}{2}\frac{\alpha_\nu}{\bar{\alpha}} + \beta_\nu} \frac{\sigma_\nu}{\alpha_\nu}. \tag{9.20}$$

We see that in the given case the quantity $1-r_\nu$ is proportional to the line absorption coefficient σ_ν. The coefficient in front of σ_ν can be considered to be frequency independent.

In the foregoing paragraph expressions were derived for the absorption coefficient in the outer portions of the line. Using these expressions and Eq. (9.20), one can determine the quantity $1-r_\nu$ in the wings of strong lines. In particular, if σ_ν is determined by radiation damping, then /112

$$1-r_\lambda=\frac{D_1}{(\Delta\lambda)^2}, \tag{9.21}$$

and if σ_ν is determined by the Stark effect, then

$$1-r_\lambda=\frac{D_2}{(\Delta\lambda)^{3/2}}, \tag{9.22}$$

where D_1 and D_2 are some constants. It must, however, be remembered that only the effect of protons is taken into consideration in Eq. (9.22). If, however, the effect of electrons is also taken into account, then, as one can conclude on the basis of Eq. (8.48) for the absorption coefficient, in sufficiently remote line wings the quantity $1-r_\lambda$ is again given by Eq. (9.21) (with, of course, another value for the constant D_1). The value of $\Delta\lambda$, at which it is necessary to switch from one formula for $1-r_\lambda$ to the other in the case of the influence of the Stark effect, depends on the electron density and temperature.

Equation (9.20) is approximate since it is based on the approximate formula (9.15) and on the assumption that the quantity σ_ν/α_ν does not change in the atmosphere. When the inequality $\sigma_\nu \ll \alpha_\nu$ is satisfied, however, one can obtain a simplified formula for r_ν without making these assumptions.

On the basis of Eqs. (9.11) and (9.12) we have

$$r_\nu=\frac{\int_0^\infty B_\nu(T)\,E_2 t_\nu\,dt_\nu}{\int_0^\infty B_\nu(T)\,E_2 \tau_\nu\,d\tau_\nu} \tag{9.23}$$

Let us examine the numerator of this expression. Making use of the equation

$$dt_\nu=\left(\frac{\sigma_\nu}{\alpha_\nu}+1\right)d\tau_\nu$$

we can represent it in the form of a sum:

$$\int_0^\infty B_\nu(T)\,\mathrm{E}_2\,t_\nu\,dt_\nu = \int_0^\infty B_\nu(T)\,\mathrm{E}_2\,t_\nu\,d\tau_\nu + \int_0^\infty B_\nu(T)\,\mathrm{E}_2 t_\nu \frac{\sigma_\nu}{\alpha_\nu}\,d\tau_\nu. \tag{9.24}$$

For the first term we find /113

$$\int_0^\infty B_\nu(T)\,\mathrm{E}_2\,t_\nu\,d\tau_\nu = \int_1^\infty \frac{dz}{z^2}\int_0^\infty B_\nu(T)\,e^{-t_\nu z}\,d\tau_\nu =$$

$$= -\int_1^\infty \frac{dz}{z^2}\int_0^\infty e^{-(t_\nu-\tau_\nu)z}\,d\tau_\nu \frac{d}{d\tau_\nu}\int_{\tau_\nu}^\infty B_\nu(T')\,e^{-\tau_\nu' z}\,d\tau_\nu' =$$

$$= \int_0^\infty B_\nu(T)\,\mathrm{E}_2\,\tau_\nu\,d\tau_\nu - \int_0^\infty \frac{\sigma_\nu}{\alpha_\nu}\,d\tau_\nu \int_{\tau_\nu}^\infty B_\nu(T')\,\mathrm{E}_1\tau_\nu'\,d\tau_\nu' \tag{9.25}$$

(integration by parts is used here). In the second term, however, when $\sigma_\nu \ll \alpha_\nu$, one can simply replace t_ν by τ_ν. Therefore, instead of the relation (9.24) we obtain

$$\int_0^\infty B_\nu(T)\,\mathrm{E}_2 t_\nu\,dt_\nu = \int_0^\infty B_\nu(T)\,\mathrm{E}_2\tau_\nu\,d\tau_\nu -$$

$$- \int_0^\infty \frac{\sigma_\nu}{\alpha_\nu}\,d\tau_\nu \left[\int_{\tau_\nu}^\infty B_\nu(T')\,\mathrm{E}_1\tau_\nu'\,d\tau_\nu' - B_\nu(T)\,\mathrm{E}_2\tau_\nu\right]. \tag{9.26}$$

Substitution of (9.26) into (9.23) yields

$$1 - r_\nu = \int_0^\infty \frac{\sigma_\nu}{\alpha_\nu}\,G(\tau_\nu)\,d\tau_\nu, \tag{9.27}$$

where

$$G(\tau_\nu) = \frac{\int_{\tau_\nu}^\infty B_\nu(T)\,\mathrm{E}_1\tau_\nu\,d\tau_\nu - B_\nu(T)\,\mathrm{E}_2\tau_\nu}{\int_0^\infty B_\nu(T)\,\mathrm{E}_2\tau_\nu\,d\tau_\nu}. \tag{9.28}$$

Equation (9.28) can also be rewritten in the form

$$G(\tau_\nu) = \frac{\int_{\tau_\nu}^{\infty} \frac{dB_\nu(T)}{d\tau_\nu} E_2 \tau_\nu \, d\tau_\nu}{\int_0^{\infty} B_\nu(T) E_2 \tau_\nu \, d\tau_\nu}. \tag{9.29}$$

Thus, for the desired quantity r_ν we derived Eq. (9.27), in which the function $G(\tau_\nu)$ is given by Eq. (9.29). It is easy to see that when Eq. (9.15) is assumed for $B_\nu(T)$ and the quantity σ_ν/α_ν is assumed constant in the atmosphere, Eq. (9.27) passes over to the Eq. (9.20) given above. /114

In Eq. (9.27) the function $G(\tau_\nu)$ represents the weighting function for the quantity σ_ν/α_ν. It is advantageous to use this formula for computations because the weighting function depends only on quantities characterizing continuous spectra (but not lines), and is slightly frequency dependent. Therefore the weighting function for a given atmosphere can be tabulated beforehand and then the profiles of the different lines can be computed from Eq. (9.27).

The problem of computing the quantity r_ν for weak lines and for the wings of strong lines was first considered by Unsold (see [7]). We discussed above the "weighting function method", proposed by him, for the case when the local thermodynamic equilibrium assumption is made. However, this method, with various modifications, is also used in other cases.

4. Deviations from thermodynamic equilibrium. The assumption we have made concerning local thermodynamic equilibrium greatly simplifies the theory of stellar spectra. An important question arises, however, concerning to what extent this assumption is valid.

Let us turn, first of all, to a comparison of theory with observations. From Eq. (9.7) it follows that in going from the center of the disk to the edge the intensity of the continuous spectrum at the edge of the disk, i.e.,

$$I_\nu(0, \vartheta) \to B_\nu(T_0) \quad \text{as} \quad \vartheta \to \frac{\pi}{2}. \tag{9.30}$$

In other words, the absorption lines should disappear at the edge of the disk. This is seen especially clearly from Eq. (9.18), from which it follows that $r_\nu(\vartheta) \to 1$ as $\vartheta \to \pi/2$.

However, observational data on the variation of line profiles at the Sun's disk show that in actuality the lines do not disappear at the edge of the disk.

It is easy to understand what gives rise to this discrepancy between theory and observations. In the deep atmosphere layers atom excitation occurs primarily as a result of collisional effects. Because of the Maxwellian velocity distribution of the particles, a Boltzmann distribution of excited atomic levels is established. This, in turn, leads to the fact that the ratio of the emission coefficient ε_ν to the absorption coefficient α_ν will be equal to the Planckian intensity for a temperature equal to the kinetic temperature of the gas. Thus, one can assume local thermodynamic equilibrium exists in the deep atmosphere layers. However, as one passes to the shallower layers, the role of collisions in atom excitation decreases, and in the uppermost layers excitation is produced primarily by radiation. Because, however, the density of this radiation differs drastically from the Planckian density, the distribution of atomic states will no longer be determined by the Boltzmann equation. Therefore the Kirchhoff-Planck law will not be obeyed. /115

Thus, appreciable deviations from local thermodynamic equilibrium should exist in the upper atmosphere layers. This also explains why the line profiles computed under the assumption of the existance of local thermodynamic equilibrium do not agree with the observed line profiles.

From what has been said it follows that in solving the problem of the formation of absorption lines in stellar spectra the line emission coefficient ε_ν cannot be specified by Eq. (9.3), and it must be determined in the course of solving the problem itself. More precisely, the determination of absorption line profiles must be based on a concentration of radiation diffusion in the spectral lines. This we will do in the following paragraphs. For the present, however, let us note that a rigorous solution of the problem of stellar line spectra formation involves considerable difficulty. Therefore, the formulas given above, based on the assumption of local thermodynamic equilibrium, are nevertheless often used for line profile calculations. This approximation can, evidently, be made for weak lines arising in relatively deep atmosphere layers.

Let us mention again that the problem of deviations from thermodynamic equilibrium in stellar atmospheres has been examined in many investigations (see Bohm's paper in [8]). Here, different aspects of this problem were studied: 1) deviations from a Maxwellian particle velocity distribution, 2) deviations from a Boltzmann atomic energy level distribution, 3) deviations from the distribution of atomic ionization states given by the Saha formula. Here, however, we cannot dwell on these investigations. Let us only mention that the fully detailed explanation of this problem is just as difficult as a rigorous solution of the problem of stellar spectra formation.

10. Absorption Lines in Presence of Coherent Scattering /116

1. Schwarzschild-Schuster model. In the foregoing paragraph we made an assumption concerning local thermodynamic equilibrium in stellar atmospheres and, in accordance with this, Eq. (9.3) was used for the line emission coefficient ε_ν. This assumption, however, is not corroborated by observations and, therefore, we must consider the actual physical processes which give rise to the quantity ε_ν. As already stated, atom excitation in the outer layers of stars is

caused primarily by radiation. Consequently, the energy, radiated by any volume, depends on the radiation energy absorbed by this volume. Therefore, in order to write an expression for ε_ν one must know the fraction of energy, radiated at frequency ν within a given line, of the total amount of absorbed radiant energy.

To determine the quantity ε_ν let us first make the following two assumptions:

1. We will assume that the amount of energy, emitted by a volume element in a given line, is exactly equal to the amount of energy absorbed by this volume in the same line, i.e., there is no energy redistribution between lines and, also, there are no other processes leading to the appearance or disappearance of quanta in the line being considered. In such a case one speaks of pure radiation scattering in the spectral line.

2. We will assume that the energy, absorbed by a volume element at a given frequency within the line, is radiated by it at exactly the same frequency, i.e., there is no frequency redistribution of the radiation within the line. This process is called coherent radiation scattering.

These assumptions were made as long ago as in the first papers on the theory of stellar spectra and have been used for a long time. Subsequently, it was ascertained that they are far from being realistic. This led to different refinements of the theory, which we will discuss later.

From the assumptions made it follows that each volume element radiates as much energy at a given frequency within the line as it absorbs. Thus, we assume that a monochromatic radiative equilibrium is achieved in the stellar atmosphere. The equation, expressing this equilibrium, is obviously written thus:

$$4\pi\varepsilon_\nu = \sigma_\nu \int I_\nu d\omega, \tag{10.1}$$

where the integration is done over all solid angles.

As already stated in the introduction to this chapter, an abrupt boundary /117
between photosphere and atmosphere was initially assumed to exist in the theory of stellar spectra. In this it was assumed that no absorption lines are present in the radiation coming from the photosphere, and these lines appear as the radiation passes through the atmosphere. This model of the outer layers of a star is called the Schwarzschild-Schuster model.

Using this model, we must set the continuous spectrum absorption and emission coefficients equal to zero in the radiative transfer Eq. (9.1). In this case the radiative transfer equation assumes the form

$$\cos\vartheta \frac{dI_\nu}{dr} = -\sigma_\nu I_\nu + \varepsilon_\nu. \tag{10.2}$$

Let us introduce the optical depth at frequency ν

$$t_\nu = \int_r^\infty \sigma_\nu \, dr \tag{10.3}$$

and let us designate

$$\varepsilon_\nu = \sigma_\nu S_\nu. \tag{10.4}$$

Then, instead of Eqs. (10.1) and (10.2), we obtain

$$\left.\begin{aligned} \cos\vartheta \frac{dI_\nu(t_\nu, \vartheta)}{dt_\nu} &= I_\nu(t_\nu, \vartheta) - S_\nu(t_\nu), \\ S_\nu(t_\nu) &= \frac{1}{2}\int_0^\pi I_\nu(t_\nu, \vartheta)\sin\vartheta \, d\vartheta. \end{aligned}\right\} \tag{10.5}$$

Let us note that Eqs. (10.5) are formally no different from Eqs. (2.8) in photosphere theory. The Eqs. (2.8), however, refer to the integrated radiation, and Eqs. (10.5)—to radiation of a definite frequency ν within the line.

Boundary conditions must be added to the system of Eqs. (10.5). The condition at the upper limit of the atmosphere (for $t_\nu = 0$) expresses the absence of radiation incident on the star from the outside:

$$I_\nu(0, \vartheta) = 0 \quad \text{for} \quad \vartheta > \frac{\pi}{2}. \tag{10.6}$$

The condition at the lower limit of the atmosphere (for $t_\nu = t_\nu^0$) must express the intensity of the radiation, entering the atmosphere from the photosphere, is given and is equal to the continuous spectrum intensity at frequency ν (obviously, one can consider it equal to the intensity of the radiation emanating from the atmosphere in the vicinity of the line). Denoting, just as before, this intensity by $I_\nu^0(0, \vartheta)$, we have /118

$$I_\nu(t_\nu^0, \vartheta) = I_\nu^0(0, \vartheta) \quad \text{for} \quad \vartheta < \frac{\pi}{2}. \tag{10.7}$$

Thus, the problem consists of solving the system of Eqs. (10.5) under the boundary conditions (10.6) and (10.7).

The methods proposed in Chapter I can be used to solve the system of equations that has been derived. Let us apply the first approximation method (i.e., the Schwarzschild-Schuster method) to it.

Denoting the mean intensity of the upward directed radiation by I_ν' and the mean intensity of the downward directed radiation by I_ν'', instead of the system

of Eqs. (10.5), we obtain

$$\left.\begin{aligned} &\frac{1}{2}\frac{dI_\nu'}{dt_\nu} = I_\nu' - S_\nu, \quad -\frac{1}{2}\frac{dI_\nu''}{dt_\nu} = I_\nu'' - S_\nu, \\ &S_\nu = \frac{1}{2}(I_\nu' + I_\nu''). \end{aligned}\right\} \tag{10.8}$$

From Eqs. (10.8) it follows that

$$I_\nu' - I_\nu'' = F_\nu, \quad I_\nu' + I_\nu'' = 2F_\nu t_\nu + C_\nu, \tag{10.9}$$

where F_ν and C_ν are arbitrary constants.

In the given case the boundary conditions (10.6) and (10.7) assume the form

$$I_\nu'' = 0 \text{ for } t_\nu = 0, \quad I_\nu' = \bar{I}_\nu^0 \text{ for } t_\nu = t_\nu^0, \tag{10.10}$$

where I_ν^0 is the mean intensity of the radiation entering the atmosphere from the photosphere. With the aid of (10.10) we find

$$C_\nu = F_\nu, \quad F_\nu = \frac{\bar{I}_\nu^0}{1 + t_\nu^0}. \tag{10.11}$$

Knowing the arbitrary constants permits one to obtain the following expression for the function S_ν from Eqs. (10.8) and (10.9):

$$S_\nu = \frac{I_\nu^0}{1 + t_\nu^0}\left(\frac{1}{2} + t_\nu\right). \tag{10.12}$$

The intensity of the radiation, leaving the atmosphere, is equal to /119

$$I_\nu(0, \vartheta) = \int_0^\infty S_\nu(t_\nu) e^{-t_\nu \sec\vartheta} \sec\vartheta \, dt_\nu + I_\nu^0(0, \vartheta) e^{-t_\nu^0 \sec\vartheta}. \tag{10.13}$$

in the case being considered. If we substitute here the expression determined for S_ν and we make use of Eq. (9.10), then we obtain the desired quantity $r_\nu(\vartheta)$, characterizing the absorption line profile at an angular distance of ϑ from the center of the disk.

In order to determine the quantity r_ν, characterizing the line profile in the total stellar spectrum, one must find the radiative flux emanating from the atmosphere at frequency ν within the line and in the continuous spectrum in the neighborhood of the line. In the approximation that has been assumed, these

quantities are equal to

$$H_\nu = \pi F_\nu, \quad H_\nu^0 = \pi \bar{I}_\nu^0. \tag{10.14}$$

Substituting (10.14) into (9.11) and utilizing the second of Eqs. (10.11), we obtain

$$r_\nu = \frac{1}{1 + t_\nu^0}. \tag{10.15}$$

Let us note that the quantity $1/(1 + t_\nu^0)$ is the fraction of the photosphere radiation at frequency ν passing through the atmosphere (after multiple scattering, generally speaking). The quantity $t_\nu^0/(1 + t_\nu^0)$ is the fraction of this radiation reflected back into the photosphere.

We can rewrite Eq. (10.15) in a somewhat different form. The quantity t_ν^0 entering into it, representing the optical thickness of the atmosphere at frequency ν, is equal to

$$t_\nu^0 = \int_{r_0}^{\infty} \sigma_\nu \, dr, \tag{10.16}$$

where r_0 is the radius of the base of the atmosphere. Let us represent the volume absorption coefficient in the form $\sigma_\nu = nk_\nu$, where n is the number of atoms in the lower state for a given line (or, as it is sometimes called, the number of absorbing atoms) in 1 cm^3 and k_ν is the absorption coefficient calculated for one atom. Then, assuming that k_ν is independent of position in the atmosphere, instead of (10.16) we obtain

$$t_\nu^0 = k_\nu N, \tag{10.17}$$

where

$$N = \int_{r_0}^{\infty} n(r) \, dr. \tag{10.18}$$

The quantity N is the number of absorbing atoms in a column with a 1 cm^2 cross section above the photosphere. Substituting (10.17) into (10.15), we obtain /120

$$r_\nu = \frac{1}{1 + k_\nu N}. \tag{10.19}$$

If we would have used the second approximation method (i.e., the Eddington method) to solve the system of Eqs. (10.5), then the following expression

would be obtained for the quantity r_ν:

$$r_\nu = \frac{1}{1 + \frac{3}{4} k_\nu N}. \tag{10.20}$$

As we see, it is not too different from Eq. (10.19).

2. Eddington method. The assumption made above concerning the division of the outer portions of a star into two layers, photosphere and atmosphere, is quite crude. We will now discard this assumption and we will assume that both continuous spectrum and line energy absorption and emission occur in each volume element. We will call this model of the outer star layers the Eddington model.

Strictly speaking, when the Eddington model is adopted, the problems of the formation of the continuous and line spectra of stars must be considered simultaneously. However, the effect of line absorption and emission on the formation of the continuous spectrum is slight, and in a first approximation it can be ignored (this effect, as we known from Section 8, is taken into consideration in the second approximation in the form of the so-called "blanketing effect"). Consequently, in solving the problem of the formation of stellar line spectra, all the quantities relating to the continuous spectrum can be assumed to be known.

The equations determining the radiation intensity within the line in the case of the Eddington model have already been derived above. One of them is the radiative transfer Eq. (9.1), and the other is the radiative equilibrium Eq. (10.1). Equation (9.1) can be rewritten in the form

$$\cos\vartheta \frac{\partial I_\nu}{\partial r} = -(\sigma_\nu + \alpha_\nu) I_\nu + \varepsilon_\nu + \alpha_\nu B_\nu(T). \tag{10.21}$$

Here we have made use of the relation (9.2) since we are assuming the assumption of local thermodynamic equilibrium is valid for the continuous spectrum. Substituting (10.1) into (10.21), we obtain one integral-differential equation for determining the quantity I_ν: /121

$$\cos\vartheta \frac{dI_\nu}{dr} = -(\sigma_\nu + \alpha_\nu) I_\nu + \sigma_\nu \int I_\nu \frac{d\omega}{4\pi} + \alpha_\nu B_\nu(T). \tag{10.22}$$

Introducing the continuous spectrum optical depth τ_ν by means of the relation $d\tau_\nu = -\alpha_\nu dr$, instead of (10.22) we obtain

$$\cos\vartheta \frac{dI_\nu}{d\tau_\nu} = (\eta_\nu + 1) I_\nu - \eta_\nu \int I_\nu \frac{d\omega}{4\pi} - B_\nu(T). \tag{10.23}$$

where

$$\eta_\nu = \frac{\sigma_\nu}{\alpha_\nu}. \tag{10.24}$$

Generally speaking, the quantity η_ν is a very complicated function of the depth; however, in what follows we will assume for simplicity that η_ν = const.

Let us apply the Eddington method (see Section 2) to determine an approximate solution of (10.23). Beforehand, let us introduce the notations:

$$\bar{I}_\nu = \int I_\nu \frac{d\omega}{4\pi}, \quad \bar{H}_\nu = \int I_\nu \cos\vartheta \frac{d\omega}{4\pi}. \tag{10.25}$$

The quantity $\bar{I}_\nu$ represents the mean radiation intensity at a given point, and $4\pi H_\nu$ is the radiation flux.

After first multiplying Eq. (10.23) by $d\omega/4\pi$ and then by $\cos\vartheta d\omega/4\pi$ and integrating over all solid angles, we find

$$\frac{d\bar{H}_\nu}{d\tau_\nu} = \bar{I}_\nu - B_\nu, \tag{10.26}$$

$$\frac{1}{3}\frac{d\bar{I}_\nu}{d\tau_\nu} = (1+\eta_\nu)\bar{H}_\nu. \tag{10.27}$$

Here we have used the approximation

$$\int I_\nu \cos^2\vartheta \frac{d\omega}{4\pi} = \frac{1}{3}\bar{I}_\nu. \tag{10.28}$$

From Eqs. (10.26) and (10.27) we obtain the following equation for determining $\bar{I}_\nu$:

$$\frac{d^2\bar{I}_\nu}{d\tau_\nu^2} = 3(1+\eta_\nu)(\bar{I}_\nu - B_\nu) \tag{10.29}$$

For the quantity $B_\nu(T)$, just as before, let us take Eq. (9.15), i.e., we will consider it to be a linear function of τ_ν. In this case the particular solution of Eq. (10.29) will be simply equal to $B_\nu(T)$. As the general solution of this equation, however, we obtain /122

$$\bar{I}_\nu = C_\nu e^{-\tau_\nu\sqrt{3(1+\eta_\nu)}} + D_\nu e^{\tau_\nu\sqrt{3(1+\eta_\nu)}} + B_\nu, \tag{10.30}$$

where C_ν and D_ν are arbitrary constants.

It is obvious that in the deep atmosphere layers, where spectral lines are absent, $\bar{I}_\nu = \bar{B}_\nu$. Therefore one must have $D_\nu = 0$. Consequently, we have

$$\bar{I}_\nu = C_\nu e^{-\tau_\nu\sqrt{3(1+\eta_\nu)}} + B_\nu(T_0)(1+\beta_\nu^*\tau_\nu), \tag{10.31}$$

where $\beta_\nu^* = \beta_\nu\bar{\alpha}/\alpha_\nu$. With the aid of (10.27) we obtain

$$\bar{H}_\nu = \frac{1}{3(1+\eta_\nu)}\left[-C_\nu e^{-\tau_\nu\sqrt{3(1+\eta_\nu)}}\sqrt{3(1+\eta_\nu)} + B_\nu(T_0)\beta_\nu^*\right]. \tag{10.32}$$

The boundary condition (10.6) must be used to determine the constant C_ν. In the approximation that has been adopted, it can be written in the form

$$\bar{I}_\nu = 2\bar{H}_\nu \quad (\text{for } \tau_\nu = 0). \tag{10.33}$$

Substituting (10.31) and (10.32) into (10.33), we obtain

$$C_\nu\sqrt{3(1+\eta_\nu)} = -\frac{3(1+\eta_\nu) - 2\beta_\nu^*}{\sqrt{3(1+\eta_\nu)}+2}B_\nu(T_0). \tag{10.34}$$

Since our problem is to determine the absorption line profile in the stellar spectrum, we must find the radiant flux emanating from the star, i.e., the quantity $H_\nu(0) = 4\pi\bar{H}_\nu(0)$. Assuming $\tau_\nu = 0$ in Eq. (10.32) and taking (10.34) into consideration, we obtain

$$H_\nu(0) = 4\pi B_\nu(T_0)\frac{1+\dfrac{\beta_\nu}{\sqrt{3(1+\eta_\nu)}}}{\sqrt{3(1+\eta_\nu)}+2}. \tag{10.35}$$

Outside the spectral line $\eta_\nu = 0$. Consequently, the continuous spectrum radiation in the neighborhood of the line is equal to

$$H_\nu^0(0) = 4\pi B_\nu(T_0)\frac{1+\dfrac{\beta_\nu^*}{\sqrt{3}}}{\sqrt{3}+2}. \tag{10.36}$$

From (10.35) and (10.36) we obtain /123

$$r_\nu = \frac{H_\nu(0)}{H_\nu^0(0)} = \frac{1+\dfrac{\beta_\nu^*}{\sqrt{3(1+\eta_\nu)}}}{1+\dfrac{\beta_\nu^*}{\sqrt{3}}}\cdot\frac{\sqrt{3}+2}{\sqrt{3(1+\eta_\nu)}+2}; \tag{10.37}$$

This formula determines the desired absorption line profile in the stellar spectrum.

Let us note that $\eta_\nu \gg 1$ in the central portions of strong lines. Therefore, in the given case we have

$$r_\nu \simeq \frac{\sqrt{3}+2}{\sqrt{3}+\beta_\nu^*} \cdot \frac{1}{\sqrt{\eta_\nu}}. \tag{10.38}$$

We see that the quantity r_ν depends on β_ν^* only by virtue of the continuous spectrum flux. In the central portions of the line, however, the flux is practically independent of β_ν^*. This is explained by the fact that the central portions of strong lines are formed at the very surface layers of the atmosphere [where one can assume that $B_\nu(T) = B_\nu(T_0)$].

In the outer portions of the line $\eta_\nu \ll 1$. In this case Eq. (10.37) yields

$$r_\nu = 1 - \frac{\eta_\nu}{2}\left(\frac{\beta_\nu^*}{\sqrt{3}+\beta_\nu^*} + \frac{\sqrt{3}}{\sqrt{3}+2}\right). \tag{10.39}$$

Thus, the quantity $1-r_\nu$ is proportional to the line absorption coefficient σ_ν [as stated by Eq. (9.20) also].

With the aid of Eq. (10.21) and the expression derived for the quantity $\bar{I}_\nu$, we can also determine the quantity $r_\nu(\vartheta)$, but we will not discuss this.

3. Fluorescence in stellar atmospheres. The expressions derived above for r_ν define the theoretical absorption line profiles. However, these profiles (both in the case of the Schwarzschild-Schuster model and in the case of the Eddington model) do not agree well with the observed profiles. The discrepancy between them in the ratio of the central line intensities is especially large. The theoretical values of r_ν for strong lines are much smaller than the observed values (see Section 11 for a detailed comparison of theory with observations).

These discrepancies mean that the assumptions, made by us in formulating Eq. (10.1), are not borne out in reality. One of these assumptions involved the /124 fact that pure radiation scattering occurs at each line. In reality, fluorescence processes, i.e., a redistribution of radiation between lines as well as between lines and the continuous spectrum, also occur in stellar atmospheres. Let us now try to take these processes into consideration.

The problem of radiation redistribution between lines has not been considered in detail up to the present time. It is obvious, however, that this process

cannot lead to an increase of the central intensities of all lines: if the intensity of one line increased, then the intensities of the other lines must decrease.

The situation is different in the case of radiation redistribution between lines and the continuous spectrum. For simplicity, let us consider an atom having only three energy levels (1, 2 and 3), with the first two being discrete and the third corresponding to ionization. In addition to the pure spectral line scattering process ($1 \rightarrow 2 \rightarrow 1$), previously discussed, the following two mutually opposed cyclical processes are also possible: 1) the $\rightarrow 3 \rightarrow 2 \rightarrow 1$ transition, i.e., ionization of the atom from the first state, capture of an electron in the second state and line emission of a quantum; 2) the $1 \rightarrow 2 \rightarrow 3 \rightarrow 1$ transition, i.e., line absorption of a quantum, ionization from the second state and capture of an electron in the first level. Processes of the first kind obviously lead to the appearance of quanta in lines, and processes of the second kind—to the disappearance of these quanta. In the deep layers of the atmosphere, where thermodynamic equilibrium can be assumed to exist, these processes balance each other. In the outer layers of the atmosphere, however, processes of the first kind predominate over processes of the second kind. This is explained by the fact that the probability of processes of the first kind depends only on the density of radiation beyond the fundamental series limit, and the probability of processes of the second kind—both on the density of radiation beyond the second series limit and on the spectral line radiation density. The continuous spectrum radiation density obviously does not change in the atmosphere. However, the spectral line radiation density decreases from the deep layers outward.

Thus, radiation redistribution between lines and the continuous spectrum in stellar atmospheres leads more frequently to the appearance of line quanta than to their disappearance. In particular, the central intensities of the absorption lines must increase because of this process.

In order to determine line profiles when the effect of this fluorescence mechanism is taken into account, we must formulate and solve the appropriate radiative transfer equation. We will do this by following Stromgren's work [9].

We will use the Eddington atmosphere model and we will start from Eq. (10.21). However, instead of Eq. (10.1), defining the quantity ε_ν, we will write /125

$$\varepsilon_\nu = (1-\gamma)\sigma_\nu \int I_\nu \frac{d\omega}{4\pi} + \varepsilon_\nu', \tag{10.40}$$

where ε_ν' is the volume emission coefficient, caused by processes of the first kind, and γ denotes the fraction of the spectral line quanta experiencing true absorption (i.e., the fraction of atoms ionized from the second state); processes of the second kind are taken into account by the introduction of the quantity γ.

Employing the considerations discussed above, it is easy to find an expression for the quantity ε_ν'. In the deep atmosphere layers, where the number

of processes of the first kind is equal to the number of processes of the second kind,

$$\varepsilon_\nu' = \gamma\sigma_\nu \bar{I}_\nu. \tag{10.41}$$

Moreover, in these same layers $\bar{I}_\nu = B(T)$. Therefore instead of (10.41) we have

$$\varepsilon_\nu' = \gamma\sigma_\nu B_\nu(T). \tag{10.42}$$

One can assume that the expression derived for ε_ν' remains valid as one goes from the deep atmosphere layers to the shallower since the density of the radiation, producing ionization of the atoms from the ground state, does not vary in the atmosphere. However, in order to take account of a possible difference between the density of this radiation in the stellar atmosphere and the density in the presence of thermodynamic equilibrium, let us introduce some correction factor Q on the right side of Eq. (10.42). Then we obtain

$$\varepsilon_\nu = (1-\gamma)\sigma_\nu \bar{I}_\nu + Q\gamma\sigma_\nu B_\nu(T). \tag{10.43}$$

Substituting (10.43) into (10.21) and changing variables from r to τ_ν, we obtain

$$\cos\vartheta \frac{dI_\nu}{d\tau_\nu} = (1+\eta_\nu) I_\nu - (1-\gamma)\eta_\nu \bar{I}_\nu - (1+Q\gamma\eta_\nu) B_\nu(T), \tag{10.44}$$

when η_ν is defined by Eq. (10.24).

We will obtain an approximate solution of Eq. (10.44), assuming that $\eta_\nu =$ = const. From this equation we have

$$\frac{d\bar{H}_\nu}{d\tau_\nu} = (1+\gamma\eta_\nu)\bar{I}_\nu - (1+Q\gamma\eta_\nu) B_\nu, \tag{10.45}$$

$$\frac{d\bar{I}_\nu}{d\tau_\nu} = 3(1+\eta_\nu)\bar{H}_\nu. \tag{10.46}$$

From this the following equation is obtained for determining $\bar{I}_\nu$: /126

$$\frac{d^2\bar{I}_\nu}{d\tau_\nu^2} = 3(1+\eta_\nu)[(1+\gamma\eta_\nu)\bar{I}_\nu - (1+Q\gamma\eta_\nu)B_\nu]. \tag{10.47}$$

The solution of Eq. (10.47) has the form

$$\bar{I}_\nu = C_\nu e^{-b_\nu\tau_\nu} + \frac{1+Q\gamma\eta_\nu}{1+\gamma\eta_\nu} B_\nu(T_0)(1+\beta_\nu^*\tau_\nu), \tag{10.48}$$

where

$$b_\nu^2 = 3(1+\eta_\nu)(1+\gamma\eta_\nu), \tag{10.49}$$

and C_ν is an arbitrary constant. The constant associated with $e^{b_\nu \tau_\nu}$ is equal to zero since $\bar{I}_\nu$ cannot increase exponentially with an increase in τ_ν. Substituting (10.48) into (10.46), we obtain

$$\bar{H}_\nu = \frac{1}{3(1+\eta_\nu)}[-b_\nu C_\nu e^{-b_\nu \tau_\nu} + B_\nu(T_0)\beta_\nu^*]. \tag{10.50}$$

Determining the constant C_ν from the condition (10.33), we obtain the following expression for the radiation flux of interest to us at the star boundary:

$$H_\nu(0) = 4\pi B_\nu(T_0)\frac{1+Q\gamma\eta_\nu}{1+\gamma\eta_\nu}\cdot\frac{b_\nu+\beta_\nu^*}{3(1+\eta_\nu)+2b_\nu} \tag{10.51}$$

From this it follows that

$$r_\nu = \frac{1+Q\gamma\eta_\nu}{1+\gamma\eta_\nu}\cdot\frac{b_\nu+\beta_\nu^*}{1+\frac{\beta_\nu^*}{\sqrt{3}}}\cdot\frac{\sqrt{3}+2}{3(1+\eta_\nu)+2b_\nu}. \tag{10.52}$$

The formula derived for r_ν is an extension of Eq. (10.37) to the case when fluorescence is present.

In order to make use of Eq. (10.52), the quantity γ must be determined. As already stated, it is equal to the ratio of the number of ionizations from the second state to the sum of the number of ionizations and the number of spontaneous transitions from this state. With the aid of the Einstein transition coefficients (see Section 8) the quantity γ is represented in the form

$$\gamma = \frac{B_{23}\rho_{23}}{B_{23}\rho_{23}+A_{21}}. \tag{10.53}$$

In this formula

$$B_{23}\rho_{23} = c\int_{\nu_{23}}^{\infty}\rho_\nu k_{2\nu}\frac{d\nu}{h\nu}, \tag{10.54}$$

where ν_{23} is the frequency of ionization from the second state, $k_{2\nu}$ is the absorption coefficient beyond the second series limit. /127

One can proceed as follows for a rough estimate of the quantity γ. We will assume that the quantity $B_{23}\rho_{23}$ is actually the product of the radiation

intensity ρ_{23} immediately beyond the second series limit and the Einstein transition coefficient [determined in accordance with Eq. (10.54)]. Then, representing ρ_{23} and A_{21} in the form

$$\rho_{23} = \frac{\sigma_{23}}{e^{\frac{h\nu_{23}}{kT}} - 1}, \tag{10.55}$$

$$A_{21} = \frac{g_1}{g_2} \sigma_{12} B_{12}, \tag{10.56}$$

where

$$\sigma_{ik} = \frac{8\pi h \nu_{ik}^3}{c^3}, \tag{10.57}$$

and assuming the approximations $g_2 \approx g_1$, $\sigma_{12} \approx \sigma_{23}$, $B_{12} \approx B_{23}$, we obtain

$$\gamma \approx e^{-\frac{h\nu_{23}}{kT}}, \tag{10.58}$$

A calculation of the quantity γ from Eq. (10.58) for atoms with about a 3 eV ionization potential from the excited state (for example, for Na I and Ca I) gives $\gamma \approx 10^{-3}$ for the temperature of the Sun. Calculations from Eqs. (10.53) and (10.54) lead to values of the same order of magnitude ($\gamma = 0.0015$ for the sodium D_1 and D_2 lines and $\gamma = 0.0004$ for the λ 4227 Ca I line).

We will use Eq. (10.52) for r_ν and the estimates made of the quantity γ below (in Section 11) in discussing the problem of the central intensities of absorption lines.

4. Exact solution of the problem. The problem, being considered by us, concerning the determination of absorption line profiles in the stellar spectra under the assumptions made above can be solved exactly. To obtain such a solution, we will employ the method proposed in Section 3.

Let us take the radiative transfer equation in the form of (10.21), and we will specify the emission coefficient ε_ν by Eq. (10.43), i.e., we will take fluorescence into consideration. These equations can be rewritten in the form

$$\cos\vartheta \frac{dI_\nu}{dt_\nu} = I_\nu - S_\nu, \tag{10.59}$$

where $dt_\nu = -(\sigma_\nu + \alpha_\nu)\, dr$ and /128

$$S_\nu = (1-\gamma)\frac{\eta_\nu}{1+\eta_\nu}\int I_\nu \frac{d\omega}{4\pi} + \frac{1+Q\gamma\eta_\nu}{1+\eta_\nu} B_\nu(T). \tag{10.60}$$

Just as before, we will represent the function $B_\nu(T)$ by Eq. (9.15). Changing from τ_ν to t_ν in it, we have

$$B_\nu(T) = B_\nu(T_0)\left(1 + \frac{\beta_\nu^*}{1+\eta_\nu} t_\nu\right), \tag{10.61}$$

where $B_\nu^* = B_\nu \frac{\bar{\alpha}}{\alpha_\nu}$.

Solving Eq. (10.59) in terms of I_ν and substituting the derived expression for I_ν in terms of S_ν into Eq. (10.60) (i.e., proceeding in the same manner as in Section 2 in deriving Milne's equation), we arrive at the following integral equation for determining the function $S_\nu(t_\nu)$:

$$S_\nu(t_\nu) = \frac{\lambda_\nu}{2}\int_0^\infty \mathrm{Ei}\,|t_\nu - t_\nu'|\, S_\nu(t_\nu')\, dt_\nu' + \frac{1+Q\gamma\eta_\nu}{1+\eta_\nu} B_\nu(T), \tag{10.62}$$

where

$$\lambda_\nu = (1-\gamma)\frac{\eta_\nu}{1+\eta_\nu}. \tag{10.63}$$

Let us rewrite Eq. (10.62) in the form

$$S(t) = \frac{\lambda}{2}\int_0^\infty \mathrm{Ei}\,|t - t'|\, S(t')\, dt' + g(t), \tag{10.64}$$

omitting, for simplicity, the subscript ν for awhile. The free term of this equation is a linear function of t, i.e.,

$$g(t) = c_0 + c_1 t. \tag{10.65}$$

We see that Eq. (10.64) belongs to the type of equations discussed in detail in Section 3. If we set

$$K(t) = \frac{\lambda}{2}\mathrm{Ei}\, t = \frac{\lambda}{2}\int_1^\infty e^{-tx}\frac{dx}{x}, \tag{10.66}$$

in Eq. (3.1), then we will obtain Eq. (10.64). When the kernel K(t) is represented in the form of (3.17), we have $A(x) = \lambda/2x$.

According to the method proposed in Section 3, the solution of Eq. (10.64) must begin with a determination of the function S(0, x), defined by Eq. (3.20). In the given case, assuming $x = 1/\mu$ and $S(0, x) = \varphi(\mu)$, instead of (3.20) we have /129

$$\varphi(\mu) = 1 + \frac{\lambda}{2}\varphi(\mu)\mu\int_0^1 \frac{\varphi(\mu')}{\mu+\mu'}d\mu'. \tag{10.67}$$

When $\lambda = 1$, the previously discussed Eq. (3.53) is obtained from (10.67).

The function $\varphi(\mu)$, first introduced by V. A. Ambartsumyan, was then investigated in detail by a number of authors. Values of this function are given in Table 11, and in Table 12—values of its moments [i.e., the quantities defined by Eq. (3.59)].

TABLE 11. VALUES OF THE FUNCTION $\varphi(\mu)$

μ \ λ	0	0,4	0,6	0,8	0,85	0,90	0,925	0,95	0,975	1
0	1,00	1,00	1,00	1,00	1,00	1,00	1,00	1,00	1,00	1,00
0,1	1,00	1,06	1,09	1,14	1,15	1,17	1,18	1,20	1,21	1,25
0,2	1,00	1,09	1,15	1,23	1,26	1,29	1,31	1,34	1,37	1,45
0,3	1,00	1,11	1,19	1,30	1,34	1,39	1,42	1,46	1,51	1,64
0,4	1,00	1,13	1,22	1,36	1,41	1,48	1,52	1,57	1,64	1,83
0,5	1,00	1,14	1,25	1,41	1,48	1,56	1,61	1,67	1,76	2,01
0,6	1,00	1,15	1,27	1,46	1,53	1,63	1,69	1,77	1,88	2,19
0,7	1,00	1,16	1,29	1,50	1,58	1,69	1,76	1,85	1,98	2,37
0,8	1,00	1,17	1,31	1,54	1,63	1,75	1,83	1,93	2,08	2,55
0,9	1,00	1,18	1,32	1,57	1,67	1,81	1,89	2,01	2,18	2,73
1,0	1,00	1,18	1,34	1,60	1,71	1,85	1,95	2,08	2,27	2,91

TABLE 12. VALUES OF THE MOMENTS OF THE FUNCTION $\varphi(\mu)$

λ	0	0,4	0,6	0,8	0,85	0,90	0,925	0,95	0,975	1
α_0	1,00	1,13	1,23	1,38	1,44	1,52	1,57	1,63	1,73	2,00
α_1	0,50	0,58	0,64	0,74	0,77	0,83	0,86	0,90	0,96	1,15
α_2	0,33	0,39	0,43	0,50	0,53	0,57	0,59	0,63	0,67	0,82

Commas represent decimal points.

The function S(t), a solution of Eq. (10.64), can be expressed in terms of the function $\varphi(\mu)$. However, right now only the absorption line profiles are of interest to us. Therefore we must determine only the intensity of the radiation /130

emanating from the atmosphere, i.e., the quantity $I(0, \mu)$. As we know, the quantity $I(0, \mu)$ is also expressed directly in terms of the function $\varphi(\mu)$.

In the given case, i.e., when g(t) is a linear function of t, we must use Eqs. (3.41) and (3.48) to determine the radiation intensity $I(0, \mu)$. The first of these is obtained when $g(t) = 1$, the second—when $g(t) = t$. As seen from Eq. (3.27), for a kernel of the form of (10.66)

$$S(0,0) = \frac{1}{\sqrt{1-\lambda}}. \tag{10.68}$$

Therefore we find

$$I(0,\mu) = \frac{\varphi(\mu)}{\sqrt{1-\lambda}}\left[c_0 + c_1\left(\mu + \frac{\lambda}{2}\frac{\alpha_1}{\sqrt{1-\lambda}}\right)\right], \tag{10.69}$$

where α_1 is the first moment of the function $\varphi(\mu)$.

Comparing the free term of Eq. (10.60) and Eq. (10.65) for the function g(t), we obtain the following expression for the intensity of the radiation emanating from the atmosphere at frequency ν:

$$I_\nu(0,\mu) = \frac{\varphi_\nu(\mu)}{\sqrt{1-\lambda_\nu}}\frac{1+Q\gamma\eta_\nu}{1+\eta_\nu}\times \\ \times B_\nu(T_0)\left[1 + \frac{\beta_\nu^*}{1+\eta_\nu}\left(\mu + \frac{\lambda_\nu}{2}\frac{\alpha_{\nu 1}}{\sqrt{1-\lambda_\nu}}\right)\right] \tag{10.70}$$

Here $\varphi_\nu(\mu)$ denotes the function $\varphi(\mu)$, defined by Eq. (10.67) for the λ value given by Eq. (10.63).

The intensity of the radiation, emanating from the atmosphere in the continuous spectrum in the neighborhood of the line, is obtained from (10.70) for $\eta_\nu = 0$. It is equal to

$$I_\nu^0(0,\mu) = B_\nu(T_0)(1 + \beta_\nu^*\mu). \tag{10.71}$$

From (10.70) and (10.71) it follows that the quantity $r_\nu(\mu)$, determining the absorption line profile at an angular distance of arccos μ from the center of the disk, is given by the formula

$$r_\nu(\mu) = \frac{I_\nu(0,\mu)}{I_\nu^0(0,\mu)} = \frac{\varphi_\nu(\mu)}{(1+\beta_\nu^*\mu)\sqrt{1-\lambda_\nu}}\times \\ \times \frac{1+Q\gamma\eta_\nu}{1+\eta_\nu}\left[1 + \frac{\beta_\nu^*}{1+\eta_\nu}\left(\mu + \frac{\lambda_\nu}{2}\frac{\alpha_{\nu 1}}{\sqrt{1-\lambda_\nu}}\right)\right]. \tag{10.72}$$

For a homogeneous atmosphere (i.e., when $\beta_\nu^* = 0$) and in the absence of fluorescence (i.e., when $\gamma = 0$), from Eq. (10.72) we obtain /131

$$r_\nu(\mu) = \frac{\varphi_\nu(\mu)}{\sqrt{1+\eta_\nu}}. \tag{10.73}$$

Equation (10.72) (for Q = 1) was first derived by Chandrasekhar [10].

11. Absorption Lines in Presence of Noncoherent Scattering

1. Frequency redistribution within the line. During the discussion in the preceding paragraph of the problem of the formation of absorption lines in stellar spectra, two assumptions were made: 1) concerning pure scattering in the spectral line (i.e., concerning the absence of energy redistribution between the lines as well as between the lines and the continuous spectrum), 2) concerning coherent scattering (i.e., concerning the absence of frequency redistribution of the radiation within the line). However, the line profiles calculated with these assumptions are very much different from observed profiles. This means that these assumptions do not hold up in reality and they must be discarded. Taking flurorescence (more precisely, radiation redistribution between lines and continuous spectrum) into account, already done above, appreciably reduces the discrepancy between theory and observations. Now we will also take into consideration the noncoherency of the scattering, i.e., the change in the radiation frequency due to the elementary scattering act.

Let us first enumerate the causes leading to the frequency redistribution of radiation within a line.

1. Natural broadening of the atomic energy levels. If the levels are broadened, then the atom can absorb photons of one frequency, and emit photons of some other frequency, with the atom returning, after the scattering process, to a state not exactly the same as the initial state. This effect plays a role in the case of subordinate series lines, for which both the upper and lower levels are broadened. In the case of the fundamental series, however, for which the lower level can be considered to be infinitely narrow (if only because an atom is not often removed from the ground state for any reasons), the frequency of the emitted photon is the same as the frequency of the absorbed photon.

2. Thermal motion of the atoms. Let a moving atom absorb a photon with a certain frequency. Since this atom can emit a photon in any direction, then /132 because of the Doppler effect the frequency of the emitted photon can be different for a stationary observer. Therefore, the frequencies of photons absorbed and emitted by a moving atom are not, generally speaking, identical. This is true even when light scattering by a stationary atom occurs without a change in frequency.

3. Pressure effects. At the instant of photon absorption by an atom, let there be a perturbing particle near the atom. During the time in which the atom remains in the upper level, the particle can move away from the atom so that the energy level shift caused by it is changed. Under this condition the frequency

of the emitted photon will differ from the frequency of the absorbed photon. The difference in photon energies is carried away by the perturbing particle.

Let us denote by $p(\nu, \nu')d\nu$ the probability that a volume element, after having absorbed photons of frequency ν', subsequently emits photons in the frequency interval from ν to $\nu + d\nu$. The function $p(\nu, \nu')$ is determined by the causes that have been enumerated and, generally speaking, is extremely complicated.

As long ago as 1929, Eddington pointed out the necessity of taking noncoherent scattering into account in the theory of stellar spectra. Subsequently, astrophysicists carried out many analyses to determine the function $p(\nu, \nu')$. Considerable work on this subject has recently been done by Hummer [11].

We will not now concern ourselves with a detailed discussion of the function $p(\nu, \nu')$, but let us only mention two special cases. Let us first assume that pressure effects play no role, i.e., the function $p(\nu, \nu')$ is the result of natural broadening of the levels (in other words, radiation damping) and of the thermal motion of the atoms only. In this case, the following formula, defining $p(\nu, \nu')$, was obtained for the resonance line:

$$p(\nu, \nu')\sigma_{\nu'} = \frac{nk_0}{\pi\Delta\nu_D}\int_0^\infty e^{-(y+r)^2}\left[\arctan\frac{y+s}{a} + \arctan\frac{y-s}{a}\right]dy, \quad (11.1)$$

where

$$s = \frac{u+u'}{2}, \qquad r = \frac{|u-u'|}{2}, \quad (11.2)$$

σ_ν is the volume absorption coefficient, equal to $\sigma_\nu = nk_\nu$. The quantity k_ν is defined by Eq. (8.17), and the other quantities in (11.1) have the same meaning as in (8.17). In the exact formula for $p(\nu, \nu')$, the scattering angle also enters. Equation (11.1) can be derived from the exact formula by integrating over the angle.

In the other special case, let us assume that pressure effects exert the principal influence on the form of the function $p(\nu, \nu')$. If, during the lifetime of an atom in an excited state, the perturbing field changes very drastically, then one can assume that the frequency ν of the emitted photon is independent of the frequency ν' of the absorbed photon. In this case the function $p(\nu, \nu')$, which we can denote simply as p_ν, is very easy to determine. /133

The function $p(\nu, \nu')$ must obviously satisfy the condition

$$\int p(\nu, \nu')d\nu = 1, \quad (11.3)$$

where the integration is carried out over all frequencies. Moreover, the relation

$$p(\nu, \nu')\sigma_{\nu'} = p(\nu', \nu)\sigma_\nu, \quad (11.4)$$

expressing the "reciprocity principle" for optical phenomena, must be satisfied.

If the function $p(\nu, \nu')$ does not depend on ν', then from (11.4) it follows that $p_\nu = c\sigma_\nu$, where c is a constant. Determining c from Eq. (11.3), we obtain

$$p_\nu = \frac{\sigma_\nu}{\int \sigma_{\nu'} d\nu'}. \tag{11.5}$$

We will say that in the case given a complete frequency redistribution of the radiation occurs during the elementary act of scattering. We will call such radiation scattering completely noncoherent.

The formulas presented for the function $p(\nu, \nu')$ correspond to different pressure values: at low pressures Eq. (11.1) should be used, at high—Eq. (11.5). Equation (11.1) should obviously be used in studying radiation diffusion in gas nebulae. Even in the case of nebulae, however, complete frequency redistribution of the radiation is usuallv assumed since some calculations have shown that the replacement of Eq. (11.1) by (11.5) does not lead to a big difference in the results (see Chapter V).

Using the function $p(\nu, \nu')$, we can write an expression for the emission coefficient ε_ν. If it is assumed that pure radiation scattering occurs in the line, then we have

$$\varepsilon_\nu = \int p(\nu, \nu') \sigma_{\nu'} d\nu' \int I_{\nu'} \frac{d\omega}{4\pi}. \tag{11.6}$$

When $p(\nu, \nu') = \delta(\nu - \nu')$, where δ is the Dirac function, from (11.6) it follows that /134

$$\varepsilon_\nu = \sigma_\nu \int I_\nu \frac{d\omega}{4\pi}, \tag{11.7}$$

i.e., the expression for ε_ν in the case of coherent radiation scattering.

Substituting into (11.6) the expression for $p(\nu, \nu')$, given by Eq. (11.5), we obtain

$$\varepsilon_\nu = \sigma_\nu \frac{\int \sigma_{\nu'} d\nu' \int I_{\nu'} \frac{d\omega}{4\pi}}{\int \sigma_{\nu'} d\nu'}. \tag{11.8}$$

The absorption coefficient for completely noncoherent scattering is determined by this formula.

Below we will assume that completely noncoherent spectral line radiation scattering occurs in stellar atmospheres.

2. Radiative transfer equation and its solution. After consideration of the processes, occurring during the elementary act of scattering, let us pass over to a determination of absorption line profiles. Here, as already stated, we assume complete frequency redistribution of the radiation.

For simplicity, we will assume fluorescence is absent. In this case we must take the radiative transfer equation in the form of (10.21), and the expression for the emission coefficient—in the form of (11.8).

We will introduce the continuous spectrum optical depth τ with the aid of the relation $d\tau = -\alpha_\nu dr$ (to simplify the notation we omit the subscript ν on τ). Then these equations assume the form

$$\mu \frac{dI_\nu(\tau, \mu)}{d\tau} = (\eta_\nu + 1) I_\nu(\tau, \mu) - \eta_\nu S(\tau) - B_\nu(T) \tag{11.9}$$

and

$$S(\tau) = \frac{1}{2} \int p_\nu d\nu \int_{-1}^{+1} I_\nu(\tau, \mu) d\mu, \tag{11.10}$$

where $\mu = \cos \vartheta$, $\eta_\nu = \sigma_\nu / \alpha_\nu$ and (11.5) is used.

Previously we took the quantity $B_\nu(T)$ in the form of a linear function of τ; however, now we will assume, for simplicity, it is constant and equal to $B_\nu(T_0)$. /135

From Eq. (11.9) it follows that the desired intensity of the radiation, coming from the atmosphere, is equal to

$$I_\nu(0, \mu) = \frac{\eta_\nu}{\eta_\nu + 1} \int_0^\infty S(\tau) e^{-x\tau} x \, d\tau + \frac{B_\nu(T_0)}{\eta_\nu + 1}, \tag{11.11}$$

where

$$x = \frac{\eta_\nu + 1}{\mu}. \tag{11.12}$$

To formulate the integral equation, defining the function $S(\tau)$, let us find the radiation intensity I_ν from (11.9) and substitute it into (11.10). As a result we obtain

$$S(\tau) = \frac{1}{2} \int p_\nu d\nu \int_0^\infty [\eta_\nu S(\tau') + B_\nu(T_0)] \operatorname{Ei}[|\tau - \tau'| (\eta_\nu + 1)] d\tau'. \tag{11.13}$$

Equation (11.13) can be rewritten in the form

$$S(\tau)=\int_0^\infty K(|\tau-\tau'|)S(\tau')d\tau'+g(\tau), \tag{11.14}$$

where

$$K(\tau)=\frac{1}{2}\int p_\nu\eta_\nu d\nu\int_{\eta_\nu+1}^\infty e^{-x\tau}\frac{dx}{x} \tag{11.15}$$

and

$$g(\tau)=B_\nu(T_0)\left[\int\frac{p_\nu d\nu}{\eta_\nu+1}-\frac{1}{2}\int p_\nu d\nu\int_{\eta_\nu+1}^\infty e^{-x\tau}\frac{dx}{x^2}\right]. \tag{11.16}$$

Changing the order of integration in (11.15), we obtain

$$K(\tau)=\int_1^\infty e^{-x\tau}A(x)dx, \tag{11.17}$$

where /136

$$A(x)=\frac{1}{x}\int_{\nu(x)}^\infty p_\nu\eta_\nu d\nu, \tag{11.18}$$

and $\nu(x)=\nu_0$ if $x>\eta_{\nu_0}+1$, and $\eta_{\nu(x)}+1=x$ if $x<\eta_{\nu_0}+1$ (ν_0 is the central line frequency).

Analogously we obtain

$$g(\tau)=B_\nu(T_0)\left[\int\frac{p_\nu d\nu}{\eta_\nu+1}-\frac{1}{2}\int_1^\infty e^{-x\tau}A_1(x)dx\right], \tag{11.19}$$

where

$$A_1(x)=\frac{1}{x^2}\int_{\nu(x)}^\infty p_\nu d\nu \tag{11.20}$$

and the lower limit of the integration is determined the same as in (11.18).

Equation (11.14) can be solved by the method discussed in Section 3. However, the function $s(\tau)$ itself is not of interest to us, but only the intensity of

the radiation coming from the atmosphere. This quantity can be found from the formulas given in Section 3 without determining the function $S(\tau)$ beforehand. Here, it will be expressed by the function $S(0, x)$, defined by Eq. (3.20).

From Eq. (11.19) we see that the free term of Eq. (11.14) comprises two parts: a constant and a superposition of exponents. Therefore, denoting the solution of Eq. (11.14) by $S(\tau, x)$ for the free term $e^{-x\tau}$, we obtain

$$S(\tau) = B_\nu(T_0)\left[S(\tau, 0)\int \frac{p_\nu\, d\nu}{\eta_\nu + 1} - \frac{1}{2}\int_1^\infty S(\tau, x) A_1(x)\, dx\right]. \tag{11.21}$$

Substituting (11.21) into (11.11) and utilizing Eq. (3.19), we find

$$I_\nu(0, \mu) = \frac{\eta_\nu}{\eta_\nu + 1} B_\nu(T_0) S(0, x)\left[S(0, 0)\int \frac{p_\nu}{\eta_\nu + 1} d\nu - \right.$$

$$\left. - \frac{x}{2}\int_1^\infty \frac{S(0, y)}{x + y} A_1(y)\, dy\right] + \frac{B_\nu(T_0)}{\eta_\nu + 1}. \tag{11.22}$$

The quantity $S(0, 0)$ entering into Eq. (11.22) can be found with the aid of relation (3.27). Taking (11.17) into consideration, instead of this relation we have /137

$$S^2(0, 0)\left[1 - 2\int_0^\infty K(\tau)\, d\tau\right] = 1. \tag{11.23}$$

Substituting Eq. (11.15) here, we obtain

$$S^2(0, 0)\int \frac{p_\nu\, d\nu}{\eta_\nu + 1} = 1. \tag{11.24}$$

Therefore Eq. (11.22) assumes the form

$$I_\nu(0, \mu) = \frac{\eta_\nu}{\eta_\nu + 1} B_\nu(T_0) S(0, x)\left[\sqrt{\int \frac{p_\nu\, d\nu}{\eta_\nu + 1}} - \right.$$

$$\left. - \frac{x}{2}\int_1^\infty \frac{S(0, y)}{x + y} A_1(y)\, dy\right] + \frac{B_\nu(T_0)}{\eta_\nu + 1}. \tag{11.25}$$

The desired intensity of the radiation, coming from the atmosphere within a spectral line, is also given by Eq. (11.25). Outside the line the radiation

intensity in the given case is equal to $B_\nu(T_0)$. Therefore for the quantity $r_\nu(\mu)$ we have

$$r_\nu(\mu) = \frac{I_\nu(0, \mu)}{B_\nu(T_0)}. \tag{11.26}$$

The function S(0, x), in terms of which the radiation intensity I_ν (0, μ) is expressed, is defined by Eq. (3.20). Assuming x = 1/z and S(0, x) = φ(z), instead of this equation we obtain

$$\varphi(z) = 1 + z\varphi(z) \int_0^1 \frac{\varphi(z')}{z + z'} A\left(\frac{1}{z'}\right) \frac{dz'}{z'}. \tag{11.27}$$

In the new notation the formula for $r_\nu(\mu)$ is written in the form

$$r_\nu(\mu) = \frac{1}{\eta_\nu + 1} + \frac{\eta_\nu}{\eta_\nu + 1} \varphi(z) \left[\sqrt{\int \frac{p_\nu d\nu}{\eta + 1}} - \right.$$
$$\left. - \frac{1}{2} \int_0^1 \frac{\varphi(z')}{z + z'} A_1\left(\frac{1}{z'}\right) \frac{dz'}{z'} \right]. \tag{11.28}$$

In order to calculate the quantity $r_\nu(\mu)$ from Eq. (11.28), the function φ(z) must be determined from Eq. (11.27). This is easily done by numerical methods. /138

Equation (11.28) gives the final expression for the quantity $r_\nu(\mu)$, determining the absorption line profile for completely noncoherent scattering. This formula was first derived [12] by another method. Then it was extended to the case when the function $B_\nu(T)$ is represented in the form of a linear function of τ and fluorescence is taken into consideration. Exact expressions for the quantity $r_\nu(\mu)$ in terms of the function φ(z) have also been derived in the papers of Busbridge [13] and Ueno [14].

It should be mentioned again that the problem of the formation of absorption lines in the presence of noncoherent light scattering has been solved in many analyses by approximation methods.

3. Central intensities of absorption lines. Until now we have not concerned ourselves with a comparison of the theory being discussed for the formation of stellar line spectra with the results of observations. Let us do this now with respect to the central intensities of the absorption lines.

Observations show that the central intensities are quite high even for very strong lines. Expressed as fractions of the continuous spectrum intensity, they amount to a few hundredths or tenths (i.e., $r_{\nu 0} \approx 0.01$–0.1). Let us see to what values of $r_{\nu 0}$ the theory discussed above leads.

Let us first consider the line profiles for noncoherent light scattering and in the absence of fluorescence. In this case the quantity r_ν is determined by Eq. (10.37). We see that the line profile depends on the quantity η_ν, which is equal to

$$\eta_\nu = \frac{nk_\nu}{\alpha_\nu}, \tag{11.29}$$

where n is the number of absorbing atoms in 1 cm^3 and k_ν is the absorption coefficient, calculated for one atom. The quantity k_ν can be assumed to be known, and the quantity n/α_ν can be determined from the line width (for example, by comparing the theoretical and observed distances from the line center for $r_\nu = 1/2$). This provides the possibility of finding the value of the quantity η_ν at the line center. For strong lines the η_{ν_0} values turn out to be very large—of the order of 10^6.

The following approximate value for the quantity r_{ν_0} results from Eq. (10.37) when $\eta_{\nu_0} \gg 1$:

$$r_{\nu_0} \approx \frac{1}{\sqrt{\eta_{\nu_0}}}. \tag{11.30}$$

When $\eta_{\nu_0} \approx 10^6$, Eq. (11.30) gives $r_{\nu_0} \approx 10^{-3}$. This value of r_{ν_0} is much less than the values obtained from observations. /139

As already stated, this discrepancy between theory and observations made it necessary to take fluorescence into consideration. In this case, Eq. (10.52) was derived for the quantity r_ν. For $\eta_{\nu_0} \approx 10^6$ and for $\gamma \approx 10^{-3}$ (this estimate of the quantity γ was made above), we have $\gamma\eta_{\nu_0} \gg 1$. Therefore from Eq. (10.52) we obtain the approximation

$$r_{\nu_0} \approx Q\sqrt{\gamma}. \tag{11.31}$$

When $\gamma \approx 10^{-3}$ and $Q \approx 1$, it follows from Eq. (11.31) that $r_{\nu_0} \approx 0.03$. Thus, Eq. (11.31) gives much higher values of r_{ν_0} than Eq. (11.30). In other words, taking fluorescence into account drastically increases the theoretical value of the central line intensity.

However, for Q = 1 the theoretical values of r_{ν_0} are nevertheless smaller than the observed. For example, for the sodium D_1 and D_2 and the λ 4227 Å calcium lines in the solar spectrum the theoretical and observed values of r_{ν_0} differ by a factor of 2–4. For the H and K lines of ionized calcium this discrepancy is much greater since the value of γ in this case is very small. In order

to bring theory into agreement with observations, it must be assumed that the hypothetical factor Q introduced above is considerably greater than unity. The Sun, producing ionization of atoms from the ground state, should surpass the radiation intensity, given by Planck's formula, many times. However, as we will see in Chapter III, we have no basis for such an assumption.

In view of what has been said, the question arises whether taking noncoherent scattering into account can lead to higher theoretical values for the central absorption line intensities. To answer this question we must return to Eq. (11.28), which defines the quantity $r_\nu(\mu)$ for completely noncoherent scattering. One can show that the second term within the square brackets of Eq. (11.28) is smaller than the first by at least a factor of two. For the line center the coefficient in front of the brackets is close to unity (since $z = \mu/(1 + \eta_\nu)$, and for very small z, as seen from Eq. (11.27), $\varphi(z) \approx 1$). In the given case, therefore, we have the approximation

$$r_{\nu_0} \approx \sqrt{\int \frac{p_\nu d\nu}{\eta_\nu + 1}}. \tag{11.32}$$

In evaluating the quantity $r_{\nu 0}$ from Eq. (11.32), for the line absorption coefficient let us take its usual expression, given by Eq. (8.17). Then we obtain /140

$$r_{\nu_0} \approx \left(\frac{a}{\eta_{\nu_0}}\right)^{1/4}. \tag{11.33}$$

For $a \approx 10^{-2}$ and $\eta_{\nu_0} \approx 10^6$, Eq. (11.33) gives $r_{\nu_0} \approx 10^{-2}$. With coherent scattering, however, we previously obtained $r_{\nu_0} \approx 10^{-3}$ from Eq. (11.30). Thus, the central absorption line intensities can be much higher for noncoherent scattering than for coherent.

The high values of $r_{\nu 0}$, given by Eq. (11.33), are explained by a frequency redistribution of the radiation within the line: in the outer layers of the atmosphere, absorption of the intense radiation occurs in the line wings followed by the emission of energy in the central portions of the line.

As already stated, a formula has been derived for the quantity $r_\nu(\mu)$ that takes account of noncoherent scattering and fluorescence simultaneously (see [12]). For the quantity $r_{\nu 0}$ this formula gives

$$r_{\nu_0} \approx \sqrt{\left(\frac{a}{\eta_{\nu_0}}\right)^{1/2} + \gamma}. \tag{11.34}$$

We see that if the inequality

$$\left(\frac{a}{\eta_{\nu_0}}\right)^{1/2} \gg \gamma, \tag{11.35}$$

is satisfied, then the quantity r_{ν_0} is caused primarily by frequency redistribution of radiation within the line. However, when this inequality is reversed, fluorescence plays the major role in the formation of the central portions of the line.

One can assume that the inequality (11.35) holds for some lines of the solar spectrum. For these lines the value of the quantity r_ν, calculated from Eq. (11.34), will be greater than the value given by the Eq. (11.31) for Q = 1, i.e., in this case theory can agree with observations. In order to verify this assumption, however, precise values of the parameters a, η_{ν_0} and γ must be found, which is difficult at the present time.

It should be mentioned again that the central portions of the strong absorption lines are formed in the outermost layers of the atmosphere. It is possible that for some lines these layers are the chromosphere. Since, however, the conditions in the chromosphere are very unusual (see Chapter III), this must also affect the central portions of the lines.

4. Variation of line profiles over the solar disk. A good method for checking the theory of stellar line spectra is to study the variation of line profiles as one goes from the center of the solar disk to its edge. Moreover, such a study can provide some information on the structure of the solar atmosphere. /141

We will now consider only the behavior of the far wings of strong lines. Just as before, let us assume that the ratio of the line absorption coefficient to the continuous spectrum absorption coefficient, denoted by η_ν, is constant in the atmosphere Obviously, the quantity $1-r_\nu(\mu)$ in the line wings is proportional to η_ν. Therefore it is convenient to characterize the behavior of the line wings over the solar disk by the quantity

$$C(\mu) = \lim_{\eta_\nu \to 0} \frac{1 - r_\nu(\mu)}{\eta_\nu}. \tag{11.36}$$

Let us determine the quantity $C(\mu)$ for different line formation mechanisms. In the case of local thermodynamic equilibrium we have, on the basis of Eq. (9.18),

$$C(\mu) = \frac{\beta_\nu \mu}{1 + \beta_\nu \mu}. \tag{11.37}$$

To determine the quantity $C(\mu)$ under the assumption of coherent light scattering we must make use of Eq. (10.72). The function $\varphi_\nu(\mu)$ entering into this

formula, is determined by Eq. (10.67), and the quantity λ_ν—by Eq. (10.63). For $\eta_\nu \ll 1$, from Eq. (10.67) it follows that

$$\varphi_\nu(\mu) = 1 + \frac{1-\gamma}{2}\eta_\nu \mu \ln\frac{1+\mu}{\mu}. \tag{11.38}$$

Therefore from Eq. (10.72) we obtain (for Q = 1):

$$C(\mu) = \frac{3}{2} - \frac{\gamma}{2} - \frac{1-\gamma}{2}\mu \ln\frac{1+\mu}{\mu} - \frac{1}{1+\beta_\nu^* \mu}\left[1 + \frac{\beta_\nu^*}{2}(1-\gamma)\right]. \tag{11.39}$$

Under the assumption of completely noncoherent scattering, from Eq. (11.28) we obtain

$$C(\mu) = 1 - \varphi(\mu)\left[\sqrt{\int \frac{p_\nu d\nu}{\eta_\nu + 1}} - \frac{1}{2}\int_0^1 \frac{\varphi(z')}{\mu + z'} A_1\left(\frac{1}{z'}\right)\frac{dz'}{z'}\right], \tag{11.40}$$

where the function $\varphi(z)$ is determined by Eq. (11.27). This formula applies to the case $\beta_\nu^* = 0$ and $\gamma = 0$; however, one can derive a more general expression for the quantity $C(\mu)$ (see [12]). /142

The theoretical expressions that have been presented for the quantity $C(\mu)$ can be compared with observational data. Such a comparison shows that the theory agrees best with observations when the assumption of noncoherent light scattering is made. Even in this case, however, the agreement between them is not complete. This is explained, apparently, by the fact that the quantity η_ν is not actually constant in the atmosphere.

Detailed observational data on the variation of the profiles of different lines over the solar disk are presented in Houtgast's paper [15]. In the interpretation of these data Houtgast first made the assumption of completely noncoherent light scattering in a spectral line.

12. Chemical Composition of Stellar Atmospheres

1. Equivalent line widths. One of the most important characteristics of an absorption line is its equivalent width, i.e., the width of an adjacent portion of the continuous spectrum having an energy equal to the energy absorbed in the line. The equivalent line width is defined by the formula

$$W = \int (1 - r_\nu)\, d\nu, \tag{12.1}$$

where $r_\nu = H_\nu / H_\nu^0$ (see Section 9).

Substituting the theoretical expression for the quantity r_ν into Eq. (12.1), we can obtain the relationship between the equivalent line width and the number of absorbing atoms. This relationship, plotted on a graph, is usually called the "curve of growth". With the aid of the curve of growth one can determine the

number of absorbing atoms from the measured equivalent line width. These determinations serve as the basis for finding the chemical composition of the stellar atmosphere. This represents a very important (but not the only) purpose of the curve of growth.

An atmosphere model must be specified in order to calculate the quantity W from Eq. (12.1). In the case of the Schwarzschild-Schuster model the quantity r_ν is defined by Eq. (10.19). Substituting (10.19) into (12.1), we obtain a relationship between W and N. Strictly speaking, however, the quantities which are parameters in the expression for the absorption coefficient k_ν must still enter into this relationship. If Eq. (8.18) is taken for k_ν, then these parameters will be k_0, $\Delta\nu_D$ and a. Obviously, in the given case the equivalent line width depends on the product k_0N and on the parameters $\Delta\nu_D$ and a, i.e., /143

$$W = F_1(k_0N, \Delta\nu_D, a). \tag{12.2}$$

In the Eddington model with the simplifying assumptions, the quantity r_ν is given by Eq. (10.37) in which $\eta_\nu = k_\nu n/\alpha_\nu$. In the given case we have

$$W = F_2\left(k_0\frac{n}{\alpha_\nu},\ \Delta\nu_D,\ a\right). \tag{12.3}$$

for the equivalent line width.

It is easy to see that the quantity n/α_ν has the same physical meaning as the quantity N, i.e., it represents the number of absorbing atoms in a column with a 1 cm^2 cross section above the atmosphere. In fact we have

$$N = \int_{r_0}^{\infty} n\,dr = \frac{n}{\alpha_\nu}\int_{r_0}^{\infty}\alpha_\nu\,dr = \frac{n}{\alpha_\nu}\tau_\nu. \tag{12.4}$$

But since the continuous spectrum optical depth τ_ν of the base of the atmosphere is about unity, then the quantities n/α_ν and N must be of the same order of magnitude.

From what has been said it follows that the parameters k_0, $\Delta\nu_D$ and a must be known in order to determine the number of absorbing atoms with the aid of the curve of growth. In most cases, however, these parameters are poorly known, and therefore attempts are made to determine them by means of the curve of growth. This can be done because the stellar spectrum usually contains many lines of the given atom, i.e., we have many relations of the type (12.2) or (12.3) in which the values of the quantity W are known from observations.

Thus, a number of problems can be solved with the aid of the curve of growth. We will now enumerate some of them.

1. The determination of the number of absorbing atoms N (or n/α_ν), i.e., the number of atoms in states such that transitions from them give rise to a given line. In this manner a value is arrived at for the number of atoms, of the element being considered, in all states. The chemical composition of the atmosphere is found in this way.

2. The determination of the number of atoms in different states (if lines, arising from different states, are observed in the stellar spectrum). When these numbers are represented by the Boltzmann formula, the "excitation temperature" of the atoms in the atmosphere is determined.

3. The determination of the Doppler half-width of the line, equal to

$$\Delta\nu_D = \nu_0 \frac{v}{c}, \tag{12.5}$$

where v is the average velocity of random atomic motion (thermal and turbulent). /144
The value of the velocity v can be determined from this.

4. The determination of the parameter a, which is given by Eq. (8.27). The role of collisions in radiation damping is thereby determined.

5. The determination of the quantity k_0, related to the Einstein spontaneous transition coefficient A_{ki} by Eq. (8.16). Expressing the coefficient A_{ki} in terms of the oscillator strength f, we obtain

$$k_0 = \frac{\sqrt{\pi}\, e^2}{m\nu_0 v} f, \tag{12.6}$$

where m is the electron mass and e is its charge. Consequently, knowing k_0, one can determine the oscillator strength for a given line.

Below we will derive theoretical curves of growth in explicit form and we will report the results of their application to the determination of the chemical composition of stellar atmospheres. The problems of determining other atmosphere parameters with the aid of the curve of growth will be considered briefly in the following section. A more detailed discussion of these problems can be found in the monographs [7] and [8] cited above.

2. Curve of growth for the Schwarzschild-Schuster model. In order to determine the dependence of the equivalent line width on the number of absorbing atoms in the case of the Schwarzschild-Schuster model, Eq. (10.19) must be substituted into Eq. (12.1). After doing this, we obtain

$$W = \int \frac{k_\nu N}{1 + k_\nu N} d\nu. \tag{12.7}$$

Let us take Eq. (8.18) for the absorption coefficient k_ν. Since the integral of (12.7) is not stated in the general form, let us consider three special cases corresponding to three portions of the curve of growth (this was first done by Menzel [16]).

1. Let N be small so that $k_\nu N \ll 1$ for all frequencies. In this case Eq. (12.7) can be rewritten in the form

$$W = N \int k_\nu \, d\nu. \tag{12.8}$$

Substituting Eq. (8.18) here, we obtain

$$W = \sqrt{\pi} \frac{\nu_0 v}{c} k_0 N. \tag{12.9}$$

This formula is valid only for very weak lines.

2. Let N be large so that $k_{\nu_0} N \gg 1$, but $k_\nu N \ll 1$ in those portions of the line where k_ν is determined by radiation damping. In the given case, Eq. (8.24) can be taken for k_ν. Substituting it into Eq. (12.7), we have /145

$$W = k_0 N \frac{\nu_0 v}{c} \int_{-\infty}^{+\infty} \frac{e^{-u^2}}{1 + k_0 N e^{-u^2}}. \tag{12.10}$$

An approximate calculation of the integral yields

$$W = 2 \frac{\nu_0 v}{c} \sqrt{\ln k_0 N}. \tag{12.11}$$

Let us note that Eq. (12.11) can also be derived from the following considerations. We find the distance $\Delta\nu$, from the line center, at which r = 1/2. According to Eq. (10.19), at this distance we must have $k_\nu N = 1$ or

$$k_0 N e^{-\left(\frac{c}{v} \frac{\Delta\nu}{\nu_0}\right)^2} = 1. \tag{12.12}$$

From this we obtain

$$\Delta\nu = \nu_0 \frac{v}{c} \sqrt{\ln k_0 N}. \tag{12.13}$$

Since $W = 2\Delta\nu$ approximately, we again arrive at Eq. (12.11).

3. Finally, let N be so large that the inequality $k_\nu N \gg 1$ is satisfied even in those portions of the line, far from the center, where k_ν is determined by radiation damping. Obviously, in this case Eq. (8.25) can be used for k_ν for computing the integral of (12.7) over the entire extent. Substituting (8.25) into (12.7), we obtain

$$W = \frac{a}{\sqrt{\pi}} k_0 N \frac{\nu_0 v}{c} \int_{-\infty}^{+\infty} \frac{du}{u^2 + \frac{a}{\sqrt{\pi}} k_0 N}, \tag{12.14}$$

or, after integration,

$$W = \pi^{3/4} \frac{\nu_0 v}{c} \sqrt{a k_0 N}. \tag{12.15}$$

Summarizing the results obtained, we can state that the equivalent line width W increases with an increase in the number of absorbing atoms, first as N, then approximately as $\sqrt{\ln N}$ and, finally, as $\sqrt{N}$. /146

The relationship between W and N is usually changed somewhat for practical use. First of all, a conversion is made from equivalent width W_ν in terms of frequency (we have designated this simply as W in the foregoing paragraphs) to equivalent width in terms of wavelength W_λ. These quantities are interrelated by the relation

$$\frac{W_\lambda}{\lambda} = \frac{W_\nu}{\nu}. \tag{12.16}$$

Further, a change is made from the number of absorbing atoms N to the quantity

$$X_0 = k_0 N, \tag{12.17}$$

representing, approximately, the optical depth of the atmosphere at the line center (since k_ν differs little from k_0 when $a \ll 1$).

Taking into consideration what has been said, the formulas derived above can be rewritten in the following form:

for small X_0

$$\frac{W_\lambda}{\lambda} = \sqrt{\pi} \frac{v}{c} X_0, \tag{12.18}$$

for large X_0

$$\frac{W_\lambda}{\lambda} = 2 \frac{v}{c} \sqrt{\ln X_0}, \tag{12.19}$$

for very large X_0

$$\frac{W_\lambda}{\lambda} = \pi^{3/4} \frac{v}{c} \sqrt{aX_0}. \tag{12.20}$$

Instead of the last formula we can also write

$$\frac{W_\lambda}{\lambda} = \frac{\pi^{1/4}}{2} \sqrt{\frac{v\Gamma}{c\nu_0} X_0}, \tag{12.21}$$

where Γ is the damping constant (caused both by radiation damping and collisional damping). Here, we have made use of the relation

$$a = \frac{c\Gamma}{4\pi\nu_0 v}, \tag{12.22}$$

resulting from the definition of a given by Eq. (8.27).

As already stated, the curve representing the dependence of W on N (or $\ln W_\lambda/\lambda$ on $\ln X_0$) is called the curve of growth. Both the formulas (12.18)—(12.20) presented above, as well as the results of a numerical determination of the integral of (12.7) for intermediate values of X_0, are used for plotting the curves of growth.

All the curves of growth comprise a family, depending on two parameters: the average velocity v of random atomic motion and the damping constant Γ (or the quantity a).

3. Curve of growth for Eddington model. To derive the dependence of the equivalent line width on the number of absorbing atoms in the case of the Eddington model we must take Eq. (10.37) for r_ν [or the more general expression (10.52)]. Substituting this expression into Eq. (12.7), one can obtain the dependence of W on $k_0 n/\alpha_\nu$. We will not carry out the calculations, but will only present their results. It turns out that the equivalent line width W first increases as $k_0 n/\alpha_\nu$, then as $\sqrt{\ln k_0 n/\alpha_\nu}$ and, finally, as $\sqrt{k_0 n/\alpha_\nu}$. In other words, the curve of growth in the case of the Eddington model has approximately the same form as in the case of the Schwarzschild-Schuster model. Let us remember that the quantity n/α_ν is analogous to the quantity N in its physical meaning.

Using the exact expression for the quantity r_ν, given by Eq. (10.72), we can obtain the exact curve of growth for the Eddington model. For simplicity let us assume that fluorescence is absent, i.e., $\gamma = 0$. In such a case Eq. (10.72) assumes the form

$$r_\nu(\mu) = \frac{\varphi_\nu(\mu)}{(1+\beta_\nu^* \mu)\sqrt{1+\eta_\nu}} \times \left[1 + \frac{\beta_\nu^*}{1+\eta_\nu}\left(\mu + \frac{\alpha_{\nu 1}\eta_\nu}{2\sqrt{1+\eta_\nu}}\right)\right] \tag{12.23}$$

where $\eta_\nu = k_\nu n/\alpha_\nu$, the function $\varphi_\nu(\mu)$ is defined by Eq. (10.67) and $\alpha_{\nu 1}$ is its first moment.

The line profile at an angular distance of arccos μ from the disk center is determined by Eq. (12.23). With the aid of this formula one can obtain the following expression for the quantity r_ν, which determines the line profile in the total stellar spectrum:

$$r_\nu = \frac{1}{\left(\frac{1}{2} + \frac{1}{3}\beta_\nu^*\right)\sqrt{1+\eta_\nu}} \left[\alpha_{\nu 2} + \frac{\beta_\nu^*}{1+\eta_\nu}\left(\alpha_{\nu 2} + \frac{\alpha_{\nu 1}^2 \eta_\nu}{2\sqrt{1+\eta_\nu}}\right)\right], \qquad (12.24)$$

where $\alpha_{\nu 2}$ is the second moment of the function $\varphi_\nu(\mu)$.

Substitution of Eq. (12.23) or (12.24) into Eq. (12.7) and carrying out the integration should give the desired curve of growth. This integration was done numerically in Wruble's paper [17], who presented his results in the form of tables and graphs. /148

One of the curves of growth obtained by Wrubel is given in Fig. 12. Along the abscissa axis is plotted the quantity $\eta_0 = k_0 n/\alpha_\nu$, and along the ordinate axis—the quantity $W_\lambda c/\lambda v$. At high η_0 values the curve branches out into a series of curves, corresponding to different values of the parameter a.

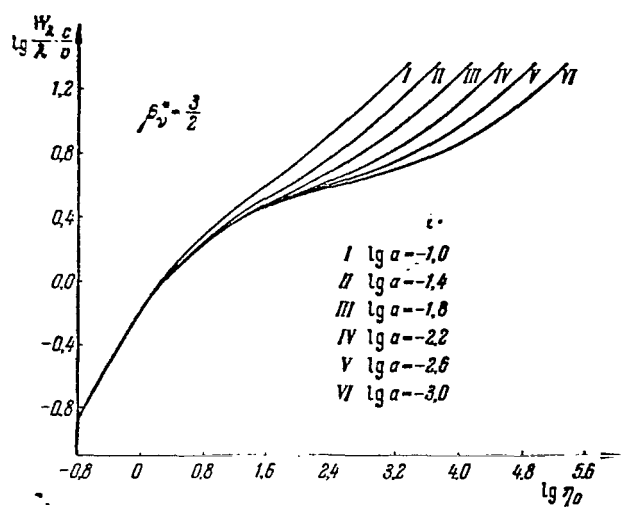

Figure 12.

The curve of growth, depicted in Fig. 12, refers to the case when $\beta_\nu^* = 3/2$. Let us remember that $\beta_\nu^* = B_\nu \bar{\alpha}/\alpha_\nu$, where β_ν is defined by Eq. (6.7).

Consequently, the quantity β_ν^*, and with it the curve of growth, can vary markedly in passing from one portion of the spectrum to another.

4. Plotting of curves of growth from observational data. The theoretical curves of growth depend on a number of parameters (k_0, α, v), which are not accurately known beforehand. Therefore the observed equivalent line widths must be used to determine these parameters. To this end, the empirical curve of growth is plotted for a given star from the lines of the atom of interest. The values of the parameters cited above are determined by comparing this curve with the theoretical curve of growth. /149

The possibility of plotting the curve of growth from observational data is based on the presence of multiplets in the stellar spectrum. For multiplet lines having a common lower level the number N is the same, and the oscillator strengths are often known. Therefore for these lines the values of the quantity lg X_0, which according to Eqs. (12.17) and (12.6) is equal to

$$\lg X_0 = \lg f + \lg \frac{\sqrt{\pi}\, e^2}{m \nu_0 v} N, \qquad (12.25)$$

differ from each other only by an unknown constant term. This circumstance makes it possible to plot, from the observed equivalent widths of the lines entering into the multiplets, a portion of the curve of growth with, however, an unknown zero point on the abscissa axis. Corresponding portions of the curve of growth can also be plotted from the lines of other multiplets. Then the total curve of growth can be determined by shifting the portions of the curves of growth, that have been obtained, along the abscissa axis to achieve agreement among them. The curve of growth, plotted by D. Kuliev from the Fe I lines (points), Ca Ca I (crosses) and Na I (circles) in the spectrum of α Perseus, is given in Fig. 13 as an example.

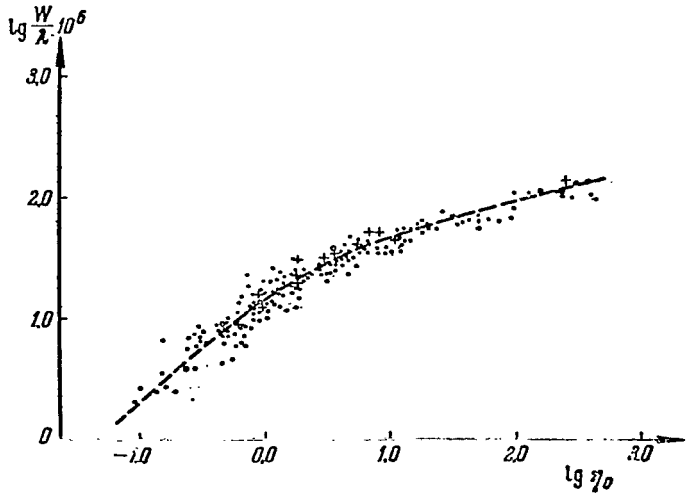

Figure 13.

A comparison of the empirical curves of growth with the family of theoretical curves provides the possibility of selecting that one of them which most nearly corresponds to the observations. In this way the values of the parameters v and a (or Γ) are determined for the atoms being considered in the atmosphere of a given star. The number of absorbing atoms N can also be determined from the curve of growth obtained in this manner. /150

A study of stellar atmospheres with the aid of curves of growth leads to very interesting results. Let us point out, for example, that for supergiant stars the values of the parameter v are often several times greater than the average thermal velocities of the atoms. This is explained by the turbulent motions in the atmospheres of stars (Section 13).

In the case of dwarf stars the values of the parameter Γ found from observations are many times larger (in the case of the sun, for example, 5-10 fold) than the corresponding theoretical values, determined with only radiation damping taken into account. This means that collisional damping also plays a large role in stellar atmospheres. The large value of Γ for dwarf stars is explained by the relatively high density of their atmospheres.

Many authors have investigated the atmospheres of the Sun and stars with the aid of the curves of growth. O. A. Mel'nikov and his co-workers have done a great deal of work in this field.

5. Amounts of different atoms in the atmospheres. The major purpose of the curve of growth is its use for determining the chemical composition of stellar atmospheres. From the equivalent line width the curve of growth gives the number of absorbing atoms, i.e., the number of atoms in the lower state for a given line. In most cases this state is excited. In order to convert to the number of atoms in the ground state, the Boltzmann formula is usually used. It often happens that lines, arising from excited states of the neutral atom, are observed in the stellar spectrum; but most atoms of a given element are in an ionized state (or vice versa). In such a case the Saha ionization formula must also be used for finding the total number of atoms of this element. The free electron density, entering into this formula, must be determined beforehand by one of the methods described in the following paragraph.

The method given for determining the chemical composition of stellar atmospheres is quite simple and is often used in practice. It must, however, be borne in mind that it is associated with two errors. The first of these arises because of the deviation of the atomic state distribution from the distribution given by the Boltzmann and Saha formulas. The source of the other error is the use of the mean temperature and electron density values for the entire atmosphere, whereas these quantities vary considerably in the atmosphere. /151

For these reasons, at the present time the determination of the chemical composition of stellar atmospheres with the aid of the curve of growth is considered to be only a first approximation. In subsequent approximations (with the aim of eliminating the second of the errors cited) stellar photosphere model calculations, made to be applicable to a given star (see Section 6), are used. The results of such calculations give the temperature and density distribution

in the surface layers of the star. This makes it possible to calculate, more or less accurately, the profile of any line of the element being considered for different assumptions concerning its content. The amount of this element in the stellar atmosphere is determined by a comparison of the calculated and observed equivalent line widths.

Special formulas have been derived for calculating the profiles and equivalent widths of absorption lines with the variation of the physical conditions with depth taken into consideration. The weighting function method, discussed in Section 10, has been extended for this. The formulas proposed by Pecker [18] are widely used in practice.

The chemical composition of the atmospheres of different stars has been determined in many investigations. Let us now introduce some results taken from Aller's paper [8].

Information on the chemical composition of the Sun's atmosphere is contained in Table 13. Here, the total concentration of the atoms of a given element is denoted by n. Values of lg n are given in the table, with lg n = 12 being arbitrarily adopted for hydrogen.

TABLE 13. CHEMICAL COMPOSITION OF THE SUN'S ATMOSPHERE

Element	lg n	Element	lg n	Element	lg n	Element	lg n
H	12,00	S	7,30	Cu	5,04	Rh	0,78
Li	0,96	K	4,70	Zn	4,40	Pd	1,21
Be	2,36	Ca	6,15	Ga	2,36	Ag	0,14
C	8,72	Sc	2,82	Ge	3,29	Cd	1,46
N	7,98	Ti	4,68	Rb	2,48	In	1,16
O	8,96	V	3,70	Sr	2,60	Sn	1,54
Na	6,30	Cr	5,36	Y	2,25	Sb	1,94
Mg	7,40	Mn	4,90	Zr	2,23	Ba	2,10
Al	6,20	Fe	6,57	Nb	1,95	Yb	1,53
Si	7,50	Co	4,64	Mo	1,90	Pb	1,33
P	5,34	Ni	5,91	Ru	1,43		

Commas represent decimal points.

Table 13 contains no information on the number of helium atoms in the solar atmosphere because of the absence of helium absorption lines in the visible portion of the solar spectrum. Only helium lines arising from excited states can be observed in this portion of the spectrum. The helium excitation potential is, however, very high so that at the relatively low temperature of the Sun there are few helium atoms in the excited states and they do not give rise to pronounced absorption lines. Intense helium absorption lines are present only in the spectra of hot stars (B and O classes).

However, as we will see below, helium emission lines are observed in the spectrum of the solar chromosphere. From the ratio of the intensities of the

helium and hydrogen emission lines it could be determined that the number of helium atoms amounts to about 0.2 of the number of hydrogen atoms.

Thus, hydrogen is the most abundant element in the solar atmosphere. Helium is the next in abundance. Then come the light elements: carbon, nitrogen, oxygen. The number of metal atoms, taken together, amounts to about one ten-thousandth of the number of hydrogen atoms.

Data on the chemical composition (more precisely, values of lg n) of the atmospheres of class B stars are given in Table 14. This table, like the preceding one, is taken from the cited paper of Aller, who used the published results of a number of authors. These results are obtained partly with the aid of the curves of growth and partly with the aid of photosphere models. Two results are presented for the star τ Scorpion. The discrepancy between them is caused both by the differences in the observational data and by differences in the methods used to determine the chemical composition.

TABLE 14. CHEMICAL COMPOSITION OF THE ATMOSPHERES OF CLASS B STARS

Element	γ Peg	ζ Per	τ Sco		10 Lac	55 Cyg
H	12,00	12,00	12,00	12,00	12,00	12,00
He	11,17	11,31	11,23	—	11,23	11,18
C	8,58	8,26	8,37	7,70	8,37	8,41
N	8,01	8,31	8,57	8,26	8,37	8,63
O	8,63	9,03	9,12	8,63	8,77	8,98
Ne	8,73	8,61	8,72	8,86	8,72	—
Mg	7,95	7,76	7,73	8,30	8,22	—
Al	5,76	6,78	6,58	6,40	7,07	—
Si	7,03	7,96	7,95	7,63	7,75	7,46

Commas represent decimal points.

From Tables 13 and 14 it is seen that the chemical composition of stellar atmospheres does not differ, in general features, from the chemical composition of the Sun's atmosphere. As we will learn later, the chemical composition of gaseous nebulae is also approximately the same. The conclusion concerning the common chemical composition of different types of stars and nebulae has immense value for astrophysics. /153

The problem of the appearance of real differences in the chemical composition of stellar atmospheres is of considerable interest. From the observational data it follows that stars with approximately the same surface temperature sometimes have vastly different spectra. As an example one can cite the Wolf-Rayet type of star, the spectra of which are divided quite markedly into two series: nitrogen and carbon. Stars of the later classes, whose spectra are divided into oxygen and carbon branches (the first of these is characterized by TiO bands, and the second—by C_2, CN and CH bands), can serve as another example. The existence of stars with very weak hydrogen spectral lines ("hydrogen-

poor stars") and stars with very strong lines of some metals ("metallic stars") has also been established by observations. Apparently, in most of these cases the spectral anomalies are caused by peculiarities in the excitation and ionization of atoms in stellar atmospheres.

13. Physical Conditions in Atmospheres

1. Atom excitation and ionization. As is known, in the presence of thermodynamic equilibrium the degree of atom excitation and ionization is determined by the Boltzmann and Saha formulas. Strictly speaking, thermodynamic equilibrium does not exist in stellar atmospheres. Even in this case, however, the Boltzmann and Saha formulas are still used as a first approximation. Therefore in considering the physical conditions in stellar atmospheres we must first of all discuss these formulas.

Let E_i be the energy of the i-th atomic level and g_i be its statistical weight (or the level multiplicity). Let us denote by n_i the number of atoms with energy E_i in 1 cm^3 in the presence of thermodynamic equilibrium. The fundamental formula of statistical physics gives

$$n_i = Ce^{-\frac{E_i}{kT}}, \tag{13.1}$$

where C is some constant.

From Eq. (13.1) we obtain /154

$$\frac{n_i}{n_1} = \frac{g_i}{g_1} e^{-\frac{\chi_1 - \chi_i}{kT}}, \tag{13.2}$$

where $E_i = -\chi_i$. The quantity χ_i represents the ionization energy from the i-th level, and the quantity $\chi_1 - \chi_i$ is the excitation energy of this level. Equation (13.2) is usually called the Boltzmann formula.

Equation (13.1) can also be applied to states with positive energies in which the electron is not bound to the atom. This provides the possibility of determining the ratio of the number of ions to the number of neutral atoms. The formula, defining this ratio (the so-called Saha formula), has the form

$$n_e \frac{n^+}{n_1} = \frac{g^+}{g_1} \frac{2(2\pi mkT)^{3/2}}{h^3} e^{-\frac{\chi_1}{kT}}, \tag{13.3}$$

where n^+ is the number of ionized atoms in the ground state in 1 cm^3, g^+ is the statistical weight of this state, n_e is the number of free electrons in 1 cm^3.

Analogous formulas also serve for determining the number of atoms in subsequent ionization stages. In particular, the ratio of the number of doubly ionized atoms to the number of singly ionized atoms is given by the formula

$$n_e \frac{n^{++}}{n^{+}} = \frac{g^{++}}{g^{+}} \frac{2(2\pi mkT)^{3/2}}{h^3} e^{-\frac{\chi_1'}{kT}}, \tag{13.4}$$

where n^{++} is the number of doubly ionized atoms in the ground state in 1 cm^3, g^{++} is the statistical weight of this state, χ_1' is the ionization energy of a singly ionized atom from the ground state.

As an example, we will apply the formulas that have been presented to the hydrogen atom. In this case $g_i = 2i^2$ and $\chi_i = \chi_1/i^2$. Therefore Eq. (13.2) assumes the form

$$\frac{n_i}{n_1} = i^2 e^{-\frac{\chi_1}{kT}\left(1-\frac{1}{i^2}\right)}. \tag{13.5}$$

In particular, for the second level we have

$$\frac{n_2}{n_1} = 4e^{-\frac{117\,800}{T}}. \tag{13.6}$$

From Eq. (13.6) it follows that for the temperatures, in thousands of degrees, prevailing in stellar atmospheres an overwhelming majority of the hydrogen atoms are in the ground state. However, with an increase in temperature the degree of atomic excitation increases rapidly. /155

From Eq. (13.5) it is also seen how the number of excited atoms varies with an increase in the level number i. If the temperature is not very high, then the quantity n_i/n_1 decreases at first with an increase in i, and then increases, with it increasing approximately proportional to i^2 at very high i. From this it follows that if all atomic levels were realizable, the total number of atoms in excited states would be infinite. In reality, however, because of perturbations caused by foreign particles the high atomic levels are not attainable. Therefore the number of atoms in all excited states is usually much less than the number of atoms in the ground state.

When the ionization formula (13.3) is applied to the hydrogen atom, we must set $g^{+} = 1$, $g_1 = 2$, $\chi_1/k = 157,200$. As a result we obtain

$$n_e \frac{n^{+}}{n_1} = 2{,}24 \cdot 10^{15} T^{3/2} e^{-\frac{157\,200}{T}}. \tag{13.7}$$

The degree of ionization depends not only on the temperature T but also on the density of free electrons n_e. Since, however, the quantity n_e is relatively small in stellar atmospheres, the degree of ionization can be high even at not very high temperatures. For example, assuming $n_e \approx 10^{12}$, from Eq. (13.7) we find that at $T \approx 10,000°$ the quantity n^+/n_1 for hydrogen will already be of the order of 300.

In practical calculations the ionization formula (13.3) is often used in the form

$$p_e \frac{n^+}{n_1} = 2 \frac{g^+}{g_1} \frac{(2\pi m)^{3/2}(kT)^{5/2}}{h^3} e^{-\frac{\chi_1}{kT}}, \tag{13.8}$$

where p_e is the electron pressure, equal to

$$p_e = n_e kT. \tag{13.9}$$

Taking the logarithm, instead of (13.8) we obtain

$$\log p_e \frac{n^+}{n_1} = -\frac{5040}{T}\chi_1 + 2.5 \log T - 0.48 + \lg \frac{2g^+}{g_1}. \tag{13.10}$$

Here, the electron pressure p_e is expressed in bars (1 bar = 1 dyne/cm^2), and /156
the ionization energy χ_1 is in electron volts. An electron volt is the energy which an electron acquires in traversing a potential difference of 1 volt (1 eV = $= 1.60 \cdot 10^{-12}$ erg).

Values of the ionization energy of neutral and singly ionized atoms are listed in Table 15. From the table it is seen that metals (Na, Ca, Fe, etc.) possess the lowest ionization energies from neutral atoms. In stellar atmospheres they are already ionized at temperatures of order of 5000°. With an increase in temperature, hydrogen undergoes ionization. The highest temperature is required for helium ionization.

As already stated, the Boltzmann and Saha formulas can be applied to stellar atmospheres as a first approximation. In those cases when more precise formulas are required to determine the quantities n_i/n_1 and n^+/n_1, the specific processes of atomic excitation and ionization due to the effects of radiation and due to the effect of collisions (as well as the reverse processes), must be examined. In such cases Eqs. (13.2) and (13.3) with certain correction factors /157
are used to determine the degree of atomic excitation and ionization. For stellar atmospheres these factors usually are not greatly different from unity. For many other astrophysical objects, however, the deviation of these factors from unity is very large. Gaseous nebulae, which we will consider later (see Section 23 and 24), can serve as an example.

TABLE 15. TO BE TRANSLATED (2 lines)
xxxxxxxxxxx

Element	x_1	x_1'	Element	x_1	x_1'	Element	x_1	x_1'
H	13,60		A	15,75	27,6	Br	11,84	21,6
He	24,58	54,4	K	4,34	31,8	Kr	14,00	24,6
Li	5,39	76,6	Ca	6,11	11,9	Rb	4,18	27,4
Be	9,32	18,2	Sc	6,56	12,8	Sr	5,69	11,0
B	8,30	25,1	Ti	6,83	13,6	Y	6,6	12,3
C	11,26	24,4	V	6,74	14,6	Zr	6,95	14,0
N	14,54	29,6	Cr	6,76	16,5	Nb	6,77	13,5
O	13,61	35,1	Mn	7,43	15,6	Mo	7,18	15,2
F	17,42	35,0	Fe	7,90	16,2	Tc	7,45	15
Ne	21,56	41,1	Co	7,86	17,0	Ru	7,5	16,4
Na	5,14	47,3	Ni	7,63	18,2	Rh	7,7	18,1
Mg	7,64	15,0	Cu	7,72	20,3	Pd	8,33	19,9
Al	5,98	18,8	Zn	9,39	18,0	Ag	7,57	22,0
Si	8,15	16,3	Ga	6,00	20,5	Cd	8,99	16,9
P	10,55	19,6	Ge	7,88	15,9	In	5,78	18,9
S	10,36	23,4	As	9,85	20,2	Sn	7,33	14,6
Cl	13,01	23,8	Se	9,75	21,4			

Commas represent decimal points.

2. Density of free electrons. The density of free electrons n_e must be known in order to determine the degree of atom ionization from Eq. (13.3). This quantity depends on the depth and must be determined on the basis of a stellar photosphere model calculation (see Section 6). In some cases, however, only the average value of the free electron density in the atmosphere is of interest. This quantity, which we will denote by $\bar{n}_e$, is usually determined by one of two methods.

The first method can be used when lines of the same atom in different stages of ionization are observed in the stellar spectrum. Let us assume, for example, that the lines of neutral and singly ionized atoms are observed. In such a case one can, with the aid of the curve of growth and Boltzmann's formula, find the numbers n_1 and n^+. Then the desired quantity $\bar{n}_e$ is determined from the ionization formula.

In the Sun's spectrum, Ca and Ca^+ lines, as well as Sr and Sr^+, are present. Application of the above-mentioned method in both cases gives approximately the same result, namely, $\bar{n}_e \approx 10^{12}$ cm^{-3}.

The second method of determining the quantity $\bar{n}_e$ is based on counting the number of hydrogen Balmer series lines observed in the stellar spectrum. As already stated, the high atomic levels are not attainable in real life because of the effect of foreign particles. Therefore an upper limit should exist for the number of lines observed. Let us denote the number of the last attainable level by i and the orbital radius corresponding to it—by r_i. Let us also denote the

mean distance between particles by r_0. Obviously, $r_i < r_0$. But for the hydrogen atom $r_i = r_1 i^2$, where r_1 is the radius of the first Bohr orbit ($r_1 = 0.53 \cdot 10^{-8}$ cm), and the average distance between the particles is equal to

$$r_0 = \left(\frac{3}{4\pi n}\right)^{1/3}, \tag{13.11}$$

where n is the particle concentration. Therefore we obtain

$$r_1 i^2 < \left(\frac{3}{4\pi n}\right)^{1/3}, \tag{13.12}$$

or /158

$$\lg n < 24{,}21 - 6 \lg i. \tag{13.13}$$

The inequality (13.13) allows one to estimate the upper limit for the particle concentration n (including the free electron density $\bar{n}_e$) from the observed number of Balmer lines.

For a sufficiently large number of charged particles (ions and free electrons), however, they produce a perturbing influence on the atom so that the number of attainable levels is reduced even further. The charged particles, because of the Stark effect, also produce a broadening of the lines. In this situation the high terms of the Balmer series merge with each other and they cannot be distinguished from the continuum. With the merging of lines taken into consideration, Inglis and Teller derived the following formula for determining the charged particle density n in terms of the number of the upper level of the last observable Balmer line:

$$\lg n = 23{,}26 - 7{,}5 \lg i. \tag{13.14}$$

Here, for low temperatures ($T < 10^5/i$) n should be construed as the density of ions and free electrons, and for high temperatures ($T > 10^5/i$)—as the density of ions only. If one can assume that the ions and free electrons are formed only through the ionization of hydrogen atoms, then in the first case $n = 2\bar{n}_e$, and in the second $n = \bar{n}_e$.

The methods described for determining the mean density of free electrons in stellar atmospheres are not distinguished by high accuracy (if only because of the uncertainty in the concept of the quantity $\bar{n}_e$ itself. In practice, however, these methods are used very frequently for a rough estimate of $\bar{n}_e$. In particular, it is easy to distinguish dwarf stars from giant stars by the number of observable Balmer lines in the stellar spectra. In the atmospheres of dwarfs the particle density is much greater than in the atmospheres of giants, and this means that the quantity i must be smaller. An especially small number of observable lines

should be present in the spectra of white dwarfs, which is in complete agreement with observations.

3. Turbulence in atmospheres. The study of stellar atmospheres by the curve of growth method has shown that for many stars the values of the parameter v are somewhat greater than the average thermal velocity of the atoms. Thus, the idea emerged that another type of random gas movement is present in stellar atmospheres in addition to the thermal motion. This motion was called "turbulent" (although it can be distinguished from turbulent motion in the aerodynamic sense). Thus, the total velocity of random motion of the gas atoms in /159 a stellar atmosphere is defined by the formula

$$v = \sqrt{v_0^2 + v_t^2}, \tag{13.15}$$

where v_0 is the average velocity of thermal motion, equal to

$$v_0 = \sqrt{\frac{2kT}{m_a}}, \tag{13.16}$$

and v_t is the turbulent motion velocity.

Especially high turbulent velocities have been found in supergiant stars. For example, as determined by Struve, in the atmosphere of ε Auriga v_t = = 20 km/sec, and in the atmosphere of 17 Leporis v_t = 67 km/sec. For comparison, the average thermal velocities of metal atoms in stellar atmospheres are about 1 km/sec.

Because of the turbulent motions in stellar atmospheres a change also occurs in the absorption line profiles, namely—a line broadening. In the spectra of some supergiants the weak lines turn out to be broad and fine, and the strong lines are broadened in their centers but stripped of their wings (this is how they are distinguished from the lines of dwarf star spectra).

For a number of stars, however, large discrepancies are observed between the turbulence velocities, determined from the equivalent widths, (i.e., from the curve of growth), and from the absorption line half-widths. For example, in a study of the δ Canis Majoris star a value of v_t = 5 km/sec was derived from the equivalent width and a value of v_t = 30 km/sec from the half-width. To explain these discrepancies it has been proposed that the turbulence elements can have different sizes within stellar atmospheres. If the linear dimensions of the turbulence elements are small compared with the thickness of the atmosphere, then the turbulence motion exerts absolutely the same effect on the absorption line as thermal motions. In this case the turbulence velocities found from the equivalent widths and from the absorption line half-widths should not be different. If, however, the linear dimensions of the turbulent elements are greater than the atmosphere thickness, then the turbulent motion should broaden the absorption lines but it cannot increase their equivalent widths. In this case the effect of turbulence on the absorption line is similar to

the effect of star rotation. According to this hypothesis, the turbulent motion in the atmosphere of δ Canis Majoris approaches that of the second case.

A detailed study of turbulence in stellar atmospheres has been made by O. Struve and S. S. Huang. In particular, they were concerned with determining the size of the turbulence elements on the basis of the relationship between the equivalent width and half-width of an absorption line (see, for example, [8]). /160

4. Rotation of stars. The rotation of a star about its own axis can be ascertained from the form of the spectrum. If a star is rotating, then the portion of the disk, receding from us, gives absorption lines shifted toward the red end of the spectrum, and the portion of the disk, approaching us, gives lines shifted toward the ultraviolet. On the whole, a rotating star gives an absorption line that is broadened with respect to the absorption line in the spectrum of a stationary star. Star rotation obviously causes a broadening of all the lines. Therefore the rotation effect is easy to differentiate from, for example, the Stark effect, which causes a noticeable broadening of only those lines which are especially sensitive to an electric field.

Let us first consider the problem of the effect of rotation on the absorption line profile. Let the rotational velocity of the star at the equator to equal to v, and let the axis of rotation form an angle with the line of sight. Let us take a rectangular coordinate system x, y, z with its origin at the center of the star, with the z-axis directed toward the observer, and with the y-axis lying in the plane passing through the axis of rotation and the line of sight (Fig. 14). To simplify the notation, we will assume that the star radius is equal to unity.

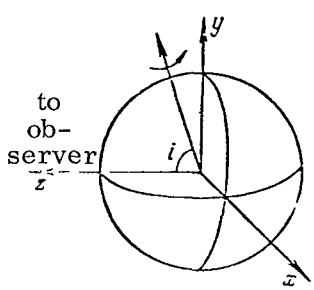

Figure 14.

We will denote by $I(x, y, \nu - \nu_0)$ the intensity of the radiation coming from a point with coordinates x, y on the disk of a nonrotating star within a line at a distance of $\nu - \nu_0$ from its center. If the star is rotating, then in the expression for the radiation intensity one must substitute, instead of ν_0, the central frequency for the point being considered, which is equal to $\nu_0 + \nu_0 v_z/c$, where v_z is the radial velocity of this point. It is easy to derive that

$$v_z = -xv \sin i. \tag{13.17}$$

Therefore the intensity of the radiation, coming from the point with coordinates x, y on the rotating stellar disk, will be $I(x, y, \nu - \nu_0 + \nu_0 \frac{v}{c} x \sin i)$ at the frequency ν.

Furthermore, let us denote the intensity of the continuous spectrum radiation, coming from the point with the coordinates x, y on the stellar disk, by $I_0(x, y)$. Then the ratio of the energy, emitted by the star at frequency ν within

the line, to the energy, emitted in the continuous spectrum by the star, will be equal to /161

$$\bar{r}(\nu-\nu_0)=\frac{\int_{-1}^{+1}dx\int_0^{\sqrt{1-x^2}}I\left(x,y,\nu-\nu_0+\nu_0\frac{v}{c}x\sin i\right)dy}{\int_{-1}^{+1}dx\int_0^{\sqrt{1-x^2}}I_0(x,y)\,dy}. \tag{13.18}$$

The profile of the absorption line in the spectrum of the rotating star is also defined by this formula.

With an increase in the rotational velocity of the star, the absorption line width increases. At the same time, however, the line becomes shallower. This circumstance is related to the fact that the equivalent line width does not change: at any rotational velocity it is equal to the equivalent line width in the spectrum of the nonrotating star. This result, which is understandable from physical considerations, is also easy to derive from Eq. (13.18).

To simplify Eq. (13.18) let us make the assumption that the absorption line profile is the same in all parts of the disk of the nonrotating star, i.e.,

$$I(x,\ y,\ \nu-\nu_0)=r(\nu-\nu_0)I_0(x,\ y). \tag{13.19}$$

Substituting (13.19) into (13.18), we obtain

$$\bar{r}(\nu-\nu_0)=\int_{-1}^{+1}r\left(\nu-\nu_0+\nu_0\frac{v}{c}x\sin i\right)A(x)\,dx, \tag{13.20}$$

where

$$A(x)=\frac{\int_0^{\sqrt{1-x^2}}I_0(x,y)\,dy}{\int_{-1}^{+1}dx\int_0^{\sqrt{1-x^2}}I_0(x,y)\,dy}. \tag{13.21}$$

Let us express the distance from the line center at the maximum Doppler widths, caused by rotation, i.e., let us set

$$t=\frac{\nu-\nu_0}{\nu_0}\frac{c}{v\sin i}, \tag{13.22}$$

and instead of $r(\nu - \nu_0)$ and $\bar{r}(\nu - \nu_0)$ we will simply write r(t) and $\bar{r}$(t). Then, instead of Eq. (13.20) we obtain /162

$$\bar{r}(t) = \int_{-1}^{+1} r(t - x) A(x)\, dx. \tag{13.23}$$

Equation (13.23) makes it possible to calculate the line profile in the spectrum of a rotating star from the line profile in the spectrum of a nonrotating star if the quantity A(x) is known. In order to determine this quantity, it is necessary to know the continuous spectrum radiation intensity distribution over the stellar disk. Let us adopt, as usual,

$$I_0 = C(1 + \beta \cos \vartheta), \tag{13.24}$$

where ϑ is the angular distance from the center of the disk. Since $\sin \vartheta = x^2 + y^2$, then instead of (13.24) we have

$$I_0(x, y) = C(1 + \beta\sqrt{1 - x^2 - y^2}). \tag{13.25}$$

Substituting (13.25) into (13.21) and performing the integration, we obtain

$$A(x) = \frac{\frac{2}{\pi}\sqrt{1 - x^2} + \frac{\beta}{2}(1 - x^2)}{1 + \frac{2}{3}\beta}. \tag{13.26}$$

It is obvious that the quantity A(x) defines the line profile in the spectrum of a rotating star if the line width in the spectrum of a nonrotating star is very small, If, however, this width is not small (i.e., compared with the width of the rotation-broadened line), then Eqs. (13.23) and (13.26) must be used to determine the line profile in the spectrum of the rotating star.

The formulas that have been presented allow one to determine the star rotation velocity (more precisely, the quantity v sin i) from the line profiles. To do this, one takes the line profile in the spectrum of a nonrotating star of the spectral class of interest and constructs, with the aid of Eq. (13.23), the rotation-broadened line profiles for different values of the parameter v sin i. A /163
comparison of these profiles with the line profile in the spectrum of the given star permits one to determine the desired value of v sin i.

The profile of the helium 4026 Å line in the spectrum of the nonrotating star i Hercules, as well as the rotation-distorted line profiles found with Eq. (13.23), are shown in Fig. 15 as an example. It should be noted that a reliable determination of the quantity v sin i is possible only when it attains a value of the order of several tens of kilometers per second. Otherwise, it is difficult to isolate the rotation effect from other effects that influence the line profile.

The values of v sin i have been determined for many stars by this method. It was found that only stars of the early spectral classes—O, B, A and early F—possess a high rotational velocity. Type Be stars rotate the fastest (with velocities up to 500-600 km/ /sec). The rotational velocities of types B and A stars amount to 400-500 km/sec, and of type F stars—to 200-300 km/sec. Stars of classes later than F5 do not exhibit a pronounced rotation. Conversion from v sin i values to rotational velocities v is accomplished statistically with the assumption that the axis of rotation is uniformly distributed in direction.

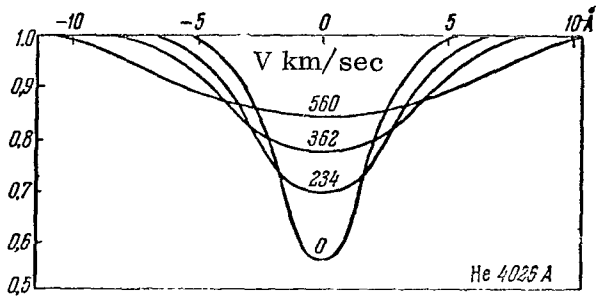

Figure 15.

Fast rotation of a star exerts a significant effect on the physical conditions in the stellar atmosphere since centrifugal force is added to the forces acting in the atmosphere. Since the centrifugal force depends on the latitude, then the physical conditions in the atmosphere of a rotating star also depend on the latitude. In particular, the temperature and density distribution in the atmosphere must be different at different latitudes. Moreover, there must also be differences in the degree of atomic excitation and ionization, and, consequently, in the form of the spectrum also. Calculations show that the spectra, forming at the equator and at the pole, can correspond to very different spectral subclasses. And since we observe the spectrum of the entire star, it must exhibit the features of each subclass. The relative role of these features obviously depends on the inclination angle of the axis of rotation to the line of sight. The observed spectra of some stars actually exhibit features of different subclasses. To explain such spectra one can assume that in these cases we are dealing with stars that are rotating rapidly and whose polar regions are turned toward us (otherwise the relative role of the spectra of the polar regions will be small). /164

For each star there exists a critical rotational velocity v_0 at the equator at which the gravitational force is balanced by the centrifugal force. This velocity is defined by the formula

$$v_c^2 = G\frac{M}{R}, \tag{13.27}$$

where M is the stellar mass, R is its radius and G is the gravitational constant. As an example let us take a class B5 star for which $M = 6M_\odot$ and $R = 4R_\odot$. For this star Eq. (13.27) gives $v_c = 530$ km/sec.

If the rotational velocity of the star at the equator exceeds the velocity v_c, then an outflow of material will occur from the equatorial region, leading to the

formation of a gaseous ring rotating around the star. Class Be stars, in the opinion of Struve, have such rings. This opinion is corroborated by the fact that the rotational velocities of class Be stars are the highest and are close to the velocity v_c. Moreover, the existence of a gas ring near the star can explain the presence of emission lines in the stellar spectrum (see Chapter VI). In reality, the ejection of material from a star occurs not because of the rotation but due to the effect of other mechanisms (for example, in the form of prominences). A rapid stellar rotation, however, facilitates this process.

5. Magnetic fields of stars. The study of the magnetic fields of stars is based on the Zeeman effect, comprising, as is known, a splitting of the spectral lines in a magnetic field. In the simplest case a single line is split into three components in a magnetic field, one of which is undisplaced while the other two are displaced an equal distance on both sides of it. The amount of displacement is proportional to the field intensity H. All line components are polarized, with the character of the polarization depending on the angle between the field direction and the line of sight. In more complicated cases the line splits into a greater number of components.

The absorption lines in stellar spectra are usually considerabley broadened because of a number of reasons (thermal motion of the atoms, Stark effect, turbulence, star rotation). Therefore the Zeeman line components merge with each other even at a very high magnetic field intensity. In order to detect the magnetic field, it is necessary to employ special methods based on the use of /165 polarized light analyzers. With the aid of such analyzers it is possible, to some degree, to isolate the Zeeman line components from each other and to determine the field intensity from their displacement.

The magnetic field was first detected by Babcock in 1947 for the star 78 Virginis, belonging to the spectral class A2p. Babcock assumed that the strong magnetic field is associated with a rapid rotation of the star. It is, however, very difficult to detect the Zeeman effect from rotation-broadened lines. Therefore a class A star with narrow spectral lines, about which one can surmise that it is rotating very rapidly, like other class A stars, but is viewed from the polar side, was selected for observations. In subsequent years Babcock extended his observations, and at the present time his catalog (see [8]) contains information on 89 "magnetic stars".

An examination of the aforementioned catalog leads to several conclusions.

1. The magnetic field intensity at the surface of a star is about 1000 gauss. However, such values of H are evidently much greater than the mean value since it is impossible to measure field intensities of less than 200 gauss with the current method.

2. Most of the stars in the catalog (70 of 89) belong to spectral class A (more precisely, to the interval B8-F0). Here, however, the selection of observations is affected, to a considerable extent, by the preferential choice of stars similar to the star 78 Virginis.

3. Nearly all magnetic stars have "peculiar" spectra in which some lines are suppressed and others are enhanced with respect to normal spectra.

4. The magnetic fields of all the stars studied are varying. In some cases the field changes periodically; in most cases, however, it changes irregularly.

The facts enumerated have considerable value for clarifying the problem of the character of stellar magnetic fields and of their origin. A number of hypotheses have been proposed up to now. Some of them relate the presence of magnetic fields to stellar rotation.

For a solution of the various problems of stellar magnetism, there must first of all be an increase in observational data. Moreover, a theory must be developed for the formation of absorption lines in a magnetic field. This theory is also required for studying the magnetic fields of sun spots, and a number of investigations have recently been carried out (see Section 15).

14. Stars of Different Spectral Classes /166

1. Temperature dependence of the spectrum. Up to now we have been concerned with the problem of how the spectrum of a star is formed. Now we will briefly discuss the entire ensemble of stellar spectra.

As is known, in a first approximation stellar spectra form a linear sequence. All spectral properties (for example, equivalent line widths) vary smoothly along the sequence. This is explained by the fact that the stellar spectrum is primarily a function of one parameter—temperature. With a change in temperature the degree of atomic excitation and ionization in the stellar atmosphere is altered, so that line intensities also change.

In practice, all stellar spectra are divided into several classes. Arranged in the order of decreasing temperature, these classes are: O—B—A—F—G—K—M. At the end the spectral sequence divides: spectral classes R—N (with carbon and cyanogen bands) and spectral class S (with zirconium oxide bands) are distinguished in addition to spectral class M (with titanium oxide bands). This branching is evidently caused by a difference in the chemical composition of the stars.

Let us trace the change in spectrum as the stellar temperature increases. In the spectra of the coldest stars (class M and others), molecular bands and the lines of neutral metal atoms are present. With an increase in temperature, the molecules dissociate so that the molecular bands disappear (class K). Moreover, the metals are gradually ionized. The very complex class G spectra contain a vast number of lines of neutral and ionized metals. With a further temperature increase the intensity of the lines of the ionized metals increases (class F). In class A the Balmer series of hydrogen lines are the most intense. Helium lines are present in class B (since a fairly high temperature is required for excitation of the helium lines lying in the visible portion of the spectrum. Finally, the ionized helium lines become intense in class O.

One can also trace the variation in the intensities of the individual lines as the stellar temperature increases. For example, let us take the lines forming

through the transition of electrons from the excited state of a neutral atom. At low temperatures these lines are very weak since most atoms exist in the ground state. With an increase in temperature the atomic excitation gradually increases, which implies an increase in the equivalent widths of the lines being considered. The increase in the number of atoms in the excited state continues, however, only up to a certain temperature. With a further increase in temperature the number /167 of atoms in the excited state decreases because of the transition of atoms into the ionized state. Therefore the equivalent widths of the lines being considered decreases. Thus, as the star temperature increases, the equivalent widths of lines, arising from the transition of electrons from the excited state of a neutral atom, increase at first and then decrease.

The equivalent widths of the lines of ionized atoms change similarly with a rise in temperature (i.e., they increase at first and then decrease). Only the lines of the principal series of the neutral atom behave otherwise with an increase in temperature: their equivalent widths decrease (if the formation of molecules at low temperatures is disregarded).

The qualitative considerations that have been discussed are confirmed by appropriate calculations. They are based on using the Boltzmann and Saha formulas, which determine the degree of atomic excitation and ionization. As we recall, these formulas have the form

$$\frac{n_i}{n_1} = \frac{g_i}{g_1} e^{-\frac{\chi_1 \chi_i}{kT}}, \tag{14.1}$$

$$n_e \frac{n^+}{n_1} = f e^{-\frac{\chi_1}{kT}}, \tag{14.2}$$

where

$$f = \frac{g^+}{g_1} \frac{2(2\pi mkT)}{h^3}. \tag{14.3}$$

Saha [19] explained the spectral classification as a result of applying Eqs. (14.1) and (14.2) to stellar atmospheres.

We will use these formulas for calculating the temperature dependence of the equivalent line width. Just as before, let us consider a line arising from the transition of an electron from the excited state of the neutral atom. When the Eddington model is used, the equivalent line width will be greater, the greater the ratio n_i/α_ν, where n_i is the number of atoms in the i-th state in 1 cm^3 and α_ν is the continuous spectrum volume absorption coefficient (see Section 12).

Let us represent the quantity α_ν in the form

$$\alpha_\nu = \varkappa_\nu \rho, \tag{14.4}$$

where $\varkappa_\nu$ is the absorption coefficient calculated per unit mass, and ρ is the density. Furthermore, let us denote by q the fraction of a given element in the total density ρ, i.e., let us set /168

$$q\rho = m_a n, \tag{14.5}$$

where n is the number of atoms of the given element in 1 cm^3, and m_a is the mass of a single atom. With the aid of (14.4) and (14.5) we obtain

$$\frac{n_i}{\alpha_\nu} = \frac{q}{m_a \varkappa_\nu} \frac{n_i}{n}. \tag{14.6}$$

We will assume that $n = n_1 + n^+$, i.e., we will ignore the number of excited atoms as well as the number of doubly ionized atoms. Then, using Eqs. (14.1) and (14.2), we find

$$\frac{n_i}{\alpha_\nu} = \frac{q}{m_a \varkappa_\nu} \frac{\frac{g_i}{g_1} e^{-\frac{\chi_1 - \chi_i}{kT}}}{1 + \frac{f}{n_e} e^{-\frac{\chi_1}{kT}}}. \tag{14.7}$$

This formula also expresses the dependence of the quantity n_i/α_ν on the temperature T. With the aid of the curve of growth, relating the equivalent line width W and the quantity n_i/α_ν, we can also find the dependence of W on T.

Analogous formulas can also be derived for lines of the ionized atoms.

From what has been said it follows that the temperature of the stellar atmosphere can be determined from the form of the stellar spectrum (more precisely, from the equivalent absorption line widths). This is called the ionization temperature.

Fowler and Milne [20] proposed the following method for determining the ionization temperatures. Using Eq. (14.7), let us find the temperature at which the quantity n_i/α_ν (and, therefore, the quantity W) has a maximum, and let us assign this temperature to a star of that spectral class in which the given line actually attains a maximum equivalent width. Assuming that $\varkappa_\nu$ = const and $p_e = n_e kT$ = const, from Eq. (14.7) we obtain the following equation for determining the ionization temperature:

$$p_e = \frac{\chi_i + \frac{5}{2} kT}{\chi_1 - \chi_i} f kT e^{-\frac{\chi_i}{kT}} \tag{14.8}$$

The aforementioned authors, after having solved Eq. (14.8) (and analogous equations for the lines of ionized atoms) in terms of T and after having compared these T values with the data of observations, obtained a scale of ionization temperatures. A portion of their results is given in Table 16. In it, it is assumed that $p_e = 10^{-6}$ atm for all stars. /169

TABLE 16. IONIZATION TEMPERATURES OF STARS

Spectral class	Line maximum	Ionization temperature
K5	Na, $1^2P - m^2D$	3900°
G5	Mg, $1^3P - m^3S$	5250
G0	CaII, $1^2S - m^2P$	6290
A0	H, Balmer ser.	10000
B2	He, $2^3P - m^2D$	16100
B1	SiIII, OII	19000
O5	HeII, λ 4686, Pickering ser.	35000

However, the ionization temperatures found by this method correspond only on the temperature T but also on the parameters $\varkappa_\nu$ and n_e. These parameters, in turn, are expressed in terms of the temperature T and the gravitational acceleration g. Therefore the equivalent line width also depends not only on T but also on g. Of course, the quantity W depends much more heavily on T than on g, which also explains the existence of the linear sequence of stellar spectra in a first approximation. But the dependence of W on g must also be taken into consideration.

2. Effect of gravitational acceleration on the spectrum. With the aid of Eq. (14.7) one can plot graphs giving the equivalent line width W in the form of a function of the temperature T. These graphs are different for different gravitational accelerations g (because of the dependence of the quantities $\varkappa_\nu$ and n_e not only on T but also on g). Here it turns out that the greater g, the greater the temperature required to achieve lines of maximum equivalent width.

In the atmospheres of giant stars the g values are much less than in the atmospheres of dwarf stars. Therefore for a given equivalent line width the temperature of a giant should be less than the temperature of a dwarf. In other words, giant stars should be colder than dwarf stars of the same spectral class. This theoretical conclusion is qualitatively confirmed by the results by observations. However, the differences, from observations, in the spectra of giants and dwarfs are much greater than those predicted by the theory based on the use of Eq. (15.7) and an analogous formula for n^+/α_ν. To considerable extent this is explained by the fact that a change in the gravitational acceleration affects the equivalent line width not only because of a change in the degree of atom ionization but also because of a change in the role of pressure effects which directly influence the line width. /170

The fact that the equivalent line width depends not only on the temperature T, but also on the gravitational acceleration g, requires refinements in the spectral classification. Each stellar spectrum must be characterized by the specification of not one parameter, but two, related in a definite fashion to T and g. In other words, the spectral classification must be two-dimensional rather than one-dimensional. Empirical two-dimensional stellar spectrum classifications

have been proposed in several papers; however, from a theoretical viewpoint they have not been adequately substantiated.

Let us note that the influence of the gravitational acceleration force on the stellar spectrum is usually called an absolute magnitude effect. This is explained by the fact that for a given temperature the gravitational acceleration g is uniquely associated with a stellar luminosity L. In fact, we have

$$g = G\frac{M}{R^2} \tag{14.9}$$

and

$$L = 4\pi R^2 \sigma T_e^4. \tag{14.10}$$

Moreover, the quantities L and M are related by an empirical massluminosity relationship of the type

$$L \sim M^n, \tag{14.11}$$

where n is some constant (of the order of 3-4). When T_e = const, from the formulas that have been presented we obtain

$$g \sim L^{-1+\frac{1}{n}}. \tag{14.12}$$

Thus, g is greater, the smaller L.

The fact that the effect of gravitational acceleration on the lines of neutral and ionized atoms is different is of considerable interest. This makes it possible to determine, from the ratio of the equivalent line widths of an ion and a neutral atom in the spectrum of a star, the gravitational acceleration at its surface and, /171 therefore, the absolute stellar magnitude. The distance to a star can also be found by a comparison of the absolute stellar magnitude with its visual magnitude. The method for determining the so-called spectral parallaxes is based on this. This method began to be used some time ago and has yielded several valuable results. In practice, for each spectral class those ion and neutral atom lines are selected for which the intensity ratio is especially sensitive to the absolute magnitude.

3. Stars of different spectral classes. The hydrogen Balmer lines are very intense in the spectra of stars of the early classes. As seen from Table 16, they reach maximum intensity in spectral class AO, i.e., at a temperature of about 10,000°. With a decrease in temperature these lines weaken because of a decrease in the number of atoms in the second state. With an increase in temperature the lines weaken because of an increase in atom ionization.

The profiles and equivalent widths of the Balmer lines in the spectra of giants and dwarfs are significantly different. This attests to the strong effect of gravitational acceleration on the Balmer lines. In a given case, however,

this effect is caused not so much by a change in the degree of atom ionization as by the Stark effect. As one goes from the giants to the dwarfs, the solid matter in the atmosphere increases so that the influence of the Stark effect is enhanced. For this reason the equivalent widths of the Balmer lines are appreciably greater in the spectra of dwarfs than in the spectra of giants.

The strong influence of gravitational acceleration on the Balmer lines provides the possibility of determining the value of g for a given star by comparing the theoretical and observed line profiles. The theoretical profiles must be determined on the basis of photosphere model calculations for an effective stellar temperature and for different g values. A comparison of theory with observations makes it possible to select the most suitable g value. As already stated above, knowing g makes it possible to find the stellar luminosity and then its parallax. This constitutes one method for determining the spectral parallaxes of stars.

From the spreading of the Balmer lines due to the Stark effect one can also roughly estimate the average electron density value in a stellar atmosphere. With the Stark effect taken into account, Eq. (8.46) was derived above for the absorption coefficient in the wings of the Balmer lines. Using the fact that in the atmospheres of hot stars the number of ions is equal to the number of free electrons (since the hydrogen is completely ionized), we can rewrite this expression in the form /172

$$k_\lambda = \frac{4\pi}{3} C \frac{e^{3/2} n_e}{(\lambda - \lambda_0)^{3/2}}. \tag{14.13}$$

For simplicity we will assume that the absorption lines are formed in the presence of local thermodynamic equilibrium. Then the quantity r_λ, characterizing the line profile, is defined by Eq. (9.19). From this formula we obtain

$$1 - r_\lambda = A \frac{\sigma_\lambda}{\sigma_\lambda + \alpha_\nu}, \tag{14.14}$$

where

$$A = \frac{\beta_\nu}{\frac{3}{2}\frac{\alpha_\nu}{\bar{\alpha}} + \beta_\nu}. \tag{14.15}$$

The quantity σ_λ, entering into Eq. (14.14), represents the volume line absorption coefficient, equal to $\sigma_\lambda = n_2 k_\lambda$, where n_2 is the number of hydrogen atoms in the second state in 1 cm^3. Using Eq. (14.13), instead of Eq. (14.14) we find

$$1 - r_\lambda = \frac{A}{1 + \left(\frac{\lambda_0 - \lambda_0}{D}\right)^{3/2}}, \tag{14.16}$$

where

$$D = \left(\frac{4\pi}{3} C e^{3/2} \frac{n_2 \bar{n}_e}{\alpha_\nu}\right)^{2/3} \tag{14.17}$$

and $\bar{n}_e$ denotes the average free electron density in the atmosphere.

The profile of the absorption line, broadened by the Stark effect, is determined by Eq. (14.16). Strictly speaking, this formula is only applicable to the wings of the line. For the central portions of the line, however, the values of the quantity σ_λ are not significant since for them $\sigma_\lambda \gg \alpha_\nu$ and, consequently, the quantity $\sigma_\lambda/(\sigma_\lambda + \alpha_\nu)$ is close to 1.

With the aid of Eq. (14.16) the following expression is derived for the equivalent line width:

$$W = \int (1 - r_\lambda)\, d\lambda = 2.64AD. \tag{14.18}$$

The equivalent width W and the quantity A, representing the center line intensity (since $A \approx 1 - r_{\lambda_0}$), can be found for each Balmer line from observations. Using these values of W and A, from Eq. (14.18) one can find the quantity D and, therefore, the product $n_2 \bar{n}_e/\alpha_\nu$. /173

The quantity n_2/α_ν must be found beforehand in order to determine the electron density $\bar{n}_e$. To do this, one can use the high terms of the Balmer series. Since the absorption coefficient decreases rapidly with an increase in line number, then for sufficiently high series terms the inequality $\sigma_\lambda \ll \alpha_\nu$ will be satisfied. In this case the equivalent line width is equal to

$$W = A \frac{n_2}{\alpha_\nu} \int k_\lambda d\lambda = A \frac{n_2}{\alpha_\nu} \frac{h}{\nu_0} B_{2k}. \tag{14.19}$$

Equation (14.19) makes it possible to find the quantity n_2/α_ν, and Eq. (14.17)—the quantity $\bar{n}_e$.

This method of determining the quantity $\bar{n}_e$ has, however, the disadvantage that the Balmer lines for which the inequality $\sigma_\lambda \ll \alpha_\nu$ is satisfied cannot be observed in real life because of the merging of these lines, caused by pressure effects. As we recall, another method of finding the quantity $\bar{n}_e$ is based just on determining the number of the last observable Balmer line. A comparison of the different methods of determining the average electron density in the atmospheres of hot stars can be found in I. M. Kopylov's paper [21].

Intense lines of helium, which, as is known, follows hydrogen in abundance, are present in the spectra of class B and O stars in addition to the hydrogen

lines. The helium spectrum is much more complex than the hydrogen spectrum; however, it has been studied in considerable detail. Many helium lines are subject to the Stark effect (quadratic in some cases, linear in others) and from the spreading of these lines one can draw a conclusion concerning the gravitational acceleration in the stellar atmosphere. The influence of the Stark effect on the line of ionized helium, present in the spectra of class O stars, can be studied quantitatively in the same way as for the hydrogen lines.

As already stated (in Section 5), radiation scattering by free electrons plays some role in energy transfer in the surface layers of hot stars. This process can markedly influence the energy distribution in the continuous stellar spectrum. In some cases it is also necessary to take this into account in studying the line spectra of hot stars.

4. Stars of the late spectral classes. Numerous metal lines are present in the spectra of stars of the late classes. Since the excitation potentials of metals are relatively low, there are quite a few atoms in the excited states. With /174 electron transitions from these states, lines appear in the visible portion of the spectrum. At very low temperatures, a large number of molecules is also formed in stellar atmospheres. Therefore intense molecular bands are seen in the spectra of stars of the latest classes.

The "dissociation formula", analogous to the ionization formula (14.2), is used to determine the number of molecules in the stellar atmosphere. Let the molecule AB be formed when the atoms A and B collide. Let us denote the concentrations of these atoms and molecules by n_A, n_B and n_{AB}. In the presence of thermodynamic equilibrium we have

$$\frac{n_A n_B}{n_{AB}} = \frac{g_A g_B}{g_{AB}} \left(\frac{2\pi M}{h^2}\right)^{3/2} \frac{(kT)^{1/2} h^2}{8\pi^2 I} \left(1 - e^{-\frac{h\nu_0}{kT}}\right) e^{-\frac{U}{kT}}, \tag{14.20}$$

where g_A, g_B, g_{AB} are the statistical weights of the ground states of the atoms A and B and of the molecules AB, M is the reduced mass, I is the moment of inertia, ν_0 is the fundamental oscillation frequency of the atoms in the molecule, U is the dissociation energy of the molecule. The quantities M and I, as is known, are equal to

$$M = \frac{M_A M_B}{M_A + M_B}, \qquad I = M r_0^2, \tag{14.21}$$

where r_0 is the equilibrium distance between the nuclei of atoms A and B.

Values of the parameters entering into Eq. (14.20) are listed in Table 17 for some molecules. Here, the dissociation energy U is given in electron volts, the reduced mass M—in atomic mass units, the distance between nuclei r_0—in angstroms.

Calculations from Eq. (14.20) show that in the atmospheres of cold stars (with temperatures of about 2000-3000°) many different molecules should be

found. With an increase in temperature the number of molecules in the atmospheres decreases. However, even at temperatures of about 5000° there should still be a sufficient number of molecules in the atmospheres so that they could be detected through observations. In fact, a large number of weak molecular bands is observed in the solar spectrum.

TABLE 17. SOME MOLECULAR PARAMETERS

Molecule	Dissociation energy	Reduced mass	Distance between nuclei
H_2	4.48	0.504	0.742
C_2	3.6	6.002	1.312
CH	3.47	0.930	1.120
CO	11.11?	6.858	1.209
CN	7	6.464	1.172
NH	3.6	0.940	1.038
O_2	5.08	8.000	1.207
OH	4.37	0.948	0.971
TiO	6	11.998	1.620
ZrO	7	13.584	1.42

To analyze the molecular spectra of stars it is necessary not only to determine the number of molecules in the atmospheres, but also to know the structure of the spectra and the band absorption coefficients. For most molecules such information is only approximate at the present time. Nevertheless, using the available data, one can calculate the change in the intensities of the bands of various molecules with a change in stellar temperature. If it is assumed that stellar atmospheres are not markedly different from the solar atmosphere in chemical composition, then the calculated molecular spectra agree, in general /175 features, with the molecular spectra of class G—K—M stars.

It is significant that the molecular spectra of stars are inherently dependent on the pressure in the atmosphere (since the number of molecules n_{AB} is proportional to the numbers of atoms n_A and n_B). Therefore the band intensities of the same molecules are very different in the spectra of giants and dwarfs. Thus, one can draw a conclusion on the gravitational acceleration in the atmospheres from the character of the molecular spectra of stars.

As already noted, a branching of the spectral sequence occurs in the late class region, which is explained by differences in the chemical composition of stellar atmospheres. In the atmospheres of class M stars, oxygen is more abundant than carbon so that the oxygen is combined primarily with titanium, forming TiO molecules. In the atmospheres of class R and N stars, however, carbon is more abundant than oxygen. Therefore the oxygen combines not with titanium but with carbon, forming a CO molecule (not having a band in the visible portion of the spectrum). Other carbon atoms enter into CH, CN and C_2 molecules, characteristic of class R and N spectra.

5. White dwarfs. The spectra of white dwarfs are drastically different from the spectra of stars of the main sequence. Their primary feature is a very small number of absorption lines. An appreciable portion of the white dwarfs do not generally contain absorption lines in their spectra (these spectra belong to the class DC). In the spectra of class DB white dwarfs only some helium lines are present. Most of the white dwarfs that have been studied possess class DA spectra in which only a few of the first terms of the hydrogen Balmer series are /176 present. The H and K lines of Ca II and some Fe I lines are also present in the spectra of class DF, DG and DK white dwarfs.

The study of the spectra of white dwarfs is fraught with considerable difficulty because of the low luminosities of these stars. Only recently, Greenstein, with the aid of a 200-inch telescope, has obtained the spectrograms of several white dwarfs, making it possible to measure the absorption line profiles and equivalent widths (see [8]).

Greenstein assumes that white dwarfs occur in two sequences. The stellar atmospheres of one of them consist primarily of hydrogen (spectral classes DA, DF, DK), and the stellar atmospheres of the second—primarily of helium (spectral classes DB and DC). Hot stars of the second sequence contain helium lines in their spectra and belong to class DB. In the spectra of cold stars of the second sequence, however, no helium lines can be observed and these stars belong to class DC.

The basic features of the spectra of white dwarfs are explained by the enormous gravitational forces in their atmospheres (of the order of 10^6-10^{10} cm/ /sec^2). This leads to high particle densities in the atmospheres and, consequently, to a strong Stark effect. For this reason the Balmer lines in the spectra of white dwarfs are very broad (their equivalent widths amount to tens of angstroms). Moreover, the high terms of the Balmer series are merged and we see only a few of the first terms of the series (usually no more than five). The weakness of the metal lines in the spectra of white dwarfs is more difficult to explain. The gravitational separation of atoms, i.e., the fact that heavy atoms occur in deeper layers of the atmosphere than the light ones, may play a role here.

The profiles and equivalent widths of the Balmer lines in the spectra of white dwarfs can be calculated approximately from Eqs. (14.16) and (14.18), derived with the Stark effect taken into account. The quantities A and D, entering into these formulas, depend on the physical conditions at the "effective" level of line formation. We will assume that the continuous spectrum optical depth at this level is equal to 1/3, i.e.,

$$\alpha_\nu \Delta r = \frac{1}{3}, \tag{14.22}$$

where Δr is the "thickness of a uniform atmosphere." Furthermore, from the equation of hydrostatic equilibrium we have

$$\Delta r = \frac{kT}{\mu m_H g}, \tag{14.23}$$

where μ is the average molecular weight. Using, also, the usual formula relat- /177
ing the temperature to the optical depth, we obtain

$$T = T_0\left(1 + \frac{\bar{\alpha}}{2\alpha_\nu}\right)^{1/4}, \tag{14.24}$$

where T_0 is the surface temperature of the star. If values of the quantities T_0 and g are specified, as well as the chemical composition of the atmosphere, then with the aid of the last three formulas one can determine the quantities Δr, ρ and T at the level of interest (values of the absorption coefficient α_ν as a function of ρ and T are given in special tables). Then the desired quantities A and D for a given line can be found.

As a result of such calculations the profiles and equivalent widths of the Balmer lines have been determined for stars with high gravitational forces in the atmospheres [22]. Graphs, giving the equivalent widths of the H_γ line as a function of the quantity $\vartheta = 5040/T_0$, are presented in Fig. 16 for different g values. From the figure it is seen that the equivalent line width increases with an increase in g. This is explained by the density increase in the atmosphere and, consequently, by the increased Stark effect. The graphs presented also show that the quantity W is strongly dependent on the temperature T_0.

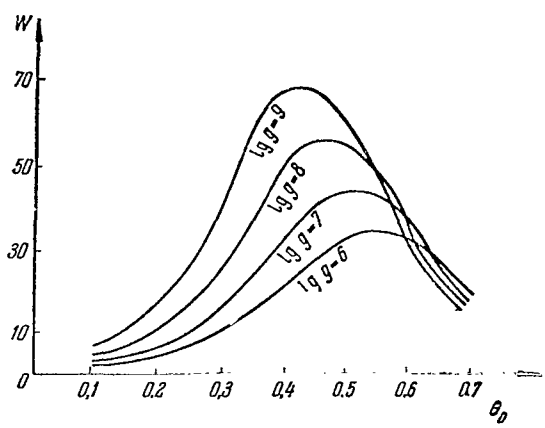

Figure 16.

A diagram, taken from Greenstein's paper and plotted on the basis of observational data, is shown in Fig. 17 for comparison. In it, values of the equivalent line width are plotted along the ordinate axis, and along the abscissa axis—values of the color index U-V. Since the quantity U-V is an approximately linear function of the quantity ϑ_0, then from a comparison of Figs. 16 and 17 we can draw a conclusion concerning the approximate agreement of theory with observations. /178

The absorption line profiles, calculated from Eq. (14.16), are very different for different temperatures. At high T_0 values, the quantity A is small, and the quantity D is large, i.e., the line is wide but weak. The smallness of the quantity β_ν at high temperatures and by the large values of the quantity $\alpha_\nu/\bar{\alpha}$ at high temperatures and for high gravitational forces. Absorption lines are difficult to detect in the spectra of very hot white dwarfs. At low temperatures the quantity D is small, i.e., the line is narrow. Such an absorption line character, determined theoretically, also agrees with observational data.

More precise calculations of the Balmer line profiles in the spectra of white dwarfs have been made in Weideman's paper [23] on the basis of stellar photosphere model calculations. The quantities T_0 and g for a number of white dwarfs are estimated by a comparison of theoretical and observed H_γ line profiles.

The question of the effect of star rotation on the absorption line profile in the spectra of white dwarfs is of interest. This problem is, however, very difficult since the lines in the spectra of white dwarfs are considerably broadened by the Stark effect. Only very high velocity values can be measured. White dwarfs, to be sure, can in principle rotate very rapidly since the escape velocity for them amounts to several thousand kilometers per second.

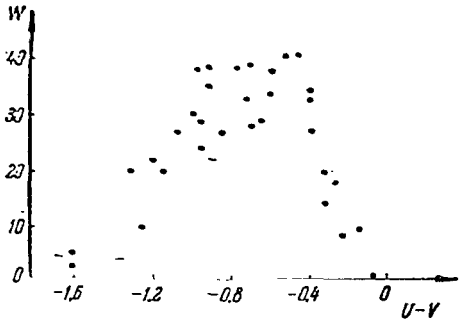

Figure 17.

One can even assume that the rapid rotation of white dwarfs makes the absorption lines in their spectra unobservable. Calculations show that this is hardly possible in the case of hydrogen lines with a large equivalent width. Narrower lines, however, can be completely unobservable because of the rotation. In order to show this, let us use Eq. (13.20), which allows one to determine the line profiles in the spectrum of a rotating star from the line profiles in the spectrum of a nonrotating star for different rotational velocities. Applying this formula to the line center, we can write it in the form /179

$$1-\bar{r}(0)=\int_{-1}^{+1}\left[1-r\left(\nu_0\frac{v}{c}x\sin i\right)\right]A(x)\,dx, \tag{14.25}$$

where the quantity A(x) is defined by Eq. (13.26). Using the defined equivalent line width, from (14.25) we obtain

$$1-\bar{r}(0)<A(0)\frac{W_\lambda c}{\lambda v\sin i}. \tag{14.26}$$

If $W \approx 1$ Å and $v \sin i \approx 1000$ km/sec, then from the inequality (14.26) it follows that $1-\bar{r}(0) < 0.05$. However, lines with such a low intensity are difficult to observe. Therefore it is possible that just the star rotation causes the absence of observable absorption lines of the metals in the spectra of white dwarfs (with the exception, for example, of the H and K lines of Ca II, which have an appreciable equivalent width).

It should be noted that the question of white dwarf rotation is also of interest from the viewpoint of cosmogony. According to present opinions, a white dwarf is the final stage of evolution of a star, formerly on the upper portion of the main sequence and then passing through the giant and supergiant stages. Stars of the upper portion of the main sequence, however, rotate very rapidly. Therefore an investigation of the rotation of white dwarfs should contribute to an understanding of the evolution paths of a star.

REFERENCES

1. Heitler, W. The quautum theory of radiation, Oxford, 1954 (Russ. translation: W. Heitler. The quantum theory of radiation, Izd-vo inostr. lit., 1956).
2. Coll. "Present-day problems of astrophysics and solar physics," Izd-vo inostr. lit., 1951.
3. Sobel'man, I. I. Introduction to the theory of atomic spectra, Fizmatgiz, 1963.
4. Holtsmark, J. Spectral line broadening. Über die Verbreiterung von Spectrallinien. I and II. Physik Z. 20, 162, 1919; 25, 73, 1924.
5. Griem, H., A. C. Kolb and K. Y. Shen. Stark broadening of hydrogen lines in a plasma, Phys. Rec. 116, 4, 1959. /180
6. Jager, C. de and L. Neven. Astronomical researches of the Utrecht observator, Spectroscopic data for 50 model photospheres, Recherches astronomiques de l'observatoire d'Utrecht, XIII(4), 1957.
7. Unsöld, A. The physics of stellar atmospheres, 1938 (Russ. translation: A. Unsöld. The physics of stellar atmospheres, Izd-vo inostr. lit., 1949).
8. Stellar Atmospheres, ed. J. L. Greenstein, 1960 (Russ. translation: "Stellar atmospheres," Izd-vo inostr. lit., 1963).
9. Strömgren, B. The influence of electron Capture on the contours of Fraunhofer lines. Zeitschrift für Astrophysik 10, 237, 1935.
10. Chandrasekhar, S. On the Radiative Equilibrium of a Stellar Atmosphere, Ap. J. 106, 145, 1947.
11. Hummer, D. G. Noncoherent scattering, MN 125, 21, 1962.
12. Sobolev, V. V. Noncoherent scattering of light in stellar atmospheres, Aston. Zh., 26, 129, 1949; 31, 231, 1954.
13. Busbridge, I. W. Coherent and noncoherent scattering in the theory of line formation, MN 113, 52, 1953.
14. Ueno, S. The formation of absorption lines by coherent and noncoherent scattering, Contr. Inst. Astrophys. Kyoto, N 64, 1956.
15. Houtgast, J. The variations in the profiles of strong Fraunhofer lines along a radius of the solar disk, Utrecht, 1942.
16. Menzel, D. The Theoretical Interpretation of Equivalent Bredths of Absorption Lines, A. J. 84, 462, 1936.
17. Wrubel, M. Exact Curves of Growth for the Formation of Absorption Lines According to the Milne—Eddington Model, Ap. J. 109, 66, 1949; 111, 157, 1950.
18. Pecker, J. C. The calculation of the strong absorption lines in stellar spectra, Ann. d'Astroph. 14, 383, 1951.
19. Saha, M. N. On a physical theory of stellar spectra, Proc. Roy. Soc. Lond. (A)99, 135, 1921.
20. Fowler, R. H. and E. A. Milne. The intensities of Absorption Lines in Stellar Spectra, and the Temperatures and Pressures in the Reversing Layers of Stars, MN 83, 403, 1923.
21. Kopylov, I. M. Electron densities in the atmospheres of hot stars, Izv. Krymskoy astrofiz. obs. 26, 232, 1961.
22. Sobolev, V. V. The spectra of low luminosity hot stars, Uchen. zap. LGU, No. 328, 1965.
23. Weidman, V. Effective temperature and high gravitational acceleration of white dwarfs, Zs, f. Aph. 57, 87, 1963.

CHAPTER III

THE SOLAR ATMOSPHERE

The Sun is a star, and therefore much of what has been said in the preceding chapters about stars also refers to the Sun. However, the extreme nearness of the Sun to us permits a much more detailed study of it than of the other stars. In particular, the Sun is the only star whose disk we see. This makes it possible to study the brightness distribution over the solar disk and the change in spectral lines as one goes from the center of the disk to the edge (this has already been discussed above). Moreover, observations of the solar disk reveal very important details on it: spots, granulation, etc. Unfortunatley such details are also characteristic of other stars, but we cannot observe them. The various phenomena on the solar disk will be briefly discussed at the beginning of this chapter. /181

Most of the attention in this chapter will be devoted to the outermost layers of the solar atmosphere: the chromosphere and corona. There are facts indicating that these layers exist in other stars also; however, considerable difficulty is encountered in trying to study them. In the case of the Sun, however, it is relatively easy to study the chromosphere and corona, especially on the basis of observations made during eclipses. The problem of solar radio emission, the source of which is these same outer layers of its atmosphere, is discussed briefly at the end of the chapter.

The physical processes occurring in the Sun are of immense interest for astrophysics. Moreover, a study of them has considerable practical value because of the important role the Sun plays with respect to the Earth. However, many problems in solar physics, lying outside the basic objective of this book, will not be considered in detail here. One can learn about them from appropriate monographs (see, for example, [1] and [2]). In particular, Waldmeier [3] has devoted a monograph to the Sun-Earth problem.

Recently, magnetohydrodynamics, very important for explaining some solar phenomena, has undergone considerable development. Its fundamentals have been discussed in S. B. Pikel'ner's book [4]. /182

15. General Information

1. Solar photosphere. A theoretical model of the solar photosphere can be constructed by solving the equations presented in Section 6. Up to the present time a number of such models have been derived, differing from each other in the specification of chemical composition and also in the mathematical assumptions which are made during the calculations.

TABLE 18. THEORETICAL MODEL OF SOLAR PHOTOSPHERE

$\bar{\tau}$	T	lgp	lgp_e	$\rho \cdot 10^3$	h
0,01	4650°	3,74	9,85	1,4	515
0,02	4700	4,01	0,09	2,7	428
0,04	4740	4,19	0,27	3,9	370
0,06	4790	4,30	0,36	5,0	333
0,08	4840	4,38	0,44	6,0	307
0,10	4890	4,43	0,50	6,6	290
0,20	5090	4,60	0,71	9,4	232
0,40	5400	4,77	0,96	13,1	170
0,60	5660	4,86	1,15	15,4	135
0,80	5870	4,91	1,32	16,6	115
1,00	6070	4,94	1,48	17,3	103

Commas represent decimal points.

The results of a solar photosphere model calculation, obtained by Munch, with the additions of Minnaert (see [1]), are given in Table 18 as an example. This model is one of the first in which there is taken into consideration the correct fundamental source of absorption in the solar photosphere, i.e., a negative ion of hydrogen. In the calculations, the following basic parameters were taken: $T_e = 5713°$, $g = 2.74 \cdot 10^4$ cm/sec^2, $\log A = 3.8$ (A denotes the ratio of the number of hydrogen atoms to the number of metal atoms).

The optical depth, corresponding to the average absorption coefficient, is given in the first column; in the second—the temperature T; in the third and fourth—the logarithms of the total pressure p and of the electron pressure p_e, respectively; in the fifth—the density of g/cm^3; and in the last—the geometrical altitude in kilometers, measured from some level.

An empirical photosphere model can also be constructed for the Sun. This possibility is based on the fact that in the case of the Sun we have observational data on the brightness distribution over the disk for different frequencies. As is known, the intensity of the radiation, leaving the photosphere at an angular distance of ϑ from the center of the disk, is given by the formula /183

$$I_\nu(0, \vartheta) = \int_0^\infty B_\nu(T) e^{-\tau_\nu \sec\vartheta} \sec\vartheta \, d\tau_\nu, \tag{15.1}$$

where $B_\nu(T)$ is the Planckian intensity at the temperature T and τ_ν is the optical depth at frequency ν. Assuming the temperature T is a function of τ_ν, we can consider the relation (15.1) as an integral equation for determining the quantity $B_\nu(T)$.

To derive an approximate solution of Eq. (15.1) the quantity $B_\nu(T)$ is usually represented in the form of an expression in terms of some function of τ_ν

with undefined coefficients. For example, one can set

$$B_\nu(T) = a_\nu + b_\nu\tau_\nu + c_\nu\tau_\nu^2. \tag{15.2}$$

Substituting (15.2) into (15.1) and integrating, we obtain

$$I_\nu(0, \vartheta) = a_\nu + b_\nu \cos\vartheta + 2c_\nu \cos^2\vartheta. \tag{15.3}$$

The coefficients a_ν, b_ν and c_ν are determined from the values of the quantity $I_\nu(0, \vartheta)$ obtained from observations. Instead of Eq. (15.2) Kourganoff suggested using the formula

$$B_\nu(T) = a_\nu + b_\nu\tau_\nu + c_\nu E_2\tau_\nu, \tag{15.4}$$

giving more accurate results both when $\tau_\nu \to 0$ when $\tau_\nu \to \infty$. Substituting (15.4) into (15.1), we have

$$I_\nu(0, \vartheta) = a_\nu + b_\nu \cos\vartheta + c_\nu[1 - \cos\vartheta \ln(1 + \sec\vartheta)]. \tag{15.5}$$

Equations (15.2) and (15.4) interrelate the quantities τ_ν and T, i.e., they give the optical depth at different frequencies at one and the same level in the photosphere (characterized by the temperature T). On the basis of the definition of the optical depth, we have

$$\alpha_\nu = -\frac{d\tau_\nu}{dr} = -\frac{d\tau_\nu}{dT}\cdot\frac{dT}{dr}. \tag{15.6}$$

Consequently, if the quantity τ_ν is known as a function of T, then one can also find the quantity α_ν as a function of T (accurate to within a constant coefficient /184
of dT/dr for a given layer). In this way the empirical dependence of α_ν on the frequency ν is found at different depths.

Chalonge and Kourganoff [5] made a detailed study of the absorption coefficient at different depths in the solar photosphere. The empirical dependence of α_ν on ν, found by them, was compared with the theoretical expression for α_ν due to the negative hydrogen ion. Such a comparison confirmed, without a doubt, the validity of the assumption made concerning the cause of absorption in the solar photosphere.

After the dependence of the temperature T on τ_ν is determined, the dependence of the pressure p on τ_ν can be found. To do this we must make use of the hydrostatic equilibrium Eq. (4.52), which together with Eq. (15.6) gives

$$\frac{dp}{d\tau_\nu} = \frac{g\rho}{\alpha_\nu}. \tag{15.7}$$

For the absorption coefficient α_ν let us take the theoretical expression (5.14), after representing it in the form $\alpha_\nu = \rho p_e f_\nu(T)$ (since $n_1 = \rho/m_H$ because of the weak ionization of hydrogen in the solar photosphere). Therefore instead of Eq. (15.7) we obtain

$$\frac{dp}{d\tau_\nu} = \frac{g}{p_e f_\nu(T)}. \tag{15.8}$$

For a given chemical composition the electron pressure p_e can be expressed in terms of p and T with the aid of the ionization formula. This allows one to integrate Eq. (15.8), i.e., to find p in the form of a function of τ_ν. Then the density ρ is determined from the gas equation of state. For ascertaining the relationship between optical and geometrical distances in the photosphere one can use the expression

$$r - r_0 = -\int \frac{d\tau_\nu}{\alpha_\nu}, \tag{15.9}$$

where r_0 is an arbitrary constant. Since α_ν depends on p and T, then to carry out the integration in (15.9) it is necessary to use the derived expressions in terms of τ_ν for these quantities.

A number of authors have engaged in the construction of empirical models of the solar photosphere: Barbier, de Jager and others. In general features these models agree with the theoretical models; however, there are differences between them. In part, these differences are caused by deficiencies in the work on photosphere theory in which certain important effects were ignored (the blanketing effect, convection, etc.). /185

2. Convection and granulation. In stellar photosphere theory it is usually assumed that radiative equilibrium occurs in the photosphere. We made such an assumption in Chapter I, and on its basis the photosphere structure was determined and the radiative field in it was calculated. In particular, the results of the solar photosphere model calculation, presented in Table 18, we obtained under the assumption of radiative equilibrium of the photosphere. A problem arises, however, as to whether such a photosphere condition will be stable, i.e., whether a volume element, removed in any fashion from its equilibrium condition, will revert to it due to the effect of forces present in the photosphere. If this will not occur, then gas masses in the photosphere are set in motion, i.e., convection occurs.

Let us determine the condition for the onset of convection in the photosphere. For this we will assume that some volume element experiences an upward movement. We will assume that the volume expands adiabatically during this movement. Then the temperature and density in the volume will change in a definite manner (in accordance with the adiabatic equation). If the temperature in the volume is lower than the temperature of the surrounding gas (and, therefore, the density in the volume is greater than the density of the gas), then the volume re-

turns to the original position due to the effect of gravity. If, however, the temperature in the volume is greater than the temperature of the surrounding gas, then the volume will continue to rise. In the latter case convection begins.

Thus the condition for the onset of convection means that the adiabatic temperature gradient must be less than the temperature gradient for the radiative equilibrium, i.e.,

$$\left|\frac{dT}{dr}\right|_{\text{ad}} < \left|\frac{dT}{dr}\right|_{\text{rad}} \tag{15.10}$$

This inequality can be put into a more convenient form. To do this we make use of the hydrostatic equilibrium Eq. (4.42) and the equation of state of an ideal gas (4.43). From these equations it turns out that

$$\frac{dp}{dr} = -\frac{g\mu p}{R_* T}. \tag{15.11}$$

Therefore we obtain

$$-\frac{dT}{dr} = -\frac{dT}{dp}\frac{dp}{dr} = \frac{g\mu}{R_*}\frac{d\ln T}{d\ln p} \tag{15.12}$$

Consequently, instead of (15.10) we have /186

$$\left(\frac{d\ln T}{d\ln p}\right)_{\text{ad}} < \left(\frac{d\ln T}{d\ln p}\right)_{\text{rad}} \tag{15.13}$$

The condition for the onset of convection in the form of the inequality (15.13) was derived by Schwarzschild in 1905.

Let us see whether the inequality (15.13) is satisfied in the photosphere. To do this let us calculate its left and right sides separately.

As is known, for an adiabatic change of state the relation

$$p^{1-\gamma}T^{\gamma} = \text{const}, \tag{15.14}$$

is satisfied, where $\gamma = c_p/c_v$, c_p is the specific heat of the gas for constant pressure, and c_v is the specific heat of the gas for constant volume. From (15.14) it follows that

$$\left(\frac{d\ln T}{d\ln p}\right)_{\text{ad}} = \frac{\gamma - 1}{\gamma} \tag{15.15}$$

For a monatomic gas $\gamma = 5/3$. Therefore in the given case

$$\left(\frac{d\ln T}{d\ln p}\right)_{ad} = \frac{2}{5}. \tag{15.16}$$

To calculate the right side of the inequality (15.13) let us make use of Eq. (4.49), defining the quantity dT/dr for radiative equilibrium in the case $\varkappa$ = const. On the basis of Eqs. (15.12) and (4.49) we have

$$\left(\frac{d\ln T}{d\ln p}\right)_{rad} = \frac{1}{4}. \tag{15.17}$$

From a comparison of Eqs. (15.16) and (15.17) it is seen that the inequality (15.13) is not satisfied, i.e., convection does not appear in the photosphere. Subsequent investigations have established, however, that convection can nevertheless occur in photospheres for two reasons: 1) because of a change in the absorption coefficient $\varkappa$ with depth, 2) because of a change in the degree of atomic ionization with depth. The latter circumstance is associated with the fact that atomic ionization processes will lead to a change in the specific heat of the gas, more precisely to a decrease in the effective value of the quantity γ. Since hydrogen is the most abundant element in photospheres, then the ionization of hydrogen atoms exerts the greatest effect on the quantity $(d \ln T/d \ln p)_{ad}$. Calculations show that convection appears in the photosphere when the hydrogen ionization reaches a certain level. The degree of hydrogen ionization increases with an increase in depth. /187
When the hydrogen becomes almost completely ionized, convection ceases.

Thus, convective zones, caused by the partial ionization of hydrogen, exist in stellar photospheres. In these zones the temperature gradient is adiabatic. To determine the temperature gradient in going from the radiative equilibrium zone to the convective zone one can use the graphs of the quantity $(d \ln T/d p)_{ad}$ as a function of T and p, given by Unsöld [6].

The depth at which the convective zone begins is different for different stars. In the photospheres of later class stars the convective zone is located relatively deep (and it is deeper, the colder the star). In the solar photosphere the convective zone beings at an optical depth in the visible portion of the spectrum of about 2. For class A stars the convective zone moves to the outermost photosphere layers.

Since the convective zone in the solar photosphere occurs at a relatively shallow optical depth, it can have an effect on some of the observed characteristics of the Sun. According to Siedentopf [7], the existence of convection is explained by the form itself of the Sun's surface, namely, the so-called granulation, i.e., the grainy structure of the surface. A granule is identified with a convective cell in which heated matter rises upward (and it flows downward in the spaces between granules).

As observations show, granule dimensions amount to 500 km on the average, and their average lifetime is equal to approximately 8 minutes. Crude theoretical estimates of these quantities lead to about the same values. These estimates are

based on the concept that in an atmosphere with a density gradient the convective elements must have diameters of the same order as the local height of the homogeneous atmosphere. Rising, the convective elements expand adiabatically and merge with other elements. New elements of smaller diameters are formed in their place (since the height of the homogeneous atmosphere decreases as one goes to solar layers nearer the outside). Such a model for the evolution of granulation is confirmed by motion pictures of the Sun's surface.

3. Sunspots. Dark formations—sunspots—are observed periodically on the solar disk. The linear dimensions of the spots range up to 100,000 km. Their life varies drastically: from several hours to several months. Each spot consists of a darker central area (or umbra) and a brighter rim, the so-called penumbra. However, the spots appear dark only in contrast with the photosphere; /188 in reality they are extremely hot. The effective temperature of a spot is about 4500° (and the effective photosphere temperature, as is known, is equal to 5785°). The spectrum of a spot belongs to class K0, whereas the spectral class of the photosphere is G3.

Spectroscopic study of the spots has made it possible to draw a conclusion about gas motion in them. The velocities of this motion are of the order of 2 km/sec in the penumbral region. In the lower layers of the spot material flows out of it, and the upper-into it (the Evershed effect). With the existence of such flows taken into consideration, one could conclude that essentially a convective survey transfer occurs in the spot. In reality, however, radiation plays a major role in the energy transfer in a spot, just as in the photosphere. A comparison of theoretical and observational data on the intensity of the radiation coming from a spot leads to such a conclusion. In a spot (as in the photospheres of cold stars in general) light absorption is produced primarily by the negative hydrogen ion. Therefore it can be assumed, approximately, that in the visible portion of the spectrum the absorption coefficient does not depend on the wavelength, and the intensity of the radiation, coming from the spot, is determined by Eq. (4.39) in the case of radiative equilibrium. This formula gives: 1) the energy distribution in the spot spectrum for a given angle ϑ, 2) the change in the radiation intensity at a given frequency ν with a change in the location of the spot on the solar disk. The values of the radiation intensity $I_\nu(0, \vartheta)$, computed from Eq. (4.39), agree satisfactorily with the results of spot observations. However, the agreement between theory and observations ceases to exist when convective equilibrium of the spot is assumed.

The physical conditions in spots are investigated by the same methods as the conditions in stellar atmospheres. In particular, the construction of curves of growth and the analysis of spectral line profiles are employed. The degree of atomic excitation and ionization, the electron density, the velocities of the gases and other characteristics of the spots are determined as a result.

The most important feature of sunspots is the presence of magnetic fields in them. No field-free spots are observed. Moreover, weak magnetic fields are sometimes observed before the appearance of a spot at a given point of the photosphere (or for some time after its disappearance).

The magnetic fields of spots are studied on the basis of observing the Zeeman effect, representing a splitting of the spectral lines in a magnetic field.

The splitting pattern depends on the angle between the field direction and the line of sight. The magnetic fields of spots are usually perpendicular to the solar surface. Therefore the longitudinal Zeeman effect occurs for a spot in the central portion of the disk. In this case the line is split into two circularly polarized components, separated from the normal location of the line by the amount /189

$$\Delta\lambda = 4.7 \cdot 10^{-5} g\lambda^2 H, \tag{15.18}$$

where the wavelength λ is expressed in centimeters, the field intensity H is in gauss and g is the Lande factor. A determination of the intensity of the magnetic fields of spots with the aid of Eq. (15.18) leads to values of the order of several hundred and thousands of gauss.

In most cases the Zeeman line components are not observed individually, and they are merged, i.e., the line is broadened in the presence of the magnetic field. In this situation an increase in the equivalent width occurs for lines of average intensity so that the curve of growth is raised in its "flat" portion. The magnetic field intensity can be estimated from the curve of growth for spots.

For a detailed interpretation of the spectra of sunspots a theory of absorption line formation in a magnetic field is required. This theory has recently been developed by a number of authors: Unno, V. E. Stepanov, D. N. Rachkovskiy, and others. In Rachkovskiy's paper [8] the problem of absorption line formation in a magnetic field was considered for fairly general assumptions (in particular, noncoherent light scattering is taken into consideration).

The cause of sunspot formation is not completely clear. Undoubtedly their appearance is associated with the appearance of magnetic fields within the convective zone which are carried outward in some manner. As is known, the magnetic energy density is equal to $H^2/8\pi$. In the deep layers this energy is less than the convective kinetic energy $\frac{1}{2}\rho v^2$ and the magnetic field does not hinder convection. But the reverse inequality exists in the outer portions of spots, i.e.,

$$\frac{H^2}{8\pi} > \frac{1}{2}\rho v^2, \tag{15.19}$$

and the magnetic field inhibits convection. It is possible for the outer portions of spots to be colder than the photosphere surrounding them because of the absence of convective energy transfer.

Groups of spots are usually surrounded by faculae, which are bright formations on the solar disk. As a rule, faculae appear somewhat before spots and exist, on the average, three times as long. Faculae are especially visible at the edge of the disk where the photosphere is less bright than at the center. This fact is explained by the fact that the facula temperature in the surface layers is higher than the photosurface temperature (by about 1000°). It is assumed that energy transfer in faculae occurs primarily by convection. /190

4. Solar activity. Besides faculae and spots, other transient processes are observed on the Sun. The most outstanding of these are chromosphere flares and prominences.

A chromosphere flare is a sudden increase in brightness of some portion of the solar surface (approximately equal in area to a spot). A flare usually rises to maximum brightness in a few minutes but it fades more slowly. Sometimes flares can be observed in white light, but for the most part they are observed in the H_α line and in some other lines by means of a spectroheliograph. In most cases a flare occurs over spot groups or not far from them. From the observed energy of flares it is found that the density of material in flares is much greater than in neighboring portions of the chromosphere. Different hypotheses associate the cause of flares with the character of the magnetic fields over spot groups.

The study of flares has great significance for geophysics since they exert a strong influence on the state of the earth's ionosphere. During flares, streams of fast particles and high-frequency radiation (ultraviolet and x-ray) flow from the Sun. These particles and photons, striking the earth's ionosphere, cause magnetic storms, disruption of radio communications and many other phenomena.

The study of prominences, which are gas clouds observable above the edge of the solar disk, also occupies an important place in the physics of the solar atmosphere. More precisely, prominences are above the chromosphere—in the corona. The spectrum of a prominence consists of discrete bright lines of hydrogen, ionized calcium, etc. Since prominences are projected onto the photosphere, there is practically no continuous background in their spectra and absorption lines are absent.

Prominences can, however, also be observed on the solar disk. In this case they reveal themselves because of light absorption in discrete lines. Prominences on the solar disk can be detected with the aid of spectroheliograph, which allows one to photograph the Sun in light of a specific wavelength. Dark filaments (or, as they are sometimes called, dark flocculi) are seen in spectroheliograms recorded in the bright lines of helium, ionized calcium, etc. These formations represent prominences projecting onto the solar disk.

Prominences differ widely in shape, size and the character of their movement. In a crude classification one can distinguish between quiescent prominences (not changing noticeably over a period of hours and days) and eruptive prominences (moving with enormous velocities ranging up to 1000 km/sec). There is also a separate class of prominences associated with sunspots. /191

Very valuable data on the motion of prominences have been obtained through motion pictures, made at a number of observatories. In particular, it was ascertained in this manner that eruptive prominences arise from quiescent because of a sudden increase in velocity. It has also been established that many prominences are formed through the condensation of coronal matter, which then moves downward in the form of streamers. The motion of prominences is undoubtedly associated with magnetic fields existing in the Sun. In many cases it has the character of the motion of charged particles along magnetic force lines. The motion of prominences has been studied in detail by A. B. Severny at the Crimean astrophysical observatory (see, for example, [9]). The problems of prominence luminosity are of great interest. However, we will not dwell on this here since they are similar to the problems of chromosphere luminosity, which will be considered in detail in the following section.

Sunspots, faculae, flares and prominences are the most characteristic examples of the appearance of solar activity. As is known, this activity varies markedly with time, with the approximate period of variation being 11 years. However, solar activity has no effect on the stellar character of the Sun. In other words, the appearance of spots and prominences on Sun-like stars is not observable. Moreover, this does not exclude the fact that such phenomena occur for other star types on a larger scale and, therefore, are reflected in the observed variations in the stellar brightness and spectrum.

16. Chromosphere

1. Line intensities. During solar eclipses, when the Moon covers the entire solar disk, we can observe a spectrum consisting of bright lines on a dark background. These lines belong to the chromosphere, which is the outermost layer of the solar atmosphere (if the corona is disregarded). In composition the line spectrum of the chromosphere is similar to the usual Fraunhofer spectrum of the solar disk, i.e., there are bright lines in the chromosphere spectrum at the same locations where absorption lines appear in the disk spectrum (with some exceptions, which will be indicated below).

The character itself of the chromosphere spectrum is quite clear. As we recall, the upper layers of the solar atmosphere yield practically no continuous spectrum radiation, but do cause light scattering in spectral lines. Therefore /192 during observations of the photosphere along a tangent to the photosphere we do not see a continuous spectrum and we see only bright lines. When, however, the solar disk is observed, then a continuous spectrum with absorption lines, arising because of the fact that line radiation, scattered by the atmosphere, is returned to an appreciable degree to the photosphere, is seen.

From the observational data one can find the total radiation intensity in any line at a height h from the edge of the disk. Let us designate this quantity by I(h). It obviously represents the amount of energy radiated in a line by a column with a cross sectional area of 1 cm^2 passing through unit solid angle at a distance h from from the photosphere during 1 sec (Fig. 18).

The quantity I(h) decreases with an increase in h, and after an analysis of the results of observations of it, it is usually represented in the form

$$I(h) = I(0)e^{-\beta h}, \qquad (16.1)$$

where I(0) and β are some parameters.

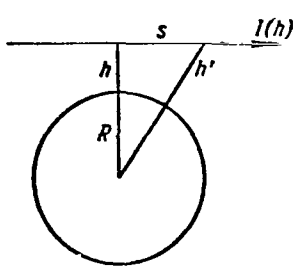

Figure 18.

Knowing the quantity I(h) for a given line, we can determine the volume emission coefficient in this line. Denoting it by $\varepsilon(h)$, we have the following equation

$$I(h) = \int_{-\infty}^{+\infty} \varepsilon(h')\,ds, \qquad (16.2)$$

where h' is the height of an arbitrary point in the line of sight and s is the distance measured along the line of sight.

If R is the Sun's radius, then from Fig. 18 it follows that

$$s^2 = (R + h')^2 - (R + h)^2. \tag{16.3}$$

Since the atmosphere thickness is small compared to R, instead of (16.3) we can write

$$s^2 = 2R(h' - h). \tag{16.4}$$

With (16.4) taken into account, Eq. (16.2) assumes the form

$$I(h) = \sqrt{2R}\int_h^\infty \frac{\varepsilon(h')\,dh'}{\sqrt{h' - h}}. \tag{16.5}$$

Equation (16.5) is the integral Abel equation for the desired function ε(h). /193
The solution of this equation is given by the formula

$$\varepsilon(h) = -\frac{1}{\pi\sqrt{2R}}\frac{d}{dh}\int_h^\infty \frac{I(h')\,dh'}{\sqrt{h' - h}}. \tag{16.6}$$

Substituting (16.1) into (16.6), we find

$$\varepsilon(h) = \varepsilon(0)\,e^{-\beta h}, \tag{16.7}$$

where

$$\varepsilon(0) = I(0)\sqrt{\frac{\beta}{2\pi R}}. \tag{16.8}$$

Thus, with the aid of Eq. (16.7) and the quantities I(0) and β derived from observations the emission coefficient ε can be determined for each line at any height h.

The quantities ε(h) were determined on the basis of observations of many solar eclipses. A portion of the results obtained by Menzel and Cillie [10] is presented in Table 19.

These results are of considerable interest for ascertaining the physical conditions in the upper layers of the solar atmosphere.

2. Self-absorption in lines. In writing Eq. (16.2) we assumed that the chromosphere is transparent to self-radiation. Such an assumption, however, is valid only for the upper chromosphere. When considering the lower chromosphere, however, it is necessary to take account of self-absorption in spectral lines.

TABLE 19. CHROMOSPHERE RADIATION IN DIFFERENT SPECTRAL LINES

Atom	Wave-length	$\beta \cdot 10^8$	$\lg \varepsilon(0)$	Atom	Wave-length	$\beta \cdot 10^8$	$\lg \varepsilon(0)$
H	4861 (H_β)	1,16	—1,63	He^+	4686	0,30	—5,88
	4340 (H_γ)	1,16	—2,22	Mg	3838	1,81	—2,90
	3970 (H_δ)	1,16	—2,56	Ti^+	4572	1,58	—3,79
He	5016	0,58	—4,96	Ca	4227	2,11	—3,19
	4026	0,67	—4,49	Ca^+	3968	0,69	—2,93
					3934	0,69	—2,85

Commas represent decimal points.

Let us denote by $\varepsilon_\nu(h)$ and $\sigma_\nu(h)$ the emission and absorption coefficients at frequency ν within a given line at a height h above the photosphere. Then the intensity of the radiation at frequency ν, passing to the observer at a distance h from the edge of the disk, will be equal to /194

$$I_\nu(h) = \int_{-\infty}^{+\infty} \varepsilon_\nu(h') e^{-t_\nu} ds, \tag{16.9}$$

where t_ν is the optical distance, measured along the line of sight, i.e.,

$$t_\nu = \int_s^\infty \sigma_\nu ds'. \tag{16.10}$$

We will assume that the quantity

$$\frac{\varepsilon_\nu}{\sigma_\nu} = S \tag{16.11}$$

does not depend on the frequency within the line. This, in particular, is the situation for completely noncoherent light scattering.

It is obvious that the quantity S is determined by specifying the ratio of the numbers of atoms in the upper and lower states for a given line, i.e., the ratio n_k/n_i. In fact, with the aid of (16.11) we can write

$$n_k A_{ki} h\nu_{ik} = 4\pi S \int \sigma_\nu d\nu. \tag{16.12}$$

Moreover, on the basis of Eq. (8.12) we have

$$\int \sigma_\nu d\nu = \frac{h\nu_{ik}}{c}(n_i B_{ik} - n_k B_{ki}), \tag{16.13}$$

where, in the interests of generality, negative absorption is taken into consideration. From Eqs. (16.12) and (16.13), using the expressions (8.5) that interrelate the Einstein transition coefficients, we obtain

$$S = \frac{2h\nu_{ik}^3}{c^2} \frac{1}{\frac{g_k}{g_i}\frac{n_i}{n_k} - 1}. \tag{16.14}$$

The quantity n_i/n_k, of course, varies in the chromosphere. However, for simplicity we will assume it is constant (corresponding to some average "excitation temperature"). Then the quantity S will be a constant in the chromosphere.

Using Eq. (16.11) and the assumption that S is constant, instead of Eq. (16.9) we obtain /195

$$I_\nu(h) = S \int_{-\infty}^{+\infty} \sigma_\nu(h') e^{-t_\nu} ds, \tag{16.15}$$

or, after integration,

$$I_\nu(h) = S[1 - e^{-t_\nu^0(h)}], \tag{16.16}$$

where $t_\nu^0(h)$ is the optical thickness along the line of sight.

Representing the quantity σ_ν in the form $\sigma_\nu = n_i k_\nu$, where k_ν is the absorption coefficient, calculated for one atom, we can write

$$t_\nu^0 = \int_{-\infty}^{+\infty} \sigma_\nu ds = k_\nu \int_{-\infty}^{+\infty} n_i ds. \tag{16.17}$$

Introducing the notation

$$N_i(h) = \int_{-\infty}^{+\infty} n_i(h') ds, \tag{16.18}$$

instead of (16.16) we obtain

$$I_\nu(h) = S[1 - e^{-k_\nu N_i(h)}]. \tag{16.19}$$

Integration of Eq. (16.19) over all frequencies yields

$$I(h) = S \int_0^\infty [1 - e^{-k_\nu N_i(h)}] d\nu, \tag{16.20}$$

where I(h) is the total line intensity.

Equation (16.20) provides the possibility of determining the quantity $N_i(h)$ from the radiation intensity I(h) obtained from observations. The quantity $N_i(h)$ represents the number of atoms in the i-th state, in a column with a 1 cm^2 cross section, flowing at a height h from the disk edge. This quantity is related to the atom concentration $n_i(h)$ by Eq. (16.18), which can be rewritten in the form

$$N_i(h) = \sqrt{2R}\int_h^\infty \frac{n_i(h')}{\sqrt{h'-h}}\,dh'. \tag{16.21}$$

Solving this Abelian equation, we can determine the desired quantity $n_i(h)$.

This method for finding the atom density in the chromosphere cannot be considered accurate since it is based on the assumption that S is constant, which is /196 not true in reality. The latter is seen to be so if only because Eq. (16.16) gives a line with maximum intensity at its center whereas observed line profiles often have a saddle-shaped form. Therefore there is interest in the problem of determining from Eq. (16.9) not only the atom density $n_i(h)$ but also the quantity S(h) (or the quantities $n_i(h)$ and $n_k(h)$). At the present time, however, the values of the function $I_\nu(h)$ available to use (characterizing the profiles of chromosphere lines at different heights), which are required for solving this problem, are scarcely sufficiently accurate.

It should be emphasized that the presence of self-absorption in the chromosphere still says nothing about a greater chromosphere optical thickness along the radius. Let us consider chromosphere layers, higher than h. The optical thickness of this layer along a radius is equal to

$$\tau_\nu(h) = k_\nu\int_h^\infty n_i(h')\,dh'. \tag{16.22}$$

Assuming that the atom density decreases with height as $e^{-\beta h}$, we obtain

$$\tau_\nu(h) = k_\nu\frac{n_i(h)}{\beta}. \tag{16.23}$$

However, the optical thickness of the chromosphere for a ray, passing at a distance h from the disk edge, on the basis of Eq. (16.17) is equal to

$$t_\nu^0(h) = k_\nu n_i(h)\sqrt{\frac{2\pi R}{\beta}}. \tag{16.24}$$

Therefore we have

$$\tau_\nu(h) = \frac{t_\nu^0(h)}{\sqrt{2\pi R\beta}}. \tag{16.25}$$

Substituting $\beta \approx 10^{-8}$ into the formula derived, we find $\tau_\nu(h) \approx 0.015\, t_\nu^0(h)$. Consequently, the quantity $\tau_\nu(h)$ can be less than unity even for large values of $t_\nu^0(h)$, i.e., for strong line self-absorption. One can assume that in such a case only single scattering of the spectral line light occurs in the chromosphere. For some strong lines of the chromosphere spectrum (for example, for the Balmer lines and the H and K Ca^+ lines), however, the optical thickness of the chromosphere along a radius is evidently greater than unity.

3. Distribution of atoms with height. The distribution of atoms with height can be found on the basis of the chromosphere spectral radiation. Let us assume that line self-absorption is absent. Then the volume line emission coefficient is determined by Eq. (16.17). Utilizing the relation /197

$$4\pi\varepsilon(h) = n_k(h) A_{ki} h\nu_{ik}, \tag{16.26}$$

we obtain

$$n_k(h) = n_k(0) e^{-\beta h}, \tag{16.27}$$

where

$$n_k(0) = \frac{4\pi\varepsilon(0)}{A_{ki} h\nu_{ik}}. \tag{16.28}$$

To pass from the number of atoms in the i-th state to the number of atoms in the ground state, the Boltzmann formula is usually used with some average atom excitation temperature T (although an appreciable error is possible in this situation since T can vary in the chromosphere). After making such a conversion, we have

$$n_1(h) = n_1(0) e^{-\beta h}, \tag{16.29}$$

where

$$n_1(0) = n_k(0) \frac{g_1}{g_k} e^{\frac{\chi_1 - \chi_k}{kT}}. \tag{16.30}$$

The variation of concentration with height for any atom can be found from Eq. (16.29). The parameters $n_1(0)$ and β, entering into this formula, are determined on the basis of observational data (for example, the data presented in Table 19).

Let us compare Eq. (16.29) with the barometric height formula

$$n_1(h) = n_1(0) e^{-\frac{m_a g h}{kT}}, \tag{16.31}$$

where m_a is the mass of a given atom and g is the gravitational acceleration in the solar atmosphere.

Although Eq. (16.29) and (16.31) are outwardly similar, they yield vastly different results. According to the barometric height formula, the greater the atomic mass, the faster the concentration falls off with height. According to Eq. (16.29), however, with values of β derived from observations, the concentration decrease with height is approximately the same for different atoms.

In addition, for any atom the value of the quantity $m_a g/kT$ is much greater than the value of β. For example, for hydrogen $m_a g/kT = 6.6 \cdot 10^{-8}$ (when $T \approx \approx 5000°$), while $\beta = 1.16 \cdot 10^{-8}$. The difference in the values of these quantities is /198 even greater for other atoms. Consequently, the fall-off in atom concentration with height in the chromosphere occurs much more slowly than the barometric height formula requires.

As is known, the barometric height formula is derived under the assumption that each volume element of gas is in equilibrium in terms of the gravitational force and the gas pressure force. Since the density distribution in the chromosphere does not satisfy the barometric height formula, then we must conclude that the chromosphere is not in equilibrium in terms of these forces. More precisely, there must be an additional force, oppositely directed to the gravitational force, present in the chromosphere.

Milne has expressed the notion that such a force in the chromosphere can be the radiation pressure in the spectral lines. On the basis of Eq. (4.56) we can write the following expression for the light pressure force acting on all atoms of a given element in a certain stage of ionization in a unit volume:

$$f = \frac{1}{c} \sum n_i k_{ik} H_{ik} \Delta\nu_{ik}, \tag{16.32}$$

where k_{ik} is the spectral line absorption coefficient calculated for one atom, H_{ik} is the radiation flux in this line, $\Delta\nu_{ik}$ is its width. In calculations of the quantity f from Eq. (16.32) it must be borne in mind that the maximum in the energy distribution curve in the solar spectrum is in the visible region, and most atoms are in the ground state. Therefore the light pressure force will be a maximum for atoms of that element for which the principal series lines lie in the visible portion of the spectrum. Only neutral sodium and ionized calcium satisfy this condition. The first of these atoms has the D_1 and D_2 resonance lines in the visible portion of the spectrum and the second—the H and K resonance lines. In the solar atmosphere the atoms of these elements exist predominantly in the singly ionized state. Therefore we come to the conclusion that the light pressure force will be a maximum for the calcium atoms. This force can be estimated from the formula

$$f = \frac{1}{c} n_1 k_{12} H_{12} \Delta\nu_{12}, \tag{16.33}$$

i.e., by considering the radiation pressure in the resonance lines only.

Calculations from Eq. (16.33) show that for calcium the light pressure force is comparable to the gravitational force. Consequently, light pressure can influence the distribution of calcium atoms with height in the chromosphere. The effect of light pressure on other atoms, however, is very slight. It is also impossible to conclude that the calcium atoms are carried away beyond the entire chromosphere itself. Thus, one must recognize that the vast extent of the chromosphere cannot be explained by the effect of light pressure. /199

Some authors have cited turbulent motions occurring in the chromosphere as an explanation for its great height. A conclusion concerning such motions must obviously be drawn on the basis of the line widths observed in the chromosphere spectrum. If it is assumed that the line widths are caused by random atomic motion, then values of about 10-20 km/sec are obtained for the velocities of this motion, i.e., greater than the average thermal velocities of the atoms. With turbulence taken into account in the barometric height formula (16.31), the quantity $v_0^2 = 2kT/m_a$ must be replaced by the quantity $v_0^2 + v_t^2$, where v_t is the turbulence velocity. In this case, instead of the barometric height formula we have

$$n_1(h) = n_1(0)\, e^{-\frac{2gh}{v_0^2+v_t^2}}. \tag{16.34}$$

For $v_t \approx 20$ km/sec, Eq. (16.34) gives approximately the same behavior of atom density with height as does Eq. (16.29), derived on the basis of observational data.

At the present time, however, the opinion that the chromosphere exists in dynamic rather than static equilibrium is the most correct. The view of a chromosphere as consisting of individual filaments or streamers (often called spicules) itself leads to such a viewpoint. These streamers are ejected from the photosphere for some reason or other. They may be associated with granulation since from a crude estimate the number of streamers is equal to the number of granules. The average lifetime of chromosphere streamers is several minutes. Their velocity is about 20 km/sec.

4. Excitation of atoms in the chromosphere. As already stated, the chromosphere spectrum, in terms of the abundance of lines, is similar to the Fraunhofer spectrum of the solar disk in its general features. There are, however, some exceptions to this. The most significant of them is the presence in the chromosphere spectrum of very intense helium lines (as is known, the element helium was discovered from these very chromosphere lines). Moreover, a weak line at λ 4686, belonging to ionized helium, is seen in the chromosphere spectrum. The presence of a large number of excited and ionized helium atoms in the chromosphere is not at all consistent with the temperature of the solar photosphere. The concentration of excited helium atoms, calculated from the Boltzmann formula for a temperature of about 6000°, is approximately a billion times less than the concentration of these atoms obtained from observations. /200

Thus, there is an anomalous excitation of atoms in the chromosphere. Initially, to explain this phenomenon a hypothesis was advanced concerning the existence of a considerable ultraviolet excess in the solar spectrum. This hypothesis,

however, cannot be accepted if only because the ultraviolet radiation coming from the photosphere would also produce atomic excitation in the deeper layers of the atmosphere, which is not observed. The same objection can be raised with respect to the assumption of atomic excitation by a flow of fast particles coming from the photosphere.

Among the other attempts to explain the anomalous atomic excitation in the chromosphere, let us mention an interesting hypothesis according to which this excitation is caused by calcium atoms. Due to the light pressure effect, atoms of ionized calcium rise rapidly in the atmosphere, and then some of these recombine with free electrons. However, the light pressure does not affect the neutral calcium atoms and they fly downward very rapidly under the influence of gravity. Excitation of helium atoms occurs through collisions with these atoms.

This last hypothesis is not confirmed by calculations, but it is interesting because the concept of helium excitation at the top of the chromosphere (toward the corona) rather than at the bottom (toward the photosphere) was first expressed in it. Subsequently, after it was found that the corona has a high temperature, this concept took on a more realistic form. The hot corona must undoubtedly strongly influence the cooler chromosphere. In the opinion of some authors the emission of the chromosphere in the helium lines can be caused by the high-frequency coronal radiation. Moreover, the corona can heat the upper chromosphere layers and the helium atoms in them can be excited by electron impact. The problem of helium atom excitation in the chromosphere has been considered in a number of papers (see, in particular, [11]).

Thus, we must conclude that the chromosphere consists of both cooler as well as warmer regions. The physical model of the chromosphere must therefore be rather complex. Several chromosphere models have been proposed up to now. In some of them it is assumed that the temperature and density in the chromosphere depend only on the height. In other models it is assumed that there are cool and warm regions at each height. An interesting model of the second type has been proposed by V. A. Krat and V. M. Sobolev [12]. We cannot describe the different chromosphere models here. Let us only mention that to select the most correct one it is necessary to use not only the results of observations in the visible portion of the spectrum, but also the results of rocket observations in the ultraviolet as well as data from radio astronomy.

5. Ultraviolet solar spectrum. Rocket flights have made it possible to obtain the solar spectrum in the ultraviolet region. The results of measurements of these spectra have been published in many papers and books (see, for example, [13] and [14]). The theoretical interpretation of ultraviolet spectra has only begun and one can expect great advancements in it in the future. /201

The solar spectrum in the near ultraviolet region (down to about 1900 Å) is similar to the spectrum in the visible portion, i.e., it is a continuous spectrum with absorption lines. Near 2100 Å the intensity of the continuous spectrum drops sharply (absorption by a number of atoms and molecules has been mentioned as a possible cause of this). Emission lines appear in the solar spectrum at about 1900 Å. With a further decrease in wavelength the continuous spectrum weakens and the emission lines become more pronounced. Beyond 1500 Å the solar spectrum consists of bright lines on a weak continuous background. The hydrogen L_α line

(1215.67 Å) is distinguished among the bright lines of the ultraviolet solar spectrum. Other lines of the Lyman series, as well as the Lyman continuum, are seen in the spectrum. In addition, the resonance line of ionized helium (303.78 Å) is very intense. Many lines of ions of C, N, O, Si, etc., (including the resonance lines) are also present in the spectrum.

Most of the bright lines of the ultraviolet solar spectrum arise in the chromosphere and in the transition region between the chromosphere and corona. Some lines arise in the corona. It is important to emphasize that we can observe these lines only because of the extreme weakness of the continuous solar spectrum in the ultraviolet. Bright lines of the same intensity in the visible portion of the spectrum cannot, as a rule, be detected since they are superimposed on a strong continuous spectrum or on an absorption line, the intensity within which is also high. Only during eclipses, when the chromosphere and corona are not projected onto the photosphere, can we observe the bright chromosphere and coronal lines in the visible portion of the spectrum. In some cases, however, the effect of chromosphere emission can be observed even in the visible portion of the spectrum of the solar disk. It appears as an increase in the intensities in the central regions of the strong Fraunhofer lines (for example, the Ca II H and K lines).

The L_α line profile in the solar spectrum has been determined through rocket observations. It is depicted in Fig. 19a. A narrow absorption line, arising because of radiation absorption by neutral hydrogen along the path from the Sun to the rocket, is seen in the center of the L_α emission line. The fact that the upper layers of the earth's atmosphere luminesce in the L_α line because of their reemission of the solar radiation absorbed in this line is confirmation of this. Digressing from this narrow /202 absorption line, we can state that the L_α line in the solar spectrum has a broad dip in the central portion.

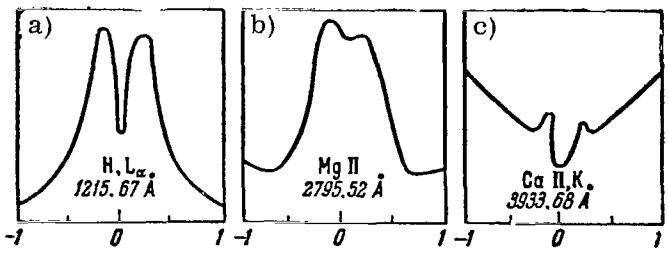

Figure 19.

The profiles of the 2796 Mg II and 3934 Ca II emission lines, very similar to the L_α line profile, are presented in Figs. 19b and c. A spectrogram with the λ 2796 line has been obtained through rocket observations. This emission line is superimposed on a wide absorption line. The λ 3934 emission line occurs at the very bottom of the very broad K absorption line and is an example of the influence of the chromosphere on the Fraunhofer spectra, which we discussed above. The L_α emission line is also superimposed on a broad absorption line, but the profile of the latter is difficult to determine because of the weakness of the continuous spectrum.

Many lines of the ultraviolet solar spectrum arise in the transition region between the chromosphere and corona, the temperature in which varies from about 10,000° to 1 million degrees. The theoretical emission of this region is a

very interesting problem of solar physics. It is obvious that the atoms of any element in a specific ionization state exist preferentially only in a very narrow layer of this region, since at a lower temperature the atoms exist in the preceding ionization state, and at a higher temperature—in the subsequent. Therefore a severe emission stratification (i.e., layering) exists in the transition region. Of the transition region models that have been proposed, let us mention the model of G.S. Ivanov-Kholodnyy and G.M. Nikol'skiy [15]. In the construction of their model these authors took into consideration not only data on the ultraviolet solar spectrum, but also the results of solar radio emission observations. Data on the radiation of the earth's ionosphere were also used since the ionization condition of the upper layers of the earth's atmosphere depends heavily on the ultraviolet solar radiation.

6. The L_α line in the solar spectrum. Above, we presented some observa- /203
tional data on the L_α line. Let us now concern ourselves with an interpretation of these data.

The L_α emission line arises in the upper layers of the chromosphere where the temperature increases with height. In these layers the atoms are excited by electron impact and spectral line quanta are formed through subsequent spontaneous transitions. In most cases, however, the L_α quanta cannot escape unhindered from the chromosphere since the optical depth of the chromosphere layers at the central frequency of this line is considerable. Therefore diffusion of the L_α radiation occurs in the chromosphere. As explained above (in Section 11), this diffusion is accompanied by a frequency redistribution of the radiation within the line. During such a process, most of the quanta escape outside in portions of the line far from the center, for which the optical depth is relatively small. In the central portions of the line, however, a small fraction of the quanta escape to the outside because of strong absorption. Consequently, the emission line must have a dip in the center. Just such a dip is observed for the L_α line of the solar spectrum.

We can make use of Eqs. (11.9) and (11.10), with some changes, to determine the theoretical L_α line profiles. These equations describe radiation diffusion in a spectral line with complete frequency redistribution for the formation of line quanta from the continuous spectrum. The absorption line contour in the stellar spectrum is determined by solving these equations. In order to take into consideration the formation of line quanta because of collisions, it is necessary to introduce some additional term into Eq. (11.10). Then we obtain an absorption line with enhanced intensity in the central portion or even an absorption line with an emission line superimposed on it. Such theoretical profiles will obviously be applicable not only to the L_α line but also to other resonance lines of the solar spectrum (in particular, to the Ca II H and K lines).

For simplicity let us determine only the profile of an emission line which is superimposed on an absorption line. In the case given, the free term of the integral equation (11.14), determining the function $S(\tau)$, is caused by collisions only.

Since this mechanism of line excitation weakens with an increase in optical depth, then let us assume that

$$g(\tau) = Ce^{-m\tau}, \tag{16.35}$$

where C and m are constants. The radiation intensity of frequency ν within a line, leaving at an angle of arccos μ to the normal, is expressed in terms of the function $S(\tau)$ by the formula /204

$$I_\nu(0, \mu) = \frac{\eta_\nu}{\eta_\nu + 1} \int_0^\infty S(\tau) e^{-x\tau} x \, d\tau, \tag{16.36}$$

where η_ν is the ratio of the line absorption coefficient to the continuous spectrum absorption coefficient and $x = (\eta_\nu + 1)/\mu$ (see Eq. [11.11) for comparison]. In the case, however, where $g(\tau)$ is an exponential, there is no need to determine the function $S(\tau)$ for finding the quantity $I_\nu(0, \mu)$. On the basis of Eq. (3.19) we have

$$I_\nu(0, \mu) = C \frac{\eta_\nu}{\eta_\nu + 1} \frac{\varphi\left(\frac{1}{m}\right) \varphi\left(\frac{\mu}{\eta_\nu + 1}\right)}{1 + m \frac{\mu}{\eta_\nu + 1}}, \tag{16.37}$$

where the function $\varphi(z)$ is determined by Eq. (11.27).

Equation (11.27) can easily be solved by numerical methods. V. V. Ivanov [17] did this for the Doppler line absorption coefficient, neglecting the continuous spectrum absorption. The emission line profiles were determined from Eq. (16.37) with the aid of the table obtained for the function $\varphi(z)$. Some results for the center of the disk ($\mu = 1$) are presented in Fig. 20 as an example. Along the abscissa axis is plotted the distance from the center of the disk in Doppler widths; along the ordinate axis—the intensity relative to the central intensity. The profiles are plotted for values of the quantity m/η_{ν_0} equal to ∞, 2, 0.5, 0.3, 0.2 and 0.15, with the line being broader, the smaller this quantity. We see that the theoretical emission line profiles are very similar to the L_α line profiles obtained from observations (see Fig. 19a).

The theory also gives the profiles of emission lines at different distances /205
from the center of the disk. It is found that the dip in the center of the line becomes deeper as one goes from the center of the disk to the edge, and the separation between the maxima increases. The L_α line profile at the solar disk changes in approximately the same way as in observations.

A comparison of theory with observations makes it possible to determine the values of the parameters C and m. This, in turn, allows one to find the electron density and temperature distribution in the upper chromosphere layers, upon which these parameters depend. It must, however, be borne in mind that in the derivation of Eq. (16.37) the profile of the absorption coefficient in the

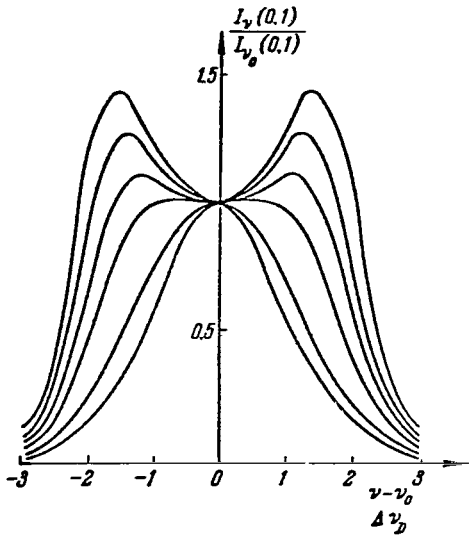

Figure 20.

chromosphere was assumed to be constant. In reality, however, it varies with depth because of a change in temperature.

A more detailed theory of resonance line formation in the solar spectrum has been developed by Jefferies and Thomas (see [11]). They have taken the various factors, influencing the population of the second atomic level, into consideration. However, the radiative transfer equation was solved approximately.

17. Corona

1. Radiation of the corona. The corona represents the outermost portion of the solar atmosphere. It is very difficult to study the corona since its brightness is much less than the sky brightness caused by the scattering of sunlight in the earth's atmosphere. Therefore coronal observations must be made during solar eclipses when the radiation of the solar disk is prevented from reaching the earth's atmosphere. To avoid scattered sky light, coronal observations are also made in high-altitude observatories with the aid of special instruments-coronagraphs. Because of the irregularity and short duration of eclipses, the second method of coronal observation yields more information about it than the first.

Observations show that the amount of energy, emitted by the corona, amounts to about one millionth of the Sun's luminosity. The coronal emission undergoes marked variations with time (increasing in years of maximum solar activity and decreasing in years of minimum activity).

The coronal spectrum in the visible portion of the spectrum differs sharply from the spectrum of the chromosphere lying below. As we recall, the chromosphere spectrum consists of bright lines, which are reversed Fraunhofer lines (with the exception of the helium lines). At the same time the corona has a continous spectrum with Fraunhofer absorption lines. In addition, bright lines are also present in the coronal spectrum, but they are not exactly the lines in the chromosphere spectrum.

More precisely, the coronal emission can be divided into three components. /206
The first component (K component) has a continuous spectrum with some number of very diffuse absorption lines corresponding to the strongest Fraunhofer lines in the spectrum of the solar disk. This emission is polarized. The second component (F component) has a continuous spectrum with Fraunhofer lines which do not differ significantly from the spectrum of the solar disk. This emission is nearly unpolarized. The third component (E component) has an emission line spectrum. The total energy, emitted by the corona in lines, amounts to about 1% of the energy leaving it in the continuous spectrum.

Curves, characterizing the relative intensities of each of the coronal emission components at different distances from the edge of the solar disk, are presented in Fig. 21, taken from Van de Hulst's paper [1]. The sky brightness of sun in three cases is denoted by the dashes in this same figure for a comparison. The first of these corresponds to a hazy sky, i.e., to the earth's atmosphere containing both molecules as well as coarse particles (the scattering indicatrices of the latter are considerably elongated in the forward direction so that a bright aureole is observed near the Sun). The second case corresponds to a blue sky, i.e., to an atmosphere containing only molecules. In the third case the dashed line gives the sky brightness during the total phase of an eclipse. The brightness is caused by the scattering of light, entering the lunar shadow region from the portion of the atmosphere illuminated by the Sun.

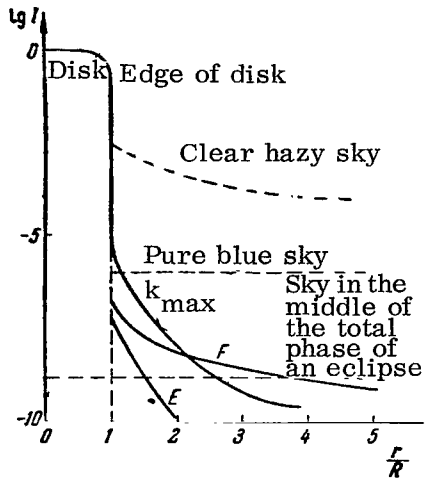

Figure 21.

As Allen and Van de Hulst (see [16]) have shown, the F component of the solar coronal emission does not actually arise in the corona itself, but in the space between Sun and Earth. This component is the result of the scattering of sunlight by particles of interplanetary dust, i.e., it has the same character as the zodiacal light. The high brightness of the F component is explained by the considerable forward elongation of the scattering indicatrix of dust particles.

Thus, the F component must be excluded from the observed coronal emission to determine the true coronal emission. From now on we will say nothing about this fictitious component of the coronal emission and we will consider only its true components K and E. /207

2. Origin of the continuous spectrum. The explanation of the origin of the continuous spectrum of the corona (more precisely, its K component) consists of the fact that it arises as the result of the scattering of the solar photosphere radiation by the free electrons of the corona. Let us introduce some facts which confirm the validity of this explanation.

1. The energy distribution of the coronal spectrum does not differ from the energy distribution in the solar spectrum. The coronal color and the Sun's color are identical. This should be the situation in the case of light scattering by free electrons because of the wavelength independence of the scattering coefficient. Some discrepancies between various observational data on the coronal spectrum and color are caused by viewing difficulties.

2. The coronal emission is polarized in accordance with the law of light polarization due to electron scattering (formulated in Section 7). Observations

yield the degree of coronal light polarization p at different distances r from the center of the solar disk (with an increase in r it increases to approximately a value of p = 40% at a distance of $r = 1.5\ r_{\odot}$, and then decreases). As is known, the theoretical value of the degree of polarization of the radiation, scattered by a volume element, is equal to

$$p = \frac{\sin^2 \gamma}{1 + \cos^2 \gamma}, \tag{17.1}$$

where γ is the angle between the directions of the incident and scattered radiation. However, radiation from different points of the photosphere strike a given volume element of the corona and each incident beam will have its own scattering angle γ and scattering plane. Therefore the expression for the degree of light polarization, scattered by a volume element of the corona, turns out to be quite complex. To determine the quantity p(r), however, the radiation from all volume elements along the line of sight must be integrated. Such calculations lead to polarization values p(r) that agree with observed values of this quantity (if, of course, the unpolarized F component is excluded from the observed coronal radiation).

3. Only a very small number of highly diffuse Fraunhofer lines are present in the coronal spectrum. This is explained by the Doppler line broadening, occurring during the scattering of sunlight by the rapidly moving free electrons /208
of the corona. If we denote by r_{ν}^{0} the relative residual line intensity in the solar spectrum and by r_{ν} the analogous quantity for the corona, then one can write the approximation

$$r_{\nu} = \frac{1}{\Delta\nu_D \sqrt{\pi}} \int_0^{\infty} e^{-\left(\frac{\nu - \nu'}{\Delta\nu_D}\right)^2} r_{\nu'}^{0} d\nu', \tag{17.2}$$

where

$$\Delta\nu_D = \frac{\nu_0}{c} \sqrt{\frac{2kT_e}{m}}, \tag{17.3}$$

and T_e is the electron temperature of the corona. Since the electron mass m is very small, then the quantity $\Delta\nu_D$ turns out to be very large. Therefore the narrow and weak Fraunhofer lines are so smeared that they become invisible. Only the very strong Fraunhofer lines (for example, H and K of ionized calcium), although very diffuse, are observed in the coronal spectrum. It should be noted that a large number of Fraunhofer lines are present in the F component of the coronal radiation spectrum, arising through light scattering by dust particles, since the velocities of the dust particles are very low.

The facts that have been enumerated attest without doubt to the fact that the continuous coronal spectrum is formed because of the scattering of light, coming

from the solar disk, by the free electrons of the corona. The following important problem arises, however: what abrupt change in the spectral character is caused by the transition from the chromosphere to the corona, i.e., why is the bright-line spectrum of the chromosphere converted into the continuous coronal spectrum? The answer, of course, to this problem is not that there are many free electrons in the corona, but that there are few in the chromosphere. In reality, with increasing distance from the solar surface the material density (including the free electron density) decreases rapidly. It is precisely this decrease which is the basic explanation of the spectral change that has been mentioned. The effect of an increase in the role of electron scattering with a decrease in density has already been mentioned in Section 5, with the photospheres of supergiant stars being introduced as an example.

In order to illustrate what has been said, let us write the expressions for the continuous spectrum and line emission coefficients. The continuous spectrum volume emission coefficient, caused by light scattering by free electrons, is given by the formula

$$\varepsilon_\nu = n_e \sigma_0 \int I_\nu^0 \frac{d\omega}{4\pi}, \tag{17.4}$$

where n_e is the free electron density, σ_0 is the scattering coefficient calculated for one electron, and I_ν^0 is the intensity of the emission coming from the photosphere. On the other hand, the line volume emission coefficient, corresponding to the transition $k \rightarrow i$, is equal to /209

$$\varepsilon_\nu' = \frac{n_k A_{ki} h\nu_{ik}}{4\pi \Delta\nu_{ik}}, \tag{17.5}$$

where n_k is the number of atoms in the k-th state in 1 cm^3, A_{ki} is the Einstein spontaneous transition coefficient and $\Delta\nu_{ik}$ is the line width. The quantity n_k, by analogy with Eq. (5.7), can be represented in the form

$$n_k = b_k n_e n^+ \frac{g_k}{g^+} \frac{h^3}{2(2\pi mkT_e)^{3/2}} e^{\frac{\chi_k}{kT_e}}, \tag{17.6}$$

where the coefficient b_k shows by how much the value of the quantity $n_k/n_e n^+$ differs from its value in the presence of thermodynamic equilibrium with temperature T_e.

Substituting (17.6) into (17.5), we see that the line emission coefficient ε_ν' is proportional to $n_e n^+$, i.e., the square of the density (if the atoms are predominantly in an ionized state). The continuous spectrum emission coefficient ε_ν, however, is proportional to n_e, i.e., the first power of the density. Therefore

in the case of a low gas density, ε_ν' is a small quantity of the first order, and ε_ν—a small quantity of the second order. Consequently, at a sufficiently low density the line emission coefficient will be less than the continuous spectrum emission coefficient, caused by scattering by free electrons.

For the ratio of the quantities ε_ν' and ε_ν we have

$$\frac{\varepsilon_\nu'}{\varepsilon_\nu} \sim n^+ \sim \rho. \tag{17.7}$$

Since the density ρ decreases with increasing distance from the solar surface, then the ratio $\varepsilon_\nu'/\varepsilon_\nu$ also decreases. At a relatively high density (in the chromosphere) $\varepsilon_\nu'/\varepsilon_\nu \gg 1$, i.e., strong lines are seen on a relatively weak continuous background. At a relatively low density (in the corona) $\varepsilon_\nu'/\varepsilon_\nu \ll 1$, i.e., a continuous spectrum is observed and almost no lines (with some exceptions).

In reality the ratio $\varepsilon_\nu'/\varepsilon_\nu$ depends not only on the density but also on the temperature. It also depends on the atomic excitation mechanism, by which the value of the coefficient b_k is determined. Therefore the variation of the quantity $\varepsilon_\nu'/\varepsilon_\nu$ with the distance r will be different for different lines. Appropriate calculations can be made for each line with the aid of Eqs. (17.4)—(17.6). /210
This will be done below for the hydrogen Balmer lines.

3. Electron density. Since the basic mechanism of the coronal emission is light scattering by free electrons, then the distribution of free electrons in the corona can be found from the measured surface brightness. In principle, this problem is solved in the same manner as the problem of determining the distribution of the emitting atoms with height in the chromosphere, considered above.

We will assume that the corona possesses spherical symmetry (although in reality this is not exactly true). Let $\varepsilon(r')$ be the volume emission coefficient at a distance r' from the center of the Sun and I(r) be the intensity of the emission coming from the corona to the observer at a distance r from the center of the disk (see Fig. 18). These quantities are interrelated by the equation

$$I(r) = \int_{-\infty}^{+\infty} \varepsilon(r')\,ds, \tag{17.8}$$

where $s = \sqrt{r'^2 - r^2}$. This equation can also be rewritten in the form

$$I(r) = 2\int_r^\infty \frac{\varepsilon(r')\,r'\,dr'}{\sqrt{r'^2 - r^2}}. \tag{17.9}$$

Since the quantity I(r) is known for observations, then, solving Eq. (17.9) (the Abel equation), we can find the emission coefficient $\varepsilon(r)$. In practice, one usually makes use of the fact that if

$$\varepsilon(r) = \frac{C}{r^m}, \tag{17.10}$$

where C and m are constant, then, as follows from (17.9),

$$I(r) = \frac{2C}{r^{m-1}} \int_0^{\frac{\pi}{2}} \cos^m \varphi \, d\varphi. \tag{17.11}$$

On this basis, assuming that $\varepsilon(r)$ is the sum of terms of the form of (17.10), the constants C and m are chosen so that the sum of terms of the form (17.11) represents the specified function I(r) sufficiently well.

If the emission coefficient $\varepsilon(r)$ is found, then, using Eq. (17.4), we can determine the electron density $n_e(r)$. Assuming that the intensity I_0 of the photosphere emission does not depend on direction, we obtain /211

$$n_e(r) = \frac{2\varepsilon(r)}{\sigma_0 I_0 \left[1 - \sqrt{1 - \left(\frac{r}{R}\right)^2}\right]}, \tag{17.12}$$

where R is the radius of the Sun.

For a more rigorous solution of the problem of determining the electron density in the corona, the darkening of the solar disk from center to edge must be taken into account. Moreover, consideration must be given to the fact that the free electrons do not scatter the radiation isotropically but with a scattering indicatrix of $x(\gamma) = 3/4(1 + \cos^2\gamma)$. An exact solution of the problem in this case has been derived by A. F. Bogorodskiy and N. A. Khinkulov.

The degree of coronal radiation polarization p(r) can be calculated after determinion of the electron density $n_e(r)$ (which has already been mentioned above). The agreement of the calculated and observed values of p(r) serves as a control on the validity of the determination of $n_e(r)$.

Let us present some results of a determination of the electron density in the corona. Baumbach (by considering the electron scattering to be isotropic) derived the following approximate formula for the quantity $n_e(r)$:

$$n_e(r) = 10^8 \left[0.036\left(\frac{R}{r}\right)^{1.5} + 1.55\left(\frac{R}{r}\right)^6 + 2.99\left(\frac{R}{r}\right)^{16}\right] \tag{17.13}$$

A detailed investigation of the coronal structure has been made by Van de Hulst (see [1]). The anisotropy of the electron scattering, the exclusion of the F component, and the polarization of the coronal radiation were taken into consideration in his work. The results obtained by Van de Hulst are presented in Table 20, containing values of the electron density both for the corona during maximum solar activity and for the corona during minimum solar activity. The "maximum" corona is assumed to be spherically symmetric, and for the "minimum" corona separate values of n_e are given for the equatorial and polar regions.

TABLE 20. ELECTRON DENSITY IN THE CORONA

$n_e(r) \cdot 10^{-6}$

r/R	"Max" corona	"Min" corona		r/R	"Max" corona	"Min" corona	
		equatorial	polar			equatorial	polar
1,00	403	227	174	1,5	14,8	8,3	1,41
1,03	316	178	127	1,7	7,11	4,0	0,542
1,06	235	132	87,2	2,0	2,81	1,58	0,196
1,1	160	90,0	53,2	2,6	0,665	0,374	0,040
1,2	70,8	39,8	16,3	3,0	0,313	0,176	0,017
1,3	37,6	21,1	5,93	4,0	0,090	0,050	0,004

Commas represent decimal points.

We can also determine the total number of free electrons in the corona for which its luminosity is adequately known. If ε is the emission coefficient, then the coronal luminosity is equal to

$$L_k = 4\pi \int \varepsilon \, dV, \tag{17.14}$$

where the integration is carried out over the entire coronal volume. Since the coronal luminosity is determined primarily by the emission of its inner portions (for which $r \approx R$), then on the basis of Eq. (17.12) one can write approximately /212

$$\varepsilon(r) = \frac{1}{2} n_e(r) \sigma_0 I_0. \tag{17.15}$$

The substitution of (17.15) into (17.14) gives

$$L_k = 2\pi\sigma_0 I_0 N_e, \tag{17.16}$$

where $N_e = \int n_e dV$.

On the other hand, the luminosity of the Sun is equal to

$$L_\odot = 4\pi R^2 \pi I_0. \tag{17.17}$$

Therefore for the ratio of the coronal luminosity to the solar luminosity we obtain

$$\frac{L_k}{L_\odot} = \frac{\sigma_0 N_e}{2\pi R^2}. \tag{17.18}$$

Equation (17.18) makes it possible to determine the total number of free electrons N_e in the corona if the quantity $L_k/L_\odot$ is known from observations. As already mentioned $L_k/L_\odot \approx 10^{-6}$. Therefore we find: $N_e \approx 5 \cdot 10^{40}$.

Incidentally, from this it follows that the number of free electrons of the corona, present in one square centimeter of the solar surface, is equal to

$$\frac{N_e}{4\pi R^2} \approx 10^{18}. \tag{17.19}$$

Multiplying this number by the scattering coefficient, calculated for one free electron, we obtain an approximate value for the optical thickness of the corona, which is equal to $\tau_0 \approx 10^{-6}$. Such a result should be expected since the approximate equality $L_k \approx \tau_0 L$ must be satisfied. /213

4. Coronal lines. About 30 emission lines are present in the visible portion of the coronal spectrum. The brightest of these is the "green" line with a wavelength of 5303 Å. The lines λ 6375 and λ 6702 Å in the red portion of the spectrum, λ 7892, λ 10747 and λ 10798 Å—in the infrared and λ 3388 Å—in the ultraviolet are also very strong lines. The relative intensities of the lines are different in different portions of the corona. The lines are fairly broad—about 1 Å.

For a long time the origin of the coronal lines was an enigma in astrophysics. Finally, in 1939 Grotian observed that the frequencies of two coronal lines coincide with the frequencies of the forbidden lines arising during transitions between sublevels of the ground state of Fe X and Fe XI ions. Then Edlen found the same agreement for the frequencies of two other coronal lines and lines of the Ca XII and Ca XIII ions. It should be noted that the forbidden lines of these ions have not been observed in the laboratory. The frequencies of these lines were determined from the term scheme constructed from the allowed lines, observed in the laboratory, lying in the ultraviolet portion of the spectrum.

Later, Edlen [16] identified most of the lines in the coronal spectrum. It was found that all of them are formed through forbidden transitions between sublevels of the first state of highly ionized atoms (iron, calcium, nickel and argon). A list of the identified coronal lines, together with different information about them, is given in Table 21.

Calculations show that the highly ionized atoms of other elements do not have lines in the visible portion of the spectrum or their lines are too weak and be observed on the background of the continuous coronal spectrum. However,

TABLE 21. CORONAL EMISSION LINES

Wave length	Observed relative intensity		Ion	Probability coefficient A_{ki} in sec^{-1}	Excitation potential in eV	Ionization potential in eV
	from Grotian	from Lee				
3328	1,0	—	Ca XII	488	3,72	589
3388	16	—	Fe XIII	87	5,96	325
3601,0	2,1	—	Ni XVI	193	3,44	455
3642.9	—	—	Ni XIII	18	5,82	350
3986,9	0,7	—	Fe XI	9,5	4,68	261
4086.3	1,0	—	Ca XIII	319	3,03	655
4231,4	2,6	—	Ni XII	237	2,93	318
4359	—	—	Ar XIV	108	2,84	682
5116,03	4,3	2,2	Ni XIII	157	2,42	350
5302,86	100	100	Fe XIV	60	2,34	355
5536	—	—	Ar X	106	2,24	421
5694,42	—	1,2	Ca XV	95	2,18	814
6374,51	8,1	18	Fe X	69	1,94	233
6701,83	5,4	2,0	Ni XV	57	1,85	422
7059,62	—	2,2	Fe XV	—	31,77	390
7891,94	—	13	Fe XI	44	1,57	261
8024,21	—	0,5	Ni XV	22	3,39	422
10746,80	—	55	Fe XIII	14	1,15	325
10797,95	—	35	Fe XIII	9,7	2,30	325

Commas represent decimal points.

some lines are present that are at the limit of visibility and in the future some method may be found to make it possible to detect them.

This identification of the coronal lines, however, immediately raises two questions: 1) what causes the existence of multiply-ionized atoms in the corona? 2) why are forbidden lines observed in the coronal spectrum? The answer to the first of these questions will be given below. Now, let us provide a brief answer to the second question (postponing a detailed consideration of the problem of the appearance of forbidden lines in the spectra of celestial bodies until Chapter V, devoted to gas nebulae).

As is known, the Einstein spontaneous transition coefficients for the allowed lines are of the order of 10^8 sec^{-1}. For the forbidden lines, however, /214
these coefficients are much smaller. For example, they are of the order of $10-10^3$ sec^{-1}, as seen from the table, for the forbidden lines in the coronal spectrum (although the exclusion in these cases is not very strong). Because of the smallness of the probabilities of forbidden transitions, special conditions are necessary in order that the forbidden lines could become fairly intense.

To ascertain these conditions, let us first of all note that if both forbidden, as well as allowed transitions, are possible from a given state, then the former occur much less frequently than the latter, and the forbidden line is much weaker than the allowed. Consequently, the forbidden lines can become relatively

intense only when the upper state is metastable, i.e., there are no downward transitions from it except forbidden.

However, unlike the usual excited states in which the atom exists for a time of the order of 10^{-8} sec, it can exist in the metastable state much longer. Therefore to achieve a spontaneous transition from a metastable state it is necessary that it not undergo external excitation over very long periods of time. In particular, the atom must not undergo frequent encounters with free electrons since the latter can transfer it downward from the metastable state without the emission of radiation of a forbidden line through a collision of the second kind. The atom must not be subjected to a strong interaction with radiation since the absorption of it can excite the atom upward from the metastable state. Thus, for the appearance of relatively intense forbidden lines in the spectrum of any object it is necessary that the matter density and the radiation density in it be quite low. /215

The very existence of forbidden lines in the coronal spectrum indicates that these conditions are fulfilled in the corona. Calculations confirm this. As we have seen, the electron density in the corona is quite low, and collisions do not prevent spontaneous transitions from metastable states (although the values of n_e in the corona are several orders of magnitude greater than in nebulae, the transition probabilities for the coronal lines are relatively high). Moreover, the condition with regard to the radiation density is also satisfied in the corona. For the ions, giving the coronal lines, to transfer upward from their metastable states, radiation in the far ultraviolet portion of the spectrum is required. However, the density of this radiation is very low in the solar atmosphere.

5. Corona temperature. Right after the identification of the coronal lines an important discovery was made in solar physics: several facts become known which attested to an extremely high coronal kinetic temperature—of the order of a million degrees. Let us now present the most significant of these facts.

1. Intense ionization of atoms in the corona. This fact should be placed first. If the corona temperature were not so high, the existence of multiply ionized atoms (such as Fe X, Ca XII, etc.) in it would be completely incomprehensible. At a temperature of the order of 10^6 degrees, however, intense ionization of atoms is caused by electron collisions (see below).

2. Blurring of absorption lines. We have already stated that Fraunhofer lines, with the exception of some severely diffuse ones, are not seen in the coronal spectrum, arising from the scattering of solar radiation by free electrons. This is explained by the Doppler broadening of the lines because of the thermal motion of the free electrons. If, however, it is assumed that the corona temperature is equal to the temperature of the reversing layer, i.e., 5000°, then the absorption line profiles calculated from Eq. (17.2) are appreciably narrower and sharper than the observed profiles. For the theory to agree with observations, it is necessary to assume that the temperature of the electron gas of the corona is no lower than 600,000°. /216

3. Emission line widths. The measured profiles of the emission lines in the coronal spectrum are well represented by curves corresponding to a Maxwellian

velocity distribution of the atoms. This makes it possible to find the average atom velocity from the line width. For the green λ 5303 Å line, belonging to Fe XIV, the width is about 1 Å, which means an average atom velocity of about 25 km/sec. From this a value of about $2 \cdot 10^6$ degrees is obtained for the kinetic temperature.

4. Absence of Balmer lines. As already mentioned, the emission lines in the coronal spectrum must be weak on the continuous spectrum background. However, the hydrogen in the outer layers of the Sun is so abundant that the Balmer lines would be observed if the corona temperature were low. The absence of these lines in the coronal spectrum, however, attests to its high temperature. The strong dependence of the intensity of the Balmer lines on the temperature is explained by the fact that these lines arise as the result of recombinations, and the recombination probability is approximately proportional to $T_e^{-3/2}$. Consequently, for $T_e = 10^6$ degrees the line intensity should be approximately 1000 times less than for $T_e = 10^4$ degrees. The ratio of the intensities of the Balmer lines to the intensity of the continuous spectrum can be found with the aid of Eqs. (17.4)—(17.6). Such calculations have shown that the H_α line will not be observable in the coronal spectrum if $T_e > 100,000°$ (see [17]).

5. Density gradient in the corona. As seen from Eq. (17.13) and Table 20, the density in the corona does not decrease very rapidly with an increase in r. In any case, this decrease occurs much more slowly than according to the barometric height formula with a temperature of 5000°. On this basis a hypothesis was put forth concerning the fact that the corona is not in hydrostatic equilibrium, and is sustained by turbulent motions. Such a hypothesis (not confirmed by observations), however, is not necessary if the corona temperature is assumed to be very high. Let us take the generalized barometric height formula

$$n_e \sim e^{\frac{GM\mu m_H}{rRkT}}, \tag{17.20}$$

differing from the usual barometric height formula (16.31) by the fact that the dependence of the gravitational acceleration on r is taken into consideration in /217
it. Here G is the gravitational constant, M is the Sun's mass, R is its radius, m_H is the mass of a hydrogen atom, μ is the mean molecular weight. It is easy to verify that Eq. (17.20) is a good representation of the observational data on the electron density, presented in Table 20, i.e., $\lg n_e$ and $1/r$ are interrelated by a linear function. For agreement between the theoretical and observed values of the angular coefficient of this function, the corona temperature must assume a value of $T \approx 1.4 \cdot 10^6$ degrees (it is derived for $\mu = 0.69$, i.e., in the case when the ratio of the number of hydrogen atoms to the number of helium atoms in the corona is equal to 5, just as in the chromosphere). Consequently, one can assume that the corona exists in hydrostatic equilibrium for the high temperature that has been cited.

6. Intensity of the solar radio emission. As we shall see in the following section, the main portion of the long-wavelength solar radio emission comes from the corona. From the measured intensities of this radio emission the electron temperature of the corona can be determined; it turns out to be of the order of 700,000°.

Thus one must assume that a corona temperature of the order of a million degrees is a well-established fact. However, the important questions of the cause of such a high corona temperature is not completely clear at present. Some hypotheses have been expressed to explain the corona heating. One of them proposes that the corona is heated because of the mechanical energy of the matter (in particular, of prominences) entering it from the chromosphere. According to another hypothesis corona heating occurs through the evolution of the Joulian heat of the electric currents created by the magnetic fields. Some authors have considered the entry of particles of interstellar matter (accretions) into the corona as a possible mechanism for corona heating. However, the most probable cause of the high corona temperature must be considered to be the existence of acoustic and magnetoacoustic waves coming from the photosphere. These waves are produced by convection and they travel through the upper photosphere and the lower chromosphere almost without loss. In the upper chromosphere and corona, however, they are converted, because of the reduction in density, into shock waves, the energy of which dissipates rapidly and changes into heat. Since the corona temperature that has been determined is established as a result of equilibrium between heating and cooling, corona cooling must also be considered in the theoretical determination of the temperature. It occurs because of the spectral line emission of the corona, because of the transfer of coronal energy to the cooler chromosphere by thermal conduction, because of the escape of fast particles, carrying some energy, from it. Calculations show that the energy /218 loss of the corona is relatively small. Because of this, the hypothetical corona heating mechanisms must not be very energetic.

In the construction of a corona theory, the mass balance must be investigated along with a consideration of the energy balance. Material enters the corona from the chromosphere and this process is compensated by the outflow of material from the corona. The dispersion of particles from a stationary corona has been investigated previously; now, however, let us assume that the entire corona is spreading out. Radar studies of the Sun have established an outward movement of gas in the corona with velocities increasing from two to several tens of km/sec. This gas movement leads to the appearance of a "solar wind" in interplanetary space.

It should be noted again that the correct corona theory must explain its observed inhomogeneity. As observations have shown, the green and red lines in the coronal spectrum (with wavelengths of 5303 Å and 6374 Å, respectively) arise in different regions of the corona. Since the first of these lines belong to Fe XIV, and the second to Fe X, then it is reasonable to assume that the "green" region of the corona is appreciably hotter than the "red". It appears that the corona temperature is below average in the polar region and above average over spots and faculae. Also of considerable interest for corona theory are its various structural formations: streamers, "arches", "necks", etc. The stability of these formations is apparently associated with the existence of magnetic fields in the corona.

6. Atomic ionization and excitation. We have already mentioned that the high corona temperature makes it possible to understand the existence of multiply ionized atoms in it. To determine, however, the degree of atomic ionization in the corona, it is necessary to use the conventional Saha ionization formula since thermodynamic equilibrium does not exist in the corona. In such cases the degree of atomic ionization is found by considering those elementary processes, which lead to ionization, and the opposite processes, i.e., recombinations. Below (in Chapters V, VI and VII) formulas will be derived for ionization in the absence of thermodynamic equilibrium for the case of nebulae and the envelopes of nonstationary stars. Now, however, let us consider rather briefly the question of the degree of atomic ionization for the coronal case (although it must be borne in mind that the ionization formulas for the nebular and coronal cases are vastly different from each other because of differences in the ionization mechanism).

Let us first consider for simplicity the ionization of hydrogen atoms. Just as before, let n_1, n^+ and n_e be the number of neutral atoms (in the first state), the number of protons and the number of free electrons in 1 cm^3, respectively. Atomic ionization can occur both through collisions (among which collisions with /219 free electrons play the largest role), and under the influence of radiation. The number of these processes, occurring in 1 cm^3 in 1 sec, we will denote by $n_1 n_e B$ and $n_1 D$, respectively. The reverse processes are recombinations through triple collisions (without radiation) and recombinations associated with radiation (both spontaneous, as well as stimulated). We will denote the number of recombinations by $n_e^2 n^+ A$ and $n_e n^+ C$, respectively. In the stationary state the number of ionizations is equal to the number of recombinations, i.e., the equality

$$n_1 n_e B + n_1 D = n_e^2 n^+ A + n_e n^+ C. \tag{17.21}$$

is satisfied.

In the presence of thermodynamic equilibrium each forward process is compensated by a reverse process. In particular, the number of ionizations through collisions is equal to the number of recombinations through collisions, i.e.,

$$n_1 B = n_e n^+ A. \tag{17.22}$$

Analogously, the number of ionizations due to the influence of radiation is equal to the number of recombinations associated with radiation, i.e.,

$$n_1 D = n_e n^+ C. \tag{17.23}$$

Equations (17.22) and (17.23) change over into the usual ionization formula (5.5) if the values of the coefficients A, B, C and D for the case of thermodynamic equilibrium are substituted into them (more precisely, for a Maxwellian distribution of free electron velocities and for a Planckian radiation density).

In the absence, however, of thermodynamic equilibrium the degree of atomic ionization is determined from Eq. (17.21) in which each term must be determined

for specific conditions. In the outer layers of stars and in nebulae, because of the low density of matter, recombinations through triple collisions occur much less frequently than recombinations associated with radiation, i.e.,

$$n_e A \ll C. \tag{17.24}$$

With regard to ionizations, they generally occur both through collisions and due to the effect of radiation. As we will see below, in nebulae ionization is caused by the radiation of hot stars. In this case the degree of atomic ionization is determined by Eq. (17.23) with an appropriate (different from Planckian) radiation density. In the corona, however, the ultraviolet radiation density is very small and it plays no role in the ionization of atoms (with the exception of the first ionization of metals). It is easy to understand that for an enormous kinetic corona /220
temperature, the ionization of atoms in it is caused by electron collision. In the given case, from Eq. (17.21) we obtain

$$\frac{n^+}{n_1} = \frac{B}{C}. \tag{17.25}$$

It is important to note that the degree of ionization in the corona does not depend on the density of matter (but depends only on the electron temperature T_e).

A theory of atomic ionization in the corona has been developed by I. S. Shklovskiy [17]. Calculations made by him from Eq. (17.25) for hydrogen led to values of the quantity n^+/n_1 of the order of 10^6 for $T_e \approx 10^5$ degrees, and of the order of 10^7 for $T_e \approx 10^6$ degrees (when $n_e \approx 10^8$ cm^{-3}). These values of the quantity n^+/n_1 are about a million times smaller than its value in the case of thermodynamic equilibrium for the same temperatures and densities.

The determination of the relative numbers of metal atoms in different ionization states can also be done with Eq. (17.25) (in which, now, n_1 must be understood to be the atom density in a given ionization state, and n^+—in the subsesequent state). In this case, however, approximate expressions must be used for the coefficients B and C since quantum mechanical calculations of these quantities are very difficult. Values of the relative numbers of iron atoms in different ionization states, obtained by I. S. Shklovskiy for different electron tempera- /221
atures, are presented in Table 22 as an example.

We see that for a given electron temperature the number of atoms first increases with an increase in the ionization state, and then decreases. For example, for $T_e = 800,000°$ the maximum number of iron atoms exists in the Fe XII state.

According to observations, the Fe X—Fe XV lines exist in the coronal spectrum, with the line radiation of the different atoms coming from different regions of the corona. On the basis of the table, one can say that the corona temperature must be of the order of a million degrees, with it being different in different regions. For example, the coronal region, emitting in the Fe X—Fe XI lines, must

TABLE 22. IONIZATION OF IRON IN THE CORONA

$T_e \cdot 10^{-6}$	0,3	0,5	0,6	0,7	0,8	1,0	1,2	1,4
Fe X / Fe IX	0,092	0,83	1,6	2,9	6,0	13	30	—
Fe XI / Fe X	—	0,29	0,77	1,1	2,7	8,0	12	22
Fe XII / Fe XI	—	0,10	0,30	0,52	1,1	3,5	7,2	12
Fe XIII / Fe XII	—	0,030	0,10	0,29	0,47	1,4	3,4	7,2
Fe XIV / Fe XIII	—	0,010	0,039	0,13	0,31	0,66	2,0	4,3
Fe XV / Fe XIV	—	0,0033	0,014	0,047	0,12	0,40	0,82	1.7

Commas represent decimal points.

have a temperature of the order of 600,000°, and the region emitting in the Fe XIII—Fe XIV lines, a temperature of the order of 1,200,000°. Lines of atoms, existing in ionization states that are very far apart, are sometimes seen in the spectrum of one and the same point of the corona. This can be explained by the fact that the line of sight traverses regions with different temperatures.

After consideration of the problem of atom ionization in the corona let us turn to the question of ion excitation. For the present we will only speak of the excitation of those levels of the ionic ground state, the transitions from which give rise to the observed forbidden lines in the coronal spectrum. The excitation of these levels occurs by two paths: 1) through collisions with free electrons, 2) through the absorption of radiation coming from the photosphere (the second excitation mechanism plays some role in the outer portions of the corona). The return of the ion to the lower level occurs both through spontaneous transitions and through collisions of the second kind. From the condition that the number of ions in each of the levels is constant, one can find the ratio of the number of ions in the k-th level to the number of ions in the first level, i.e., the quantity n_k/n_1. We will not dwell on these calculations here since the distribution of ionic levels in gas nebulae, which will be discussed in detail in Section 24, is determined in the same manner.

Knowing the ratio n_k/n_1 allows one to convert from the concentration of ions in the excited level n_k (found from the measured intensity of the emission line, as in the case of the chromosphere) to the concentration of ions in the first level n_1. Summing the numbers n_1 for all ionization states allows one to determine the total concentration of atoms of a given element. After dividing this concentration by n_e, we obtain the ratio of the number of atoms of the element being considered to the number of hydrogen atoms (since n_e is approximately equal to the proton concentration).

The ratio of the number of metal atoms to the number of hydrogen atoms in the corona was determined by this method. It was found that this ratio is independent of the height and approximately the same as in the reversing layer. /222
This fact is of considerable interest since it attests to the intermixing of material in the corona.

7. Ultraviolet and x-radiations. The coronal lines observed in the visible portion of the spectrum are formed through transitions between sublevels of the ground states of the different ions. The next states of the coronal ions are, however, very high. For example, the resonance excitation potentials of the Fe X—Fe XV ions are 30-40 V. Therefore the resonance lines of these ions lie in the far ultraviolet region of the spectrum.

Excitation of ions in the corona can occur as the result of ionizations and subsequent recombinations. However, as calculations show, an electron collision is a more effective excitation mechanism. It should be borne in mind that for a temperature of the order of a million degrees, the average energy of a free electron is about 100 eV. Therefore each free electron, in practice, can excite, through a collision, ions such as the iron ions mentioned above.

Specifying a certain coronal chemical composition, we can compute its ultraviolet spectrum. Calculations have shown that this spectrum should be very rich in emission lines. Moreover, the corona should also exhibit a continuous spectrum in the region being considered, arising from the recombinations of the most abundant atoms: hydrogen ($\lambda < 912$ Å), helium ($\lambda < 504$ Å) and ionized helium ($\lambda < 227$ Å). A continuous spectrum at even shorter wavelengths (of the order of tens of angstroms) should appear due to the recombinations of highly ionized atoms of iron, nickel, etc.

Observations, made with the aid of rockets, provided the possibility of determining the ultraviolet solar spectrum. This spectrum has already been described in the previous section. There, however, it was indicated that the ultraviolet solar radiation arises primarily in the upper chromosphere and the transition region between the chromosphere and corona. However, a portion of this radiation, caused by multiply ionized atoms, comes from the corona.

As is known, very short wavelength radiation (from about 0.1 Å to several tens of angstroms) belongs to the x-ray region of the spectrum. It is easy to understand that fairly intense x-radiation should appear in the corona with its high temperature. As follows from what has been said above, it can be both continuous as well as line.

Solar x-radiation has also been observed with the aid of rockets. The observations were made with filters predominantly in the 2-8, 8-18 and 44-60 Å spectral regions, i.e., in the soft x-ray region. Observations over a number /223
of years have made it possible to determine the dependence of the x-radiation intensity on the solar activity phase. It was found that in years of maximum activity the x-radiation is several times more intense than in years of minimum activity. This is explained both by an increase in the coronal density, as well as an increase in its temperature during the transition from minimum to maximum activity.

The results of solar x-radiation observations during the 1958 eclipse are of considerable interest. One of these is proof of the fact that the solar x-radiation is actually formed in the corona. The fact that the x-radiation intensity, during the total eclipse phase, amounts to a significant fraction (about 10%) of its uneclipsed intensity serves as the basis for this conclusion (at the same time the intensity of the L_α line emission, arising in the chromosphere, decreases by about a factor of a thousand). Another important result was obtained by investigating the dependence of the x-radiation intensity on the eclipse phase. It was observed that a particularly intense x-radiation comes from portions of the corona lying above the active regions of the solar surface. This result is also confirmed by x-ray photographs of the uneclipsed Sun.

The results of an observation of the x-radiation during chromosphere flares are especially interesting. In these cases streams of hard x-rays—with wavelengths of about 1 Å and less—are observed over fairly short time intervals (of the order of a few minutes). To explain such radiation one can made an assumption about the formation of very hot regions in the corona. Calculations, made by Elwert (see [14]), provided a representation of the coronal x-ray spectrum for different temperatures. For example, a temperature of about 10^7 degrees is sufficient for the appearance of radiation with a wavelength of about 3 Å. However, to explain the observed shorter wavelength radiation requires assuming the presence of a nonthermal emission mechanism in the corona. This mechanism, for example, can be the reverse Compton effect, i.e., the formation of hard photons through the scattering of radiation by relativistic electrons (which can occur in the vicinity of a flare).

18. Solar Radio Emission

1. Results of observations. Solar radio emission was discovered during the Second World War and has been very intensively investigated since then. It was very quickly established that this emission comes to us from the corona and upper chromosphere layers. Thus, from the observed solar radio emission /224 one can draw conclusions about the physical processes in its outermost portions. It is important to emphasize one significant advantage of radio observations of the corona and chromosphere over optical observations: whereas the high brightness of the photosphere interferes to a great extent with observations in the optical region, this is not the case for radio observations (since these very portions of the Sun are the "photosphere" for radio emission).

Observations of the solar radio emission from the earth's surface can be made within a fairly broad wavelength interval—from several millimeters to several tens of meters. Shorter wavelength radiation is absorbed in the earth's atmosphere (by O_2 and H_2O molecules), and longer wavelength radiation is reflected from the earth's ionosphere.

The solar radio emission has been studied with the aid of radio telescopes, allowing one to measure the solar radiation of a specific wavelength. To measure the intensities of the radio emission coming from different points of the solar disk, large-size radio telescopes or radio interferometers must be used. This is caused by the fact that the angular resolution, defined as the ratio of the

telescope aperture diameter to the radiation wavelength, is much less at radio frequencies than at optical.

Very valuable information on the brightness distribution over the disk at radio frequencies is also obtained during solar eclipses. Let us note that S. E. Khaykin and B. N. Chikhachev first proved experimentally the coronal nature of the meter wavelength solar radio emission through observations of the 1947 solar eclipse (since the radio emission during total eclipse was found equal to about 40% of the uneclipsed emission).

The measured radio emission intensity I_ν is usually characterized by the brightness temperature T_ν, i.e., it is represented in the form $I_\nu = B_\nu(T_\nu)$, where $B_\nu(T)$ is the Planckian intensity at temperature T. Since $h\nu/kT \ll 1$ for radio frequencies, Planck's formula passes over to the Rayleigh-Jeans formula:

$$B_\nu(T) = \frac{2\nu^2}{c^2} kT. \tag{18.1}$$

Therefore the brightness temperature is determined by the relation

$$I_\nu = \frac{2\nu^2}{c^2} kT_\nu. \tag{18.2}$$

The measured solar radio emission can be written in the form /225

$$H_\nu = I_\nu \Omega, \tag{18.3}$$

where $\bar{I}_\nu$ is the average emission intensity and Ω is the solid angle at which the solar disk is viewed. Denoting the Planckian intensity by $\bar{I}_\nu$, corresponding to temperature $\bar{T}_\nu$, we can consider this temperature to be a measure of the emission. The quantity $\bar{T}_\nu$ is called the effective temperature for frequency ν. Using Eq. (18.2), we have

$$H_\nu = \frac{2\nu^2}{c^2} k\bar{T}_\nu \Omega. \tag{18.4}$$

Since $\Omega = \pi(R/r)^2$, where R is the radius of the Sun and r is the distance from the Earth, then instead of (18.4) we obtain

$$H_\nu = \pi\left(\frac{R}{r}\right)^2 \frac{2\nu^2}{c^2} k\bar{T}_\nu. \tag{18.5}$$

However, the solar luminosity at frequency ν is represented in the form

$$L_\nu = 4\pi^2 R^2 \frac{2\nu^2}{c^2} k\bar{T}_\nu. \tag{18.6}$$

As observations show, solar radio emission comprises two components: 1) the radio emission of the quiet Sun (undisturbed component) and 2) the irregular radio emission of the Sun (disturbed component). The first component is almost constant (more precisely, it varies slightly during the solar activity cycle). As we shall see below, it is the thermal emission of the corona and chromosphere. The second component undergoes slow as well as very rapid variations with time. Its origin is associated with various active processes on the Sun: spots, chromosphere flares, etc.

A measurement of the solar radio emission leads to the result that the effective temperature $\bar{T}_\nu$ for the undisturbed component is about 10^4 degrees in the centimeter band and about 10^6 degrees in the meter band. With respect to the disturbed component, effective temperatures of the order of 10^8-10^9 degrees and higher are sometimes obtained for it in the meter band. In other words, the disturbed solar radio emission is sometimes 100-1000 and more times greater than the radio emission of the quiet Sun.

Below we will discuss primarily the undisturbed component of the solar radio emission, while the disturbed component will be considered very briefly. A detailed discussion of the problem of solar radio emission is contained in the already cited monographs [1], [2], [17] and especially in the book of V. V. Zheleznikov [18]. The general theory of radio emission propagation in a plasma is discussed in V. L. Ginzburg's monograph [19]. /226

2. Radio emission of quiet Sun. Proceeding toward an interpretation of the observational data on solar radio emission, let us first give an answer to the question: in what layers of the Sun does it originate? To do this, we must determine the optical depths of the different layers in the radio frequency region. It is obvious that the emission can reach the observer only from those layers whose optical depth is no greater than about unity.

The volume absorption coefficient α_ν must be known in order to find the optical depth τ_ν. As explained in Section 5, the absorption of continuous spectrum radiation occurs through photoionizations and free-free transitions. Photoionizations, however, are produced only by those quanta whose energy is greater than ionization energy ($h\nu > \chi_i$), and therefore quanta in the radio frequency region, having a low energy, cannot be absorbed through photoionizations (they could be absorbed through photoionizations from the high discrete levels, but these levels do not occur in real life). At the same time quanta of any frequencies, including very low, can be absorbed through free-free transitions. The absorption of radio emission occurs through the free-free transitions.

The volume absorption coefficient, caused by free-free electron transitions in the field of a proton, is given by Eq. (5.10).

Since hydrogen is the most abundant element in the solar atmosphere, then let us assume that the total volume absorption coefficient is approximately deter-

mined by this formula, i.e.,

$$\alpha_\nu = n_e n^+ \frac{2^4 \pi^2 e^6 k T_e}{3\sqrt{3}\, c b (2\pi m k T_e)^{3/2}} \frac{g_\nu}{\nu^3} \tag{18.7}$$

where n^+ and n_e are the concentrations of protons and free electrons, respectively, T_e is the electron gas temperature and g_ν is the Gaunt factor (about 10 in the radio frequency region).

However, negative absorption, which plays a very big role for radio emission is not taken into consideration in Eq. (18.7). On the basis of what has been said in Section 8, the factor $1 - e^{-h\nu/kT_e}$ must be introduced on the right side of Eq. (18.7) to take negative absorption into account. A factor of this form is /227 introduced for free-free transitions for the assumption of a Maxwellian velocity distribution for the free electrons.

The quantity $h\nu/kT_e$ is very small in the radio frequency region (for example, $h\nu/kT_e \approx 10^{-8}$ for $T_e \approx 10^6$ degrees and $\lambda = 100$ cm), so that this factor can be replaced by the quantity $h\nu/kT_e$. Therefore the volume absorption coefficient in the radio frequency region, when negative absorption is taken into consideration, is written in the form

$$\alpha_\nu = n_e n^+ \frac{2^4 \pi^2 e^6}{3\sqrt{3}\, c (2\pi m k T_e)^{3/2}} \frac{g_\nu}{\nu^2}. \tag{18.8}$$

Since g_ν is only very slightly dependent on ν, then one can assume that $\alpha_\nu \sim 1/\nu^2$.

Using the expression that has been derived for α_ν, we can determine the optical depth of any point in the solar atmosphere from the formula

$$\tau_\nu = \int_r^\infty \alpha_\nu\, dr = \frac{2^4 \pi^2 e^6}{3\sqrt{3}\, c (2\pi m k T_e)^{3/2}} \frac{g_\nu}{\nu^2} \int_r^\infty n^+ n_e\, dr, \tag{18.9}$$

where, for simplicity, it is assumed that T_e = const. The dependence of n_e on r must be known to calculate the integral entering into (18.9) ($n^+ = n_e$, approximately). For the corona this dependence is given by Eq. (17.13). The results of a calculation of the optical depths in the corona for different wavelengths are given in Table 23, taken from I.S. Shklovskiy's book [17].

From the table it is seen that for meter waves the optical thickness of the corona exceeds unity, i.e., the solar radio emission in the meter wave region comes to the observer primarily from the corona. The corona is transparent, to an appreciable degree, to shorter wavelength radiation, and therefore this /228

TABLE 23. OPTICAL DEPTHS IN THE CORONA FOR RADIO EMISSION

$\frac{r}{R}$	Wavelength λ cm							
	50	100	150	187	300	400	800	1200
1,04	0,183	0,73	1,65	2,58	6,6	11,7	47	107
1,1	0,061	0,26	0,59	0,93	2,4	4,2	17	38
1,2	0,017	0,068	0,154	0,24	0,62	1,09	4,4	10
1,4	0,004	0,015	0,035	0,053	0,14	0,25	1,0	2,3
1,6	0,0006	0,002	0,005	0,008	0,02	0,03	0,14	0,82

Commas represent decimal points.

radiation comes to the observer not only from the corona but also from the chromosphere.

The radio emission absorption process that has been discussed occurs through the transitions of free electrons from one hyperbolic orbit to another in the field of an ion. The emission of quanta in the radio frequency regions occurs through reverse transitions. Such transitions are the source of the quiet Sun radio emission. Thus, this emission is the usual thermal emission of the electron gas. In terms of its origin, the undisturbed solar emission is no different from solar radiation in the optical region of the spectrum. Solar radio emission, however, comes to the observer from the corona and chromosphere, and the emission in the optical portion of the spectrum—from deeper photosphere layers. This difference is explained by the drastic increase in the absorption coefficient with a decrease in radiation frequency.

If we know the volume absorption coefficient α_ν, then we can also easily determine the volume emission coefficient ε_ν. For this, let us make use of the known relation

$$\varepsilon_\nu = \alpha_\nu B_\nu(T_e), \tag{18.10}$$

which is valid for free-free transitions for a Maxwellian velocity distribution of the free electrons. Substituting Eqs. (18.1) and (18.8) into Eq. (18.10), we obtain

$$\varepsilon_\nu = n_e n^+ \frac{2^5 \pi^2 e^6 k T_e}{3\sqrt{3}\, c^3 (2\pi m k T_e)^{3/2}} g_\nu. \tag{18.11}$$

Knowing the absorption and emission coefficients allows one to calculate the intensity of the radiation coming to the observer at any distance from the center of the solar disk. We will perform this calculation below, but for now let us derive an approximate formula for the solar luminosity at radio frequencies. Let us denote by R_ν the radius of the solar disk for the radio emission frequency ν (it is defined from the condition that the optical path of the ray, coming at a

distance R_ν from the center of the disk, is equal to unity). Then, assuming that T_e = const, for the solar luminosity at frequency ν we have

$$L_\nu = 4\pi R_\nu^2 \pi B_\nu(T_e). \tag{18.12}$$

Substituting Eq. (18.1) here, we find

$$L_\nu = 4\pi^2 R_\nu^2 \frac{2\nu^2}{c^2} kT_e. \tag{18.13}$$

We will apply Eq. (18.13) to the solar radio emission at meter wavelengths, which, as was explained above, comes to us from the corona. As seen from this formula, the solar luminosity is proportional to the frequency squared, which is confirmed by observations. From the value of the luminosity, found from observations, one can determine the electron temperature T_e of the corona with the aid of Eq. (18.13). /229

As already stated, the effective temperature of the Sun $\overline{T}_\nu$ in the meter region is about 10^6 degrees. Comparing Eqs. (18.6) and (18.3), we see that $\overline{T}_\nu \approx$ $\approx T_e$ (since R_ν differs little from R). Therefore the electron temperature of the corona must also be about 10^6 degrees. The measurement of the solar luminosity at radio frequencies was one of the first proofs in favor of a high corona temperature. If the corona temperature were equal to the photosphere temperature, then the solar luminosity in the meter band would be hundreds of times lower than what is observed (since $L_\nu \sim T_e$).

The centimeter wave solar radio emission comes primarily from the upper chromosphere layers. The measured effective temperature of this emission (about 10,000°) is approximately equal to the electron temperature of these layers.

It should be emphasized that Eq. (18.13) is valid only when T_e = const. Therefore it cannot be applied to the centimeter wave solar radio emission, which comes to use partly from the corona and partly from the chromosphere. The formula for the solar luminosity in this case will be derived below.

3. Distribution of radio emission over the disk. Knowing the mechanism of quiet Sun radio emission permits one to find the intensity distribution of this emission over the disk. Generally speaking, the radio emission of a given frequency comes to the observer both from the corona and from the chromosphere.

Let us denote the corona temperature by T_1 and the chromosphere temperature by T_2, and we will assume they are constant. Let us also assume that the corona and chromosphere have spherical symmetry, with the boundary between them being a sphere of radius R.

The intensity of emission of frequency ν, coming to an observer at a distance r from the center of the disk, is given by the formula

$$I_\nu(r) = \int_{-\infty}^{+\infty} B_\nu(T_e) e^{-t_\nu} \alpha_\nu \, ds, \tag{18.14}$$

where t_ν is the optical distance of a given point in the solar atmosphere to the observer [compare with Eq. (16.9)]. If r > R, then the radiation comes only from the corona, and Eq. (18.14) assumes the form /230

$$I_\nu(r) = B_\nu(T_1)[1 - e^{-t_\nu^0(r)}], \tag{18.15}$$

where

$$t_\nu^0(r) = 2\int_r^\infty \frac{\alpha_\nu(r') r' \, dr'}{\sqrt{r'^2 - r^2}}. \tag{18.16}$$

If r < R, then chromosphere radiation (weakened by absorption in the corona), as well as corona radiation, reaches the observer. In this case, instead of (18.14) we have

$$I_\nu(r) = B_\nu(T_1)[1 - e^{-t_\nu^0(r)}] + B_\nu(T_2) e^{-t_\nu^0(r)}, \tag{18.17}$$

where

$$t_\nu^0(r) = \int_R^\infty \frac{\alpha_\nu(r') r' \, dr'}{\sqrt{r'^2 - r^2}}, \tag{18.18}$$

and it is assumed that the optical thickness of the chromosphere is infinitely great.

Equation (18.8) for the absorption coefficient α_ν must be substituted into Eqs. (18.16) and (18.18). Then a law must be specified for the variation of the electron density in the corona for calculating the quantity $t_\nu^0(r)$. Substitution of the calculated values of $t_\nu^0(r)$ into Eqs. (18.15) and (18.17) gives the theoretical distribution of the thermal radio emission over the solar disk.

The results of these calculations are inherently dependent on the emission wavelength. For radiation with a wavelength of about 1 cm and less, the optical thickness of the corona is very small and, therefore, as is seen from Eq. (18.17),

$$I_\nu(r) \approx B_\nu(T_2),$$

i.e., the radio emission intensity is the same over the entire disk and corresponds to the chromosphere temperature. With an increase in wavelength, the optical thickness of the corona increases and, in addition, the role of coronal radio

emission increases. As one goes out from the center of the disk, the intensity of this radiation increases at first, and decreases, reaching a maximum for r = = R (since the optical path length in the corona is a maximum for r = R). For meter waves, the optical thickness of the corona exceeds unity. In this case, as seen from Eqs. (18.17) and (18.15), the emission intensity is constant and corresponds to the corona temperature for r < R, and then decreases slowly with an increase in r.

The described results of calculations of the radio emission distribution over the solar disk agree, in general features, with observational data. The observed intensity distribution of 7.5-cm radiation is shown in Fig. 22 as an example. From the figure it is seen that the observations, just like the calculations, give a maximum brightness for r ≈ ≈ R. Some discrepancies between the proposed simple theory and the observations are explained by the fact that in reality the corona and chromosphere temperatures are not constant and the corona is not spherically symmetrical. /231

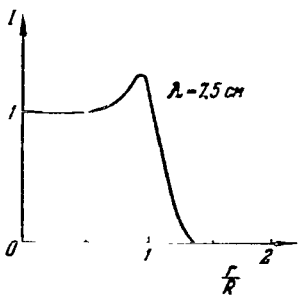

Figure 22.

By using the formulas that have been derived for the solar radio emission intensity, one can determine the solar luminosity at radio frequencies. Obviously, the solar luminosity at frequency ν is equal to

$$L_\nu = 4\pi \cdot 2\pi \int_0^\infty I_\nu(r) r\, dr. \tag{18.19}$$

Substituting, here, Eqs. (18.15) and (18.17), we find

$$L_\nu = 8\pi^2 \left\{ B_\nu(T_1) \int_0^\infty [1 - e^{-t_\nu^*(r)}] r\, dr + B_\nu(T_2) \int_0^R e^{-t_\nu^*(r)} r\, dr \right\}, \tag{18.20}$$

or

$$L_\nu = 4\pi^2 R^2 [a_\nu B_\nu(T_1) + b_\nu B_\nu(T_2)], \tag{18.21}$$

where

$$a_\nu = \frac{2}{R^2} \int_0^\infty [1 - e^{-t_\nu^*(r)}] r\, dr, \tag{18.22}$$

$$b_\nu = \frac{2}{R^2} \int_0^R e^{-t_\nu^*(r)} r\, dr. \tag{18.23}$$

Expressing the solar luminosity L_ν in terms of the effective temperature $\bar{T}_\nu$ with the aid of Eq. (18.6), and also using Eq. (18.1) for the quantity $B_\nu(T)$, instead of (18.21) we obtain

$$\bar{T}_\nu = a_\nu T_1 + b_\nu T_2. \tag{18.24}$$

Equation (18.24) expresses the effective temperature $\bar{T}$ of solar radio emission of frequency ν in terms of the corona temperature T_1 and the chromosphere temperature T_2.

The quantities a_ν and b_ν are easily determined numerically. In particular /232
according to the calculations of I. S. Shklovskiy and S. B. Pikel'ner (see [17]),

$$\begin{array}{llll} a_\nu = 1, & b_\nu = 0.0019 & \text{for} & \lambda = 3 \text{ см}, \\ a_\nu = 0.99, & b_\nu = 0.021 & \text{for} & \lambda = 10 \text{ см}, \\ a_\nu = 0.96, & b_\nu = 0.088 & \text{for} & \lambda = 21 \text{ см}, \\ a_\nu = 0.82, & b_\nu = 0.37 & \text{for} & \lambda = 50 \text{ см}. \end{array}$$

By specifying the corona and chromosphere temperatures ($T_1 \approx 10^6$ degrees and $T_2 \approx 10^4$ degrees), we can find the theoretical dependence of the effective temperature $\bar{T}_\nu$ on frequency. The values of $\bar{T}_\nu$, obtained from observations, approximately satisfy this relationship.

4. Radio wave propagation in the corona. In determining the radio emission brightness distribution over the solar disk, we assumed that the radiation is propagated rectilinearly. In reality, however, the radio emission can undergo refraction in the surface layers of the Sun. An expression for the refractive index of radio waves in a plasma must be known in order to explain the role of refraction.

Considering the motion of a free electron in the field of a radio wave, one can derive (see [19]) an expression for the absorption coefficient α_ν as well as an expression for the refractive index n. The expression for the absorption coefficient has already been given above by Eq. (18.8). Insofar as the refractive index is concerned, it turns out to be equal to

$$n = \sqrt{1 - \frac{\nu_n^2}{\nu^2}}, \tag{18.25}$$

where the quantity ν_n, representing the normal oscillation mode of the plasma, is defined by the formula

$$\nu_n^2 = \frac{e^2 n_e}{\pi m}. \tag{18.26}$$

We see that $n < 1$, i.e., the plasma has a lower refractive index for radio waves than a vacuum. With an increase in n_e the refractive index decreases, and for each frequency ν there is a critical value n_e' of the electron density for which $n = 0$. The radiation does not pass through the level where $n = 0$, but undergoes total reflection. Consequently, the radio emission comes only from solar atmosphere layers above this level. /233

On the other hand, as we know, radiation comes to the observer primarily from those layers whose optical depth is less than unity. Let us denote by n_e'' the value of the electron density for $\tau_\nu = 1$. Then one can say that if $n_e' \gg n_e''$ (i.e., the level with $n = 0$ lies below the level with $\tau_\nu = 1$), refraction has little effect on the radiation coming to the observer. Calculations show that this is the case for centimeter and decimeter waves. For example, for $\lambda = 10$ cm, as seen from Eq. (18.26), $n_e' \approx 10^{11}$ cm^{-3}, and $n_e'' \approx 10^9$ cm^{-3}. In this case $n \approx 1$ throughout the entire region where $\tau_\nu < 1$. For meter waves, however, $n_e' \ll \ll n_e''$ and refraction plays a very large role.

To determine the ray trajectory when refraction is considered, one must use the known relation

$$n(r')r' \sin\vartheta = r, \tag{18.27}$$

where $n(r')$ is the refractive index at a distance r' from the center of the Sun, ϑ is the angle between the radiation direction and the radius vector, r is the distance from the center of the Sun to the tangent to the direction of the radiation coming from the corona. Substitution of Eq. (18.25) into Eq. (18.27) gives a ray trajectory that is convex toward the center of the Sun (Fig. 23).

The optical path in the corona is obviously determined by the formula

$$t_\nu^0(r) = 2\int_{r_0}^{\infty} \alpha_\nu(r') \sec\vartheta \, dr', \tag{18.28}$$

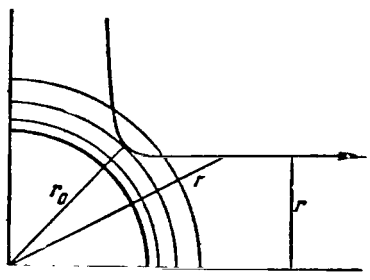

Figure 23.

where r_0 is determined from the condition: $n(r_0)r_0 = r$. Using Eq. (18.27), we obtain

$$t_\nu^0(r) = 2\int_{r_0}^{\infty} \frac{\alpha_\nu(r')\,dr'}{\sqrt{1 - \left[\frac{r}{n(r')r'}\right]^2}}. \tag{18.29}$$

The quantity $t_\nu^0(r)$, defined by Eq. (18.29), must also be substituted into Eq. (18.15) to calculate the intensity of the radiation coming from the corona at meter waves. The radio emission intensity distribution over the solar disk, /234

found as a result of such calculations, differs significantly from the distribution obtained when refraction is ignored.

Let us note that for a medium with a varying refractive index the radiation transfer equation has the form

$$n^2 \frac{d}{ds}\left(\frac{I_\nu}{n^2}\right) = -\alpha_\nu I_\nu + \varepsilon_\nu. \tag{18.30}$$

Since, in the presence of thermodynamic equilibrium, the radiation intensity is equal to $n^2 B_\nu(T)$, where $B_\nu(T)$ is the Planckian intensity, the relationship between the emission coefficient ε_ν and the absorption coefficient α_ν is given by the formula

$$\varepsilon_\nu = n^2 \alpha_\nu B_\nu(T). \tag{18.31}$$

Substituting (18.31) into Eq. (18.30) and integrating it for T = const, we again arrive at Eq. (18.15) for the intensity of the radiation, coming from the corona, in which the quantity $t_\nu^0(r)$ is given by Eq. (18.29).

5. Sporadic radio emission. The Sun is rarely quiet at radio frequencies. The disturbed emission, which can be divided into two components, is usually superimposed on the radio emission of the quiet Sun. The first of these varies relatively slowly (over a period of hours, days and months), the second—very rapidly (over a period of seconds and minutes).

The slowly varying component of the disturbed solar radio emission is observed primarily in centimeter and decimeter waves. Its intensity is comparable to the intensity of the radiation of the quiet Sun. From observations it follows that the origin of this component is associated with the formation of sunspots (since the greater the spot area, the more intense the radio emission). More precisely, the sources of the slowly varying solar radio emission are regions located over spots and faculae. A direct comparison of solar images, made at radio frequencies and in the optical portion of the spectrum, confirms this. The local radio emission sources rotate together with the Sun, and since they are located above spots, they rise earlier and set later than the spots. On this basis the heights of the sources above the photosphere, which are of the order of 0.05 $R_\odot$, can be determined.

Observations (performed especially during eclipses) provide the possibility of determining the location, size and effective temperature of the local sources. An examination of these data lead to the conclusion that the slowly varying disturbed solar radio emission is the thermal emission of coronal condensations, /235
i.e., it originates through free-free electron transitions in the field of ions (or, in other words, it represents the bremsstrahlung during the collisions of charged particles). Since the density in coronal condensations appreciably exceeds the density in the corona and the absorption coefficient for free-free transitions, according to Eq. (18.11), is proportional to the density squared, then fairly intense

radiation comes from the condensations, although they occupy a relatively small portion of the corona volume.

Observations show that the radio emission of local sources is partially polarized. This is explained by the effect of the magnetic fields of the spots above which the sources are located. A plasma in a magnetic field possesses the property of birefringence, with the refractive indices and the absorption coefficients of the two rays (ordinary and extraordinary) being different. Because of this the radiation is elliptically polarized. It is possible that in some cases the radio emission of local sources arises through the deceleration of electrons in a magnetic field, i.e., there is magnetoretardation.

The rapidly varying component of the solar radio emission is observed throughout the entire radio range (from millimeter to meter waves). It appears in the form of bursts of radio emission of different duration and intensity. Some bursts occur within a time of the order of 1 sec with an effective temperature that is several times greater than the effective temperature of the quiet Sun. However, much more intense bursts are also observed—with a duration of several minutes with an effective temperature of 10^8-10^9 and sometimes even 10^{12} degrees.

Radio emission bursts obviously cannot have a thermal origin. Therefore nonthermal emission mechanisms are included to explain the bursts. One of these indicated by I. S. Shklovskiy) consists of the excitation of plasma oscillations by a beam of fast particles. In this situation longitudinal plasma waves are formed which are then converted into transverse electromagnetic waves. The frequencies of the normal plasma oscillations are determined by Eq. (18.26). From the latter it is seen that for the electron densities, characteristic of the corona, meter waves appear at which intense radio emission bursts are observed. It is possible that fast particles, forming during chromosphere flares, are the cause of plasma oscillations. The fact that intense radio emission bursts are observed for several minutes after chromosphere flares favors this hypothesis. Bursts are observed initially at the shorter wavelengths, and then at longer and longer /236 wavelengths. This can be explained by the movement of fast particles, causing plasma oscillations, from the more dense to the less dense regions of the corona. The bremsstrahlung of relativistic electrons in a magnetic field, i.e., the so-called synchrotron radiation (see Section 31 about this), has been cited as another possible mechanism of radio emission bursts. Since bursts are very diverse, one can conclude that they arise due to the effect of different mechanisms. The fundamental problems associated with solar radio emission bursts are discussed in S. A. Kaplan's book [20].

6. Supercorona of the Sun. The solar corona can be investigated not only from its radio emission but also from the attenuation of the coronal radiation coming from sources located beyond it. By fortuitous chance one of the most powerful galactic sources of radio emission, the Crab nebula, lies very close to the ecliptic (at a distance of about 4.5 angular solar radii). Therefore every year the Crab nebula is eclipsed by the outer portions of the corona. Observations of this phenomenon, first made by V. V. Vitkevich, led to the discovery of portions of the corona at distances of several tens of solar radii from the center of the Sun.

The outer portion of the corona (usually called the supercorona) attenuates the radiation of the Crab nebula because of the scattering of radio waves by electron irregularities. When a ray passes through an inhomogeneity, the ray is deflected because of a difference in the refractive indices of the inhomogeneity and the surrounding medium. Simple calculations allow one to determine the decrease in the intensity of the radiation, passing through the corona at different distances from the center of the solar disk, as a function of the number of inhomogeneities, their size and the electron density in them. From a comparison of theory with observations it is found, for example, that in the corona at a distance of 20 solar radii the linear dimensions of the inhomogeneities amount to about 10^{10} cm, and the electron densities in them—to about 10^{3} cm^{-3}.

It should be noted that the supercorona can also be observed in the optical portion of the spectrum. Michard, in 1952, and Blackwell, in 1954, made such observations during solar eclipses (to reduce the effect of light, scattered by the earth's atmosphere, the latter observations were made from an airplane). These observations also led to a determination of the density of free electrons at different distances from the center of the Sun. A comparison of observational data, obtained in the visible portion of the spectrum and at radio frequencies, permitted V. V. Vitkevich to conclude that the solar supercorona has a two-component structure. He assumes that the supercorona consists of a diffuse /237 component with a density that decreases rapidly as r increases and a radial component, penetrating into it, whose density decreases more slowly. The radial component represents plasma flows, moving in radial directions from the Sun. The radio emission is scattered by the inhomogeneities of the radial corona component.

On the basis of the observed slow density decrease in the corona with increasing distance from the Sun, the notion arose that interplanetary space is nothing more than an extension of the corona. At first the properties of interplanetary space at different distances from the Sun were determined by considering a model of a static corona. Then Parker [21] made a detailed hydrodynamic examination of an "expanding corona", i.e., a corona consisting of particles moving from the Sun. This movement occurs with enormous velocities (at large distances from the Sun—of the order of hundreds of kilometers per second) and gives rise to the existence of a "solar wind" in interplanetary space. The solar wind evidently exerts a considerable effect on the outer portions of planetary atmospheres, on comet tails and on certain other objects in the solar system.

REFERENCES

1. The Sun, ed. G. Kuiper, Chicago, 1953. (Russ. translation: The Sun, IL, 1957).
2. de Jager, C. Structure and dynamics of the Solar Atmosphere, 1959. (Russ. translation: C. de Jager, Structure and dynamics of the solar atmosphere, Izd-vo inostr. lit., 1962).
3. Waldmeier, M. Results and problems of solar research, 1941. (Russ. translation: M. Waldmeier, Results and problems of solar research, Izd-vo inostr. lit., 1950).
4. Pikel'ner, S. B. Fundamentals of space electrodynamics, 2nd ed., "Nauka", 1966.

5. Chalonge, D. and V. Kourganoff. Studies of the continuous solar spectrum, Ann. d'Ap. 9, 69, 1946.
6. Unsöld, A. The physics of stellar atmospheres, 2nd ed., 1955.
7. Siedentopf, H. Convection in stellar atmospheres, AN 247, 297, 1933; 249, 53, 1933; 255, 157, 1935.
8. Rachkovskiy, D. N. Theory of the structure of absorption lines in a magnetic field, Izv. Krymskoy astrofiz. obs. 30, 267, 1963.
9. Severnyy, A. B. Magnetohydrodynamic phenomena at the Sun's surface, Izv. Krymskoy astrofiz. obs. 11, 129, 1954.
10. Menzel, D. H. and G. G. Cillié. The physical state of the Solar Chromosphere, Harvard Coll. Obs. Circ. N 410, 1936.
11. Thomas, R. N. and R. G. Athay. Physics of the Solar Chromosphere, New York, 1961. (Russ. translation: R. Thomas and R. Athay, Physics of the solar chromosphere "Mir", 1965).
12. Krat, V. A. and V. M. Sobolev. The solar chromosphere, Izv. GAO, No. 160, 116, 1957. /238
13. Space Astrophysics, ed. W. Liller, 1961. (Russ. translation: Space astrophysics, ed. W. Liller, Izd-vo inostr. lit., 1962).
14. Compilation "Ultraviolet radiation of the Sun and interplanetary space", Izd-vo inostr. lit., 1962.
15. Ivanov-Kholodnyy, G. S. and G. M. Nikol'skiy. Ultraviolet radiation of the Sun and the transition layer between chromosphere and corona, Astron. Zh. 38, 45, 1961.
16. Astrophysical compilation, IL, 1949.
17. Shklovskiy, I. S. The physics of the solar corona. Fizmatgiz, 1962.
18. Zheleznyakov, V. V. Solar and planetary radio emission, "Nauka", 1964.
19. Ginzburg, V. L. The propagation of electromagnetic waves in a plasma, Fizmatgiz, 1960.
20. Kaplan, S. A. Elementary radio astronomy, "Nauka", 1966.
21. Parker, E. N. Interplanetary dynamical Processes, 1963. (Russ. translation: E. N. Parker, Dynamic processes in interplanetary space, "Mir", 1965).

CHAPTER IV

PLANETARY ATMOSPHERES

As is known, the planets are luminous because of the reflection of sunlight by them. A complex process of multiple light scattering occurs in planetary atmospheres, as a result of which the radiant energy partially undergoes true absorption (i.e., changes into another form of energy), and partially escapes outward from the atmosphere. From the radiation, diffusely reflected by a planetary atmosphere, we can learn about the optical properties of the atmosphere and about the physical nature of the particles composing it. /239

The atmospheres of some planets (for example, Venus and Jupiter) have a very large optical thickness and the surface of the planet is not visible through the atmosphere. Other planets (for example, Mars) are surrounded by atmospheres of small optical thickness. In this case information can be gathered not only about the atmosphere but also about the planet's surface by studying the radiation from the planet.

This chapter is devoted primarily to the theory of multiple light scattering in planetary atmospheres along with its application to individual planets. The results of photometric and spectroscopic observations of planets are used in this. This theory is discussed in more detail in specific papers [1-3].

Recently, very valuable information about planets has been obtained with the aid of rockets. The results of radio emission studies of planets are also of considerable interest. These results will be indicated briefly at the end of the chapter.

19. Light Scattering in Planetary Atmospheres

1. Basic equations. Because of the thinness of the atmosphere in comparison with the radius of a planet, one can make the approximation that the atmosphere consists of plane-parallel layers. In addition, one can assume that the atmosphere is illuminated by parallel sunbeams. We will denote the angle of incidence of the sunbeams on the atmosphere at a given point by ϑ_0, and the illumin-

ance perpendicular to its surface—by πF. Our problem will be one of determining the intensity of the radiation coming from the atmosphere in different directions after the process of multiple scattering in it. /240

To solve the problem that has been set forth, we must make use of the radiative transfer equation. As shown in Section 1, in the case of plane-parallel layers this equation has the form

$$\cos\vartheta \frac{dI}{dz} = -\alpha I + \varepsilon, \tag{19.1}$$

where I is the radiation intensity, α is the absorption coefficient, ε is the emission coefficient, z is the height above the planet's surface, ϑ is the angle between the radiation direction and the normal to the atmosphere layers (Fig. 24). The quantities I, α and ε depend on the radiation frequency, but to simplify the notation we will omit the index ν.

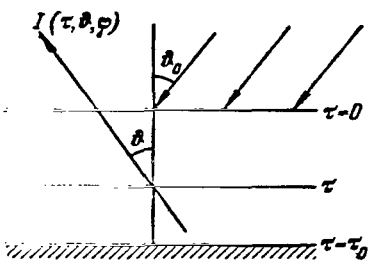

Figure 24.

The quantity ε, entering into Eq. (19.1), is caused by light scattering occurring in a volume element. We will assume that a fraction λ of the total amount of radiant energy absorbed in this volume is scattered by it. In this case the quantity λ will be represent the scattering coefficient, and the quantity $(1 - \lambda)\alpha$—the true absorption coefficient. Generally speaking, the probability of radition scattering is not the same in different directions. Let us denote by $x(\gamma)d\omega/4\pi$ the probability of radiation scattering in a direction, forming an angle γ with the direction of the radiation incident on the volume, within a solid angle $d\omega$. The quantity $x(\gamma)$ is called the scattering indicatrix. If radiation scattering occurs with equal probability in all directions, then $x(\gamma) = 1$. In this case the scattering indicatrix is said to be spherical.

To obtain an expression for the quantity ε, let us consider a volume element with unit area base and a thickness dz located at a height z. This volume is illuminated both by radiation coming directly from the Sun and by radiation scattered by the atmosphere. Let us denote the optical depth of this volume element by τ, i.e., let us say

$$\tau = \int_z^\infty \alpha(z)\,dz. \tag{19.2}$$

Then the amount of energy incident on the volume directly from the Sun will be /241
to $\pi F e^{-\tau \sec\vartheta_0} \cos\vartheta_0$. A fraction $\alpha dz \sec\vartheta_0$ of this amount of energy is absorbed by the volume, and a fraction $\lambda x(\gamma)d\omega/4\pi$ is scattered by it at an angle γ to the

direction of the sunlight in the solid angle $d\omega$. Therefore for the emission coefficient, caused by first order scattering, we obtain

$$\varepsilon_1 = \frac{\lambda}{4} aFx(\gamma) e^{-\tau \sec \vartheta_0}. \tag{19.3}$$

An additional term, resulting from higher order scattering, must be added to Eq. (19.3). As a result, for the total emission coefficient we obtain

$$\varepsilon = \lambda a \int Ix(\gamma') \frac{d\omega'}{4\pi} + \frac{\lambda}{4} aFx(\gamma) e^{-\tau \sec \vartheta_0}, \tag{19.4}$$

where the integration is done over all directions of radiation incidence on the volume and γ' is the angle between any of these directions and the direction of the radiation scattered by the volume.

Instead of the emission coefficient ε in Eqs. (19.1) and (19.4), let us introduce the quantity S by means of the relation

$$\varepsilon = aS. \tag{19.5}$$

For an arbitrary scattering indicatrix the quantities S and I depend on the optical depth τ, the zenith distance ϑ and the azimuth φ. Therefore instead of Eqs. (19.1) and (19.4) we can write

$$\cos \vartheta \frac{dI(\tau, \vartheta, \varphi)}{d\tau} = I(\tau, \vartheta, \varphi) - S(\tau, \vartheta, \varphi), \tag{19.6}$$

$$S(\tau, \vartheta, \varphi) = \frac{\lambda}{4\pi} \int_0^{2\pi} d\varphi' \int_0^{\pi} x(\gamma') I(\tau, \vartheta', \varphi') \sin \vartheta' d\vartheta' + \frac{\lambda}{4} Fx(\gamma) e^{-\tau \sec \vartheta_0}, \tag{19.7}$$

where

$$\left.\begin{aligned} \cos \gamma' &= \cos \vartheta \cos \vartheta' + \sin \vartheta \sin \vartheta' \cos (\varphi - \varphi'), \\ \cos \gamma &= -\cos \vartheta \cos \vartheta_0 + \sin \vartheta \sin \vartheta_0 \cos \varphi, \end{aligned}\right\} \tag{19.8}$$

and the azimuth of the sunlight direction is taken equal to zero.

Thus, the problem of light scattering in a planetary atmosphere reduces to a solution of Eqs. (19.6) and (19.7). Boundary conditions must still be added to these equations. The condition at the upper boundary of the atmosphere (i.e., for $\tau = 0$) must express the fact that there is no diffuse radiation incident on the atmosphere from outside. The condition at the lower boundary (i.e., for $\tau = \tau_0$) must take account of radiation reflection by the planet's surface. /242

Solving the equations that have been presented, one can find the intensities or the radiation coming from the atmosphere. A comparison of the theoretical

and observed values of these intensities allows one to draw conclusions about the optical properties of the atmosphere, i.e., about the quantities τ_0, λ and $x(\gamma)$.

From the optical properties of the atmosphere, in turn, one can learn about the nature of the particles which comprise it. To do this the theory of light scattering by individual particles is used (see, for example, [4]). This theory, developed in particular detail for spherical particles, defines the absorption coefficient α, the particle albedo λ and the scattering indicatrix $x(\gamma)$ as a function of the ratio of the particle radius to the radiation wavelength and of the refractive index of the particle material.

Let us note that in the case of light scattering by molecules the scattering indicatrix is determined by the Rayleigh formula

$$x(\gamma)=\frac{3}{4}(1+\cos^2\gamma). \tag{19.9}$$

If, however, the light scattering is done by particles whose radii are comparable to the radiation wavelength, then the scattering indicatrix usually is greatly elongated forward.

2. Semi-infinite atmosphere. As already indicated, the atmospheres of some planets have an optical thickness in excess of unity. In this case, to determine the intensity of the radiation, diffusely reflected by the atmosphere, one can assume the approximation $\tau_0 = \infty$.

Let us first assume that isotropic light scattering occurs in the atmosphere, i.e., $x(\gamma) = 1$. Then the quantity S will be a function of τ only, and the radiation intensity I—a function of τ and ϑ only. Therefore Eqs. (19.6) and (19.7) can be rewritten in the form

$$\mu\frac{dI(\tau,\mu,\mu_0)}{d\tau}=I(\tau,\mu,\mu_0)-S(\tau,\mu_0), \tag{19.10}$$

$$S(\tau,\mu_0)=\frac{\lambda}{2}\int_{-1}^{+1}I(\tau,\mu,\mu_0)\,d\mu+\frac{\lambda}{4}Fe^{-\frac{\tau}{\mu_0}}, \tag{19.11}$$

where $\cos\vartheta = \mu$, $\cos\vartheta_0 = \mu_0$ and the dependence of the quantities I and S on the parameter μ_0 is emphasized.

From Eqs. (19.10) and (19.11) one integral equation can be derived for determining the function $S(\tau, \mu_0)$. Proceeding in the same manner as in the derivation of Eq. (2.47), we obtain /243

$$S(\tau,\mu_0)=\frac{\lambda}{2}\int_0^{\infty}\mathrm{Ei}\,|\tau-t|\,S(t,\mu_0)\,dt+\frac{\lambda}{4}Fe^{-\frac{\tau}{\mu_0}}, \tag{19.12}$$

where $\mathrm{Ei}\,\tau$ is the first integral exponential function.

If the function $S(\tau, \mu_0)$ is known, then the intensity of the radiation coming from the atmosphere, i.e., the quantity $I(0, \mu, \mu_0)$, can easily be determined. Assuming

$$I(0, \mu, \mu_0) = F\rho(\mu, \mu_0)\mu_0, \tag{19.13}$$

we have

$$\rho(\mu, \mu_0) = \frac{1}{F}\int_0^\infty S(\tau, \mu_0) e^{-\frac{\tau}{\mu}} \frac{d\tau}{\mu\mu_0}. \tag{19.14}$$

The quantity $\rho(\mu, \mu_0)$ is called the atmosphere brightness coefficient.

The integral equation (19.12) reduces to an equation like (3.1), considered in detail in Section 3. In the given case the kernel of Eq. (3.1) is given by Eq. (3.17) in which $A(x) = \lambda/2x$, $a = 1$, $b = \infty$, and the free term has the form $g(\tau) = (\lambda/4)Fe^{-\tau/\mu_0}$. Using Eqs. (3.19) and (3.20), we obtain for the brightness coefficient the expression

$$\rho(\mu, \mu_0) = \frac{\lambda}{4}\frac{\varphi(\mu)\varphi(\mu_0)}{\mu + \mu_0}, \tag{19.15}$$

in which the function $\varphi(\mu)$ is defined by the equation

$$\varphi(\mu) = 1 + \frac{\lambda}{2}\mu\varphi(\mu)\int_0^1 \frac{\varphi(\mu')}{\mu + \mu'} d\mu'. \tag{19.16}$$

As we recall, the function $\varphi(\mu)$ has already been encountered in the theory of stellar photospheres (in Section 3) and in the theory of stellar spectra formation (in Section 10). Now we see that the brightness coefficient of a planet's atmosphere is expressed in terms of the same function. Values of the function $\varphi(\mu)$ for different values of the parameter λ are presented in Table 11 (p. 129).

We derived Eqs. (19.15) and (19.16) with the aid of Eq. (19.12); however, V.A. Ambartsumyan has shown that they can also be derived without using this equation, namely—by means of the so-called "invariance principle". According to this principle the reflectivity of a semi-infinite medium is not altered if some /244 layer with the same optical properties is added to it. By adding to a semi-infinite medium a layer of infinitely small optical thickness, determining all the changes in the intensity of the radiation introduced by this layer, and equating them to zero, we also arrive at the stated relations (see [1]).

The brightness coefficient for an arbitrary scattering indicatrix was also found by means of the invariance principle. By way of an example, let us present the result obtained for a very simple nonspherical scattering indicatrix

$$x(\gamma) = 1 + x_1 \cos\gamma, \tag{19.17}$$

where x_1 is some parameter.

In the case given the brightness coefficient is defined by the formula

$$\rho(\mu, \mu_0, \varphi) = \rho_0(\mu, \mu_0) + \rho_1(\mu, \mu_0)\cos\varphi, \tag{19.18}$$

and the quantities $\rho_0(\mu, \mu_0)$ and $\rho_1(\mu, \mu_0)$ have the following structure:

$$\rho_0(\mu, \mu_0) = \frac{\lambda}{4}\frac{\varphi_0^0(\mu)\varphi_0^0(\mu_0) - x_1\varphi_1^0(\mu)\varphi_1^0(\mu_0)}{\mu + \mu_0}, \tag{19.19}$$

$$\rho_1(\mu, \mu_0) = \frac{\lambda}{4}x_1\frac{\varphi_1^1(\mu)\varphi_1^1(\mu_0)}{\mu + \mu_0}. \tag{19.20}$$

In turn, the auxiliary functions $\varphi_0^0(\mu)$ and $\varphi_1^0(\mu)$ are determined from the system of equations

$$\varphi_0^0(\mu) = 1 + \frac{\lambda}{2}\mu\int_0^1 \frac{\varphi_0^0(\mu)\varphi_0^0(\mu') - x_1\varphi_1^0(\mu)\varphi_1^0(\mu')}{\mu + \mu'}d\mu', \tag{19.21}$$

$$\varphi_1^0(\mu) = \mu - \frac{\lambda}{2}\mu\int_0^1 \frac{\varphi_0^0(\mu)\varphi_0^0(\mu') - x_1\varphi_1^0(\mu)\varphi_1^0(\mu')}{\mu + \mu'}d\mu', \tag{19.22}$$

and the auxiliary function $\varphi_1^1(\mu)$—from the equation

$$\varphi_1^1(\mu) = \sqrt{1-\mu^2} + \frac{\lambda}{4}x_1\mu\varphi_1^1(\mu)\int_0^1 \frac{\varphi_1^1(\mu')}{\mu + \mu'}\sqrt{1-\mu'^2}\,d\mu'. \tag{19.23}$$

The functions $\varphi_0^0(\mu)$, $\varphi_1^0(\mu)$ and $\varphi_1^1(\mu)$ have been tabulated so that the computation of the brightness coefficient from Eqs. (19.18)—(19.20) represents no problem.

3. Atmosphere of finite optical thickness. Let us now consider light scattering in an atmosphere of arbitrary optical thickness τ_0. Assuming for simplicity that the scattering indicatrix is spherical, we obtain the following equation /245 for determining the function $S(\tau, \mu_0)$:

$$S(\tau, \mu_0) = \frac{\lambda}{2}\int_0^{\tau_0} \mathrm{Ei}|\tau - t|S(t, \mu_0)\,dt + \frac{\lambda}{4}Fe^{-\frac{\tau}{\mu_0}}. \tag{19.24}$$

Here, for the present, we have neglected light reflection by the planet surface.

Our problem consists of determining the intensities of the radiation diffusely reflected and diffusely transmitted by the atmosphere. Instead of these we will

look for the corresponding brightness coefficients $\rho(\mu, \mu_0)$ and $\sigma(\mu, \mu_0)$, expressed in terms of the function $S(\tau, \mu_0)$ by means of the formulas

$$F\rho(\mu, \mu_0)\mu_0 = \int_0^{\tau_0} S(\tau, \mu_0) e^{-\frac{\tau}{\mu}} \frac{d\tau}{\mu}, \tag{19.25}$$

$$F\sigma(\mu, \mu_0)\mu_0 = \int_0^{\tau_0} S(\tau, \mu_0) e^{-\frac{\tau_0-\tau}{\mu}} \frac{d\tau}{\mu}. \tag{19.26}$$

To find the quantities $\rho(\mu, \mu_0)$ and $\sigma(\mu, \mu_0)$, however, there is no necessity to determine the function $S(\tau, \mu_0)$ beforehand. Just as in the case of $\tau_0 = \infty$, one can obtain equations directly defining the brightness coefficients. To do this, we proceed in the following manner.

Let us rewrite Eq. (19.24) in the form

$$S(\tau, \mu_0) = \frac{\lambda}{2}\int_0^{\tau} \mathrm{Ei}(\tau - t) S(t, \mu_0) dt + \\ + \frac{\lambda}{2}\int_{\tau}^{\tau_0} \mathrm{Ei}(t - \tau) S(t, \mu_0) dt + \frac{\lambda}{4} F e^{-\frac{\tau'}{\mu_0}}. \tag{19.27}$$

After setting $\tau - t = x$ in the first integral and $t - \tau = x$ in the second, we obtain

$$S(\tau, \mu_0) = \frac{\lambda}{2}\int_0^{\tau} \mathrm{Ei}\, x S(\tau - x, \mu_0) dx + \\ + \frac{\lambda}{2}\int_0^{\tau_0-\tau} \mathrm{Ei}\, x S(\tau + x, \mu_0) dx + \frac{\lambda}{4} F e^{-\frac{\tau}{\mu_0}}, \tag{19.28}$$

Differentiating this equation with respect to τ, we obtain /246

$$S'(\tau, \mu_0) = \frac{\lambda}{2}\int_0^{\tau_0} \mathrm{Ei}|\tau - t| S'(t, \mu_0) dt - \frac{\lambda F}{4\mu_0} e^{-\frac{\tau}{\mu_0}} + \\ + \frac{\lambda}{2} S(0, \mu_0) \mathrm{Ei}\, \tau - \frac{\lambda}{2} S(\tau_0, \mu_0) \mathrm{Ei}(\tau_0 - \tau). \tag{19.29}$$

Comparing Eqs. (19.24) and (19.29), we see that they have the same kernels and differ only in their free terms. But since the function $\mathrm{Ei}\, \tau$ is defined by the formula

$$\mathrm{Ei}\, \tau = \int_0^1 e^{-\frac{\tau}{\mu}} \frac{d\mu}{\mu}, \tag{19.30}$$

then the free term of Eq. (19.29) represents a superposition of the free terms of Eq. (19.24). Therefore, because of the linearity of the equations being considered, we have

$$S'(\tau, \mu_0) = -\frac{1}{\mu_0} S(\tau, \mu_0) + \frac{2}{F} S(0, \mu_0) \int_0^1 S(\tau, \mu') \frac{d\mu'}{\mu'} - \\ - \frac{2}{F} S(\tau_0, \mu_0) \int_0^1 S(\tau_0 - \tau, \mu') \frac{d\mu'}{\mu'}. \tag{19.31}$$

The relation (19.31) also provides us the possibility of obtaining equations determining the quantities $\rho(\mu, \mu_0)$ and $\sigma(\mu, \mu_0)$. Multiplying this relation by $e^{-\tau/\mu} d\tau/\mu$, integrating with respect to τ over the limits from zero to τ_0 and taking Eqs. (19.25) and (19.26) into account, we obtain

$$F\rho(\mu, \mu_0)(\mu + \mu_0) = S(0, \mu_0)\varphi(\mu) - S(\tau_0, \mu_0)\psi(\mu), \tag{19.32}$$

where

$$\varphi(\mu) = 1 + 2\mu \int_0^1 \rho(\mu, \mu') d\mu', \tag{19.33}$$

$$\psi(\mu) = e^{-\frac{\tau_0}{\mu}} + 2\mu \int_0^1 \sigma(\mu, \mu') d\mu'. \tag{19.34}$$

After the multiplication of Eq. (19.31) by $e^{-(\tau_0 - \tau)/\mu} d\tau/\mu$ and integration, we obtain similarly /247

$$F\sigma(\mu, \mu_0)(\mu - \mu_0) = S(0, \mu_0)\psi(\mu) - S(\tau_0, \mu)\varphi(\mu). \tag{19.35}$$

On the other hand, from Eq. (19.24) it follows

$$S(0, \mu_0) = \frac{\lambda}{2} \int_0^{\infty} S(t, \mu_0) dt \int_0^1 e^{-\frac{t}{\mu}} \frac{d\mu}{\mu} + \frac{\lambda}{4} F = \\ = \frac{\lambda}{2} \int_0^1 d\mu \int_0^{\infty} S(t, \mu_0) e^{-\frac{t}{\mu}} \frac{dt}{\mu} + \frac{\lambda}{4} F = \\ = \frac{\lambda}{4} F \left[1 + 2\mu_0 \int_0^1 \rho(\mu, \mu_0) d\mu \right]. \tag{19.36}$$

From the same equation we find analogously

$$S(\tau_0, \mu_0) = \frac{\lambda}{4} F\left[e^{-\frac{\tau_0}{\mu_0}} + 2\mu_0 \int_0^1 \sigma(\mu, \mu_0) d\mu \right]. \tag{19.37}$$

Making use of the symmetry of the quantities $\rho(\mu, \mu_0)$ and $\sigma(\mu, \mu_0)$ with respect to μ and μ_0 (which will be demonstrated below) and the definitions of (19.33) and (19.34), we obtain

$$S(0, \mu_0) = \frac{\lambda}{4} F\varphi(\mu_0), \quad S(\tau_0, \mu_0) = \frac{\lambda}{4} F\psi(\mu_0). \tag{19.38}$$

Substitution of Eqs. (19.38) into Eqs. (19.32) and (19.35) yields

$$\rho(\mu, \mu_0) = \frac{\lambda}{4} \frac{\varphi(\mu)\varphi(\mu_0) - \psi(\mu)\psi(\mu_0)}{\mu + \mu_0}, \tag{19.39}$$

$$\sigma(\mu, \mu_0) = \frac{\lambda}{4} \frac{\psi(\mu)\varphi(\mu_0) - \varphi(\mu)\psi(\mu_0)}{\mu - \mu_0}. \tag{19.40}$$

Substituting, however, Eqs. (19.39) and (19.40) into Eqs. (19.33) and (19.34), we find /248

$$\varphi(\mu) = 1 + \frac{\lambda}{2}\mu \int_0^1 \frac{\varphi(\mu)\varphi(\mu') - \psi(\mu)\psi(\mu')}{\mu + \mu'} d\mu', \tag{19.41}$$

$$\psi(\mu) = e^{-\frac{\tau_0}{\mu}} + \frac{\lambda}{2}\mu \int_0^1 \frac{\psi(\mu)\varphi(\mu') - \varphi(\mu)\psi(\mu')}{\mu - \mu'} d\mu'. \tag{19.42}$$

Equations (19.39)—(19.42) are what we have sought. Equations (19.39) and (19.40) define the structure of the brightness coefficients, and Eqs. (19.41) and (19.42) serve to define the auxiliary functions $\varphi(\mu)$ and $\psi(\mu)$.

For a scattering indicatrix of arbitrary form the brightness coefficients are also expressed in terms of the auxiliary functions, depending only on one argument, and these functions are determined by systems of equations similar to Eqs. (19.41) and (19.42) (see, for example, [2]).

The symmetry of the brightness coefficients with respect to the angles of incidence and reflection (or transmission) still remains to be proved. To do

this let us consider the integral equation

$$S(\tau, \mu_0) = \int_0^1 K(|\tau - t|) S(t, \mu_0)\, dt + g(\tau, \mu_0) \tag{19.43}$$

with an arbitrary kernel, depending on the modulus of the difference of two arguments, and with an arbitrary free term, depending on the parameter μ_0. Equation (19.24) is a special case of Eq. (19.43).

Assuming that $g(\tau, \mu)$ represents the free term of Eq. (19.43), in which μ_0 is replaced by μ, we obtain

$$\int_0^{\tau_0} S(\tau, \mu_0) g(\tau, \mu)\, d\tau =$$

$$= \int_0^{\tau_0} S(\tau, \mu_0) \left[S(\tau, \mu) - \int_0^{\tau_0} K(|\tau - t|) S(t, \mu)\, dt \right] d\tau =$$

$$= \int_0^{\tau_0} S(\tau, \mu_0) S(\tau, \mu)\, d\tau - \int_0^{\tau_0} S(t, \mu)\, dt \int_0^{\tau_0} S(\tau, \mu_0) K(|\tau - t|)\, d\tau. \tag{19.44}$$

From this, turning again to Eq. (19.43), we obtain /249

$$\int_0^{\tau_0} S(\tau, \mu_0) g(\tau, \mu)\, d\tau = \int_0^{\tau_0} S(\tau, \mu) g(\tau, \mu_0)\, d\tau. \tag{19.45}$$

Analogously, one can obtain:

$$\int_0^{\tau_0} S(\tau, \mu_0) g(\tau_0 - \tau, \mu)\, d\tau = \int_0^{\tau_0} S(\tau, \mu) g(\tau_0 - \tau, \mu_0)\, d\tau. \tag{19.46}$$

Assuming $g(\tau, \mu_0) = e^{-\tau/\mu_0}$ and taking Eqs. (19.25) and (19.26) into account, from (19.45) and (19.46) we have

$$\rho(\mu, \mu_0) = \rho(\mu_0, \mu), \quad \sigma(\mu, \mu_0) = \sigma(\mu_0, \mu). \tag{19.47}$$

These relations, which we have already used before, are what we were to prove.

Equations (19.47) play an extremely important role in the theory of light scattering. From a physical point of view they express the "reciprocity principle" for optical phenomena. Minnaert [5] first applied this principle to planet atmospheres.

4. Light reflection by the planet's surface. We have assumed above that the coefficient of light reflection by the planet's surface is equal to zero. Now

we will take the reflection effect into account, with our assuming, for simplicity, that the intensity of the reflected light is independent of direction (i.e., the reflection is isotropic). Let us designate the albedo of the planet surface by A. The scattering indicatrix of light in the planet atmosphere, just as before, will be assumed to be spherical.

In the case given the atmosphere is illuminated not only by direct sunlight from above, but also by diffuse radiation coming from the planet surface below. We will now designate the ratio of the emission coefficient to the absorption coeffecient by $\bar{S}(\tau, \mu_0)$ and instead of Eq. (19.24) we obtain

$$\bar{S}(\tau, \mu_0) = \frac{\lambda}{2}\int_0^{\tau_0} \mathrm{Ei}|\tau - t|\bar{S}(t, \mu_0)\,dt + \frac{\lambda}{4}Fe^{-\frac{\tau}{\mu_0}} + \frac{\lambda}{2}I(\mu_0)\int_0^1 e^{-\frac{\tau_0-\tau}{\mu}}\,d\mu, \qquad (19.48)$$

where $\bar{I}(\mu_0)$ is the intensity of the radiation reflected from the surface. /250

We must find the brightness coefficients $\bar{\rho}(\mu, \mu_0)$ and $\bar{\sigma}(\mu, \mu_0)$, defined by the formulas

$$F\bar{\rho}(\mu, \mu_0)\mu_0 = \int_0^{\tau_0} \bar{S}(\tau, \mu_0)e^{-\frac{\tau}{\mu}}\frac{d\tau}{\mu} + I(\mu_0)e^{-\frac{\tau_0}{\mu_0}}, \qquad (19.49)$$

$$F\bar{\sigma}(\mu, \mu_0)\mu_0 = \int_0^{\tau_0} \bar{S}(\tau, \mu_0)e^{-\frac{\tau_0-\tau}{\mu}}\frac{d\tau}{\mu}. \qquad (19.50)$$

The last term of Eq. (19.49) takes account of radiation reflected by the surface and passing through the atmosphere.

The quantity $\bar{I}(\mu_0)$, entering into the equation, is also not known a priori. It obviously depends on the unknown radiation intensity, incident on the surface, or on the corresponding brightness coefficient $\bar{\sigma}(\mu, \mu_0)$. To find the stated relationship, one must first of all write the expression for the surface illumination. It is easy to see that the illumination by direct sunlight is equal to $\pi Fe^{-\tau_0/\mu_0}\mu_0$, and the illumination by the diffuse radiation of the atmosphere is equal to $2\pi F\mu_0\int_0^1 \bar{\sigma}(\mu, \mu_0)\mu d\mu$. Multiplying the total illumination by the surface albedo A, we obtain the amount of energy reflected by the surface. On the other hand, this amount of energy is equal to $\pi\bar{I}(\mu_0)$. Therefore we have

$$I(\mu_0) = AF\mu_0\left[e^{-\frac{\tau_0}{\mu_0}} + 2\int_0^1 \bar{\sigma}(\mu, \mu_0)\mu\,d\mu\right]. \qquad (19.51)$$

To determine the quantities $\bar{\rho}(\mu, \mu_0)$ and $\bar{\sigma}(\mu, \mu_0)$, we equate Eqs. (19.24) and (19.48). From this equation it is seen that

$$\bar{S}(\tau, \mu_0) = S(\tau, \mu_0) + \frac{2}{F} \bar{I}(\mu_0) \int_0^1 S(\tau_0 - \tau, \mu') d\mu'. \tag{19.52}$$

Multiplying (19.52) by $e^{-\tau/\mu} d\tau/\mu$, integrating over the limits from zero to τ_0 and using Eqs. (19.25), (19.26) and (19.49), we obtain /251

$$\bar{\rho}(\mu, \mu_0) = \rho(\mu, \mu_0) + \frac{\bar{I}(\mu_0)}{F\mu_0} \left[e^{-\frac{\tau_0}{\mu}} + 2 \int_0^1 \sigma(\mu, \mu') \mu' d\mu' \right]. \tag{19.53}$$

Analogously, we obtain

$$\bar{\sigma}(\mu, \mu_0) = \sigma(\mu, \mu_0) + \frac{\bar{I}(\mu_0)}{F\mu_0} 2 \int_0^1 \rho(\mu, \mu') \mu' d\mu'. \tag{19.54}$$

To determine the quantity $\bar{I}(\mu_0)$, we multiply (19.54) by $2\mu d\mu$ and we integrate over the limits from zero to 1. With the aid of (19.51) this yields

$$\bar{I}(\mu_0) = \frac{A}{1 - AC} \left[e^{-\frac{\tau_0}{\mu_0}} + 2 \int_0^1 \sigma(\mu, \mu_0) \mu d\mu \right] F\mu_0, \tag{19.55}$$

where

$$C = 4 \int_0^1 \mu d\mu \int_0^1 \rho(\mu, \mu') \mu' d\mu'. \tag{19.56}$$

Also introducing the definitions

$$M(\mu) = e^{-\frac{\tau_0}{\mu}} + 2 \int_0^1 \sigma(\mu, \mu') \mu' d\mu', \tag{19.57}$$

$$N(\mu) = 2 \int_0^1 \rho(\mu, \mu') \mu' d\mu' \tag{19.58}$$

and substituting (19.55) into (19.53) and (19.54), we obtain

$$\bar{\rho}(\mu, \mu_0) = \rho(\mu, \mu_0) + \frac{A}{1 - AC} M(\mu) M(\mu_0), \tag{19.59}$$

$$\bar{\sigma}(\mu, \mu_0) = \sigma(\mu, \mu_0) + \frac{A}{1 - AC} N(\mu) M(\mu_0). \tag{19.60}$$

Thus, we have arrived at formulas by means of which the brightness coefficients $\bar{\rho}(\mu, \mu_0)$ and $\bar{\sigma}(\mu, \mu_0)$ for $A \neq 0$ are expressed in terms of the brightness coefficients $\rho(\mu, \mu_0)$ and $\sigma(\mu, \mu_0)$ for $A = 0$. /252

The quantities $M(\mu)$ and $N(\mu)$ entering into Eqs. (19.59) and (19.60) can be expressed in terms of the same auxiliary functions $\varphi(\mu)$ and $\psi(\mu)$, in terms of which the quantities $\rho(\mu, \mu_0)$ and $\sigma(\mu, \mu_0)$ were previously expressed. By means of Eqs. (19.39) and (19.40), as well as Eqs. (19.41) and (19.42), we obtain

$$M(\mu) = \left(1 - \frac{\lambda}{2} \alpha_0\right) \psi(\mu) + \frac{\lambda}{2} \beta_0 \varphi(\mu), \tag{19.61}$$

$$N(\mu) = 1 - \left(1 - \frac{\lambda}{2} \alpha_0\right) \varphi(\mu) - \frac{\lambda}{2} \beta_0 \psi(\mu), \tag{19.62}$$

where the definitions

$$\left.\begin{aligned} \alpha_i &= \int_0^1 \varphi(\mu) \mu^i d\mu, \\ \beta_i &= \int_0^1 \psi(\mu) \mu^i d\mu, \end{aligned}\right\} \tag{19.63}$$

are used, i.e., α_0 and β_0 are the zero moments of the functions $\varphi(\mu)$ and $\psi(\mu)$.

It is easy to see that the quantities $M(\mu_0)$ and $N(\mu_0)$ have a simple physical meaning. The first of them represents the ratio of the planet surface illumination to the illumination of the upper boundary of the atmosphere, and the second—the ratio of the illumination of the upper boundary from below to the illumination of the upper boundary from above (for $A = 0$).

5. Planet albedo. The formulas derived above for the intensity of the radiation, diffusely reflected by the planet atmosphere, make it easy to determine the planet albedo. First, let us find the so-called planar albedo, i.e., the planet albedo at a given point for a certain incidence angle of the sunlight on a planar layer, which is the form in which the atmosphere is represented. It is obvious that the radiation flux, coming from the atmosphere, is equal to $2\pi F\mu_0 \int_0^1 \bar{\rho}(\mu, \mu_0) \mu d\mu$, and the solar radiation flux, incident on the atmosphere, is equal to $\pi F\mu_0$.

Therefore the planar albedo, being the ratio of the fluxes mentioned, is equal to /253

$$A_1(\mu_0) = 2\int_0^1 \bar{\rho}(\mu, \mu_0)\mu\, d\mu. \tag{19.64}$$

To calculate the quantity $A_1(\mu_0)$, we substitute Eq. (19.59) into Eq. (19.64). Taking Eqs. (19.58) and (19.61) into account, we obtain

$$A_1(\mu_0) = N(\mu_0) + \frac{A}{1-AC}[(2-\lambda\alpha_0)\beta_1 + \lambda\beta_0\alpha_1]M(\mu_0), \tag{19.65}$$

where, just as before, A is the planet surface albedo, and α_1 and β_1 are the first moments of the functions $\varphi(\mu)$ and $\psi(\mu)$. As seen from Eqs. (19.56), (19.58) and (19.62), the quantity C is equal to

$$C = 1 - (2-\lambda\alpha_0)\alpha_1 - \lambda\beta_0\beta_1. \tag{19.66}$$

Let us note that the quantities α_0 and β_0, entering into the formulas presented, are interrelated by a simple expression. To obtain it, let us integrate Eq. (19.41) with respect to μ over the limits from zero to 1. As a result we obtain

$$\alpha_0 = 1 + \frac{\lambda}{2}\int_0^1 \mu\, d\mu \int_0^1 \frac{\varphi(\mu)\varphi(\mu') - \psi(\mu)\psi(\mu')}{\mu+\mu'} d\mu', \tag{19.67}$$

or, after the substitution $\mu/\mu + \mu' = 1 - \mu'/\mu + \mu'$,

$$\alpha_0 = 1 + \frac{\lambda}{2}(\alpha_0^2 - \beta_0^2) - \frac{\lambda}{2}\int_0^1 d\mu \int_0^1 \frac{\varphi(\mu)\varphi(\mu') - \psi(\mu)\psi(\mu')}{\mu+\mu'}\mu'\, d\mu'. \tag{19.68}$$

The desired relation follows from the last two formulas:

$$\alpha_0 = 1 + \frac{\lambda}{4}(\alpha_0^2 - \beta_0^2). \tag{19.69}$$

Let us consider two special cases of Eq. (19.65), determining the planar albedo.

1. Let us assume that the optical thickness of the atmosphere is infinitely great ($\tau = \infty$). In this case the function $\varphi(\mu)$ is determined by Eq. (19.16), and /254
$\psi(\mu) = 0$. Therefore Eq. (19.65) assumes the form

$$A_1(\mu_0) = 1 - \left(1 - \frac{\lambda}{2}\alpha_0\right)\varphi(\mu_0). \tag{19.70}$$

But from the relation (19.69) in the case given (i.e., for $\beta_0 = 0$) we obtain

$$\alpha_0 = \frac{2}{\lambda}(1 - \sqrt{1-\lambda}). \tag{19.71}$$

Consequently, instead of (19.70) we have

$$A_1(\mu_0) = 1 - \varphi(\mu_0)\sqrt{1-\lambda}. \tag{19.72}$$

2. We will assume that pure radiation scattering occurs in the atmosphere, i.e., $\lambda = 1$. In the case cited, as follows from (19.69)

$$\alpha_0 = 2 - \beta_0, \tag{19.73}$$

therefore

$$C = 1 - \beta_0(\alpha_1 + \beta_1). \tag{19.74}$$

It is easy to see that Eq. (19.65) can now be rewritten in the form

$$A_1(\mu_0) = 1 - \frac{\beta_0}{2}[\varphi(\mu_0) + \psi(\mu_0)]\frac{1-A}{1-AC}. \tag{19.75}$$

In the study of planets, the so-called spherical albedo, representing the ratio of the energy reflected by the entire planet to the energy incident on the planet from the Sun, is used in addition to the planar albedo. If the planar albedo is known, then it is easy to find the spherical albedo also.

Let us denote the planet radius by R (Fig. 25). Then the energy, striking the planet from the Sun, will be equal to $\pi R^2 \pi F$. On the other hand, denoting the distance of a given point on the planet's disk from the center of the disk by r, we find that the energy reflected by the planet will be equal to $2\pi\int_0^R A_1(\mu_0)\pi F r dr$. Since $r dr = R^2 \mu_0 d\mu_0$, then the last expression can be rewritten in the form

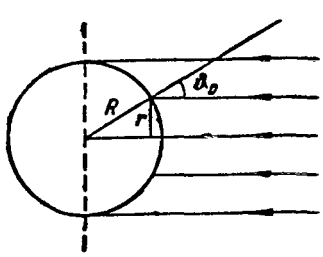

Figure 25.

$$2\pi R^2 \pi F \int_0^1 A_1(\mu_0)\mu_0 d\mu_0,$$

Therefore, denoting the spherical albedo by A_*, we obtain /255

$$A_* = 2\int_0^1 A_1(\mu_0)\mu_0 d\mu_0. \tag{19.76}$$

Substituting (19.65) into (19.76), we obtain

$$A_* = C + \frac{A}{1-AC}[(2-\lambda\alpha_0))\beta_1 + \lambda\beta_0\alpha_1]^2 \tag{19.77}$$

where C is determined by Eq. (19.66).

Let us apply the formula derived for the spherical albedo to the two cases considered above. In the first of these cases (i.e., for $\tau_0 = \infty$) we have

$$A_* = 1 - 2\alpha_1\sqrt{1-\lambda}, \tag{19.78}$$

and in the second (i.e., for $\lambda = 1$)

$$A_* = 1 - \frac{(1-A)(1-C)}{1-AC}. \tag{19.79}$$

To calculate the quantities $A_1(\mu_0)$ and A_* it is necessary to have tables of the functions $\varphi(\mu)$ and $\psi(\mu)$ and of their zero and first moments. Such tables are contained in a number of papers, in particular the paper of Sobouti [6].

Listed in Table 24 are the values of the spherical albedo, found from Eq. (19.79), i.e., for the case when pure light scattering occurs in an atmosphere of optical thickness τ_0 and the atmosphere is bounded by a surface with albedo A.

TABLE 24. SPHERICAL ALBEDO A_*

	A										
	0	0,1	0,2	0,3	0,4	0,5	0,6	0,7	0,8	0,9	1
0	0,00	0,10	0,20	0,30	0,40	0,50	0,60	0,70	0,80	0,90	1,00
0,1	0,08	0,17	0,26	0,34	0,43	0,52	0,61	0,71	0,80	0,90	1,00
0,2	0,15	0,22	0,30	0,38	0,46	0,54	0,63	0,72	0,81	0,90	1,00
0,3	0,21	0,27	0,34	0,41	0,48	0,56	0,64	0,72	0,81	0,90	1,00
0,5	0,30	0,35	0,40	0,46	0,52	0,59	0,66	0,73	0,82	0,90	1,00
1,0	0,45	0,48	0,51	0,55	0,60	0,64	0,70	0,76	0,83	0,91	1,00
2,0	0,61	0,63	0,65	0,67	0,69	0,72	0,75	0,80	0,85	0,92	1,00
3,0	0,70	0,71	0,72	0,73	0,75	0,77	0,79	0,82	0,86	0,92	1,00
∞	1,00	1,00	1,00	1,00	1,00	1,00	1,00	1,00	1,00	1,00	1,00

Commas represent decimal points.

20. Optical Properties of Planetary Atmospheres

1. The Venusian atmosphere. With the aid of light scattering theory, the results of photometric observations of the planets can be interpreted. The optical properties of planetary atmospheres can be determined by comparing theory with observations. Let us do this first for the Venusian atmosphere [7]. /256

Since the planet's surface is not visible through the Venusian atmosphere, then as an approximation it is assumed that the optical thickness of the atmosphere is infinitely great ($\tau_0 = \infty$). To determine the other quantities characterizing the optical properties of the atmosphere (in particular, the scattering indicatrix $x(\gamma)$ and the parameter λ), the observed brightness distribution over the planetary disk for different phase angles must be used. Especially large amounts of observational data can be obtained for Venus since in this case the phase angle (i.e., the angle at the planet between the directions to the Sun and Earth) assumes all possible values—from 0° to 180°. Conclusions about the optical properties of the Venusian atmosphere can also be drawn on the basis of the curve of variation of the planetary brightness with phase angle, which we will now do.

Let us find the theoretical relationship between the stellar magnitude m of the planet and the phase angle α. Let us denote by μ_0 the cosine of the angle of incidence of sunlight at a given point of the planet, by μ—the cosine of the reflection angle and by φ—the difference in the azimuths of the incident and reflected beams. Let us introduce the planetocentric coordinates ω and ψ (Fig. 26). The quantities μ_0, μ, φ are obviously related to ω, ψ and α by the formulas

$$\left.\begin{aligned} &\mu_0 = \cos\psi\cos(\alpha-\omega), \quad \mu = \cos\psi\cos\omega, \\ &\cos\alpha = \mu\mu_0 - \sqrt{(1-\mu^2)(1-\mu_0^2)}\cos\varphi. \end{aligned}\right\} \quad (20.1)$$

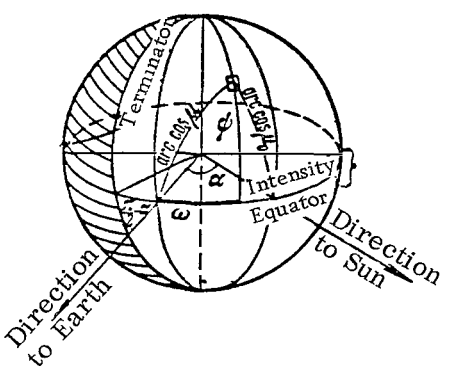

Figure 26.

Let πF be the illumination of an area perpendicular to the sunlight at the upper boundary of the planet atmosphere, and $\rho(\mu, \mu_0, \varphi)$—the atmosphere brightness coefficient. Then the intensity of the radiation, diffusely reflected by the atmosphere, will be equal to $F\rho(\mu, \mu_0, \varphi)\mu_0$, and the amount of energy coming from the area element $d\sigma$ in unit solid angle will be equal to $F\rho(\mu, \mu_0, \varphi)\mu\mu_0 d\sigma$. Since $d\sigma = R^2\cos\psi\, d\psi\, d\omega$, where R is the planet radius, then this amount of energy can be written in the form

$$FR^2\rho(\mu, \mu_0, \varphi)\cos(\alpha-\omega)\cos\omega\cos^3\psi\, d\psi\, d\omega.$$

To obtain the total amount of energy coming from Venus toward Earth in unit solid angle, the last expression must be integrated with respect to ψ over the limits from $-\pi/2$ to $+\pi/2$ and with respect to ω over the limits from $\alpha - \pi/2$ to $\pi/2$, i.e., from the terminator to the edge of the disk. Denoting the distance from Venus to Earth by Δ, for the illumination of Earth from Venus we obtain

$$E_V = 2F\frac{R^2}{\Delta^2}\int_{\alpha-\frac{\pi}{2}}^{\frac{\pi}{2}}\cos(\alpha-\omega)\cos\omega\, d\omega\int_0^{\frac{\pi}{2}}\rho(\mu, \mu_0, \varphi)\cos^3\psi\, d\psi \quad (20.2)$$

The illumination of Earth from the Sun is obviously equal to $E_s = \pi F(r_1/r_2)^2$, where r_1 is the distance from the Sun to Venus and r_2 is the distance from the Sun to Earth, and $E_V/E_S = 2.512^{m_\odot - m}$, where $m_\odot$ is the stellar magnitude of the Sun. Therefore we obtain

$$2.512^{m_\odot - m} = \frac{2}{\pi}\left(\frac{r_2 R}{r_1 \Delta}\right)^2 \int_{\alpha-\frac{\pi}{2}}^{\frac{\pi}{2}} \cos(\alpha - \omega) \times$$

$$\times \cos\omega \, d\omega \int_0^{\frac{\pi}{2}} \rho(\mu, \mu_0, \varphi) \cos^3\psi \, d\psi. \qquad (20.3)$$

Equation (20.3) gives the desired theoretical dependence of m on α, i.e., it enables one to construct the theoretical curve of planet brightness. The expression for $\rho(\mu, \mu_0, \varphi)$ must be substituted into Eq. (20.3) and Eqs. (20.1) must be used. Since the brightness coefficient $\rho(\mu, \mu_0, \varphi)$ depends on the quantities $x(\gamma)$ and λ, then these quantities can be determined by comparing the theoretical and observed brightness curves. The relation

$$\frac{1}{2}\int_0^{\pi} x(\gamma) \sin\gamma \, d\gamma = 1, \qquad (20.4)$$

must also be taken into consideration; (20.4) expresses the normalization condition of the scattering indicatrix. /258

To determine the theoretical brightness curve, it is convenient to isolate, in the expression $\rho(\mu, \mu_0, \varphi)$, the term that takes first order scattering into account. In this case we have

$$\rho(\mu, \mu_0, \varphi) = \frac{\lambda}{4} \frac{x(\gamma)}{\mu + \mu_0} + \Delta\rho(\mu, \mu_0, \varphi), \qquad (20.5)$$

where $\gamma = \pi - \alpha$ and $\Delta\rho$ is a term that takes higher order scattering into account. Since the exact expression for the quantity $\Delta\rho$ for an arbitrary scattering indicatrix is very complex, we will determine this quantity approximately, retaining only the first two terms of the Legendre polynomial expansion of the scattering indicatrix. In other words, let us find the quantity $\Delta\rho$ not for the actual scattering indicatrix $x(\gamma)$, but for the scattering indicatrix

$$x(\gamma) = 1 + x_1 \cos\gamma, \qquad (20.6)$$

where

$$x_1 = \frac{3}{2}\int_0^{\pi} x(\gamma)\cos\gamma\sin\gamma\, d\gamma. \tag{20.7}$$

As shown before, the brightness coefficient $\rho(\mu, \mu_0, \varphi)$ for a scattering indicatrix in the form of Eq. (20.6) is given by Eqs. (19.18)-(19.20). Using them, we obtain

$$\Delta\rho = \frac{\lambda}{4}\frac{\varphi_0^0(\mu)\varphi_0^0(\mu_0) - x_1\varphi_1^0(\mu)\varphi_1^0(\mu_0) - 1}{\mu + \mu_0} + \\ + \frac{\lambda x_1}{4}\frac{\varphi_1^1(\mu)\varphi_1^1(\mu_0)\cos\varphi + \cos\alpha}{\mu + \mu_0}, \tag{20.8}$$

where the auxiliary functions $\varphi_0^0(\mu)$, $\varphi_1^0(\mu)$ and $\varphi_1^1(\mu)$ are defined by Eqs. (19.21)-(19.23). As already stated, these functions have been tabulated. Let us also note that when the role of pure absorption is small in the atmosphere (i.e., for λ values near 1), the following asymtotic formulas follow from Eqs. (19.21) and (19.22):

$$\varphi_0^0(\mu) = \varphi(\mu)\left(1 - 3\sqrt{\frac{1-\lambda}{3-x_1}}\,\mu\right), \tag{20.9}$$

$$\varphi_1^0(\mu) = \varphi(\mu)\,\mu\sqrt{\frac{3(1-\lambda)}{3-x_1}}, \tag{20.10}$$

where $\varphi(\mu)$ is a function defined by Eq. (19.16) for $\lambda = 1$. Equations (20.9) and (20.10) can be used in the case of Venus since the albedo of this planet is very high (about 0.7) and, consequently, the quantity $1-\lambda$ is very small. For a spherical scattering indicatrix this is seen from Eq. (19.78), and for a forward-elongated scattering indicatrix the quantity $1-\lambda$ will be even smaller. /259

Let us now substitute Eq. (20.5) into Eq. (20.3). The result of this substitution can be written in the form

$$x(\pi - \alpha)f(\alpha) + g(\alpha) = h(\alpha), \tag{20.11}$$

where the following definitions are introduced

$$f(\alpha) = \frac{1}{4}\int_{\pi-\frac{\pi}{2}}^{\frac{\pi}{2}} \frac{\cos\omega\cos(\alpha-\omega)}{\cos\omega + \cos(\alpha-\omega)}\, d\omega \int_0^{\frac{\pi}{2}} \cos^2\psi\, d\psi = \\ = \frac{\pi}{16}\left(1 - \sin\frac{\alpha}{2}\operatorname{tg}\frac{\alpha}{2}\ln\operatorname{ctg}\frac{\alpha}{4}\right), \tag{20.12}$$

$$g(\alpha) = \int_{\alpha-\frac{\pi}{2}}^{\frac{\pi}{2}} \cos\omega \cos(\alpha - \omega)\, d\omega \int_{C}^{\frac{\pi}{2}} \Delta\rho \cos^3\psi\, d\psi, \tag{20.13}$$

$$h(\alpha) = \frac{\pi}{2}\left(\frac{r_1\Delta}{r_2 R}\right)^2 2.512^{m_\odot - m} \tag{20.14}$$

The left side of Eq. (20.11) is determined from theoretical data, and the right side depends only on observational data. If these data are known, then, using Eq. (20.11) as well as Eqs. (20.4) and (20.7), one can find the quantities $x(\gamma)$ and λ.

The dependence of the function $h(\alpha)$ on the phase angle α is specified by the observed curve of planet brightness variation. This curve has been determined by a number of authors for Venus. For example, on the basis of Mueller's data the visual stellar magnitude of Venus can be represented in the form

$$m = -4.71 + 0.01322\,\alpha + 0.000\,000\,425\,\alpha^3 \tag{20.15}$$

in the interval from $\alpha = 24°$ to $\alpha = 156°$ when the distance from Venus to earth is one astronomical unit.

The scattering indicatrix in the Venusian atmosphere, determined by the method cited, is given in Table 25. The average of the values obtained by Mueller and Danzhon was taken for the quantity m. For the given scattering indicatrix, the quantity x_1, defined by Eq. (20.7) and characterizing the elongation of the scattering indicatrix, was equal to $x_1 = 1.43$. The albedo of the particles in the Venusian atmosphere was found equal to $\lambda = 0.987$, i.e., very close to 1. The scattering indicatrix in the Earth's atmosphere (determined by the method described below) is presented in the same table for comparison. /260

TABLE 25. SCATTERING INDICATRICES IN THE VENUSIAN AND EARTH ATMOSPHERES

γ	15	30	45	60	75	90	105	120	135	150	165
Venus	9,20	2,80	1,22	0,53	0,26	0,18	0,24	0,38	0,61	0,92	1,23
Earth	3,30	1,90	1,30	0,94	0,75	0,64	0,65	0,72	0,85	1,03	1,10

Commas represent decimal points.

As seen from Table 25, the scattering indicatrix in the Venusian atmosphere is very severely elongated in the forward direction (being considerably more than the scattering indicatrix in the Earth's atmosphere). This means

that light scattering in the Venusian atmosphere is done primarily by large particles. The Venusian atmosphere does, of course, contain some molecules (spectroscopic studies indicate this). However the role of molecular light scattering is not large in the Venusian atmosphere since its scattering indicatrix differs considerably from the Rayleigh scattering indicatrix. If it is assumed that the Venusian atmosphere consists of a cloud layer and a gas layer above it, then on the basis of what has been said the optical thickness of the gas layer must be very small.

The last conclusion is also confirmed by the results of studies of the polarization of the light from Venus. Observations have shown that Venusian radiation is only slightly polarized (not exceeding 4%). The change in the degree of polarization with phase angle has been determined. This change cannot, however, be explained by Rayleigh light scattering in a gas layer. Therefore it must be assumed that polarization of the light of Venus occurs primarily during the scattering by large particles.

2. The Martian atmosphere. The surface of the planet Mars is quite visible through its atmosphere so that one can assume that the optical thickness of the atmosphere in the visible portion of the spectrum is less than unity. On the /261 basis of photometry of Mars, conclusions can be drawn about the optical properties of its atmosphere and surface. In some respects, however, the study of Mars is more difficult than that of Venus since its phase angle only varies within the limits from 0° to 47°. Therefore, in particular, it is impossible to completely determine the scattering indicatrix in the Martian atmosphere.

Mars is usually observed at opposition time, i.e., when the phase angle is close to zero. At such periods many investigators have photographed Mars in various lines. This has made it possible to determine the brightness distribution over the planet's disk within a fairly broad range of wavelengths.

In interpreting Mars observations, in a first approximation it can be assumed that only single scattering of light occurs in the atmosphere. In such a case, as seen from Eq. (19.3), the function S, representing the ratio of the emission coefficient to the absorption coefficient, is equal to

$$S = \frac{\lambda}{4} F x(\gamma) e^{-\frac{\tau}{\mu_0}}. \tag{20.16}$$

Substituting this expression into Eq. (19.25), we obtain the following formula for the brightness coefficient, caused by first order scattering:

$$\rho(\mu, \mu_0, \varphi) = \frac{\lambda}{4} x(\gamma) \frac{1 - e^{-\tau_0\left(\frac{1}{\mu} + \frac{1}{\mu_0}\right)}}{\mu + \mu_0}. \tag{20.17}$$

In Eq. (20.17), however, the reflection of light by the planet's surface is ignored. We will assume that the surface is illuminated only by direct sunlight and reflects the radiation orthogonally with an albedo A. Then the intensity of the radiation, reflected from the surface and leaving the atmosphere at an angle

of arccos μ to the normal will obviously be equal to

$$AFe^{-\tau_0\left(\frac{1}{\mu}+\frac{1}{\mu_0}\right)}\mu_0.$$

Therefore the expression for the brightness coefficient, when light reflection by the planet's surface is taken into account, assumes the form

$$\rho(\mu, \mu_0, \varphi) = \frac{\lambda}{4}x(\gamma)\frac{1-e^{-\tau_0\left(\frac{1}{\mu}+\frac{1}{\mu_0}\right)}}{\mu+\mu_0}+Ae^{-\tau_0\left(\frac{1}{\mu}+\frac{1}{\mu_0}\right)}. \tag{20.18}$$

Applying Eq. (20.18) to the planet at opposition, we must set $\mu_0 = \mu$, $\varphi = \pi$, $\gamma = \pi$. Consequently, in the case given we have /262

$$\rho(\mu, \mu, \pi) = \frac{\lambda x(\pi)}{8\mu}\left(1-e^{-\frac{2}{\mu}\tau_0}\right)+Ae^{-\frac{2}{\mu}\tau_0}. \tag{20.19}$$

This formula defines the brightness coefficient at an angular distance of arccos μ from the center of the disk.

Equation (20.19) is also usually used in the interpretation of photometric observations of Mars (see [8]). Since the quantity $\rho(\mu, \mu, \pi)$ is known from observations, then, using this formula, one can attempt to find the unknown quantities $\lambda x(\pi)$, τ_0 and A (assuming they do not depend on μ). In a first approximation true absorption in the atmosphere can be assumed to be absent and the scattering indicatrix is Rayleigh, i.e., it is assumed that $\lambda x(\pi) = 3/2$. In such a case only two quantities—the optical thickness τ_0 of the atmosphere and the surface albedo A—need to be matched for there to be agreement of the theoretical and observed values of the brightness coefficient at the planet disk.

With the method cited it was found that in the visible portion of the spectrum the optical thickness of the Martian atmosphere is about 0.03, i.e., about 10 times less than the optical thickness of the Earth's atmosphere. Moreover, values of about 0.1-0.3 (different for the "continents", "maria" and "polar caps") were obtained for the surface albedo of the planet.

The values of τ_0 and A, found for Mars, are strongly dependent on the wavelength. The quantity τ_0 increases from the red to the violet portion of the spectrum. This increase, however, occurs more slowly than $\tau_0 \sim \nu^4$, which is the case for purely molecular light scattering, so that it must be assumed that light scattering by large particles plays some role in the Martian atmosphere.

For those spectral regions in which the optical thickness of the atmosphere is of the order of unity and greater, Eq. (20.18) cannot be used since in this case higher order scattering must be taken into consideration. An exact expression

for the brightness coefficient, valid for any value of τ_0, was derived above. It is given by Eq. (19.39) for A = 0 and by Eq. (19.59) for A $\neq$ 0. In deriving these formulas it was assumed that the light scattering is isotropic. With the aid of these formulas, however, an approximate expression can also be derived for the brightness coefficient for an arbitrary scattering indicatrix. In this, first order scattering will be taken into precise account, and higher order scattering—approximately, with it being determined for a spherical scattering indicatrix rather than the given one. In this case we obtain the expression /263

$$\rho(\mu, \mu_0, \varphi) = \frac{\lambda}{4} x(\gamma) \frac{1 - e^{-\tau_0\left(\frac{1}{\mu} + \frac{1}{\mu_0}\right)}}{\mu + \mu_0} + \Delta\rho(\mu, \mu_0). \tag{20.20}$$

for the brightness coefficient, where, on the basis of Eqs. (19.39) and (19.59),

$$\Delta\rho(\mu, \mu_0) = \frac{\lambda}{4(\mu + \mu_0)} [\varphi(\mu)\varphi(\mu_0) - \psi(\mu)\psi(\mu_0) - 1 + e^{-\tau_0\left(\frac{1}{\mu} + \frac{1}{\mu_0}\right)}] + \frac{A}{1 - AC} M(\mu) M(\mu_0). \tag{20.21}$$

Equation (20.20) can be used, in particular, for studying the radiation of Mars in the violet portion of the spectrum. When Mars is observed in violet light, the details which are seen in red light are usually not seen, but sometimes they become pronounced. On this basis it was concluded that particles with strong light absorption in the violet portion of the spectrum are present in the Martian atmosphere, but sometimes the number of these particles decreases and the atmosphere clears up. The existence of a "violet layer" in the Martian atmosphere is presumably explained by the fact that it consists of dust or carbon dioxide crystals (molecules of which have been detected spectroscopically in the Martian atmosphere).

3. The Earth's atmosphere. The optical properties of the Earth's atmosphere have been studied extremely thoroughly and the results are discussed in many monographs (see, for example, [9] and [10]). Here we will discuss only those properties of the Earth's atmosphere which are determined on the basis of the simplest photometric observations and with the aid of the formulas of light scattering theory presented in the foregoing section.

The optical thickness of the Earth's atmosphere is found most simply by measuring the intensity of the solar radiation, penetrating the atmosphere, at different solar zenith distances. This intensity is determined by the formula

$$I = I_0 e^{-\tau_0 \sec \vartheta_0}, \tag{20.22}$$

where I_0 is the solar radition intensity at the upper boundary of the atmosphere. At least two measurements of the quantity I at different solar zenith distances ϑ_0 are required (in order to eliminate I_0) to determine the optical thickness τ_0

of the atmosphere with the aid of Eq. (20.22). For a clear sky the optical thickness of the atmosphere in the visible portion of the spectrum is about 0.3, with /264 its value increasing with a decrease in wavelength. The latter fact, as is known, explains the reddening of the Sun as it approaches the horizon and the blue color of the sky. The relative role of light scattering by molecules and by large particles on the Earth's atmosphere can be judged from the deviation of the wavelength variation of τ_0 from the $\tau_0 \sim \nu^4$ law.

A measurement of the brightness distribution over the sky provides the possibility of finding the scattering indicatrix in the atmosphere. To do this we must make use of the formula defining the intensity of the radiation, diffusely transmitted by the atmosphere, or its corresponding brightness coefficient $\sigma(\tau, \tau_0, \varphi)$. If only first order scattering is taken into consideration, then Eq. (20.16) must be substituted into Eq. (19.26) in order to find the quantity $\sigma(\mu, \mu_0, \varphi)$. As a result we have

$$\sigma(\mu, \mu_0, \varphi) = \frac{\lambda}{4} x(\gamma) \frac{e^{-\frac{\tau_0}{\mu}} - e^{-\frac{\tau_0}{\mu_0}}}{\mu - \mu_0}. \tag{20.23}$$

Scattering of higher orders can be taken into account just as in Eq. (20.20), i.e., for a spherical scattering indicatrix. In this case, instead of Eq. (20.23) we obtain

$$\sigma(\mu, \mu_0, \varphi) = \frac{\lambda}{4} \frac{e^{-\frac{\tau_0}{\mu}} - e^{-\frac{\tau_0}{\mu_0}}}{\mu - \mu_0} + \Delta\sigma(\mu, \mu_0), \tag{20.24}$$

where, as follows from Eqs. (19.40) and (19.60),

$$\Delta\sigma(\mu, \mu_0) = \frac{\lambda}{4(\mu - \mu_0)} [\psi(\mu)\varphi(\mu_0) - \psi(\mu_0)\varphi(\mu) - $$
$$- e^{-\frac{\tau_0}{\mu}} + e^{-\frac{\tau_0}{\mu_0}}] + \frac{A}{1 - AC} N(\mu) M(\mu_0). \tag{20.25}$$

The scattering indicatrix of the Earth's atmosphere, found in the manner cited (with some other formula used for the quantity $\Delta\sigma$), is given in the last line of Table 25. In the case given it was assumed that $\lambda = 1$. The considerable difference between the derived and the Rayleigh scattering indicatrix is explained by the presence of a large number of large particles, besides molecules, in the /265 atmosphere (dust, water droplets, etc.).

The determination of the optical properties of clouds is also of considerable interest. For solid clouds it can be assumed that light scattering occurs in a plane layer whose optical thickness is very great. In this case only radiation that has undergone a very large number of scatterings reaches an observer

standing on the earth's surface. Therefore the determination of the optical properties of clouds (characterizing light scattering in a volume element) involves considerable difficulties.

As an example, let us apply Eq. (20.24) to a cloudy sky. For $\tau_0 \gg 1$ the first term on the right side of this formula is negligibly small, and simple asymptotic formulas can be derived for the second term (see [3]). In particular, for $\lambda = 1$ and $A = 0$ we have

$$\sigma(\mu, \mu_0) = \frac{1}{4} \frac{\varphi(\mu)\varphi(\mu_0)}{\tau_0 + b}, \tag{20.26}$$

where $\varphi(\mu)$ is a function defined by Eq. (19.16) (for $\lambda = 1$), and $b = 2\alpha_2/\alpha_1$, where α_1 and α_2 are the first and second moments of this function. Calculations give $b = 1.42$. From Eq. (20.26) it is seen that the relative brightness distribution over a cloudy sky is determined by the function $\varphi(\mu)$, i.e.,

$$I(\mu) \sim \varphi(\mu). \tag{20.27}$$

As shown in Section 3, the relative brightness distribution over the stellar disk is also given by Eq. (20.27). The result obtained is entirely understandable since in both cases we are dealing with light scattering in a medium consisting of plane-parallel layers for radiation sources at a very large optical distance from the boundary.

If $A \neq 0$, then to determine the quantity $\sigma(\mu, \mu_0)$ we must find the functions $M(\mu)$ and $N(\mu)$. For $\lambda = 1$, as seen from formulas (19.61), (19.62) and (19.73),

$$N(\mu) = 1 - M(\mu). \tag{20.28}$$

For $\tau_0 \gg 1$ substitution of (20.26) into (19.57) yields

$$M(\mu) = \frac{\varphi(\mu)}{(\tau_0 + b)\sqrt{3}}, \tag{20.29}$$

where it is taken into consideration that $\alpha_1 = 2/\sqrt{3}$ (see Section 3). Using Eqs. (19.56) and (19.58), as well as the last two formulas, we obtain

$$C = 1 - \frac{4}{3(\tau_0 + b)}. \tag{20.30}$$

Writing the quantity $\sigma(\mu, \mu_0)$ in the form

$$\sigma(\mu, \mu_0) = \frac{1}{4} \frac{\varphi(\mu)\varphi(\mu_0)}{\tau_0 + b} + \frac{A}{1 - AC} N(\mu) M(\mu_0). \tag{20.31}$$

and substituting the expressions obtained for the quantities $N(\mu)$, $M(\mu)$ and C into Eq. (20.31), we obtain

$$\sigma(\mu, \mu_0) = \frac{\sqrt{3}}{4}\varphi(\mu_0)\frac{4A + \sqrt{3}(1-A)\varphi(\mu)}{4A + 3(1-A)(\tau_0 + b)}. \tag{20.32}$$

Similar formulas for the quantity $\sigma(\mu, \mu_0, \varphi)$ can be derived even in more complex cases, i.e., for arbitrary values of λ and different scattering indicatrices. Some results in this direction have been obtained by S. Piotrowski [11]. Formulas can also be given for the brightness coefficient $\rho(\mu, \mu_0, \varphi)$, characterizing the brightness distribution of clouds for observations from above. The quantity $\rho(\mu, \mu_0, \varphi)$ is approximately determined by Eqs. (20.5) and (20.8), which we used for studying Venus. A comparison of theoretical and observed values of the brightness coefficients $\sigma(\mu, \mu_0, \varphi)$ and $\rho(\mu, \mu_0, \varphi)$ makes it possible to obtain information about τ_0, λ and $x(\gamma)$ for clouds.

4. Interpretation of planet spectra. The spectroscopic study of planets can give very valuable information about planetary atmospheres. Such a study, however, represents considerable difficulty. In part this is caused by the fact that planet radiation occurs because of the scattering of solar radiation by them and therefore all the lines of the solar spectrum are contained in planet spectra. Moreover, telluric lines, arising from the passage of the radiation through the earth's atmosphere, are also present in planet spectra. This complexity of planet spectra severely hinders the identification of lines forming in the planet's atmosphere. This refers especially to the lines of gases contained in the earth's atmosphere (in particular, oxygen and water vapor). The presence of these gases in a planet's atmosphere can be judged only from an enhancement of the telluric lines. From what has been said it is seen how important it is for planet spectroscopy to take astronomical instruments beyond the earth's atmosphere by means of artificial satellites and rockets.

Let us present some results of planetary spectral observations made from the earth's surface. In 1932 Adams and Dunham discovered carbon dioxide (CO_2) gas absorption bands in the infrared portion of the Venusian spectrum. As laboratory studies have shown, bands of the same intensity are produced when radiation passes through a 100-1000 m thick gas layer at a pressure of 760 mm and a temperature of 0°C. Recently weak oxygen and water vapor absorption bands have also been detected in the spectrum of Venus. Kuiper discovered carbon dioxide absorption bands in the spectrum of Mars. The equivalent gas layer thickness under normal conditions, producing such bands, is equal to 4.4 m. Methane (CH_4) and ammonia (NH_3) absorption bands are present in the spectra of Jupiter and Saturn. A few years ago H_2 lines, produced by quadrupole transitions, were also found in the spectrum of Jupiter, attesting to the presence of large numbers of hydrogen molecules in the planet's atmosphere. The spectra of Uranus and Neptune contain strong methane bands and weak molecular hydrogen bands. It should be noted that some gases do not appear spectro-

scopically in the spectral regions that are accessible to observation. Among these, for example, is molecular nitrogen which apparently exists in large quantities in planet atmospheres.

The same formulas, which were used above in the interpretation of photometric data about planets, can be used for a quantitative interpretation of planet spectra. We will now write down expressions for the radiation intensity within a planet spectral line in some very simple cases.

Above we assumed that scattering and true absorption of light in a continuous spectrum occur in each volume element of the atmosphere (due to the presence of molecules and large particles in the atmosphere). The scattering coefficient was denoted by $\lambda\alpha$, and the true absorption coefficient by $(1-\lambda)\alpha$, where λ is the particle albedo and α is the absorption coefficient. Now let us assume that true spectral line absorption also occurs in each volume element in addition to the processes mentioned. We will neglect scattering of light in the lines (this obviously cannot be done for the resonance band). Let us denote by α_ν the true absorption coefficient at frequency ν within a line.

With the notations that have been adopted the radiative transfer equation in a spectral line is written in the form

$$\cos\vartheta \frac{dI_\nu}{dx} = -(\alpha + \alpha_\nu) I_\nu + \varepsilon_\nu, \tag{20.33}$$

where

$$\varepsilon_\nu = \lambda\alpha \int I_\nu \frac{d\omega}{4\pi} + \lambda\alpha \frac{F}{4} e^{-\tau_\nu \sec\vartheta_0}, \tag{20.34}$$

and τ_ν is the optical depth at frequency ν, i.e., /268

$$\tau_\nu = \int_x^\infty (\alpha + \alpha_\nu) dx. \tag{20.35}$$

For simplicity in Eq. (20.34) it is assumed that the light scattering is isotropic.

Introducing the notation

$$S_\nu = \frac{\varepsilon_\nu}{\alpha + \alpha_\nu}, \tag{20.36}$$

instead of Eqs. (20.33) and (20.34) we obtain

$$\cos\vartheta \frac{dI_\nu}{d\tau_\nu} = I_\nu - S_\nu, \tag{20.37}$$

$$S_\nu = \lambda_\nu \int I_\nu \frac{d\omega}{4\pi} + \lambda_\nu \frac{F}{4} e^{-\tau_\nu \sec \theta_0}, \tag{20.38}$$

where

$$\lambda_\nu = \frac{\lambda a}{a + a_\nu}. \tag{20.39}$$

We see that Eqs. (20.37) and (20.38) formally agree with the Eqs. (19.10) and (19.11) considered earlier. Outside a spectral line, i.e., when $\alpha_\nu = 0$, $\tau_\nu = \tau$ and $\lambda_\nu = \lambda$, the first set of equations passes over to the second.

Let us first consider the case when the continuous spectrum optical thickness of the atmosphere is an order of magnitude less than unity. In this case, on the basis of Eq. (20.18), the intensity of the continuous spectrum radiation coming from the atmosphere is equal to

$$I(\mu, \mu_0) = \left[\frac{\lambda}{4} \frac{1 - e^{-\tau_0\left(\frac{1}{\mu} + \frac{1}{\mu_0}\right)}}{\mu + \mu_0} + A e^{-\tau_0\left(\frac{1}{\mu} + \frac{1}{\mu_0}\right)}\right] F\mu_0. \tag{20.40}$$

where A is the albedo of the planet surface. Replacing, here, λ by λ_ν and τ_0 by τ_ν^0, we obtain an expression for the intensity of the radiation coming from the atmosphere at frequency ν within a spectral line:

$$I_\nu(\mu, \mu_0) = \left[\frac{\lambda_\nu}{4} \frac{1 - e^{-\tau_\nu^0\left(\frac{1}{\mu} + \frac{1}{\mu_0}\right)}}{\mu + \mu_0} + A e^{-\tau_\nu^0\left(\frac{1}{\mu} + \frac{1}{\mu_0}\right)}\right] F\mu_0. \tag{20.41}$$

The ratio of these intensities, i.e., the quantity /269

$$r_\nu(\mu, \mu_0) = \frac{I_\nu(\mu, \mu_0)}{I(\mu, \mu_0)}, \tag{20.42}$$

characterizes the absorption line profile at an angular distance of arccos μ from the center of the planet disk.

If the continuous spectrum optical thickness of the atmosphere is very small ($\tau_0 \to 0$), then from the formulas presented it follows that

$$r_\nu(\mu, \mu_0) = e^{-\tau_\nu^0\left(\frac{1}{\mu} + \frac{1}{\mu_0}\right)} \tag{20.43}$$

This formula expresses the fact that an absorption line arises from the passage of a ray through the atmosphere, its reflection from the planet surface and a second passage through the atmosphere toward the observer. Therefore the line

has the same residual intensity as when radiation passes through a gas layer with an optical thickness $\tau_\nu^0(1/\mu + 1/\mu_0)$. In the case given the "equivalent gas layer thickness", found from observations, directly characterizes the amount of gas in the atmosphere. Equation (20.43) is obviously applicable to the red portion of the Martian spectrum.

Let us now consider the case when the optical thickness of the atmosphere is very large (we will assume $\tau_0 = \infty$). Let us assume the quantities λ and λ_ν are constant in the atmosphere. As follows from Eq. (19.15), the intensity of the continuous spectrum radiation leaving the atmosphere is equal to

$$I(\mu, \mu_0) = \frac{\lambda}{4} \frac{\varphi_\lambda(\mu)\varphi_\lambda(\mu_0)}{\mu + \mu_0} F\mu_0, \tag{20.44}$$

where by $\varphi_\lambda(\mu)$ we mean the function defined by Eq. (19.16). Replacing λ by λ_ν, we find that the intensity of the spectral line radiation coming from atmosphere is given by the formula

$$I_\nu(\mu, \mu_0) = \frac{\lambda_\nu}{4} \frac{\varphi_{\lambda_\nu}(\mu)\varphi_{\lambda_\nu}(\mu_0)}{\mu + \mu_0} F\mu_0. \tag{20.45}$$

Substituting (20.44) and (20.45) into (20.42), we obtain

$$r_\nu(\mu, \mu_0) = \frac{\lambda_\nu \varphi_{\lambda_\nu}(\mu)\varphi_{\lambda_\nu}(\mu_0)}{\lambda \varphi_\lambda(\mu)\varphi_\lambda(\mu_0)}. \tag{20.46}$$

We will assume that the quantities λ and λ_ν are close to 1. Then, as follows from Eq. (20.9) for $x_1 = 0$, the function $\varphi_\lambda(\mu)$ is represented in the form /270

$$\varphi_\lambda(\mu) = \varphi(\mu)[1 - \mu\sqrt{3(1-\lambda)}], \tag{20.47}$$

where the function $\varphi_\lambda(\mu)$ for $\lambda = 1$ is designated $\varphi(\mu)$. A similar expression can also be written for the function $\varphi_{\lambda_\nu}(\mu)$. Substituting these expressions into Eq. (20.46) and neglecting terms of the order of $1-\lambda$ and $1-\lambda_\nu$, we obtain

$$r_\nu(\mu, \mu_0) = 1 - \sqrt{3}(\mu + \mu_0)(\sqrt{1-\lambda_\nu} - \sqrt{1-\lambda}). \tag{20.48}$$

Obviously, in this case the "equivalent gas layer thickness", obtained from observations, no longer has the simple physical meaning it had in the case of Eq. (20.43). Using the expression derived for the quantity $r_\nu(\mu, \mu_0)$, one can de-

termine the equivalent absorption line width from the formula

$$W(\mu, \mu_0) = \int [1 - r_\nu(\mu, \mu_0)] d\nu. \tag{20.49}$$

Since the line absorption coefficient α_ν is proportional to the concentration n of absorbing molecules, Eq. (20.49) gives the dependence of W on n (more precisely on n/α). Therefore a comparison of the observed and theoretical values of W allows one to find the molecule concentration n in the planet atmosphere.

If Eq. (20.49) is applied to the different lines of a molecular band, then the relative number of molecules in different rotational-vibrational levels can be determined. Assuming that a Boltzmann distribution of excited molecular levels is established because of collisions, one can determine the gas temperature. In this manner Chamberlain and Kuiper [12] determined the temperature in the Venusian atmosphere from CO_2 absorption bands; it turned out to be equal to 285°K. Equation (20.48) for the quantity $r_\nu(\mu, \mu_0)$ was used in this temperature determination. In other words, it was assumed that molecules and large particles are mixed at a constant ratio in the atmosphere. This assumption is evidently approximately true since the dependence of the equivalent width of the CO_2 band on the phase, calculated on the basis of it, agrees with the analogous dependence obtained from observations.

21. Structure of Planetary Atmospheres

1. Planetary temperatures. In the study of planets other observations, besides the observations in the optical region of the spectrum considered above, are made. Very important among these are observations for the purpose of measuring planet temperatures. Before reporting the results of such measurements, let us ascertain what temperatures should be expected on the planets. /271

Let us assume that the sunlight illuminates an absolutely black plate oriented perpendicular to it. If L is the solar luminosity and r is the distance to the plate from the center of the Sun, then the plate illumination is equal to

$$E = \frac{L}{4\pi r^2}. \tag{21.1}$$

The plate absorbs the solar radiation and re-emits it in accordance with Planck's law with a temperature T_1, defined by the condition

$$E = \sigma T_1^4. \tag{21.2}$$

Since

$$L = 4\pi r^2_\odot \sigma T_\odot^4, \tag{21.3}$$

where $r_\odot$ is the Sun's radius and T_e is its effective temperature, then from the formulas that have been presented we obtain

$$T_1 = T_e \left(\frac{r_\odot}{r}\right)^{1/2}. \tag{21.4}$$

Values of the temperature T_1 for the different planets can be calculated from Eq. (21.4). These values of T_1 are listed in the last column of Table 26. Values of the distance r in astronomical units and of the illumination E in cal/ /cm^2-min are given in the first two columns (the value of E, listed in the table for the Earth, represents the so-called solar constant).

TABLE 26. VALUES OF THE QUANTITIES E AND T_1 FOR THE VARIOUS PLANETS

Planet	r	E	T_1	Planet	r	E	T_1
Mercury	0,387	12,7	631	Saturn	9,539	0,0208	128
Venus	0,723	3,64	464	Uranus	19,191	0,0052	89
Earth	1,000	1,90	392	Neptune	30,071	0,0021	72
Mars	1,524	0,81	316	Pluto	39,52	0,0012	62
Jupiter	5,203	0,0702	173				

Commas represent decimal points.

The value of T_1 calculated from Eq. (21.4) characterizes the temperature of a planet devoid of atmosphere in the case when the Sun is at the zenith and the planet absorbs all the solar radiation incident upon it. If, however, the sunlight /272 angle of incidence is ϑ_0 and the planet albedo in the visible portion of the spectrum (where the Sun radiates most of its energy) is equal to A, then the temperature T_1 will obviously be defined by the formula

$$T_1 = T_e \left[\frac{r_\odot^2 (1-A)\cos\vartheta_0}{r^2}\right]^{1/4}. \tag{21.5}$$

In reality the angle ϑ_0 for a given point changes with time because of the planet rotation about its own axis and about the Sun. Therefore the temperature value T_1 also varies. To determine the temperature for a given point and a given instant of time, the slowness of the heating and cooling of the planet surface must also be taken into account.

If the planet has an atmosphere, then the problem of radiative transfer through the atmosphere must be solved for a theoretical determination of the atmosphere and planet surface temperature. This problem will be considered below, but for now let us note that even then temperatures of the same order as those presented in Table 26 are obtained. Since these temperatures are much

less than the temperature of the Sun, the major portion of the energy radiated by a planet is not in the visible but in the far infrared portion of the spectrum (nearly all planet radiation in the visible portion of the spectrum represents the reflection of solar radiation). More precisely, the thermal radiation of a planet has a wavelength λ_m determined from the Wien displacement law

$$\lambda_m T = 0.290 \text{ cm-deg},$$

and at temperatures, characteristic of planets, the values of λ_m are about 5-50 μ.

Sensitive thermocouples and special filters, transmitting radiation in the infrared spectral region, are used to measure the thermal radiation of the planets. In doing this, use is made of the fact that the Earth's atmosphere has a "transparent window" in the 8-15 μ interval. In calculating the temperature from the radiation measurements it is assumed that the energy distribution in the planet spectrum is given by Planck's formula.

Let us present some results of planet temperature determinations (for more details see [13] and [14]).

The thermal radiation has been measured as a function of phase angle for Mercury. This has permitted calculating the temperature at a sunlit point of the planet; it was found to be equal to 613°K. This temperature agrees well with the value of T_1 determined from Eq. (21.5) for $\vartheta_0 = 0$ and $A = 0.07$.

The measured temperature of Venus is approximately equal to 230°K. Especially interesting is the fact that there is no marked difference between the temperatures of the illuminated and dark hemispheres. Since the Venusian atmosphere has a large optical thickness, this temperature value refers to the outer atmosphere layers. /273

For Mars similar data are obtained for temperatures at different points of the disk and for different times. Let us only indicate that the temperature of a sunlit point at perihelion is equal to 300° and at aphelion 273°K. The difference between these temperatures agrees with Eq. (21.5) (i.e., with the change of T_1 as a function of r). The measured temperature values are, however, somewhat lower than the values of T_1 found from Eq. (21.5), which is evidently explained by the presence of an atmosphere around the planet.

The measured temperatures of Jupiter and Saturn at sunlit points are equal to approximately 150° and 125°K respectively. The temperatures of the more remote planets are uncertainly determined.

2. Planetary radio emission. The study of planetary radio emission has considerable value for explaining the physical conditions on planets. Radio emission of different wavelengths comes to us from different atmospheric layers, making it possible to draw conclusions about the change of physical conditions with depth in the atmosphere. For some wavelengths in the radio band the atmosphere can be perfectly transparent although it is opaque in the optical portion of the spectrum. From the radio emission of these wavelengths information about

the invisible planetary surface can be obtained. At the present time Venus and Jupiter have been studied in most detail by radioastronomy methods. Such an investigation has led to a number of important and unexpected results.

Especially interesting is the fact that a very high brightness temperature—about 600°K—is obtained for Venus in the centimeter band. This temperature is much higher than that found from the radiation in the infrared portion of the spectrum (equal, as we know, to about 230°K). The radio emission of Venus is apparently thermal in nature since it does not exhibit systematic variations and does not contain any appreciable polarized component. The most probable explanation for such a high temperature from radio emission observations is that it is the temperature of the planet's surface; surface heating, however, is caused by the so-called "greenhouse effect" (which we will discuss below).

In the millimeter band the Venusian temperature is about 300-400°K. According to the interpretation that has been given, this is the temperature of intermediate layers of the atmosphere.

The radio emission observed from Venus depends on the phase angle, with the temperature on the illuminated side of the planet being higher than on the dark. These results, however, are not very reliable. If they are confirmed, then from them one can conclude, in particular, that the rotational velocity of Venus about its axis is not very great since otherwise large temperature differences could not be established between different points of the planet*. /274

The radio emission of Jupiter is very complex. For $\lambda < 3$ cm the brightness temperature is about 140°K, i.e., it is close to the temperature found from the radiation in the infrared portion of the spectrum. On this basis the Jovian emission at $\lambda < 3$ cm can be assumed to be thermal. However, observations of the radio emission of Jupiter in the interval from 3 cm to 70 cm have shown that the intensity of this emission per unit frequency interval depends slightly on the wavelength. Meanwhile the thermal emission intensity (for constant temperature and constant source dimensions) should decrease rapidly with an increase in wavelength since the thermal emission intensity is determined by Eq. (18.1). Therefore it was concluded that the radio emission of Jupiter in the band being considered is nonthermal in character. It is difficult to assume that this emission is thermal and comes to us from layers with a different temperature since for $\lambda = 70$ cm the brightness temperature is 50,000°, i.e., very high.

The assumption of the nonthermal nature of Jovian emission in the wavelength interval from 3 to 70 cm is corroborated by the following important facts: 1) the intensity of this emission varies with time, 2) this emission is linearly polarized (the polarization is about 30% at 31-cm wavelength, and the electric vector is approximately parallel to the planet equator), 3) the dimensions of the emitting region are approximately three times greater than the optical diameter of Jupiter. The last fact deserves special attention because it lies at the base of the concept of the Jovian radiation belts (similar to the Earth's radiation

*According to the latest radar observations the Venusian period of rotation is 247 ± 5 days.

belts discovered by means of artificial satellites). It is assumed that the radiation belts are formed by the capture of charged particles by the magnetic field of the planet and the observed decimeter radio emission of Jupiter is the magneto-bremsstrahlung radiation of electrons.

Observations also show that an intense sporadic radio emission comes from Jupiter. Radio emission bursts, about 1 sec in duration, are observed at wave- /275 lengths equal to a few tens of meters. This emission is polarized and appears at certain localized sources. The same mechanisms are proposed for explaining the sporadic radio emission of Jupiter as for explaining the sporadic solar radio emission, i.e., magnetic bremsstrahlung radiation of electrons and the normal plasma oscillations.

3. Planetary atmosphere models. The results of observations of planets in different spectral regions (visible, infrared and radio band) serve as the basis for constructing planetary atmosphere models. Such models have recently been developed for several planets (Venus, Mars, Jupiter). At the moment, however, their status is not completely certain, and therefore here let us only briefly consider, by way of an example, the models proposed for the Venusian atmosphere.

In the development of a planetary atmosphere model some scheme of atmosphere structure, its chemical composition and energy transfer mechanism, is specified. The density and temperature distribution in the atmosphere is determined through calculations. This allows one to compute the optical depths in the atmosphere for different frequencies, and then the intensities of the radiation coming from the atmosphere in different spectral regions. A comparison of theoretical and observed radiation intensities provides the possibility of checking the analytical model.

For the Venusian atmosphere the greenhouse model, the essence of which is included below, is assumed to be the most probable. Solar radiation, incident on the atmosphere, is partially reflected by it, and partially transmitted through it (generally speaking, after multiple scatterings, which were discussed in Section 19). The solar radiation, passing through the atmosphere, heats the surface and thermal radiation in the far infrared spectral region flows out from the latter. However, the optical thickness of the atmosphere is very great in the infrared region of the spectrum. Therefore a considerable portion of the infrared radiation returns to the surface from the atmosphere so that it is heated even further. As a result of the radiative transfer process and equilibrium condition is established whereby the thermal radiation energy, coming outward from the atmosphere, is equal to the solar radiation incident on the planet's surface. Similar processes occur in greenhouses (in which, however, the glass does not absorb the thermal radiation coming from the ground so much as it prevents convection).

It is easy to find an approximate temperature distribution in the atmosphere. Since the absorption of infrared radiation in the atmosphere occurs in molecular bands, the frequency dependence of the absorption coefficient is very complex. /276 For simplicity let us introduce the average absorption coefficient and its corresponding optical depth τ. The amount of energy, incident on the planet's surface from the Sun, we will denote by E_1. This amount of energy, is transferred

outward through the atmosphere in the form of infrared radiation. We will assume that local thermodynamic equilibrium exists in the atmosphere. Then the dependence of the temperature T on the optical depth τ will be defined by the formula

$$\frac{ac}{4}T^4 = E_1\left(\frac{1}{2}+\frac{3}{4}\tau\right), \tag{21.7}$$

written in analogy to Eq. (4.16), derived in the Eddington approximation in photosphere theory. We have only replaced the radiant flux πF in the stellar photosphere by the radiant flux E_1 in the planet's atmosphere.

If the optical thickness of the atmosphere is denoted by τ_1, then the temperature of the planet's surface will be equal to

$$T_1 = \left[\frac{4E_1}{ac}\left(\frac{1}{2}+\frac{3}{4}\tau_1\right)\right]^{1/4}. \tag{21.8}$$

Equation (21.8), of course, is very crude and it only illustrates the action of the "greenhouse effect". In reality, when considering radiative transfer through the atmosphere, the frequency dependence of the absorption coefficient, determined by the assignment of chemical composition and physical conditions (i.e., temperature and density), must be taken into consideration. The possibility of convective energy transfer in the atmosphere must also be taken into consideration.

Sagan developed a greenhouse model applicable to the Venusian atmosphere (see [15]). He assumed that the atmosphere consists of CO_2 and H_2O molecules and selected their content such that the atmosphere opacity in the infrared portion of the spectrum led to a planet surface temperature of 600°K. According to this model, at a height of about 40 km from the surface the temperature is equal to 220-235°K and clouds, consisting of ice crystals, are formed at that height. The fact that the energy distribution in the infrared spectrum of the Venusian clouds differs little from the energy distribution in the spectra of laboratory-produced ice crystals is a point in favor of this conclusion.

Figure 27 is a schematic representation of the greenhouse model of the Venusian atmosphere, with those regions of the atmosphere from which radiation in different spectral regions reaches the observer being indicated by the arrows. /277
Diffusely reflected sunlight in the visible portion of the spectrum and the infrared self-radiation of the atmosphere come to us from the clouds. Millimeterwave radio emission comes from atmosphere layers beneath the clouds, and centimeter-wave—from the planet's surface.

Öpik proposed another Venusian atmosphere model to explain the same observational data. It assumes that the planet's surface is heated to a temperature of 600°K not by radiation, but by winds carrying energy from the upper atmosphere layers to the lower. There is much dust in the lower atmosphere layers

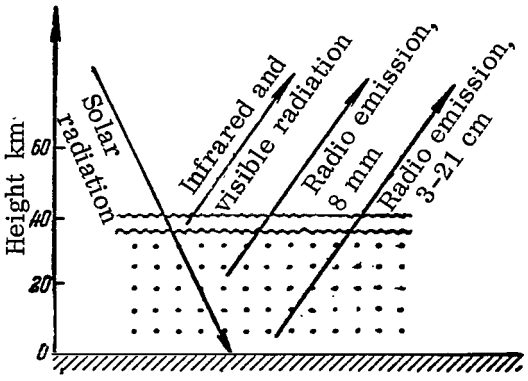

Figure 27.

and solar radiation does not reach the planet's surface. This atmosphere model is called the "eolosphere" (from the word "eol"—wind).

In both Venusian atmosphere models (greenhouse and eolosphere) it is assumed that the temperature of the planet's surface is very high. Therefore if either model is correct, life, as we know it on Earth, cannot exist on Venus. A third Venusian atmosphere model—the ionospheric—gives considerable chance for such life. According to this model, the radio emission at 3-21 cm with a brightness temperature of about 600°K comes to us not from the planet surface, but from its ionosphere, above the cloud layer. The planet surface temperature can be considerably less than 600°K.

In order for the ionosphere to emit strong radio emission, its optical depth must be quite large. As we recall, the optical depth at radio frequencies is determined by Eq. (18.9). From it it is seen that the value of τ_ν is inherently dependent on the value of the integral $\int n_e n^+ dr$, taken over the entire ionosphere /278 thickness. As calculations show, the ionosphere can give the observed emission in 3-21 cm waves only in the case when the value of this integral will be of the order of 10^{26} cm^{-5}. From this it follows that the density of free electrons in the Venusian ionosphere must be several orders of magnitude greater than in the Earth's ionosphere. It is very difficult, however, to explain such a large value of n_e. Ionization in the Earth's ionosphere is caused by ultraviolet solar radiation, but at Venus the intensity of this radiation is only twice as large as at the Earth. In view of this, the possibility of ionization by the corpuscular stream, coming from the Sun, was considered. This stream does not reach the Earth's ionosphere (except at the polar regions) since it is deflected by the Earth's magnetic field. If, however, Venus has a weak magentic field, then the solar corpuscles can enter the upper layers of its atmosphere and cause ionization. However, much stronger corpuscular streams are required than those obtainable on the basis of other data to explain high electron densities in the Venusian ionosphere.

A derivation of the radio emission distribution over the planetary disk from observations can serve as one method of checking the validity of the proposed Venusian atmosphere models. If the ionosphere model is correct, then the emission intensity must increase as one goes from the center of the disk to the edge because of the increased ionospheric path length. However, observations do not corroborate this, i.e., they contradict the ionosphere model. Observations, made at the Pulkovo observatory at a wavelength of 3 cm, led to the conclusion that the Venusian disk darkens as one goes from center to edge. The same result was also obtained from observations with the Mariner II space rocket at a

wavelength of 1.9 cm. Similar observations must be continued for the purpose of refining the results.

4. Upper layers of the atmosphere. Purely gaseous layers, consisting of molecules, are present in the earth's atmosphere above the clouds. It is reasonable to assume that this is also the case for other cloud-covered planets (in particular, Venus and Jupiter). The gaseous layers can be studied by different methods. The polarimetric method, already described above, is one of these methods. Radiation becomes polarized through scattering by molecules, with the degree of polarization being close to unity at scattering angles close to 90°. Therefore from a comparison of the polarization of the light of a planet with the polarization caused by molecular scattering one can draw a conclusion about the role of the gaseous layer in radiation scattering. In this manner it is found that for Venus the optical /279 thickness of the gaseous layer in the visible portion of the spectrum is very small (no greater than 0.03). For Jupiter polarization studies are made difficult by the fact that its phase angle only varies from 0 to 12°. The detailed results of a study of the planets by the polarimetric method are contained in the book by Dollfus [13].

The spectroscopic method of investigation of planetary atmospheres gives much more valuable results. As already stated, the molecule concentrations in the atmosphere and its temperature can be found by comparing the theoretical and observed equivalent line widths. Let us also note that the pressure in the atmosphere can also be determined by the method cited. This possibility is associated with the fact that the equivalent line width depends not only on the concentration of the molecules being considered, but also on the concentration of all particles in the atmosphere (i.e., on the pressure), since the collisions of particles with molecules affects the line absorption coefficient. A pressure determination for the Venusian atmosphere was made from the CO_2 bands. It is not completely clear, however, to what level of the atmosphere the results obtained must be applied. At first it was thought that molecular bands arise only in the gas layer above the clouds, but, evidently, they are also formed in the clouds where true line absorption of light and scattering by large particles occur. In this case the determination of the optical properties of the above-the-clouds layer by the spectroscopic method is fraught with difficulties.

Very important information on the structure of the upper layers of planetary atmospheres can also be obtained from observation of star occultations by the planets. When a planet passes in front of a star, a gradual weakening of the stellar brightness occurs, caused by the passage of its radiation through more and more dense layers of the planetary atmosphere. The height dependence of the density in the atmosphere can obviously be found from the observed curve of stellar brightness variation.

As elementary calculations show, the decrease in stellar brightness, when its radiation passes through the planetary atmosphere, is primarily caused not by light absorption in the atmosphere but by the differential refraction effect. Parallel stellar rays, incident on the planetary atmosphere, diverge because of refraction in it. For an observer on earth, therefore, the illumination E from the star during its eclipse by the planetary atmosphere will be less than the illumination E_0 from the star when it is not occulted (Fig. 28).

Let us find the ratio E/E_0. Let r be the distance from the center of the planet at which a stellar ray would pass in the absence of refraction. Because of refraction the ray is bent in the atmosphere and upon its exit from the atmosphere it makes an angle δ with the initial ray. If the distance between two rays before entering the atmosphere is equal to dr, then for an observer on earth it will obviously be equal to /280

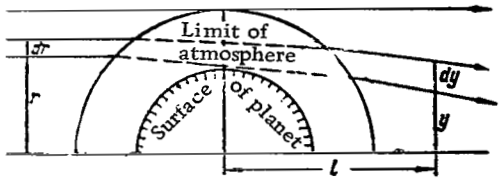

Figure 28.

$$dy = \left(1 - l\frac{d\delta}{dr}\right)dr, \tag{21.9}$$

where l is the distance from the planet to Earth (let us note that $d\delta/dr < 0$). Since

$$E_0\, dr = E\, ay, \tag{21.10}$$

for the desired ratio of intensities we obtain

$$\frac{E_0}{E} = 1 - l\frac{d\delta}{dr}. \tag{21.11}$$

The quantity δ is given as a function of r by the theory of refraction. As is known, the ray trajectory in the atmosphere is determined by the equation

$$n(r')r'\sin\vartheta = r, \tag{21.12}$$

where ϑ is the angle between the ray and the radius vector, and n(r') is the refractive index at a distance r' from the center of the planet. Using Eq. (21.12), one can obtain the following formula for the quantity δ:

$$\delta = 2\int_1^{n(r_0)} \operatorname{tg}\vartheta\frac{dn}{n}, \tag{21.13}$$

where r_0 is the minimum distance of the ray from the center of the planet.

In calculating the quantity δ, we assume that the density in the upper layers of the atmosphere decreases exponentially with an increase in r', i.e.,

$$\rho(r') = \rho(R)e^{-\beta(r'-R)}, \tag{21.14}$$

where β is some constant and R is the radius of the upper boundary of the cloud layer. Then the refractive index can be represented in the form /281

$$n(r') = 1 + ke^{-\beta(r'-R)}, \tag{21.15}$$

where k is a constant, proportional to the quantity $\rho(R)$.

Using Eqs. (21.12) and (21.15), and also taking into account the smallness of the quantity k in comparison with 1, from (21.13) we obtain approximately

$$\delta = k\sqrt{2\pi\beta R}\, e^{-\beta(r-R)}. \tag{21.16}$$

We must substitute this expression for δ into Eq. (21.11). As a result we obtain

$$\frac{E_0}{E} = 1 + lk\beta^{3/2}\sqrt{2\pi R}\, e^{-\beta(r-R)}. \tag{21.17}$$

From observations the quantity E_0/E is obtained as a function of time which can be represented as a function of the distance y when the occultation of the star by the planet is taken into consideration. Therefore we must replace the theoretical relationship (21.17) between the quantity E_0/E and r by a relationship between E_0/E and y. Differentiating (21.17) with respect to y and taking (21.10) into consideration, we obtain

$$\frac{d}{dy}\left(\frac{E_0}{E}\right) = -\beta\left(\frac{E_0}{E} - 1\right)\frac{E_0}{E}. \tag{21.18}$$

Integration of this equation gives

$$\frac{E_0}{E} + \ln\left(\frac{E_0}{E} - 1\right) = -\beta y + \text{const}. \tag{21.19}$$

The value of the parameter β can be determined from a comparison of the observed and theoretical dependence of E_0/E on y. If it is assumed that the density in the atmosphere changes in accordance with the barometric law, then

$$\beta = \frac{\mu m_H g}{kT}, \tag{21.20}$$

where μ is the mean molecular weight and g is the gravitational acceleration in the atmosphere. Therefore the quantity μ can be found from the quantity β with the aid of Eq. (21.20). This allows one to formulate some idea about the chemical composition of the atmosphere.

The cited method of studying the upper layers of planetary atmospheres has been applied to Jupiter and Venus. In 1952 Baum and Code observed the occultation of the star σ Aries by Jupiter and determined that $\beta = 0.12\ \text{km}^{-1}$. Assuming /282
$g = 2600\ \text{cm/sec}^2$ and $T = 86°K$ for Jupiter, from Eq. (21.20) they found a value of $\mu = 3.3$ for the average molecular weight. Such a low value of μ can be explained by the fact that the upper layers of the Jovian atmosphere are composed primarily of molecular hydrogen and helium.

An occultation of Regulus by Venus was observed in 1959. Comparing the observed and theoretical stellar brightness curves, Vaucouleurs found that the "homogeneous atmosphere height" of Venus is equal to approximately 6 km, i.e., $\beta \approx 0.17\ \mathrm{km}^{-1}$. Since $g = 850\ \mathrm{cm/sec}^2$ and $T \approx 230°K$ for Venus, Eq. (21.20) gives $\mu \approx 38$. This value of μ does not differ greatly from the molecular weight of carbon dioxide gas ($\mu = 44$), which has been detected spectroscopically in the Venusian atmosphere.

REFERENCES

1. Ambartsumyan, V.A. Scientific proceedings, v. I, Izd-vo AN Arm. SSR, 1960.
2. Chandrasekhar, S. Radiative Transfer, Oxford, 1950. (Russ. translation: S. Chandrasekhar, Radiative transfer, Izd-vo inostr. lit., 1953).
3. Sobolev, V.V. Radiative energy transfer in stellar and planetary atmospheres, Gostekhizdat, 1956.
4. Shifrin, K.S. Light scattering in a turbid medium, Gostekhizdat, 1951.
5. Minnaert, M. The reciprocity principle in lunar photometry, Ap. J. 93, 403, 1941.
6. Sobouti, Y. Chandrasekhar's X-, Y-, and related functions, Ap. J. Suppl. N 72, 411, 1963.
7. Sobolev, V.V. A study of the Venusian atmosphere, Astron. Zh., 41, No. 1, 1964.
8. de Vaucouleurs, C. Physics of the planet Mars, Paris, 1951) (Russ. translation: C. de Vaucouleurs, Physics of the planet Mars, Izd-vo inostr. lit., 1956).
9. The atmospheres of the earth and planets, ed. G.P. Kuiper, Chicago, 1947. (Russ. translation: The atmospheres of the earth and planets, coll. ed. G.P. Kuiper, Izd-vo inostr. lit., 1951).
10. Kondrat'ev, K.Ya. Actonometry, Gidrometeoizdat, 1965.
11. Piotrowski, S. Asimptotic case of the diffusion of light through an optically thick scattering layer, Acta Astronomica 6, N 2, 61, 1956.
12. Chamberlain, J.W. and G.P. Kuiper. Rotational temperature and phase variation of the carbon dioxide bands of Venus, Ap. J. 124, 399, 1956.
13. Planets and Satellites, Chicago, 1961. (Russ. translation: Planets and Satellites, Izd-vo inostr. lit., 1963).
14. Sharonov, V.V. Nature of the planets, Fizmatgiz, 1958.
15. Kellog, W. and C. Sagan. The atmospheres of Mars and Venus, 1961. (Russ. translation: W. Kellogg and C. Sagan. The atmospheres of Mars and Venus, Izd-vo inostr. lit., 1962).

CHAPTER V

GASEOUS NEBULAE

The physics of gaseous nebulae is pertinent to a number of the most developed branches of astrophysics. This is due to the extremely simple physical conditions in nebulae: low density of matter and low radiation density. Under such conditions many processes occur in a "pure" form, free of foreign influences. /283

The luminosity of gaseous nebulae is caused by the radiation of hot stars. A nebula absorbs the high-frequency stellar radiation and re-emits it in lower frequency quanta. The bright lines in nebular spectra arise in this manner. In principle, the bright lines in the spectra of Be and Wolf-Rayet stars, novae and other objects arise in the same manner (although more complex in some respects). Therefore the results of the study of gaseous nebulae are widely used in various branches of astrophysics.

The conversion process, occurring in gaseous nebulae, of high-frequency stellar radiation into lower frequency quanta indicates a drastic deviation from thermodynamic equilibrium for the nebulae. This sharply distinguishes nebulae from stellar atmospheres for which the assumption of the existance of thermodynamic equilibrium proves to be adequate as a first approximation to reality. In the study of nebulae we will no longer be able to use the Boltzmann and Saha formulas for calculating the numbers of atoms in different states and the Planck formula for computing the radiation intensity at different frequencies. These quantities must be determined in each separate case by a consideration of the elementary processes which occur in real nebulae. We will usually make use of the assumption that nebulae are stationary, i.e., the distribution of atomic states and the radiation field in a nebula do not change with time. In this case, of course, we must know the probabilities of the various elementary processes (i.e., the probabilities of photoionizations, recombinations, collisions, etc.), which are calculated in theoretical physics.

22. Emission Mechanism of Nebulae

1. Observational data. A thorough discussion of the results of observations of gaseous nebulae is contained in the books of B. A. Vorontsov-Vel'yaminov [1], L. Aller [2] and G. A. Gurzadyan [3]. Now we will direct our attention to only basic facts. /284

The gaseous nebulae in our Galaxy are divided into two groups. The so-called planetary nebulae belong to the first group. When observed in a telescope they mostly appear in the form of circular or oval disks, resembling the disks of planets, and also in the form of rings. A hot star, usually called the nucleus of the nebula, is at the center of the planetary nebula. Diffuse nebulae, not having a regular shape, comprise the second group. Stars of the early spectral classes (one or several) are observed in the diffuse nebula itself or near it.

The dimensions of individual planetary nebulae are not known with much accuracy because of parallax uncertainties. The average diameter of a planetary nebula amounts to about 10,000 astronomical units. Diffuse nebulae are often much larger in size.

The spectra of gaseous nebulae consist of individual bright lines on a weak continuous background. The bright lines belong to hydrogen, helium, ionized helium, as well as several other atoms and ions. However, the so-called principal nebular lines N_1 and N_2 with wavelengths of 5006 and 4959 Å, respectively, are most characteristic of the spectra of gaseous nebulae. These lines, previously unknown on Earth, were assigned to the element "nebulium"; however, in 1928 Bowen [4] showed that they are the forbidden lines of doubly ionized oxygen. Many other forbidden lines are also observed in the spectra of gaseous nebulae.

The number of gaseous nebulae known at the present time amounts to a few hundred. The disks of many of the recently discovered planetary nebulae are not visible in a telescope and their nature was deduced from the form of the spectrum. They are either very small or very distant nebulae. The number of known diffuse nebulae has grown considerably as a result of the work of G. A. Shayn and V. F. Gaze [5]. By taking sky photographs in a narrow spectral region, including the H_α line, they observed a large number of weakly luminous diffuse nebulae.

In spite of the fact that the energy emitted by gaseous nebulae is contained predominantly in individual spectral lines, the nebular luminosities are very high. Thus, the average absolute photographic magnitude of planetary nebulae is equal to $M_n = -0.5$. It is important to note that planetary nebulae are, as a /285 rule, considerably brighter than the nuclei themselves, i.e., $M_* - M_n > 0$. Sometimes this difference amounts to seven stellar magnitudes. On the average, however, $M_* - M_n \approx 3$.

The stars, producing the luminosity of gaseous nebulae, belong to the earliest spectral classes. About half the nuclei of planetary nebulae possess type

WR spectra (however, these stars are different from the usual Wolf-Rayet stars of much lower brightness). About one-fourth of the nuclei of planetary nebulae have spectra without any noticeable lines. Calculations show that stars with high surface gravitational forces and high temperatures can exhibit such spectra (see Section 14). The remaining nuclei of planetary nebulae belong to spectral classes O and Of.

Diffuse nebulae shine because of the radiation of stars of spectral classes O, WR and BO, located in the nebula itself or near it. No diffuse nebulae, whose luminosity is caused by stars of spectral classes later than BO, have been observed. This is explained by the fact that the high-frequency radiation of these stars is inadequate to produce an observable nebular luminosity in the visible portion of the spectrum.

As observations show, the material comprising planetary nebulae moves away from the nucleus, i.e., the nebulae are expanding. The nebular expansion velocities are equal to several tens of kilometers per second. Initially, the conclusion about the expansion of planetary nebulae was based on spectral observations. The emission lines in nebular spectra are relatively narrow at the edge of the nebula and broader, or even split, at its center. When an expanding nebula is assumed, this is explained by the fact that at the edge of the nebula the line of sight is passing through that portion of it which is moving with a zero radial velocity, and at the center it passes through regions that are both approaching and receding from us. The latter aspect of the expansion of planetary nebulae was confirmed by a direct comparison of photographs of certain nebulae, obtained at intervals over several decades. This fact served as the basis for the hypothesis concerning the formation of a planetary nebula as the result of an ejection of matter from its nucleus.

2. Cause of nebular emission. As already stated, in gaseous nebulae high-frequency radiation of stars is converted into lower frequency quanta. We must now ascertain what is the cause of this process. In order to do this, let us first consider the properties of the radiation coming from a star at a given point of the nebula.

We will assume that the star radiates as an absolute blackbody of temperature T_*. If the entire sky were completely covered with such stars, the radiation density at a given point of the nebula would be equal to the radiation density in the presence of thermodynamic equilibrium, i.e., it would be expressed by Planck's formula: /286

$$\rho_\nu^* = \frac{8\pi h\nu^3}{c^3}\frac{1}{e^{\frac{h\nu}{kT_*}}-1}. \tag{22.1}$$

In reality, the radiation density in the nebula is much less than ρ_ν^*. We will represent it in the form

$$\rho_\nu = W\rho_\nu^*, \tag{22.2}$$

where W is the so-called radiation dilution (attenuation) factor. It is obvious that

$$W = \frac{\Omega}{4\pi}, \tag{22.3}$$

where Ω is the solid angle subtended at the observer by the star at a given point of the nebula (Fig. 29). Let us denote the star radius by r_* and the distance from the point being considered to the center of the star—by r. Since

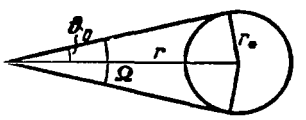

Figure 29.

$$\Omega = 2\pi \int_0^{\vartheta_0} \sin\vartheta \, d\vartheta = 2\pi(1 - \cos\vartheta_0),$$

and $\sin\theta_0 = r_*/r$, then we obtain

$$W = \frac{1}{2}\left[1 - \sqrt{1 - \left(\frac{r_*}{r}\right)^2}\right]. \tag{22.4}$$

At a point on the surface of the star, the radiation comes from a hemisphere. Therefore in this case (i.e., for $r = r_*$) $W = 1/2$.

For points at large distances from the star (i.e., for $r \gg r_*$), from Eq. (22.4) we obtain

$$W = \frac{1}{4}\left(\frac{r_*}{r}\right)^2. \tag{22.5}$$

Let us note that in this case the dilution factor can be represented as the ratio of the area πr_*^2 of the stellar disk to the area of a sphere of radius r, i.e., $4\pi r^2$.

The average radii of planetary nebulae are about 10^{17} cm, and the radii of /287
their nuclei—about 10^{10} cm. Therefore the radiation density in a planetary nebula is attenuated by about a factor of 10^{14} compared with the radiation density at the stellar surface.

After integrating the relation (22.2) over all frequencies and making use of the Stefan-Boltzmann formula for the integrated radiation density in the presence of thermodynamic equilibrium, we obtain the following expression for the integrated radiation density in the nebula

$$\rho = WaT_*^4. \tag{22.6}$$

After representing the quantity ρ in the form $\rho = aT_1^4$, we obtain

$$T_1 = W^{1/4}T_*. \tag{22.7}$$

Since the temperatures of the stars producing the luminosity of nebulae are of the order of several ten thousand degrees and the values of W in nebulae, as we have just determined, are of the order of 10^{-14}, then the values of the temperature T_1, corresponding to the integrated radiation density in nebulae, are only of the order of a few tens of degrees.

Thus, the integrated density of the radiation coming from a star in the nebula is extremely small. On the other hand, as seen from Eq. (22.2), the relative frequency distribution of this radiation is the same as that coming from the star, i.e., it corresponds to a very high temperature T_*. Thus, the radiation coming from a star in the nebula is characterized by an immense discrepancy between the integrated density and the spectral composition.

If radiation, possessing such a property, interacts with matter, then, as is known from thermodynamics, a frequency redistribution of the radiation occurs in the direction of establishing the most probable distribution. In other words, a conversion of higher frequency quanta into lower frequency quanta must occur. This provides a qualitative explanation of the radiation conversion process in gaseous nebulae.

3. Rosseland theorem. Passing on to a consideration of the emission process of nebulae from a quantitative viewpoint, let us first assume that the atoms have only three energy levels (1, 2 and 3). Of the various transitions occurring under the influence of stellar radiation, let us consider the two mutually opposed cyclical processes:

$$\text{I. } 1 \to 3 \to 2 \to 1, \quad \text{II. } 1 \to 2 \to 3 \to 1.$$

The first of these processes is associated with the absorption of one quantum of frequency ν_{13} and with the emission of two quanta of lower frequencies ν_{12} and ν_{23}, and the second—with the absorption of two quanta of frequencies ν_{12} and ν_{23} and the subsequent emission of one quantum of higher frequency ν_{13}. /288

Let us find the number of processes of the first and second kind occurring in a unit volume of the nebula in 1 sec. To do this, we utilize the Einstein transition coefficients A_{ki}, B_{ik} and B_{ki} and we denote the radiation density of frequency ν_{ik} by ρ_{ik}.

If n_1 is the number of atoms in the first state in 1 cm^3, then the number of transitions from the first state into the third, occurring in 1 cm^3 in 1 sec, will be equal to $n_1 B_{13} \rho_{13}$. Transitions (spontaneous and induced) are possible from the third state, both into the first state and into the second. The fraction of transitions into the second state of interest to us is equal to

$$\frac{A_{32} + B_{32}\rho_{23}}{A_{31} + B_{31}\rho_{13} + A_{32} + B_{32}\rho_{23}}.$$

Of the atoms appearing in the second state, a portion jumps backward into the third state, when radiation is absorbed, and a portion jumps into the first state (spontaneously or under the influence of radiation). The ratio of the number of transitions from the second state into the first to the total number of transitions from the second state is equal to

$$\frac{A_{21}+B_{21}\rho_{12}}{B_{23}\rho_{23}+A_{21}+B_{21}\rho_{12}}.$$

Thus, for the number of processes of the first kind we obtain

$$N_{\mathrm{I}}=n_1B_{13}\rho_{13}\frac{A_{32}+B_{32}\rho_{23}}{A_{31}+B_{31}\rho_{13}+A_{32}+B_{32}\rho_{23}}\times$$
$$\times\frac{A_{21}+B_{21}\rho_{12}}{B_{23}\rho_{23}+A_{21}+B_{21}\rho_{12}}. \tag{22.8}$$

The number of processes of the second kind is found in an analogous manner. It is found equal to

$$N_{\mathrm{II}}=n_1B_{12}\rho_{12}\frac{B_{23}\rho_{23}}{A_{21}+B_{21}\rho_{12}+B_{23}\rho_{23}}\times$$
$$\times\frac{A_{31}+B_{31}\rho_{13}}{A_{31}+B_{31}\rho_{13}+A_{32}+B_{32}\rho_{23}}. \tag{22.9}$$

The following formula for the ratio of the number of processes of the second kind to the number of processes of the first kind results from Eqs. (22.8) and (22.9): /289

$$\frac{N_{\mathrm{II}}}{N_{\mathrm{I}}}=\frac{B_{12}\rho_{12}B_{23}\rho_{23}(A_{31}+B_{31}\rho_{13})}{B_{13}\rho_{13}(A_{32}+B_{32}\rho_{23})(A_{21}+B_{21}\rho_{12})}. \tag{22.10}$$

To simplify the formula that has been derived, let us introduce the Einstein ratios:

$$A_{ki}=B_{ik}\frac{g_i}{g_k}\sigma_{ik},\qquad B_{ki}=\frac{g_i}{g_k}B_{ik}, \tag{22.11}$$

where

$$\sigma_{ik}=\frac{8\pi h\nu_{ik}^3}{c^3}, \tag{22.12}$$

and g_i is the statistical weight of the i-th state (see Section 8). Moreover, let us write the quantity ρ_{ik} in the form

$$\rho_{ik}=W\sigma_{ik}\bar{\rho}_{ik}, \tag{22.13}$$

where

$$\bar{\rho}_{ik} = \frac{1}{e^{\frac{h\nu_{ik}}{kT_*}} - 1}. \tag{22.14}$$

As a result, Eq. (22.10) is transformed to

$$\frac{N_{II}}{N_I} = W \frac{\bar{\rho}_{12}\bar{\rho}_{23}(1 + W\bar{\rho}_{13})}{\bar{\rho}_{13}(1 + W\bar{\rho}_{12})(1 + W\bar{\rho}_{23})}. \tag{22.15}$$

When W = 1, Eq. (22.15) gives

$$\frac{N_{II}}{N_I} = \frac{\frac{1}{\bar{\rho}_{13}} + 1}{\left(\frac{1}{\bar{\rho}_{12}} + 1\right)\left(\frac{1}{\bar{\rho}_{23}} + 1\right)} = \frac{e^{\frac{h\nu_{13}}{kT_*}}}{e^{\frac{h\nu_{12}}{kT_*}} \cdot e^{\frac{h\nu_{23}}{kT_*}}}. \tag{22.16}$$

But $\nu_{12} + \nu_{23} = \nu_{13}$. Therefore in the case given $N_{II}/N_I = 1$, just as one should expect.

If $W \ll 1$, then, taking into account that the factor $\bar{\rho}_{12}\bar{\rho}_{23}/\bar{\rho}_{13}$ has a value of about unity, we obtain

$$\frac{N_{II}}{N_I} \approx W. \tag{22.17}$$

Thus, the ratio of the number of processes of the second kind to the number of processes of the first kind turns out to be of the order of W. This result is usually called Rosseland's theorem. /290

In planetary nebulae $W \approx 10^{-14}$. Therefore in the case given the number of processes of the second kind can be completely neglected compared with the number of processes of the first kind. In other words, conversion processes of high-frequency quanta into lower frequency quanta occur in comparably more frequently than the reverse processes.

4. Determination of stellar temperatures from the hydrogen lines. Above, we assumed that a nebula consists of atoms having only three energy levels. Now let us consider the emission of a real nebula consisting of hydrogen atoms.

Because of the extremely small radiation density in nebulae the overwhelming majority of the atoms are in the ground state. Therefore nebulae are opaque to radiation in the Lyman series and perfectly transparent to radiation in the Balmer, Paschen and other subordinate series. Thus, the nebula absorbs stellar energy at frequencies of the Lyman series and instead emits quanta in the subordinate series (and, in particular, in the Balmer series which we observe), which emerge unhindered from the nebula. When the optical thickness of the nebula is sufficiently great beyond the Lyman series limit, it will emit in the hydrogen lines

primarily because of the stellar energy beyond the limit of this series (since the energy absorbed by the nebula in the Lyman lines will be much less).

More precisely, the nebular hydrogen emission process occurs in the following manner. Hydrogen atom ionization, i.e., a proton and free electron are formed, occurs under the influence of stellar radiation beyond the Lyman series limit. After some period of time the free electron is captured by some proton. Let us assume that the capture occurred in one of the high levels. The quantum that thereby appears beyond the limit of the corresponding subordinate series leaves the nebula. Further, there follows a chain of "cascade" electron transitions from level to level. Because of the extremely low radiation and matter density in nebulae, this chain of transitions is not interrupted in the vast majority of cases. The quanta of the subordinate series lines formed during these transitions also leave the nebula. If, however, the electron passed into the first level, then the Lyman line quantum that is produced is absorbed in the nebula and the electron is in the previous level again. Therefore from a given level (only if it is not the second) the electron sooner or later effects a transition that is not into the /291
first level. It is easy to understand that this chain of transitions must be terminated by a transition into the second level with the formation of a Balmer quantum and a subsequent transition from the second level into the first with the formation of an L_α line quantum. The Balmer quantum escapes unhindered from the nebula. The L_α quantum also escapes from the nebula after, however, a prolonged diffusion process.

From what has been said it follows that one Balmer quantum and one L_α-line quantum are necessarily formed from each Lyman continuous quantum absorbed and converted by the nebula (and some number of quanta in the other subordinate series can also be formed).

We will now assume that the optical thickness of the nebula beyond the Lyman series limit is appreciably greater than unity. In this case the nebula will absorb and convert all stellar L_c quanta. In the given case, therefore, the number of L_c quanta emitted by a star will be equal to the number of Balmer quanta emitted by the nebula.

Thus, information about the star beyond the Lyman series limit can be determined from the nebular emission in the Balmer series. By comparing the nebular emission in the Balmer series with the stellar emission in the visible portion of the spectrum, we are, in essence, comparing the stellar emission in two widely separated spectral regions (ultraviolet and visible). Therefore the stellar temperature can be determined from this comparison.

Let us denote the average intensity of the radiation, coming from the star, by I_ν^*. Then the number of quanta, emitted by the star in the frequency interval from ν to $\nu + d\nu$, will be equal to

$$4\pi r_*^2 \frac{\pi I_\nu^*}{h\nu} d\nu,$$

and this means that the total number of L_c quanta emitted by the star will be determined by the formula

$$N_{L_c}^* = 4\pi r_*^2 \int_{\nu_0}^{\infty} \frac{\pi I_\nu}{h\nu} d\nu, \tag{22.18}$$

where ν_0 is the frequency of the Lyman series limit.

On the other hand, the number of Balmer quanta, emitted by the nebula, is equal to

$$N_{Ba} = \sum_{Ba} \frac{E_i}{h\nu_i}, \tag{22.19}$$

where E_i is the total energy emitted by the nebula in the i-th Balmer line, and /292
$h\nu_i$ is the corresponding photon energy. Let us denote by E_i^* the energy emitted by the star in unit frequency interval near the i-th Balmer line, and let us formulate the dimensionless ratio

$$A_i = \frac{E_i}{\nu_i E_i^*}, \tag{22.20}$$

which can be determined from observations. Substituting (22.20) into (22.19) and considering that

$$E_i^* = 4\pi r_*^2 \pi I_{\nu_i}^*, \tag{22.21}$$

we obtain

$$N_{Ba} = 4\pi r_*^2 \sum_{Ba} A_i \frac{\pi I_{\nu_i}^*}{h}. \tag{22.22}$$

In the case when the optical thickness of the negula beyond the Lyman series limit appreciably exceeds unity,

$$N_{Ba} = N_{L_c}^*. \tag{22.23}$$

Therefore, with the aid of Eqs. (22.18) and (22.22) we have

$$\int_{\nu_0}^{\infty} I_\nu^* \frac{d\nu}{\nu} = \sum_{Ba} A_i I_{\nu_i}^*. \tag{22.24}$$

We will assume that the radiation intensity I_ν^* is given by Planck's formula with temperature T_*. Then instead of (22.24) we obtain

$$\int_{\nu_0}^{\infty} \frac{\nu^2 d\nu}{e^{\frac{h\nu}{kT_*}}-1} = \sum_{\text{Ba}} A_i \frac{\nu_i^3}{e^{\frac{h\nu_i}{kT_*}}-1}. \tag{22.25}$$

After making the substitution

$$\frac{h\nu}{kT_*} = x, \quad \frac{h\nu_i}{kT_*} = x_i, \quad \frac{h\nu_0}{kT_*} = x_0, \tag{22.26}$$

we finally obtain

$$\int_{x_0}^{\infty} \frac{x^2 dx}{e^x - 1} = \sum_{\text{Ba}} A_i \frac{x_i^3}{e^{x_i} - 1}. \tag{22.27}$$

The summation on the right side of this formula extends over all lines of the Balmer series and over the Balmer continuum. /293

As already stated, the quantities A_i must be found from observations. Then the stellar temperature T_* can be determined from Eq. (22.27).

The method that has been discussed for determining the temperature of stars was proposed by Zanstra [6]. He also applied this method to a determination of the temperatures of three planetary nebulae nuclei (NGC 6543, 6572, 7009). It was found that the temperatures of these stars are very high (39,000, 40,000 and 55,000° respectively).

In the derivation of Eq. (22.27) it was assumed that all stellar energy in the Lyman continuum is absorbed by the nebula. If this is not so, then instead of Eq. (22.27) we obviously have

$$\int_{x_0}^{\infty} \left[1 - e^{-\tau_0 \left(\frac{x_0}{x}\right)^2} \right] \frac{x^2 dx}{e^x - 1} = \sum_{\text{Ba}} A_i \frac{x_i^3}{e^{x_i} - 1}, \tag{22.28}$$

where τ_0 is the optical thickness of the nebula immediately beyond the Lyman series limit. Here it is taken into consideration that the absorption coefficient of hydrogen is inversely proportional to the frequency cubed. When $\tau_0 = \infty$, Eq. (22.28) passes over to Eq. (22.27). If $\tau_0 \ll 1$ for a given nebula and we still use Eq. (22.27) to determine the stellar temperature, then, as is easily seen, a temperature lower than the true value is obtained.

The determination of the stellar temperature from Eq. (22.28) requires a preliminary determination of the nebular optical thickness τ_0, which is a fairly

difficult problem. Equation (22.28) is sometimes used to determine the quantity τ_0 after a stellar temperature value found by some other method has been assumed.

5. Stellar radiation in the ultraviolet region of the spectrum. The emission of gaseous nebulae in the lines of many atoms (but, as we will see below, not all) occurs in the same fashion as the hydrogen line emission resulting from photoionization and subsequent recombinations. These atoms absorb stellar energy beyond the limits of their principal series and radiate it partially in the visible portion of the spectrum. Thus, in particular, nebulae emit in the lines of hydrogen, helium and ionized helium. We recall that the ionization energies of H, He I and He II are equal to 13.6, 24.6 and 54.4 eV, respectively, whereas the energy of visible quanta is about 2-3 eV. Consequently, the nebular emission in the lines of these atoms occurs because of stellar energy in the far ultraviolet region of the spectrum. /294

From the intensities of the various atomic lines appearing as the result of photoionizations and recombinations, one can determine the star temperature in the same manner as from the hydrogen line intensities. We will assume that the nebula absorbs all stellar photons beyond the principal series limit of the given atom. Then the number of these photons (just as in the case of the hydrogen atom) will be equal to the number of photons emitted by the nebula in the second series. Therefore, for determining the stellar temperature we obtain the following equation, which is an extension of Eq. (22.27):

$$\int_{x_0}^{\infty} \frac{x^2 dx}{e^x - 1} = Q \sum A_i \frac{x_i^3}{e^{x_i} - 1}. \qquad (22.29)$$

Here $x_0 = h\nu_0/kT_*$, and ν_0 is the ionization frequency of the ground state of the atom of interest. The summation on the right side of Eq. (22.29) is taken over the lines of this atom in the visible portion of the spectrum, and the factor Q is the ratio of the number of photons in the second series to the number of photons in the lines observed. For hydrogen Q = 1, if all the Balmer series lines are observed. For other atoms the quantity Q can be evaluated on the basis of theoretical determinations of emission line intensities (see Section 24). It should be noted that a precise knowledge of the quantity Q is not required since a large change in the integral on the left side of Eq. (22.29) corresponds to a small change in temperature.

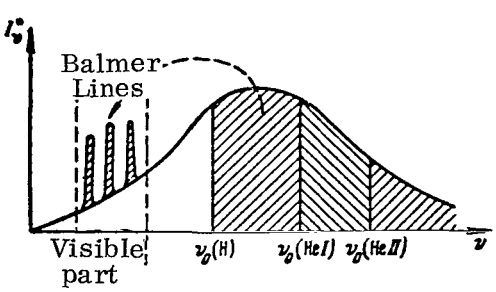

Figure 30.

Stellar temperature determination from the lines of different atoms leads, generally speaking, to different results. For example, for the nucleus of the NGC 7009 nebula a temperature of 55,000° is obtained from the hydrogen lines and 70,000° from the ionized helium lines. In some cases the temperature discrepancy is even greater. /295

To explain such results we must assume that the stellar radiation intensity cannot be represented by Planck's formula with the same temperature in all spectral regions. Moreover, the difference in the temperatures determined from the lines of different atoms can be caused by the incomplete absorption by the nebula of stellar radiation beyond the limits of the principal series of some atoms. In the last case, as explained above, Eq. (22.29) gives reduced temperature values.

In the practical application of the method that has been discussed to stellar temperature determination, considerable difficulty arises in finding the quantities A_i from a comparison of the nebular and stellar spectra. Therefore the possibility of determining T_* from the ratio of the line intensities of any two atoms in the nebular spectrum is of considerable interest. It is obvious that in this case the quantity T_*, in essence, is found from a comparison between the stellar spectral regions beyond the limits of the principal series of these atoms.

This possibility was first employed by V. A. Ambartsumyan, who suggested determining the stellar temperature from the ratio of the intensities of the hydrogen H_β lines and λ 4686 Å of ionized helium in the nebular spectrum. To relate this ratio with the quantity T_*, we can make use of Eq. (22.29), by writing it first for hydrogen and then for ionized helium. In the first case we restrict ourselves to the H_β lines on the right side of Eq. (22.29), and in the second—to the λ 4686 Å line. The corresponding values of Q in both of these cases will be similar since the H and He^+ atoms are similar, and the Einstein probability coefficients for the $4 \rightarrow 2$ and $4 \rightarrow 3$ transitions (by means of which the lines of interest are produced) are almost identical. Therefore, after dividing one of these equations by the other, we obtain (with an accuracy to within a coefficient near unity)

$$\frac{\int_{x_0}^{4x_0} \frac{x^2 dx}{e^x - 1}}{\int_{4x_0}^{\infty} \frac{x^2 dx}{e^x - 1}} = \frac{E_{H_\beta}}{E_{\lambda 4686}} \tag{22.30}$$

where x_0 is the quantity defined by Eq. (22.26) for hydrogen.

The stellar temperatures determined with the aid of Eq. (22.30) are very high. For example, a temperature of 115,000° was obtained for the nucleus of the NGC 7009 nebula. Such high temperature values are apparently explained primarily by the incomplete absorption by the nebula of stellar radiation beyond the Lyman series limit. Such an explanation seems probable because the hydrogen should be highly ionized in nebulae in which the helium is doubly ionized. As a result, the optical thickness of the nebula beyond the Lyman series limit can be less than unity. /296

The lines of other atoms (N III, C IV, etc.), besides those of hydrogen, helium and ionized helium, can be used to determine stellar temperatures from the emission lines in nebular spectra. Instead of temperatures, the number of

photons, emitted by the star beyond the limits of the principal atomic series, can also be determined simply. In this case the possibility of incomplete absorption of such photons by the nebula must be taken into consideration for atoms with low ionization potentials (H, He). Photons beyond the principal series limits of atoms with high ionization potentials are usually completely absorbed by the nebula. Thus, we can find the energy distribution in the far ultraviolet region of the stellar spectrum from the intensities of the emission lines of different atoms in the visible spectrum.

6. Determination of stellar temperatures of "nebular" lines. As already mentioned, the gaseous nebula emission mechanism (photoionizations with subsequent recombinations) considered above is not the only one. Another mechanism, causing emission in the principal lines N_1 and N_2, as well as in other "nebular" lines, is also present in nebulae.

The fact that nebular emission in the N_1 and N_2 lines occurs not as a result of photoionizations is corroborated by the following considerations:

1. If the photons in the N_1 and N_2 lines were to arise because of stellar radiation beyond the principal series limit of doubly ionized oxygen, the stellar temperatures would be extremely high, more than a million degrees in some cases.

2. There are a number of planetary nebulae in whose spectra there are no ionized helium lines, which is explained by the weakness of the radiation of the nucleus beyond the principal series limit of this ion. If the N_1 and N_2 lines were to arise because of photoionizations, then in the case given they also would be absent since the ionization potentials of He^+ and O^{++} are nearly identical. However, the N_1 and N_2 lines are the most intense in the spectra of all planetary nebulae.

In actuality the emission of gaseous nebulae in "nebular" lines is caused /297
by the excitation of atoms through collisions with free electrons. The excitation potentials of states, in transitions from which photons are emitted in the lines being discussed, are very low (for example, 2.5 V for the N_1 and N_2 lines). Therefore there is a large number of free electrons in the nebulae whose energies are sufficient to excite these states. In the final analysis, of course, the emission of nebulae in the "nebular" lines occurs because of the stellar radiation since the free electrons acquire their energy through photoionizations.

The stellar temperatures can be determined from the emission of nebulae in the "nebular" lines, just as they can be determined from the emission in lines having a recombination origin. Appropriate formulas have been derived in the previously cited work of Zanstra [6]. In this the following assumptions were made: 1) most of the free electrons arise through photoionization of hydrogen atoms, 2) all the L_c photons of the star are absorbed by the nebula, 3) all the energy received by the electrons during ionization enters into the excitation of the "nebular" lines.

As is known, when an atom is ionized by radiation of frequency ν, the kinetic energy of the freed electron is equal to

$$\frac{1}{2}mv^2 = h\nu - h\nu_0,$$

where ν_0 is the ionization frequency of the atom (hydrogen in the case given). If the nebula absorbs all stellar radiation beyond the Lyman series limit, then the energy acquired by the free electrons in 1 second will be equal to

$$4\pi r_*^2 \int_{\nu_0}^{\infty} \frac{\pi I_\nu^*}{h\nu}(h\nu - h\nu_0)\,d\nu.$$

On the other hand, the energy emitted by the nebula in the "nebular" lines in 1 second can be represented in the form

$$4\pi r_*^2 \sum_{\text{Neb}} A_i \pi I_{\nu_i}^* \nu_i,$$

where A_i are the quantities defined by Eq. (22.20), and the summation is taken over all "nebular" lines excited by electron impact.

Under the assumptions made, the last two quantities must be equal to each other, i.e., /298

$$\int_{\nu_0}^{\infty} I_\nu^*(\nu - \nu_0)\frac{d\nu}{\nu} = \sum_{\text{Neb}} A_i I_{\nu_i}^* \nu_i. \tag{22.31}$$

Replacing the quantity I_ν^* here by the Planckian intensity, we obtain

$$\int_{\nu_0}^{\infty} \frac{\nu^2(\nu - \nu_0)}{e^{\frac{h\nu}{kT_*}} - 1}\,d\nu = \sum_{\text{Neb}} A_i \frac{\nu_i^4}{e^{\frac{h\nu_i}{kT_*}} - 1}, \tag{22.32}$$

or, using the notations of (22.26)

$$\int_{x_0}^{\infty} \frac{x^2(x - x_0)}{e^x - 1}\,dx = \sum_{\text{Neb}} A_i \frac{x_i^4}{e^{x_i} - 1}. \tag{22.33}$$

Equation (22.33) provides the possibility of determining the stellar temperature T_*, if the quantities A_i for the "nebular" lines are known from observations.

After applying this method to the determination of the temperatures of the nuclei of planetary nebulae, Zanstra obtained a temperature of 39,000°for NGC

6543, 38,000° for NGC 6552 and 50,000° for NGC 7009. We see that these temperature values are very close to the T_* values, found from the hydrogen lines, presented above.

For a crude estimate of stellar temperatures Zanstra used the method discussed in a simplified form. Using Eq. (22.33) and the fact that the N_1 and N_2 lines determine the major portion of the visible luminosity of a nebula, he derived the relationship between the stellar temperature T_* and the difference of the stellar magnitudes of the nucleus and nebula $m_* - m_n$. It is obvious that the greater this difference, the higher the stellar temperature. The temperatures of a large number of nebular nuclei were determined from observed values of the difference $m_* - m_n$. It was found that in some cases these temperatures reach 100,000°. The high stellar temperatures, obtained by this method, are confirmed, as a rule, by other signs, in particular the high intensity of the He II lines in nebular spectra.

The methods presented in this section for determining stellar temperatures are widely used in astrophysics. With the aid of these methods not only are the temperatures of nebular nuclei determined, but also the temperatures of stars with bright lines in their spectra: Be and Wolf-Rayet class stars, novae, etc.

23. Ionization of Atoms

1. Number of recombinations. As explained, atomic ionization due to the effect of the radiation of hot stars occurs in gaseous nebulae. At the same time, reverse processes also occur in the nebulae—capture of free electrons by ions, i.e., atom recombinations. The number of ionizations can be determined with the aid of the continuous spectrum absorption coefficient introduced in Section 5. We will now derive formulas for determining the number of recombinations. /299

Let n^+ and n_e be the number of ions and the number of free electrons in 1 cm^3, respectively, and f(v)dv is the fraction of the electrons with velocities from v to v + dv. Let us denote by $\beta_i(v)$ the effective capture cross section of an electron with velocity v in the i-th level. Then the number of captures of electrons with velocities from v to v + dv, occurring in 1 cm^3 in 1 sec, will be equal to

$$n^+ n_e \beta_i(v) f(v) v dv.$$

Let us represent the total number of recombinations in 1 cm^3 in 1 sec in the i-th level in the form $n_e n^+ C_i(T_e)$, where T_e is the electron gas temperature. It is obvious that

$$C_i(T_e) = \int_0^\infty \beta_i(v) f(v) v\, dv. \qquad (23.1)$$

The quantity $\beta_i(v)$ is related to the continuous spectrum absorption coefficient of atoms in the i-th state. To establish this relationship let us examine

the state of thermodynamic equilibrium. In this case detailed balance occurs, whereby any process is counterbalanced by an opposite process. In particular, the number of ionizations, occurring from the i-th level upon absorption of photons with frequencies from ν to $\nu + d\nu$, must be equal to the number of captures at this level of electrons with velocities from v to v + dv, where

$$h\nu = \frac{1}{2} m v^2 + \chi_i. \tag{23.2}$$

The number of ionizations from the i-th level, upon absorption of photons with frequencies from ν to $\nu + d\nu$, in 1 cm^3 in 1 sec is equal to

$$n_i k_{i\nu} \left(1 - e^{-\frac{h\nu}{kT}}\right) \frac{c\rho_\nu}{h\nu} d\nu,$$

where n_i is the number of atoms in the i-th state, $k_{i\nu}$ is the absorption coefficient /300
calculated for one atom (the expression within the parentheses takes negative absorption into account), ρ_ν is the density of radiation of frequency ν. On the basis of the detailed balance principle we have

$$n_e n^+ \beta_i(v) f(v) v\, dv = n_i k_{i\nu} \left(1 - e^{-\frac{h\nu}{kT}}\right) \frac{c\rho_\nu}{h\nu} d\nu. \tag{23.3}$$

As is known, in the presence of thermodynamic equilibrium the function f(v) is determined by Maxwell's formula, the radiation density ρ_ν—by Plancks' formula, and the atomic state distribution—by the Boltzmann and Saha formulas. From Eq. (23.3), with the aid of the formulas that have been enumerated, we obtain

$$\beta_i(v) = \frac{h^2\nu^2}{c^2 m^2 v^2} \frac{g_i}{g^+} k_{i\nu}, \tag{23.4}$$

where g_i is the statistical weight of the i-th state of a given atom, and g^+ is the statistical weight of the ground state of the ion.

Equation (23.4) also gives the desired relationship between the quantities $\beta_i(v)$ and $k_{i\nu}$. Although thermodynamic equilibrium was assumed in its derivation, it is not always correct (since the quantum absorption and emission probabilities are independent of the atomic state and quantum frequency distributions).

Substituting (23.4) into (23.1), we obtain the following expression for the recombination coefficient:

$$C_i(T_e) = \frac{g_i}{g^+} \frac{h^2}{c^2 m^2} \int_0^\infty \frac{\nu^2}{v} k_{i\nu} f(v)\, dv. \tag{23.5}$$

Here the function f(v) is given by Maxwell's formula for the temperature T_e, i.e.,

$$f(v)=\frac{4\pi m^3}{(2\pi mkT_e)^{3/2}}e^{-\frac{mv^2}{2kT_e}}v^2. \tag{23.6}$$

To compute the quantity $C_i(T_e)$ from Eq. (23.5), the absorption coefficient for the given atom must be known. Let us now find $C_i(T_e)$ for hydrogen. In this /301 case the absorption coefficient $k_{i\nu}$ is given by Eq. (5.6). Substituting (5.6) into (23.5) and also using Eqs. (23.2) and (23.6), we obtain

$$C_i(T_e)=\frac{2^9\pi^5}{(6\pi)^{3/2}}\frac{e^{10}}{m^2\cdot{}^3h^3}\left(\frac{m}{kT}\right)^{3/2}\frac{1}{i^3}e^{\frac{\chi_i}{kT_e}}\mathrm{Ei}\left(\frac{\chi_i}{kT_e}\right), \tag{23.7}$$

where Eix is the integral exponential function.

Equation (23.7) can be rewritten in the form

$$C_i(T_e)=3{,}22\cdot10^{-6}M_i(T_e), \tag{23.8}$$

where

$$M_i(T)=\frac{1}{T^{3/2}i^3}e^{\frac{\chi_i}{kT}}\mathrm{Ei}\left(\frac{\chi_i}{kT}\right). \tag{23.9}$$

Values of the function $M_i(T) \times 10^8$, taken from Cillié's paper [7], are listed in Table 27.

TABLE 27. VALUES OF THE FUNCTION $M_i(T) \times 10^8$

i	T					i	T				
	1000	5000	10000	20000	50 000		1000	5000	10 00	20:00	50000
1	20	8,8	6,0	3,9	2,3	5	3,5	1,1	0,64	0,34	0,13
2	9,8	3,9	2,7	1,6	0,78	6	2,9	0,86	0,46	0,23	0,088
3	6,4	2,5	1,4	0,83	0,37	7	2,3	0,66	0,35	0,17	0,032
4	4,7	1,6	0,94	0,52	0,21	8	1,9	0,52	0,23	0,13	0,046

Commas represent decimal points.

The recombination coefficients for other atoms can be found in an analogous fashion.

2. Degree of ionization in a nebula. In the presence of thermodynamic equilibrium the degree of atomic ionization is determined by Saha's formula. There is no thermodynamic equilibrium in nebulae; therefore we must derive a new ionization formula. To do this, we make use of the fact that nebulae are stationary, i.e., the physical conditions in them do not change with time (a change does occur in reality, but very slowly). More precisely, we will assume that in any volume the number of ionizations is equal to the number of recombinations.

Since atom ionization in nebulae occurs predominantly from the ground state, the number of ionizations completed in 1 cm^3 in 1 sec due to the effect of radiation of frequency in the frequency interval from ν to $\nu + d\nu$ is equal to /302

$$n_1 k_{1\nu} \frac{c\rho_\nu}{h\nu} d\nu.$$

The radiation density ρ_ν in a nebula is determined by Eq. (22.2). Therefore, for the total number of ionizations occurring in a unit volume per unit time we obtain

$$n_1 W \int_{\nu_1}^{\infty} k_{1\nu} \frac{c\rho_\nu}{h\nu} d\nu,$$

where ν_1 is the frequency of ground state ionization.

Recombinations, on the other hand, occur at all levels. Therefore the total number of recombinations occurring in 1 cm^3 per 1 sec will be equal to

$$n_e n^+ \sum_1^{\infty} C_i(T_e).$$

Equating the last two expressions, we have

$$n_1 W \int_{\nu_1}^{\infty} k_{1\nu} \frac{c\rho_\nu}{h\nu} d\nu = n_e n^+ \sum_1^{\infty} C_i(T_e). \tag{23.10}$$

This formula also provides the possibility of determining the degree of atom ionization in a nebula if the quantities $k_{1\nu}$ and $C_i(T_e)$ are known. It can be simplified considerably, however, by making use of the relation (23.5).

First, let us rewrite Eq. (23.10) in the form

$$p n_1 W \int_{\nu_1}^{\infty} k_{1\nu} \frac{c\rho_\nu}{h\nu} d\nu = n_e n^+ C_1(T_e), \tag{23.11}$$

where the fraction of the captures in the first level is denoted by p. Taking Eq. (23.5) into consideration, as well as assuming that the quantity ρ_ν^* is given by Planck's formula with temperature T_*, and the quantity f(v)—by Maxwell's formula with temperature T_e, instead of (23.11) we obtain

$$pn_1W\int_{\nu_1}^{\infty} k_{1\nu}\frac{\nu^2 d\nu}{e^{\frac{h\nu}{kT_*}}-1} = \frac{g_1}{g^+}n_e n^+\frac{mh^3}{2(2\pi mkT_e)^{3/2}}\int_0^{\infty} k_{1\nu}v^2 e^{-\frac{mv^2}{2kT_e}}v\,dv. \qquad (23.12)$$

To order to evaluate the integrals entering into Eq. (23.12), the frequency dependence of $k_{1\nu}$ must be known. This dependence is different for different atoms; however, let us assume that $k_{1\nu} \sim 1/\nu^2$ for all atoms. The error resulting from this is relatively small, and the calculations are greatly simplified. After integration, Eq. (23.12) assumes the form /303

$$\frac{n_e n^+}{n_1} = \frac{g^+}{g_1}pW\sqrt{\frac{T_e}{T_*}}\frac{2(2\pi mkT_*)^{3/2}}{h^3}\ln\left(1-e^{-\frac{h\nu_1}{kT_*}}\right)^{-1} \qquad (23.13)$$

In normally encountered practical cases $h\nu_1/kT_* \gg 1$. Therefore instead of (23.13) we have

$$n_e\frac{n^+}{n_1} = \frac{g^+}{g_1}pW\sqrt{\frac{T_e}{T_*}}\frac{2(2\pi mkT_*)^{3/2}}{h^3}e^{-\frac{h\nu_1}{kT_*}} \qquad (23.14)$$

This is the final form of the formula for ionization in nebulae.

We see that Eq. (23.14) differs from the Saha formula by the presence of the factor $pW\sqrt{T_e/T_*}$ on the right side. This factor is very small for gaseous nebulae. This does not mean, however, that the degree of ionization n^+/n_1 is also small. In fact, the degree of ionization can be extremely high in nebulae since the dilution factor W is compensated by the smallness of the free electron density n_e.

In planetary nebulae, as we know, $W \approx 10^{-14}$, and it will be shown below that $n_e \approx 10^4$ cm^{-3}. In this case Eq. (23.14) shows that for hydrogen the degree of ionization will be greater than unity when $T_* > 20,000°$. In the same situation for helium $n^+/n_1 > 1$ when $T_* > 33,000°$.

3. Ionization in nebulae of large optical thickness. Equation (23.14) is valid only when the optical thickness of the nebula beyond the principal series limit of a given atom is less than unity. In the opposite case stellar radiation absorption must be taken into account, as well as the presence of diffuse nebular radiation occurring from recombinations in the first level.

The absorption of stellar radiation along the path to a given point of the nebula can be taken into account by introducing a factor $e^{-\tau}$ in the right side of Eq. (23.14), where τ is the optical distance from the star beyond the principal series limit, corresponding to some average absorption coefficient. Ionizations due to the diffuse nebular radiation can be taken into account approximately by discarding, on the right side of Eq. (23.10), the terms corresponding to recombinations at the first level (since in nebulae of large optical thickness recombinations at the first level are compensated by ionizations due to the absorption of the diffuse radiation). It is easy to see that in this case the factor p/(1-p) must be introduced on the right side of Eq. (23.14) in place of the factor p. For the hydrogen atom the fraction of captures in the first level is about one-half so that the factor p/ /(1-p) is near unity. We will assume that this factor is approximately equal to unity for other atoms also. Taking into consideration all that has been said, Eq. (23.14) can be rewritten in the following form: /304

$$n_e \frac{n^+}{n_1} = \frac{g^+}{g_1} W \sqrt{\frac{T_e}{T_*}} \frac{2(2\pi mkT_*)^{3/2}}{h^3} e^{-\frac{h\nu_1}{kT_*}} \cdot e^{-\tau}. \tag{23.15}$$

Of interest is the question: how does the degree of ionization n^+/n_1 change with a change in the distance r from the star? To simplify the consideration of this question, let us take a planetary nebula whose thickness is small compared with its radius. In this case the dilution factor in the nebula can be considered to be constant (W = const). Moreover, let us assume that the atom density in the nebula is also constant (n = const).

Our analysis will pertain to hydrogen. In principle, however, the results will be valid for all atoms which produce strong absorption beyond the limits of their principal series in nebulae.

Let us denote the fraction of ionized atoms by x, i.e., let us set

$$n^+ = xn, \qquad n_1 = (1-x)n, \qquad n_e = xn. \tag{23.16}$$

Then instead of Eq. (23.15) we obtain

$$\frac{x^2}{1-x} = \frac{g^+}{g_1} \frac{W}{n} \sqrt{\frac{T_e}{T_*}} \frac{2(2\pi mkT_*)^{3/2}}{h^3} e^{-\frac{h\nu_1}{kT_*}} \cdot e^{-\tau}. \tag{23.17}$$

The optical thickness τ entering into this formula is equal to

$$\tau = nk \int_{r_1}^{r} (1-x)\, dr, \tag{23.18}$$

where k is the average absorption coefficient and r_1 is the radius of the inner boundary of the nebula.

From Eqs. (23.17) and (23.18) it is easy to derive a differential equation relating the quantities x and r. Taking the logarithm and then differentiating Eq. (23.17), we find /305

$$\left(\frac{2}{x}+\frac{1}{1-x}\right)dx=-d\tau. \tag{23.19}$$

From this, with the aid of (23.18), we have

$$\left(\frac{2}{x}+\frac{1}{1-x}\right)\frac{dx}{1-x}=-nk\,dr. \tag{23.20}$$

Integrating Eq. (23.20) yields

$$2\ln\frac{x_0}{1-x_0}\frac{1-x}{x}+\frac{1}{1-x_0}-\frac{1}{1-x}=nk(r-r_1), \tag{23.21}$$

where x_0 is the value of x when $\tau = 0$.

Values of the quantity $nk(r - r_1)$, calculated from Eq. (23.21) for different x values, are listed in Table 28 as an example. Here it is assumed that $1 - x_0 = 0.001$. The values of τ, found from the formula

$$\tau=\ln\left(\frac{x_0}{x}\right)^2\frac{1-x}{1-x_0} \tag{23.22}$$

resulting from (23.17) are the same.

TABLE 28. FRACTION IONIZED ATOMS x AS A FUNCTION OF r AND τ

x	$nk(r-r_1)$	τ
0,999	0	0
0,997	669	1,1
0,990	907	2,3
0,970	963	3,5
0,900	999	4,7
0,700	1009	6,4
0,500	1012	7,6

Commas represent decimal points.

From the formula presented and from the table it is seen that the quantity x remains near unity up to the value of r defined by the formula

$$nk(r-r_1)\approx\frac{1}{1-x_0}, \tag{23.23}$$

after which it decreases rapidly for a relatively small change in r. The values of r given by Eq. (23.23) correspond to τ values of a few units.

The result obtained is completely understandable from physical considerations. When the optical distance τ becomes of the order of unity, a decrease occurs in the degree of ionization, i.e., the number of neutral atoms increases. The increase in the number of neutral atoms leads, in turn, to an increase in the optical distance.

Thus, a nebula can be divided into two regions: an inner region in which which the degree of ionization is high ($n^+/n_1 \gg 1$), and an outer region in which /306

the degree of ionization is low ($n^+/n_1 \ll 1$), with a very sharp boundary between them. The first region emits in the lines of a given atom which appear as a result of photoionizations and recombinations; the second does not emit in these lines. For the hydrogen atom case, the first of these regions is usually called the H II zone, the second—the H I zone (Fig. 31).

If the temperature of the star is sufficiently high to produce a second ionization of a given atom, then the nebula can be divided into three regions. Primarily doubly ionized atoms exist in the first region nearest the star and the emission occurs in the lines of the singly ionized atom. Primarily singly ionized atoms exist in the next region and it emits in the lines of the neutral atom. Only neutral atoms are present in the last region and it does not emit at all in the lines of the given atom that have a recombination origin.

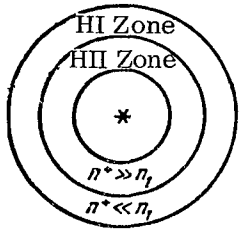

Figure 31.

What we have said means that radiation "stratification" (i.e., layering) must exist in nebulae. This theoretical conclusion is confirmed by observations: the images of planetary nebulae, obtained with the aid of a slitless spectrograph, have a nonuniform magnitude at the different lines. Just as one should expect, the dimensions of the imate are smaller, the higher the atomic ionization potential. For example, the image dimensions of nebulae are considerably smaller in the ionized helium lines than in the neutral helium lines.

4. Energy balance of free electrons. In the derivation of the ionization formula we assumed that the number of free electrons in each elementary volume of the nebula does not change with time. Now we will consider once again the important stationarity equation, expressing the energy conservation law of free electrons. This permits one to derive the relationship between the stellar temperature and the electron temperature of the nebula [8].

We will assume that the free electrons arise from photoionization of hydrogen atoms. Let us denote by ε the average energy acquired by an electron during photoionization. Since the number of ionizations must be equal to the number of recombinations, then the amount of energy acquired by the electrons in 1 cm^3 in /307
I second will be equal to $\sum_1^\infty$.

The free electrons expend their energy by different means. Some portions of their energy is expended in continuous spectrum radiation during recombinations and free-free transitions. Let us denote this portion of the energy by

$$n_e n^+ \left(\sum_1^\infty C_i \varepsilon_i + f \right),$$

where ε_i is the average energy of a free electron, bound in the i-th level. Another portion of the energy of the free electrons, which we will denote by E, is expended in the excitation of radiation in the "nebular" lines (in the foregoing section it was assumed, as an approximation, that all the energy acquired by free electrons through photoionizations goes into this). Finally, the free electrons can expend their energy in the excitation of hydrogen atoms. Although the energy required for the excitation of a hydrogen atom is not large, there are many of these atoms so that the energy loss of free electrons through collisions with them must be taken into consideration. Let us denote by $n_1 n_e D_i$ the number of excitations of the i-th hydrogen level and by $n_1 n_e D_c$—the number of hydrogen atom ionizations occurring in 1 cm^3 in 1 second because of collisions with free electrons. Then the energy lost by the free electrons through these collisions will be equal to

$$n_1 n_e \left(\sum_2^{\infty} D_i h\nu_{1i} + D_c h\nu_{1c} \right)$$

On the basis of the law of energy conservation we have

$$\varepsilon n_e n^+ \sum_1^{\infty} C_i = n_e n^+ \left(\sum_1^{\infty} C_i \varepsilon_i + f \right) + E + \\ + n_1 n_e \left(\sum_2^{\infty} D_i h\nu_{1i} + D_c h\nu_{1c} \right) \tag{23.24}$$

For simplicity we will assume that the temperature is the same throughout the nebula. Then, integrating Eq. (23.24) over the entire volume of the nebula, we obtain /308

$$\bar{\varepsilon} \sum_1^{\infty} C_i \int n_e n^+ dV = \left(\sum_1^{\infty} C_i \varepsilon_i + f \right) \int n_e n^+ dV + \\ + \int E\, dV + \left(\sum_2^{\infty} D_i h\nu_{1i} + D_c h\nu_{1c} \right) \int n_1 n_e\, dV, \tag{23.25}$$

where $\bar{\varepsilon}$ is the energy, acquired by an electron during photoionization, averaged for the entire nebula.

The energy, emitted by the nebula in "nebular" lines, can be expressed in terms of the energy emitted by the nebula in any Balmer line, for example, in the H_β line. Doing this, we have

$$\int E\, dV = \frac{I_{\text{Neb}}}{I_{H_\beta}} A_{k2} h\nu_{2k} \int n_k\, dV, \tag{23.26}$$

where $I_{Neb}/I_{H\beta}$ is the ratio of the intensities of the "nebular" and H_β lines in the spectrum of the nebula. But the quantity n_k, representing the number of hydrogen atoms in the k-th state in 1 cm^3, must be proportional to $n_e n^+$ since filling of the hydrogen atom levels occurs as a result of recombinations. Therefore, introducing the notation $n_k = z_k n_e n^+$ (see following section concerning the definition of the numbers z_k), instead of (23.26) we obtain

$$\int E\,dV = \frac{I_{Neb}}{I_{H_\beta}} A_{i2} h\nu_{2i} z_i \int n_e n^+ dV. \tag{23.27}$$

Substituting (23.27) into (23.25), we obtain

$$\bar{\varepsilon} \sum_1^\infty C_i = \sum_1^\infty C_i \varepsilon_i + f + \frac{I_{Neb}}{I_{H_\beta}} A_{i2} h\nu_{2i} z_i + \frac{\bar{n}_1}{n^+}\left(\sum_2^\infty D_i h\nu_{1i} + D_c h\nu_{1c}\right), \tag{23.28}$$

where

$$\frac{\bar{n}_1}{n^+} = \frac{\int n_1 n_e\,dV}{\int n_e n^+ dV}. \tag{23.29}$$

Equation (23.28) can be discussed for two limiting cases. In the first case let us assume that the optical thickness of the nebula in the Lyman continuum is small ($\tau_0 \ll 1$). Then the ionization of hydrogen atoms will occur primarily due /309
to the effect of radiation coming directly from the star, and the quantity $\bar{\varepsilon}$ will be equal to

$$\bar{\varepsilon} = \frac{\int_{\nu_1}^\infty (h\nu - h\nu_1) \frac{\rho_\nu^*}{h\nu} k_{1\nu}\,d\nu}{\int_{\nu_1}^\infty \frac{\rho_\nu^*}{h\nu} k_{1\nu}\,d\nu}. \tag{23.30}$$

For hydrogen, as is known, $k_{1\nu} \sim 1/\nu^3$. Therefore, representing the quantity $\bar{\varepsilon}$ in the form

$$\bar{\varepsilon} = AkT., \tag{23.31}$$

where k is the Boltzmann constant, for the quantity A we obtain

$$A = \frac{\int\limits_{x_0}^{\infty} \frac{dx}{e^x - 1}}{\int\limits_{x_0}^{\infty} \frac{dx}{x(e^x - 1)}} - x_0, \tag{23.32}$$

where $x_0 = h\nu_1/kT_*$.

In the second case, let us assume that the optical thickness of the nebula beyond the Lyman series is large ($\tau_0 \gg 1$). In this case ionization is caused both by radiation coming directly from the star and by the diffuse radiation of the nebula itself. For large values of τ_0, however, one can assume that all the quanta emitted during electron captures in the first level are absorbed in the nebula, i.e., the number of ionizations occurring due to the effect of the diffuse radiation is equal to $C_1 \int n_e n^+ dV$, and the energy which the electrons acquire is equal to $C_1 \varepsilon_1 \int n_e n^+ dV$. Therefore the diffuse radiation of the nebula can be ignored in the case given. The quantities C_i and $C_i \varepsilon_i$ in Eq. (23.28) need only be summed from 2, and not from 1. For the quantity A we now obtain

$$A = \frac{\int\limits_{x_0}^{\infty} \frac{x^3 dx}{e^x - 1}}{\int\limits_{x_0}^{\infty} \frac{x^2 dx}{e^x - 1}} - x_0. \tag{23.33}$$

The values of the quantity A, calculated from Eqs. (23.32) and (23.33), are listed in Table 29. /310

From this table it is seen that in the assumed interval of stellar temperatures of energy $\bar{\varepsilon}$ in the second case is approximately twice as large as in the first. And since the number of captures in the first level amounts to about one-half of the total number of captures, Eq. (23.28) should give similar results in both cases.

Considering the second of the cases examined (although it is certainly not always achieved in reality), in addition to the equality (23.31) we set

$$\sum_2^{\infty} C_i \varepsilon_i + f = BT_e k \sum_2^{\infty} C_i, \tag{23.34}$$

TABLE 29. VALUES OF THE QUANTITY A

$T_*/1000$	I		II	
	A	$AT_*/1000$	A	$AT_*/1000$
20	0,90	18	1,24	25
40	0,83	33	1,46	58
60	0,77	46	1,63	98
80	0,71	57	1,76	141

Commas represent decimal points.

$$A_{i2}h\nu_{2i}z_i = Ck\sum_2^\infty C_i, \qquad (23.35)$$

$$\sum_2^\infty D_i h\nu_{1i} + D_c h\nu_{1c} = Dk\sum_2^\infty C_i. \qquad (23.36)$$

Then instead of Eq. (23.28) we obtain

$$AT_* = BT_e + C\frac{I_{\text{Neb}}}{I_{\text{H}_\beta}} + D\frac{\bar{n}_1}{n^+}. \qquad (23.37)$$

Equation (23.37) is what we are looking for. It interrelates the stellar temperature T_* and the electron temperature T_e of the nebula. The coefficient A entering into this relation depends only on T_* and is given in Table 29. The coefficients B, C and D depend only on T_e and are listed in Table 30. /311

The electron temperature T_e of the nebula can be found with the aid of Eq. (23.37) if the stellar temperature T_* is known. To do this the quantities $I_{\text{Neb}}/I_{\text{H}\beta}$ and n_1/n^+ must also be known from observations. Since the N_1 and N_2 lines are the brightest in nebular spectra, we have the approximation $I_{\text{Neb}}/I_{\text{H}_\beta} \approx I_{N_1} + N_2/I_{\text{H}_\beta} = 4I_{N_2}/I_{\text{H}_\beta}$. Using Eq. (23.29) and (23.15), we can represent the quantity n_1/n^+ in the form

TABLE 30. COEFFICIENTS B, C AND D

$T_e/1000$	B	$BT_e/1000$	C/1000	D/1000
5	1,02	5	3	0,001
7,5	1,04	8	3	3,0
10	1,06	11	3	$2,5\cdot10^2$
12,5	1,08	14	3	$2,5\cdot10^3$
15	1,10	17	3	$1,6\cdot10^4$

Commas represent decimal points.

$$\frac{\bar{n}_1}{n^+} = \left(\frac{n_1}{n^+}\right)_0\left[\ln\left(\frac{n^+}{n_1}\right)_0 + 1\right], \qquad (23.38)$$

where $(n^+/n_1)_0$ is the degree of ionization, defined by the ionization formula (i.e., Eq. (23.15) for $\tau = 0$). It should be noted that the quantity n_1/n^+ need only be known approximately since the coefficient D changes very rapidly with a change in the electron temperature.

The results of using Eq. (23.37) to determine the electron temperatures of a a number of planetary nebulae are listed in Table 31. The nebula number is given in the first column, the value of T_e in the second, in the next three columns—the free electron energy fractions expended, respectively, in continuous spectrum radiation, in "nebular" line excitation and in inelastic collisions with hydrogen atoms.

TABLE 31. ELECTRON TEMPERATURES OF NEBULAE AND THE TEMPERATURES OF THEIR NUCLEI

No.	T_e	Continuous spectrum	Nebular	Hydrogen	T_* from nebular lines	T_* revised
NGC 7672	14000°	0,10	0,30	0,60	59000	76000
NGC 7009	10000	0,15	0,55	0,30	40000	45000
NGC 6572	13000	0,15	0,40	0,45	40000	48000
NGC 6826	9000	0,25	0,60	0,15	27000	29000
ICII 4593	10000	0,30	0,60	0,10	24000	25000
NGC 6543	11000	0,20	0,30	0,50	33000	41000

Commas represent decimal points.

The assumed values of the temperatures of nebular nuclei, from the "nebular" lines, i.e., from Eq. (22.33), are presented in the next to last column of Table 31. As we recall, in writing down this equation it was assumed that all the energy acquired by free electrons in photoionizations goes to excite the "nebular" lines. In reality, only a fraction of the energy, equal to $CI_{Neb}/AT_*I_{H\beta}$, goes for this purpose. Therefore we can refine the method of determining stellar temperatures from the "nebular" lines by inserting this fraction as a coefficient in the left side of Eq. (22.33). The nuclei temperatures, found after this refinement, are presented in the last column of Table 31. It is easy to see that the refined method of determining stellar temperatures from the "nebular" lines becomes equivalent to the method of determining stellar temperatures from the hydrogen lines. /312

As seen from Table 31, the electron temperatures of the planetary nebulae are much lower than the temperatures of their nuclei. This is explained by the fact that a considerable portion of the energy acquired by the free electrons through photoionizations is expended by them in inelastic collisions with various atoms. Collisions with atoms having low excitation potentials (especially with O^{++} ions) play the major role in the cooling of the electron gas.

The T_e values determined by us represent the average electron temperatures in the H II zones. The T_e values can, however, differ significantly from one portion of the nebula to another. This is caused both by differences in the values of the quantity ε and in the concentrations of these atoms and ions, through collisions with which cooling of the electron gas occurs. As calculations show, the electron temperatures in the H I zone are much lower than in the H II zone.

Other methods of determining the electron temperatures of nebulae (from the ratio of the intensities of forbidden lines) will be discussed in Section 25. The T_e values, found by these methods, turn out to be approximately the same as the values presented in Table 31. If the electron temperature of the nebula is assumed to be known, then the stellar temperature can be determined from Eq. (23.37). It should be emphasized that this temperature will be characterized /313

by the stellar energy in the Lyman continuum itself, and not by its ratio to the energy in the visible portion of the spectrum, like the temperature found by Zanstra's method.

As we will see below (in Chapter VII), a consideration of the energy balance of the free electrons is also used in the study of the interstellar gas (primarily for the determination of the electron temperatures).

24. Excitation of Atoms

1. Excitation through photoionizations and recombinations. The excitation of atoms in nebulae occurs either through photoionizations and subsequent recombinations or through collisions. Let us now consider the first of these mechanisms, applying it, for simplicity, to the hydrogen atom. The role of collisions in the excitation of atoms will be considered later.

A calculation of the degree of atom excitation in nebulae is not too difficult. Under nebular conditions the probabilities of transitions from excited states due to the effect of radiation and collisions are much less than the probabilities of spontaneous transitions (with the exception of transitions from very high levels). Therefore after the photoionization and recombination of the atom, only "cascade" transitions from level to level occur (i.e., a chain of spontaneous transitions from the excited state to the first). The photons in the subordinate series lines, formed through these transitions, leave the nebula unhindered. As a result, the intensities of the emission lines are easily computed after a determination of the level populations.

To determine the number of atoms in the different states we must formulate the steady-state equations expressing the fact that the number of transitions into a given state is equal to the number of transitions from this state.

The number of transitions into the i-th state, occurring in 1 cm^3 in 1 sec, is equal to

$$n_e n^+ C_i(T_e) + \sum_{k=i+1}^{\infty} n_k A_{ki} + n_1 B_{1i} \rho_{1i}.$$

Here the first term represents the number of captures directly into the i-th level, the second—the number of spontaneous transitions from the upper-lying discrete states, the third—the number of transitions from the first state due to the effect of Lyman line radiation.

Practically only spontaneous transitions occur downward from the i-th state. The number of these transitions in 1 cm^3 in 1 sec is equal to /314

$$n_i \sum_{k=1}^{i-1} A_{ik}.$$

Equating the last two expressions, we obtain

$$n_i \sum_{k=1}^{i-1} A_{ik} = n_e n^+ C_i(T_e) + \sum_{k=i+1}^{\infty} n_k A_{ki} + n_1 B_{1i} \rho_{1i} \qquad (i = 2, 3, 4, \ldots). \tag{24.1}$$

The quantity ρ_{1i}, representing the Lyman line radiation density, is not known to us a priori. Let us therefore consider two limiting cases of (24.1).

In case A we will assume that the optical thickness of the nebula in the Lyman lines is very small compared to 1. Then the radiation density ρ_{1i} will also be small. Therefore, neglecting the last term in each of Eqs. (24.1), we find

$$n_i \sum_{k=1}^{i-1} A_{ik} = n_e n^+ C_i(T_e) + \sum_{k=i+1}^{\infty} n_k A_{ki} \qquad (i = 2, 3, 4, \ldots). \tag{24.2}$$

In case B (which is much closer to reality than the foregoing case for the negulae that have been observed) the optical thickness of the nebula in the Lyman lines is assumed to be very large. In this case nearly all the photons emitted through the transition $i \to 1$ are absorbed in the reverse transition, i.e., $n_i A_{i1} = n_1 B_{1i} \rho_{1i}$. Consequently, instead of the system of Eqs. (24.1) we have

$$n_i \sum_{k=2}^{i-1} A_{ik} = n_e n^+ C_i(T_e) + \sum_{k=i+1}^{\infty} n_k A_{ki} \qquad (i = 3, 4, 5, \ldots). \tag{24.3}$$

Thus, in both cases we have come to a system of linear algebraic equations in terms of the numbers $z_i = n_i / n_e n^+$.

The system of Eqs. (24.3) was solved approximately for hydrogen by Cillié [7] who used the first 12 equations ($i = 3, 4, \ldots, 14$) are discarded the rest. The recombination coefficient $C_i(T_e)$ is found from Eq. (23.7). /315

Later Menzel and Becker [9] considered the systems of Eqs. (24.2) and (24.3), after taking a more exact expression for the recombination coefficient (with a Gaunt factor different from unity) and after taking higher levels into consideration. Values of the quantity b_i, defined by the relation

$$n_i = b_i n_e n^+ \frac{i^2 h^3}{(2\pi m k T_e)^{3/2}} e^{\frac{\chi_i}{kT_e}}, \tag{24.4}$$

i.e., showing by what factor the value of $n_i/n_e n^+$ in nebulae differs from the value of $n_i/n_e n^+$ in the thermodynamic equilibrium condition with temperature T_e, are presented in their tables.

Seaton [10] has recently derived more exact solutions of the systems of Eqs. (24.2) and (24.3). The desired quantity z_i was represented in the form

$$z_i = \frac{C_i + \sum_{k=i+1}^{\infty} Q_{ki} C_k}{\sum_{k=k_0}^{i-1} A_{ik}}, \tag{24.5}$$

where $k_0 = 1$ in case A and $k_0 = 2$ in case B, and the quantities Q_{ki} (depending only on the Einstein spontaneous transition coefficients and on the value of k_0) comprise the elements of the "cascade matrix". The quantity Q_{ki} obviously determines the probability of an atom entering level i from level k by any means. The values of the quantity $b_i e^{(\chi_i/kT_e)}$, calculated by Seaton, listed in Table 32.

TABLE 32. VALUES OF THE QUANTITY $b_i e^{(\chi_i/kT_e)}$

i	T_e				i	T_e			
	Case A		Case B			Case A		Case B	
	10 000°	20 000°	10 000°	20 000°		10 000°	20 000°	10 000°	20 000°
2	0,193	0,315	—	—	9	0,360	0,480	0,552	0,730
3	0,213	0,332	0,668	1,013	10	0,376	0,494	0,563	0,735
4	0,244	0,364	0,540	0,792	15	0,434	0,547	0,605	0,756
5	0,273	0,394	0,519	0,739	20	0,472	0,580	0,635	0,772
6	0,299	0,421	0,520	0,725	25	0,499	0,603	0,656	0,785
7	0,322	0,443	0,529	0,722	30	0,520	0,621	0,673	0,795
8	0,341	0,463	0,540	0,725					

Commas represent decimal points.

We see that the quantity b_i does not differ greatly from unity (and for $i \to \infty$, as should be expected, $b_i \to 1$). On this basis some notion can be gathered with respect to the atomic state distribution of the nebula near thermodynamic equilibrium. In reality this is true only with respect to the quantities $n_i/n_e n^+$ (for $i \geq 2$ in case A and for $i \geq 3$ in case B). If, however, the degree of atomic excitation n_i/n_1 is considered, then this quantity is very far from its value in the

presence of thermodynamic equilibrium. In fact, from Eqs. (23.14) and (24.4) we obtain

$$\frac{n_i}{n_1} = pW\frac{T_*}{T} b_i \frac{g_i}{g_1} e^{\frac{\chi_i}{kT_*} - \frac{\chi_1}{kT_*}}, \tag{24.6}$$

Equation (24.6) differs considerably from Boltzmann's formula. The presence of the small factor W on the right side of Eq. (24.6) is especially significant. Because of this the number of excited atoms in the nebula is much less than the number of atoms in the ground state. /316

It should be noted that the system of Eqs. (24.3) [just like (24.2)], determining the populations of the hydrogen atom levels, is not completely exact. The azimuthal degeneracy of the levels, i.e., the presence of a number of states with different azimuthal numbers l in association with the principal quantum number i, was not taken into consideration in writing down this system. In reality instead of the system (24.3) we must write the following system of equations for determining the numbers n_{il}:

$$n_{il}\left[\sum_{k=l}^{i} A_{ilk(l-1)} + \sum_{k=l+2}^{i} A_{ilk(l+1)}\right] =$$

$$= \sum_{k=l}^{\infty} \left[n_{k(l+1)} A_{k(l+1)il} + n_{k(l-1)} A_{k(l-1)il}\right] + n_e n^+ C_{il}(T_e) \tag{24.7}$$

$$(i = 3, 4, 5, \ldots, \; l = 0, 1, 2, \ldots, i-1)$$

Here it is assumed that the only transitions allowed are those for which the number l changes by one. The system of Eqs. (24.7) has been discussed in a number of papers. One of the results obtained is that the replacement of the system (24.3) by the system (24.7) does not lead to significant changes in the numbers of atoms n_i (nor in the emission line intensities). /317

Equations, determining the level populations, can be formulated not only for hydrogen but also for other atoms. However, for other atoms (except hydrogenlike ions) it is very difficult to find the quantities A_{ki} and $C_i(T_e)$. Therefore the level populations in these cases were only computed approximately. Such calculations have been made in the papers of A. A. Nikitin [11] for several atoms (He I, N III, etc.).

2. Intensities of emission lines. Knowing the atomic level populations makes it possible to calculate the emission line intensities. These calculations are greatly facilitated by the complete transparency of nebulae for radiation in the subordinate series lines. The intensities of lines, appearing in nebular spectra as the result of recombinations, depend only on the recombination coefficients $C_i(T_e)$ and the spontaneous transition coefficients A_{ki}. Therefore by comparing

theory with observations one can, in particular, check the correctness of the quantum mechanical calculations of these coefficients. Such a check (of special interest in the case of complex atoms) is possible only in the study of nebulae because of the extreme simplicity of the physical conditions existing in them.

Let us now find the hydrogen emission line intensities. The amount of energy, emitted by the nebula in the line corresponding to the transition $k \rightarrow i$ in 1 sec, is equal to

$$E_{ki} = A_{ki} h\nu_{ik} \int n_k \, dV, \tag{24.8}$$

where the integration is performed over the entire volume of the nebula. Let us represent the number of atoms n_k in the form $n_k = z_k(T_e) n_e n^+$, where the quantity $z_k(T_e)$ is determined from the system of Eqs. (24.2) or (24.3). If it is assumed that the electron temperature does not vary in the nebula, then instead of Eq. (24.8) we have

$$E_{ki} = z_k A_{ki} h\nu_{ik} \int n_e n^+ dV. \tag{24.9}$$

The integral entering into the formula that has been derived is unknown, but it is common to all lines. Therefore Eq. (24.9) provides the possibility of calculating the relative emission line intensities.

In particular, with the aid of Eq. (24.9) the relative intensities of the Balmer lines, i.e., the so-called Balmer decrement, can be found. Expressing the intensities of the Balmer lines in terms of the intensity of the H_β line (as it is usually done), we obtain /318

$$\frac{E_{k2}}{E_{i2}} = \frac{z_k A_{k2} \nu_{2k}}{z_i A_{i2} \nu_{2i}}. \tag{24.10}$$

The theoretical Balmer decrement (calculated by Seaton) is listed in Table 33.

TABLE 33. BALMER DECREMENT

T_e	Case A		Case B		Observed
	10 000°	20 000°	10 000°	20 000°	
H_α	1,91	1,99	2,71	2,79	2,77
H_β	1,00	1,00	1,00	1,00	1,00
H_γ	0,539	0,569	0,506	0,491	0,50
H_δ	0,378	0,356	0,298	0,282	0,26
H_ε	0,253	0,238	0,192	0,178	0,18

Commas represent decimal points.

We see that the theoretical Balmer decrement in each of the cases considered is slightly dependent on the electron temperature and can practically be considered constant. However, the observed Balmer decrement varies markedly from nebula to nebula, and is greater than theory predicts (for example, for many nebulae the ratio of the H_α and H_β line intensities is equal to approximately 5). As has been established, the difference between theory and observations are

explained primarily by the selective absorption of light in space, leading to the reddening of distant objects. As a result, the observed ratio of the H_α and H_β line intensities appears greater than it actually is. After taking account of light absorption, the theory (in case B) and observations agree satisfactorily. This is seen, for example, from Table 33, in the last column of which is listed the observed Balmer decrement with light absorption taken into account (averaged for 17 nebulae).

It is obvious that light absorption in the Galaxy can be determined by comparing the theory and observed line intensities in nebular spectra. In such determinations it is expedient to use data for the Paschen as well as for the Balmer lines.

Besides the relative intensities of hydrogen lines in nebular spectra, at the present time the relative intensities of the lines of some other atoms (in particular, He I and N III) have also been calculated approximately. /319

3. Role of collisions. The free electrons, appearing through the photoionization of atoms, have a fairly high kinetic energy. They can expend this energy in the excitation of atoms through collisions. It is obvious that the lower the atomic excitation potential, the larger the fraction of free electrons that can excite this atom. Therefore atoms having low excitation potentials are excited primarily by electron collisions in nebulae. In particular, the excitation of the "nebular" line emission of nebulae occurs in this fashion. The electron collisions cannot, however, markedly affect the level populations of atoms with high excitation potentials. Let us now consider the question of hydrogen atom excitation by electron collisions (the excitation potentials of which must be considered to be appreciable, although not very high). The collisions leading to the "nebular" line emission of nebulae, will be examined in detail in the following section.

As before, let $n_1 n_e D_i(T_e)$ be the number of excitations and $n_1 n_e D_c(T_e)$ be the number of ionizations from the ground state through collisions in 1 cm^3 in 1 sec. The values of the quantities $D_i(T_e)$ and $D_c(T_e)$ for hydrogen, calculated by Chamberlain [12], are presented in Table 34. For $i > 6$ the quantity D_i is approximately determined by the formula

$$D_i = D_6\left(\frac{6}{i}\right)^{3.20}. \tag{24.11}$$

To determine the numbers of atoms in different states due to collisional excitation, we must formulate the steady-state equations, analogous to Eqs. (24.3). In the case given the number of collisions $n_1 n_e D_i$ must be written instead of the number of recombinations $n_e n^+ C_i$. Therefore instead of Eq. (24.3) we obtain /320

$$n_i \sum_{k=2}^{i-1} A_{ik} = n_1 n_e D_i(T_e) + \sum_{k=i+1}^{\infty} n_k A_{ki} \qquad (i = 3, 4, 5, \ldots). \tag{24.12}$$

By solving Eqs. (24.12) the quantities $n_i/n_1 n_e$, and then the relative emission line intensities, can be determined. Miyamoto, S. A. Kaplan and S. I. Gopasyuk, Chamberlain and others have discussed Eq. (24.12). The Balmer decrement calculated by Chamberlain is listed in Table 35.

TABLE 34. VALUES OF THE QUANTITIES $D_i(T_e)$ AND $D_c(T_e)$ FOR HYDROGEN

T_e	10000°	20000°	40000°
D_2	$231 \cdot 10^{-15}$	$89 \cdot 10^{-12}$	$23{,}2 \cdot 10^{-10}$
D_3	6,32	6,65	3,05
D_4	1,50	1,86	0,92
D_5	0,435	0,69	0,404
D_6	0,201	0,36	0,218
D_c	25,7	5,31	6,25

Commas represent decimal points.

TABLE 35. BALMER DECREMENT FOR COLLISION EXCITATION

T_e	10 000°	20 000°	40 000°
H_α	5,76	4,79	4,06
H_β	1,00	1,00	1,00
H_γ	0,291	0,347	0,383
H_δ	0,136	0,169	0,194
H_ε	0,076	0,097	0,112

Commas represent decimal points.

From a comparison of Tables 33 and 35 it is seen that in the case of collisional atom excitation the Balmer decrement is greater than in the case of excitation by ionizations and recombinations. Because of this it has been suggested that the observed magnitude of the Balmer decrement in the spectra of planetary nebulae is caused not only by light absorption in the Galaxy but also by the effect of collisions on the population of the atomic levels. However, as it is easy to show, this effect cannot be large if the free electrons arise from photoionization of hydrogen atoms. In fact, one Balmer quantum is formed from each L_c photon of the star absorbed by the nebula, whereas by far not every free electron causes a collision leading to the appearance of such a photon. This is explained, first of all, by the fact that for a stellar temperature of the order of several ten thousand degrees the average energy of the freed electron amounts to only a small /32
portion of the excitation energy of the hydrogen levels. Moreover, an appreciable portion of the free electron energy goes into the excitation of the "nebular" line emission of the nebula. Finally, as seen from Table 34, for inelastic collisions of free electrons with hydrogen atoms the major portion of the energy is expended in the excitation of the L_α line, and not in the excitation of the Balmer lines. Thus, it must be recognized that the free electron energy is insufficient to produce by collisions the same Balmer line emission as is caused by recombinations.

4. Masses and densities of nebulae. The hydrogen atom concentration in the nebula can be determined from the hydrogen line emission of the nebula. To do this, Eq. (24.9), determining the energy emitted by the nebula in a given line,

must be used. Applying this formula to the Balmer line, corresponding to the $k \rightarrow 2$ transition, we have

$$E_{k2} = z_k A_{k2} h\nu_{2k} \int n_e n^+ dV. \tag{24.13}$$

Since hydrogen is the most abundant element and it exists predominantly in an ionized state in the luminous portion of the nebula, then one can assume that $n_e = n^+$. Therefore Eq. (24.13) can be rewritten in the form

$$E_{k2} = z_k A_{k2} h\nu_{2k} n^{+2} V, \tag{24.14}$$

where n^+ is the average number of protons in 1 cm^3, and V is the volume of the luminous portion of the nebula. From Eq. (24.14) we obtain

$$n^+ = \sqrt{\frac{E_{k2}}{z_k A_{k2} h\nu_{2k} V}}. \tag{24.15}$$

A calculation of the quantity n^+ in planetary nebulae from Eq. (24.15) leads to values of the order of several thousand. With these values of n^+ the ionization formula gives $n^+/n_1 \approx 10^3$ for the degree of hydrogen atom ionization. Consequently there are several neutral hydrogen atoms in 1 cm^3, on the average.

Knowing the quantity n^+ provides the possibility of determining the mass of the luminous portion of the nebula, which is equal to

$$M = m_H n^+ V, \tag{24.16}$$

where m_H is the mass of a hydrogen atom. Substituting (24.15) into (24.16) we find /322

$$M = m_H \sqrt{\frac{E_{k2} V}{z_k A_{k2} h\nu_{2k}}}. \tag{24.17}$$

The energy emitted by the nebula in a given Balmer line amouts to some fraction δ_{2k} of the visual luminosity L of the nebula, i.e., $E_{k2} = \delta_{2k} L$. Therefore instead of Eqs. (24.15) and (24.17) we have

$$\rho = m_H n^+ = C\sqrt{\frac{L}{V}}, \tag{24.18}$$

$$M = C\sqrt{LV}, \tag{24.19}$$

where

$$C = m_H \sqrt{\frac{\delta_{2k}}{z_k A_{k2} h\nu_{2k}}}. \tag{24.20}$$

For most nebulae one can assume that the visual luminosities are determined primarily by radiation in the N_1 and N_2 lines (nebulae with an intense continuous spectrum, which will be considered in Chapter VII, are an exception). Then, roughly speaking, the quantity δ_{2k} represents the ratio of the intensity of a given line to the intensity of the lines $N_1 + N_2$. For example, in the case when the N_2 line is three times brighter than H_β, the quantity δ_{24} is equal to 1/12. In this case $C = 1.5 \cdot 10^{-12}$. Finally, the quantity δ_{24} varies somewhat for nebula to nebula; however, this has little effect on the value of C since δ_{2k} enters Eq. (24.20) under the square root sign. Therefore in a first approximation the coefficient C can be assumed to be constant for all nebulae of interest.

Equations (24.18) and (24.19) were first derived by V. A. Ambartsymyan [13]. Their application to the determination of planetary nebular masses and densities gave the following results:

$$M \approx 0.01\, M_\odot,$$
$$\rho \approx 10^{-20}\ г/см^3.$$

These values of M and ρ are averages. The masses and densities of individual planetary nebulae can differ from these average values by a factor of ten.

The densities of diffuse gaseous nebulae are, on the average, somewhat less than the densities of planetary nebulae (by about one to two orders of magnitude). The masses of diffuse nebulae lie within a very broad interval—from a small fraction of a solar mass to several thousand times the mass of the Sun. For example, the mass of the "Omega" nebula is about 500 $M_\odot$. /323

It should be emphasized that Eq. (24.19) gives the value of the mass of only that portion of the nebula which emits in the hydrogen lines. This value is the mass of the entire nebula only in the case when the optical thickness of the nebula beyond the Lyman series limit is less than unity.

To determine the densities and masses of nebulae from Eqs. (24.18) and (24.19) the distances from them must be known. However, the distances from planetary nebulae are poorly known so that their densities and masses are determined with some errors. Denoting the distance from the nebula by R, we see from the formulas cited that $\rho \sim R^{-1/2}$ and $M \sim R^{5/2}$. Consequently an error in the distance has a small effect on the density value, but a very large effect on the mass value.

It is interesting to note that the weak dependence of R on M made it possible for I. S. Shklovskiy [14] to use Eq. (24.19) for determining the distances from planetary nebulae under the assumption that their mass is a constant. We obviously have

$$V \sim r^3 \sim R^3\varphi^3$$

and

$$L \sim r^2 I \sim R^2\varphi^2 I,$$

where r is the radius of the nebula, φ is its radius in angular measure, I is the surface brightness of the nebula. Therefore from Eq. (24.19) we obtain

$$R \sim \frac{M^{1/2}}{\varphi I^{1/2}}. \tag{24.21}$$

Using Eq. (24.21), I.S. Shklovskiy assembled a catalog of distances to planetary nebulae. In this the proportionality constant in Eq. (24.21) was determined with the aid of statistical parallaxes. Moreover, as already indicated, the mass M was assumed constant for all nebulae. However, for a nebula the quantity M changes with an increase in the H II zone in proportion to the expansion of the nebula. The quantity M remains constant with time only for nebulae with a small optical thickness in the Lyman continuum. Therefore the catalog cited above refers just to these nebulae.

For some of the nebulae that are nearest to use, it was possible to determine the distances by trigonometric means. These agreed satisfactorily with the distances found from Eq. (24.21). This indicates that the masses of planetary nebulae do not differ from each other by very much. /324

25. Forbidden Lines

1. Necessary conditions for the appearance of forbidden lines. In the spectra of gaseous nebulae there are many forbidden lines, belonging to various atoms and ions: O O, O II, O III, N I, N II, S II, etc. The most intense of these are the principal nebular lines N_1 and N_2 of doubly ionized oxygen (with wavelengths of 5006 and 4959 Å, respectively). Of the other forbidden lines one should mention the 4363 Å line of doubly ionized oxygen, the 3726 abd 3729 Å violet doublet of singly ionized oxygen, the 6548 and 6584 Å red doublet of singly ionized notrogen. The energy level diagrams of these ions are shown in Fig. 32.

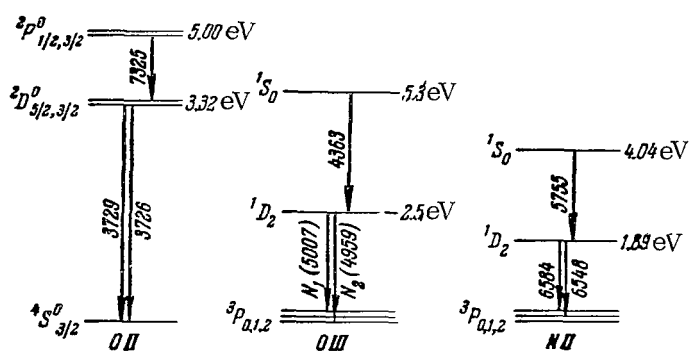

Figure 32.

As is known, "forbidden" lines differ from "allowed" lines by the extreme smallness of the transition probabilities. The Einstein spontaneous transition

probability coefficients of allowed lines are about 10^8 sec^{-1}; for forbidden lines they are a million and billion times smaller. Values of the spontaneous transition coefficients for some of the forbidden lines of the O III, O I and N II ions (calculated by Garstang) are given in Table 36 as an example.

TABLE 36. SPONTANEOUS TRANSITION PROBABILITY COEFFICIENTS FOR SOME FORBIDDEN LINES

Transition	O III		N II		O I	
	λ	A	λ	A	λ	A
$^3P_2—^1D_2$	5006,84	0,021	6583,4	0,0030	6300,23	0,0069
$^3P_1—^1D_2$	4958,91	0,0071	6548,1	0,00103	6363,88	0,0022
$^3P_0—^1D_2$	4931,0	$1,9\cdot10^{-6}$	6527,4	$4,2\cdot10^{-7}$	6392	$1,1\cdot10^{-6}$
$^1D_2—^1S_0$	4363,21	1,6	5754,8	1,08	5577,35	1,28

Commas represent decimal points.

Forbidden lines are not observed in the normal stellar spectra. In the spectra of gaseous nebulae, however, they have intensities comparable to those of the allowed lines. What causes this difference?

As we recall, forbidden lines (belonging, to be sure, to altogether different ions) are present in the spectrum of the solar corona. In discussing the corona (in Section 17) we elucidated the conditions necessary for the appearance of forbidden lines. Similar conditions obviously also must exist in gaseous nebulae. /325

As has been established, intense forbidden lines can arise from metastable states only, i.e., from those states for which there are no other transitions downward except forbidden (in the opposite case allowed transtions occur much more frequently than forbidden). But the lifetime of an atom in a metastable state is very long (for example, it is 38 seconds for the O^{++} ion in the $^1D_2$ state from which the N_1 and N_2 lines emanate). Consequently for a spontaneous transition from a metastable state to occur, the atom must not be subject to any disturbances for a long period of time: neither an interaction with radiation, nor collisions. This means that a low radiation density and a low density of matter are required for the appearance of forbidden lines.

The absence of forbidden lines in stellar spectra indicates that these conditions are not fulfilled in stellar atmospheres. On the other hand, on the basis of the presence of numerous and very intense forbidden lines in the spectra of gaseous nebulae one can conclude that the radiation and matter densities in these objects are extremely low.

The conditions necessary for the appearance of forbidden lines can be expressed in the form of certain inequalities. To derive these let us consider an atom having three energy levels. Here we will assume that a transition from the /326

second state to the first is forbidden (i.e., the second state is metastable), and transitions from the third state downward are allowed. In this case $A_{21} \ll A_{31}$, A_{32}.

Atom excitation can occur both because of the effect of radiation and also by means of collisions. The number of second level excitations will obviously be of the same order as the number of third level excitations. Consequently the forbidden line will be comparable in intensity to that of the allowed lines if primarily spontaneous transitions will occur from the second state.

The number of spontaneous transitions from the second state in 1 cm^3 in 1 sec is equal to n_2A_{21}. In addition to these, transitions from the second state can also occur due to the effect of radiation; of these, in a given case the upward transitions will be much more frequent than the downward (since the B_{ik} coefficients are proportional to the A_{ki} coefficients). The number of $2 \rightarrow 3$ transitions due to the absorption of radiation is equal to $n_2B_{23}\rho_{23}$. Consequently, in order that emission by spontaneous transitions from the metastable state not be hindered, the condition

$$A_{21} \gg B_{23}\rho_{23}. \tag{25.1}$$

must be satisfied. Let us represent the radiation density in the form $\rho_{23} = W\rho_{23}^*$, where ρ_{23}^* is the radiation density in the stellar atmosphere and W is the radiation dilution factor. Then instead of the inequality (25.1) we obtain

$$A_{21} \gg WB_{23}\rho_{23}^*. \tag{25.2}$$

Transitions through collisions with free electrons are also possible from the second state. Let us denote the number of collisions of the first kind in 1 cm^3 in 1 sec by n_2b_{23}, and the number of collisions of the second kind—by n_2a_{21}. Since collisions of the first kind can be caused only by those electrons whose energy exceeds the atomic excitation energy $h\nu_{23}$, and collisions of the second kind—by electrons with any energy, then usually $a_{21} \gg b_{23}$. Thus, in order that collisions not prevent the emission of forbidden line photons, the inequality

$$A_{21} \gg a_{21}. \tag{25.3}$$

must be satisfied. The quantity a_{21} can be represented in the form $a_{21} = n_e\sigma_{21}v$, where n_e is the free electron density, σ_{21} is the average effective cross section for collisions of the second kind, v is the average free electron velocity. Therefore instead of (25.3) we have

$$A_{21} \gg n_e\sigma_{21}v. \tag{25.4}$$

The inequalities (25.2) and (25.4) express the conditions necessary for the appearance of forbidden lines, comparable in intensity to the allowed lines. /327

The quantities W and n_e are extremely small in gaseous nebulae. Because of this, the inequalities (25.2) and (25.4) are satisfied even for lines with very small values of A_{21}, i.e., forbidden by very strong selection rules.

From the presence of forbidden lines in the nebular spectrum one can evaluate the upper limits of the quantities W and n_e with the aid of the inequalities that have been presented. For example, on the basis of Table 36 we have $A_{21} = 0.028$ sec^{-1} for the N_1 and N_2 lines. Furthermore, for a rough estimate one can assume: $\sigma_{21} \approx 10^{-16}$ cm^2, $v \approx 10^8$ cm/sec. Therefore from the inequality (25.4) we find that $n_e \ll 10^6$ cm^{-3} in a nebula. The N_1 and N_2 lines will, of course, be visible even for $n_e \approx 10^6$ cm^{-3}, but in this case the population of the second level will already be reduced by collisions of the second kind. When $n_e \gg 10^6$ cm^{-3}, collisions of the second kind will "quench" these lines.

As we have seen, the conditions in nebulae are such that the atoms entering the metastable state can exist in it for a very long time (until a spontaneous downward transition). Therefore an enormous number of atoms must be stored in the metastable states. This process must obviously occur not only in nebulae but also in other objects with small values of the quantities W and n_e.

Let us emphasize that intense forbidden lines are emitted only because of the accumulation of atoms in metastable states since the line intensity is proportional to the number of atoms in the initial state and the probability of the corresponding spontaneous transition, and the probabilities of spontaneous transitions from the metastable states are very small.

Moreover, the accumulation of atoms in metastable states can lead to the appearance of absorption lines for which these states are the lower levels. The λ 3889 Å absorption line, having the metastable 2^3S helium state as the lower level, can serve as an example. In particular, this line is observed in the spectrum of the ϑ_1 Orion star in the Orion nebula.

The question of the conditions necessary for the appearance of forbidden lines and of the accumulation of atoms in metastable states has been examined in detail by V. A. Ambartsumyan [15]. This question is encountered not only in the study of gaseous nebulae but also of other objects: nova envelopes, comets, etc.

2. Collision probabilities. Most of the forbidden lines in the spectra of gaseous nebulae appear because of the excitation of atoms by an electron collision. Therefore for all the calculations associated with forbidden line emission /328
of nebulae it is necessary to know the probabilities of inelastic collisions of atoms with free electrons.

Let us consider atomic transitions between states i and j due to the effect of electron collisions. We will denote the number of collisions of the first kind in 1 cm^3 in 1 sec by $n_i b_{ij}$. For such collisions atomic transitions occur from the lower state i to the upper state j because of the electron energy. Let us denote the number of collisions of the second kind in 1 cm^3 in 1 sec by $n_j a_{ji}$. For such collisions the opposite transitions occur, with the excitation energy of the atom being transferred to the electron.

The quantities b_{ij} and a_{ji}, characterizing the probabilities of inelastic collisions, are interrelated by a simple expression. To derive this relationship we will consider the thermodynamic equilibrium condition. In this case, on the basis of the principle of detailed equilibrium, we have

$$n_i b_{ij} = n_j a_{ji}. \tag{25.5}$$

But in the presence of thermodynamic equilibrium the distribution of atomic states is given by the Boltzmann formula. Therefore from (25.5) we obtain

$$b_{ij} = a_{ji} \frac{g_j}{g_i} e^{-\frac{h\nu_{ij}}{kT}}. \tag{25.6}$$

Obviously the relationship that has been derived is valid in all cases when the electron velocity distribution is Maxwellian for the temperature T.

The quantity a_{ji} is very slightly dependent on the electron gas temperature since collisions of the second kind can be caused by electrons with any velocity (in this case the electron does not lose energy, but acquires it). On the other hand, the quantity b_{ij} is very strongly temperature dependent, with b_{ij} being greater, the greater T. This is caused by the fact that collisions of the first kind can be caused only by those electrons whose energy is greater than the atomic excitation energy. In Eq. (25.6) the temperature dependence of b_{ij} is given primarily by the exponential term.

The quantities a_{ji} and b_{ij} are expressed in terms of the effective cross sections for the collisions of atoms with electrons. Let $\sigma_{ij}(v)$ be the effective cross section for a collision of the first kind between an atom and a free electron with a velocity v, and $n_e f(v)dv$—the number of electrons with velocities from f to v + dv in 1 cm^3. Obviously we have

$$b_{ij} = n_e \int_{v_0}^{\infty} \sigma_{ij}(v) v f(v) dv, \tag{25.7}$$

where $mv_0^2/2 = h\nu_{ij}$. Analogously, for the quantity a_{ji} we obtain /329

$$a_{ji} = n_e \int_0^\infty \sigma_{ji}(v) v f(v) dv. \tag{25.8}$$

On the basis of quantum mechanical calculations one can assume that in the case of the metastable states the effective collision cross sections are inversely proportional to the electron energy. Therefore the quantity $\sigma_{ij}(v)$ can be represented in the form

$$\sigma_{ij}(v) = \frac{h^2}{4\pi m^2} \frac{\Omega(i,j)}{g_i v^2}, \tag{25.9}$$

whre $\Omega(i, j)$ is the dimensionless effective cross section (of the order of unity). The quantity $\sigma_{ji}(v)$ is given by an analogous formula with g_i replaced by g_j.

Substituting (25.9) into (25.7) and using the Maxwellian expression (23.6) for the function f(v), we obtain

$$b_{ij} = n_e \frac{h^2}{2\pi m^2} \left(\frac{m}{2\pi k T_e} \right)^{1/2} \frac{\Omega(i,j)}{g_i} e^{-\frac{h\nu_{ij}}{kT_e}} = \\ = 8.54 \cdot 10^{-6} \frac{n_e}{\sqrt{T_e}} \frac{\Omega(i,j)}{g_i} e^{-\frac{h\nu_{ij}}{kT_e}} \tag{25.10}$$

For the quantity a_{ji} we find

$$a_{ji} = 8.54 \cdot 10^{-6} \frac{n_e}{\sqrt{T_e}} \frac{\Omega(i,j)}{g_j}. \tag{25.11}$$

The values of the quantities $\Omega(i, j)$ for several ions have been calculated by Seaton. A portion of his results are presented in Table 37.

The values of the quantities $\Omega(i, j)$ that have been calculated obviously differ by no more than 40% from the exact values, the estimates (numbers in parentheses)—by no more than a factor of two.

3. Intensities of forbidden lines. If the probabilities of the collisions giving rise to the metastable states are known along with the Einstein probability coefficients for spontaneous transitions from these states, then we can easily calculate the intensities of the forbidden lines. Such calculations are greatly simplified because of the complete transparency of nebulae for radiation in the forbidden lines, caused by the extreme smallness of the atomic absorption coefficient in these lines.

The populations of the energy levels must be found to determine the line intensities. We will now limit our consideration to only the three lowest atomic levels. As seen from Fig. 32, this is entirely adequate in the cases of most interest. /330

Taking into consideration the transitions due to the effect of collisions and the spontaneous transitions, we obtain the following steady-state equations for the second and third atomic states:

$$\begin{aligned} n_2(A_{21} + a_{21} + b_{23}) &= n_1 b_{12} + n_3(A_{32} + a_{32}), \\ n_3(A_{31} + A_{32} + a_{31} + a_{32}) &= n_1 b_{13} + n_2 b_{23}. \end{aligned} \tag{25.12}$$

Solving these equations with respect to the quantities n_2 and n_3, we find

$$n_2 = n_1 \frac{(A_{31} + A_{32} + a_{31} + a_{32}) b_{12} + (A_{32} + a_{32}) b_{13}}{(A_{31} + A_{32} + a_{31} + a_{32})(A_{21} + a_{21}) + (A_{31} + a_{31}) b_{23}}, \tag{25.13}$$

$$n_3 = n_1 \frac{b_{13}(A_{21} + a_{21} + b_{23}) + b_{12} b_{23}}{(A_{31} + A_{32} + a_{31} + a_{32})(A_{21} + a_{21}) + (A_{31} + a_{31}) b_{23}}. \tag{25.14}$$

Equations (25.13) and (25.14) are valid for any free electron density n_e, upon which the quantities a_{ji} and b_{ij} are dependent. In the two limiting cases—for large and small values of n_e—these formulas are greatly simplified.

For large values of n_e we can disregard the spontaneous transitions in comparison with transitions due to collisional effects. It is easy to see that in this case, as should be expected, a Boltzmann distribution of atomic states is obtained. For example, from Eq. (25.13), when Eq. (25.6) is used, we obtain /331

$$n_2 = n_1 \frac{(a_{31} + a_{32}) b_{12} + a_{32} b_{13}}{(a_{31} + a_{32}) a_{21} + a_{31} b_{23}} = n_1 \frac{g_2}{g_1} e^{-\frac{h\nu_{12}}{kT_e}}. \tag{25.15}$$

For small n_e values we can disregard all transitions from excited states due to collision effects in comparison with spontaneous transitions. In the case given Eqs. (25.13) and (25.14) assume the form

$$n_2 = \frac{n_1}{A_{21}} \left(b_{12} + \frac{A_{32}}{A_{31} + A_{32}} b_{13} \right), \tag{25.16}$$

$$n_3 = \frac{n_1 b_{13}}{A_{31} + A_{32}}. \tag{25.17}$$

In gaseous nebulae (with some exceptions) the second of these cases occurs, i.e., the populations of the metastable states are determined by Eqs. (25.16) and (25.17).

With the aid of the expressions derived for the level populations, we can determine the forbidden line intensities. Let us find, for example, the ratio of the intensities of the lines arising from the 2 → 1 and 3 → 2 transitions. Using Eqs. (25.13) and (25.14), we obtain

$$\frac{E_{21}}{E_{32}} = \frac{n_2 A_{21} \nu_{12}}{n_3 A_{32} \nu_{23}} = \frac{\nu_{12} A_{21}}{\nu_{23} A_{32}} \frac{(A_{31} + A_{32} + a_{31} + a_{32}) b_{12} + (A_{32} + a_{32}) b_{13}}{b_{13}(A_{21} + a_{21} + b_{23}) + b_{12} b_{23}}. \tag{25.18}$$

For high free electron densities it follows from this formula that

$$\frac{E_{21}}{E_{32}} = \frac{\nu_{12} A_{21}}{\nu_{23} A_{32}} \frac{g_2}{g_3} e^{\frac{h\nu_{23}}{kT_e}}. \tag{25.19}$$

For small n_e values Eq. (25.18) gives

$$\frac{E_{21}}{E_{32}} = \frac{\nu_{12}}{\nu_{23}} \left[\left(\frac{A_{31}}{A_{32}} + 1 \right) \frac{b_{12}}{b_{13}} + 1 \right]. \tag{25.20}$$

The formulas that have been found for the forbidden line intensities will be applied later not only to gaseous nebulae but also to the envelopes of novae. /332

As already stated, for small n_e values (and at the same time for small values of W) a heavy buildup of atoms in metastable states occurs. This is well evident from Eqs. (25.16) and (25.17), according to which the population of an excited level is greater, the lower the probability of spontaneous transitions from it. If we were to consider the downward transition from the second state to be forbidden, and transitions from the third state allowed, then the number of atoms in the second state would be much greater than in the third. In other words, the population of the metastable level appreciably exceeds the population of the normal level. The forbidden line intensity, then as seen from Eq. (25.20), is about of the same order as the allowed line intensity.

TABLE 37. EFFECTIVE COLLISION CROSS SECTIONS

Configuration	Ion	Ω (1,2)	Ω (1,3)	Ω (2,3)
$2p^2$	NII	2,39	0,223	0,46
	OIII	1,73	0,195	0,61
	FIV	(1,21)	(0,172)	(0,58)
	NeV	(0,84)	(0,157)	0,53
$2p^3$	OII	1,44	0,218	1,92
	FIII	(1,00)	(0,221)	(3,11)
	NeIV	(0,68)	(0,234)	(3,51)
	NaV	0,43	(0,255)	(3,49)
$2p^4$	FII	(0,95)	(0,057)	0,17
	NeIII	0,76	0,077	0,27
	NaIV	(0,61)	(0,092)	(0,30)
	MgV	0,54	(0,112)	(0,30)

Commas represent decimal points.

4. Electron temperatures and densities. The forbidden line intensity of any atom in the nebular spectrum depends on the number of these atoms, on the free electron density and on the electron gas temperature. Therefore the values of these quantities can be determined from observations of the forbidden line intensities in the nebular spectrum.

A method based on the measurement of the relative intensities of the forbidden lines of the O III ion is widely used to determine the electron temperature of a nebula. This ion has two metastable states, transitions from which give rise to the lines λ 4363 Å and $N_1 + N_2$ (see Fig. 32). These states are excited by electron collisions. Since the electron must have a higher energy to excite emission in the λ 4363 Å line than to excite emission in the N_1 and N_2 lines, the ratio of the intensities of these lines (i.e., the quantity $E_{\lambda\,4363}/E_{N_1+N_2}$) must increase with an increase in T_e.

The formulas derived above for the metastable state populations and for the forbidden line intensities can be applied directly to the O III ion. Let us call the three bottom states of this ion (the ground and two metastable states) states 1, 2 and 3. If it is assumed that the free electron density in the nebula is small, then the ratio of the intensities of the $N_1 + N_2$ and λ 4363 Å lines will be determined by Eq. (25.20).

Let us now convert from the quantities b_{ij} to the quantities a_{ji} with the aid of relation (25.6). This allows us to express the temperature dependence of the ratio of the intensities of the $N_1 + N_2$ and λ 4363 Å lines since the quantities a_{ji} are nearly independent of T_e. After completing this conversion, we find /333

$$\frac{E_{N_1+N_2}}{E_{\lambda\,4363}} = \frac{\nu_{12}}{\nu_{32}}\left[\left(\frac{A_{31}}{A_{32}}+1\right)\frac{g_2 a_{21}}{g_3 a_{31}}e^{\frac{h\nu_{21}}{kT_e}}+1\right]. \qquad (25.21)$$

Equation (25.21) was first derived by V. A. Ambartsumyan [13]. Since the effective collision cross sections were unknown then, he assumed $g_2a_{21}/g_3a_{31} \approx 1$. Now on the basis of Eq. (25.11) and Table 37 we obtain $g_2a_{21}/g_3a_{31} = \Omega(1, 2)/\Omega(1, 3) = 8.9$. Also taking into account that in the given case $A_{31}/A_{32} = 0.14$, instead of (25.21) we have

$$\frac{E_{N_1+N_2}}{E_{\lambda\,4363}} = 8.74e^{\frac{33000}{T_e}}. \qquad (25.22)$$

This formula also provides the possibility of determining T_e from the ratio of the intensities of the $N_1 + N_2$ and λ 4363 Å lines obtained from observations.

The method that has been discussed for determining electron temperatures of nebulae was employed in the works of Menzel and co-workers [9] and Seaton [16]. They obtained T_e values in the interval from 7000 to 25,000° for a large number of nebulae. These values differ little from those which were found by considering the free electron energy balance (see Section 23).

If the electron density in the nebula is not low, then collisions of the second kind affect the population of the metastable levels. In this case the ratio of the intensities of the $N_1 + N_2$ and λ 4363 Å lines will be determined by Eq. (25.18). Using Eqs. (25.10) and (25.11), and also Tables 36 and 37, instead of Eq. (25.18) we obtain the approximation

$$\frac{E_{N_1+N_2}}{E_{\lambda 4363}} = 0.0753 e^{\frac{33000}{T_e}} \frac{1 + 2.67 \cdot 10^5 \frac{\sqrt{T_e}}{n_e}}{1 + 2300 \frac{\sqrt{T_e}}{n_e}}. \tag{25.23}$$

Just as should be expected, for low electron densities (approximately for $n_e < 10^5$ cm^{-3}, if T_e is about 10^4 degrees) Eq. (25.23) converts into Eq. (25.22). With an increase in n_e the role of collisions of the second kind increases and the ratio of the intensities of the lines becomes dependent not only on T_e but also on n_e. For large n_e values (approximately for $n_e > 10^7$ cm^{-3}), however, the ratio of the line /334
intensities again depends only on T_e and is defined by the formula

$$\frac{E_{N_1+N_2}}{E_{\lambda 4363}} = 0.0753 e^{\frac{33000}{T_e}}. \tag{25.24}$$

This formula can also be derived directly from Eq. (25.19) when the numerical values of the parameters are substituted into it. In the case given the transitions due to collision effects occur more frequently than spontaneous transitions and the distribution of atomic levels is Boltzmann.

Other ions besides the O III ion can be used to determine the electron temperature of a nebula from the ratio of the forbidden line intensities. Among these, in particular, is the N II ion, having two metastable states from which the λ 5755 Å line and the λ 6548 and λ 6584 Å doublet are emitted. Applying Eq. (25.18) to the N II ion, we obtain

$$\frac{E_{\lambda 6560}}{E_{\lambda 5755}} = 0.0162 e^{\frac{25000}{T_e}} \frac{1 + 1.94 \cdot 10^5 \frac{\sqrt{T_e}}{n_e}}{1 + 320 \frac{\sqrt{T_e}}{n_e}} \tag{25.25}$$

For small and large n_e values the temperature T_e can be found without knowing n_e with the aid of this formula.

In the case of intermediate n_e values (when collisions of the second kind affect the population of the metastable levels, but a Boltzmann distribution of atomic levels was still not established) the ratio of forbidden line intensities depends not only on T_e but also on n_e. In this case one can attempt to determine both the electron temperature and the electron density through the simultaneous use of Eqs. (25.23) and (25.25). Seaton [16] has made such determinations. However, this method of finding T_e and n_e can be used only infrequently since in most nebulae the electron density is low (as was explained in Section 24, $n_e \approx 10^3$-10^4 cm^{-3}).

It is more convenient to determine the electron density in nebulae from the ratio of the intensities of the λ 3276 and λ 3729 Å lines, belonging to the O II ion. If the initial levels of these lines are considered to be states 2 and 3, then the ratio of line intensities will be given by a formula analogous to Eq. (25.18) (with $\nu_{23}A_{32}$ replaced by $\nu_{13}A_{31}$). Upon substitution of the numerical values of the parameters into this formula we obtain /335

$$\frac{E_{\lambda\,3729}}{E_{\lambda\,3726}} = 0.35\,\frac{1+43\dfrac{\sqrt{T_e}}{n_e}}{1+10\dfrac{\sqrt{T_e}}{n_e}}. \qquad (25.26)$$

We see that the exponential term containing the temperature, which is characteristic of Eqs. (25.23) and (25.25), does not enter into Eq. (25.26). This is explained by the close proximity of states 2 and 3 to each other so that $h\nu_{23} \ll kT_e$. With the aid of Eq. (25.26) the electron density can be determined without precise knowledge of the electron temperature. However, Eq. (25.26) is valid only for relatively low temperatures. At higher temperatures it is also necessary to take account of the next two higher levels, i.e., to consider an atom having five energy levels. Seaton and Osterbrock [17] made a determination of electron densities by this method.

It is interesting to note that the electron density, obtained from the ratio of forbidden line intensities, is independent of the distance from the nebula. At the same time the electron density, determined from the Balmer line intensities, i.e., from Eq. (24.15), does depend on this distance. Therefore there is the possibility of finding the distance from the nebula by comparing the electron densities determined by the methods cited. While this method does not give accurate results, it can evidently be refined.

5. Chemical composition of nebulae. From the ratio of the intensities of the lines in a nebular spectrum, belonging to different atoms, one can determine the relative abundance of these atoms in the nebula. Such determinations can be

accomplished both from lines appearing as the result of collisions, and also from lines having a recombination origin.

Let E_{21} be the amount of energy emitted by a nebula in 1 sec in the forbidden lines corresponding to the $2 \rightarrow 1$ transition of the given atom. This quantity can be represented in the form

$$E_{21} = n_2 A_{21} h\nu_{12} V, \tag{25.27}$$

where n_2 is the number of atoms in the second state in 1 cm^3 and V is the volume of the nebula radiating in the line being considered (as we know from Section 23, the atoms in different stages of ionization are in different zones of the nebula).

If the nebula density is low, then the number of atoms n_2 is determined by Eq. (25.16). The first term in parentheses in this formula corresponds to collisions exciting the second level directly, and the second term—to collisions, exciting the third level, and to subsequent transitions of the atom into the second level. The second term is usually considerably smaller than the first. Therefore instead of Eq. (25.27) we obtain (approximately) /336

$$E_{21} = n_1 b_{12} h\nu_{12} V. \tag{25.28}$$

A similar formula can be written for any other atom. From these formulas we have

$$\frac{E_{21}}{E_{21}'} = \frac{n_1 b_{12} \nu_{12} V}{n_1' b_{12}' \nu_{12}' V'}, \tag{25.29}$$

where the primes denote quantities belonging to the second atom. From observations one can find the ratio of line intensities E_{21}/E_{21}' and the ratio V/V' of the volumes emitting in these lines. Therefore Eq. (25.29) makes it possible for one to determine the quantity n_1/n_1', representing the ratio of the densities of the atoms being considered. It is obvious that the probabilities of exciting collisions (and for more precise calculations with the use of Eq. (25.16)—the spontaneous transition probabilities) must be found beforehand theoretically for such determinations.

The emission of nebulae in lines arising as the result of photoionizations and recombinations was discussed in Section 24. On the basis of Eq. (24.9), the amount of energy, emitted by the nebula in 1 sec in the hydrogen Balmer lines, can be written in the form

$$E_{k2} = z_k A_{k2} h\nu_{2k} n_e n^+ V_H, \tag{25.30}$$

where z_k are quantities determined by the system of Eqs. (24.3), and V_H is the volume of the nebula, emitting in the Balmer lines. Similar formulas can also be written down for other atoms whose lines originate in an analogous fashion.

With the aid of these formulas, just as before, the relative atom densities can be found. In order to do this one must know the probabilities of spontaneous transitions and recombinations.

It should be noted that the concentration of atoms in a specific stage of ionization is determined by the method that has been discussed (for example, from the N_1 and N_2 lines—the concentration of doubly ionized oxygen atoms). The ionization formula must be used in order to estimate the fraction of the atoms of the element of interest in other states of ionization.

Aller and Menzel [10] determined the chemical composition of planetary nebulae from the emission line intensities. The data obtained by them on the relative numbers of atoms of various elements are listed in Table 38 (the number of hydrogen atoms is arbitrarily taken as 1000). Data on the relative numbers of atoms in the atmosphere of the Sun and of the star τSco, obtained by an entirely different method—from the intensities of absorption lines, are given in the same table for comparison. /337

TABLE 38. CHEMICAL COMPOSITION OF PLANETARY NEBULAE AND OF STELLAR ATMOSPHERES

Element	Planetary nebula	Sun	τ Sco	Element	Planetary nebula	Sun	τ Sco
Hydrogen	1000	1000	1000	Fluorine	0,0001		
Helium	100	222	175	Neon	0,01		0,1
Carbon	0,6	0,04	0,17	Sulfur	0,036	0,037	
Nitrogen	0,2	0,12	0,3	Chlorine	0,002		
Oxygen	0,25	0,37	1,0	Argon	0,0015		

Commas represent decimal points.

We see that there are no great differences in the chemical composition of nebulae and of stellar atmospheres. In particular, hydrogen is the most abundant element in nebulae. The number of helium atoms amounts to about one tenth of the number of hydrogen atoms, and the number of all other atoms, besides these, is about one thousandth.

26. Continuous Spectrum

1. Recombinations and free-free transitions. As already stated, the spectra of gaseous nebulae consist of emission lines on a weak continuous background. The origin of this continuous background is explained to an appreciable extent by recombinations and free-free transitions of electrons in ion fields. Hydrogen, as the most abundant element in nebulae, plays the prime role in the origin of this radiation.

To calculate the amount of energy emitted by a nebula in the continuous spectrum, we must know the emission coefficients caused by recombinations and

free-free transitions. Since the continuous spectrum absorption coefficients are known (see Section 5), we can easily find the emission coefficients that we require, using the usual method, i.e., considering the thermodynamic equilibrium condition. /338

Let us denote by $\varepsilon_{i\nu}$ the volume emission coefficient for recombinations in the i-th level, and by $\alpha_{i\nu}$—the volume absorption coefficient with the i-th level. In the presence of thermodynamic equilibrium we have

$$\varepsilon_{i\nu} = \alpha_{i\nu} \frac{2h\nu^3}{c^2} \frac{1}{e^{\frac{h\nu}{kT}} - 1}. \tag{26.1}$$

Let us represent the volume absorption coefficient in the form $\alpha_{i\nu} = n_i k_{i\nu}$, where n_i is the number of atoms in the i-th state in 1 cm^3 and $k_{i\nu}$ is the absorption coefficient, calculated for one atom. In the presence of thermodynamic equilibrium the quantity n_i is expressed in terms of the ion concentration n^+ and the free electron density n_e by Eq. (5.7), resulting from the Boltzmann and Saha formulas. For hydrogen the absorption coefficient $k_{i\nu}$ is given by Eq. (5.6) (in which the factor $1-e^{-h\nu/kT}$ must again be inserted to take account of the negative absorption). Using the formulas cited, from (26.1) we obtain

$$\varepsilon_{i\nu} = n_e n^+ \frac{2^7\pi^4}{(6\pi)^{3/2}} \frac{e^{10}}{m^2c^3h^2} \left(\frac{m}{kT}\right)^{3/2} \frac{g_{i\nu}}{i^3} e^{\frac{\chi_i - h\nu}{kT}}, \tag{26.2}$$

where $h\nu > \chi_i$. This formula is always correct when the free electron velocities have a Maxwellian distribution with a temperature T.

With the aid of Eq. (26.2) we can, incidentally, find the total number of recombinations in the i-th level. This number is equal to

$$n_e n^+ C_i = 4\pi \int_{\nu_i}^{\infty} \frac{\varepsilon_{i\nu}}{h\nu} d\nu. \tag{26.3}$$

When $g_{i\nu} = 1$, Eq. (26.7) for the recombination coefficient C_i is obtained from this.

The volume emission coefficient, caused by recombinations at all levels, is obviously equal to

$$\varepsilon_\nu' = n_e n^+ \frac{2^7\pi^4}{(6\pi)^{3/2}} \frac{e^{10}}{m^2c^3h^2} \left(\frac{m}{kT}\right)^{3/2} \sum_{i=j}^{\infty} \frac{g_{i\nu}}{i^3} e^{\frac{\chi_i - h\nu}{kT}}. \tag{26.4}$$

Here one must assume that j = 1 beyond the Lyman series limit, j = 2 from the Balmer series limit to the Lyman series limit, etc.

The volume emission coefficient ε_ν'', caused by free-free transitions, can be found in an analogous fashion. Using Eq. (5.10) for the volume absorption coeffeicient α_ν'' and the Kirchhoff-Planck law, we obtain /339

$$\varepsilon_\nu'' = n_e n^+ \frac{2^5\pi^2}{(6\pi)^{3/2}} \frac{e^6}{m^2c^2} \left(\frac{m}{kT}\right)^{1/2} g_\nu e^{-\frac{h\nu}{kT}}. \tag{26.5}$$

Adding Eqs. (26.4) and (26.5), we arrive at the following formula for the volume emission coefficient caused both by recombinations and by free-free transitions:

$$\varepsilon_\nu = n_e n^+ \frac{2^5\pi^2}{(6\pi)^{3/2}} \frac{e^6}{m^2c^2} \left(\frac{m}{kT_e}\right)^{1/2} \left(g_\nu + 2\frac{\chi_1}{kT_e} \sum_{i=j}^{\infty} \frac{g_{i\nu}}{i^3} e^{\frac{\chi_i}{kT_e}}\right) e^{-\frac{h\nu}{kT_e}}. \tag{26.6}$$

Having in mind the application of this formula to gaseous nebulae, we replaced the temperature T in it by the electron temperature T_e of the nebula.

The energy distribution in the continuous spectrum, given by Eq. (26.6), is characterized by the fact that at the series limits the emission intensity increases discontinuously as one goes from lower to higher frequencies. This is explained by the presence of a new term in Eq. (26.6), caused by recombinations at the lower level.

As seen from Eq. (26.6), the emission in the visible portion of the continuous spectrum is caused in approximately equal amounts by recombinations and free-free transitions (for $T_e \approx 10,000°$). On the other hand, as we know from Section 22, each recombination in the third and higher levels necessarily leads to the appearance of one photon in the Balmer lines. Consequently, the number of photons in the Balmer lines must be equal in order of magnitude to the number of photons in the continuous spectrum. But the line emission is concentrated in very narrow frequency intervals. Therefore the continuous spectrum being considered must only play the role of a weak background for the emission lines. Let us find, for example, the ratio of the number of photons in the H_β line to the number of photons in the Balmer continuum (assuming for simplicity that it increases only with captures in the second level). This ratio is obviously equal to

$$\frac{n_i A_{i2}}{n_e n^+ C_2(T_e)} = z_i \frac{A_{i2}}{C_2(T_e)},$$

and, as calculations show, it is about unity. Thus, almost as many photons are emitted in the one H_β line as in the entire Balmer continuum.

The theory that has been discussed agrees qualitatively with the results of observations. As is known, the continuous spectrum of gaseous nebulae is actually very weak. Moreover an intensity discontinuity is observed at the Balmer series limit, characteristic of recombination spectra. However there is no quantitative agreement between theory and observations. /340

From Eq. (26.6) it is seen that the theoretical energy distribution in the continuous spectrum follows the law

$$H_\nu \sim e^{-\frac{h\nu}{kT_e}}. \tag{26.7}$$

Substituting this expression for the radiant flux H_ν into Eq. (6.18), we obtain the following relationship between the spectrophotometric temperature T_s and the electron temperature T_e:

$$-\frac{h}{kT_e} = \frac{3}{\nu} - \frac{h}{kT_s}\frac{1}{1-e^{-\frac{h\nu}{kT_s}}}. \tag{26.8}$$

Neglecting here the quantity $e^{-h\nu/kT_s}$ compared with 1, for the portion of the spectrum near the H_β line we find

$$\frac{1}{T_s} - \frac{1}{T_e} = \frac{1}{10000}. \tag{26.9}$$

For $T_e = 10,000°$ this relation gives $T_s = 5000°$. However, the observed spectrophotometric temperatures of nebulae are appreciably higher. In addition the observed intensity of the continuous spectrum of nebulae in the visible region markedly exceeds its theoretical intensity (with respect to the intensity of the Balmer lines). Therefore one can conclude that some supplementary source of radiation in the continuous spectrum exists in the nebulae.

One can arrive at the same conclusion by considering the Balmer discontinuity. The theoretical Balmer discontinuity, as seen from Eqs. (6.19) and (26.6), is given by the expression

$$D = \lg \frac{1 + 2\frac{\chi_1}{kT_e}\sum_{i=3}^{\infty}\frac{1}{i^3}e^{\frac{\chi_i}{kT_e}}}{1 + 2\frac{\chi_1}{kT_e}\sum_{i=2}^{\infty}\frac{1}{i^3}e^{\frac{\chi_i}{kT_e}}}, \tag{26.10}$$

where it is assumed $g_\nu = 1$ and $g_{i\nu} = 1$. We see that in the case given $D < 0$. The quantity D depends only on the electron temperature and can be calculated for each /341

nebula (for the T_e value obtained from the forbidden line intensities). However, the observed values of the quantity D are greater than the calculated. This can obviously be explained by the effect of the supplementary radiation.

Values of the Balmer discontinuity D, taken from Greenstein's paper [18], are presented in Table 39 as a function of the electron temperature T_e and the quantity C/Ba_s, representing the ratio of the intensity of the supplementary continuous spectrum to the intensity of the continuous spectrum, caused by recombinations and free-free transitions, beyond the Balmer series limit. For C = 0 the Balmer discontinuity is calculated from Eq. (26.10). From the table it is seen how the quantity D increases with an increase in the quantity C/Ba_s for a constant electron temperature.

TABLE 39. BALMER DISCONTINUITY D (WITH OPPOSITE SIGN)

T_e	$\frac{C}{Ba_s}$				T_e	$\frac{C}{Ba_s}$			
	0	0,1	0,2	0,3		0	0,1	0,2	0,3
5000°	2,34	1,02	0,77	0,63	20000	0,72	0,58	0,49	0,42
7500	1,68	0,96	0,73	0,61	25000	0,60	0,49	0,42	0,37
10000	1,31	0,87	0,68	0,57	30000	0,51	0,41	0,36	0,32
15000	0,93	0,70	0,57	0,49	40000	0,38	0,33	0,29	0,26

Commas represent decimal points.

The paper by Greenstein that has been cited is devoted to a study of the continuous spectrum of the Orion nebula. From observations he found that D = = -0.64. If it is assumed that the quantity D is defined by Eq. (26.10), then, as seen from Table 39, the electron temperature will be equal to T_e = 22,000°. Such an electron temperature is too high for a nebula. In order to obtain T_e = = 12,000° for the value of D that has been found, one must assume C/Bs_s = 0.2.

From what has been said it follows that the origin of the continuous spectrum of gaseous nebulae cannot be explained only by recombinations and free-free transitions. Dust, scattering the stellar radiation, plays some role in the origin of the continuous spectrum in connection with diffuse nebulae. In planetary nebulae, however, dust is apparently completely absent. A supplementary mechanism for the formation of the continuous spectrum of purely gaseous nebulae will be indicated below.

2. Two-photon emission. Besides spontaneous transitions with the emission of one photon, spontaneous transitions with the emission of two photons are also possible from each excited state of the atom. Usually the probability of the first transitions (one-photon) is much greater than the probability of the second (two-photon). However, in the case of metastable states, from which the /342

probability of all one-photon transitions is small, the opposite can be true. In particular, this is the case with the metastable 2s hydrogen state. As calculations show, the 2s → 1s transition is more probable with the emission of two photons than of one.

The energies of the quanta emitted in the two-photon 2s → 1s transition can be arbitrary, but their sum is constant and equal, obviously, to the energy of the L_α quantum. Thus, for two-photon transitions the energy is emitted in a continuous spectrum. In gaseous nebulae after photoionizations, recombinations and cascade transitions an appreciable portion of the hydrogen atoms enter the metastable 2s state. As we know, the conditions in nebulae are such that neither radiation nor collisions remove the atoms from the metastable states (or remove them very infrequently). Therefore the hydrogen atoms, entering the 2s state, in most cases (if the density is not very great) complete transitions into the 1s state with the emission of photons in the continuous spectrum. The significant role of these processes in the formation of the continuous spectrum of gaseous nebulae was first mentioned in the papers of A. Ya. Kipper [19] and Spitzer and Greenstein [20].

Let us designate the frequencies of the two photons emitted during the 2s → → 1s transition as $y\nu_{12}$ and $(1 - y)\nu_{12}$, where ν_{12} is the L_α frequency and y is any number from zero to 1. Let A(y)dy be the transition probability coefficient, associated with the emission of a photon in the frequency interval from $\nu_{12}y$ to $\nu_{12}(y + dy)$. Representing the quantity A(y) in the form

$$A(y) = \frac{9\alpha^6\nu_0}{2^{10}}\psi(y), \tag{26.11}$$

where ν_0 is the hydrogen ionization frequency and $\alpha = 2\pi e^2/hc$ is the fine structure constant, the authors cited above obtained the values listed in Table 40 for the function $\psi(y)$. Since $\psi(y) = \psi(1-y)$, then in the table y varies only from zero to 1/2. The energy emitted in unit frequency interval is proportional to the quantity $h\nu A(y)$ or $y\psi(y)$. Values of the function $y\psi(y)$ are also given in the table. The Einstein coefficient of the two-photon 2s → 1s transition is equal to

$$A_{2s,1s} = \frac{1}{2}\int_0^1 A(y)\,dy = 8.227\,\text{sec}^{-1}. \tag{26.12}$$

With the aid of the quantity A(y) one can easily write an expression for the volume emission coefficient ε_ν, caused by two-photon transitions. Let us denote by n_{2s} the number of hydrogen atoms in the 2s state in 1 cm^3. Then, obviously, we have /343

$$4\pi\varepsilon_\nu d\nu = n_{2s}A(y)\,dy\cdot h\nu,$$

or

$$\varepsilon_\nu = n_{2s}\frac{h}{4\pi}A(y)\,y. \tag{26.13}$$

TABLE 40. THE QUANTITIES $\psi(y)$ AND $y\psi(y)$, CHARACTERIZING TWO-PHOTON EMISSION

y	λ (Å)	$\psi(y)$	$y\psi(y)$	y	λ (Å)	$\psi(y)$	$y\psi(y)$
0,00		0	0	0,30	4052	4,546	1,363
0,05	24313	1,725	0,0863	0,35	3473	4,711	1,649
0,10	12157	2,783	0,2783	0,40	3039	4,824	1,929
0,15	8105	3,481	0,5222	0,45	2702	4,889	2,200
0,20	6078	3,961	0,7922	0,50	2403	4,907	2,454
0,25	4862	4,306	1,077				

Commas represent decimal points.

To find the quantity n_{2s}, the steady-state equation for the 2s state must be formulated. Hydrogen atoms enter the 2s state after recombinations and subsequent cascade transitions. Let us designate by X the fraction of all recombinations at high levels, starting with the second, which lead to the appearance of atoms in the 2s state. Then the number of transitions into the 2s state in 1 cm^3 in 1 sec will be equal to $Xn_e n^+ \sum_2^\infty C_i(T_e)$. Calculations show that X = 0.32, approximately (the quantity X depends slightly on the electron temperature). On the other hand, atoms leave the 2s state because of two-photon transitions. The number of such transitions in 1 cm^3 in 1 sec is equal to $n_{2s}A_{2s,1s}$. On the basis of what has been said, we obtain

$$n_{2s}A_{2s,1s} = Xn_e n^+ \sum_2^\infty C_i(T_e). \tag{26.14}$$

Substituting the quantity n_{2s} from (26.14) into (26.13), we find

$$\varepsilon_\nu = Xn_e n^+ \sum_2^\infty C_i(T_e) \frac{hA(y)y}{4\pi A_{2s,1s}}. \tag{26.15}$$

The desired quantity ε_ν can be calculated from Eq. (26.15) with the aid of Table 40. /344

It is obvious that the total number of photons, emitted in the 2s → 1s two-photon transitions in 1 cm^3 in 1 sec, is equal to

$$2Xn_e n^+ \sum_2^\infty C_i(T_e).$$

This number is comparable, in order of magnitude, to the number of photons emitted during recombinations. Therefore two-photon transitions must play a significant role in the formation of the continuous spectrum of gaseous nebulae.

Adding Eq. (26.15) to the previously derived Eq. (26.6) leads to a continuous spectrum energy distribution which agrees better with observational data than the energy distribution given by Eq. (26.6). However, before a detailed comparison of theory with observations, let us examine certain processes which affect the intensity of the two-photon emission.

3. Effect of collisions. It was assumed above that all atoms, entering into the metastable 2s state, complete a spontaneous transition from it into the 1s state with the emission of two photons. However, transitions due to the effect of collisions are also possible from the 2s state. Calculations show that the most probable of them are transitions into the 2p state very near the 2s (Fig. 33), with these transitions being caused primarily by collisions with protons. Then an atom spontaneously jumps from the 2p state into the 1s state with the emission of an L_α photon. Such processes lead to a decrease in the population of the 2s level compared with that determined previously, leading also to a decrease in the intensity of the two-photon emission.

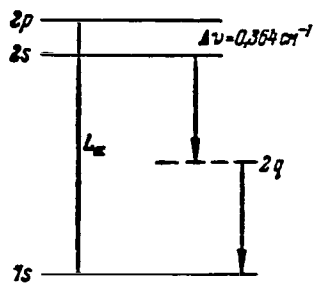

Figure 33.

Moreover, reverse processes can also occur in nebulae. An atom, entering into the 2p state, instead of a spontaneous transition into the 1s state with the emission of an L_α photon can jump into the 2s state due to the effect of a collision, and then into the 1s state with the emission of two photons. At first glance it appears that such processes occur extremely rarely since the 2p → 1s transition has a very high probability. In reality, however, the situation is not so simple. In an overwhelming majority of cases the L_α photon does not leave the nebula immediately upon its formation, but only after many scatterings. This leads to a considerable increase in the residence time of an atom in the 21 state. One can assume that on the average it is equal to $N/A_{2p,1s}$, where N is the average number of scatterings of the L_α photon in the nebula. It is obvious that the greater N, the greater the probability of the 2p → 2s transition due to the effect of collisions and the subsequent two-photon 2s → 1s transition. /345

To explain the role of these processes, we must take them into consideration in the determination of the population of the 2s state. Let us write the steady-state equations for the 2s and 2p states. Denoting the atom densities in these states by n_{2s} and n_{2p}, we have

$$\left.\begin{aligned} n_{2s}(A_{2s,1s}+b_{2s,2p}) &= XR + n_{2p}a_{2p,2s}, \\ n_{2p}\left(\frac{A_{2p,1s}}{N}+a_{2p,2s}\right) &= (1-X)R + n_{2s}b_{2s,2p}. \end{aligned}\right\} \qquad (26.16)$$

Here XR and (1 - x)R are the numbers of atoms entering the 2s and 2p states, respectively, after recombinations and cascade transitions in 1 cm^3 in 1 sec, and $R = n_e n^+ \sum_2^\infty C_i$. The number of 2s → 2p transitions, produced through the effect of collisions in 1 cm^3 in 1 sec, is denoted by $n_{2s} b_{2s,2p}$; and the number of opposite transitions—by $n_{2p} a_{2p,2s}$. Instead of the quantity $A_{2p,1s}$, we have written the quantity $A_{2p,1s}/N$ in order to take approximate account of the multiple scattering of L_α photons in the nebula.

Starting from Eqs. (26.16) for the quantity n_{2s}, we obtain the following expression for the desired number of two-photon transitions:

$$n_{2s} A_{2s,1s} = \frac{X + a_{2p,2s} \dfrac{N}{A_{2p,1s}}}{1 + a_{2p,2s} \dfrac{N}{A_{2p,1s}} + \dfrac{b_{2s,2p}}{A_{2s,1s}}} R. \tag{26.17}$$

This formula should replace Eq. (26.14) when account is taken of the collisions removing atoms from the 2s state into the 2p state and vice versa.

Let us substitute the numerical values of the parameters into Eq. (26.17): $A_{2p,1s} = 6.24 \cdot 10^8$, $A_{2s,1s} = 8.23$, $b_{2s,2p} = n_e 5 \cdot 10^{-4}$, $a_{2p,2s} = n_e 1.5 \cdot 10^{-4}$ sec^{-1}. Then we obtain

$$\bar{n}_{2s} A_{2s,1s} = \frac{X + 2.4 \cdot 10^{-13} n_e N}{1 + 2.4 \cdot 10^{-13} n_e N + 6 \cdot 10^{-5} n_e} R. \tag{26.18}$$

We see that when the number of scatterings of L_α photons in the nebula is small, namely /346

$$2.4 \cdot 10^{-13} n_e N \ll 1, \tag{26.19}$$

Eq. (26.18) assumes the form

$$n_{2s} A_{2s,1s} = \frac{X}{1 + 6 \cdot 10^{-5} n_e} R. \tag{26.20}$$

In this case the 2s → 2p transitions occur more frequently than the opposite transitions, and the intensity of the two-photon emission decreases with an increase in n_e.

When, however, the average number of scatterings of L_α quanta in the nebula satisfies the inequality

$$N \gg 2.5 \cdot 10^8, \tag{26.21}$$

then instead of Eq. (26.18) we obtain

$$n_{2s} A_{2s,1s} = \left[X + (1 - X) \frac{2.4 \cdot 10^{-13} n_e N}{1 + 2.4 \cdot 10^{-13} n_e N} \right] R. \tag{26.22}$$

This formula gives, for the number of two-photon transitions, approximately the same value, or greater, as Eq. (26.14). This means that the 2p → 2s transitions balance the 2s → 2p transitions or even predominate over them.

If the inequality (26.21) can be supplemented by the inequality

$$2.4 \cdot 10^{-13} n_e N \gg 1, \tag{26.23}$$

then we obtain

$$n_{2s} A_{2s,1s} = R, \tag{26.24}$$

i.e., the number of two-photon transitions is equal to the number of recombinations in all levels, starting with the second. In the case given, all L_α photons are transformed into two-photon emission.

As we will see in the following section, the quantity N is very large in nebulae. However, it is apparently not so large that the inequality (26.21) is satisfied. Therefore it must be assumed that the number of two-photon transitions in nebulae is determined by Eq. (26.20).

Equation (26.20) can be replaced by Eq. (26.14), with the quantity X in it being defined as

$$X = \frac{0.32}{1 + 6 \cdot 10^{-5} n_e}. \tag{26.25}$$

Correspondingly, Eq. (26.15) can also be used for the emission coefficient ε_ν, assuming that X in it is given by Eq. (26.25).

4. Comparison of theory with observations. We have already stated that the theory of the formation of the continuous spectrum do nebulae, when only recombinations and free-free transitions are taken into consideration, cannot satisfactorily explain the results of observations. From a comparison of this theory with observations it must be concluded that some supplementary continuous spectrum source exists in nebulae. If two-photon emission is assumed as this source, then the agreement between theory and observations will be considerably better. /347

A comparison of the observed energy distribution in the spectra of nebulae with the theoretical distribution has been made by Seaton. Its results, with respect to the Balmer discontinuity, are presented in Table 41.

TABLE 41. THEORETICAL AND OBSERVED VALUES OF THE BALMER DISCONTINUITY IN NEBULAR SPECTRA

Nebula	$10^{-4}\ T_e$	$10^{-4}\ n_e$	$-D_{obs.}$	$-D_{theor.}$		
NGC 6543	1,0	3	0,98	1,26	0,70	0,95
NGC 6572	1,3	5	0,79	1,00	0,59	0,84
NGC 6826	1,1	3	0,61	1,15	0,66	0,89
NGC 7009	1,4	3	0,82	0,90	0,56	0,73
NGC 7662	1,3	5	0,81	0,80	0,59	0,79
IC 418	1,9	0,8	0,48	0,69	0,45	0,50
average			0,75	0,98	0,59	0,78

Commas represent decimal points.

The numbers of the nebulae from the NGC and IC catalogs are given in the first column, in the second and third—the values of T_e and n_e from Seaton's determinations, in the fourth—the observed values of the Balmer discontinuity. In the last columns are given the theoretical values of the Balmer discontinuity for three cases: 1) when recombinations and free-free transitions are taken into account; 2) when two-photon emission with $X = 0.32$ is taken into account at the same time; 3) when two-photon emission with the quantity x defined by Eq. (26.25) is taken into account at the same time.

From the table it follows that two-photon emission has a significant effect on the magnitude of the Balmer discontinuity. In addition one can ascertain a better agreement between observations and theory for values of the quantity X found from Eq. (26.25).

Observations also give the curves of the variation of the emission intensity with frequency in the visible portion of nebular spectra. In a number of planetary nebulae the emission intensity was approximately constant within a considerable spectral region (from 3600 to 4800 Å). This fact does not correspond to an exponential decrease of the emission intensity with an increase in frequency, which follows from Eq. (26.6). On the other hand, as seen from Eq. (26.15) and Table 40, the intensity of the two-photon emission in the visible portion of the spectrum increases somewhat with an increase in frequency. Therefore, taking two-photon emission into account explains, to a considerable extent, the energy distribution in the continuous spectrum of planetary nebulae. Some discrepancies between theory and observations are possibly caused by inaccuracy in the observations. /348

In a number of planetary nebulae, however, the observed energy distribution in the continuous spectrum differs quite drastically from the theoretical distribution (taking two-photon emission into account). Such cases have been examined in detail by G. A. Gurzadyan [3], who assumes the existence of still another

continuous spectrum source is possible in nebulae. In his opinion synchroton radiation can be such a source.

27. Radiation Diffusion in Nebulae

1. L_c radiation field. In determining the emission line intensities we assumed that the nebulae are transparent for radiation in these lines. There is no doubt about this assumption with respect to the lines of the subordinate series since there are very few atoms in excited states. It is also valid with respect to the forbidden lines (even if the lower state is the ground state) because of the extreme smallness of the absorption coefficient, calculated for one atom, for them.

Generally speaking, however, nebulae are not transparent for radiation at the frequencies of the principal series. This greatly complicates the radiation field at these frequencies since the radiative transfer equation must be applied in this situation. Let us now calculate the radiation field at the frequencies of the hydrogen Lyman series. This problem was first considered by V. A. Ambartsumyan [21]. Several authors then refined and broadened the solution obtained by him.

The geometrical model of the nebula has significant value in a study of radiation transfer in nebulae. Let us assume that the nebula is bounded by two concentratic spheres with radii r_1 and r_2, and the nucleus of the nebula is at the center of these spheres. The nebula thickness will be assumed to be small in comparison with its distance from the nucleus (i.e., $r_2 - r_1 \ll r_1$). In such a case the nebula can be considered to consist of plane-parallel layers, and the radiation dilution factor is constant.

Let us first consider the radiation field in the Lyman continuum. When L_c photons, coming from a star in the nebula, are absorbed, hydrogen atoms are ionized and during subsequent recombinations at the first level L_c photons are emitted. Such processes of L_c photon absorption and emission can be continued even further. Consequently, diffusion of the L_c radiation occurs in the nebula. In this situation the "survival" probability of a photon during an elementary scattering act is equal to the ratio of the number of recombinations at the first level to the number of recombinations at all levels. /349

In order to determine the density of the diffuse L_c radiation, we write the radiative transfer equation and the radiative equilibrium equation. In the case given the radiative equilibrium equation must express the fact that the number of ionizations in each volume element of the nebula is equal to the number of recombinations. Consequently, we have

$$n_e n^+ \sum_1^\infty C_i = n_1 \int_{\nu_1}^\infty k_{1\nu} \frac{d\nu}{h\nu} \int (I_\nu + I_\nu^0)\, d\omega, \qquad (27.1)$$

where I_ν is the intensity of the diffuse radiation and I_ν^0 is the intensity of the radiation arriving at a given point of the nebula directly from the star. Previously (in Section 23) we wrote a similar equation, ignoring diffuse radiation.

Let us denote by p the fraction of recombinations at the first level. Moreover, let us take into consideration the fact that for hydrogen the absorption coefficient on the basis of Eq. (5.6) changes with frequency in accordance with the law

$$k_{1\nu} = k_{1\nu_1}\left(\frac{\nu_1}{\nu}\right)^3. \tag{27.2}$$

Then instead of Eq. (27.1) we obtain

$$\frac{n_e n^+ C_1}{n_1 k_{1\nu_1}} = p\int_{\nu_1}^{\infty}\left(\frac{\nu_1}{\nu}\right)^3 \frac{d\nu}{h\nu}\int (I_\nu + I_\nu^0)\,d\omega. \tag{27.3}$$

In the case of a nebula consisting of plane-parallel layers, the radiative transfer equation has the form

$$\cos\vartheta\frac{dI_\nu}{dr} = -n_1 k_{1\nu} I_\nu + \varepsilon_{1\nu}, \tag{27.4}$$

where $\varepsilon_{1\nu}$ is the volume emission coefficient for recombinations at the first level. As follows from Eq. (26.2), the quantity $\varepsilon_{1\nu}$ can be represented in the form /350

$$\varepsilon_{1\nu} = \varepsilon_{1\nu_1} e^{-\frac{h(\nu-\nu_1)}{kT_e}} \tag{27.5}$$

Let τ be the optical distance at any point in the nebula from its inner boundary at frequency ν_1, i.e.,

$$\tau = \int_{r_1}^{r} n_1 k_{1\nu_1}\,dr. \tag{27.6}$$

With the aid of Eqs. (27.2), (27.5) and (27.6) instead of Eq. (27.4) we obtain

$$\cos\vartheta\frac{dI_\nu}{d\tau} = -\left(\frac{\nu_1}{\nu}\right)^3 I_\nu + \frac{\varepsilon_{1\nu_1}}{n_1 k_{1\nu_1}} e^{-\frac{h(\nu-\nu_1)}{kT_e}}. \tag{27.7}$$

The quantities C_1 and $\varepsilon_{1\nu_1}$ must obviously be interrelated. Substitution of (27.5) into (26.3) gives

$$n_e n^+ C_1 = 4\pi\frac{\varepsilon_{1\nu_1}}{h}\,\mathrm{Ei}\left(\frac{\chi_1}{kT_e}\right) e^{\frac{\chi_1}{kT_e}}. \tag{27.8}$$

Let us introduce the notation

$$S_c(\tau) = \frac{n_e n^+ C_1}{4\pi n_1 k_{1\nu_1}}. \tag{27.9}$$

Then Eqs. (27.7) and (27.3) assume the form

$$\cos\vartheta \frac{dI_\nu}{d\tau} = -\left(\frac{\nu_1}{\nu}\right)^3 I_\nu + \frac{h}{\mathrm{Ei}\left(\frac{\chi_1}{kT_e}\right)} e^{-\frac{h\nu}{kT_e}} S_c(\tau) \tag{27.10}$$

and

$$S_c(\tau) = p \int_{\nu_1}^{\infty} \left(\frac{\nu_1}{\nu}\right)^3 \frac{d\nu}{h\nu} \int I_\nu \frac{d\omega}{4\pi} + S_c^0(\tau), \tag{27.11}$$

where

$$S_c^0(\tau) = p \int_{\nu_1}^{\infty} \left(\frac{\nu_1}{\nu}\right)^3 \frac{d\nu}{h\nu} \int I_\nu^0 \frac{d\omega}{4\pi}. \tag{27.12}$$

The intensity of the radiation, arriving from the star at a given point of the nebula, is obviously equal to /351

$$I_\nu^0 = I_\nu^* e^{-\tau\left(\frac{\nu_1}{\nu}\right)^3}, \tag{27.13}$$

where I_ν^* is the intensity of the radiation leaving the stellar atmosphere. Therefore we obtain

$$S_c^0(\tau) = pW \int_{\nu_1}^{\infty} \left(\frac{\nu_1}{\nu}\right)^3 I_\nu^* e^{-\tau\left(\frac{\nu_1}{\nu}\right)^3} \frac{d\nu}{h\nu}, \tag{27.14}$$

where W is the radiation dilution factor.

Thus, we have derived two Eqs. (27.10) and (27.11), for determining the two quantities $I_\nu(\tau, \vartheta)$ and $S_c(\tau)$ that we are seeking. Still to be added to these equations are boundary conditions, which in the case given have the form

$$\left.\begin{aligned} I_\nu(0, \vartheta) &= I_\nu(0, \pi - \vartheta), \\ I_\nu(\tau_0, \vartheta) &= 0 \text{ for } \vartheta > \frac{\pi}{2}. \end{aligned}\right\} \tag{27.15}$$

The first of these conditions, existing at the inner boundary of the nebula (at $\tau = 0$), means that the intensity of the radiation leaving the nebula is equal to the intensity of the radiation entering the nebula. This occurs because the radiation entering the nebula at any point on the inner boundary at an angle of ϑ to the normal is no different from the radiation leaving the nebula at an angle $\pi - \vartheta$ on the opposite side (Fig. 34). The second condition shows, however, that there is no incoming radiation at the outer boundary (at $\tau = \tau_0$).

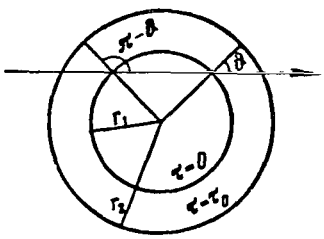

Figure 34.

An expression for the radiation intensity $I_\nu(\tau, \vartheta)$ in terms of the function $S_c(\tau)$ can be found from Eq. (27.10) for the boundary conditions (27.15). Substituting this expression into Eq. (27.11), we obtain the following integral equation for determining the function $S_c(\tau)$:

$$S_c(\tau) = \frac{p}{2}\int_0^{\tau_0} [K(|\tau-\tau'|) + K(\tau+\tau')] S_c(\tau')\, d\tau' + S_c^0(\tau), \tag{27.16}$$

where /352

$$K(\tau) = \frac{\int_{\nu_1}^{\infty} \left(\frac{\nu_1}{\nu}\right)^3 \mathrm{Ei}\left[\tau\left(\frac{\nu_1}{\nu}\right)^3\right] e^{-\frac{h\nu}{kT_e}} \frac{d\nu}{\nu}}{\mathrm{Ei}\left(\frac{\chi_1}{kT_e}\right)}. \tag{27.17}$$

Equation (27.16) can be investigated by the methods discussed in Section 3. In particular, an exact solution of this equation in explicit form can be derived for $\tau_0 = \infty$.

To simpifiy the problem being considered the average absorption coefficient for the entire Lyman continuum is sometimes inserted and its corresponding optical distance is taken for τ. Then, as it is easy to see, instead of Eq. (27.16) we have

$$S_c(\tau) = \frac{p}{2}\int_0^{\tau_0} [\mathrm{Ei}|\tau-\tau'| + \mathrm{Ei}(\tau+\tau')] S_c(\tau')\, d\tau' + S_c^0(\tau). \tag{27.18}$$

The quantity $S_c^0(\tau)$ can then be represented in the form

$$S_c^0(\tau) = p\frac{N_c}{4\pi} e^{-\tau}, \tag{27.19}$$

where N_c is the number of Lyman continuum photons arriving from the star on 1 cm^2 of the inner boundary of the nebula in 1 sec.

When $\tau_0 = \infty$ the exact solution of Eq. (27.18), derived by the method cited above, has the form

$$S_c(\tau) = p\frac{N_c}{4\pi}\left\{e^{-\tau} + \frac{1}{2}\int_0 \Phi(\tau')[e^{-|\tau-\tau'|} + e^{-(\tau+\tau')}]d\tau'\right\} \tag{27.20}$$

where

$$\Phi(\tau) = 4p\int_1^\infty \frac{xe^{-x\tau}dx}{(p\pi)^2 + \left(2x + p\ln\frac{x-1}{x+1}\right)^2} + \frac{2k(1-k^2)}{p+k^2-1}e^{-k\tau} \tag{27.21}$$

and k is determined from the equation

$$\frac{p}{2k}\ln\frac{1+k}{1-k} = 1. \tag{27.22}$$

Values of the quantity $4\pi S_c(\tau)/p$, calculated with the aid of Eq. (27.20), are presented in Table 42.

TABLE 42. VALUES OF THE QUANTITY $4\pi S_c(\tau)/p$

τ \ p	0,0	0,3	0,4	0,5	0,6	0,7	0,8	0,9
0,0	1,00	1,13	1,20	1,30	1,42	1,61	1,93	2,68
0,2	0,82	0,97	1,04	1,14	1,27	1,46	1,79	2,54
0,4	0,67	0,81	0,87	0,96	1,09	1,27	1,59	2,32
0,6	0,55	0,67	0,71	0,81	0,92	1,10	1,40	2,11
0,8	0,45	0,55	0,60	0,68	0,78	0,94	1,23	1,91
1,0	0,37	0,46	0,50	0,57	0,66	0,81	1,08	1,73
1,5	0,22	0,28	0,32	0,36	0,43	0,55	0,76	1,34
2,0	0,14	0,17	0,20	0,23	0,28	0,37	0,54	1,03
2,5	0,08	0,11	0,12	0,15	0,18	0,25	0,38	0,80
3,0	0,05	0,06	0,08	0,09	0,12	0,16	0,27	0,62

Commas represent decimal points.

For $\tau \gg 1$ the following asymptotic expression for the function $S_c(\tau)$ can be derived from Eq. (27.20): /35

$$S_c(\tau) = \frac{N_c}{2\pi}\frac{kp}{p+k^2-1}e^{-k\tau}. \tag{27.23}$$

Values of the quantity k, found from Eq. (27.22), are presented in the table:

p	0	0.5	0.6	0.7	0.8	0.9	1.0
k	1.00	0.96	0.91	0.82	0.70	0.52	0

From Table 42 it is seen that the role of the diffuse radiation depends intrinsically on the magnitude of the parameter p. In the case L_c radiation diffusion this parameter is equal to

$$p = \frac{C_1(T_e)}{\sum_1^\infty C_i(T_e)}. \tag{27.24}$$

Calculations from Eq. (27.24) give:

T_e	5000	10 000	20 000	50 000
P	0.39	0.44	0.49	0.57

As we know, the electron temperatures of nebulae are about 10,000°. Therefore from Table 42 it follows that about the same number of photons of diffuse L_c radiation is contained in nebulae as the number of L_c photons arriving directly from the star. Thus, it must be recognized that the role of diffuse L_c radiation in nebulae is not very great (although it is a maximum in the case $\tau_0 = \infty$ considered by us). /354

Such a result is explained by the fact that the fraction of captures at the first level, i.e., the quantity p, is relatively small. If p would be close to unity, then diffuse radiation would predominate over direct. This would be especially noticeable when $\tau \gg 1$ because of the smallness of the quantity k.

After a determination of the function $S_c(\tau)$ we can, by using Eq. (27.10), also find the quantity $I_\nu(\tau, \vartheta)$, i.e., the intensity of the diffuse L_c radiation at any point of the nebula. As seen from Eq. (27.10), the frequency distribution of the diffuse L_c radiation depends strongly on the electron temperature T_e.

At each point of the nebula the diffuse L_c radiation supplements the L_c radiation arriving directly from the star. The intensity of the radiation arriving from the star is given by Eq. (27.13). Obviously the spectral composition of the

total L_c radiation (i.e., diffuse and arriving from the star) must change significantly from one point of the nebula to another.

2. L_α radiation field in a stationary nebula. The optical thicknesses of nebulae in the Lyman series lines are much greater than in the Lyman series lines are much greater than in the Lyman continuum. Even in those cases when the nebula is transparent for L_c radiation, it can be fairly opaque for Lyman radiation. Therefore the diffuse radiation in these lines must be considered to determine the radiation density in the Lyman lines.

It is obvious that the radiation density in the high terms of the Lyman series (starting with L_β) cannot be great. This is explained by the fact that spontaneous transitions from high atomic states (starting with the third) can occur not only into the first state, but also into others. Therefore photons in the lines being considered are converted into other photons (in particular, into L_α quanta) after a small number of scatterings.

The situation with L_α line radiation is different. From the second atomic state a spontaneous transition occurs only into the first state with the emission of an L_α photon, and transitions from the latter, due to the interaction of radia- /355
tion and collisions, occur extremely rarely (under nebula conditions they are infrequent even from metastable states). Therefore an L_α photon that is formed cannot vanish in the nebula. However this photon will escape from the nebula only after a large number of scatterings because of the very great optical thickness of the nebula in the L_α line. This leads to a very high density of L_α radiation in nebulae.

In considering the diffusion of L_α radiation in nebulae let us adopt the same geometrical model of a nebula as before (see Fig. 34). The radiative transfer equation at any frequency ν within a line can be written in the form

$$\cos\vartheta \frac{dI_\nu}{dr} = -n_1 k_\nu I_\nu + \varepsilon_\nu, \tag{27.25}$$

where k_ν is the absorption coefficient, calculated for one atom, and ε_ν is the volume emission coefficient.

The radiative equilibrium equation for L_α radiation can be derived from the steady-state equation for the second level of the hydrogen atom. As we know, hydrogen atoms enter the second state as the result of absorption of L_c photons and subsequent recombinations. Each recombination at a high level (starting with the second) leads to the entry of an atom into the second state. Therefore

as the steady-state equation for this state we have

$$n_2 A_{21} = n_1 B_{12} \rho_{12} + n_e n^+ \sum_2^\infty C_i. \tag{27.26}$$

It is obvious that

$$n_2 A_{21} = \frac{4\pi}{h\nu_{12}} \int \varepsilon_\nu \, d\nu \tag{27.27}$$

and

$$B_{12}\rho_{12} = \frac{1}{h\nu} \quad k_\nu d\nu \quad I_\nu \, d\omega, \tag{27.28}$$

where $h\nu_{12}$ is the energy of an L_α quantum. Moreover, using Eq. (27.9), we obtain

$$n_e n^+ \sum_2^\infty C_i = \frac{1-p}{n} n_e n^+ C_1 = 4\pi \frac{1-p}{p} n_1 k_{1\nu_1} S_c(\tau), \tag{27.29}$$

where the function $S_c(\tau)$ is defined by Eq. (27.16). Substitution of the last three relations into Eq. (27.26) gives

$$\int \varepsilon_\nu d\nu = n_1 \int k_\nu d\nu \int I_\nu \frac{d\omega}{4\pi} + \frac{1-p}{n} n_1 k_{1\nu_1} S_c(\tau) h\nu_{12}. \tag{27.30}$$

As explained in the theory of absorption line formation (in Section 11), radiation diffusion in a spectral line is accompanied by a frequency redistribution of the radiation during an elementary scattering act. As a good approximation to reality one can assume complete frequency redistribution of the radiation (or completely noncoherent scattering), for which the emission coefficient ε_ν is proportional to the absorption coefficient k_ν. After making such an assumption, we can represent the quantity ε_ν in the form /356

$$\varepsilon_\nu = n_1 k_\nu S, \tag{27.31}$$

where S is frequency independent.

In fulfilling the relation (27.31) the radiative transfer Eq. (27.25) and the radiative equilibrium Eq. (27.30) can be rewritten as:

$$\cos\vartheta \frac{dI_\nu}{dr} = n_1 k_\nu (S - I_\nu) \tag{27.32}$$

and

$$S \int k_\nu \, d\nu = \int k_\nu \, d\nu \int I_\nu \frac{d\omega}{4\pi} + \frac{1-p}{p} k_{1\nu_1} S_c h\nu_{12}. \tag{27.33}$$

Let us denote the absorption coefficient at the center of the L_α line by k_0 and let us introduce the nebular optical distances:

$$t = \int_{r_1}^{r} n_1 k_0 \, dr, \qquad t_0 = \int_{r_1}^{r_2} n_1 k_0 \, dr. \tag{27.34}$$

Moreover, let us represent the absorption coefficient in the form

$$k_\nu = k_0 \alpha(x), \tag{27.35}$$

where x is a dimensionless frequency, representing the ratio of the distance from the line center to the Doppler half-width of the line, i.e.,

$$x = \frac{\nu - \nu_0}{\Delta\nu_D}. \tag{27.36}$$

For the notations that have been adopted, instead of Eqs. (27.32) and (27.33) we have

$$\cos\vartheta \frac{dI_\nu}{dt} = \alpha(x)(S - I_\nu) \tag{27.37}$$

and

$$S = A \int_{-\infty}^{+\infty} \alpha(x) dx \int I_\nu \frac{d\omega}{4\pi} + \frac{1-p}{n} \frac{Aqh\nu_{12}}{\Delta\nu_D} S_c(\tau), \tag{27.38}$$

where

$$q = \frac{k_{1\nu_1}}{k_0} \text{ and } A \int_{-\infty}^{+\infty} \alpha(x) dx = 1. \tag{27.39}$$

Equations (27.37) and (27.38) must be solved with boundary conditions analogous to (27.15). Using these conditions, from the equations presented we obtain the following integral equation for determining the function S(t):

$$S(t) = \frac{1}{2} \int_0^{t_0} [K(|t-t'|) + K(t+t')] S(t') dt' + S_0(t), \tag{27.40}$$

where

$$K(t) = A \int_{-\infty}^{+\infty} \alpha^2(x)\, \mathrm{Ei}\,[t\alpha(x)]dx \tag{27.41}$$

and

$$S_0(t) = \frac{1-p}{p} \frac{Aqh\nu_{12}}{\Delta\nu_D} S_c(\tau). \tag{27.42}$$

Let us note that an obvious relationship exists between the optical distances t and τ:

$$\tau = qt, \qquad \tau_0 = qt_0. \tag{27.43}$$

As calculations show, $q \approx 10^{-4}$. Therefore we see that when the nebular optical thickness immediately beyond the Lyman series limit is of the order of unity (such τ_0 values must be assumed for the H II zone), the nebular optical thickness at the L_α line center will be of the order of ten thousand.

Calculation of the function S(t) from Eq. (27.40) completely determines the L_α radiation field in the nebula since then the radiation intensity $I_\nu(t, \vartheta)$ can be found from Eq. (27.37). Other physical quantities, associated with L_α radiation, can also be expressed in terms of the function S(t). For example, from Eqs. (27.27) and (27.31) we obtain the following expression for the degree of excitation of the second level of the hydrogen atom:

$$\frac{n_2}{n_1} = \frac{g_2}{g_1} \frac{c^2}{2h\nu_{12}^3} S(t). \tag{27.44}$$

Here we have also made use of Eqs. (8.12) and (8.5).

The kernel of the integral Eq. (27.40) is expressed in terms of the function K(t), which in turn depends on the quantity $\alpha(x)$. Therefore the desired function S(t) will depend intrinsically on the quantity $\alpha(x)$, characterizing the absorption coefficient profile. /358

A rectangular absorption coefficient profile was initially assumed in the theory of L_α radiation diffusion in nebulae, i.e., it was assumed that $\alpha(x) = 1$ for $|x| \leq 1$ and $\alpha(x) = 0$ for $|x| > 1$. In this case Eq. (27.40) has the form

$$S(t) = \frac{1}{2} \int_0^{t_0} [\mathrm{Ei}\,|t-t'| + \mathrm{Ei}\,(t+t')] S(t')\, dt' + S_0(t). \tag{27.45}$$

We will not concern ourselves here with the solution of this equation, and we will only point out that very large values are obtained for the L_α radiation

density in the nebula. This means that the L_α photon undergoes a very large number of scatterings in the nebula; namely, the average number of scatterings turns out to be of the order of the square of the optical thickness of the nebula at the L_α line center, i.e.,

$$N \approx t_0^2. \tag{27.46}$$

Consequently, for $t_0 \approx 10^4$, $N \approx 10^8$.

However, the assumption of a rectangular absorption coefficient profile is very crude. In reality the absorption coefficient is maximum at the line center and decreases gradually as one goes out from the center. Because of this, the diffusion of spectral line radiation possesses the following special property. Each photon, absorbed at any point of the nebula, can then be emitted at any distance from the line center (since $\varepsilon_\nu \sim k_\nu$). In particular, it can be emitted with such a frequency that the optical thickness of the nebula at this frequency will be much less than unity (i.e., $t_\nu^0 = t_0\alpha(X) \ll 1$). Such a photon leaves the nebula unhindered. Consequently, for each photon, absorbed at any point of the nebula, there is a definite probability of escaping outside the nebula immediately after re-emission. Such a process obviously cannot occur in the case of a rectangular profile absorption coefficient. In this case the photon escapes from the nebula only after a lengthy diffusion, approaching the edge of the nebula.

This special feature of the diffusion of spectral line radiation makes it possible to easily obtain an approximate solution of Eq. (27.40). From what has been said above it follows that an L_α photon, appearing at any point of the nebula, escapes out of it after diffusion within a relatively small region. Consequently, the L_α radiation density at a given point depends little on the radiation density /359
in portions of the nebula far removed from it. Therefore in Eq. (27.40) for an approximation we can remove the value of the function $S(t')$ for $t' = t$ outside the integral sign. After doing this, we obtain

$$S(t)\left[1-\int_0^\infty K(u)\,du+\frac{1}{2}\int_{t_0-t}^\infty K(u)\,du+\frac{1}{2}\int_{t_0+t}^\infty K(u)\,du\right]=S_0(t). \tag{27.47}$$

But from (27.41) it follows that

$$\int_0^\infty K(u)\,du = 1. \tag{27,48}$$

Therefore from (27.47) we obtain

$$S(t)=\frac{2S_0(t)}{L(t_0-t)+L(t_0+t)}, \tag{27.49}$$

where

$$L(t) = \int_t^{\infty} K(u)\,du = A \int_{-\infty}^{+\infty} \alpha(x) E_2[\alpha(x) t]\,dx, \tag{27.50}$$

and $E_2 t$ is the second integral exponential function.

It is easy to see that the quantity $1/2[L(t_0 - t) + L(t_0 + t)]$ represents the fraction of L_α photons, leaving the nebula, of the total number of L_α photons emitted at an optical distance t from the inner boundary of the nebula. Consequently, Eq. (27.49) expresses the equality between the number of L_α quanta, originating in a given volume of L_c radiation, and the number of L_α photons being emitted by this volume and leaving the nebula.

We can assume that the ratio $S(t)/S_0(t)$ approximately defines the average number of scatterings undergone by an L_α photon originating at an optical distance t. From Eq. (27.49) it follows that this number is approximately equal to

$$N(t) = \frac{2}{L(t_0 - t) + L(t_0 + t)}. \tag{27.51}$$

Equation (27.51) is also easily understood on the basis of the physical significance of the quantity L(t).

As an example let us consider the case when the absorption coefficient has a Doppler profile, i.e., $\alpha(x) = e^{-x^2}$. In this case /360

$$K(t) = \frac{2}{\sqrt{\pi}} \int_0^{\infty} e^{-2x^2} \mathrm{Ei}(te^{-x^2})\,dx \tag{27.52}$$

and

$$L(t) = \frac{2}{\sqrt{\pi}} \int_0^{\infty} e^{-x^2} E_2(te^{-x^2})\,dx. \tag{27.53}$$

For $t \gg 1$, the following asymptotic formulas result from (27.52) and (27.53):

$$K(t) = \frac{1}{2\sqrt{\pi}\, t^2 \sqrt{\ln t}} \tag{27.54}$$

and

$$L(t) = \frac{1}{2\sqrt{\pi}\, t \sqrt{\ln t}}. \tag{27.55}$$

Substituting Eq. (27.55) into Eqs. (27.49) and (27.51), we obtain approximate formulas for the quantities S(t) and N(t), respectively. In particular, the average number of scatterings of an L_α photon, originating at the inner boundary of the nebula, is approximately equal to

$$N(0) = 2\sqrt{\pi t_0}\sqrt{\ln t_0}. \tag{27.56}$$

We see that Eq. (27.56) gives much smaller values for the quantity N than does Eq. (27.46). For example, for $t_0 = 10^4$ a value of $N \approx 10^5$ is obtained from Eq. (27.56) instead of the value of 10^8 given by Eq. (27.46). Such a result is completely understandable: for a Doppler profile absorption coefficient the photon can escape at the outer portions of the line upon emission at any point of the nebula, whereas for a rectangular profile absorption coefficient it is deprived of this possibility. In addition it should be noted that the average number of L_α photon scatterings in a nebula, given by Eq. (27.56), remains very large nevertheless. This is explained by the smallness of the fraction of photons which can escape from the nebula in the outer portions of the line (i.e., at the point where $t_0\alpha(x) \ll 1$) for a large nebular optical thickness at the line center.

If the function S(t) is known, then with the aid of Eq. (27.37) one can find the intensity of the L_α line radiation leaving the nebula, i.e., the quantity $I_\nu(t, \vartheta)$, and also the radiation flux $H_\nu(t_0)$ that is leaving. The L_α line profile in the nebular spectrum is determined in this manner. As explained, L_α photons leave the nebula primarily in the outer portions of the line. Therefore the L_α line should have /361
a double-peaked profile. It is obvious that the separation of the peaks will be greater, the greater the optical thickness t_0 of the nebula.

The problem of the diffusion of L_α radiation in a nebula for complete frequency redistribution of the radiation and for a Doppler profile absorption coefficient was first considered in Zanstra's paper [22]. This same problem was subsequently considered for more general assumptions. In particular, the true radiation frequency redistribution law, expressed by Eq. (11.1), was used. In addition, the methods of the modern multiple scattering theory of radiation, discussed in Section 3, were used in solving this problem (see [23, 24], etc.).

It should also be noted that we encounter the problem of the diffusion of resonance line radiation in a number of fields of physics (in particular, in plasma physics and in gas discharge theory). An integral equation of the type (27.40), in which the function K(t) is defined by Eq. (27.52), applies to these cases also. L. M. Biberman [25] first derived such an equation, and it has then been investigated by many authors.

3. L_α radiation field in an expanding nebula. Until now we have assumed that the nebula is stationary. In reality different portions of nebulae can move with respect to each other. In particular, as already stated, planetary nebulae expand with velocities of the order of several tens of kilometers per second.

The relative motion of matter in nebulae should be taken into consideration in discussing the diffusion of radiation in them. The motion of matter affects the radiation field because of the Doppler effect. This effect is obviously very small in the continuous spectrum case, but very large in the case of spectral lines.

Let us now examine the diffusion process for L_α radiation in an expanding nebula. Here, just as before, we will represent the nebula in the form of a thin spherical layer.

Let us first assume that the expansion velocity v is independent of the distance r from the center of the star. In this case the expansion of the nebula will be expressed in the statement of the boundary condition for $r = r_1$. When we were considering a stationary nebula, then we assumed that the intensity of the radiation leaving the nebula through the inner boundary is exactly equal to the intensity of the radiation entering the nebula in the opposite direction. In the case of an expanding nebula, however, these two radiations are displaced in frequency with respect to each other so that this equality will not be true. If we assume that the expansion velocity is much greater than the average thermal velocity of an atom /362
(i.e., $v \gg u$), then the radiation coming into the nebula from its opposite side will no longer be absorbed in the nebula. Therefore the intensity of this radiation can be considered equal to zero. Thus, instead of the boundary conditions (27.15), existing for a stationary nebula, we must write the following boundary conditions for a nebula expanding with a high velocity:

$$\left.\begin{aligned} I_\nu(0,\vartheta) &= 0 \text{ for } \vartheta < \frac{\pi}{2}, \\ I_\nu(t_0,\vartheta) &= 0 \text{ for } \vartheta > \frac{\pi}{2}. \end{aligned}\right\} \tag{27.57}$$

If, of course, the expansion velocity of the nebula is comparable to the average thermal velocity of an atom, then the first of these conditions must be suitably altered.

From Eqs. (27.37) and (27.38) for the boundary conditions (27.57) we obtain the following integral equation for determining the function S(t):

$$S(t) = \frac{1}{2}\int_0^{t_0} K(|t-t'|)S(t')\,dt' + S_0(t), \tag{27.58}$$

where the function K(t) is defined by Eq. (27.41). The approximate solution of this equation has the form

$$S(t) = \frac{2S_0(t)}{L(t)+L(t_0-t)} \tag{27.59}$$

where L(t) is given by Eq. (27.50). The L_α radiation density in an expanding nebula will obviously be less than in a stationary one.

We will now assume that the expansion velocity of the nebula depends on r. In this case the Doppler effect must be taken into account in the radiative transfer equation and in the radiative equilibrium equation (see [26]).

Let us consider radiation of frequency ν, the direction of which forms an angle ϑ with the normal to the plane-parallel layers of the nebula. Along this path the central frequency for the absorption coefficient will vary in accordance with the relationship

$$\nu_0' = \nu_0 + \nu_0 \frac{v(t)}{c} \cos\vartheta, \tag{27.60}$$

where ν_0 is the central line frequency for a stationary observer. Therefore the absorption coefficient can be represented in the form

$$k_\nu = k_0 a\left(\frac{\nu - \nu_0'}{\Delta\nu_D}\right) = k_0 a\left[x - \frac{v(t)}{u}\cos\vartheta\right] \tag{27.61}$$

where it has been taken into consideration that $x = \frac{\nu - \nu_0}{\Delta\nu_D}$ and $\nu_0 \frac{u}{c}$. Assuming, as before, that radiation diffusion is accompanied by a frequency redistribution during the elementary scattering act, we take Eq. (27.31) for the emission coefficient ε_ν. On the basis of what has been said, we have

$$\cos\vartheta \frac{dI_\nu}{dt} = a\left[x - \frac{v(t)}{u}\cos\vartheta\right](S - I_\nu). \tag{27.62}$$

as the radiative transfer equation. The radiative equilibrium equation will now have the form

$$S(t) = A\int_{-\infty}^{+\infty} dx \int a\left[x - \frac{v(t)}{u}\cos\vartheta\right] I_\nu \frac{d\omega}{4\pi} + S_0(t). \tag{27.63}$$

For v = 0 the last two equations transform into Eqs. (27.37) and (27.38).

An integral equation for determining the function S(t) can be derived from Eqs. (27.62) and (27.63) for the boundary conditions (27.15) or (27.57). For simplicity we assume that the expansion velocity v increases linearly with an increase in the optical distance t, i.e., v(t) = v(0) + dv/dt· t, where dv/dt = const and dv/dt > 0. Then the function S(t) will be defined by Eq. (27.40) or (27.58), in which the function K(t) is equal to

$$K(t) = A\int_0^1 \frac{d\mu}{\mu} \int_{-\infty}^{+\infty} a(x)\, a(x + \gamma t\mu)\, e^{-\int_0^t a(x+\gamma t\mu)\frac{dx}{\mu}}\, dx, \tag{27.64}$$

where

$$\gamma = \frac{1}{u}\frac{dv}{dt}. \tag{27.65}$$

An approximate solution of the equations cited is given by Eqs. (27.49) or (27.59), in which

$$\begin{aligned} L(t) &= A\int_0^1 d\mu \int_{-\infty}^{+\infty} a(x)\, e^{-\int_0^t a(x+\gamma z\mu)\frac{dz}{\mu}}\, dx = \\ &= A\int_0^1 d\mu \int_{-\infty}^{+\infty} a(x)\, e^{-\frac{1}{\gamma\mu^2}\int_x^{x+\gamma t\mu} a(y)\,dy}\, dx. \end{aligned} \tag{27.66}$$

In gaseous nebulae the quantity γ is usually very small, and the quantity t is very large. Let us therefore consider two special cases of Eq. (27.66).

1. We will assume that $\gamma t \ll 1$, i.e., the nebula is expanding with a small velocity gradient. In the limiting case we can set $\gamma = 0$. Then Eq. (27.66) transforms into Eq. (27.50), and the L_α radiation field in the nebula is determined by the escape of photons in the line wings from it (in the same manner as was considered in detail above).

2. Let us assume that $\gamma t \gg 1$, i.e., the velocity gradient in the nebula is large. In the limiting case we set $t = \infty$. Then it will be impossible for photons in the line wings to escape, and the L_α radiation field in the nebula is determined by the escape of photons from it because of the Doppler effect. In the case given Eq. (27.66) assumes the form

$$L = A\gamma \int_0^1 \left(1 - e^{-\frac{1}{A\gamma\mu^2}}\right)\mu^2 d\mu. \tag{27.67}$$

When $A\gamma \ll 1$, from (27.67) we obtain

$$L = \frac{1}{3}A\gamma. \tag{27.68}$$

It should be noted that the quantity $A\gamma$ does not depend on the absorption coefficient profile. In fact, we have

$$\int k_\nu d\nu = k_0 \Delta\nu_D \int_{-\infty}^{+\infty} a(x)\,dx = \frac{k_0 \nu_0 u}{cA}. \tag{27.69}$$

Therefore, using Eq. (8.12), we obtain

$$\frac{k_0 u}{A} = hB_{12}. \tag{27.70}$$

Consequently, /365

$$A\gamma = \frac{A}{n_1 u k_0}\frac{dv}{dr} = \frac{1}{n_1 h B_{12}}\frac{dv}{dr}. \tag{27.71}$$

In the case being considered the approximate expression for the function S(t) has the form

$$S(t) = \frac{3S_0(t)}{A\gamma}. \tag{27.72}$$

This formula, of course, can only be used for nebular regions far from the boundaries (as also, in general, the expressions for S(t) derived by the method that has been discussed).

It is of interest to ascertain under what conditions these special cases of Eq. (27.66) occur in reality. As already established, the answer to this problem depends on the value of the quantity

$$\delta = \gamma t = \frac{t}{u}\frac{dv}{dt}. \tag{27.73}$$

If $\delta \gg 1$, then line photons leave the nebula primarily because of the Doppler effect, and the function S(t) is defined by Eq. (27.72). If, however, $\delta \ll 1$, then photons leave the nebula primarily in the line wings. This conclusion is completely understandable since the quantity δ, on the basis of Eqs. (27.55) and (27.68), is equal (in order of magnitude) to the ratio of the fraction of photons, leaving the nebula because of the Doppler effect, and the fraction of photons leaving in the line wings.

We can rewrite Eq. (27.73) in the form

$$\delta = \frac{\Delta r}{r}\cdot\frac{dv}{dr}, \tag{27.74}$$

where Δr is the nebula thickness. It is very difficult to evaluate the quantity dv/dr; however, it must be remembered that for real nebulae $\overline{dv}/ds$ must be taken instead of dv/dr, i.e., the velocity gradient averaged over all directions. As will be shown in Section 28, $\overline{dv}/ds \approx v/r$ in nebulae always (because of the curvature of the layers). Therefore instead of Eq. (27.74) we obtain

$$\delta \approx \frac{\Delta r}{r}\frac{v}{u}. \tag{27.75}$$

We will apply Eq. (27.75) to planetary nebulae. Since the nebular thickness amounts to a few tenths of its radius, and the nebular expansion velocity is several times greater than the average thermal velocity of an atom, then in the case given δ is of the order of unity. Consequently, the function L(t) is defined by Eq. (27.66) itself, and not by its limiting cases. In other words, the escape of a photon in the line wings, as well as the escape because of the Doppler effect, must be taken into consideration in determining the L_α radiation field in a nebula. /366

Also of interest is the problem of finding the L_α radiation field in the envelopes of novae. The expansion velocity of these envelopes is much greater than the expansion velocity of planetary nebulae. Therefore the inequality $\delta \gg 1$ will be satisfied in the given case. Consequently, the L_α radiation field in nova envelopes is determined primarily by the escape of photons from the envelope because of the Doppler effect.

4. Radiation pressure in nebulae. The determination of the L_α radiation field in the nebula gives the possibility of calculating the pressure caused by this radiation. V. A. Ambartsumyan [21] first made such a calculation, indicating the large role of the L_α radiation pressure in the dynamics of nebulae. The intensity of the radiation pressure is especially large at the boundaries of the nebula, where the radiation flux reaches a maximum value. The intensity of the radiation pressure is different at the boundaries of stationary and expanding nebulae. If the nebula is stationary, then the L_α radiation flux at the inner boundary is equal to zero and the radiation pressure acts only at the outer boundary with it being directed outward. In an expanding nebula, however, the radiant flux differs from zero not only at the outer but also at the inner boundary. In the given case, therefore, the radiant pressure acts at both boundaries, with it being directed from the star at the outer boundary, and toward the star at the inner boundary. In both cases the L_α radiation diffusing in the nebula leads to an increase in the thickness of the nebula by its very pressure.

The radiation pressure force in the L_α line, acting per unit volume in 1 sec, is equal to

$$f_r = \frac{n_1}{c} \int k_\nu H_\nu d\nu \tag{27.76}$$

where n_1 is the number of hydrogen atoms in 1 cm^3, k_ν is the absorption coefficient calculated for one atom, H_ν is the radiant flux and c is the velocity of light.

At first we will assume that the nebula is stationary or is expanding with no velocity gradient. For a rectangular profile absorption coefficient instead of Eq. (27.76) we have /367

$$f_r = \frac{n_1 k_0 H}{c}, \tag{27.77}$$

where H is the total radiant flux in the L_α line. A determination of the quantity f_r from Eq. (27.77) for the nebular boundaries is not difficult since the number of L_α photons, leaving the nebula, is equal to the number of stellar L_c photons, absorbed in the nebula. Calculations show that under the influence of radiation pressure in the L_α line the outer portions of a stationary nebula should undergo an acceleration of about 1 km/sec in 10 years. The layers of an expanding nebula, nearest the star, should undergo a deceleration of approximately the same magnitude.

As we know, however, the assumption of a rectangular absorption coefficinet profile is very crude. In reality the radiation pressure force in the L_α line must be determined not from Eq. (27.77), but from Eq. (27.76). In this situation the problem of the diffusion of line radiation must be solved beforehand for the real absorption coefficient profile and when the radiation frequency redistribution is taken into account. As explained previously, during radiation diffusion there occurs a transition of photons from the central portions of the line into its wings. Therefore for a large nebular optical thickness at the center of the L_α line the radiant flux H_ν is great in the line wings and small in its central portions. On the other hand the absorption coefficient k_ν is large in the central portions of the lines and small in its wings. Because of what has been said, Eq. (27.76) gives a much lower value for the radiation pressure force at the boundary of the nebula than does Eq. (27.77) (by about a factor of 100, according to Zanstra's calculations [22], for a nebular optical thickness of about 10^4 at the center of the L_α line).

In a nebula, expanding with a velocity gradient, the radiation pressure force in the L_α line will also be much less than the value found from Eq. (27.77) (see [26]).

To explain the meaning of the results obtained, it must be borne in mind that a planetary nebula cannot exist for a long time. Because of the nebula expansion the density in it decreases and the nebula ceases to be visible. If the nebula is expanding with a velocity of 30 km/sec, then during a time of about 10^4 years its radius becomes about 10^{18} cm, and its density—about 10^{-24} g/cm^3, i.e., about the same as the average density of interstellar space. During this same time, as follows from these calculations, the radiation pressure in the L_α line can give rise to a velocity difference of about 10 km/sec in the nebula. Even through this effect is not very great, it must be taken into consideration in the solution of certain problems.

The results that have been presented apply to a nebula which has no H I zone. In such nebulae most of the hydrogen atoms are in an ionized state. On the other hand, only neutral hydrogen atoms are subject to the radiation pressure in the L_α line. Therefore the acceleration of a volume element, caused /368

by radiation pressure, is not very great. More precisely, this acceleration w is defined by the equation

$$(n_1 + n^+) m_H w = \frac{n_1}{c} \int k_\nu H_\nu d\nu, \tag{27.78}$$

and in the H II zone the inequality $n^+ \gg n_1$ is satisfied.

The opposite relation holds in the H I zone, i.e., $n_1 \gg n^+$. However, almost no L_α photons originate in this zone so that the radiant flux H_ν is very small. However, the radiation in the L_α line, coming from the H II zone, is not absorbed in the H I zone for the most part, and this means no radiation pressure is produced. This is explained by the fact that the Doppler line width $\Delta\nu_D$ in the H I zone is very small because of the smallness of the temperature T_e. Therefore the radiation pressure in the L_α line in the H I zone cannot be appreciable.

It is interesting to note that in nebulae having H II and H I zones the radiation pressure in the L_α line reaches a maximum in the transition region between these zones. As calculations show, in those cases when the mass of the H I zone is relatively small, the radiation pressure can even cause this zone to move with respect to the H II zone. In the opinion of G. A. Gurzadyan [3] planetary nebulae, comprising two envelopes, are formed in this fashion.

G. A. Gurzadyan, engaging in a study of the spatial shapes of planetary nebulae, divided them into three groups: planet-like, two-envelope and ring-shaped. He assumes that these nebular types are successive stages in their development. As the nebula expands, its optical thickness beyond the Lyman series limit decreases. At first $\tau_0 \gg 1$, i.e., the nebula has H II and H I zones. At this time the nebula is planet-like. When the quantity τ_0 becomes of the order of unity, the H I zone begins to separate from the H II zone due to the effect of radiation pressure in the L_α line. The two-envelope nebula is formed in this situation. With further expansion of the nebula the second envelope disperses and ceases to be visible. The first envelope (for which $\tau_0 \ll 1$), receding at a great distance from the star, is observed by us in the form of a ring. This representation of the evolution of planetary nebulae is corroborated by several facts. One of them is that nebular sizes increase, on the average, as one goes from planet-like nebulae, to two-envelope, and then to ring-shaped.

Thus, we see that the radiation pressure in the L_α line can cause appreciable relative displacements in nebulae. This is explained both by the large number of L_α photons in the nebula, and also by the large value of the absorption coefficient at the L_α line. As we know, certain effects, associated with radiation diffusion (the drift of photons into the line wings, the Doppler effect /369

caused by the presence of a velocity gradient), reduce the L_α radiation pressure in nebulae, but it still remains significant.

Besides the radiation pressure in the L_α line, the L_c radiation pressure also plays some role in nebulae. However, unlike the L_α radiation pressure which causes relative movements in the nebula, the radiation pressure in the Lyman continuum causes an accelerated expansion of the entire nebula. It is obvious that the magnitude of this acceleration is defined by the equation

$$Mw = \frac{E_c}{c}, \tag{27.79}$$

where M is the mass of the nebula and E_c is the energy emitted by the star in the Lyman continuum in 1 sec (or a portion of this energy if the optical thickness of the nebula beyond the Lyman series limit does not exceed unity). The quantity w can easily be calculated. As we know, the mass of a planetary nebula is about 0.01 $M_\odot$, and the quantity E_c should be of the order of 10^{36} ergs/sec. Therefore from Eq. (27.79) we find that the expansion velocity of the nebula should increase by about 1 km/sec in 1000 years due to the effect of the L_c radiation pressure, i.e., by a fairly noticeable amount during the lifetime of the nebula. One can assume that this conclusion is confirmed by observational data since the expansion velocity v of the nebula is greater, on the average, the smaller the value of the dilution factor in the nebula.

The observed expansion of planetary nebulae renders the assumption that a nebula forms as the result of a star shedding its outermost layers very probable. As confirmation of this hypothesis one can mention the fact that the mass of the nebula amounts to only a small fraction of the mass of the star. At the present time, however, we are unable to explain the stellar catastrophe which leads to the formation of a planetary nebula. At one time it was thought that nebulae originate in the outbursts of novae or supernovae. A comparison of the expansion velocities of the envelopes that are ejected (about 1000 km/sec) with the expansion velocities of nebulae (which are only about 10 km/sec) contradicts /370
this notion. Moreover, the mass of nova envelopes is much less (by about 1000 times) than the mass of a planetary nebula. In view of this the assumption was expressed that planetary nebulae are formed in the detachment of an envelope with a low velocity from any unstable stars (for example, from red supergiants). An entirely different point of view consists of the fact that the planetary nebula, along with its nucleus, originates from prestellar matter (see [3]).

It should again be noted that the cosmogonic role of planetary nebulae is evidently quite significant. Up to the present time about 300 such nebulae have been observed; however, their total number in the Galaxy is probably at least 10,000. As a nebula expands, it ceases to be visible and, as already mentioned, the average lifetime of a nebula is about 10,000 years. From this it follows that on the average one nebula vanishes (i.e., it becomes unobservable) each year in the Galaxy. Moreover, each year one nebula must obviously form. And since

the age of our Galaxy is about 10^{10} years, then in all the Galaxy about 10^{10} nebulae should have formed (and then vanished). We can, therefore, conclude that a considerable number of the stars were once the nuclei of planetary nebulae.

REFERENCES

1. Vorontsov-Vel'yaminov, B. A. Gaseous nebulae and novae, Izd-vo AN SSSR, 1948.
2. Aller, L. H. Gaseous Nebulae, 1956.
3. Gurzadyan, G. A. Planetary nebulae, Fizmatgiz, 1962.
4. Bowen, I. The origin of the nebular lines and the structure of the planetary nebulae, Ap. J. 67, 1, 1928.
5. Shayn, G. A. and V. F. Gaze. Some results of a study of luminous galactic nebulae, Izv. Krymskoy astrofiz. obs. 6, 3, 1951; Second list of diffuse nebulae, Izv. Krymskoy astrofiz. obs. 7, 93, 1951.
6. Zanstra, H. The radiation processes of planetary nebulae and the temperatures of the central star, Zs. f. Astrophys. 2, 1, 1931.
7. Cillié, G. The theoretical capture spectrum of hydrogen, MN 96, 771, 1936.
8. Sobolev, V. V. Determination of the electron temperatures of planetary nebulae and refinement of the temperatures of their nuclei, Trudy Astron. obs. LGU 12, 3, 1941.
9. Menzel, D. et al., Physical processes in gaseous nebulae, Izd-vo inostr. lit., 1948.
10. Seaton, M. J. The solution of capture-cascade equation for hydrogen, MN 119, 90, 1959.
11. Nikitin, A. A. An investigation of the recombination spectrum of stars and nebulae, Vestn. Leningr. un-ta, No. 1, 1963.
12. Chamberlain, J. W. Collision exitation of hydrogen in a gaseous nebulae, Ap. J. 117, 387, 1953.
13. Ambartsumyan, V. A. Theoretical astrophysics, GONTI, 1939.
14. Shklovskiy, I. S. A new scale of distances to planetary nebulae, Astron. Zh. 33, No. 2, 1956.
15. Ambartsumyan, V. A. The excitation of the metastable states in the gaseous nebulae, Tsirk. Pulkovskoy obs., No. 6, 1933. /371
16. Seaton, M. J. Electron temperatures and electron densities in planetary nebulae, MN 114, 154, 1954.
17. Seaton, M. J. and D. E. Osterbrock. Relative [OII] intensities in gaseous nebulae, Ap. J. 125, 66, 1957.
18. Greenstein, J. L. Continuous emission in the Orion nebula, Ap. J. 104, 414, 1946.
19. Kipper, A. Ya. The continuous spectrum of planetary nebulae, Coll. "The growth of Soviet science in the Estonian SSR 1940-1950", 1950.
20. Spitzer, L. and J. Greenstein. Continuous emission from planetary nebulae, Ap. J. 114, 407, 1951.
21. Ambartsumyan, V. A. On the radiative equilibrium of a planetary nebula, Izv. Pulkovskoy obs., 13, 31, 1933.
22. Zanstra, H. On scattering with redistribution and radiation pressure in a stationary nebula, Bull. Astr. Inst. Netherlands, XI, N 401, 1949.
23. Sobolev, V. V. The scattering of frequency-shifted radiation, Vestn. Leningradsk. un-ta, No. 5, 1955; No. 11, 1955; No. 19, 1957.

24. Ivanov, V. V. The scattering of resonance emission in stellar and nebular atmospheres, Astron. Zh., 39, 1020, 1962; 40, 257, 1963.
25. Biberman, L. M. Theory of resonance emission scattering, ZhETF, 17, 416, 1947.
26. Sobolev, V. V. Scattering of L_α emission in nebular and stellar envelopes, Astron. Zh. 34, 694, 1957.

CHAPTER VI

VARIABLE STARS

The vast majority of stars exhibit absorption spectra that do not change with time. The atmospheres of these stars have been examined in detail in Chapters I and II. In accordance with observational data it was assumed that there were no nonstationary processes in the atmospheres. The example of the Sun, to be sure, indicates that such processes do occur in reality (spots, prominences, etc.). They occur, however, on a relatively small scale and they have no effect on the observable characteristics of the star as a whole. /372

At the same time, a large number of stars with drastic and rapid changes in spectrum and brightness have been detected by observers. A characteristic feature of these stars is the presence of bright lines in their spectra. It is obvious that nonstationary processes are occurring on an appreciable scale in the outer layers of these stars. As detailed investigations have shown, these processes are associated with the ejection of large amounts of matter from the star. As a result, an expanding envelope, in which bright spectral lines also originate, is formed around the star.

Stars, ejecting matter, are extremely diverse. Some stars eject matter more or less continuously over a long time. Among these, in particular, are the Wolf-Rayet, P Cygni and Be types. In other cases the ejection of material from the star is explosive in nature. We encounter such a process in the outbursts of novae. Especially large amounts of matter and energy are evolved in the outburst of a supernova, representing one of the most magnificent phenomena in the Galaxy.

Stars of these types are the most outstanding representatives of variable stars. Their study constitutes a very important problem of astrophysics since it contributes, to a large degree, to an explanation of the nature of stars and of the course of their evolution.

The physical conditions in the envelopes of variable stars are similar in certain respects to the conditions in gaseous nebulae. Therefore, in the dis- /373

cussion of variable stars we will frequently make use of the results set forth in the preceding chapter.

28. Stars with Bright Spectral Lines

1. Early class stars with bright lines. Stellar spectra with bright lines predominantly belong either to the very earliest or very latest classes (we are not now speaking of novae and related stars). Of these, early class stars with bright lines, i.e., Wolf-Rayet, P Cygni and Be type stars, have been studied most thoroughly. This is explained primarily by the simplicity of the physical processes occurring in the atmospheres of these stars.

Wolf-Rayet (WR) type stars correspond to spectral class O in degree of atomic excitation and ionization. Their spectra consist of wide emission bands of H, He I, He II, C III, N III and other atoms with very high ionization potentials superimposed on a continuous background. Weak absorption lines are seen on the violet side of some of the bright bands. The width of the bright bands amounts to several tens of angstroms, and the intensity within a band is sometimes 10-20 times greater than the intensity of the continuous spectrum. Therefore the energy, emitted in the bright lines by the star, is comparable to the energy emitted in the continuous spectrum (in the visible or ultraviolet regions).

In the work of Beals [1] it was established that the spectra of WR stars are divided into two sequences: nitrogen and carbon. Bands of nitrogen in various stages of ionization are found in the spectra of the first sequence, but no carbon or oxygen bands; bands of carbon and oxygen in various stages of ionization are found in the spectra of the second sequence, but no nitrogen bands. The degree of atomic excitation and ionization is about the same in both sequences. Subsequently, WR type spectra with nitrogen and carbon bands were discovered. Nevertheless it should be assumed that the nitrogen lines are more intense in some WR spectra, in others—the carbon lines.

WR stars are often found to be components of spectroscopic binary systems. Some of them are eclipsing variables. The study of such systems has provided much valuable information on WR stars. Thus, it has been found that their masses are about 10 solar masses.

The absolute visual magnitudes of WR stars are about -3^m. These stars are some of the brightest objects of the Galaxy. However, novae, several years after outburst, and some nuclei of planetary nebulae also exhibit WR spectra. These stars are appreciably weaker than true WR stars. Their absolute visual /374
magnitudes are equal to $+5^m$, on the average.

P Cygni type stars, belonging to spectral class B, are adjacent to the WR stars. Bright lines, approximately symmetrical about their center frequencies and bounded by absorption lines on the violet side (Fig. 35a), are seen in the spectra of these stars, just as in the spectra of WR stars. In this case, however, unlike in the WR spectra the width of the bright lines is not so great and the absorption lines, on the other hand, are much more intense.

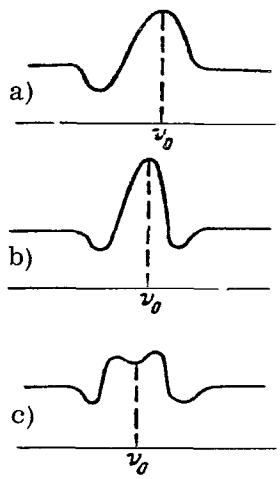

Figure 35.

Besides the P Cygni type stars, other stars of spectral class B also exhibit emission lines. They are simply called Be type stars. The line profiles in the spectra of type Be stars can be characterized in the following manner: a narrower emission line, which in some cases is a single line and in others—split (Fig. 35b and c), is superimposed on a broad and shallow absorption line. The spectra of type Be stars undergo pronounced changes with time. For example, the relative intensities of the bright line components vary. Sometimes the bright lines vanish completely and the type Be star becomes a normal class B star. Small variations in the stellar brightness are also observed along with the spectral changes.

The explanation of the emission spectra of the stars being considered is based on the hypothesis that material is ejected from the star, leading to the formation of an extended moving envelope around it. Since the emission dilution factor in the envelope is small, then, based on Rosseland's theorem (see Section 22), we can verify that the envelope should absorb the high-frequency photons coming from the star and convert them into low-frequency photons. In other words, the envelope emission occurs, in principle, the same as the emission of a gaseous nebula, i.e., because of the ultraviolet energy of the star. For the appearance of bright lines in the stellar spectrum it is clearly necessary that its temperature be quite high (greater than approximately 20,000°, as simple calculations show). Therefore the bright lines, appearing because of the ultraviolet energy of the star, are also observed only in the spectra of the hottest stars (classes O and B).

The nature of the ejection of material from the star can be judged from the profiles of the bright lines in the stellar spectra. After Beal's work [1] it has been assumed that there is a continuous ejection of material from type WR stars with an approximately constant intensity in all directions. Such a movement of matter must lead to the observed line profiles, symmetrical with respect to the center frequency. The material, receding from us, gives the portion of the line extending toward the red portion of the spectrum, and the material approaching us—the ultraviolet portion of the line. Since the spectra of type WR stars do not undergo pronounced changes with time, it must be assumed that the ejection of matter from them is stationary. /375

The explanation of the line profiles in the spectra of type Be stars is more complex. According to Struve [2] these stars are rotating very rapidly so that broad absorption lines are also observed in their spectra. Judging from the width of these lines, the rotational velocities of the stars at the equator amount to several hundred kilometers per second. Struve assumed that because of the rotation, matter is ejected from the equatorial plane of the star, leading to the formation of a gaseous ring rotating about the star. Bright lines, superimposed on broad absorption lines, also appear in the gaseous ring. Since the rotational velocity of the ring is less than the rotational velocity of the star (because of the

conservation of angular momentum), the bright line appears narrower than the absorption lines. In fact, the rapid rotation of type Be stars apparently contributes to the ejection of matter from them, but it is not the reason for the ejection. This follows from the fact that the emission spectrum of type Be stars undergoes irregular changes with time (and sometimes disappears entirely). Therefore the ejection of matter from these stars must exhibit an irregular character.

A theory for the formation of the spectral lines in the extended moving envelopes of stars is needed to interpret the spectra of type WR, P Cygni and Be stars (and of other variable stars). The fundamentals of the theory will be discussed below (for more details see [3] and [4]).

2. Emission line profiles. The envelope motion velocities usually amount to tens and hundreds of kilometers per second, i.e., they are much greater than the average thermal velocities of atoms. Therefore one can assume that the emission line profiles are determined primarily by the envelope movement. The effect of other factors on the line profile can be neglected in a first approximation.

Let us now derive a formula determining the emission line profile for an arbitrary field of velocities in the envelope. We will also take into consideration the possible opacity of the envelope to the emission line.

We will consider a line, arising through a transition from the k-th state in a given i-th atom. The absorption coefficient α_{ik} and the emission coefficient /376
ε_{ik} will be considered constant in the interval $\nu_{ik} - \Delta\nu_{ik}/2 < \nu < \nu_{ik} + \Delta\nu_{ik}/2$ and equal to zero outside this interval. Here ν_{ik} is the central frequency of the line, $\Delta\nu_{ik} = 2\frac{u}{c}\nu_{ik}$, where u is the average thermal velocity of an atom, c is the velocity of light.

Let us take an xyz coordinate system with origin at the center of the star and the z-axis pointed toward the observer. Let us denote the velocity of atoms in the envelope by v(x, y, z), and its projection on the z-axis by $v_z(x, y, z)$. We will assume that $v \gg u$.

It is clear that under the assumptions that have been made with respect to α_{ik} and ε_{ik}, radiation of frequency ν will be transmitted to the observer not by entire envelope but only by some region of it located on both sides of the plane of equal radial velocities, defined by the equation

$$\nu = \nu_{ik} + \frac{\nu_{ik}}{c} v_z(x, y, z). \tag{28.1}$$

The boundaries of this region are from the surface of (28.1) along the line of sight (i.e., along the z-axis) to a distance corresponding to a $\Delta\nu_{ik}/2$ change in

frequency. Denoting the limiting values of z by z_1 and z_2 and making use of the smallness of u with respect to v, we obtain

$$\Delta \nu_{ik} = \frac{\nu_{ik}}{c} \left| \frac{\partial v_z}{\partial z} \right| (z_2 - z_1), \tag{28.2}$$

or

$$z_2 - z_1 = \frac{2u}{\left| \frac{\partial v_z}{\partial z} \right|}. \tag{28.3}$$

Let $I_{ik}(x, y, \nu)$ be the intensity of the radiation coming from a point on the stellar disk with coordinates x, y at a frequency ν within the line. Since the "thickness" of the layer giving the emission at frequency ν (i.e., the distance $z_2 - z_1$) is relatively small (with the exception of isolated points), then the quantities α_{ik} and ε_{ik} can be assumed to be constant in this layer along the z-axis and equal to their values at the surface (28.1). Therefore, for the intensity $I_{ik}(x, y, \nu)$ we have

$$I_{ik}(x, y, \nu) = \frac{\varepsilon_{ik}}{\alpha_{ik}} [1 - e^{-\alpha_{ik}(z_2 - z_1)}]. \tag{28.4}$$

The total energy, emitted by the envelope at frequency ν into a unit solid angle, is given by the formula

$$E_{ik}(\nu) = \int\int I_{ik}(x, y, \nu)\, dx dy. \tag{28.5}$$

Using (28.3) and (28.4), instead of (28.5) we obtain

$$E_{ik}(\nu) = \iint \frac{\varepsilon_{ik}}{\alpha_{ik}} [1 - e^{-\frac{2u}{\left| \frac{\partial v_z}{\partial z} \right|} \alpha_{ik}}]\, dx\, dy. \tag{28.6}$$

The integration here is done over the surface (28.1). Equation (28.6) also defines the desired emission line profile.

As an approximation the envelope can be divided into two regions: opaque to radiation in the line being considered and transparent to this radiation. In the first region the quantity $\frac{2u}{\left| \frac{\partial v_z}{\partial z} \right|} \alpha_{ik}$ is greater than unity; in the second it is less than unity. The integral in (28.6) in the first region is equal to

$$E'_{ik}(\nu) = \int\int \frac{\varepsilon_{ik}}{\alpha_{ik}} dx\, dy, \tag{28.7}$$

and in the second

$$E''_{ik}(\nu) = \int\int \varepsilon_{ik} \frac{2u}{\left|\frac{\partial v_z}{\partial z}\right|} dx\, dy. \tag{28.8}$$

The quantities α_{ik} and ε_{ik} entering into these formulas are expressed in terms of the concentration n_i of absorbing atoms and the concentration n_k of emitting atoms in the follow manner:

$$\varepsilon_{ik} = \frac{n_k A_{ki} h\nu_{ik}}{4\pi\Delta\nu_{ik}}, \tag{28.9}$$

$$\alpha_{ik} = \frac{n_i B_{ik} h\nu_{ik}}{\Delta\nu_{ik} c}\left(1 - \frac{g_i}{g_k}\frac{n_k}{n_i}\right), \tag{28.10}$$

where A_{ki} and B_{ik} are the Einstein transition coefficients. Taking account of the relationship between A_{ki} and B_{ik}, we obtain

$$\frac{\varepsilon_{ik}}{\alpha_{ik}} = \frac{2h\nu_{ik}^3}{c^2} \frac{1}{\frac{g_k}{g_i}\frac{n_i}{n_k} - 1} \tag{28.11}$$

Equation (28.11), just as it should, passes over to Planck's formula when n_k/n_i is defined by the Boltzmann formula.

Thus, to calculate the emission line profile it is necessary to know both the velocity distribution in the envelope, as well as the distribution of absorbing and emitting atoms. It will be shown below how the quantities n_i and n_k can be found. Thereby the problem of calculating emission line profiles will finally be solved.

As an example of the application of Eqs. (28.7) and (28.8) let us find the profiles of emission lines, formed by an envelope that is expanding with a velocity that is constant for all layers (v = const). Let us denote the distance of a given volume from the center of the star by r, and the angle between the direction of motion of the atoms and the observer's direction—by ϑ. The we will have /378

$$v_z = v\cos\vartheta, \quad \frac{\partial v_z}{\partial z} = \frac{v}{r}\sin^2\vartheta, \tag{28.12}$$

and the surface of equal radial velocities, corresponding to frequency ν, will be defined by the equation

$$\nu = \nu_{ik} + \frac{\nu_{ik}}{c} v \cos \vartheta. \tag{28.13}$$

Let us first assume that the envelope is transparent to the line emission. Then from Eq. (28.8), taking into account that $dxdy = 2\pi \sin^2 \vartheta \, rdr$, we obtain

$$E''_{ik}(\nu) = 4\pi \frac{u}{v} \int \varepsilon_{ik} r^2 dr. \tag{28.14}$$

Thus, a transparent envelope gives an emission line with a rectangular profile (i.e., the intensity within the line is constant). The line width clearly corresponds to twice the envelope expansion velocity.

If the envelope is opaque to the line emission, then from Eq. (28.7) in the case being considered we obtain

$$E'_{ik}(\nu) = 2\pi \sin^2 \vartheta \int \frac{\varepsilon_{ik}}{\alpha_{ik}} r \, dr. \tag{28.15}$$

or, taking (28.13) into consideration,

$$E'_{ik}(\nu) = 2\pi \left[1 - \left(\frac{\nu - \nu_{ik}}{\nu_{ik}} \frac{c}{v} \right)^2 \right] \int \frac{\varepsilon_{ik}}{\alpha_{ik}} r \, dr. \tag{28.16}$$

Consequently, an opaque envelope gives an emission line with a parabolic profile.

The profiles of emission lines, formed by an envelope in which the expansion velocity v depends on r, can be determined analogously. As is easily understood, for a transparent envelope in this case the line profiles will be symmetrical with an intensity that decreases with distance from the line center (since they are obtained by the overlapping of rectangular profiles of various widths). These profiles are very similar to the profiles of lines formed by an opaque envelope for v = const. Therefore before drawing conclusions about the velocity distribution in the envelope from the line profiles, it is necessary to ascertain whether the envelope is transparent or opaque to line emission.

To answer this question, a few of the emission lines of one and the same atom in the stellar spectrum can be examined. In the case of a transparent envelope the profiles of all these lines must clearly be similar to each other. If, however, the envelope is partially opaque to line radiation, then different parts of the envelope will be opaque to different lines so that the profiles of the lines being considered should differ from each other. /379

In those cases when the envelope is close to the star (for example, when it is formed as a result of the stationary ejection of matter from the star), the effect of screening by the star of a part of the envelope must be taken into con-

sideration in determining the emission line profiles. The lines become asymmetrical because of this effect.

If the envelope is opaque to line radiation, then in that portion of the envelope that lies between the star and the observer, an absorption line forms. In the case of radial ejection of matter from the star, this line is shifted toward the violet end of the spectrum. The emission line, forming in the envelope, is partially superimposed on the absorption line.

With the aid of Eq. (28.6) one can also determine the profiles of emission lines formed by an envelope that is being ejected from a rotating star. This problem has significance for interpreting the spectra of type Be stars.

3. Emission line intensities. The intensities of emission lines for the gaseous nebula case were determined in Section 24. As we recall, the problem reduced to solving a system of linear algebraic equations

$$n_i \sum_{k=2}^{i-1} A_{ik} = \sum_{k=i+1}^{\infty} n_k A_{ki} + n_e n^+ C_i(T_e), \tag{28.17}$$

expressing the stationarity conditions for each of the excited atomic states. Here n_i, n_e, n^+ are the densities of atoms in the i-th state, free electrons and ions respectively, $n_e n^+ C_i(T_e)$ is the number of electron captures of ions at the i-th level in 1 cm^3 per 1 sec. In writing these equations it was assumed that the nebulae are transparent to radiation in the subordinate series lines since the degree of atomic excitation in nebulae is very low.

The emission lines in the spectra of WR, P Cygni and Be type stars arise, in principle, in the same way as the emission lines in nebular spectra, i.e., as a result of photonionization and recombinations. However, the degree of atomic excitation in the envelopes of the stars being discussed is not as low as in nebulae so that the envelopes can be opaque to radiation in the subordinate series lines. Therefore Eq. (28.17) cannot always be used to determine emission line /380 intensities in the stellar spectra. Generally speaking, in a given case a new system of equations must be formulated and solved, taking account of the opacity of the envelope for line radiation, i.e., including the radiative transfer equations for each line together with the stationarity equations for each level.

The need to take into consideration the envelope movement complicates the problem even more. If, however, the velocity gradient in the envelope is quite large (and in the envelopes being considered this is the case), then the problem is greatly simplified. This is explained by the fact that in the presence of a velocity gradient in the envelope line quanta can emanate not only from its boundary regions but also from the inner regions because of the Doppler effect. Roughly speaking, the envelope becomes transparent, to some degree, to the line radiation because of the velocity gradient. In this case the problem of determining the emission line intensities again reduces to some system of algebraic equations (but not linear, as in the case of nebulae).

In order to formulate the equations cited above, the following processes must be taken into consideration: 1) the ionization of atoms from each state due to the stellar radiation; 2) recombination at each level; 3) spontaneous transitions from upper states to lower; 4) transitions from lower states to upper through the absorption of photons in the lines emitted by the envelope.

The number of spontaneous transitions from the k-th into the i-th, occuring in 1 cm^3 in 1 sec, is equal to $n_k A_{ki}$. If the envelope is transparent to radiation in a given line, then the quanta emitted during this transition escape to the outside unhindered, and the reverse transitions do not occur at all. If the envelope is not transparent to the line radiation and there is no velocity gradient in it, then nearly all the line quanta are absorbed in the envelope and the number of transitions from the k-th state to the i-th is almost exactly equal to the number of transitions from the i-th state to the k-th. In the presence, however, of a velocity gradient in the envelope some fraction of the line quanta escape from the envelope because of the Doppler effect. We will denote this fraction by β_{ik}. Then the number of $k \rightarrow i$ transitions will be greater then the number of reverse transitions by the amount $n_k A_{ki} \beta_{ik}$.

Since the number of atomic transitions from the k-th state into all other states must be equal to the number of transitions into the i-th state, then we have

$$n_i\left(\sum_{k=1}^{i-1} A_{ik}\beta_{ki} + B_{ic}\rho_{ic}\right) = \sum_{k=i+1}^{\infty} n_k A_{ki}\beta_{ik} + n_e n^+ C_i(T_e), \qquad (28.18)$$

where $n_i B_{ic} \rho_{ic}$ is the number of ionizations from the i-th state. The quantities ρ_{ic} are assumed to be known and equal to /381

$$\rho_{ic} = W\rho_{ic}^*, \qquad (28.19)$$

where ρ_{ic}^* is the emission density beyond the i-th series limit in the stellar atmosphere and W is the radiation dilution factor.

In determining the quantities β_{ik} we assume, just as before, that both the absorption coefficient α_{ik} and the emission coefficient β_{ik} for a line of frequency ν_{ik} are nonzero and constant within the interval $\Delta\nu_{ik} = 2\frac{u}{c}\nu_{ik}$ and equal to zero outside this interval. Moreover, let us assume that the region of the envelope, in which a given line radiation is absorbed, is relatively small (because of a large velocity gradient) so that the density of matter and the velocity gradient in the region can be assumed to be constant.

Let us consider line radiation of frequency ν_{ik}, emanating from some volume element in the direction s within a solid angle $d\omega$. Along the path from s to

s + ds the following fraction of the emitted photons will be absorbed:

$$e^{-\alpha_{ik}s}\left(1-\frac{|\nu'_{ik}-\nu_{ik}|}{\Delta\nu_{ik}}\right)\alpha_{ik}\,ds, \tag{28.20}$$

where the factor $e^{-\alpha_{ik}s}$ takes account of radiation absorption along the path from zero to s, and the factor $1-\frac{|\nu'_{ik}-\nu_{ik}|}{\Delta\nu_{ik}}$ is the change in the radiation frequency because of the Doppler effect. Here

$$\nu'_{ik}-\nu_{ik}=\frac{\nu_{ik}}{c}\frac{\partial v_s}{\partial s}s. \tag{28.21}$$

The fraction of the photons absorbed along their entire path in the envelope will be equal to

$$\int_0^{s_1} e^{-\alpha_{ik}s}\left[1-\frac{1}{2u}\left|\frac{\partial v_s}{ds}\right|\cdot s\right]\alpha_{ik}\,ds, \tag{28.22}$$

where the quantity s_1 is determined from the condition

$$\frac{1}{2u}\left|\frac{\partial v_s}{\partial s}\right| s_1=1. \tag{28.23}$$

Multiplying Eq. (28.22) by $d\omega/4\pi$ and integrating over all solid angles, we obtain the fraction, absorbed in the envelope, of the total number of photons emitted by a given volume. In the nomenclature that has been adopted this fraction is equal to $1 - \beta_{ik}$. Therefore, for the quantity β_{ik} we obtain /382

$$\beta_{ik}=\int\left(1-e^{-\frac{2u}{\left|\frac{\partial v_s}{\partial s}\right|}\alpha_{ik}}\right)\frac{1}{2u\alpha_{ik}}\left|\frac{\partial v_s}{\partial s}\right|\frac{d\omega}{4\pi}. \tag{28.24}$$

If the envelope at a given point is opaque in all directions, then

$$\beta_{ik}=\frac{1}{2u\alpha_{ik}}\overline{\left|\frac{\partial v_s}{\partial s}\right|}, \tag{28.25}$$

where $\overline{\left|\frac{\partial v_s}{\partial s}\right|}$ is the quantity $\left|\frac{\partial v_s}{\partial s}\right|$, averaged over all directions. If the envelope at a given point is transparent in all directions (i.e., $\frac{2u}{\overline{\left|\frac{\partial v_s}{\partial s}\right|}}\alpha_{ik}\ll 1$), then $\beta_{ik}=1$, just as it should be.

Thus, for determining the quantities n_i we derived the system of Eqs. (28.18), in which the quantities β_{ik} are defined by the relations (28.24). The absorption coefficients α_{ik} entering into these relations are given by Eq. (28.10), presented above.

If Eqs. (28.18) are solved for different parts of the envelope, then we can determine the total amount of energy emitted by the envelope in any spectral line. The following equation serves this purpose:

$$E_{ki} = A_{ki} h \nu_{ik} \int n_k \beta_{ik} \, dV, \tag{28.26}$$

where the integration is done over the entire envelope volume. For a transparent envelope $\beta_{ik} = 1$ and Eq. (28.26) passes over to Eq. (24.8) of the preceding chapter.

The system of Eqs. (28.18) can be solved numerically. To do this the values of four parameters must be specified: the stellar temperature T_* (on which $\rho_{ic}{}^*$ depends), the electron temperature T_e (on which C_i depends), the dilution factor W and the quantity β_{12}. Values of the Balmer decrement, determined for $T_* = 20,000°$, $T_e = 20,000°$, $\beta_{12} = 0.001$ and for two values of the dilution factor: $W = 0.01$ (case I) and $W = 0.1$ (case II), are listed in Table 43 as an example.

TABLE 43. THEORETICAL BALMER DECREMENT IN THE SPECTRA OF MOVING ENVELOPES OF STARS

Line	Case I	Case II	Nebular case
H_α	1,61	0,97	2,79
H_β	1,00	1,00	1,00
H_γ	0,44	0,80	0,49
H_δ	0,24	0,50	0,28
H_ϵ	0,15	0,32	0,18

Commas represent decimal points.

Values of the Balmer decrement for the case of transparent envelopes (for example, of nebulae) for $T_e = 20,000°$ are given in the same table for a comparison. They are obtained by solving the system of Eqs. (28.17), which is a special case of the system of Eqs. (28.18) for $\beta_{1k} = 0$, $\beta_{ik} = 1$ ($i = 2, 3, \ldots$) and when ionizations from the excited states are ignored.

In the case of nebulae the Balmer decrement depends only on the temperature T_e and changes very little for a change in it. In the case, however, of envelopes moving with a velocity gradient, the Balmer decrement depends on several parameters and can assume very different values. /383

Observations indicate that in the spectra of WR, P Cygni, Be and nova type stars the Balmer decrement changes markedly from one star to another and in Be and nova type stars it also changes with time within the spectrum of an individual star. This can be explained by the fact that in the envelopes of these stars the values of the parameters W and β_{12}, upon which the Balmer decrement depends heavily, are changing.

To calculate the parameter β_{12} the velocity field in the envelope must be known. Let us assume, for example, that the atoms are moving in a radial direction with velocity v, depending on r. It is easy to show that in such a case

$$\frac{\partial v_s}{\partial s} = \frac{dv}{dr}\cos^2\vartheta + \frac{v}{r}\sin^2\vartheta, \tag{28.27}$$

where ϑ is the angle between the radius vector direction and the direction of a ray. From Eq. (28.27) it is seen that even when dv/dr = 0, a velocity gradient exists in the envelope (caused by the curvature of the layers). In this case

$$\overline{\frac{\partial v_s}{\partial s}} = \frac{2}{3}\frac{v}{r} \tag{28.28}$$

After a determination of $\overline{\partial v_s}/\partial s$ the quantity β_{12} is found from the formula

$$\beta_{12} = \frac{1}{2un_1k_{12}}\left|\overline{\frac{\partial v_s}{\partial s}}\right|, \tag{28.29}$$

where n_1 is the number of atoms in the ground state in 1 cm^3 and k_{12} is the absorption coefficient at the resonance line, calculated for one atom.

An evaluation of the quantity β_{12} from the formulas presented leads to the values which are necessary for explaining the observed Balmer decrement. /384

Recently, many authors have determined the Balmer decrement by solving the system of Eqs. (28.18) and subsequent application of Eq. (28.26). Especially detailed calculations of this nature have been made by A. A. Boyarchuk [5].

4. Type Be stars. As already stated, to explain the line profiles in the spectra of type Be stars the assumption is made that these stars are rotating rapidly and matter is being ejected from them. Profiles of the emission lines, arising in the envelope ejected from a rotating star, can be determined from Eq. (28.6) for the appropriate velocity field in the envelope. These profiles prove to be very similar to the emission line profiles in the spectra of type Be stars. The observed changes in line profiles can be explained by a change in the rate of election of matter from the star. Here, in particular, a change in the ratio between transparent and opaque portions of the envelope plays a role.

The relative intensities of the Balmer emission lines in the spectra of Be type stars usually do not agree with the intensities calculated for the case of nebulae. They can, however, be explained by means of the theory proposed above, in which envelope opacity and the presence of a velocity gradient are taken into consideration. Envelope opacity has considerable significance for the first terms of the Balmer series. The envelopes can be assumed to be transparent for the high terms of this series.

The hydrogen atom concentration in the envelopes can be determined from the observed Balmer emission line intensities. Let us assume, for simplicity, that the envelope is transparent for the line corresponding to the transition $k \rightarrow 2$. Then in Eq. (28.26) one can assume that $\beta_{2k} = 1$ and $n_k = z_k n_e n^+$, where z_k is found from the system of Eqs. (28.17) (see Section 24 for more details about this). In the case given Eq. (28.26) assumes the form

$$E_{k2} = A_{k2} h\nu_{2k} z_k \int n_e n^+ dV. \tag{28.30}$$

Let us assume that the hydrogen atoms in the envelope are predominantly in an ionized state and the density of matter decreases in it in inverse proportion to the square of the distance from the center of the star (although the last assumption is crude for envelopes of type Be stars). Then we will have

$$n_e = n^+ = n_e^0 \left(\frac{r_0}{r}\right)^2, \tag{28.31}$$

where r_0 is the radius of the star and n_e^0 is the free electron density near the surface of the star. Now, instead of Eq. (28.30) we obtain /385

$$E_{k2} = 4\pi A_{k2} h\nu_{2k} z_k n_e^{02} r_0^3. \tag{28.32}$$

On the other hand, the energy emitted by the envelope in the lines can be represented in the form

$$E_{k2} = \frac{8\pi^2 r_0^2 hc^2}{\lambda_{2k}^5} \frac{W_{2k}}{e^{\frac{h\nu_{2k}}{kT_*}} - 1}, \tag{28.33}$$

where W_{2k} is the equivalent line width (expressed in centimeters). Equating the last two equations, we find

$$n_e^{02} = \frac{2\pi c}{r_0 A_{k2} z_k \lambda_{2k}^4} \frac{W_{2k}}{e^{\frac{h\nu_{2k}}{kT_*}} - 1}. \tag{28.34}$$

Equation (28.34) provides the possibility of determining the density of free electrons (and this means protons also) in the envelope from the measured equivalent line width. Then the concentration of neutral hydrogen atoms can be found from the ionization formula (23.14). In this way it was determined for several Be type stars that on the average $n_e^0 \approx 10^{11}$ cm^{-3} and $n_1^0 \approx 10^5$ cm^{-3}.

Be type stars differ from B class stars not only in the presence of bright lines in their spectra but also in certain anomalies in the continuous spectrum. As observations have show, Be type stars with emission are, on the average, redder than B class stars without emission. Moreover, the Balmer discontinuity

for Be type stars was found to be smaller than for B class stars. These differences are clearly caused by the existence of envelopes for Be type stars. As a result of the conversion of the high-frequency stellar radiation in the envelope, photons are produced both in the lines and in the continuous spectrum.

A determination of the amount of energy emitted in the continuous spectrum by a Be type star is not difficult. Since the envelope is transparent to the frequencies of the continuous spectrum (the star itself is seen through the envelope), then the energy emitted by a Be star at frequency ν can be represented in the form of the sum

$$L_\nu = L_\nu^* + L_\nu^{\text{env}}, \tag{28.35}$$

where L_ν^* is the energy emitted by the star itself (without the envelope), and L_ν^{env} is the energy emitted by the envelope. It is obvious that

$$L_\nu^* = 4\pi^2 r_0^2 \frac{2h\nu^3}{c^2} \frac{1}{e^{\frac{h\nu}{kT_*}} - 1}. \tag{28.36}$$

To find the quantity L_ν^{env}, however, we must make use of Eq. (26.6) for the volume emission coefficient, caused by recombinations and free-free transitions. Integrating this expression over all solid angles and over the entire volume of the envelope and using Eq. (28.31), we obtain /386

$$L_\nu^{\text{env}} = 4\pi^2 r_0^3 n_e^2 \frac{2^7\pi^3}{(6\pi)^{3/2}} \frac{e^6}{m^2c^2} \left(\frac{m}{kT_e}\right)^{1/2} \times$$
$$\times \left(1 + 2\frac{\chi_1}{kT_e} \sum_{i=j}^{\infty} \frac{1}{i^3} e^{\frac{\chi_i}{kT_e}}\right) e^{-\frac{h\nu}{kT_e}}. \tag{28.37}$$

From the formulas presented it follows that the following changes should be observed with an increase in the ejection of matter from a star:

1) the visual brightness of the star should increase;
2) the spectrophotometric temperature should be reduced (since the spectrophotometric temperature of the envelope is low);
3) the Balmer discontinuity should be reduced (since the Balmer discontinuity of the envelope is negative).

The last two conclusions are made on the basis of Eqs. (26.9) and (26.10) of the previous chapter.

With an increase in the matter ejected from the star, an increase in the energy emitted in spectral lines by the envelope should be observed along with the changes cited in the continuous spectrum. All these effects will be greater, the higher the stellar temperature and the greater the optical thickness of the envelope beyond the Lyman series limit.

A detailed interpretation of the continuous spectrum of Be stars can be given with the aid of the formulas written above. V. G. Gorbatskiy [6] did this for the star γ Cassiopeiae, among the best known of the stars under consideration. From 1936 to 1941 very drastic changes occurred in the brightness and spectrum of this star. During that period of time the stellar brightness increased three times. Along with the increase in brightness there also occurred a decrease in the spectrophotometric temperature, a decrease in the magnitude of the Balmer discontinuity and an increase in the intensity of the Balmer lines (Fig. 36). All this can be explained by the fact that the rate of ejection of matter from the star increased three times, and then decreased. In other words, the star ejected three envelopes from itself in sequence. From a comparison of theory with observations the fundamental parameters of the star and envelope were determined. It was found that the radius of the star is equal to three solar radii, the stellar temperature is equal to 34,000°, the number of hydrogen atoms in 1 cm^3 near the surface of the star is about 10^{12}-10^{13} and the average electron temperature of the envelope is $T_e \approx 15{,}000$-$20{,}000°$.

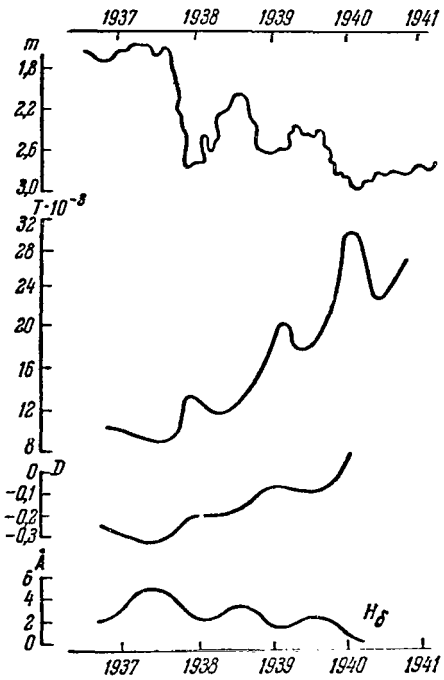

Commas represent decimal points.

Figure 36.

The continuous spectra of many Be type stars have been studied in detail by Tsoy Dyay O [7], who measured the Balmer discontinuity and the spectrophotometric temperature in different regions of the spectrum (with interstellar absorption taken into account). On the basis of these data he determined the energy emitted by the star and by the envelope, the atom density in the envelope and the amount of matter ejected by the star per year (about 10^{-7} $M_\odot$ for Be type stars of various subclasses). /387

5. Wolf-Rayet type stars. The presence, in the spectra of WR type stars, of broad bright lines that do not vary noticeably with time led to a hypothesis concerning the unchanging ejection of matter from these stars. Since the bright line is symmetrical with respect to the center frequency and is sometimes bounded on the violet side by an absorption line, then it is reasonable to assume that the ejection of matter is radial. In this situation the bright line is produced through the entire depth of the envelope, and the absorption line—in the portion of the envelope approaching the observer. We have already seen that in the case of ejection of matter with a constant velocity the bright line should have a rectangular profile. Lines with such profiles are actually found in the spectra of WR

stars. More frequently, however, lines are observed with rounded profiles, which can be explained with the aid of Eq. (28.6) both by accelerated or decelerated motion of the ejected atoms and by the opacity of the envelope to the line emission.

The weakness of the absorption lines in the spectra of WR stars can be caused not only by the small optical thickness of the envelope for lines, but also by a filling-in of the absorption line with an emission line. In those cases, however, when the lower level is metastable, the absorption line is extremely strong. /388 The λ 3889 Å absorption line, arising from the metastable 2^3S state of neutral helium, can serve as an example. The strong absorption in these lines is explained by the buildup of atoms in metastable states because of the smallness of the radiation dilution factor and the density of matter throughout the envelope.

It is clear that in the case of radial ejection of matter from a star, the width $\Delta\lambda$ of the emission line must be proportional to the wavelength λ. Such a relationship between these quantities is actually observed for the spectra of WR stars (which is one of the strongest arguments in favor of the ejection hypothesis).

Measured and computed values of $\Delta\lambda$ for three WR stars are listed in Table 44 as an example (the proportionality coefficient assumed between $\Delta\lambda$ and λ is given under the star number). The ejection velocities of matter from WR stars, found from the width of the emission lines, are about 1000-2000 km/sec.

TABLE 44. WIDTHS OF EMISSION LINES IN SPECTRA OF WR STARS (IN ANGSTROMS)

λ, Å	192163 k = 0,00833		50896 k = 0,00961		191765 k = 0,00883	
	meas.	calc.	meas.	calc.	meas.	calc.
6563	58,0	54,7	74,2	63,1	57,5	57,9
4861	41,2	40,5	44,8	46,7	43,9	42,9
4340	33,4	36,2	36,0	41,7	37,8	38,3

Commas represent decimal points.

The matter ejected from a star can be decelerated or accelerated under the influence of stellar attraction and radiation pressure. The function describing the change in velocity v with increasing distance r from the center of the star determines the matter density distribution in the envelope. To find the dependence of the density ρ on the velocity v, let us consider the flow of matter through a sphere of radius r. The amount of matter, flowing through this sphere during time dt, will obviously be equal to

$$dM = 4\pi r^2 \rho(r) v(r) dt. \tag{23.38}$$

When the motion of the matter is stationary, $dM/dt = \text{const}$ and therefore from (28.38) we have

$$\rho(r) \sim \frac{1}{r^2 v(r)}. \tag{28.39}$$

If the velocity of movement is constant, then /389

$$\rho(r) \sim \frac{1}{r^2}. \tag{28.40}$$

In the case of decelerated motion the density decreases more slowly with an increase in r than according to (28.40); in the case of accelerated motion—more rapidly.

The problem of the dependence of the velocity v on the distance r in the envelopes of WR stars can be solved in the following manner. Since the envelopes, in principle, shine the same as gaseous nebulae, then the envelopes, just as in nebulae, an emission stratification should exist. This means that the lines of atoms with high ionization potentials are formed in envelope layers nearer the star than the lines of atoms with low ionization potentials. Therefore when the velocity changes appreciably in the envelope, the lines of atoms with different ionization potentials should have different widths. Observations indicate that line widths in the spectra of WR stars are greater, the lower the ionization potential. This is especially evident in the case of the He I and He II lines. For example, for star HD 192103 the expansion velocity of the envelope is equal to 1290 km/sec according to the He I lines and 975 km/sec according to the He II lines. Thus, we must conclude that the atoms ejected from a WR star are accelerated. Because of this, as seen from Eq. (28.39), the density of matter in the envelope decreases more rapidly than in inverse proportion to the square of the distance from the center of the star. As calculations show, accelerated motion of the atoms, ejected from WR stars, can be explained by the effect of radiation pressure on them (especially beyond the limits of the fundamental He II series).

Using Eq. (28.38), we can find the amount of matter ejected by a WR star per year. This amount of matter is equal to

$$M = 4\pi r_0^2 \rho(r_0) v(r_0) \cdot 3.16 \cdot 10^7, \tag{28.41}$$

where the radius of the lower boundary of the envelope is denoted by r_0 (coinciding with the photosphere radius for WR stars). The quantity $\rho(r_0)$ for the envelopes of WR stars can be determined in the same way as for the envelopes of Be stars, i.e., by means of Eq. (28.34). Assuming, also, that $r_0 \approx 5r_\odot$ and $v \approx 10^8$ cm/sec, from Eq. (28.41) we find that a WR star in one year loses a mass equal to about 10^{-5} of the solar mass.

This result is of considerable interest for cosmogony. Since the mass of WR stars is about 10 solar masses, then a star cannot remain in the WR stage more than a million years. If, however, it is taken into consideration that we know of no stars whose mass exceeds the mass of the WR stars (with the exception of the related /390 class O stars), then we can make the assumption that the stars being considered have arisen directly from a prestellar phase of matter and, moreover, quite recently. Such an assumption is corroborated by the fact that most WR stars enter into the structure of stellar associations which, as is known, are considered to be very young formations in terms of a number of criteria.

Equation (28.41) also makes it possible to estimate the mass lost annually by P Cygni and Be type stars. It turns out to be about 10^{-5} $M_{\odot}$ for P Cygni type stars and about 10^{-6}-10^{-8} $M_{\odot}$ for Be type stars. These stars, just like WR stars, are also characteristic members of the stellar associations.

From the relative intensities of the emission lines in the spectra of WR stars one can obtain some information about the chemical composition of their envelopes. This is done by comparing the observed line intensities with the theoretical intensities determined on the basis of solving the system of Eqs. (28.17) or (28.18). In this manner, in particular, it was found that the number of helium atoms in the envelopes of WR stars is several times greater than the number of hydrogen atoms (see paper of S. G. Slyusarev [8]). Envelopes of WR stars, in this regard, are considerably different from the atmospheres of ordinary stars and gaseous nebulae in which the ratio of the number of helium atoms to the number of hydrogen atoms is the reverse. Another anomaly of the envelopes of WR stars, as we recall, is that in some of them there is much nitrogen but little carbon and oxygen, and in others—much carbon and oxygen but little nitrogen. Thus, the chemical composition of the envelopes of WR stars must be considered to be very anomalous.

Temperatures of WR stars can be determined from the ratio of the emission line intensities to the intensity of the continuous spectrum. Zanstra's method, discussed in detail in the previous chapter, is used for this. More precisely, the stellar temperature is found from Eq. (22.29), applied to different atoms. Temperatures of WR stars, determined by B. A. Vorontsov-Vel'yaminov [9], are listed in Table 45. The star number from the HD catalog is given in the first column; subsequent columns give the stellar temperatures (in thousands of degrees) found from the lines of different atoms (the ionization potential in volts is given below the atomic symbols).

We see that the temperatures of WR stars, determined by this method, are very high. Moreover, it is seen from the table that the temperatures of a single star, found from different atomic lines, are different. This is caused primarily by a lowering of the temperatures determined from lines with relatively low ionization potentials. Such atoms (in particular, hydrogen and helium) are heavily ionized in the envelopes of WR stars and therefore absorb only a small portion /391 of the stellar energy beyond the limits of their fundamental series. For example, calculations show that the optical thickness of an envelope of a WR star beyond the Lyman series limit is about 0.01. Therefore the temperatures determined from the hydrogen lines are very low for the stars being considered—about

TABLE 45. TEMPERATURE OF WR STARS
(IN THOUSANDS OF DEGREES)

Star	He I 24.5	C III or N III 47.4	He II 54.2	C IV 64.2	N IV 77.0	T_c
HD 192163	32	65	73	—	84	15
HD 191765	35	62	69	—	75	15
HD 193077	29	51	59	—	74	13
HD 193576	29	48	60	—	62	14
HD 192103	33	64	63	69	—	12
HD 192641	—	59	55	70	—	7

20,000°. Another reason for the differences between the temperatures found from different atomic lines can be a deviation of the energy distribution in the stellar spectrum from Planck's law. It must also be noted that Eq. (22.29) is not completely applicable for determining the temperatures of WR stars because of the great complexity of the radiation processes of their envelopes in comparison with the radiation processes of gaseous nebulae.

Spectrophotometric temperature values for WR stars are listed in the last column of Table 45. We see that they are much lower than the temperatures found by Zanstra's method. This is explained by the fact that in the envelopes of WR stars, as a result of the conversion of high-frequency radiation, not only are the emission lines transformed but also the continuous spectrum, the energy distribution in which corresponds to a very low temperature. In the case of WR stars, however, the continuous spectrum is transformed in a more complex manner than in the case of Be stars. This is caused by the large extent of the envelopes of WR stars, because of which they play the role of "atmosphere" as well as "photosphere". The continuous spectrum of WR stars can be explained on the basis of the special theory of extended photospheres, which was discussed in Section 7.

6. Late class stars with bright lines. In addition to the WR, P Cygni and Be type stars considered above, emission lines are also observed in the spectra of stars of the late classes. Among these are the long-period variables, Z Andromedae type stars, etc.

The variation in brightness and spectrum of long-period variables occurs with periods of about a year. The amplitudes of the brightness variation amount to several stellar magnitudes. Near the time of maximum brightness, bright lines of hydrogen and ionized iron are seen in the spectrum, near the time of minimum brightness—bright lines of neutral iron. Most of the long-period variables belong to spectral class M; approximately 80% of these have bright lines in the spectra. /392

As observations indicate, the bright lines in the spectra of long-period variables form in deeper layers of the atmosphere than the absorption lines and bands. This follows from the fact that the line emission of hydrogen is partially absorbed in the stellar atmosphere. Some Balmer lines are decomposed into a series of

components which is caused by the absorption of radiation in these lines by metal atoms. An unusual intensity distribution among the Balmer series members is observed in the spectra of Me stars, explainable by the absorption of hydrogen radiation in the titanium oxide bands. In the spectra of Ne and Se stars the titanium oxide bands are absent and in them the Balmer decrement is normal.

The different behavior of the radial velocity curves, determined from these lines, attests to the formation of emission and absorption lines in different layers of the atmosphere. It is found that the difference in the radial velocities from bright and dark lines is always negative. In addition, the K-term determined from the emission lines is negative and equal to about -15 km/sec, and the k-term determined from the absorption lines is close to zero. From these data it follows that the layer in which the bright lines are forming is moving toward the observer.

The spectra of Z Andromedae type stars are combinations of the later class spectrum with absorption lines and the early class spectrum with emission lines belonging to atoms with high ionization potentials (for example, He II). The spectral brightnesses of these stars exhibit irregular variations. In addition to Z Andromedae, the stars R Aquarii, V Sagittae, etc. belong in this group.

The major problem arising in the interpretation of the spectra of the late class stars with bright lines consists of explaining the reasons for the appearance of bright lines in the spectra of such cool stars. As we know, emission lines appear in the spectra of hot stars because of the conversion of high-frequency stellar radiation in the extended envelopes. However, the high-frequency energy of late class stars is too low for the emission lines in their spectra to be formed in the same manner.

To explain the spectra of Z Andromedae type stars the hypothesis was advanced that these are double stars composed of one hot star and one cold. Furthermore, brightness variation curves of the hypothetical components were deduced from the observational data. It is possible that some of these stars are actually double; however, as yet there is no definite confirmation of the double-star hypothesis. This hypothesis is inapplicable to the long-period variables. /393

Another hypothesis proposed for explaining the spectra of late class stars with bright lines considers them to be single hot stars having extended envelopes of great optical thickness in the continuous spectrum [3]. We have already seen above that in the cases of Be and WR type stars the temperatures found from the bright lines are appreciably higher than the spectrophotometric temperatures. With an increase in the optical thickness of the envelope, this temperature difference should increase. If we assume that the optical thickness of the envelope is great (this will be the case when the density in the envelope decreases slowly with an increase in distance from the center of the star), then the following processes will occur in the envelope. The inner portions of the envelope will absorb nearly all the stellar radiation and convert it into low-frequency photons. The continuous late class spectrum forms here and emission lines, corresponding in intensity to the temperature of the star itself, appear. In the outer portions of the envelope, which will be primarily under the influence of the low-temperature radiation of its inner portions, unionized metal atoms and molecular compounds will exist. The late class absorption spectrum forms here.

According to the proposed hypothesis, Z Andromedae type stars are class O stars, having envelopes with a slow decrease in density along the radius. However, the optical thicknesses of these envelopes in the continuous spectrum are still not very great. Therefore we see "combination spectra" which are the superposition of two spectra: of the star and of the envelope. In this situation, roughly speaking, the violet end of the continuous spectrum belongs to the star, and the red—to the envelope. The brightness and spectral variations in these stars can be explained by a change in the rate of matter ejection from them.

If the optical thickness of the envelope becomes very great, then no emission lines will be observed. The "normal" cold supergiants are possibly formed in this manner. As is known, the mass and brightness of class M supergiants and class O and B stars are approximately the same. By itself this forces one to think that these stars differ only in envelope configuration.

Finally, a third hypothesis views the cause of the appearance of bright lines /394 in the spectra of certain types of cold stars as due to a shock wave. As indicated by V. G. Gorbatskiy [4], this hypothesis is very probable with respect to long-period variables. With the passage of a shock wave through the atmosphere of a star, a heating of the gas occurs, leading to an increase in the ionization of the atoms. After passage of the shock wave the gas luminesces, i.e., recombinations occur and then luminescence in the spectral lines. Therefore the movement of a shock wave in a stellar atmosphere appears as the movement of a luminous layer of gas. The change in the spectrum, occurring in this situation, is very similar to the change in the spectrum of a long-period variable. From the observed shift of the bright lines in the stellar spectrum, one can determine the velocity of the shock wave. This makes it possible to find the temperature in the layer of heated gas and the amount of energy emitted by it in the spectral lines. For long-period variables the calculated energy and that obtained from observations agree in order of magnitude.

In addition to the stars considered above, exhibiting high luminosities, late class dwarf stars with emission lines have also been detected by observations. The most interesting of these are type T Tauri variable stars. These stars belong to spectral classes G - M and have the bright lines of H, Ca II, Fe II, etc. Absorption lines are seen on the violet side of the bright lines. Judging from the profiles of the spectral lines, ejection of matter occurs from type T Tauri stars. Nearly all type T Tauri stars known to us are in stellar clusters (so-called T-clusters), which serves as the basis for concluding these stars are young.

V. A. Ambartsumyan [10] directed his attention to a surprising feature of type T Tauri and related stars. This feature is that during the rise in stellar brightness an extremely strong continuous spectrum, superimposed on the normal continuous spectrum with absorption lines, also appears along with the appearance and intensification of the emission lines. The fact that the new continuous spectrum weakens all the absorption lines and does not involve the appearance of new absorption lines indicates that it arises in the outermost layers of the stellar atmosphere. The appearance of emission lines together with emission absorption in the continuous spectrum corroborate this.

In the case of UV Ceti stars the flare-up occurs in a period of several minutes, with the stellar brightness increasing by several stellar magnitudes during this time. Such a rapid and intense increase in the stellar brightness cannot be explained by a transfer of energy outward from the interior of the star by thermal conduction nor by radiation transfer. Therefore it must be assumed that the /395 energy radiated during the flare-up of a type UV Ceti star is transferred from the inner layers of the star to the upper layers of the atmosphere by some still-unknown process.

An examination of the emission of several stars with additional continuous spectrum emission led V. A. Ambartsumyan to conclude that in all these cases we are dealing with the ejection from the inner layers of the star of some portion of the material that is serving as the source of stellar energy. Apparently the intrastellar matter ejected outwards undergoes a rapid disintegration here, similar to nuclear disintegration, with the release of some energy, which is then converted into radiation. One can assume that during the disintegration of the intrastellar matter, atoms of various elements are also formed. This explains the presence, in stellar atmospheres, of technetium, deuterium and other atoms having a short lifetime.

Type T Tauri stars are frequently associated with nebulae, resembling comet tails in outward appearance. These nebulae, usually called "cometary", possess the characteristic that they are variable. However, the nebular brightness varies independently of the change in stellar brightness. In a number of cases the continuous spectrum of the nebula is considerably more intense in the blue and violet regions than the spectrum of the star associated with it. V. A. Ambartsumyan assumes that the continuous spectrum of cometary nebulae arises in the same way as the additional continuous spectrum of type T Tauri stars, i.e., as the result of the outward ejection of intrastellar matter and its subsequent disintegration.

29. Novae

1. Observational data. The discovery of each bright nova is an important event in astronomy and they are studied intensively by many observatories. Therefore the observational data on novae are extremely voluminous. Here we will mention some of these data; the details, however, can be found in specific monographs (see [9] and [11]).

To begin with, attempts have been made to determine the nova brightness curve from observations. These curves are very different for different stars. In general, however, the rise in brightness is extremely rapid and its decay is very slow, frequently accompanied by large fluctuations. The "flare-up" of a nova usually occurs in a period of a few days, and the "fading"—in a period of several years. Finally the star returns to a brightness not much different from what it had before flare-up. The brightness curve of a typical nova is shown in Fig. 37 /396 as an example.

At the moment of maximum brightness, novae are the brightest objects of the Galaxy (if supernovae are ignored). On the average their absolute magnitudes

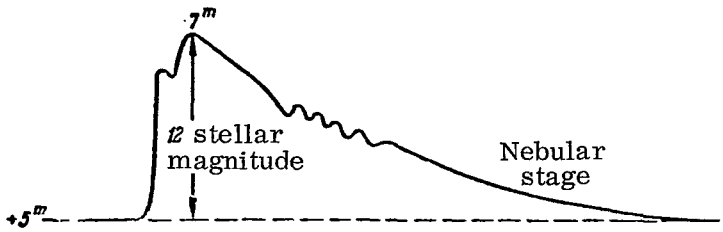

Figure 37.

at maximum are equal to -7^m. In its "normal" state, i.e., before the outburst and many years after outburst, novae have absolute magnitudes of about $+5^m$ (with a fairly large dispersion). Consequently, the average amplitude of the brightness change of a nova amounts to 12^m. Some information on the most studied novae are listed in Table 46.

TABLE 46. SOME CHARACTERISTICS OF NOVAE

Star	Amplitude of brightness change	Absolute magnitude at maximum	Distance in parsecs	Displacement of absorption lines in mm/sec
Nova Aurigae 1891	9^m	—5,3	800	—
Nova Persei 1901	13,3	—8,4	480	800
Nova Aquilae 1918	11,9	—9,3	430	1250
Nova Cygni 1920	14,2	—8,9	1470	380
Nova Pictoris 1925	11,5	—7,3	500	64
Nova Herculis 1934	12,6	—5,5	230	180
Nova Lacertae 1936	13,2	—8,6	1350	600
Nova Puppis 1942	17	—8,5	500	—

Commas represent decimal points.

Vast changes occur in the spectra of novae along with the change in brightness. However, we do not know the complete spectroscopic history of any nova since we have no data on the spectra at the start of the outburst and before it. The spectrum before outburst of Nova Aquilae 1918, indicating it belongs to an /397
early class (probably O), was found on only one random spectrogram, obtained with an objective prism. The first spectrograms of novae are usually obtained not long before the moment of maximum brightness. They show that the spectra of novae at this time can belong to classes A or F. A characteristic feature of these spectra is the drastic shift of all lines toward the violet. Expressed in velocities, it usually amounts to a few hundred kilometers per second. The line shifts of the pre-maximum spectrum of novae are listed in the last column of Table 46.

Immediately after the maximum brightness of the star is reached, broad emission bands appear in its spectrum. They are approximately symmetrical with respect to the center frequency and are bordered by absorption lines on the

violet side. The absorption lines of the new spectrum (usually called principal) are shifted toward the violet by a greater amount than the lines of the pre-maximum spectrum. Sometimes somewhat of a system of absorption lines with different shifts is observed in the stellar spectrum. Initially the bright lines belong to atoms with low ionization potentials (primarily hydrogen and ionized metals), then the lines of high-ionization atoms appear (for example, He II, N IV, O V). In addition to these changes in the bright line spectrum, a gradual weakening of the continuous spectrum and absorption lines occurs.

Bright forbidden lines, characteristic of the spectra of gaseous nebulae (including the N_1 and N_2 "nebular" lines), are observed in the nova spectrum some months after outburst. With the appearance of these lines the nova enters the "nebular stage" of its evolution, which lasts for many years. Gradually the nebular spectrum disappears and the star returns to its initial brightness. At this time it has a class O spectum, sometimes with weak emission lines.

A nebula, surrounding the star, is seen on photographs of a nova some years after outburst. This nebula expands with an enormous velocity and then is dissipated in space. The existence of such nebulae leaves no doubt that during the nova outburst the outer layers of the star are detached from it. Below it will be shown that the changes in nova brightness and spectrum are explained by the gradual expansion of the detached envelope.

The observational data that have been presented refer to a typical nova. However, some other stars undergo similar outbursts. Of these, repeating novae are the most closely related to the typical nova. Unlike typical novae, which have undergone an outburst only once in all the time of their observation, repeating novae suffer many outbursts. Approximately the same phenomena occur during an outburst of a repeating nova as during the outburst of a typical nova, but they are on a different scale. A list of all the repeating novae that are known at the present time is given in Table 47. /398

TABLE 47. REPEATING NOVAE

Star	Dates of outburst	Limits of stellar magnitude variation
N Orionis	1677, 1750, 1892	6^m—11^m
T Pyxidis	1890, 1902, 1920, 1941	6 —14
U Scorpii	1863, 1906, 1935	9 —>17
RS Ophiuchi	1898, 1933	4 —12
T Coronae	1866, 1946	2 —11
N Sagittae	1913, 1946	7 —15
N Sagittarri	1901?, 1919	<7 —14

The so-called novalike variables, in turn, are related to the repeating novae. In their change in brightness and spectrum they also resemble novae. The novalike variables differ, however, from repeating novae not only in the small scale of the phenomena characterizing nova outbursts, but they are also less distinct. Star clusters of the types U Gemini, Z Andomedae, etc. are distinguished among the novalike variables.

The external similarity between repeating and typical novae permits one to suppose that the typical novae also undergo many outbursts; however, the time

between outbursts exceeds the period of the observations. Such a supposition is corroborated by two statistical results. The first of these, first found by B. V. Kukarkin and P. P. Parenago, interrelates the lengths of time between outbursts with the amplitudes of the brightness change for novalike variables and repeating novae. It is found that the greater the first of these quantities, the greater the second, on the average. Extrapolating this dependence to typical novae, the authors mentioned have found that in this case the time between outbursts should amount to several thousand years.

The second of the statistical results cited above refers to calculations of the number of outbursts. Every year, 1-2 nova outbursts are observed in the Galaxy. Since these stars are found only in the immediate vicinity of the Sun, the total number of nova outbursts in the Galaxy apparently amounts to about 100 per /399 year. During the entire lifetime of the Galaxy, estimated at 10^{10} years, about 10^{12} outbursts should have occurred. But the total number of stars in the Galaxy is equal to about 10^{11}. Consequently, each nova should have suffered an average of 10 outbursts. On the other hand, we know for certain that for $2 \cdot 10^9$ years the Sun has not suffered such a catastrophe since it would have led to the melting of the earth's crust, which, however, has not occurred in that length of time. One can assume that other stars, like the Sun, have not suffered outbursts in the same length of time. This increases the number of outbursts occurring at each of the remaining stars. What has been said forces one to conclude that there exists a special class of stars, each of which suffers many nova outbursts.

2. Explanation of outburst. As already stated, during a nova outburst the envelope is detached from it and it then expands at a rapid rate. It is easy to show that the envelope expansion must lead to the observed changes in the brightness and spectrum of a nova.

At the moment of outburst, let the envelope, which has an optical thickness much greater than unity in the continuous spectrum, be detached from the star. With the expansion of the envelope its optical thickness will decrease. However, until it becomes of the order of unity, the envelope will serve not only as a reversing layer but also as a photosphere. In such a case the envelope expansion behaves like a rise in stellar brightness. Because, however, of the approach toward the observer of the reversed portion of the envelope, the absorption lines will be shifted toward the violet end of the spctrum. Just such a spectrum is observed during the increase in nova brightness.

At the moment maximum brightness is reached, the optical thickness of the envelope in the continuous spectrum becomes of the order of unity. At this time radiation directly from the star begins to reach the outer portions of the envelope, and bright lines flare up in the envelope. The reason for the appearance of bright lines is the same as in the case of gaseous nebulae, i.e., fluorescence. Moreover, bright lines can also arise as the result of collisions of the envelope with matter impinging on it, which is ejected from the star after detachment of the envelope.

Line emission reaches the observer not only from the portion of the envelope approaching him but also from the receding portion. It is not absorbed by the envelope because of the Doppler effect. The width of the bright lines is found therefore by the corresponding expansion velocity of the envelope. An absorption line, arising in the portion of the envelope approaching the observer and screening star, is found on the violet side of the bright line. The scheme for the formation of the spectral lines in the expanding envelopes of novae is given in Fig. 38. /400

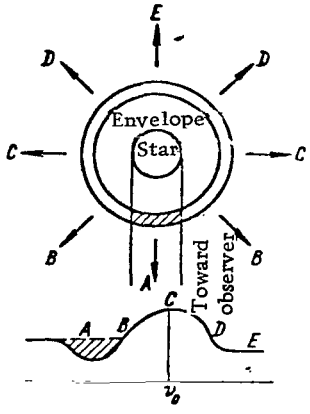

Figure 38.

After maximum brightness, with further expansion of the envelope its optical thickness at the spectral lines decreases. Because of this the dim components of the bright lines fade, and then disappear. At some stage the conditions required for the appearance of forbidden lines, i.e., the radiation density and the density of matter become sufficiently low, exist in the envelope. Starting with the appearance of the forbidden lines, the "nebular stage" lasts for quite a long time—until the brightness of the dispersing envelope (caused primarily by radiation in the emission lines) becomes less than the brightness of the star itself. The spectrum of the star, belonging now to type WR, shows that the ejection of matter from the star is still continuing. When the process is completed, the star assumes a class O spectrum without emission lines.

The explanation set forth for the phenomena occurring during outburst well satisfies, in general aspects, the observations in all stages of nova evolution. However, E.R. Mustel' [13] considers that there is another point of view, with respect to the question of the detachment of the envelope from the star, besides the one that has been discussed. It consists of the fact that at the instant the outburst begins, the entire star starts to expand and the envelope (small optical thickness in the continuous spectrum) is detached from the star only at the moment of maximum brightness, after which the star starts to contract. At the present time it is difficult to choose between these points of view. It should only be mentioned that at times far removed from the instant of maximum brightness there is practically no difference between them.

On the basis of the explanation given for nova outbursts, simple methods can be given for determining their parallaxes. These methods are very important since the trigonometric parallaxes of novae are totally unreliable because of their smallness.

One method of determining nova parallax is based on a comparison of the absorption line shifts with the rate of increase of the brightness before maximum. From observations one can find the visual magnitudes m_1 and m_2 and temperatures T_1 and T_2 (from the spectral class) for two instants of time t_1 and t_2. Using the /401

known formula relating the absolute stellar magnitude M with its temperature T and radius R, / 401

$$M = \frac{29500}{T} - 5 \lg R - 0.08, \tag{29.1}$$

and also the fact that the difference in the visual magnitudes of a star is equal to the difference in its absolute magnitudes, i.e., $m_2 - m_1 = M_2 - M_1$, we obtain the following formula defining the ratio of the stellar radii at times t_1 and t_2:

$$\lg \frac{R_2}{R_1} = \frac{5900}{T_2} - \frac{5900}{T_1} - \frac{m_2 - m_1}{5}. \tag{29.2}$$

On the other hand, for the difference in radii at times t_1 and t_2 we have

$$R_2 - R_1 = v(t_2 - t_1), \tag{29.3}$$

where v is the rate of expansion of the photosphere, determined from the shift of the absorption lines. Each of the quantities R_1 and R_2 is determined separately from Eqs. (29.2) and (29.3). This provides the possibility of finding, from Eq. (29.1), the absolute magnitude of the nova and then from a comparison of it with the visual magnitude, the parallax.

Another method of determining the parallax of a nova is based on a measurement of the expansion rate of its envelope. This rate can be measured, on the one hand, from the width of the bright bands in the spectrum and expressed in kilometers per second, and, on the other hand, from an observation of the expansion of the nebular envelope and expressed in an angular measure. This method is more precise than the previous one. The distances and absolute magnitudes at maximum, presented in Table 46 for several novae, are determined by this method.

The parallax of Nova Persei 1901 was found in an interesting manner. The nebula observed around this star was expanding so rapidly that it was completely impossible to distinguish it from the envelope ejected during the outburst. Therefore it was assumed that Nova Persei 1901 burst within a dust nebula and created a luminous region around itself, expanding with the velocity of light. This assumption was confirmed by the fact that the nebular spectrum obtained one and one-half years after the outburst was the same as the stellar spectrum at the moment of maximum brightness.

The parallax of Nova Persei 1901 was determined by the second of the methods given above with consideration given to the fact that the "expansion" of the luminous region was equal to the velocity of light, i.e., 300,000 km/sec. Subsequently a second nebula, expanding much more slowly than the first, was discovered around Nova Persei. This was the "genuine" envelope, detached from the star during outburst.

3. First period of outburst. Going over to a more detailed interpretation of the spectrum of a nova, let us first discuss the period from the start of the outburst to the moment of maximum brightness. During this time the nova possesses a continuous spectrum with absorption lines. From the line profiles one can attempt to answer certain questions relating to the outburst. To do this is obviously necessary to determine theoretically beforehand the profiles of the absorption lines arising in the expanding atmosphere. The vast extent of the atmosphere, i.e., the slow radial decrease in density, must be taken into consideration. /402

For simplicity we will assume that the outer portions of the star comprise the "photosphere" and "atmosphere", i.e., let us adopt the Schwarzschild-Schuster model. The intensity of the radiation coming to an observer from the photosphere at an angular distance ϑ from the center of the disk, we will denote by $I(\vartheta)$ (within the line limits this quantity can be considered to be independent of the frequency). The intensity of the radiation coming from the atmosphere at frequency ν within a line at the same angular distance from the center of the disk we will denote by $I_\nu(\vartheta)$. If only true line absorption is taken into account, then we will have

$$I_\nu(\vartheta) = I(\vartheta)\, e^{-\tau_\nu(\vartheta)}, \tag{29.4}$$

where $\tau_\nu(\vartheta)$ is the optical path length in the atmosphere.

Let n(r) be the density of absorbing atoms at the distance r from the center of the star and $k(\nu - \nu_0)$ be the absorption coefficient calculated for one atom. In the case given we must write the frequency $\nu_0 + \nu_0 \frac{v(r)}{c} \cos\vartheta'$ instead of the center frequency ν_0, where v(r) is the rate of expansion of the atmosphere and ϑ' is the angle between the radiation direction and the radius vector. Therefore for the quantity $\tau_\nu(\vartheta)$ we obtain

$$\tau_\nu(\vartheta) = \int_{r_0}^{\infty} n(r)\, k\left[\nu - \nu_0 - \nu_0 \frac{v(r)}{c} \cos\vartheta'\right] \sec\vartheta'\, dr, \tag{29.5}$$

where r_0 is the photosphere radius.

Let us assume, for example, that

$$v = \text{const} \quad \text{and} \quad n = n_0 \left(\frac{r_0}{r}\right)^2. \tag{29.6}$$

Then

$$\tau_\nu(\vartheta) = N r_0 \int_{r_0}^{\infty} k\left(\nu - \nu_0 - \nu_0 \frac{v}{c} \cos\vartheta'\right) \sec\vartheta' \frac{dr}{r^2}, \tag{29.7}$$

where the number of absorbing atoms in a 1 cm^2 cross section column above the photosphere is denoted by N, i.e., /403

$$N = \int_{r_0}^{\infty} n(r)\,dr = n_0 r_0. \tag{29.8}$$

In Eq. (29.7) let us change from the integration variable r to a new integration variable ϑ' by means of the relation $r_0 \sin\vartheta = r \sin\vartheta'$. After doing this, we obtain

$$\tau_\nu(\vartheta) = \frac{N}{\sin\vartheta} \int_0^{\vartheta} k\left(\nu - \nu_0 - \nu_0 \frac{v}{c} \cos\vartheta'\right) d\vartheta'. \tag{29.9}$$

In order to find the profile of an absorption line in the spectrum of the entire star, the radiant flux H_ν must be determined. Using Eqs. (29.4) and (29.9), we find

$$H_\nu = 2\pi \int_0^{\frac{\pi}{2}} I(\vartheta)\, e^{-\frac{N}{\sin\vartheta}\int_0^{\vartheta} k\left(\nu-\nu_0-\nu_0\frac{v}{c}\cos\vartheta'\right)d\vartheta'} \cos\vartheta \sin\vartheta\, d\vartheta. \tag{29.10}$$

The radiant flux in the continuous spectrum near the line is clearly equal to

$$H = 2\pi \int_0^{\frac{\pi}{2}} I(\vartheta) \cos\vartheta \sin\vartheta\, d\vartheta. \tag{29.11}$$

The quantity $r_\nu = H_\nu/H$, which also characterizes the line profile, can be determined with the aid of Eqs. (29.10) and (29.11).

The absorption line profiles calculated from the formulas presented are very similar to the line profiles in the spectra of novae. From a comparison of the theoretical and observed profiles one can determine the atmosphere expansion velocity v.

After finding the quantity r_ν, we can also calculate the equivalent line width W, for which Eq. (12.1) must be used. In the case given W depends not only on the number of absorbing atoms N, but also on the expansion velocity v. Therefore we obtain a family of "curves of growth", representing the dependence of W on N for different values of the parameter v. Curves of growth, constructed by M.A. Arakelyan with the aid of the formulas given for some values of the ratio of expansion velocity v to the average thermal velocity u of the atoms, are given in Fig. 39 as an example. Here the absorption coefficient was calculated from Eq. (8.18) for a = 0.01. From the observed values of W and v one can determine, with the aid of the appropriate curve of growth, the number of absorbing atoms N. /404 Such determinations allow one to draw conclusions about the chemical composition

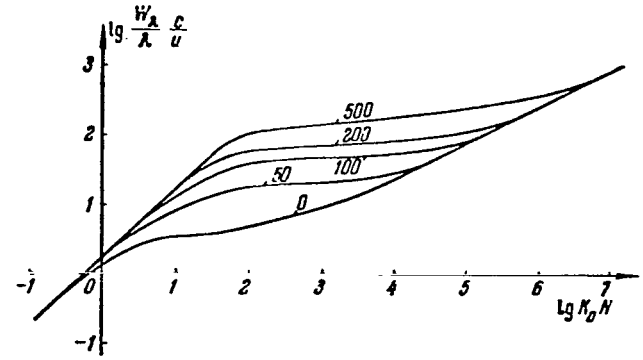

Figure 39.

of the atmosphere. It must be noted that in the case given the use of the usual curve of growth (found in Section 12 for stationary atmospheres) leads to large errors in the chemical composition.

From observations it is concluded that in the pre-maximum spectra of many novae a decrease occurred in the shift of the absorption lines with time. At first an attempt was made to explain this effect in terms of a slowing down of the envelope because of stellar gravitation. In this case extremely large values were obtained for the masses of novae (of the order of hundreds and thousands of solar masses). Then, however, it was ascertained that nova masses are of the same order as the masses of other stars. Therefore the explanation given above had to be discarded. It is possible that in reality the decrease in the absorption line shift in nova spectra is not entirely caused by a change in the envelope velocity, but by a change in the effective level of the absorbing material in the envelope, in which the velocity depends on the distance from the center of the star. If the outer layers of the envelope are expanding with a greater velocity than the inner, then as the outer layers disperse, the effective level of the absorbing material will approach the inner boundary and the absorption line shift will decrease. It should be noted that such behavior must always be taken into consideration in interpreting a change in the shifts of the absorption lines.

The spectra of novae immediately after the moment of maximum brightness are extremely complex and their theoretical interpretation meets with great difficulty. Apparently the ejection of matter from the star, beginning after detachment of the envelope from it, plays a large role in the formation of these spectra. /405 This process leads to the formation of an extended atmosphere around the star, which absorbs the ultraviolet radiation of the star and converts it into lower frequency photons. It must be taken into account that the extended atmosphere possesses, at this time, a fairly large optical thickness in the continuous spectrum since its absorption and emission spectra are characteristic of stars of the relatively late classes (so-called diffuse spark spectra). Judging from the shift of the absorption lines (or from the width of the emission lines), the outward velocity of material from the star exceeds the velocity of the envelope. Therefore the ejected material overtakes the envelope and produces emission lines in it because

of collisions. Moreover, the ejected material, added to the envelope, increases its velocity (see Section 30 concerning this), so that the shift of the absorption lines increases, as noticed in observations. It should also be considered that after the detachment of the primary envelope from the star, in some cases additional envelopes are detached from the star. This can explain the appearance of secondary maxima on the descending branch of the nova brightness curve and also the appearance of additional systems of absorption lines in its spectrum.

As time passes, the rate of matter ejection from the star decreases and the extended atmosphere becomes transparent to the ultraviolet radiation of the star. Then the envelope shines primarily because of this radiation. At first, however, this emission occurs in a more complex fashion than in nebulae because of the opacity of the envelope to line radiation. Therefore in the case given the intensity of the emission lines must be calculated on the basis of the theory discussed in Section 28. Such calculations lead to theoretical and observed Balmer decrements that are in agreement.

It is interesting to note that a completely anomalous Balmer decrement has been observed in the spectra of some novae for some months after start of the outburst. Thus, for example, in the spectrum of Nova Lacertae 1936 the H_α line was 5-6 times brighter than the H_β line, and in the spectrum of RS Ophiuchi 1933—10-12 times brighter. This phenomenon is explained by the fact that in the period being considered the envelope was opaque to radiation in the Lyman and Balmer series lines and transparent to lines of the other series. The solution of Eqs. (28.18) for the case given leads to precisely these large values of the ratio of the intensities of the H_α and H_β lines. As the envelope expands, it becomes transparent to radiation in the lines of all series, except Lyman, and the Balmer decrement in the nova spectrum is the same as in the spectrum of a gaseous nebula.

4. Nebular phase. With the appearance of forbidden lines in the spectrum of a nova, the nebular phase of its evolution begins. From this time the conditions in the envelope become similar to the conditions in gaseous nebulae and, therefore, the envelope can be investigated by the methods discussed in Chapter V. In particular, nova temperatures (which turn out to be very high—about 50,000°) can be determined by the Zanstra methods. From the envelope emission in the lines of various atoms one can find the concentration of these atoms in the envelope, its electron temperature, mass, etc. We will not discuss all of these questions here, but will consider only some of them. /406

As established in Section 25, in order for forbidden lines to appear in the spectrum of any object it is necessary for the radiation density and the density of matter in them to be quite low. One can show that in the envelopes of nova the first of these conditions (regarding the radiation density) starts to be satisfied sooner than the second. Consequently, forbidden lines appear in the spectrum of a nova at a density of matter in the envelope when the number of spontaneous transitions in these lines becomes comparable to the number of collisions of the second kind. In other words, at this time the condition

$$A_{21} \approx n_e \sigma_{21} v, \qquad (29.12)$$

is satisfied, where A_{21} is the Einstein spontaneous transition coefficient in the forbidden line, n_e is the density of free electrons in the envelope, σ_{21} is the effective cross section for collisions of the second kind, v is the average velocity of a free electron.

If the quantities A_{21} and σ_{21} are known for a given forbidden line, then, using Eq. (29.12), one can find the free electron density n_e in the envelope for that moment when this line appears in the nova spectrum (before this moment the quantity n_e is larger than the value determined from Eq. (29.12), and after—smaller). On the other hand, the envelope volume V for this same moment can be calculated from the envelope expansion velocity and from the time interval elapsed since the start of the outburst. This gives the possibility of determining the envelope mass from the formula

$$M = m_H V n_e \tag{29.13}$$

(since the number of free electrons is equal to the number of protons, and the hydrogen in the envelope is predominantly in the ionized state).

The mass of the nova envelope can also be found by the same method used for determining the masses of gas nebulae. This method is based on using the hydrogen line emission of the envelope, arising, as we know, as a result of photoioni tions and subsequent recombinations. In Section 24 the following formula /407
for the envelope mass was derived by using the theoretical expressions for the intensities of the Balmer lines:

$$M = C\sqrt{LV}, \tag{29.14}$$

where L is the luminosity of the envelope in the visible portion of the spectrum and C is some constant.

The use of these methods for determining the envelope masses of novae leads to values of about 10^{28}-10^{29}g. In other words, during each outburst a nova ejects a mass of about 10^{-5}-10^{-4} solar mass.

In the nebular stage of a nova it is also easy to determine the electron temperature of the envelope. The simplest way to do this is to use the observed ratio of the intensities of the $N_1 + N_2$ and λ 4363 Å lines, belonging to doubly ionized oxygen. The forbidden lines in nova spectra are excited by electron collision and their intensities depend on the electron temperature T_e and the electron density n_e. When, however, the envelope density is so low that spontaneous transitions occur much more frequently than collisions of the second kind, the ratio of the intensities of these lines depends only on T_e and, as is shown in Section 25, is determined by Eq. (25.22). In nova spectra, as in the spectra of gaseous nebulae,

the N_1 and N_2 lines are usually much brighter than the λ 4363 Å line (by about a factor of 100). Therefore values of about 10,000° are obtained for the electron temperatures of envelopes.

It should, however, be noted that at the start of the nebular stage the N_1 and N_2 lines are weaker than the λ 4363 Å line. This is explained by the fact that at the time of appearance of forbidden lines in the nova spectrum, the role of collisions of the second kind is still important. Let us assume, for example, that collisions of the second kind predominate over spontaneous transitions. Then the populations of the atomic energy levels are determined by Boltzmann's formula and the ratio of the intensities of the lines being considered is given by Eq. (25.24). From this formula it is seen that the N_1 and N_2 lines will actually be weaker than the λ 4363 Å line only if the envelope temperature is very low.

Interesting information on the envelopes of novae can be obtained through a study of the profiles of the emission lines in their spectra. In the nebular stage the envelope is transparent to line radiation so that analysis of the line profiles is significantly simplified. Since the expansion velocities of envelopes are much greater than the average thermal velocity of the atoms, the profiles of the emission lines are determined primarily by the motion of the envelope. As shown in Section 28, when the envelope possesses spherical symmetry and all its layers are /408 moving with the same velocity, the emission line profile is rectangular. Such line profiles are actually observed for a number of novae, which indicates their envelopes are approximately spherical. Usually, however, the emission lines in nova spectra have a very complex structure. In particular, in some cases (for example, in the spectrum of Nova Herculis 1934) the emission lines would be split, i.e., be saddle-shaped. As we already known, such profiles cannot be explained by a velocity dispersion in a spherically symmetrical envelope. Therefore one must conclude that the envelopes of some novae do not possess spherical symmetry, i.e., the ejection of material from the star occurs with different intensities in different directions.

This conclusion is confirmed by photographs of nova envelopes in which individual blobs of material are visible in the envelopes. Such blobs were first observed in the envelope of Nova Pictoris 1925 (on the basis of this the subsequently unjustified hypothesis was made concerning the formation of multiple stars during nova outbursts). Two bright blobs were also observed in the envelope of Nova Herculis 1934. The splitting of emission lines in the nova spectrum is explained by the movement of these blobs with different radial velocities.

To interpret the deviations of nova envelopes from sphericity, E.R. Mustel' set forth an assumption concerning the strong magnetic fields of these stars. If for example it is assumed that the field is dipole in nature, then the ionized gas ejected from the star will undergo minimum deceleration in the polar directions where the gas is moving approximately parallel with the lines of force. Therefore the amount of ejected matter will be a maximum in the polar direction.

One can also conclude that the deviation of nova envelopes from sphericity is caused by the entry of these stars into intimate binary systems. Nova Herculis

1934 is a component of such a system. Several other cases of nova doubling have been discovered recently.

5. Herculis nova of 1934. One of the most interesting and thoroughly studied novae is Nova Herculis 1934. It must be classed as a "special" nova since it is markedly different from most novae in terms of the variations in its brightness and spectrum.

The light curve of Nova Herculis 1934 is depicted in Fig. 40. The brightness of the star, increasing initially from $14\text{-}15^m$ to $1^m.3$ (22 decades), then slowly decreased over a period of three months. At this time the spectrum of the star belonged to class F with the emission lines of H, Fe II, Ca II, etc. In April 1935 the nova brightness rapidly fell to $13^m.1$ and then increased by approximately 7^m, after which it again began to decrease slowly. After the April minimum the nova /409 spectrum became typical of gaseous nebulae. The increase in the intensities of the lines of this spectrum caused an increase in the nova brightness by seven stellar magnitudes.

The explanation of the brightness and spectral changes of Nova Herculis 1934, given by Grotrian, consists in the following. During the first three months after start of the outburst, a great deal of matter was ejected from the star, leading to the formation of a very extended atmosphere around it. However, the outermost portions of the envelope did not shine at this time since the ultraviolet radiation of the star was not reaching them. This radiation was absorbed very near the star in envelope layers which converted it into lower frequency radiation in the continuous spectrum, i.e., played the role of an extended photosphere. In April the amount of material being ejected from the star decreased suddenly, the extended photosphere dispersed and the brightness of the nova in the visible portion of the spectrum fell drastically. This exposed a very hot star (with a temperature of about 70,000°); the ultraviolet radiation of this star then caused the outermost rarefied portions of the envelope to shine, similarly to the shining of gaseous nebulae, so that the brightness of the nova in the visible portion of the spectrum began to increase again. This process of increasing nova brightness continued as long as the intensity of the emission lines of the envelope spectrum did not equal that of the ultraviolet radiation of the star. The subsequent slow decrease in nova brightness is associated with the gradual dispersion of the nebular envelope.

An examination of the radiation of the Nova Herculis envelope after the April brightness minimum is of great interest. The point is that in theoretical astrophysics an assumption is usually made concerning the existence of radiative equilibrium in stellar envelopes. Even in those cases when a very rapid change occurs /410 in the physical conditions in envelopes, it is nevertheless assumed that radiative equilibrium tends to be established. In other words, envelope evolution is thought of as a sequence of equilibrium states. In some cases, however, envelopes radiate in the absence of radiative equilibrium. One of the most clear cut examples of such emission is the envelope of Nova Herculis after the brightness minimum in April. We have already seen that although the ultraviolet quanta of the star were reaching the nebular envelope at the time of minimum brightness, it still was not shining. Radiative equilibrium was clearly absent at this time. Subsequently the envelope evolved in the direction of establishing radiative equilibrium.

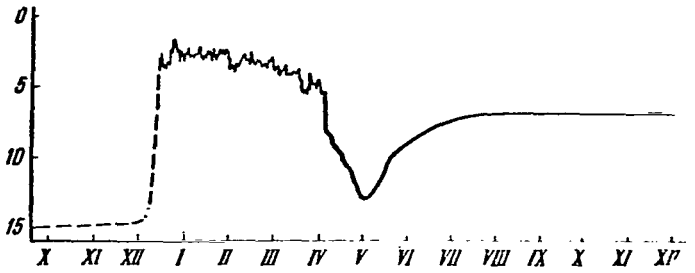

Figure 40.

This process can be considered completed only at the moment of the second brightness maximum.

Let us consider a theoretical interpretation of the emission of the Nova Herculis envelope after the April brightness minimum. For simplicity let us consider a hydrogen envelope of constant density. Let us assume that the envelope is spherically symmetrical, with its thickness being considerably less than its distance from the star ($r_2 - r_1 \ll r_1$).

Let $n_1(r, t)$ and $n^+(r, t)$ be the number of neutral and ionized atoms, respectively, in 1 cm^3 at a distance r from the star at time t, and n be the number of hydrogen atoms in 1 cm^3, so that

$$n_1(r, t) + n^+(r, t) = n. \tag{29.15}$$

At the initial instant of time, which we take as the time of the sudden temperature increase of the star, all envelope atoms are un-ionized, i.e., $n_1(r, 0) = n$ and $n^+(r, 0) = 0$.

Then ionization of the atoms occurs through the absorption of photons emitted by the star beyond the Lyman series limit. The number of these photons, incident on 1 cm^2 of the inner boundary of the envelope per second, we will denote by H. If the absorption coefficient, calculated for one atom, is denoted by k, then the total number of ionizations occurring per second in 1 cm^3 at a distance r from the star at time t will be equal to

$$n_1(r, t) k H e^{-\tau(r, t)},$$

where $\tau(r, t)$ is the optical distance of a given point from the inner edge of the envelope, i.e.,

$$\tau(r, t) = \int_{r_1}^{r} n_1(r, t) k \, dr. \tag{29.16}$$

In addition to the ionizations, reverse processes, i.e., recombinations, also occur in the envelope. The number of recombinations at the i-th level, occurring per second in 1 cm^3 at a distance r from the star at time t, is equal to /411

$$n_e(r, t) n^+(r, t) C_i(T_e),$$

where $n_e(r, t)$ is the number of free elctrons in 1 cm^3.

At each point of the envelope the change in the number of ions is equal to the difference between the number of ionizations and the number of recombinations. Therefore we have

$$\frac{\partial n^+}{\partial t} = n_1 k I I e^{-\tau} - n_e n^+ \sum_{i=2}^{\infty} C_i. \tag{29.17}$$

Recombinations at the first level and ionization due to the effect of the diffuse radiation of the envelope are ignored in Eq. (29.17) since these processes compensate each other.

Thus, the problem of determining the change in the number of ionized atoms in the envelope reduces to solving Eq. (29.17) for the conditions (29.15) and (29.16). We will not discuss the detailed solution of this equation here (see [13]), and we will give only some of the results.

Let the optical thickness of the envelope beyond the Lyman series limit at the initial instant of time be much greater than unity, i.e., $\tau(r_2, 0) \gg 1$. Further, let the stellar radiation be so intense that it is able to create a degree of ionization in the envelope considerably in excess of unity ($n^+/n_1 \gg 1$). In this case for each instant of time the envelope can be divided into two regions: "ionized" ($n^+ \gg n_1$) and "un-ionized" ($n^+ \ll n_1$) with a very sharp boundary between them, and the gradual increase in ionization in the envelope can be considered as a movement of the boundary between these regions. This boundary occurs approximately at the point where $\tau \approx 1$ for a given instant of time. Such a result is completely understandable since as long as $\tau \gg 1$ for the layer being considered, the ionizing radiation of the star does not reach it. Ionization begins in a layer only when its optical thickness becomes of the order of unity because of the ionization of the envelope portion nearest the star.

This result makes it possible to easily find how the total number of ionized atoms in the envelope varies with time, i.e., the quantity

$$N^+ = \int n^+ dV. \tag{29.18}$$

Let us integrate both sides of Eq. (29.17) over the entire envelope volume. Denoting the total number of photons, emitted by the star beyond the Lyman series

limit in 1 sec, by $\overline{H}$, we obtain /412

$$\frac{dN^+}{dt} = \overline{H} - N^+ n \sum_2^\infty C_i. \tag{29.19}$$

The last term in this equation is written on the basis of the relation

$$\int n_e n^+ dV = nN^+, \tag{29.20}$$

which follows from the fact that in the ionized region $n_e \approx n$, and in the un-ionized region $n_e \approx 0$.

The solution of Eq. (29.19), satisfying the initial condition $N^+(0) = 0$, has the form

$$N^+(t) = \overline{H} t_* (1 - e^{-\frac{t}{t_*}}), \tag{29.21}$$

where

$$t_* n \sum_2^\infty C_i = 1. \tag{29.22}$$

The quantity t_*, defined by Eq. (29.22), can be considered as the time to establish equilibrium. As is seen, it is greater, the lower the density of matter in the envelope.

To evaluate the quantity t_*, we note that for hydrogen $\sum_2^\infty C_i \approx 3 \cdot 10^{-13}$ (for $T_e = 10,000°$). This means that when $n \approx 10^{10}$ cm^{-3} the quantity t_* is of the order of several minutes. In nova envelopes $n > 10^{10}$ cm^{-3} in the initial period after maximum brightness. Therefore one can assume that in the given case the establishment of radiative equilibrium results directly from a change in the physical conditions in the envelope. In the case of Nova Herculis 1934, however, the stellar temperature increased suddenly when the density of matter in the envelope was already extremely low. It is for this reason, therefore, that the establishment of radiative equilibrium in the envelope of Nova Herculis was delayed by months.

With the aid of the formulas derived, one can find the change with time of the total amount of energy radiated by the envelope in any Balmer line. As we know, the amount of energy E_{k2} radiated by the envelope in the $k \to 2$ transition is given by Eq. (28.30). Using Eqs. (29.20) and (29.21) instead of (28.30), we find

$$E_{k2} = A_{k2} h \nu_{2k} z_k n \overline{H} t_* (1 - e^{-\frac{t}{t_*}}). \tag{29.23}$$

Values of the quantity E_{k2} for several of the Balmer lines were determined from observations of Nova Herculis. These values vary with time approximately the as the star brightness (which is completely understandable since the increase in brightness is also caused primarily by an increase in the energy emitted in the lines). The observed variation of the E_{k2} values is well represented by Eq. (29.23). Here a value of $n = 3 \cdot 10^6$ cm^{-3} must be assumed for the atom density in the envelope. /413

The change in the emission line profiles in the Nova Herculis spectrum after the April brightness minimum is also of interest. As already stated, the emission lines in the spectrum of this nova were split, which is caused by the presence of two blobs of matter, having different radial velocities, in the envelope. Observations have shown that at the time of appearance of the emission lines their red components were much weaker than the violet components and both components were of comparable intensity only at the time of the second brightness maximum. This behavior of the emission lines seemed puzzling at first and some hypotheses were made to explain it. It can, however, be easily explained on the basis of the discussed concept of envelope emission in the absence of radiative equilibrium (more precisely, with the aid of Eq. (29.23)). From observations it is seen that the intensity of the violet component increased more rapidly than the intensity of the red component. This means that radiative equilibrium was established more quickly in the blob of matter approaching us than in the blob receding from us. As already pointed out, this is the situation when the density of matter is different in the blobs (less—in the one approaching us and greater—in the one receding from us). The value, given above, of the density of atoms in the envelope is some average value for both blobs.

Knowing the atom density n and the envelope volume V provides the possibility of determining the envelope mass from Eq. (29.13). Such a mass determination method is, however, associated with some uncertainty because of possible errors in calculating the envelope volume. In order to avoid determining the volume, one can proceed in the following manner. Let us multiply both sides of Eq. (29.22) by n^+ and integrate over the entire envelope volume. As a result we obtain

$$t_* \int n_e n^+ \sum_2^\infty C_i dV = \int n^+ dV, \tag{29.24}$$

where we have replaced n by n_e since the integration, in essence, is done only in the ionized region and there $n_e \approx n^+ \approx n$. But the integral on the right side of this equation is the total number of hydrogen ions in the envelope, and the integral on the left side is the total number of recombinations at all levels, starting with the second. The latter number, however, is equal to the number of Balmer photons emitted by the envelope in 1 sec. Consequently, we have /414

$$t_* N_{Ba} = N^+. \tag{29.25}$$

Equation (29.25) allows one to determine the quantity N^+ for any instant of time t from observed values of the quantities t_* and N_{Ba}. Applying this formula to the time of the second brightness maximum, we obtain the total number of hydrogen atoms in the envelope (if it is assumed that $n^+ \gg n_1$ throughout the entire envelope at this instant of time). With the aid of Eq. (29.25) it was found that in the Nova Herculis envelope the total number of hydrogen atoms is equal to $1.4 \cdot 10^{52}$, and this means its mass is equal to $2.3 \cdot 10^{28}$ g.

Equation (29.23) determines not only the change with time of the hydrogen line intensities, but also the intensities of the lines of other atoms, arising as the result of photoionizations and recombinations. The forbidden lines, whose radiation is excited by electron collisions, behave somewhat differently since the intensities of these lines depend strongly on the electron temperature of the envelope. As we have seen in Section 23, the electron temperature level is determined primarily by the energy acquired by the free electrons through photoionizations and by energy lost by them through collisions. Since collisions occur infrequently for a low density of matter in the envelope, the establishment of an equilibrium temperature can extend over a long period of time. The problem of the change of electron temperature of the envelope with time has been examined by I. N. Minin [14]. The solution obtained has made it possible to interpret the behavior of the forbidden lines in the Nova Herculis spectrum during the time when radiation equilibrium did not exist in the envelope.

6. Novae many years after outburst. The envelope of a nova disperses to a considerable extent over a period of some decades after outburst and the brightness of the star approaches the value it had before the outburst. A study of the star during this period (possible only with the aid of the largest telescopes) has led to very interesting results. The discovery of the duality of some novae, making it possible to determine their masses, is especially important.

Duality was first discovered in Nova Herculis 1934 (Waker in 1954). Observations indicated that the star is an eclipsing variable with a period of 4 hours 39 minutes. At the primary brightness minimum the cold star eclipses the hot star (which, apparently, also flares up in the form of a nova). A lack of knowledge about the cold star prevents a precise determination of the masses of the components; in all probability, the mass of the hot star amounts to about 0.25 solar mass.

Emission lines, arising partly in the very tenuous envelope that was ejected in the 1934 outburst and partly in the denser envelope surrounding the star, are observed in the Nova Herculis spectrum in the period under consideration. The spectrum of the latter envelope changes significantly together with the eclipse phase. A study of the variations of this spectrum, undertaken by Kraft [15], showed that this envelope can be represented in the form of a "disk", rotating about the hot star with a velocity of about 500 km/sec. Apparently, this "disk" is formed as a result of the ejection of matter from the cold star. From the energy distribution in the continuous spectrum it was found that the temperature of the hot star is about 80,000°. The stellar radius, determined on the basis of the temperature and luminosity, is close to the radii of white dwarfs. A sur- /415

prising feature of the hot star is the fact that it undergoes small brightness fluctuations with a very well-defined period equal to about 71 seconds.

Besides Nova Herculis 1934, there are many other stars, which have flashed in the form of novae, that are in binary systems (in particular, Nova Persei 1901, Nova Aurgae 1891, Nova Aquilae 1918). The binary condition was found to be an extremely common phenomenon among the novae that have been examined lately. On this basis Kraft even put forth the hypothesis that the entry of a star into a binary system is a necessary condition for an outburst.

One can assume that novae exist in their normal states many years after outburst. Since data on the spectra and luminosities of stars in these states are available to us, one can pose a question about their location on the spectrum-luminosity diagram. This same question is of interest with respect to the repeating novae and novalike variables. B. A. Vorontsov-Vel'yaminov (see [9]) studied this problem first and concluded that a special sequence of stars, called blue-white by him, existed on the spectrum-luminosity diagram. This sequence starts from the class O stars, runs through the Wolf-Rayet type stars, novalike variables, repeating and ordinary novae and ends with the blue and white dwarfs.

B. A. Vorontsov-Vel'yaminov advanced the hypothesis that the blue-white sequence has an evolutionary significance: the most massive stars, losing mass, move along the sequence as they evolve, finally changing into white dwarfs. The loss of mass initially occurs in the form of a continuous ejection, and then as outbursts, with the intervals between them gradually increasing. The fact that the stellar masses do in fact decrease along the sequence (the masses of class O /416 stars amount to about 40 $M_\odot$, the masses of WR type stars—about 10 $M_\odot$, the masses of white dwarfs—of the order of $M_\odot$ and less) favors this hypothesis. The objection that the spatial and kinematic characteristics of the various star types, entering into the sequence, are different was raised against this hypothesis. These characteristics cannot change significantly during the relatively short "lifetime" of the objects under consideration (about 10^5-10^6 years for WR stars and about 10^7-10^8 years for novae) as they evolve along the sequence. Not excluded, however, is the fact that an evolutionary relationship does exists between the individual members of the blue-white sequence.

In conclusion, let us emphasize that stars, differing drastically from other stars, are subject to outbursts in the form of novae. For example, stars such as the Sun cannot flare up.

30. Motion and Luminosity of Envelopes

1. Energy released during outburst. In the previous section we were concerned primarily with interpreting the variations in nova spectra caused by the receding of the ejected envelope from the star. Now we will consider the problems associated with the ejection of the matter and with the energy released during the outburst.

Let us first find the total energy released during a nova outburst. This energy is composed of three parts: 1) radiative, 2) kinetic energy of the envelope and 3) the energy to separate the envelope from the star.

The radiative energy is determined from the formula

$$E_{rad} = \int L(t)\,dt, \tag{30.1}$$

where L(t) is the nova luminosity, and the integration extends over the entire outburst period. The integral of (30.1) can be calculated for each nova with the aid of the light curve. It turns out that $E_{rad} \approx 10^{45}$-10^{46} ergs.

The kinetic energy is equal to

$$E_{kin} = \frac{1}{2} M v^2. \tag{30.2}$$

Assuming a value of about 10^{28}-10^{29} g for the mass M of the envelope and a value of about 1000 km/sec for its velocity v, we find that $E_{kin} \approx 10^{44}$-10^{45} ergs.

To calculate the energy to separate the envelope from the star the formula /417

$$E_{sep} = G\frac{M_* M}{r_*}, \tag{30.3}$$

must be used, where G is the gravitational constant, M_* is the stellar mass and r_* is its radius. Assuming that $M_* \approx M_\odot$ and $r_* \approx 0.1\, r_\odot$, we find $E_{sep} \approx$ $\approx 10^{44}$-10^{45} ergs.

Thus, an extremely large amount of energy (of the order of 10^{45}-10^{46} ergs) is released during a nova outburst. For comparison, one can note that the Sun radiates the same amount of energy in a period of 10^5-10^6 years.

The sources of the energy, released during a nova outburst, are a very important question. To answer this question we will determine the physical conditions in the layer where the envelope is tearing away from the star. We will assume the envelope mass M is known. Assuming that the envelope is composed primarily of hydrogen, we have

$$M = 4\pi r_*^2 m_H \int_{r_*}^{\infty} n\,dr, \tag{30.4}$$

where r_* is the radius of the separation layer and n is the hydrogen atom density in the envelope.

To compute the integral of (30.4) we need to know the dependence of n on r. This dependence is given in photosphere theory (see Section 4). Since the temperature in the envelope is very high, let us take the expression

$$\alpha = C\frac{n^2}{T^{7/2}}, \tag{30.5}$$

for the volume absorption coefficient, where C is some constant (of the order of 10^{-23}). In this case, from Eqs. (4.51) and (4.52) it follows that

$$n = n_*\left(\frac{T}{T_*}\right)^{15/4} \tag{30.6}$$

and

$$\frac{dT}{dr} = -\frac{2}{17}\frac{m_H g}{k}, \tag{30.7}$$

where n_* and T_* are the values of n and T in the separation layer, g is the gravitational acceleration at the surface of the star, k is Boltzmann's constant. Substituting (30.6) into (30.4) and using (30.7), we obtain

$$M = 8\pi r_*^2\frac{k}{g}n_* T_*. \tag{30.8}$$

Equation (30.8) gives one relationship between the desired quantities n_* and T_*. To find another relationship between them, we can made use of the relation /418

$$T_*^4 = T_0^4\left(1+\frac{3}{2}\tau_*\right), \tag{30.9}$$

where T_0 is the surface temperature of the star and τ_* is the optical depth of the separation layer, i.e.,

$$\tau_* = \int_{r_*}^{\infty}\alpha\, dr. \tag{30.10}$$

Substituting Eq. (30.5) into (30.10) and taking (30.6) and (30.7) into account, we have

$$\tau_* = \frac{17}{8}\frac{Ck}{m_H g}\frac{n_*^2}{T_*^{5/2}}. \tag{30.11}$$

Equations (30.8), (30.9) and (30.11) allow one to determine the quantities n_*, T_* and τ_*. Assuming that $T_0 = 50,000°$, $r_* = 10^{10}$ cm, $g = 10^7$ cm/sec^2,

$M = 10^{28}$ g (these values must be considered to be the most probable), we find

$$n_* \approx 5 \cdot 10^{22} \text{ g/cm}^3, \quad T_* \approx 5 \cdot 10^6 \text{ deg}, \quad \tau_* \approx 10^8.$$

One source of the nova emission is the energy contained in the envelope at the start of the outburst. This energy is thermal, radiative and ionizational in nature. As the envelope expands, the energy contained in it escapes in the form of radiation, i.e., the envelope luminesces.

The amount of thermal energy in the envelope is given by the formula

$$E_{\text{ther}} = 4\pi r_*^2 \frac{3}{2} k \cdot 2 \int_0^{T_*} nT \left(-\frac{dr}{dT}\right) dT, \tag{30.12}$$

where 2n is the total number of particles (protons and free electrons) in 1 cm^3. With the aid of Eqs. (30.6)-(30.8) we obtain

$$E_{\text{ther}} = \frac{17}{7} kT_* \frac{M}{m_H}. \tag{30.13}$$

Assuming that $T_* \approx 5 \cdot 10^6$ deg and $M \approx 10^{28}$-10^{29} g, we obtain $E_{\text{ther}} \approx 10^{43}$-$10^{44}$ ergs.

The amount of radiative energy in the envelope is equal to

$$E_{\text{rad}} = 4\pi r_*^2 a \int_0^{T_*} T^4 \left(-\frac{dr}{dT}\right) dT, \tag{30.14}$$

or, with (30.7) taken into account,

$$E_{\text{rad}} = 4\pi r_*^2 \frac{17}{10} \frac{kaT_*^5}{gm_H}. \tag{30.15}$$

Assuming the values given above for the quantities r_*, T_* g, we obtain $E_{\text{rad}} \approx$ /419
$\approx 10^{42}$ ergs. Consequently the amount of radiative energy in the envelope is considerably less than the amount of thermal energy.

The amount of ionizational energy in the envelope (converting into radiation when the degree of ionization decreases) is also small in comparison with the amount of thermal energy. This follows from the fact that for temperatures of the order of a million degrees the ionization energy of the most prevalent elements (hydrogen and helium) is small compared with kT.

Thus, the internal energy of the envelope (predominantly in the form of thermal energy, as explained) is about 10^{43}-10^{44} ergs. This energy is radiated

as the envelope expands. It amounts, however, to only a small fraction of the total energy emitted during a nova outburst. As we will see later, the internal energy of the envelope plays some role in its luminosity only in the first stage of the outburst.

Another source of the nova luminosity is the emission of the star after the envelope is separated from it. Since the temperature of the separation layer is very high, the stellar luminosity immediately after envelope separation should be very high. This brightness, however, does not correspond to the energy being generated within the star, and therefore the stellar temperature should decrease gradually. This process is complicated by the continuous ejection of matter from the star. An estimate of the energy radiated by the star after the envelope separation is very difficult to arrive at; however, undoubtedly the envelope shines for some time after the start of the outburst because of this very energy.

Finally, additional energy released during the outburst, i.e., the explosion energy, can serve as a source of nova radiation. The separation of the envelope from the star and its subsequent expansion occur because of this energy. As we have seen, an energy equal to 10^{44}-10^{45} ergs is expended in this. If an equal portion of the explosion energy changes into radiation, then it can play a significant role in the nova luminosity.

2. Interpretation of light curve. Knowing the sources of the nova luminosity and the rule for envelope expansion allows one, in principle, to determine the variation of the envelope brightness with time, i.e., to construct a theoretical nova light curve. Here, the intrinsic difference in the envelope radiation mechanisms before and after the instant of maximum brightness must be kept in mind. While the light is increasing, the envelope brightness is caused by continuous spectrum radiation, i.e., the envelope is the photosphere. At maximum brightness the optical thickness of the envelope in the continuous spectrum becomes of the order of unity and bright lines appear in the nova spectrum. The relative role of the bright lines in the envelope emission increases and, after some time, it predominates. /420

Let us now discuss the period from start of the outburst to the moment of maximum brightness (see [16]) for more details). In this interval the physical conditions in the envelope are changing very rapidly with time. In particular, the optical thickness of the envelope decreases from a value of about 10^8 to a value of the order of unity. Therefore a very difficult radiation transfer problem in a medium with changing optical properties has to be solved to determine the change of envelope brightness with time. Strictly speaking, these properties are not even defined and, in turn, depend on the radiation field; however, we will ignore this fact.

The problem facing us can be formulated thus. Let the envelope radiate both because of the energy present in it at the start of the outburst, and also because of the stellar radiation after envelope separation. Let us denote the initial envelope energy by E, and the stellar luminosity by $L_*(t)$, where t is the time, measured from start of the outburst. Let r(t) be the envelope radius and $\tau_0(t)$—

its optical thickness. All the quantities mentioned are assumed to be specified. The envelope luminosity L(t) is to be determined.

To simplify the problem we will assume that the envelope thickness is small compared with its radius, and we will ignore the residence time of radiation in the envelope itself compared with its residence time in the void created by the envelope. In other words, we will replace the radiation diffusion process in the envelope by a photon transfer mechanism in this void after their nearly instantaneous reflection from the envelope. Under the assumption of the existence of radiative equilibrium in the envelope itself, the probability of reflection of a photon from it is equal to $\tau_0(t)/[1 + \tau_0(t)]$, and the probability of transmission of a photon through the envelope is equal to $1/[1 + \tau_0(t)]$. At the start of the outburst the quantity $\tau_0(t)$ is very large so that each photon, before its passage through the envelope, undergoes an enormous number of transits in the void. The quantity $\tau_0(t)$ decreases with time, the escape process of photons from the void outward is accelerated and the envelope brightness increases.

The change, with time, of the amount of energy in the void created by the envelope must be considered in determining the envelope luminosity L(t). The amount of energy in the void increases because of the stellar radiation, and decreases because of the escape of radiation outward from the envelope. On the basis of the energy conservation law, we obtain /421

$$L_*(t) - L(t) = \frac{d}{dt}\left[\frac{4}{3}\pi r^3(t)\rho(t)\right], \tag{30.16}$$

where $\rho(t)$ is the radiation density in the void (obviously independent of location).

The radiation density $\rho(t)$ can easily be related to the envelope luminosity L(t). If the intensities of the radiation, reflected and transmitted by the envelope, are denoted by $I_1(t)$ and $I_2(t)$, respectively, then we have

$$I_1(t) = \tau_0(t) I_2(t). \tag{30.17}$$

But the radiation density $\rho(t)$ is equal to

$$\rho(t) = \frac{4\pi}{c} I_1(t), \tag{30.18}$$

and the envelope luminosity L(t) is related to the quantity $I_2(t)$ by the expression

$$I_2(t) = \frac{L(t)}{4\pi^2 r^2(t)}. \tag{30.19}$$

Therefore we obtain

$$\rho(t)=\frac{L(t)\tau_0(t)}{\pi c r^2(t)}. \tag{30.20}$$

Substituting (30.20) into (30.16) leads to the following equation for determining L(t):

$$L_*(t)-L(t)=\frac{4}{3c}\frac{d}{dt}[\tau_0(t)r(t)L(t)] \tag{30.21}$$

Clearly, the solution of Eq. (30.21) must satisfy the condition

$$\int_0^\infty L(t)\,dt=E+\int_0^\infty L_*(t)\,dt. \tag{30.22}$$

Such a solution has the form

$$L(t)=\frac{3c}{4\tau_0(t)r(t)}\left[Ee^{-\frac{3c}{4}\int_0^t\frac{dt'}{\tau_0(t')r(t')}}+\right.$$
$$\left.+\int_0^t L_*(t')e^{-\frac{3c}{4}\int_{t'}^t\frac{dt''}{\tau_0(t'')r(t'')}}dt'\right]. \tag{30.23}$$

To calculate the envelope luminosity L(t) from Eq. (30.23) it is necessary to know the quantities r(t) and $\tau_0(t)$. As an example, let us take /422

$$r=vt,\qquad \tau_0=\tau_*\left(\frac{r_*}{r}\right)^k, \tag{30.24}$$

where k is some parameter. Then instead of Eq. (30.23) we obtain

$$L(t)=kbt^{k-1}\left[Ee^{-bt^k}+\int_0^t L_*(t')e^{-b(t^k-t'^k)}dt'\right], \tag{30.25}$$

where

$$b=\frac{3cv^{k-1}}{4k\tau_*r_*^k}. \tag{30.26}$$

Let us first assume that the envelope radiates only because of its own internal energy, i.e., $L_*(t) = 0$. In this case it is seen from Eq. (30.25) that the envelope luminosity initially increases and then decreases (if $k > 1$). It is easy

to derive that the luminosity reaches a maximum for an optical thickness value equal to

$$\tau_0 = \frac{3}{4(k-1)} \frac{c}{v}. \qquad (30.27)$$

Assuming $v \approx 1000$ km/sec and $k = 2$, from Eq. (30.27) we find $\tau_0 \approx 200$. When the optical thickness of the envelope becomes several times less than this value, the luminescence of the envelope is basically completed.

An examination of Eq. (30.25) shows, in general, that when the stellar luminosity $L_*(t)$ decreases, the envelope luminosity $L(t)$ initially increases (approximately as long as τ_0 does not decrease to the value given by Eq. (30.27)) and then decreases, gradually approaching the stellar luminosity $L_*(t)$ (Fig. 41).

To compare theory with observations it is convenient to convert from envelope luminosity to quantities which are directly derived from observations. Such quantities are the visual brightness of the nova and its effective temperature (or the corresponding spectral class).

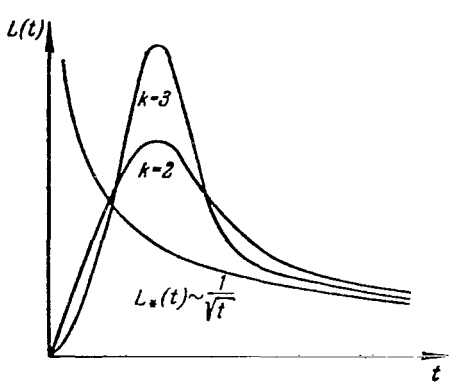

Figure 41.

The effective envelope temperature $T_e(t)$ is defined by the relation

$$L(t) = 4\pi r^2(t)\sigma T_e^4(t), \qquad (30.28)$$

from which it is seen that the quantity $T_e(t)$ slowly decreases with time (only if the envelope luminosity does not increase faster than r^2). /423

We will assume that the energy distribution in the envelope spectrum is given by Planck's formula. In this case the absolute visual magnitude of the envelope is determined by the formula

$$M_v(t) = -0{,}08 - 5\lg r(t) + \frac{29500}{T_e(t)} + 2{,}5\lg\left(1 - e^{-\frac{27000}{T_e(t)}}\right), \qquad (30.29)$$

into which T_e from (30.28) must be substituted.

From Eq. (30.29) it follows that the visual luminosity of the nova should increase rapidly with time because of the rapid increase in the surface of the envelope for a relatively slow decrease in temperature. It is of interest to note that the visual luminosity can increase even for a decrease in total brightness (since the increase in envelope surface is not compensated by a temperature decrease).

As calculations from the formulas presented show, the visual luminosity of the envelope increases rapidly at first, then slows down (caused by the luminescence of the envelope at this time) and then increases more slowly with a decreasing total brightness. This process continues until the primary brightness maximum is reached when the optical thickness of the envelope becomes of the order of unity. Then the envelope no longer absorbs all the stellar radiation, as before, but only a portion of it that decreases with time so that the nova brightness decreases.

The theoretical conclusions that have been discussed are confirmed, in general, by observational data. Observations actually show that a slow temperature decrease occurs with the increase in nova luminosity. Moreover, before the primary brightness maximum a slowing down was observed in the brightness rise for several novae, or even a slight decrease.

However, to achieve better agreement between theory and observations it is apparently necessary to assume that the envelope brightness continues to increase after the slowing down in the luminosity rise. As will be shown below, this may /424 be associated with the ejection of matter from the star, which begins after envelope separation.

3. Ejection of stellar matter. After separation of the envelopes from the star very hot stellar layers in an unstable state are revealed. The ejection of stellar matter should begin due to the effect of the radiation pressure force. When the optical thickness of the envelope in the continuous spectrum becomes less than unity, this process is observed firsthand. One can discern this from the so-called diffuse spark spectrum which appears after the maximum in nova brightness. The shift of the lines of this spectrum attests to the fact that the ejection velocity of the stellar matter exceeds the envelope velocity.

The ejection of stellar matter must obviously lead to an increase in the nova brightness. This is caused both by the luminescence of the ejected material and also by the slower cooling of the surface layers of the star itself. In addition, when the ejected material collides with the envelope, a portion of the kinetic energy is converted into thermal energy and then into radiation.

Now we will consider the problem of the motion of the envelope, which the material ejected from the star overtakes. Let us determine both the change in envelope velocity and the amount of kinetic energy that is converted into radiation.

At some fixed instant of time t_0, let the envelope have a mass M_0 and a velocity v_0. Let us assume that after envelope separation ejection of stellar matter occurs with a constant velocity u, with the amount of material ejected in 1 second being equal to au. Let us assume that $u > v_0$ and, therefore, the envelope mass M and its velocity v should increase with time.

To find the dependence of M and v on the time t, one must write the equation of motion of the envelope. Denoting the mass of material added to the

envelope in 1 second by q, we have

$$\frac{d(Mv)}{dt} = qu \tag{30.30}$$

and

$$q = \frac{dM}{dt} = a(u - v). \tag{30.31}$$

The equations that have been derived are very simple to solve. Substituting $q = dM/dt$ into (30.30) and integrating, we obtain

$$M(u - v) = M_0(u - v_0). \tag{30.32}$$

Introducing M from (30.32) into (30.31), we have

$$\frac{d}{dt}\left(\frac{1}{u - v}\right) = \frac{a(u - v)}{M_0(u - v_0)}. \tag{30.33}$$

Integration of this equation yields /425

$$v = u - \frac{u - v_0}{\sqrt{1 + \frac{2a}{M_0}(u - v_0)(t - t_0)}}. \tag{30.34}$$

Equation (30.34) defines the desired envelope velocity. Substituting v from (30.34) into (30.32), we obtain the following expression for the envelope mass as a function of t:

$$M = M_0\sqrt{1 + \frac{2a}{M_0}(u - v_0)(t - t_0)}. \tag{30.35}$$

By using Eq. (30.35) we can determine the amount of material added to the envelope in the time $t - t_0$, i.e., the quantity $Q = M - M_0$. This quantity, with the aid of Eq. (30.32), can also be represented in the form

$$Q = M\frac{v - v_0}{u - v_0}. \tag{30.36}$$

Let us now turn to a consideration of the changes in the envelope energy. The kinetic energy of the matter added to the envelope during the time $t - t_0$ is equal to $1/2\ Qu^2$. A portion of this energy goes to increase the kinetic energy of the envelope, which during the same time interval changes from a value of $1/2\ M_0v_0^2$

to a value of $1/2\,Mv^2$. The rest of the energy, however, causes an increase in the internal energy of the envelope, which is then converted into radiation. The increase in the internal energy of the envelope is clearly equal to

$$\Delta E = \frac{1}{2} M_0 v_0^2 + \frac{1}{2} Q u^2 - \frac{1}{2} M v^2. \tag{30.37}$$

Using Eqs. (30.32) and (30.36), we obtain

$$\Delta E = \frac{1}{2} M (u - v)(v - v_0). \tag{30.38}$$

This formula defines the energy radiated by the envelope as the result of collisions with the matter ejected from the star.

To compute from these formulas the changes in the velocity, mass and internal energy of the envelope, it is necessary to have data on the ejection velocity u of the stellar matter and the rate of ejection au. Prior to the moment of maximum brightness we obviously have no such data. After this moment, the diffuse spark spectrum can be observed, and the velocity u can be determined from the displacements of the lines of this spectrum. Moreover, after maximum brightness, an increase is observed in the displacements of the absorption lines of the principal spectrum, which can be interpreted as an increase in the envelope /426 velocity due to the effect of the material ejected from the star. Observations allow one to find the velocity v_0 at time t_0, which can be taken as the moment of maximum brightness, and the velocity v at some time t. The envelope mass can be determined by one of the methods cited in the foregoing paragraph. All of this allows one to calculate from Eqs. (30.36) and (30.38) the amount of matter ejected by the star and the amount of kinetic energy being converted into radiation during some time interval after maximum brightness. These results can be extrapolated into the period before maximum brightness. In this situation it is found that the energy ΔE must play a significant role in the nova luminosity in that period. Such calculations were first made by V. G. Gorbatskiy (see [17] for more details).

4. Envelope motion in interstellar space. As the envelope of a nova expands, its mass increases not only because of the material ejected from the star and overtaking the envelope but also because of the interstellar material captured by the envelope. Since the density of the interstellar medium is very low, its effect on envelope motion becomes evident only in the later stage of envelope evolution. Let us now discuss this stage, ignoring the arrival of stellar matter at the envelope.

Let us assume that a nova has flared up in a homogeneous medium with density ρ. If, at the moment of outburst, the envelope mass is equal to M_0, then at a distance r from the star it becomes equal to

$$\frac{4}{3}\pi r^3 \rho + M_0.$$

On the basis of the law of momentum conservation we have

$$\left(\frac{4}{3}\pi r^3\rho + M_0\right)v = M_0 v_0, \tag{30.39}$$

where v_0 is the envelope velocity at the initial instant of time and v is the envelope velocity at the distance r from the star.

Substituting dr/dt instead of v in Eq. (30.39) and integrating, we obtain

$$\frac{4}{3}\pi r^4\rho + M_0 r = M_0 v_0 t, \tag{30.40}$$

where t is the time elapsed since start of the outburst. Equation (30.40) defines the envelope radius r as a function of the time t.

To find how the envelope expansion velocity changes with time, one must make use of Eqs. (30.39) and (30.40). Let us find, for example, the time span during which the velocity is halved. From (30.39) it is seen that v will be equal /427 to $1/2\, v_0$ when

$$\frac{4}{3}\pi r^3\rho = M_0. \tag{30.41}$$

Substituting (30.41) into (30.40), we obtain

$$t = \frac{5}{4v_0}\left(\frac{3M_0}{4\pi\rho}\right)^{1/3}. \tag{30.42}$$

for the time span we are seeking.

Listed in Table 48 are the time intervals within which the envelope velocity decreased by one-half and by one-hundredth, as well as the envelope radii when these velocities are reached. The average value of $\rho = 3\cdot 10^{-24}$ g/cm^3 is taken for the density of interstellar space, and v_0 = 1000 km/sec—for the initial envelope velocity. The table considers three envelope mass values: 10^{-5}, 10^{-4} and 10 solar masses.

Oort [18], studying for the first time the problem under consideration, also made a comparison of theory with observations. From the table it is seen that the slowing down of nova envelopes should become noticeable after a few decades. Generally speaking, however, this is not observed. For example, the envelope of Nova Aquilae 1918 has expanded for 30 years without slowing down. The absence of a noticeable slowing down in this case is apparently explained by the relatively large envelope mass (equal to 10^{-4} $M_\odot$). Another possible expla-

TABLE 48. SLOWING DOWN OF ENVELOPES DUE TO THE DRAG EFFECT OF INTERSTELLAR SPACE

$M_e/M_\odot$	10^{-5}		10^{-4}		10	
v/v_e	0.5	0.01	0.5	0.01	0.5	0.01
t in years	48	4500	102	9800	4800	450000
r in parsecs	0.04	0.18	0.08	0.38	3.8	17.6

nation is that during the time interval between outbursts the nova does not leave the region from which the interstellar matter was swept by the previous outburst.

If the nova outburst occurred at a place with an increased density of interstellar matter, then the detection of the envelope slowing down becomes more probable. In view of this, Nova Persei 1901 is of considerable interest since it /428 flared up, as we know, within a dust nebula and illuminated it. A comparison of photographs of the envelope of this nova, taken in 1917 and 1934, showed that during that time the envelope motion did slow down and in some cases the envelope was distorted. The latter can be explained by a nonuniformity of the dust nebula. It is interesting that the distorted edge of the envelope is extremely bright. According to Oort the luminosity is caused by collisions of envelope atoms with the particles of the dust nebula. This constitutes an additional confirmation of the slowing down of the envelope.

As already stated, in studying the motion of a nova envelope both envelope acceleration by material ejected from the star and retardation by interstellar space must be taken into consideration simultaneously. This was done in I. N. Minin's work (see [4]). The laws of envelope motion, presented above, result from his solution in the form of special cases.

31. Supernovae

1. Results of observations. As we already know, the absolute magnitudes of novae at maximum brightness are equal to -7^m on the average. There are, however, some flaring stars which, at maximum brightness, are thousands and tens of thousands times brighter than novae. These stars are called supernovae.

Supernovae flare up much less frequently than novae. Only three supernovae have been observed in our Galaxy in the last thousand years. One of these, according to Chinese records, flared up in the Taurus constellation in 1054. Tycho Brahe observed the second supernova in 1572 in Cassiopeia, and Kepler observed the third in 1604 in Ophiuchus. Supernovae, because of their immense brightness, can, however, also be discovered in other galaxies. The first such supernovae was discovered in the Andromeda nebula in 1885 (S Andromedae). Tens of supernovae have since been found in other galaxies, with the spectra and light curves having been determined for many of them.

As established by Minkovskiy, supernovae are divided into two groups on the basis of the nature of brightness and spectral variations. Type I supernovae all have very similar light curves, with the brightness decreasing exponentially. The light curves of type II supernovae are distinguished by their great variety and by a certain similarity to the light curves of ordinary novae. The spectra of type I supernovae consist of bright bands, separated by darker spaces. These bands have not yet been identified. Two bands, identifiable with the λ 6300 and λ 6364 Å forbidden lines of neutral oxygen, are seen in the spectra only in the relatively later stages. From the width of these bands one can conclude that the velocity of the ejected envelope is about 1000 km/sec. Type II supernovae before /429 the moment of maximum brightness have a continuous spectrum with a high-intensity ultraviolet end (color temperature of about 40,000°). After maximum brightness is reached, broad bright bands, identifiable with known lines (H, N III, etc.), appear in the spectrum. The width of these bands indicates tremendous envelope expansion velocities—of the order of 6000 km/sec. Types I and II supernovae apparently are quite different in their physical nature.

Rapidly expanding gaseous nebulae are found at the point of supernovae flare-ups. It is difficult to doubt that they are formed as the result of the ejection of material during the supernova outbursts. The Crab nebula, expanding with a velocity of about 1100 km/sec, is observed now at the location of the supernova in 1054. If the expansion velocity is assumed constant, then the time of the start of the expansion agrees approximately with the date of the outburst. The Crab nebula has been studied very thoroughly and more will be said about it below. The remains of the 1572 and 1604 supernovae are expanding filamentary nebulae. The brightness of these nebulae is low, however, and it is difficult to study them.

The fact that the remains of supernovae are intense sources of radio emission has considerable importance in understanding their nature. The radio emission from the Crab nebula was measured first (by Bolton in 1947), and then the emission from the remains of the 1572 and 1604 supernovae. The observations show that the intensity of this emission decreases with an increase in frequency, and it is usually represented in the form

$$I_\nu \sim \nu^{-n}, \tag{31.1}$$

where $n > 0$. In particular, for the Crab nebula $n = 0.2$, and for the remains of the other two supernovae that have been mentioned $n = 0.8$. As we know (see Section 18), in the case of thermal radiation the intensity in the radio frequency band is constant for a transparent nebula and proportional to ν^2 for a nontransparent one. Therefore we must conclude that the radio emission of the supernova remains are nonthermal in origin. As we will see later, the radio emission spectrum given by Eq. (31.1) can be explained on the assumption that it has a synchrotron origin.

Besides the three supernova remains, many other discrete sources of radio emission are found in the Galaxy. Some of them are identified with diffuse gaseous nebulae and, on the basis of a number of their characteristics, they also can be considered to be the remains of supernovae. The most intense radio source in the sky, Cassiopeia A, is, in particular, one of these objects. It has been identi-

fied with a ring-shaped nebula, expanding with a velocity of about 7000 km/sec. /430
From a comparison of this velocity, determined from the spectrum, and the expansion velocity in angular measure it has been found that the nebula is at a distance of 3400 parsecs from us. This nebula is evidently the remains of a supernova that flared up in about 1700. However, the supernova could not be observed because of the vast distance to it and considerable interstellar absorption.

In all, at the present time 15 radio emission sources are known, identified with nebulae and able to be considered as the remains of supernovae. They differ considerably from each other since they are at various evolution stages. The youngest of these nebulae is Cassiopeia A, the age of which is about 260 years. Most of the known remains of supernovae are located at distances of less than 2000 parsecs, and therefore the total number of them in the Galaxy must be fairly large (of the order of 1000). Since the lifetime of a nebula, ejected during a supernova outburst, apparently does not exceed 100,000 years, then in our Galaxy one supernova should flare up about every 100 years. This estimate, of course, is very crude, but it agrees with results of calculations of supernova outbursts in other galaxies.

2. Synchrotron radiation. The mechanism of synchrotron radiation is attractive as an explanation of the origin of the radio emission of the nebulae formed during supernova outbursts. Such radiation arises from a relativistic electron moving in a magnetic field. The name of this effect is associated with the fact that it was first observed in a synchrotron, intended for producing high-energy particles.

The motion of an electron in a homogeneous magnetic field comprises a translational movement along the lines of force and a rotation about them. In this situation the electron radiates with a frequency

$$\nu_0 = \frac{eH}{2\pi mc}, \tag{31.2}$$

where H is the magnetic field component perpendicular to the velocity. At the field intensities characteristic of astrophysical objects, the frequency ν_0 is usually very low. For example, for $H \approx 10^{-5}$ oersted we find, from Eq. (31.2), that $\nu_0 \approx 30\ \mathrm{sec}^{-1}$, i.e., the radiation wavelength is of the order of 10^4 km.

Only a nonrelativistic electron radiates in this fashion. If, however, the electron is relativistic, i.e., its energy E satisfies the inequality

$$E \gg mc^2, \tag{31.3}$$

then the character of the electron radiation is altered drastically. In this case, /431
instead of energy of a single frequency ν_0, the electron radiates energy in a continuous spectrum with a maximum near the frequency

$$\nu_m = \nu_0 \left(\frac{E}{mc^2}\right)^2, \tag{31.4}$$

where ν_0 is defined by Eq. (31.2). If the inequality (31.3) is satisfied to a very high degree, then a considerable portion of the energy will be radiated in the radio frequency band.

The problem of energy radiation by a relativistic electron, moving in a magnetic field, has been treated by a number of authors. It turns out (see, for example, [20]) that the amount of energy of frequency ν, radiated by an electron with energy E in 1 sec in a unit frequency interval, is equal to

$$P(\nu, E) = \frac{16e^3H}{mc^2} p(\alpha), \tag{31.5}$$

where $\alpha = \nu/\nu_m$ II $p(\alpha)$ and $p(\alpha)$ is the function depicted in Fig. 42.

Let us note that the function $p(\alpha)$ reaches a maximum for $\alpha \approx 1/2$. When $\alpha \ll 1$, it has the form

$$p(\alpha) = 0.256\alpha^{1/3} \tag{31.6}$$

and when $\alpha \gg 1$,

$$p(\alpha) = \frac{\sqrt{\pi}}{16}\alpha^{1/2} e^{-2/3\alpha}. \tag{31.7}$$

Since the quantity $P(\nu, E)$ is known, the volume emission coefficient ε_ν can easily be determined. Let us denote the number of electrons with energy from E to E + dE in 1 cm^3 by n(E)dE. Then the amount of energy of frequency ν, radiated by these electrons in 1 sec, will be equal to $P(\nu, E)n(E)dE$. Therefore the volume emission coefficient will be defined by the formula

$$\varepsilon_\nu = \frac{1}{4\pi}\int_0^\infty P(\nu, E)n(E)dE. \tag{31.8}$$

Let us assume that the number of electrons n(E) decreases with an increase in energy E in the form of a power law, i.e.,

$$n(E) = \frac{K}{E^\gamma}, \tag{31.9}$$

where K and γ are constants. Substituting (31.5) and (31.9) into (31.8) and performing the integration, we obtain

$$\varepsilon_\nu = C(\gamma)KH^{\frac{\gamma+1}{2}}\nu^{\frac{1-\gamma}{2}}, \tag{31.10}$$

where $C(\gamma)$ is some constant depending on γ.

From Eq. (31.10) it is seen that the emission coefficient ε_ν decreases with an increase in the frequency ν, if $\gamma > 1$. The intensity of the radiation, coming from any object must exhibit the same frequency dependence if there is no absorption in this object and along the path from it to the observer. As we recall, the radio emission of the remains of supernovae is characterized by a decrease in intensity with an increase in frequency, with this relationship being represented by Eq. (31.1). Thus, the radio emission of supernova remains can be explained by the fact that it has a synchrotron nature and the velocity distribution of the relativistic electrons is given by Eq. (31.9). In particular, for the Crab nebula one must take $\gamma = 1.4$, and for the remains of the 1572 and 1604 nebulae—$\gamma = 2.6$. /432

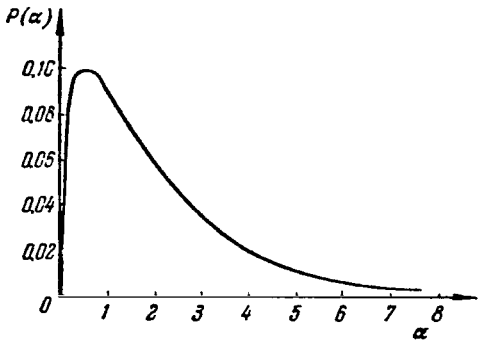

Figure 42.

Assuming the synchrotron mechanism for the origin of the radio emission of a nebula resulting from a supernova outburst, we obtain the following expression for the radio emission flux coming from it:

$$H_\nu = \frac{V}{r^2} C(\gamma) K H^{\frac{\gamma+1}{2}} \nu^{\frac{1-\gamma}{2}}, \tag{31.11}$$

where V is the volume of the nebula and r is the distance to it. Assuming the quantities H_ν, V and r are known from observations, the quantity $KH^{(\gamma+1)/2}$ can be determined from Eq. (31.11).

Knowing this last quantity allows one to estimate the density of relativistic electrons in the nebula. The emission in the radio frequency band is clearly caused primarily by electrons with energy within a certain interval. One can roughly assume that the electrons must have an energy in excess of the value

$$E_1 = mc^2\left(\frac{2\pi mc\nu}{eH}\right)^{1/2}. \tag{31.12}$$

From (31.12) it is seen that $E_1 \approx 10^9$ eV for meter waves and a field intensity of about 10^{-4} oersted.

For the density of electrons with energy $E > E_1$ we obtain the formula /433

$$n_1 = \int_{E_1}^{\infty} \frac{K}{E^{\gamma}} dE = \frac{K}{\gamma - 1} \frac{1}{E_1^{\gamma-1}}, \tag{31.13}$$

into which Eq. (31.12) for E_1 must be substituted. We see that $n_1 \sim KH^{\frac{\gamma-1}{2}}$ and, therefore, to determine n_1 the field intensity H must be known besides the quantity $KH^{(\gamma+1)/2}$ found on the basis of observational data. The value of H is usually determined from the condition that the turbulent motion energy and the magnetic energy are equal. For nebulae that are the remains of supernovae it is found, in this manner, that $H \approx 10^{-4}$ gauss. In this case an estimate of the density of electrons with an energy in excess of 10^9 eV leads to values of the order of 10^{-5} cm^{-3}. This density constitutes a negligible fraction of the total free electron density (which is about 10^3 cm^{-3}), determined from the Balmer line emission of nebulae.

It should, however, be noted that the smallness of the density of relativistic electrons gives no basis for concluding that they represent a small total energy in the nebula. Computing this value from the formula

$$U = V \int_{E_1}^{\infty} n(E) E \, dE. \tag{31.14}$$

we find that it will be of the order of 10^{46}-10^{47} ergs. Consequently, this energy can represent an appreciable portion of the total energy radiated during a supernova outburst.

3. Crab Nebula. The Crab nebula, of all the remains of supernovae, has been studied in most detail. It is not only an intense source of radio emission, but it is also quite bright in the visible spectral region (ninth magnitude).

Photographs show that the nebula consists of two parts. The inner part is an amorphous mass, and the outer—a delicate fibrous structure. The continuous spectrum arises in the amorphous part of the nebula; the fibers, however, exhibit a bright-line spectrum consisting of the hydrogen Balmer lines, the forbidden lines of N II, O II and others. The lines are split, which is explained by the expansion of the nebula. Two weak stars, one of which has no absorption lines in the spectrum, are visible at the center of the nebula. It is assumed that this is the one that flared up in the form of the supernova.

The hypothesis of synchrotron radiation was advanced to explain the radio /434
emission of the Crab nebula. This hypothesis was later confirmed by a number of facts. In particular, it should be noted that, according to theory, synchrotron

radiation should be polarized, and polarization of the radio emission of the Crab nebula was actually observed.

For some time astrophysics could not explain the origin of the intense continuous spectrum of the Crab nebula in the visible region. After having assumed it is the result of known mechanisms (i.e., recombinations and free-free transitions), extremely unusual properties had to be ascribed to the nebula (a mass of about 20 $M_\odot$ and an electron temperature of the order of hundreds of thousands of degrees). Finally, I.S. Shklovskiy [19] assumed that the continuous spectrum in the visible spectrum has a synchrotron origin, just like the radio-frequency spectrum. In other words, both of these spectra, identical in nature, are an extension of one another. The Crab nebula spectrum is depicted in Fig. 43, with the results of observations indicated by the points.

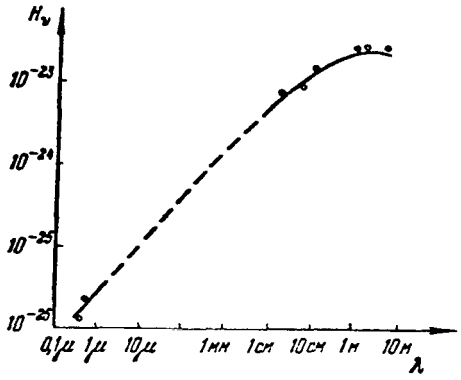

Figure 43.

As seen from Eq. (31.12), the higher the radiation frequency, the greater the energy of the relativistic electron, producing this radiation, must be. Therefore if the radio emission is caused by electrons with an energy of the order of 10^9 eV, then electrons with an energy of about 10^{11} eV are necessary to produce radiation in the visible region of the spectrum.

The results of polarization observations of the nebula are a confirmation of the validity of the proposed explanation of the continuous spectrum of the Crab nebula in the visible region. These observations have been made by many investigators: V.A. Dombrovskiy, E.E. Khachikyan, et al. It was found that the degree of polarization of the nebular emission in the visible portion of the spectrum is very high, amounting to 50% in isolated portions of the nebula.

The problem of the sources of relativistic electrons in the Crab nebula and in the remains of other supernovae is very important. One might think that the relativistic electrons appear at the time of the outburst itself. It must be kept in mind, however, that the lifetime of these electrons is not long since they lose their energy quite rapidly. In particular, a considerable fraction of the energy is expended as radiation by the electrons moving in a magnetic field. Using Eq. (31.5), we find that in the case given the change in electron energy with time is defined by the equation /435

$$\frac{dE}{dt} = -\frac{16e^3H}{mc^2}\nu_m\int_0^\infty p(\alpha)\,d\alpha. \qquad (31.15)$$

Substituting Eq. (31.4) here, we obtain

$$\frac{dE}{dt} = -AH^2E^2, \tag{31.16}$$

where A is a constant ($A \approx 2.4 \cdot 10^{-3}$ if E is expressed in ergs, H in oersteds and t in seconds). Integration of Eq. (31.16) yields

$$E = \frac{E_0}{1 + AH^2E_0t}, \tag{31.17}$$

where E_0 is the initial electron energy (for t = 0). From (31.17) it follows that the electron energy is reduced by one-half in the time

$$t_1 = \frac{1}{AH^2E_0}. \tag{31.18}$$

For $E_0 \approx 10^{11}$ eV and $H \approx 10^{-4}$ oersted we find from Eq. (31.18) that $t_1 \approx 10^4$ years. This time is an order of magnitude greater than the life of the Crab nebula; however, it must be realized that electrons can lose energy by other means also (for example, in ionization). Therefore it was assumed that relativistic electrons enter the nebula from the star for some time beyond the outburst. Possible mechanisms for the appearance of relativistic electrons in the nebula itself have also been indicated (see Section 34).

Let us say a few words about the filamentary portion of the Crab nebula. The emission of the filaments is caused by the ultraviolet radiation of the amorphous part or because of heating due to collisions with the interstellar medium. The density of free electrons in the filaments and the mass of the latter can be determined from the intensity of the bright lines. It is found that the mass of the filamentary portion of the nebula is quite large—about 0.1 $M_\odot$. The mass of the remains of the 1572 and 1604 supernovae (members, like the 1054 supernova, /436
of type I) lead to somewhat lower values. Nevertheless, one can state that much larger masses are ejected during supernova outbursts than during normal outbursts.

Evidently, even larger masses are ejected during type II supernova outbursts than during type I supernova outbursts. According to estimates that have been made, the masses of remains of type II supernovae are sometimes of the order of several tens of solar masses. It should be kept in mind, however, that both the material ejected during outburst and the material of interstellar space, captured by the expanding envelope, are included in the nebulae now observed. Taking into into account, values of the order of 1 $M_\odot$ are obtained for the mass ejected during type II supernova outbursts. If these estimates are correct, then the big difference in the envelope masses of type I and II supernovae indicates there are intrinsic differences in their physical nature.

4. Supernovae and cosmic rays. We have seen that in the nebulae formed during supernova outbursts, there are a large number of relativistic electrons. As the nebulae expand, the relativistic electrons enter the interstellar medium and begin to diffuse into it. Simultaneously, heavy particles with high energies (in particular, protons) appear in the interstellar medium. The number of heavy particles must be even greater than the number of relativistic electrons since the latter, because of radiation losses, have a shorter lifetime than the former.

On the other hand, we can deduce the presence of high energy particles in interstellar space on the basis of the cosmic ray phenomenon. Cosmic rays are known to be composed of protons, α-particles and a small number (about 1%) of nuclei of heavier atoms. Therefore the question arises as to whether supernova outbursts can be the cause for the formation of cosmic rays.

In order to answer this question, we must, first of all, estimate the average energy density of cosmic rays in the Galaxy. From the magnitude of the cosmic rays incident on the earth's atmosphere, a value of about 10^{-12} erg/cm^3 is obtained for their energy density. It should be noted that this value is relatively large: in order of magnitude it is comparable to the average radiation density in interstellar space.

Let us now see what cosmic ray energy densities can be produced by supernova outbursts. One can assume that supernova outbursts in the Galaxy occur about once every 100 years and cosmic rays with an energy of about 10^{47} ergs are produced during each outburst. The high energy particles survive for a very /437 long time in the Galaxy—about 10^8 years (it is determined by the probability of collisions with the nuclei of interstellar atoms). Therefore the total energy of the cosmic rays in the Galaxy, formed during supernova outbursts, must be of the order of 10^{53} ergs. Dividing this energy by the volume of the Galaxy, amounting to about 10^{66} cm^3, we arrive at a value of the order of 10^{-13} erg/cm^3 for the energy density. Since this value is not much different from the cosmic ray energy density determined from observations on Earth, the hypothesis that cosmic rays are produced during supernova outbursts appears very likely.

A very characteristic property of cosmic rays—their isotropy—must be noted. If the cosmic rays are coming to us directly from their sources, then one must assume that the sources are uniformly distributed throughout the sky. There is, however, no need for such a requirement since the isotropy of the cosmic rays apparently is the result of the dispersion of the particles comprising them in galactic magnetic fields.

Other hypotheses have been proposed to explain the origin of cosmic rays. In particular, some mechanisms have been mentioned for the acceleration of the particles as they move through the Galaxy.

More details on the problem of the origin of cosmic rays can be found in the book by V. L. Ginzburg and S. I. Syrovatskiy [20].

REFERENCES

1. Beals, C.S. Spectrophotometric studies of Wolf-Rayet stars and Novae, Publ. Obs. Victoria 6, N 9, 1934.
2. Struve, O. On the origin of bright lines in spectra of stars of class B, Ap. J. 73, 94, 1931.
3. Sobolev, V.V. Moving stellar clouds, Izd-vo Leningr. un-ta, 1947.
4. Gorbatskiy, V.G. and I.H. Minin. Variable stars, Fizmatgiz, 1963.
5. Boyarchuk, A.A. The Balmer decrement in moving media, Izv. KrAO 35, 45, 1966.
6. Gorbatskiy, V.G. Interpretation of variations in the γ spectrum of Cassiopeia, Astron. Zh. 26, No. 5, 1949; 28, No. 6, 1951.
7. Dyay, Tsoy O. The continuous spectrum of Be type stars, Astron Zh. 33, No. 5, 1956.
8. Slyusarev, S.G. The relative amounts of hydrogen and helium in the atmospheres of Wolf-Rayet type stars, Astron Zh. 37, No. 4, 1955.
9. Vorontsov-Vel'yaminov, B.A. Gaseous nebulae and novae, Izd-vo AN SSSR, 1948.
10. Ambartsumyan, V.A. The continuous emission phenomenon and stellar energy sources. Soobshch. Byurakanskoy obs., No. XIII, 1954.
11. Payne-Gaposchkin, C. The Galactic Novae, Amsterdam, 1957. /438
12. Mustel', E.R. Expansion mechanism for novae before maximum brightness and novae masses, Izv. Krymskoy astrofiz. obs., 4, 152, 1949.
13. Sobolev, V.V. The luminosity of stellar clouds in the absence of radiative equilibrium, Astron. Zh., 27, 81, 1950.
14. Minin, I.N. Electron temperature variation in stellar clouds in the absence of radiative equilibrium, Astron. Zh. 29, No. 2, 1952.
15. Kraft, R.P. The binary system Nova DQ Herculis, Ap.J. 130, 110, 1959.
16. Sobolev, V.V. Theory of nova brightness, Astron. Zh. 31, No. 1, 1954.
17. Gorbatskiy, V.G. Nova brightness, Parts. I and II, Vestn. LGU, No. 1, 1960; No. 13, 1960.
18. Oort, J. Some phenomena connected with interstellar matter, MN 106, 159, 1946.
19. Shklovskiy, I.S. The nature of the Crab Nebula luminosity, DAN SSSR, 90, 983, 1953.
20. Ginzburg, V.L. and S.I. Syrovatskiy. Origin of cosmic rays, Izd-vo AN SSSR, 1963.

CHAPTER VII

INTERSTELLAR SPACE

The interstellar material in our Galaxy occurs both in the form of dust and in the form of gas. The existence of interstellar dust is evidenced primarily through its absorption of star light in the continuous spectrum. This absorption is selective: it is weaker in the red portion of the spectrum than in the ultraviolet; it is for this reason that distant objects appear "reddened" to us. /439

Absorption is especially great in certain regions of the sky. This is caused by dark dust nebulae relatively near to us. Luminous dust nebulae, which shine because of the stellar radiation reflected by them, are also observed in the Galaxy.

The presence of gas in interstellar space can be deduced from the absorption lines caused by it in interstellar spectra. Near hot stars the interstellar gas is highly ionized and it shines because of the ultraviolet energy of the stars. The radiation of the interstellar gas, both line and continuous, is observed not only in the visible spectrum, but also in the radio frequency region.

Interstellar matter is quite heavily concentrated in the galactic plane. As a first approximation it is assumed that it forms a homogeneous layer or that its density decreases exponentially with distance from the galactic plane.

Actually, the interstellar matter is extremely inhomogeneous and is charterized by large density fluctuations. Sometimes it is assumed that it consists of individual clouds, moving with respect to each other. It should be noted that if the interstellar matter were homogeneous at some instant of time, regions of lower and higher density would be formed because of the motion of the stars and the light pressure caused by them.

The amount of interstellar matter in the Galaxy is very great. Its mass apparently amounts to about one-hundredth of the mass of the stars. Therefore interstellar matter should play a large role both in the physical, as well as the cosmogonic processes, occurring in the Galaxy. /440

32. Interstellar Dust

1. Relation between stars and nebulae. As already mentioned, the emission of nebulae is caused by stellar radiation. One can nearly always specify the star or group of stars which causes the emission of a given nebula. As observations show, the emission of gaseous nebulae is caused by very hot stars (spectral classes O and BO). This fact is entirely understandable since the ultraviolet radiation energy of the colder stars is too low to cause a noticeable nebular emission in the visible spectrum. From observations it also follows that dust nebulae shine primarily because of the effect of the radiation of the colder stars (spectral classes later than B1). At first glance there seems to be a strange absence of dust nebulae, reflecting the radiation of hot stars. Some hypotheses have been put forth to explain this phenomenon. According to one of them, hot stars, being also stars of high luminosity, repel dust by light pressure. According to another hypothesis, hot stars convert the dust to gas through the action of radiation. In fact, these observational data are apparently explained by the fact that there is always some quantity of gas contained in dust nebulae. If the nebula is near a cold star, then the dust shines and the gas does not. If, however, a hot star is in the vicinity of the nebula, both the dust and the gas shine. The gas, however, shines much more brightly than the dust since the ultraviolet radiation of the hot star is much more intense than its radiation in the visible spectrum. This conclusion was drawn in the paper by G. A. Shayn, V. F. Gaze and S. B. Pikel'ner [1] in which the question of the presence of dust and gas in nebulae was examined in detail.

It is of interest to clarify the nature of the relationship between a nebula and the star that is illuminating it. The nebula and star can be genetically related (i.e., of common origin), and can also have come together by chance while moving through the Galaxy. V. A. Ambartsumyan and Sh. G. Gordeladze [2] resolved this problem in the following way.

If the relationship between a nebula and a star is by chance, then the number of nebulae associated with stars of different spectral classes should be proportional to the regions of space illuminated by the stars of these classes. Let /441
us see whether such a proportionality actually exists.

Each star illuminates a volume V around itself, and the illumination within this volume exceeds some critical value E. When a nebula enters into this volume, it shines, and outside this volume it is dark. For a star of luminosity L the radius r_0 of this volume is clearly determined from the relation

$$E = \frac{L}{4\pi r_0^2}, \tag{32.1}$$

and the size of the volume itself is equal to

$$V = \frac{4}{3}\pi\left(\frac{L}{4\pi E}\right)^{3/2}. \tag{32.2}$$

Since the luminosity L is related to the absolute magnitude M of the star by the expression $L \sim 10^{-0.4M}$, then instead of (32.2) we have

$$V = V_0 10^{-0.6M}, \tag{32.3}$$

where V_0 is the value of the volume V for a star of zero absolute magnitude.

Let $\varphi(M)$ be the luminosity function for stars of a given spectral class, i.e., $\varphi(M)dM$ is the probability that the absolute magnitude of the star lies in the interval from M to M + dM. Then the average value of the volume V for stars of this class will be equal to

$$\bar{V} = V_0 \int_{-\infty}^{+\infty} \varphi(M) \cdot 10^{-0.6M} dM. \tag{32.4}$$

If we denote by n the number of stars of a given spectral class in a unit volume, then the quantity $n\bar{V}$ will be the desired fraction of space illuminated by these stars.

To compute the integral of (32.4) V. A. Ambartsuyman suggested using the fundamental integral equation of stellar statistics

$$N(m) = \Omega \int_0^{\infty} n(r) \varphi(M) r^2 dr, \tag{32.5}$$

where N(m) is the number of stars, of the spectral class being considered, with a visual stellar magnitude from m - 1/2 to m + 1/2 in the solid angle Ω. We will assume that the stars are uniformly distributed in space, i.e., n = const. Then, taking into consideration the known formula

$$M = m + 5 - 5 \lg r, \tag{32.6}$$

instead of (32.5) we obtain /442

$$N(m) = \frac{\Omega n}{5 \lg e} \int_{-\infty}^{+\infty} \varphi(M) \cdot 10^{0.6(m-M)+3} dM. \tag{32.7}$$

Here, light absorption in the Galaxy is disregarded. Equating the relation (32.4) and (32.7), we find

$$n\bar{V} = \frac{N(m) V_0}{\Omega} \cdot 10^{-3-0.6m} 5 \lg e. \tag{32.8}$$

Equation (32.8) makes it possible to determine easily the quantity $n\bar{V}$ from observational data. Values of this quantity for stars of different spectral classes are listed in Table 49. The number of nebulae, illuminated by the stars of these classes, are given in the same table for comparison.

TABLE 49. COMPARISON OF THE FRACTIONS OF SPACE ILLUMINATED BY STARS OF DIFFERENT CLASSES, WITH THE NUMBERS OF NEBULAE ILLUMINATED BY THE RADIATION OF THESE STARS

Spectral class	$n\bar{V}\cdot 10^4$	No. of nebula	Spectral class	$n\bar{V}\cdot 10^4$	No. of nebula
O	0,2	11	F	0,25	2
B0	0,6	7	G	0,18	1
B1 — B9	2,9	54	K	0,25	2
A	0,8	5	M	0,02	0

Commas represent decimal points.

We see that the numbers in the columns of Table 49 are approximately proportional to each other. From this one can conclude that the relationship between nebulae and stars is random.

Strictly speaking, the data for class O and BO stars should not be included in the table since these stars are associated with gaseous nebulae and not with dust nebulae. Therefore the volume of space illuminated by such a star will not be defined by Eq. (32.2).

One more important consequence can be drawn from the table. If we add all the numbers $n\bar{V}$, then we obtain the fraction of space illuminated by all the stars. This fraction is equal to $5\cdot 10^{-4}$. Since only those nebulae, which enter the illuminated portion of space, shine, then we are forced to the conclusion that the number of bright nebulae in the Galaxy is about 2000 times smaller than the number of dark nebulae.

Thus, the number of dark nebulae in the Galaxy is very large. After having estimated this number and after having adopted some average value for the optical thickness of a nebula, derived from observations of the known dark nebulae, /443 we can determine the value of the average absorption, caused by the nebulae, per unit path length. This value turns out to be approximately equal to the value of the total light absorption in the Galaxy found from observations (of the order of one stellar magnitude per kiloparsec in the galactic plane). Therefore we can consider that the total light absorption in the Galaxy is caused primarily by the presence in it of a large number of dust nebulae. Because of the random distribution of nebulae, light absorption in the Galaxy is very nonuniform. If a nebula is near to us and its optical thickness is relatively great, then the presence of such a nebula is detected from the marked decrease in the number of stars up to a certain magnitude in a specific region of the sky.

2. Fluctuations of the Milky Way brightness. The patchy structure of interstellar space leads to large variations in sky brightness in different directions. Given the number of nebulae (or, as they are sometimes called, clouds) per unit path length and their absorptivity, we can determine the brightness probabilities. Let us do this, following the work of V. A. Ambartsumyan [3].

For simplicity let us take the galactic plane and let us assume that the stars are uniformly distributed in it. Let us denote the star-caused emission coefficient by ε. We will assume that all nebulae possess the same transparency, equal to q. The number of nebulae, located in a given direction up to a distance s from us, we will denote by n(s). Then the intensity of the radiation coming to us in this direction will be equal to

$$\varepsilon \int_0^\infty q^{n(s)} ds.$$

The behavior of the integral function n(s) is different in different directions, so that sky brightness fluctuations result.

Let f(I) be the probability that the radiation intensity is less than I, i.e.,

$$f(I) = P\left(\varepsilon \int_0^\infty q^{n(s)} ds < I\right). \tag{32.9}$$

We will employ the following method to determine the function f(I).

Let us rewrite Eq. (32.9) in the form

$$f(I) = P\left(\varepsilon \int_0^a q^{n(s)} ds + \varepsilon q^{n(a)} \int_a^\infty q^{n(s)-n(a)} ds < I\right) \tag{32.10}$$

where a is some small distance. One can assume that the quantity n(a) has either a value n(a) = 0 or n(a) = 1. Let us denote by ν the average number of clouds per unit path length. Then the probability of the first of these n(a) values will be $1 - \nu a$, and the probability of the second will be νa. The probabilities of other values for small a can be ignored. In the first of the cases being considered, the integral $\int_0^a n(s) ds$ is obviously equal to a, and in the second case it is equal to $a\vartheta$, where $0 < \vartheta < 1$. Therefore instead of Eq. (32.10) we obtain /444

$$f(I) = (1 - \nu a) P\left(\varepsilon \int_a^\infty q^{n(s)-n(a)} ds < I - a\varepsilon\right) + \nu a P\left(\varepsilon \int_a^\infty q^{n(s)-n(a)} ds < \frac{I - a\vartheta\varepsilon}{q}\right). \tag{32.11}$$

Since the probability of measuring one brightness or another should not change when the point of observation is changed, we have

$$P\left(\varepsilon \int_a^\infty q^{n(s)-n(a)} ds < I\right) = P\left(\varepsilon \int_0^\infty q^{n(s)} ds < I\right). \tag{32.12}$$

Because of this, Eq. (32.11) assumes the form

$$f(I)=(1-\nu a)f(I-a\varepsilon)+\nu af\left(\frac{I-a\vartheta\varepsilon}{q}\right). \tag{32.13}$$

Taking advantage of the smallness of a, instead of (32.13) we obtain

$$f(I)=(1-\nu a)\,[f(I)-a\varepsilon f'(I)]+\nu af\left(\frac{I}{q}\right), \tag{32.14}$$

or

$$f(I)+\frac{\varepsilon}{\nu}f'(I)=f\left(\frac{I}{q}\right). \tag{32.15}$$

Instead of I let us introduce the dimensionless brightness u, equal to

$$u=I\frac{\nu}{\varepsilon}. \tag{32.16}$$

Then we will have the equation

$$f(u)+f'(u)=f\left(\frac{u}{q}\right). \tag{32.17}$$

for the determination of the function f(u).

Let us denote by g(u)du the probability that the dimensionless brightness u lies within the interval from u to u + du. Since g(u) = f'(u), then from Eq. (32.17) /445
we obtain

$$g(u)+g'(u)=\frac{1}{q}g\left(\frac{u}{q}\right). \tag{32.18}$$

Equation (32.18) is what we are looking for. From it one can easily derive an expression for the function g(u) in the form of some series. Equation (32.18) also provides the possibility of determining the moment of the function g(u), i.e., the quantity

$$\overline{u^k}=\int_0^\infty u^k g(u)\,du \tag{32.19}$$

without a prior determination of the function g(u).

Let us determine, for example, the quantities $\bar{u}$ and $\overline{u^2}$, which are of interest for certain theoretical applications. Multiplying Eq. (32.18) by u, integrating

with respect to u over the limits from 0 to ∞ and making use of the normalization condition of the function g(u), we obtain

$$\bar{u} = \frac{1}{1-q}. \tag{32.20}$$

After multiplying Eq. (32.18) by u^2 and integrating, we similarly obtain

$$\overline{u^2} = \frac{1}{(1-q)(1-q^2)}. \tag{32.21}$$

With the aid of (32.20) and (32.21) we obtain the following expression for the relative standard deviation:

$$\frac{\overline{(u-\bar{u})^2}}{\bar{u}^2} = \frac{\overline{u^2}}{\bar{u}^2} - 1 = \frac{1-q}{1+q}. \tag{32.22}$$

The theoretical results that have been presented can be compared with observational data. The latter are photometric maps of the Milky Way. On the basis of these maps, the average brightness $\bar{I}$ and relative standard deviation $\overline{(I-\bar{I})^2}/\bar{I}^2$ are determined. With the aid of Eqs. (32.16) and (32.20) we obtain

$$\bar{I} = \frac{\varepsilon}{\nu}\bar{u} = \frac{\varepsilon}{\nu}\frac{1}{1-q}. \tag{32.23}$$

Using Eq. (32.22) also, we find

$$\frac{\overline{(I-\bar{I})^2}}{\bar{I}^2} = \frac{1-q}{1+q}. \tag{32.24}$$

Since the left sides of these relations are known from observations, these relations allow a determination of the quantities q and ε/ν to be made. /446

With this method a value of q = 0.8 was obtained for the average cloud transparency. Consequently, when star light passes through a cloud, its brightness is reduced by 0.25 of a stellar magnitude. The value of the quantity ε/ν was also found with the aid of Eq. (32.23). With the quantity ε known from stellar computations, this permitted a determination of the quantity ν. It was found that there are, on the average, four nebulae in a path length of 1 kiloparsec. Thus, the dust nebulae in the Galaxy produce an absorption approximately equal to one stellar magnitude per kiloparsec. This result agrees with the absorption value determined from observational data on the attenuation of the light of distant objects in the galactic plane.

The presence of dust material in the Galaxy causes an absorption not only of star light, but also of the light of extragalactic nebulae (i.e., the nebulae of other galaxies). The number of extragalactic nebulae N up to a specific stellar

magnitude is known to decrease with a decrease in the galactic latitude b. The region of the sky near the galactic equator is the "avoidance zone" for extragalactic nebulae. This is explained by the fact that the optical path length of a ray in the layer of absorbing material increases with a decrease in b. From the variation of the quantity N as a function of b one can determine the optical thickness of this layer (it turns out to be about 0.5). The variation of the quantity N as a function of the galactic longitude l for a constant b can also be examined. As l changes, the quantity N exhibits appreciable fluctuations, caused by the random distribution of dust clouds in the Galaxy. V. A. Ambartsumyan developed a theory of the fluctuations in the numbers of extragalactic nebulae and, on its basis, determined the average optical thickness of one cloud.

The theories, developed by V. A. Ambartsumyan, on the Milky Way brightness fluctuations and on the fluctuations in the numbers of extragalactic nebulae have been expanded in many respects by a number of authors: Chandrasekhar and Münch [4], T. A. Agekyan [5], and others.

3. Emission of dust nebulae. Dust nebulae shine because of their reflection of stellar radiation (as a result, they are sometimes called reflective nebulae). The nature of the dust particles can be deduced from the emission of the nebulae. To do this it is obviously necessary to relate the observed brightnesses of nebulae with quantities characterizing light scattering processes in a volume element.

A theoretical determination of the brightnesses of nebulae meets with great difficulties. One of these difficulties is caused by the extremely complex geometrical shapes of the nebulae. Another difficulty is caused by the fact that each /447
volume element of a nebula scatters the radiation, entering it not only from a star but also from other parts of the nebula. In other words, multiple light scattering occurs in nebulae.

To solve, however, the problem of determining the optical properties of the dust particles, we need not consider the complicated shapes of the nebulae and can restrict ourselves to ones that are fairly simple. Let us now consider a homogeneous spherical nebula with a star located at its center. Some of the nebulae that have been observed can evidently be considered to be spherical since their isophots are nearly circular.

We will assume that a star of luminosity L is located at the center of a spherical nebula of radius r_0. We will characterize the optical properties of the nebular material by the volume absorption coefficient α, the probability of survival λ of a photon during an elementary scattering act (this quantity can also be called the particle albedo) and the scattering indicatrix $x(\gamma)$, where γ is the angle between the direction of the radiation, incident on a given volume, and the direction of the radiation, scattered by this volume. It is understood that the quantities α, λ and $a(\gamma)$ are frequency dependent.

Let us consider the process of multiple light scattering in a nebula [6]. We will denote the unknown intensity of the scattered radiation by I. It depends both on the distance r from the star and also on the angle ϑ between the radiation

direction and the radius vecor. The radiation transfer equation, defining the quantity I, has the form

$$\cos\vartheta\frac{\partial I}{\partial r}-\frac{\sin\vartheta}{r}\frac{\partial I}{\partial\vartheta}=-\alpha I+\varepsilon, \tag{32.25}$$

in the case of spherical symmetry, where ε is the volume emission coefficient. Introducing the notations $\tau=\alpha r$ and $\varepsilon=\alpha S$, instead of Eq. (32.25) we obtain

$$\cos\vartheta\frac{\partial I(\tau,\vartheta)}{\partial\tau}-\frac{\sin\vartheta}{\tau}\frac{\partial I(\tau,\vartheta)}{\partial\vartheta}=-I(\tau,\vartheta)+S(\tau,\vartheta). \tag{32.26}$$

The quantity S is determined by the scattering of the light, entering a given volume, from the star and also from the nebula. It can be represented in the form

$$S=\lambda\int Ix(\gamma)\frac{d\omega}{4\pi}+\frac{\lambda x(\vartheta)L}{16\pi^2r^2}e^{-\tau}, \tag{32.27}$$

where the integration is over all directions. Assuming that the radiation direction at a given point is characterized by the polar angle ϑ and the azimuth φ, we obtain /448

$$\cos\gamma=\cos\vartheta\cos\vartheta'+\sin\vartheta\sin\vartheta'\cos(\varphi-\varphi') \tag{32.28}$$

and $d\omega=\sin\vartheta'\,d\vartheta'\,d\varphi'$. Designating

$$\frac{1}{2}\int_0^{2\pi}x(\gamma)\,d\varphi=p(\vartheta,\vartheta') \tag{32.29}$$

and

$$\frac{L\alpha^2}{16\pi^2}=A, \tag{32.30}$$

instead of Eq. (32.27) we have

$$S(\tau,\vartheta)=\frac{\lambda}{2}\int_0^{\pi}I(\tau,\vartheta')p(\vartheta,\vartheta')\sin\vartheta'd\vartheta'+\lambda x(\vartheta)\frac{A}{\tau^2}e^{-\tau}. \tag{32.31}$$

Thus, we have Eqs. (32.26) and (32.31) for determining the unknown functions $S(\tau,\vartheta)$ and $I(\tau,\vartheta)$. A boundary condition, expressing the fact that there is no radiation striking the nebula from the outside, must still be added to these.

From Eqs. (32.26) and (32.31) we can derive an integral equation defining the function $S(\tau, \vartheta)$. To do this the quantity $I(\tau, \vartheta)$ must be found from Eq. (32.26) and substituted into Eq. (32.31).

In the case of a spherical scattering indicatrix, i.e., for $x(\gamma) = 1$, the quantity S depends only on τ. In the case given the integral equation cited is obtained in the form

$$\tau S(\tau) = \frac{\lambda}{2} \int_0^{\tau_0} [\mathrm{Ei}|\tau - \tau'| - \mathrm{Ei}(\tau + \tau')] S(\tau') \tau' d\tau' + \frac{\lambda A}{\tau} e^{-\tau}, \tag{32.32}$$

where $\tau_0 = \alpha r_0$ is the optical radius of the nebula.

When $\tau_0 = \infty$, it is easy to find an exact solution of Eq. (32.32). Introducing the function

$$U(\tau) = \int_\tau^\infty S(\tau) \tau \, d\tau, \tag{32.33}$$

we obtain the equation

$$U(\tau) = \frac{\lambda}{2} \int_0^\infty [\mathrm{Ei}|\tau - \tau'| + \mathrm{Ei}(\tau + \tau')] U(\tau') d\tau' + \lambda A \, \mathrm{Ei}\, \tau. \tag{32.34}$$

for its definition. Denoting the resolvent of Eq. (32.34) by $\Gamma(\tau, \tau')$ and assuming /449
$\Gamma(\tau, 0) = \Phi(\tau)$, we see that $U(\tau) = A\Phi(\tau)$, and this means

$$S(\tau) = -\frac{A}{\tau} \Phi'(\tau). \tag{32.35}$$

The function $\Phi(\tau)$ was defined, earlier by Eq. (27.21). Using this formula, we find

$$S(\tau) = \frac{A}{\tau} \left\{ 4\lambda \int_1^\infty \frac{x^2 e^{-x\tau} dx}{(\lambda\pi)^2 + \left(2x + \lambda \ln \frac{x-1}{x+1}\right)^2} + \frac{2k^2(1-k^2)}{\lambda + k^2 - 1} e^{-k\tau} \right\}, \tag{32.36}$$

where the quantity k is related to λ by the expression $\frac{\lambda}{2k} \ln \frac{1+k}{1-k}$. The function $s(\tau)$ contains, in the form of an additive term. the quantity

$$S_1(\tau) = \frac{\lambda A}{\tau^2} e^{-\tau}, \tag{32.37}$$

representing the function $S(\tau)$ caused by first order scattering. Values of the ratio $S(\tau)/S_1(\tau)$, computed with the aid of Eqs. (32.36) and (32.37), are listed in Table 50 for different values of the particle albedo λ.

TABLE 50. VALUES OF THE QUANTITY $S(\tau)/S_1(\tau)$

τ \ λ	0,3	0,5	0,7	0,9	1,0	τ \ λ	0,3	0,5	0,7	0,9	1,0
0	1,00	1,00	1,00	1,00	1,00	1,0	1,47	2,00	2,92	4,89	8,92
0,1	1,07	1,12	1,17	1,24	1,29	1,5	1,65	2,47	4,11	8,50	20,9
0,2	1,12	1,23	1,35	1,51	1,65	2,0	1,80	2,94	5,50	13,8	45,0
0,4	1,22	1,43	1,70	2,14	2,66	2,5	1,95	3,42	7,11	21,4	92,0
0,6	1,31	1,62	2,08	2,90	4,11	3,0	2,08	3,91	8,98	32,1	181
0,8	1,40	1,82	2,49	3,81	6,13						

Commas represent decimal points.

The table clearly shows the role of higher order scattering for different λ. For each λ there exists, around the star, a region in which higher order scattering plays a smaller role than single scattering, but outside this region the situation is reversed. The size of this region is greater, the smaller λ. It must be borne in mind, however, that in real nebulae the quantity τ_0 is finite and the scat- /450 tering indicatrix is other than spherical. Therefore the results, presented in Table 50, are only illustrative in nature insofar as nebulae are concerned.

Equations (32.26) and (32.31) can be solved by an approximation method (see [6]) for any nebular optical radius τ_0 and for an arbitrary scattering indicatrix $x(\gamma)$. In this case the quantity $S(\tau, \vartheta)$ is represented in the form

$$S(\tau, \vartheta) = \lambda x(\vartheta) \frac{A}{\tau^2} e^{-\tau} + \Delta S(\tau, \vartheta, x_1, \lambda, \tau_0), \tag{32.38}$$

where first order scattering is taken into account precisely, while the effects of higher order scattering are only approximated. In this situation the quantity ΔS depends not on the overall scattering indicatrix, but only on the parameter x_1, representing the first coefficient in a Legendre polynomial expansion of $x(\gamma)$.

If the function $S(\tau, \vartheta)$ is known, then it is easy to find the brightness distribution over the nebular disk (Fig. 44). Let us denote by $I(\rho)$ the intensity of the radiation coming from the nebula at a distance ρ from the center of the disk [in the previous notations this is $I(\tau_0, \vartheta_0)$]. As follows from the radiation transfer equation, the quantity $I(\rho)$ is equal to

$$I(\rho) = \int_{-s_0}^{s_0} S(\tau, \vartheta) e^{-\mu(s_0 - s)\alpha} ds, \tag{32.39}$$

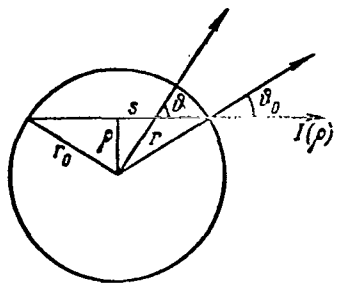

Figure 44.

where $s_0 = \sqrt{r_0^2 - \rho^2}$. Changing over to a new integration variable ϑ by means of the relations $\tau = \alpha\rho/\sin\vartheta$ and $s = \rho \operatorname{ctg}\vartheta$, we obtain

$$I(\rho) = \int_{\vartheta_0}^{\pi-\vartheta_0} S\left(\frac{\alpha\rho}{\sin\vartheta}, \vartheta e^{-\alpha(\sqrt{r_0^2-\rho^2}-\rho \operatorname{ctg}\vartheta)}\right) \frac{\alpha\rho\, d\vartheta}{\sin^2\vartheta}, \quad (32.40)$$

where $\vartheta_0 = \rho/r_0$.

Knowing the quantity $I(\rho)$ allows one to calculate the nebular luminosity, which is obviously equal to

$$L_n = 4\pi \cdot 2\pi \int_0^{r_0} I(\rho)\, \rho\, d\rho. \quad (32.41)$$

For the ratio of the nebular luminosity L_n to the observed stellar luminosity L_* we obtain /451

$$\frac{L_n}{L_*} = \frac{8\pi^2 \int_0^{r_0} I(\rho)\rho\, d\rho}{Le^{-\tau_0}}. \quad (32.42)$$

The theoretical values of the quantities $I(\rho)$ and L_n/L_* can be compared with the results of observations. By means of such a comparison one can attempt to determine the optical properties of the nebula, i.e., the quantities τ_0, λ and $x(\gamma)$.

Some information about these quantities is especially simple to obtain in those cases when the optical radius of the nebula is small ($\tau_0 \ll 1$). In this case the function $S(\tau, \vartheta)$ is defined by the formula

$$S(\tau, \vartheta) = \frac{\lambda L}{16\pi^2 r^2} x(\vartheta) \quad (32.43)$$

and instead of Eq. (32.40) we obtain

$$I(\rho) = \frac{\lambda L \alpha}{16\pi^2 \rho} \int_{\vartheta_0}^{\pi-\vartheta_0} x(\vartheta)\, d\vartheta. \quad (32.44)$$

From this it follows:

$$\frac{dI(\rho)\rho}{d\rho} = -\frac{\lambda L \alpha}{16\pi^2 \sqrt{r_0^2 - \rho^2}} [x(\vartheta_0) + x(\pi - \vartheta_0)]. \quad (32.45)$$

We see that it is impossible to find the scattering indicatrix $x(\vartheta)$ completely from Eq. (32.45), and only the sum $x(\vartheta) + x(\pi - \vartheta)$ can be obtained. In the case of light scattering by dust particles, however, the fraction of the light scattered forward is usually much greater than the fraction of the light scattered backward. Consequently, a more or less correct representation of the scattering indicatrix can be obtained from this sum.

To determine the quantity L_n/L_* for $\tau_0 \ll 1$, Eq. (32.44) must be substituted into Eq. (32.42). Doing this and performing the integration, we find

$$\frac{L_n}{L_*} = \lambda\tau_0. \tag{32.46}$$

This formula is perfectly obvious since for $\tau_0 \ll 1$ the amount of energy absorbed by the nebula is equal to $L(1 - e^{-\tau_0}) \approx L\tau_0$, and of this energy the nebula scatters the fraction λ.

I.N. Minin [7] made use of Eqs. (32.45) and (32.46) to determine the optical properties of dust nebulae. Values of the quantity $x(\gamma) + x(\pi - \gamma)$, obtained by him for the IC 431 and IC 435 nebulae, are listed in Table 51. Here, the usual scattering indicatrix normalization was used, i.e., $\int x(\gamma)d\omega/4\pi = 1$. The numbers in parentheses are found by extrapolation. /452

TABLE 51. VALUES OF THE QUANTITY $x(\gamma) + x(\pi - \gamma)$ FOR TWO NEBULAE

γ	0	10	20	30	40	50	60	70	80	90
IC 431	(35)	14	3,7	2,4	2,2	1,4	1,1	0,82	0,75	(0,69)
IC 435	(8.4)	7,3	6,4	3,8	2,5	1,4	0,96	0,79	0,73	(0,70)

Commas represent decimal points.

Values of the quantity $\lambda\tau_0$ were also obtained for these same nebulae from Eq. (32.46). They were equal to 0.063 and 0.16, respectively. Since $\tau_0 = \alpha r_0$, and $\lambda\alpha$ is the volume scattering coefficient σ, then we have $\lambda\tau_0 = \sigma r_0$. With the aid of this relation, the quantity σ was determined for these nebulae from values of the quantity $\lambda\tau_0$ and the nebular radius r_0.

As observations reveal, nebulae with nearly circular isophots comprise a fairly large percentage of the luminous diffuse nebulae. It is, however, difficult to infer that each of these is an approximately spherical nebula with a star located at its center. Most of these nebulae are, apparently, simply illuminated portions of larger nebulae. The illuminated part will obviously be approximately spherical even in the case of a formless nebula if its optical thickness exceeds unity by an order of magnitude and the density of matter does not vary greatly

in it. For determining the function $S(\tau, \vartheta)$ for these nebulae one can use the approximation $\tau_0 = \infty$, which leads to considerable simplification of the calculations.

4. Nature of dust particles. As shown above, a study of the emission of dust nebulae allows one to determine certain quantities characterizing their optical properties: the volume absorption coefficient α, the particle albedo λ and the scattering indicatrix $x(\gamma)$. In turn, knowing these quantities makes it possible to attempt to solve questions concerning the shape, size and concentration of dust particles, and also concerning the nature of the material of which they are composed.

The results of the theory of light scattering by discrete particles are used to answer these questions. Up to the present time, quite a number of calculations have been made of the quantities α, λ and $x(\gamma)$ for particles of various shapes (spheres, cylinders, disks) and with different refractive indices. Generally speaking, the refractive index is complex in form. For insulating particles the imaginary part of the refractive index is equal to zero; for metallic particles it is nonzero. In the first case the particles give rise to pure radiation scattering ($\lambda = 1$), in the second case—to scattering as well as pure absorption ($\lambda < 1$). /453

Light scattering by spherical particles has been investigated the most completely. The optical properties of these particles depend both on the refractive index and on the ratio of the particle radius to the radiation wavelength. The present status of the theory of light scattering by small particles is discussed in detail in Van de Hulst's book [8], together with the results of many calculations.

The application of this theory to the study of dust nebulae does not, however, lead to completely definite results since various assumptions have to be made. Usually the particle shape and refractive index are specified beforehand, and the particle dimensions are determined by comparing the optical properties obtained theoretically and from observations.

In his consideration of the IC 431 and IC 435 nebulae cited above, I. N. Minin assumed that they were composed of spherical, insulating particles. By comparing the values of the quantity $x(\gamma) + x(\pi - \gamma)$ found from observations (listed in Table 51) with the theoretical values of this quantity, he obtained a value of $a = 6.7 \cdot 10^{-6}$ cm for the average particle radius in these nebulae. Approximately the same values of a were found for dust nebulae by other methods. Therefore it is assumed that the average size of interstellar dust particles is of the order of 10^{-5} cm.

For a specific particle radius a and refractive index m, the theory yields a value of the scattering coefficient k, calculated for one particle. Since the volume scattering coefficient σ is known from observations, then the particle concentration n can be found from the relation $\sigma = nk$. Then the dust density in the nebula can be found from the formula

$$D = \frac{4}{3}\pi a^3 \delta n; \tag{32.47}$$

where δ is the specific gravity of the particle material. By way of an example, let us point out that density values of $2.1 \cdot 10^{-24}$ g/cm^3 and $4.5 \cdot 10^{-24}$ g/cm^3 were obtained from Eq. (32.47) for the IC 431 and IC 435 nebulae, respectively. Here /454 it was assumed that $\delta = 1$ g/cm^3, and a value of $m = 1.33$ was assumed for the refractive index (i.e., the same as for water droplets or ice crystals).

Some information on the dust particles can also be derived from a study of the polarization of the light of nebulae. Observations indicate that the degree of light polarization of dust nebulae is quite high—about 10-15%. As should be expected for light reflection by fine particles, the polarization is radial, i.e., the preferred direction of the electric vector oscillations is perpendicular to the radius vector outward from the illuminating star. The presence of appreciable radial radiation polarization points to the large role of first order scattering in regions of the nebula nearest to the star (since multiply scattered radiation is weakly polarized).

The theory of light scattering by small particles also provides the possibility of determining the degree of polarization of the reflected radiation. The comparison of observational and theoretical data on the polarization of nebular radiation began to be made only recently and henceforth it may lead to significant results (especially when data for different spectral regions are used).

As we know, numerous dark nebulae exist in the Galaxy in addition to the luminous dust nebulae. The nature of interstellar dust particles can also be deduced from a study of these nebulae in terms of the light absorption caused by them.

The investigation of interstellar light absorption has led to the conclusion that in the visible spectrum the absorption coefficient is approximately inversely proportional to the wavelength. Moreover, the magnitude of the absorption coefficient was also found. In the visible spectrum in the galactic plane the absorption amounts to one stellar magnitude per kiloparsec on the average. This means that a path length of 1 kiloparsec corresponds to approximately unit optical distance. Therefore the volume absorption coefficient of interstellar dust for visible wavelengths is equal to $\alpha \approx 3 \cdot 10^{-22}$ cm^{-1}.

On the other hand, according to the theory of light scattering by small particles the wavelength dependence of the absorption coefficient is determined by the values assigned to the particle dimensions and the refractive index. If insulating particles with a refractive index of $m = 1.33$ are assumed, then the absorption coefficient will be inversely proportional to the wavelength when the particle radius is equal to $a \sim 5 \cdot 10^{-5}$ cm.

For such a particle size the absorption coefficient, calculated for one par- /455 ticle, will be approximately equal to $k \approx \pi a^2 \approx 10^{-8}$ cm^2. Using the formula $\alpha = nk$, we obtain a value of $n \approx 3 \cdot 10^{-14}$ cm^{-3}. In this case Eq. (32.47) (for $\delta \approx 1$) yields a value of $D \approx 10^{-26}$ g/cm^3 for the average density of dust matter near the galactic plane.

As we will see below, this value of the dust density is approximately two orders of magnitude less than the gas density near the galactic plane. It should, however, be borne in mind that coarse particles, causing no noticeable light absorption but of greater total mass than the particles causing absorption in the visible spectrum, can exist in the Galaxy. Therefore the density of dust matter in the Galaxy can be somewhat greater than the value given above.

5. Polarization of starlight. Both light absorption and polarization occur when starlight passes through the interstellar dust matter. This phenomenon was discovered by V. A. Dombrovskiy and, independently, by Hiltner and Hall, and was then investigated in detail both by these authors as well as others. Observations indicate that the degree of starlight polarization is small (a fraction of a percent or a few percent), but in some cases it amounts to 10%. The plane of electric vector oscillations is close to the galactic plane. The angle between these planes is no more than 20° for approximately two-thirds of the stars for which light polarization has been measured.

Light polarization is detected only for remote stars, with a correlation existing between light polarization and absorption. The relationship between the degree of polarization p, the distance modulus m - M and the color excess E is presented in Table 52, taken from Loden's paper [9]. We see that the greater the absorption, the greater the polarization. It must be borne in mind, however, that only average values of the quantities are included in the table. In individual portions of the sky this relationship is not very pronounced.

TABLE 52. RELATIONSHIP BETWEEN THE DEGREE OF STARLIGHT POLARIZATION THE DISTANCE MODULUS AND THE COLOR EXCESS

p in %	$\overline{m-M}$	$\overline{E}$
0.0—0.4	6.53	0.048
1.5—0.9	8.41	0.032
0.0—1.4	8.56	1.158
1.5—1.9	9.45	0.298
2.0—2.4	10.50	0.394

The observed polarization of stellar radiation can be explained by the fact that the interstellar dust particles are elongated in shape. As calculations show, the fraction of the radiation absorbed by such a particle depends on the angle between its axis and the direction of the electric /456 vector oscillations (the absorption is greatest when this angle is equal to zero). Therefore radiation passing through a cloud of particles oriented in some fashion should be polarized. To explain the orientation of the dust particles, a hypothesis was advanced concerning the effect of the magnetic field of the Galaxy on them. The field intensity should be about 10^{-5} oersted. The direction of the field can be different at different points of the Galaxy; this can explain the rather complex distribution pattern of the stellar radiation polarization over the sky.

In order for the magnetic field to be able to influence the dust, the presence of some quantity of metal in them must be assumed. On the other hand, a study of the luminosity of dust nebulae leads to the conclusion that in all probability the particles in them are nonmetallic. At the present time, therefore, it is assumed that the interstellar dust particles are insulators with a small metallic impurity. The presence of graphite particles, which is similar to the metals in some of its

properties (especially electrical conductivity), in the Galaxy has also been suggested to explain interstellar light absorption and polarization.

It is interesting to note that the phenomenon of starlight polarization has been, for a considerable length of time, one of the main arguments in favor of the existence of magnetic fields in the Galaxy. Then other arguments in favor of this appeared and the intensity of the galactic magnetic field was measured directly (see Section 34).

33. Interstellar Gas

1. Ionization of interstellar hydrogen. The physical processes in gaseous nebulae have already been considered in detail in Chapter V. There, however, we restricted ourselves to only those portions of nebulae which are near hot stars. Now let us attempt to formulate an overall concept of interstellar gas, considering regions both near and far from hot stars.

First, we will discuss the question of the ionization of interstellar hydrogen. Since hydrogen is the most abundant element in the Galaxy, many processes are inherently dependent on whether the hydrogen is ionized or neutral in a given region.

Let us assume that the ionization is produced by a star with a radius r_* and temperature T_*. Then at a distance r from the star the fraction of ionized atoms /457
x will be determined by the formula

$$\frac{x^2}{1-x}=\frac{W}{n}f(T_*)e^{-\tau}, \tag{33.1}$$

where

$$f(T_*)=\left(\frac{T_e}{T_*}\right)^{1/2}\frac{g^+}{g_1}\frac{2(2\pi mkT_*)^{3/2}}{h^3}e^{-\frac{\chi_1}{kT_*}} \tag{33.2}$$

n is the concentration of hydrogen atoms, W is the dilution factor, τ is the optical distance from the star to a given point beyond the Lyman series limit. We have

$$W=\frac{1}{4}\left(\frac{r_*}{r}\right)^2 \tag{33.3}$$

and

$$\tau=k\int_{r_*}^{r}n(1-x)dr, \tag{33.4}$$

where k is the average absorption coefficient in the Lyman continuum, calculated for one atom.

Equation (33.1) was derived in Section 23. There, however, an explicit dependence of x on r was found under the assumption that W/n = const. Now we will assume that W is given by Eq. (33.3) and n = const. In reality, interstellar gas is very inhomogeneous so that the assumption that n is a constant is only a crude approximation to reality.

From the relations that have been presented it is easy to derive the following equation for determining the dependence of x on r:

$$\left(\frac{2}{x}+\frac{1}{1-x}\right)\frac{dx}{dr}+(1-x)nk+\frac{2}{r}=0. \tag{33.5}$$

Near the surface of the star $x = x_*$. The quantity x_* is close to unity for stars with a fairly high temperature.

The solution of Eq. (33.5) [just like the solution of Eq. (23.17) in Chapter V] shows that the quantity x remains close to unity up to some value $r = r_0$, and then rapidly decreases to zero. Consequently, there exists a region of radius r_0 about the star within which the hydrogen is almost completely ionized and outside of which it is almost completely un-ionized.

The transition from one region to the other occurs at the point where the optical distance τ becomes of the order of unity. On this basis it is easy to determine the radius r_0. From Eq. (33.4) we have /458

$$kn\int_{r_*}^{r_0}(1-x)\,dr=1. \tag{33.6}$$

But for $r < r_0$ Eq. (33.1) yields approximately

$$1-x=\frac{n}{Wf(T_*)}. \tag{33.7}$$

Therefore, substituting (33.7) into (33.6) and using Eq. (33.3), we obtain

$$r_0=\left[\frac{3r_*^2f(T_*)}{4kn^2}\right]^{1/3}. \tag{33.8}$$

The region in which the hydrogen is almost completely ionized is called the H II zone, and the region in which it is completely un-ionized is the H I zone. The radius of the H II zone around a given star is defined by Eq. (33.8).

We can also derive a somewhat different formula for defining the quantity r_0. To do this we make use of the fact that all stellar photons beyond the Lyman series limit are absorbed in the region of radius r_0. Ionization of a hydrogen atom occurs with the absorption of each L_c photon, and then recombination occurs.

Since this is a stationary process, we can equate the number of stellar L_c photons to the number of recombinations occurring in the region being considered. Here, obviously, recombinations at the first level must be disregarded since the L_c quanta arising from these recombinations again produce ionization.

Let us denote by I_ν^* the intensity of the stellar radiation. Then for the total number of L_c photons emitted by the star we have the expression

$$4\pi r_*^2 \int_{\nu_1}^{\infty} \pi I_\nu^* \frac{d\nu}{h\nu},$$

where ν_1 is the frequency of the Lyman series limit. On the other hand, the total number of recombinations at all levels, starting with the second, occurring in a region of radius r_0, is equal to

$$4\pi \sum_2^{\infty} C_i \int_{r_*}^{r_0} n_e n^+ r^2 dr,$$

where n^+ is the number of protons and n_e is the number of free electrons in 1 cm^3. Equating the last two expressions and making use of the fact that $n_e = n^+ \approx n$ in the region being considered, we obtain /459

$$r_0^3 n^2 \sum_2^{\infty} C_i = 3r_*^2 \int_{\nu_1}^{\infty} \pi I_\nu^* \frac{d\nu}{h\nu}. \qquad (33.9)$$

It is easily verified that when the stellar radiaton I_ν^* is given by Planck's formula with the temperature T_*, Eq. (33.9) passes over to Eq. (33.8).

The question of the ionization of interstellar hydrogen was first examined by Strömgren [10]. Table 53, taken from this paper, contains values of the quantity r_0 calculated from Eq. (33.8) for stars of various spectral classes. The values of the stellar temperature used for the calculations and their visual absolute magnitude are listed in the same table.

From the table it is seen that ionization of interstellar hydrogen is produced primarily by the hottest stars—spectral classes O and B. Class A stars play only a small role in hydrogen ionization. For example, one class 05 star ionizes hydrogen in the same region of space as 22 million class AO stars. Cold stars ionize none of the interstellar hydrogen—the hydrogen is un-ionized, for the most part, even in the inner layers of their own atmospheres. Roughly speaking, the boundaries of the ionized hydrogen zones lie within the atmospheres of these stars.

Photoionizations of hydrogen atoms and subsequent recombinations occur in the H II zones surrounding hot stars. Then cascade transition of electrons from

level to level occur, so that spectral line photons are produced. Thus, in particular, the emission of the H II zone appears in the Balmer lines, which can be observed. Initially it was precisely this emission that was observed in some /460 regions of the sky, and then Strömgren suggested the theory set forth above as an explanation of it.

The radius of the H II zone around a given star can be found from observations of the Balmer line emission. By comparing it with the theoretical value of the quantity r_0, one can estimate the average density of hydrogen atoms in interstellar space. Observations show that the radius of the H II zone around an O class star is about 100 parsecs. Therefore on the basis of Table 53 we conclude that the average density of hydrogen atoms is equal to approximately $n \approx 1\ cm^3$. From this, a value of $\rho \approx 10^{-24}\ g/cm^3$ is obtained for the average density of the interstellar gas.

TABLE 53. RADII OF THE H II ZONE AROUND STARS OF VARIOUS SPECTRAL CLASSES

Spectrum	T_*	M_{vis}	r_*	Spectrum	T_*	M_{vis}	r_*
O5	79000	—4,2	$140nc \times n^{-2/3}$	B1	23000	—2,5	$17nc \times n^{2/3}$
O6	63000	—4,1	110	B2	20000	—1,8	11
O7	50000	—4,0	87	B3	18600	—1,2	7,2
O8	40000	—3,9	66	B4	17000	—1,0	5,2
O9	32000	—3,6	46	B5	15500	—0,8	3,7
B0	25000	—3,1	26	A0	10700	+0,9	0,5

Commas represent decimal points.

The value of ρ that has been stated refers to regions near the galactic plane. The gas density decreases away from this plane. In addition, extremely large fluctuations are observed in the interstellar gas density. When the gas density in the H II zone exceeds the average density by an order of magnitude, we observe a luminous diffuse nebula. The density of hydrogen atoms in diffuse nebulae, as established in Chapter V, attains values of the order of $10^3\ cm^{-3}$.

According to the estimates that have been made, the H II zones occupy about one-tenth of galactic space. H I zones occupy the remaining space, in which the hydrogen is primarily un-ionized. The explanation of the division of the Galaxy into H II and H I zones is very important for the physics of the interstellar gas.

2. Ionization of other atoms. After having considered the ionization of hydrogen, let us now proceed to a determination of the degree of ionization of other atoms in interstellar space. Here we must keep in mind the vast difference in ionization conditions in the H II and H I zones. This difference is caused by the fact that radiation beyond the Lyman series limit does not leave the H II zone. Therefore in the H I zone only those atoms can be ionized whose ionization energy is less than the hydrogen ionization energy (equal to 13.6 eV). At the same time,

in the H II zone atoms with a higher ionization energy can be ionized if the temperature of the ionizing star is sufficiently high.

In the H II zone the ionization of all atoms is usually caused by the same star as the hydrogen atom ionization. In this case the degree of ionization is determined by Eq. (33.1), which is already known to us. In particular, the He and He^+ atoms can be ionized when the value of T_* is sufficiently high. The ionization of these atoms and their emission, caused by recombinations, occur in corresponding zones within the H II zone. All these questions have already been discussed in detail in Chapter V.

The degree of ionization of atoms in the H I zone is determined in a completely different manner. An arbitrary volume element of this zone is usually quite far from any hot star and the ionization of atoms in it is usually produced /461 by a large number of different stars. In order to formulate a concept of the average degree of ionization of any atom, we must determine beforehand the average radiation density ρ_ν in galactic space. To find the quantity ρ_ν, however, it is necessary to know the distribution of stars of the various spectral classes in the Galaxy, as well as the distribution of dust material which causes absorption of radiation in the continuous spectrum.

A determination of the average radiation density in the Galaxy has been made in a number of papers. Let us now find the quantity ρ_ν, following the work of S. A. Kaplan (see [11]); for simplicity, let us do this for the galactic plane only.

We will denote by $\varepsilon_\nu(z)$ the volume emission coefficient at a height z above the galactic plane and by $\alpha_\nu(z)$—the volume absorption coefficient at the same height. The first of these coefficients is caused by stars, the second—by dust. We will assume that the decrease of these quantities with an increase in z is represented by the formulas

$$\alpha_\nu(z) = \alpha_\nu(0)\, e^{-\frac{z}{\beta}}, \qquad \varepsilon_\nu(z) = \varepsilon_\nu(0)\, e^{-\frac{z}{\beta_*}}. \tag{33.10}$$

From observations it is known that $\beta \approx 100$ parsecs, and the values of β_* are different for stars of different spectral classes (about 50-500 parsecs).

The radiation intensity I_ν depends on the galactic latitude b and is defined by the formula

$$I_\nu(b) = \int_0^\infty \varepsilon_\nu(z)\, e^{-\frac{\tau_\nu(z)}{\sin b}} \frac{dz}{\sin b}, \tag{33.11}$$

where $\tau_\nu(z)$ is the optical distance of a point with coordinate z from the galactic plane. Using Eqs. (33.10), we obtain

$$\tau_\nu(z) = \alpha_\nu(0)\,\beta\left(1 - e^{-\frac{z}{\beta}}\right) \tag{33.12}$$

and

$$I_\nu(b) = \varepsilon_\nu(0)\int_0^\infty e^{-\frac{z}{\beta_*}-\frac{\alpha_\nu(0)\beta}{\sin b}(1-e^{-z/\beta})}\frac{dz}{\sin b}. \tag{33.13}$$

The volume emission coefficient is clearly equal to

$$\varepsilon_\nu(z) = \frac{L_\nu}{4\pi}n_*(z), \tag{33.14}$$

where L_ν is the stellar luminosity at frequency ν and $n_*(z)$ is the number of stars per unit volume at height z. This relation can also be rewritten in the form /462

$$\varepsilon_\nu(z) = r_*^2\pi I_\nu^* n_*(z), \tag{33.15}$$

where I_ν^* is the average intensity of the radiation coming from the star.

Taking Eq. (33.15) into consideration and making the substitution $1-e^{-z/\beta_*} = y$, instead of Eq. (33.13) we obtain

$$I_\nu(b) = \pi I_\nu^* r_*^2 n_*(0)\beta\int_0^1 (1-y)^{\frac{\beta}{\beta_*}-1} e^{-\frac{\alpha_\nu(0)\beta y}{\sin b}}\frac{dy}{\sin b}. \tag{33.16}$$

In a given case the radiation density is equal to

$$\rho_\nu = \frac{4\pi}{c}\int_0^{\pi/2} I_\nu(b)\cos b\, db. \tag{33.17}$$

Substituting Eq. (33.16) here, we obtain

$$\rho_\nu = \frac{4\pi}{c}r_*^2\pi I_\nu^* n_*(0)\beta\int_0^1 (1-y)^{\frac{\beta}{\beta_*}-1}\,\mathrm{Ei}[\alpha_\nu(0)\beta y]\,dy. \tag{33.18}$$

Just as in the case of the effect of a single star, to characterize the radiation density ρ_ν we can introduce the dilution factor W, defined by the relation

$$\rho_\nu = W\rho_\nu^* = W\frac{4\pi}{c}I_\nu^*. \tag{33.19}$$

Using Eq. (33.18), we obtain

$$W = \pi r_*^2 n_*(0)\beta\int_0^1 (1-y)^{\frac{\beta}{\beta_*}-1}\,\mathrm{Ei}[\alpha_\nu(0)\beta y]\,dy. \tag{33.20}$$

Equations (33.18) and (33.20) determine the desired radiation density and its corresponding dilution factor W. This density is produced by stars of a specific spectral class (characterized by the quantities r_*, I_ν^* and n_*). To find the total radiation density, Eq. (33.18) must be summed over all spectral classes.

Values of the dilution factor W, calculated from Eq. (33.20), as well as values of the quantity WI_ν^* representing the direction-averaged radiation intensity in interstellar space, are listed in Table 54. The values of the quantity WI_ν^* are given for three wavelengths in the ultraviolet portion of the spectrum. Theoretical data on the energy distribution in the stellar spectrum, obtained from stellar photosphere model calculations, were used in the computations. As already mentioned (in Section 6), these data are quite different from the observational results obtained with the aid of rockets. Therefore the values of the quantity WI_ν^* that are listed require some revision. /463

TABLE 54. AVERAGE RADIATION INTENSITY IN INTERSTELLAR SPACE

Spectrum	W	WI_ν^*		
		912 Å	1500 Å	2000 Å
O5	$2\cdot10^{-21}$			
O6—O8	$3\cdot10^{-20}$	$5.7\cdot10^{-22}$	$4.4\cdot10^{-22}$	$3.5\cdot10^{-22}$
B0—B2	10^{-17}	$4.1\cdot10^{-20}$	$3.2\cdot10^{-20}$	$2.5\cdot10^{-20}$
B3—B9	$4\cdot10^{-17}$	$4\cdot10^{-20}$	$4\cdot10^{-20}$	$4\cdot10^{-20}$
A0—A9	10^{-15}	$1.2\cdot10^{-20}$	$1.5\cdot10^{-20}$	$1.3\cdot10^{-20}$
F—M	$2\cdot10^{-13}$			
Sum		$1.0\cdot10^{-19}$	$0.9\cdot10^{-19}$	$0.8\cdot10^{-19}$

The WI_ν^* values were calculated for radiation in the wavelength interval from 912 to 2000 Å because it is this radiation that produces ionization in the H I zone. We recall that radiation with $\lambda < 912$ Å is practically nonexistent in the H I zone since it is absorbed by the hydrogen in the H II zones.

If the radiation density ρ_ν at a given point is known, then it is easy to determine the degree of ionization of any atom. To do this we must make use of the relation expressing the equality between the number of ionizations and the number of recombinations. This relation has the form

$$\frac{n_e n^+}{n_1}\sum_{i=1}^{\infty} C_i = \int_{\nu_1}^{\nu_1(\mathrm{H})} k_{1\nu}\frac{c\rho_\nu}{h\nu}\,d\nu, \qquad (33.21)$$

where ν_1 is the ionization frequency of the atom being considered and $\nu_1(\mathrm{H})$ is the hydrogen ionization frequency. The quantity ρ_ν, entering into Eq. (33.21), is given by Eq. (33.19).

The radiation density ρ_ν in interstellar space is very small. However, in addition to this the free electron density n_e is also low. Therefore the degree of ionization of many atoms in interstellar space is much greater than unity. For example, calculations with Eq. (33.21) give about 10^5 for the value of n^+/n_1 for /464 calcium (6.1 V ionization potential). Even for ionized calcium (11.9 V ionization potential) the degree of ionization, i.e., the quantity n^{++}/n^+, is about 10^2.

It should be noted that the free electron density in the H I zones is much less than in the H II zones (by about three orders of magnitude). This is explained by the fact that hydrogen, the most abundant element in the Galaxy, is not ionized in the H I zone. The same applies to the next most abundant element—helium. Free electrons appear in the H I zone only through the ionization of elements whose relative abundance is low (carbon, sodium, etc.).

3. Interstellar absorption lines. The presence of gas in interstellar space is evident not only from its emission but also from the absorption lines in stellar spectra that arise when the stellar radiation passes through the interstellar gas. The first interstellar absorption lines (H and K of ionized calcium) were detected in the spectrum of the binary star δ Orion by Hartman in 1904. The position of these lines in the spectrum did not change, whereas other lines were periodically shifted because of the rotation of one star about the other. Interstellar absorption lines were later observed in the spectra of single stars. At first it was thought that the stars are surrounded by clouds of ionized calcium. Then, however, the increase in the intensity of interstellar absorption lines with an increase in the distance from the star was discovered. This made it possible to arrive at the correct point of view that gas fills all of interstellar space. This effect began to be used for an approximate determination of the distances to stars.

Few interstellar absorption lines are observed in the visible spectrum. In addition to the H and K lines of ionized calcium already mentioned, the sodium D_1 and D_2 lines and a few others are observed. Among molecular lines, only the lines of neutral and ionized molecules of CH and of cyanogen CN are found. All these lines originate from the ground states of the atoms and molecules.

This type of interstellar gas absorption spectrum is explained by the fact that the degree of atomic and molecular excitation in interstellar space is very low. Therefore the lines originating from excited states are extremely weak and cannot be observed. The interstellar gas absorption spectrum should comprise only lines of the principal series, and we observe those which lie in the visible spectrum. The lines of the principal series of many of the abundant elements are in the ultraviolet spectrum (912 Å < λ < 2000 Å) and they can be observed with the aid of rockets. Lines lying beyond the Lyman series limit (λ < 912 Å) cannot be observed because of the absorption of the interstellar hydrogen.

The big difference in the degree of ionization and the degree of excitation of /465 atoms in interstellar space must be emphasized. As we have seen, the degree of ionization of the interstellar gas is quite large. It is explained by the fact that the

low value of the radiation density is compensated by the low density of free electrons. In other words, photoionizations of atoms occur infrequently but the reverse processes—recombinations—also occur infrequently. It is quite different in the case of atomic excitation. Atoms enter excited states (due to stellar radiation or collisions) very rarely. However, spontaneous transitions from the excited states occur quickly (independently, as opposed to recombinations, of the physical conditions. Therefore the degree of atomic excitation in interstellar space is extremely small.

A study of interstellar absorption makes it possible to determine many characteristics of the interstellar gas. This is done by comparing the theoretical and observed line profiles and their equivalent widths.

The determination of the theoretical profiles of the interstellar absorption lines does not represent great difficulty since scattered line radiation can be disregarded. Let us denote by I_0 the intensity of the radiation coming from the stellar atmosphere, and by I_λ—the intensity of the radiation with wavelength λ reaching the observer. In a given case these quantities are related by the simple expression

$$I_\lambda = I_0 e^{-\tau_\lambda}, \tag{33.22}$$

where τ_λ is the optical distance from the star to the observer. The quantity I_0 can be considered to be independent of λ if the interstellar absorption line is not superimposed on the absorption line arising in the stellar atmosphere. The equivalent width of the interstellar absorption will be defined by the formula

$$W_\lambda = \int \frac{I_0 - I_\lambda}{I_0} d\lambda = \int (1 - e^{-\tau_\lambda}) d\lambda. \tag{33.23}$$

The spectral line absorption coefficient must be known to calculate the quantities I_λ and W_λ from Eqs. (33.22) and (33.23). In stellar atmospheres it is determined by radiation attenuation and the thermal motion of the atmosphere. In the case of the interstellar gas, however, the radiation attenuation can be disregarded since absorption occurs primarily only in the central portions of the line. Therefore for the absorption coefficient, calculated for one atom, we can take the expression

$$k_\lambda = k_0 e^{-\left(\frac{\lambda - \lambda_0}{\Delta\lambda_D}\right)^2}. \tag{33.24}$$

where k_0 is the absorption coefficient at the center of the line and $\Delta\lambda_D$ is the Doppler half-width. On the basis of Eq. (12.6) we have /466

$$k_0 = \frac{\sqrt{\pi}\, e^2 \lambda_0^2}{mc^2 \Delta\lambda_D} f, \tag{33.25}$$

where f is the oscillator strength. As we will see later, the thermal velocities of the atoms are much less than the random motion velocities of the interstellar gas. As a result, in the expression for the Doppler line half-width

$$\Delta\lambda_D = \lambda_0 \frac{v}{c} \tag{33.26}$$

by v we mean the average random motion velocity.

If the quantity k_λ is given, then the optical distance τ_λ can be found from the formula

$$\tau_\lambda = k_\lambda \int_0^{r_0} n\,dr = k_\lambda N, \tag{33.27}$$

where n is the number of absorbing atoms in 1 cm^3 and r_0 is the distance between the star and the observer. For the equivalent line width we now obtain

$$W_\lambda = \Delta\lambda_D \int_{-\infty}^{+\infty} (1 - e^{-k_0 N e^{-x^2}})\,dx, \tag{33.28}$$

where $x = \lambda - \lambda_0 / \Delta\lambda_D$.

For small values of the quantity $\tau_0 = k_0 N$, from Eq. (33.28) we find

$$W_\lambda = \sqrt{\pi}\Delta\lambda_D \tau_0 \left(1 - \frac{\tau_0}{2\sqrt{2}} + \frac{\tau_0^2}{6\sqrt{3}} - \ldots\right). \tag{33.29}$$

For large values of the quantity τ_0 we have the asymptotic expansion

$$W_\lambda = 2\Delta\lambda_D \sqrt{\ln \tau_0}\left[1 + \frac{0.2886}{\ln \tau_0} - \frac{0.1355}{(\ln \tau_0)^2} + \ldots\right]. \tag{33.30}$$

If the relationship between W_λ and N, given by Eq. (33.28), is plotted on a graph, then we obtain the curve of growth for the interstellar absorption line. When $k_0 N \ll 1$, the quantity W_λ is proportional to N and is independent of $\Delta\lambda_D$. When $k_0 N \gg 1$, the quantity W_λ depends very slightly on N, but is approximately proportional to $\Delta\lambda_D$. It is obviously impossible to use Eq. (33.28) for very large values of $k_0 N$ (for $k_0 N > 10^3$, approximately) since in this case radiation attenuation must be taken into account.

Using the values of the equivalent line width and of the curve of growth obtained from observations, one can determine the values of the quantities N and $\Delta\lambda_D$. Generally speaking, we have one equation with two unknowns but, for $k_0 N \ll \ll 1$, N can be found without knowing $\Delta\lambda_D$. After dividing N by the distance r_0 to the star, we obtain the average concentration of absorbing atoms n. Passing from one stage of ionization to another with the aid of the ionization formula, we find the average concentration of a given element. The chemical composition of the interstellar gas (or, more precisely, the number of atoms of those elements which give interstellar absorption lines in the visible spectrum) is determined in this manner. /467

A determination of the quantity $\Delta\lambda_D$ from the observed values of W_λ and from the curve of growth can be made when the quantity N is estimated beforehand. There is also a method for determining the quantities $\Delta\lambda_D$ and N simultaneously. It is based on the fact that the Na I and Ca II resonance lines are doublets with a known ratio of oscillator strengths equal to 2. Therefore if the optical distance from the star to the observer is equal to τ_0 for one component of the doublet, then for the other component it is equal to $2\ \tau_0$. The quantity τ_0 can clearly be found from the ratio of the equivalent widths of the doublet components. Further, the quantity $\Delta\lambda_D$ is determined from Eq. (33.28) and the quantity N—from Eq. (33.27).

Knowing the Doppler half-width $\Delta\lambda_D$ of the line allows one to find the quantity v from Eq. (33.26), i.e., the average random velocity of the interstellar gas. A value of $v \approx 10$ km/sec is obtained for this quantity.

As already mentioned, in a first approximation the interstellar gas has a cloud-like structure. The fact that the interstellar absorption lines sometimes consist of several components is evidence of this structure. This is explained by the fact that in such cases several clouds with different radial velocities lie along the path from the star to the observer. The relative velocities of the clouds can be determined from the displacements of the line components with respect to each other. In this manner a value of the order of 10 km/sec is also obtained for the velocity v.

In determining the equivalent widths of the interstellar absorption lines above we have assumed that the random velocities of the interstellar gas have a Maxwellian distribution. From a consideration of the absorption line profiles, however, other expressions are obtained for the velocity distribution function (which falls off more slowly than the Maxwellian function with an increase in velocity). These empirical expressions are sometimes also used to construct theoretical curves of growth.

It must be reiterated that the interstellar gas takes part in the galactic rotation. This effect is evident in the profiles of the interstellar absorption lines at large distances from the stars, with it being different for different directions. This also must be taken into consideration in plotting the theoretical curves of growth. /468

4. Physical state of interstellar gas. As we have seen above, the interstellar gas is extremely rarefied. From the emission of the gas in the H II zones it was found that on the average there is only 1 hydrogen atom in 1 cm^3 of interstellar space. Approximately the same result is also obtained from the interstellar absorption lines. In this case, to be sure, the concentrations of other atoms are found directly from observations (in particular, sodium and calcium) and in the conversion to the density of hydrogen atoms assumptions must be made concerning the relative abundance of the elements in interstellar space. Observations of the galactic radio emission at a wavelength of 21 cm, which will be discussed in the following section, give very detailed information on the density of interstellar hydrogen and on its distribution in space.

Let us now briefly consider the question of the temperature of the interstellar gas. In the H II zones the temperature is determined by the methods discussed in Chapter V and is of the order of 10,000°. One of these methods, based on a consideration of the energy balance of the gas, can also be used to find the temperature in the H I zone. In the H I zone, however, the gas gains and expends energy differently than in the H II zone. As we recall, in the H II zone heating of the gas occurs primarily through the photoionization of hydrogen atoms (and, in part, of helium atoms). But in the H I zone only those atoms are ionized whose ionization potential is less than 13.6 V. Here, as simple estimates show, the gas acquires most of its energy through the ionization of carbon atoms (whose ionization potential is equal to 11.3 V). Since the number of carbon atoms is approximately 10^4 times less than the number of hydrogen atoms, then a unit volume of gas in the H I zone acquires much less energy than in the H II zone. Because of this, those gas cooling mechanisms which are completely nonexistent in the H II zone play a role in the H I zone. Electron collisions, exciting the fine structure of the principal terms of some ions (in particular, C II and Fe II), must be considered to be the most prominent of these mechanisms. From what has been said it follows that the gas temperature in the H I zone must be very low.

A detailed examination of the gas energy balance, performed by Spitzer and Savedoff [12], led to the conclusion that the temperature in the H I zone is about 60°. It is impossible to attach much faith to this value, however, since different gas heating and cooling mechanisms can exist which are difficult to take into account exactly (for example, heating through the dissipation of magnetic energy, cooling through collisions with dust particles, etc.). As we will see below, a temperature value of about 100° is obtained from the 21-cm wavelength radiation of the Galaxy. /469

Under the conditions existing in the un-ionized hydrogen zones, an appreciable number of different molecules must be present in them. In the presence of thermodynamic equilibrium the molecular concentration is determined by Eq. (14.21). Since there is no thermodynamic equilibrium in interstellar space, then the condition of equality between the number of molecules being formed and the number dissociating must be used to determine the concentration of molecules. In this manner it is found, in particular, that there should be many hydrogen molecules H_2 in interstellar space. These molecules, however, have not yet been detected through observations since all their lines, originating from the ground state, are located in the ultraviolet spectrum. As already noted, inter-

stellar absorption lines of the CH, CH^+ and CN molecules are observed in the visible spectrum of stars. From the equivalent widths of these lines, a density of about 10^{-8} cm^{-3} is obtained for these molecules in interstellar space.

5. Motion of interstellar gas. As observations of the interstellar absorption lines indicate, the gas clouds in interstellar space move with velocities of about 10 km/sec. Observations of luminous gas clouds lead to approximately the same results. In this case the cloud velocities are determined from the displacement of the emission lines in their spectra. In addition, random (turbulent) motions exist within the clouds. This is evident in the fact that the radial velocities of different elements of the gas cloud are different. In particular, the internal motions have been studied in detail in the case of the Orion nebula. It was found that the average velocity of these motions is about 7 km/sec.

The interstellar gas motions have been studied by the methods of gas dynamics (see [13] and [14]). We will mention only some of the results here.

If the gas cloud is in a vacuum, then it must, of course, expand. As Riemann has shown, the expansion velocity is equal to

$$v = \frac{2v_s}{\gamma - 1}, \tag{33.31}$$

where v_s is the velocity of sound and γ is the adiabatic exponent.

The velocity of sound, as is known, is given by the formula /470

$$v_s = \sqrt{\frac{\gamma kT}{\mu m_H}}, \tag{33.32}$$

where μ is the mean molecular weight. The interstellar gas is primarily monatomic so that $\gamma = 5/3$. One can assume that $\mu = 1$ and $T = 100°$ in the H I zone and $\mu = 1/2$ and $T = 10,000°$ in the H II aone. Therefore we obtain values of $v_s = 1.2$ km/sec and $v_s = 19$ km/sec, respectively, for the velocity of sound in these zones.

For the cited values of γ and v_s it follows from Eq. (33.31) that a cloud of ionized hydrogen should expand into the void with a velocity of the order of 60 km/sec. The expansion will occur with approximately the same velocity even when the cloud density is much greater than the density of the surrounding medium. Usually, however, the density of the H II zone does not differ greatly from the density of the H I zone adjacent to it. In this case the H II zone will expand more slowly; however, it must expand because of the large difference in the pressures in these zones, caused by the temperature difference. The expansion of the hot gas of the H II zone leads to the movement of the cold gases of the H I zone and compresses it. Moreover, the density of the hot gas is reduced and it becomes more transparent for the stellar radiation in the Lyman continuum. This radiation enters the compressed cold gases and causes its ionization. Because of this process the gas

in the outer layer of the H II zone should be denser and it should shine brighter than the gas in the inner regions. As observations show, the H II zones, in reality, are often bounded by luminous rims.

A characteristic feature of the interstellar gas movement is the formation of shock waves. This is explained by the fact that the gas velocities in interstellar space are often greater than the veolocity of sound (especially in the H I zone). Shock waves can arise through different processes: through the expansion of the H II zone (or, it is sometimes said, through the movement of an ionization front), through the collisions of interstellar clouds, through the movement of the envelopes ejected during nova and supernova outbursts.

Let us present some formulas describing the phenomena occurring during shock wave propagation. Let a dense cloud (or envelope) move with a velocity v in the interstellar un-ionized gas. In front of the cloud there will be compressed gas moving with the same velocity v. The boundary between the compressed and uncompressed gas, called the shock wave front, moves with a velocity V, greater than v. If the shock wave propagates in an ideal monatomic gas, then, as calculations show, /471

$$V = \frac{4}{3} v, \tag{33.33}$$

and the density of the compressed gas is four times greater than the density of the uncompressed gas. When the gas is compressed, its temperature increases to a value determined by the formula

$$\frac{3}{2} kT = \frac{\mu m_{\mathrm{H}} v^2}{2}. \tag{33.34}$$

It is obvious that the heating of the gas and the motion imparted to it occur because of the kinetic energy of the cloud, which gradually slows down. However, in the derivation of the formulas that have been presented the fact that the heated compressed gas can be cooled was disregarded. This cooling occurs because of the fact that atoms are excited through collisions with free electrons and then emit line quanta that leave the gas. This process is gas luminescence. The structure of the shock waves with luminescence was first considered by S. B. Pikel'ner [15], and then by other authors. The results of this theory differ from those cited above. In particular, it was found that the density of the compressed gas can exceed its initial density tenfold. It is possible that the luminosity of some diffuse nebulae is explained by the luminescence of the gas after passage of a shock wave through it.

The turbulent gas motions existing in the Galaxy have been studied by special statistical methods. A discussion of the theory of interstellar turbulence can be found in the already-cited book of S. A. Kaplan [13] in which the original results of the author, taking into consideration the interaction of the gas with a magnetic field, are also presented.

The movement of gas and dust particles in the Galaxy can be caused by a number of reasons. One of these is the radiation pressure of the stars, which has quite a strong influence on the dust particles. The expansion of nova and supernova envelopes can be cited as another reason. Apparently, the expansion of the ionized hydrogen zones, surrounding class O stars, plays the greatest role in imparting movements to the gas and dust in interstellar space.

34. Space Radio Emission

1. Emission of the H II zone. Emission of the interstellar medium is observed both in the optical spectrum and at radio frequencies. Observations in the radio frequency band provide valuable information not only about the physical state of the interstellar medium but also about its structure and movement. Especially /472 important is the fact that we can observe radio emission from very remote parts of the Galaxy which are completely unreachable for optical observations. This is explained by the fact that the interstellar dust is practically transparent at radio frequencies.

Let us first discuss the radio emission coming from the ionized hydrogen zones. This emission, observable in the centimeter and decimeter bands, is thermal (in the meter band it is supplemented with nonthermal emission, which we will discuss below). Since the radio emission of the quiet Sun is also thermal in nature, we can utilize the formulas presented in Section 18 in the consideration of the thermal radio emission of the H II zones.

We will assume that the radio emission comes to us from a cloud of ionized hydrogen and that there is no absorption along the path from cloud to observer. We will denote the volume emission coefficient by ε_ν and the volume absorption coefficient by α_ν in the cloud. If the emission is thermal, then we have

$$\frac{\varepsilon_\nu}{\alpha_\nu} = B_\nu(T_e) = \frac{2\nu^2}{c^2} kT_e, \tag{34.1}$$

where T_e is the electron gas temperature. It was established above that in the H II zones the quantity T_e is nearly constant (and close to 10,000°). Therefore for the intensity of the emission coming from the cloud we can write

$$I_\nu = B_\nu(T_e)\,(1 - e^{-\tau_\nu^0}), \tag{34.2}$$

where τ_ν^0 is the optical path length in the cloud. To calculate the quantity τ_ν^0, Eq. (18.9) should be used, on the basis of which we obtain

$$\tau_\nu^0 = \int_0^{s_0} \alpha_\nu ds = \frac{2^4\pi^2 e^6}{3\sqrt{3}c\,(2\pi mkT_e)^{3/2}} \frac{g_\nu}{\nu^2} \int_0^{\infty} n_e n^+ ds, \tag{34.3}$$

where s_0 is the geometrical "thickness" of the cloud.

As we know, the emission intensity I_ν is customarily expressed in terms of the brightness temperature T_ν by means of Eq. (18.2). Therefore Eq. (34.2) can be rewritten in the form

$$T_\nu = T_e(1 - e^{-\tau_\nu^0}). \tag{34.4}$$

Let us consider two special cases of Eq. (34.4). For $\tau_\nu^0 \gg 1$ from this formula it follows that

$$T_\nu \approx T_e, \tag{34.5}$$

and for $\tau_\nu^0 \ll 1$:

$$T_\nu \approx T_e \tau_\nu^0 \sim \nu^{-2} \tag{34.6}$$

It is easy to distinguish one case from the other by means of the observed dependence of the brightness temperature T_ν on the frequency ν. If observations show that T_ν is independent of ν, then the optical thickness of the cloud is considerable ($\tau_\nu^0 \gg 1$). In this case the measured brightness temperature is simply equal to the electron temperature of the cloud, which is thereby determined. If, however, observations indicate that $T_\nu \sim \nu^{-2}$, then the cloud has a small optical thickness ($\tau_\nu^0 \ll 1$). In the given case the value of the integral $\int_0^{s_0} n_e n^+ ds$ (sometimes called the "emission standard") can be determined from the measured brightness temperature. Knowing the value of this integral and the cloud thickness s_0 allows one to estimate the average free electron density in the cloud (since $n^+ = n_e$, approximately). /473

As seen from Eq. (34.3), the optical thickness of the nebula decreases with an increase in frequency. Therefore through observations at radio frequencies it can be shown that the brightness temperature at low frequencies will be a constant, and at high frequencies—proportional to ν^{-2}. In other words, a break is observed in the radio spectrum of a nebula at some frequency (which we denote by ν_1). The frequency ν_1 is obviously determined from the condition

$$\nu_1^2 = \frac{2^4 \pi^2 e^6 g_{\nu_1}}{3\sqrt{3} c (2\pi m k T_e)^{3/2}} \int_0^{s_0} n_e n^+ ds. \tag{34.7}$$

Instead of (34.7) we have, approximately (for $T_e \approx 10^4$),

$$\nu_1^2 \approx 10^{-7} \int_0^{s_0} n_e n^+ ds. \tag{34.8}$$

Equation (34.8) allows one to find the emission standard from the observed frequency ν_1.

The formulas that have been presented can be used only for those nebulae for which the radio emission intensity I_ν is measured. For most nebulae, however, the flux H_ν is measured and not the intensity. In order to derive a theoretical expression for H_ν, Eq. (34.2) for I_ν must be integrated over the coordinates in the plane of the figure. In this situation it is usually assumed that the nebula has a spherical shape.

Values of the electron temperatures and densities have been determined by the methods cited (or different variations of them) for many diffuse nebulae. The work of Yu. N. Pariyskiy [16], who investigated the radio emission of the Orion nebula in detail, can be cited as an example. In particular, he obtained a value /474 of 11,750° for the electron temperature of the nebula. The nebular mass, equal to 116 $M_\odot$, was also determined.

2. Nonthermal emission. From Eq. (34.4) it is seen that in the case of thermal emission the brightness temperature T_ν cannot exceed the electron temperature T_e. If, however, observations show that $T_\nu > T_e$, then one must conclude that nonthermal emission is present.

As we know, the electron temperature in the H II zones is about 10,000°. However, the brightness temperature of the Galaxy radio emission in the meter band is very high, reaching values of the order of hundreds of thousands of degrees. Therefore it is necessary to assume that a portion of the continuous spectrum radio emission is nonthermal in nature.

This conclusion is corroborated by the frequency dependence of the radio emission intensity found from observations. Usually the radio emission intensity and its brightness temperature are represented in the form

$$I_\nu \sim \nu^{-n}, \qquad T_\nu \sim \nu^{-n-2}, \tag{34.9}$$

where n is some constant. For thermal emission $n \leq 0$ (when the emitting layer is transparent, I_ν decreases with an increase in wavelength, and when it is nontransparent I_ν = const). For galactic radio emission in the meter band, however, it is found that $n \approx 0.5$, i.e., the intensity increases with an increase in wavelength.

Thus, the galactic radio emission comprises two parts: thermal and nonthermal. In the meter band nonthermal emission predominates over thermal. With a decrease in wavelength, however, the nonthermal emission intensity decreases and in the decimeter band it is of the same order as the thermal emission intensity. In the centimeter band thermal emission, coming from the ionized hydrogen zones as explained above, predominates.

It should be noted that ionized hydrogen clouds are sometimes observed in the meter band, but by virtue of their absorption, not their emission. This occurs when the H II cloud is projected onto a region of the Galaxy emitting meter waves with a very high brightness temperature.

Detailed maps of the radio emission of the Galaxy have been compiled by virtue of numerous observations. The Mills (3.5-m waves) and Westerhout (22--cm waves) maps can be cited as an example. From the maps that have been produced it is seen that the centimeter wave emission comes to us from a narrow band located along the galactic equator. It originates in H II zones in the spiral /475 arms. Meterwave emission, however, comes both from the narrow galactic band and also from a very extended region, the emission intensity of which slowly decreases with distance away from the galactic plane. This region is approximately spherical in shape and is the corona of the Galaxy.

At the present time it is assumed that the nonthermal radio emission of the Galaxy is the bremsstrahlung of relativistic electrons in a magnetic field (i.e., it is caused by the synchrotron mechanism). This concept was first proposed in 1950 by Alfven and Herlofson [17] and Kippenheuer [18]. These authors based it on the fact that an enormous number of high energy particles should exist in galactic space which produce the cosmic ray effect observed on Earth. Subsequently, the theory of the origin of the nonthermal radio emission of the Galaxy due to the synchrotron mechanism was developed in detail by V. L. Ginzburg, I. S. Shklovskiy, G. G. Getmantsev and others.

The basic formulas for determining the intensity of the synchrotron radiation were given in Section 31 during the discussion of the radio emission of discrete sources in the remains of supernovae. These formulas can also be applied to the nonthermal radio emission of the Galaxy. Since the observed frequency dependence of the radio emission intensity is expressed by Eq. (34.9), in which $n \approx 0.5$, the energy spectrum of the relativistic electrons will be determined by Eq. (31.9), in which $\gamma \approx 2$. Further, the volume emission coefficient ε_ν can be found from the radiation intensity I_ν and the path length r_0 in the Galaxy with the aid of the relation

$$I_\nu = \varepsilon_\nu r_0 \tag{34.10}$$

A comparison of this value of ε_ν with its theoretical value, given by Eq. (31.10), allows one to estimate either the density of relativistic electrons in the Galaxy, or the magnetic field intensity (if one of these quantities is given, then the other is determined). We assume that the number of relativistic electrons is about 1% of the number of high energy particles (estimated from the observed cosmic rays). Then values of the order of 10^{-6}-10^{5} oersted are obtained for the magnetic field intensity in the Galaxy. In this situation the magnetic field intensity in the galactic corona is 2-3 times lower than in the galactic disk.

If the nonthermal radio emission of the Galaxy has a synchrotron origin, then the manner in which relativistic electrons appear in it must be clarified. As already stated in Section 31, relativistic electrons can originate during supernova /476

outbursts. However, other mechanisms exist for the formation of high energy particles in the Galaxy. One of them is the "statistical mechanism" mentioned by Fermi. It involves the acceleration of charged particles through collisions with a magnetized cloud of interstellar gas. Such a collision can lead to the acceleration as well as the deceleration of a particle, with it being more efficient, the higher the particle energy. It is possible that the high energy particles, formed during supernova outbursts, are accelerated still more as the result of the action of the Fermi mechanism.

3. Monochromatic radio emission. At radio frequencies the interstellar medium radiates energy not only in a continuous spectrum but also in spectral lines. These lines originate through transitions between discrete levels that are very close together. The most important of these lines belongs to hydrogen and has a wavelength $\lambda = 21$ cm. It originates through transitions between the sublevels of the hyperfine structure of the ground state of the atom. Van de Hulst first indicated the possibility of observing this line, and then it was actually observed. Subsequently, many astrophysicists studied the galactic radio emission in this line. It should be stressed that these investigations are the major source of our information about neutral hydrogen in interstellar space (since it occurs preferentially in the H I zones where it gives no emission in the visible spectrum).

Calculations have shown (see [19]) that the Einstein spontaneous transition coefficient in the $\lambda = 21$ cm line is equal to

$$A = 2{,}85 \cdot 10^{-15} \sec^{-1}. \tag{34.11}$$

As we see, it is very small and therefore the mean lifetime of an atom in an excited sublevel of the ground state is extremely long—about 10^7 years.

Excitation of the upper sublevel occurs through collisions between atoms. Under the conditions of the interstellar medium these collisions occur extremely rarely; however, they are more frequent than spontaneous transitions between the sublevels. Therefore one can assume that the distribution of atoms in the sublevels is given by Boltzmann's formula for the kinetic gas temperature T_k. In this case the ratio of the emission coefficient to the absorption coefficient at the $\lambda = 21$ cm line will be equal to the value of Planck's function for the same temperature, i.e., the quantity $B_\nu(T_k)$.

On the basis of what has been said the emission intensity in the line being considered is represented by the formula /477

$$I_\nu' = B_\nu(T_k)\,(1 - e^{-t_\nu^0}) + I_\nu'', \tag{34.12}$$

where t_ν^0 is the total optical path of a ray at frequency ν within the line for a given direction in the Galaxy, and I_ν'' is the intensity of the continuous spectrum galactic emission at the line frequencies.

The quantity I_ν'' (caused primarily by the nonthermal emission of the Galaxy) is determined by the formula

$$I_\nu'' = \int_0^\infty \varepsilon_\nu e^{-\sigma_\nu r} dr = \frac{\varepsilon_\nu}{\sigma_\nu}(1 - e^{-t_\nu^0}), \tag{34.13}$$

where ε_ν is the volume emission coefficient in the continuous spectrum, and σ_ν is the volume absorption coefficient in the line. Let I_ν be the continuous spectrum emission intensity in the absence of line absorption. The emission coefficient ε_ν is expressed in terms of I_ν with the aid of Eq. (34.10). Using also the formula $t_\nu^0 = \sigma_\nu r_0$, instead of (34.13) we obtain

$$I_\nu'' = I_\nu \frac{1 - e^{-t_\nu^0}}{t_\nu^0}. \tag{34.14}$$

Beyond the line limits, i.e., for $t_\nu^0 \to 0$, $I_\nu' \to I_\nu$. The quantity I_ν can be found from observations of a portion of the continuous spectrum adjacent to the line.

Since the absorption coefficient at the $\lambda = 21$ cm line is very small (it is proportional to the small quantity A), then for most directions in the Galaxy the quantity t_ν^0 is less than unity. Only in certain regions of the sky (in particular, in the direction of the galaxtic center) is $t_\nu^0 \gg 1$. In the latter case the gas temperature in the H I regions can be determined from the observed line intensity, which is now close to the value $B_\nu(T_k)$. In this way a value of $T_k \approx 125°$ is obtained for this temperature.

When, however, $t_\nu^0 \ll 1$, instead of (34.12) we have

$$I_\nu' - I_\nu = B_\nu(T_k) t_\nu^0. \tag{34.15}$$

Using this formula, one can find the quantity t_ν^0 from the observed emission intensity at the $\lambda = 21$ cm line. This permits a conclusion to be drawn concerning the distribution and movement of interstellar hydrogen. The quantity t_ν^0 can be written in the form

$$t_\nu^0 = \int_0^\infty n_1(r) k(\nu - \nu_0') dr, \tag{34.16}$$

where $n_1(r)$ is the hydrogen atom density at a distance r in the direction being considered and $k(\nu - \nu_0')$ is the absorption coefficient calculated for one atom. /478

Here, ν_0' denotes the center frequency of the line, corresponding to the radial velocity v(r) of the given volume with respect to the observer, i.e.,

$$\nu_0' = \nu_0 + \nu_0 \frac{v(r)}{c}. \tag{34.17}$$

Let us assume that there is a cloud of interstellar hydrogen, moving at a velocity v with respect to the observer, at some distance in the direction being considered. Then for frequencies ν near the frequency ν_0' defined by Eq. (34.17), the value of t_ν^0 will have a maximum and a peak should be observed in the line profile. The number of hydrogen atoms in the cloud can be found from the intensity of this peak, and the cloud velocity can be found from the shift of the peak with respect to the center frequency ν_0. In reality, however, there are a large number of clouds, moving with different velocities, along the line of sight. Moreover, the interstellar gas takes part in the galactic rotation. Therefore the profiles of a given line are quite complicated.

In analyzing the profiles of the $\lambda = 21$ cm line it must be borne in mind that the emission in this line reaches us from very remote parts of the Galaxy. Therefore, of all the interstellar gas motions, the galactic rotation exerts the biggest influence on the line profile. It is easy to derive that in this case the radial velocity of some volume with respect to the observer is defined by the formula

$$v(r) = R_0[\omega(R) - \omega(R_0)] \sin(l - l_0), \tag{34.18}$$

where R and R_0 are the distances of the given volume and the Sun from the galactic center, respectively; $\omega(R)$ is the angular rotational velocity; $l - l_0$ is the difference in longitudes between the given volume and the center of the Galaxy (Fig. 45). If the function $\omega(R)$ is known, then, using Eq. (34.15), the hydrogen distribution in the Galaxy can be found from the observed line profiles. This work, performed by Oort and his colleagues, led to the conclusion concerning the preferential occurrence of hydrogen in the spiral arms. Detailed maps of the hydrogen distribution in the galactic plane now exist.

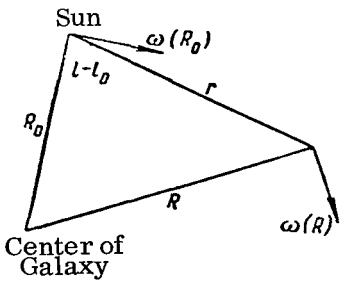

Figure 45.

If both sides of Eq. (34.15) are integrated /479
over all frequencies, then we obtain

$$\int_0^\infty (I_\nu' - I_\nu)\, d\nu = \frac{h\nu_0}{4\pi} A \int_0^\infty n_1(r)\, dr, \tag{34.19}$$

where A is given by Eq. (34.9). In the derivation of Eq. (34.19), Eq. (8.12) is used and negative absorption is taken into consideration. We see that the total

number of hydrogen atoms in a column with a 1 cm^2 cross section located along the line of sight can be determined from the observed total line intensity with the aid of Eq. (34.19). From this, given the dimensions of the Galaxy, the average hydrogen atom density can be found. A value of $\bar{n}_1 \approx 1$ cm^{-3} is obtained for this quantity, just as with other methods.

The galactic rotation velocity as a function of R can also be determined from the profiles of the $\lambda = 21$ cm line. It is obvious that, for a given ray, the volume which is nearest to the center of the Galaxy has the maximum radial velocity, equal to $R_0 \sin(l - l_0)$. On the other hand, the velocity of this volume is determined from the displacement of the edge of the line with respect to the center frequency ν_0. A comparison of these quantities, obtained by observations in different directions, allows one to find the function $\omega(R)$.

Thus, very important results are obtained through an analysis of the profiles of the $\lambda = 21$ cm line. To a considerable degree this is explained by the presence of large velocity gradients in the interstellar medium, caused by the galactic rotation. Because of the Doppler effect, the line emission coming from different parts of the Galaxy has different frequencies and is not absorbed along the path to the observer. Therefore each element of the line profile characterizes the emission coming from a specific portion of the Galaxy. This considerably facilitates the analysis of the line profile.

Besides the $\lambda = 21$ cm line, the interstellar medium also emits other radio frequency lines. In particular, hydrogen gives such lines for the transitions between the fine structure levels. For example, a line with a 3-cm wavelength arises from the $2^2P_{3/2}$-$2^2S_{1/2}$ transition. The intensity of this line, however, is low. Hydrogen also emits radio frequency lines for transitions between high levels with principal quantum numbers that are close to each other. It is easily verified that lines with a wavelength $\lambda > 1$ cm are formed for $n \rightarrow n-1$ transitions if $n > 60$. As shown by the calculations of N. S. Kardashev [20], the intensities of these lines are quite high and they can be observed.

4. Absorption lines at radio frequencies. The interstellar hydrogen gives both an emission line and an absorption line at the $\lambda = 21$ cm wavelength. The latter is produced when there is an intense source of continuous spectrum radio emission in the path. Generally speaking, the line emission intensity is determined by the formula /480

$$I_\nu' = B_\nu(T_k)(1 - e^{-t_\nu^0}) + I_\nu'' + I_\nu^0 e^{-t_\nu^0}, \tag{34.20}$$

where I_ν^0 is the emission intensity of the source, and t_ν^0 is the optical distance from source to observer. If there is no source, then Eq. (34.20) passes over to the previously discussed Eq. (34.12). If, however, the source is very intense, then instead of (34.20) we obtain

$$I_\nu' = I_\nu^0 e^{-t_\nu^0}. \tag{34.21}$$

The absorption line profile is also determined by Eq. (34.21).

The $\lambda = 21$ cm absorption line has been observed in the spectra of very bright galactic radio emission sources: Cassiopeia A, Taurus A and Sagittarius A. The location of these sources and the spiral arms, in which the hydrogen is most abundant, is depicted schematically in Fig. 46. The hydrogen atom density in the arms, as well as the kinetic temperature of the interstellar gas, were determined from the observed line profile and intensity with the aid of Eq. (34.21).

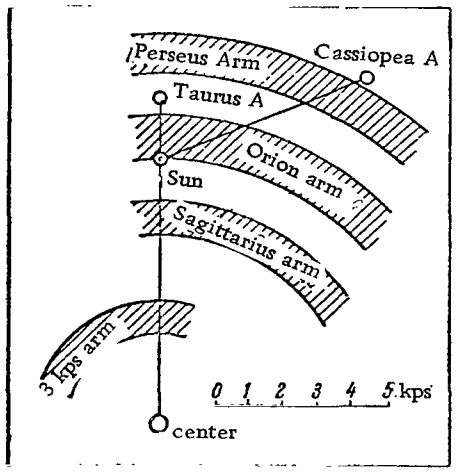

Figure 46.

Especially interesting is the fact that the magnetic field intensity in the Galaxy can be determined from the $\lambda = 21$ cm absorption line. This possibility results from the fact that the upper sublevel of the ground state of the hydrogen atom is a triplet and the $\lambda = 21$ cm line is split into three components in a magnetic field (the Zeeman effect). Because of the weakness of the magnetic field, however, the distance between the outer components is very small (it is about 30 hertz for $H \approx 10^{-5}$ oersted, whereas the Doppler line width is about 10^4 hertz). Nevertheless one can attempt to measure the magnitude of the splitting, using the polarization of the outer components for this. Such an attempt has been made at the English radio astronomy observatory of Jodrell Bank. As a result it was found that in regions of the Galaxy, lying in the directions of the three radio emission sources cited above, the magnetic field intensity amounts to 10^{-6}-10^{-5} oersted. /481

Besides the $\lambda = 21$ cm absorption line, interstellar absorption lines of certain molecules can also be observed at radio frequencies. The lines of the OH molecule were the first of these to be detected. A measurement of the profiles and intensities of these lines in the direction of the galactic center has made it possible to determine the velocity of the interstellar gas clouds and the density of OH molecules in the clouds.

5. Metagalactic radio emission. Until now we have discussed only the interstellar medium in our Galaxy. However, the results of a study of other galaxies are also of very considerable value in understanding the nature of the interstellar medium. These results are based on galactic observations in the optical portion of the spectrum as well as at radio frequencies.

The galaxies nearest to us are the Magellanic Clouds. Many gaseous nebulae, and the radiation of the hot stars causing them, have been observed in them. The S Dorado nebula, whose mass is apparently about a million solar masses, is especially large. Intense continuous spectrum radio emission, having a thermal origin, comes from this nebula. The major portion of the continuous radio emission spectrum of the Magellanic Clouds has a nonthermal (probably synchrotron)

nature. Observations of the 21-cm radio emission of the Magellanic Clouds have yielded important results. In particular, it has been possible to determine the mass of the interstellar hydrogen in them from the intensity of this emission (approximately $6 \cdot 10^8 M_\odot$ in the Large Magellanic Cloud and $4 \cdot 10^8 M_\odot$ in the Small).

The M 31 galaxy ("Andromeda nebula") is also very near to us; in many respects it is similar to the Milky Way. A study of its emission at $\lambda = 21$ cm has made it possible to determine the rotational velocity at different distances from the center and the distribution of interstellar hydrogen. The continuous spectrum radio emission of the galaxy comes from a more extended region than the optical emission. This attests to the presence of a corona, similar to the corona of our Galaxy. The frequency dependence of the emission intensity is expressed as $\nu^{-0.7}$, which can be explained by the synchrotron character of the emission.

The radio emission of many other galaxies has also been measured by various observers. The amount of interstellar hydrogen in the galaxy, determined from the $\lambda = 21$ cm emission, was found to be strongly dependent on its structure. This fact is of considerable interest from the viewpoint of the theory of galactic evolution. /482

The overwhelming majority of the galaxies emit about the same amount of energy in the radio band as the Milky Way. Among them, in particular, are the Magellanic Clouds and the Andromeda nebula. However, the amount of energy emitted by some galaxies at radio frequencies is some orders of magnitude greater. Such galaxies are commonly called radio galaxies. The radio source Cygnus A, emitting about a million times more energy than our Galaxy at the radio frequencies, is a characteristic example of a radio galaxy. On photographs this source is a very unusual galaxy with a binary nucleus. Its emission in the visible spectrum is concentrated in bright forbidden lines (O I, O II, O III, Ne II, Ne III, etc.). The widths of these lines indicates internal motions with velocities of the order of 400 km/sec. Baade and Minkovskiy, studying the Cygnus A source in detail, proposed the hypothesis that in the case given we are dealing with a collision between two galaxies. Subsequently this hypothesis was applied to other radio galaxies; however, V. A. Ambartsumyan [21] advanced persuasive objections against it. According to him, galaxies with binary nuclei are in the process of splitting and this process, at a certain stage, is accompanied by intense radio emission and by the appearance of emission in the visible spectrum.

The radio source Virgo A, appearing in visible light as a giant galaxy of nearly spherical shape, can serve as another example of a radio galaxy. An intense λ 3727 Å (O II) emission line, originating, it must be presumed, in gaseous nebulae of low density, is observed in the spectrum of the galactic nucleus. A surprising feature of this galaxy is that a bright surge of blue color emanates from its nucleus. This emission is polarized (with a 30% degree of polarization), and its spectrum is purely continuous. One can assume that the surge emission in the visible spectrum is similar to the emission of the Crab nebula, i.e., it has a synchrotron nature.

A detailed study of the radio galaxies shows the origin of their radio emission is apparently associated with the vigorous activity of their nuclei. This activity involves the ejection of material from the nucleus, leading to the appearance of relativistic electrons, gas clouds and variable stars in the galaxy. As a result, intense radio emission, blue surges and emission lines are observed in the spectra of the galaxies. /483

Recently intense radio emission sources, visually identified with star-like objects, have also been discovered. The spectra of these quasi-stellar objects (sometimes called quasars for short) contain emission lines shifted toward the red by an amount of the order of a thousand angstroms. Initially it was assumed that the "red shift" in quasar spectra has a gravitational origin. Then, however, a view was adopted in which the quasars are extragalactic objects, receding from us with velocities of the order of some tens of thousands of kilimeters per second. By using the Hubble relation between the galactic recession velocity and the distance to it, it was found that the distances to the quasi-stellar objects amount to millions of parsecs, and their brightness is some orders of magnitude greater than the galactic brightness. Quasars have stimulated a great deal of interest in astrophysics; however, their nature has not yet been explained.

REFERENCES

1. Shayn, G. A., V. F. Gaze and S. B. Pikel'ner. The presence of dust and gas in diffuse nebulae, Izv. Krymskoy astrofiz. obs. 12, 64, 1954.
2. Ambartsumyan, V. A. and Sh. G. Gordeladze. Problem of diffuse nebulae and cosmic absorption, Byull. Abastumanskoy astron. obs. No. 2, 37, 1938.
3. Ambartsumyan, V. A. Theory of brightness fluctuations in the Milky Way, DAN SSSR 44, 244, 1944.
4. Chandrasekhar, S. and G. Münch. The theory of the fluctations in brightness of the Milky Way, Ap. J. 112, 390, 1950; 112, 393, 1950; 114, 110, 1951; 115, 94, 1952; 115, 103, 1952.
5. Agekyan, T. A. Theory of the fluctuations in the number of observable galaxies, Astron. Zh. 34, 371, 1957.
6. Sobolev, V. V. The luminosity of a spherical nebula, Astron. Zh. 37, 3, 1960.
7. Minin, I. N. Optical properties of dust nebulae, Astron. Zh. 38, 641, 1961.
8. van de Hulst, H. C. Light scattering by small particles, 1957. (Russ. translation: H. van de Hulst, Light scattering by small particles, Izd-vo inostr. Lit., 1961).
9. Loden, L. O. Contribution to the discussion of interstellar polarization, Stockholms Obs. ann. 22, N 3, 1961.
10. Strömgren, B. The physical state of interstellar hydrogen, Ap. J. 89, 526, 1939. (Russ. translation in "Astrophysical compilation", Izd-vo inostr. lit., 1949).
11. Kaplan, S. A. and S. B. Pikel'ner. Interstellar space, Fizmatgiz, 1963.
12. Spitzer, L. and M. P. Savedoff. The temperature of interstellar matter, Ap. J. 111, 593, 1950.
13. Kaplan, S. A. Interstellar gas dynamics, Fizmatgiz, 1958.
14. Problems of cosmical aerodynamics, 1951. (Russ. translation: Problems of cosmic aerodynamics, Izd-vo inostr. lit., 1953).
15. Pikel'ner, S. B. Spectrophotometric study of the excitation mechanism of filamentary nebulae, Izd. Krymskoy astrofiz. obs. 12, 93, 1954.

16. Pariyskiy, Yu. N. Model of the Orion Nebula from radio observations, Astron. Zh. 38, 798, 1961.
17. Alfven, H. and N. Herlofson. Cosmic radiation and radio stars, Phys. Rev. 78, 616, 1950.
18. Kippenheuer, K. Cosmic rays as the source of general glactic radio emission, Phys. Rev. 79, 738, 1950.
19. Shklovskiy, I. S. Cosmic radio emission, Gostekhizdat, 1956.
20. Kardashev, N. S. Possibility of detecting the allowed lines of the hydrogen atom in the radio frequency range, Astron. Zh. 36, 838, 1959.
21. Ambartsumyan, V. A. The evolution of galaxies, Izv. AN Arm. SSR, seriya fiz.-matem. nauk 11, No. 5, 1958.

CHAPTER VIII

INTERNAL STRUCTURE OF STARS

The theory of the internal structure of stars is well removed from other portions of theoretical astrophysics. First of all, this is explained by the unusual nature of the physical conditions within a star, characterized by very high temperatures and high densities. The behavior of matter and energy under such conditions is not yet adequately understood. The experimental investigation of a high-temperature plasma, of which stellar interiors are composed, has really just begun. Therefore the theory of the internal structure of stars can still encounter many unexpected facts. /485

Another feature of stellar interiors is that they cannot be observed with the aid of normal astronomical methods. Therefore only indirect considerations, and not direct measurements, can be used to check the results of the theory. Theoretically, of course, a possibility does exist for obtaining direct information on the processes occurring within a star. This possibility involves the measurement of the neutrino flux coming from the star. Because of the extremely high penetration power of these particles, they escape from stellar interiors unhindered. However, it is extremely difficult to collect a neutrino, and the development of "neutron astronomy" is a thing of the future.

The basic problem of the theory of the internal structure of stars is as follows. Consider a star with radius R, mass M and luminosity L. The boundary conditions of the problem are known, i.e., the conditions in the surface layers of the star. One can assume that the star is in a steady-state condition (this is valid for the overwhelming majority of the stars). It is required to determine the structure of the star, i.e., to find the density and temperature distribution within the star.

The theory, however, must not only explain the structure of an individual star but also explain the various statistical relationships found in the examination of star clusters. Of these relationships, the following are the principal ones: 1) the mass-luminosity relation and 2) the spectrum-luminosity relation /486
(which can also be represented as the luminosity-radius relation). The theory

of internal stellar structure should also provide the necessary bases for constructing a stellar evolution theory.

Data from theoretical physics must, of course, be used to solve this fundamental problem. However, the study itself of stellar interiors can lead to the expansion of these data. As an example, let us point out that searches for the sources of stellar energy contributed to the discovery of nuclear reactions, associated with the evolution of large amounts of energy. Similar discoveries will undoubtedly occur in the future.

The theory of the internal structure of stars has passed through several stages in its evolution. Initially only mechanical equilibrium of the star under the influence of two forces was considered in the theory: gravity and gas pressure. It was assumed that the pressure is proportional to some power of the density. This theory found its fruition in Emden's book [1]. Subsequently, radiation pressure was introduced into the mechanical equilibrium equation and the energy equilibrium of the star began to be considered. Eddington's [2] investigations had considerable importance at this state. However, the fundamental problem of the theory—the problem of stellar energy sources—remained unresolved for a long time. Only in the 1940's was it established that nuclear reactions, transforming hydrogen into helium, are the prime source of stellar energy. This discovery marked the beginning of the modern stage of the theory. The study of the structure of white dwarfs, within which the gas is degenerate, occupies a special place in the theory of internal stellar structure.

In this chapter the theory of internal stellar structure is presented in the order of its evolution. The initial stages of the theory are considered very briefly since only very few of the results obtained then still retain their value.

35. Equations of Equilibrium of Stars

1. Equation of mechanical equilibrium. We will assume that the star possesses spherical symmetry and is in equilibrium under the influence of gravitational and gas pressure forces. Let P be the pressure and ρ—the density within the star. These quantities depend on the distance r from the center of the star.

The equation of equilibrium under the influence of these forces (i.e., the equation of hydrostatic equilibrium) has the from /487

$$dP = -g\rho\, dr, \tag{35.1}$$

where g is the acceleration of gravity at a given point of the star. In the case of spherical symmetry the quantity g is defined by the formula

$$g = G\frac{M_r}{r^2}, \tag{35.2}$$

where G is the gravitational constant and M_r is the mass included within a sphere of radius r, i.e.,

$$M_r = 4\pi \int_0^r \rho r^2 \, dr \tag{35.3}$$

Substituting (35.2) into (35.1), we obtain

$$\frac{dP}{dr} = -G\frac{M_r}{r^2}\rho. \tag{35.4}$$

Introducing the expression for M_r here, we arrive at the equation of mechanical equilibrium in the form

$$\frac{1}{r^2}\frac{d}{dr}\left(\frac{r^2}{\rho}\frac{dP}{dr}\right) = -4\pi G\rho. \tag{35.5}$$

Equation (35.5) is one of the fundamental equations of the theory of the internal stellar structure.

Two unknown quantities enter into Eq. (35.5): the pressure P and the density ρ. As already mentioned, in the first stage of the theory development it was assumed that these quantities are interrelated:

$$P = C\rho^k, \tag{35.6}$$

where C and k are constants. This relationship between P and ρ is called polytropic. Thus, the stars were initially considered as polytropic gaseous spheres.

With the aid of (35.6) we find

$$\frac{1}{\rho}\frac{dP}{dr} = \frac{Ck}{k-1}\frac{d\rho^{k-1}}{dr}. \tag{35.7}$$

Substituting (35.7) into (35.5) and using the notation

$$\rho^{k-1} = u, \tag{35.8}$$

we obtain

$$C(1+n)\frac{1}{r^2}\frac{d}{dr}\left(r^2\frac{du}{dr}\right) = -4\pi G u^n, \tag{35.9}$$

where n = 1/k - 1). The quantity n is called the polytropic index.

Equation (35.9), in which the one unknown function u(r) enters, can be simplified somewhat by introducing new dimensionless variables, namely: /488

$$u = u_0 y, \qquad x = \lambda r \tag{35.10}$$

and we will assume that u_0 is the value of u at the center of the star (when r = 0). Let us select the quantity λ such that when (35.10) is substituted into (35.9), all physical constants vanish. Then we obtain the relation

$$C(1+n)\lambda^2 = 4\pi G u_0^{n-1}, \tag{35.11}$$

for defining λ, and Eq. (35.9) assumes the form

$$\frac{1}{x^2}\frac{d}{dx}\left(x^2\frac{dy}{dx}\right) = -y^n. \tag{35.12}$$

The function y(x) must clearly satisfy the following two conditions at the center of the star:

$$y = 1, \; y' = 0 \quad \text{for} \quad x = 0. \tag{35.13}$$

Equation (35.12), the so-called Emden equation, played a very important role in the first stage of studying stellar structure. Many papers have been devoted to the study of this equation. However, the Emden equation could be solved in explicit form for only three values of the polytropic index (n = 0, 1, 5). These solutions, for the boundary conditions (35.13), have the form

$$y = 1 - \frac{x^2}{6} \quad \text{for} \quad n = 0, \tag{35.14}$$

$$y = \frac{\sin x}{x} \quad \text{for} \quad n = 1, \tag{35.15}$$

$$y = \frac{1}{\left(1+\frac{x^2}{3}\right)^{1/2}} \quad \text{for} \quad n = 5. \tag{35.16}$$

For the boundary conditions (35.13), Eq. (35.12) was solved numerically for other values of n. Detailed tables of solutions of the Emden equation are given in the astrophysics literature (for example, in [1]).

2. Density, pressure and temperature inside a star. If a star is assumed to be a polytropic sphere with a given polytropic index n, then, using the corresponding solution of the Emden equation, one can easily find the distribution of density, pressure and temperature inside a star.

On the basis of Eqs. (35.8) and (35.10) we have /489

$$\rho(r) = u_0^n y^n(\lambda r). \tag{35.17}$$

Consequently, the constants u_0 and λ must be known to find the function $\rho(r)$. We use the conditions at the boundary of the star to determine them.

Let us denote the value of x for r = R by x_1. The quantity x_1 is found from the condition that the function y(x) becomes zero at the surface of the star, i.e., $y(x_1) = 0$. Applying the second of Eqs. (35.10) to the stellar surface, we obtain

$$x_1 = \lambda R. \tag{35.18}$$

Later we will write the equation of hydrostatic equilibrium for the boundary of the star. From Eqs. (35.1) and (35.2) it follows that

$$\left(\frac{1}{\rho}\frac{dP}{dr}\right)_{r=R} = -G\frac{M}{R^2}, \tag{35.19}$$

where M is the stellar mass. Using Eqs. (35.7), (35.8) and (35.10), instead of (35.19) we find

$$C(1+n)u_0\lambda y'(x_1) = -G\frac{M}{R^2}. \tag{35.20}$$

Substituting into (35.20) the expression for C from (35.11) and the expression for λ from (35.18), we obtain

$$u_0^n = -\frac{x_1 M}{4\pi R^3 y'(x_1)}. \tag{35.21}$$

Thus, the unknown quantities λ and u_0 are given by Eqs. (35.18) and (35.21). After their determination, as already mentioned, the density at any point of the star can be found from (35.17).

The quantity u_0^n is obviously the density at the center of the star, i.e., $\rho_c = u_0^n$. Denoting the mean stellar density by $\bar{\rho}$, we have

$$\bar{\rho} = \frac{M}{\frac{4}{3}\pi R^3}. \tag{35.22}$$

Therefore Eq. (35.21) can be rewritten in the form

$$\rho_c = -\frac{x_1}{3y'(x_1)}\bar{\rho}. \tag{35.23}$$

Values of the quantities x_1, $x_1^2 y'(x_1)$ and $\rho_c/\bar{\rho}$ for different values of the polytropic index n are given in Table 55, taken from Chandrasekhar's book [3].

TABLE 55. THE DEPENDENCE OF CERTAIN STELLAR PARAMETERS ON THE POLYTROPIC INDEX

n	0	1	2	3	4	5
x_1	2,45	3,14	4,35	6,90	15,0	
$-x_1^2 y'(x_1)$	4,90	3,14	2,41	2,02	1,80	1,73
$\rho_c/\bar{\rho}$	1,00	3,29	11,4	54,2	622	

Commas represent decimal points.

By way of an example, let us find the density at the center of the Sun with the aid of Table 55, assuming n = 3. Since the mean density of the Sun is equal to $\bar{\rho} = 1.41$ g/cm^3, then we obtain $\rho_c = 54.2\bar{\rho} = 76.5$ g/cm^3 for the density at the center. /490

The pressure inside the star can be found from Eq. (35.6), for which the quantity C, which is assumed to be constant in the star but unknown beforehand, must be determined. With the aid of Eqs. (35.11), (35.18) and (35.21) we have

$$C = \frac{4\pi G}{1+n}\frac{R^2}{x_1^2}\left[-\frac{x_1 M}{4\pi R^3 y'(x_1)}\right]^{\frac{n-1}{n}}. \tag{35.24}$$

For the pressure at the center of the star we find

$$P_c = \frac{G}{4\pi(1+n)}\left[\frac{M}{R^2 y'(x_1)}\right]^2. \tag{35.25}$$

To find the temperature within the star, the equation of state of the stellar material, interrelating the temperature, density and pressure, must be specified. We assume that the star consists of an ideal gas. In this case we have

$$P = \frac{R_*}{\mu}\rho T, \tag{35.26}$$

as the equation of state, where R_* is the gas constant and μ is the mean molecular weight.

From Eq. (35.26), with the aid of relations (35.6) and (35.8), for the temperature T we obtain

$$T = \frac{\mu}{R_*} Cu. \tag{35.27}$$

Thus, the temperature is proportional to the quantity u introduced above.

It is easy to establish that at the center of the star the temperature is equal to

$$T_c = -\frac{\mu G}{(1+n) R_* x_1 y'(x_1)} \frac{M}{R}. \tag{35.28}$$

For the Sun with n = 3, from Eq. (35.27) we find: $T_c = 2 \cdot 10^7$ degrees (if it is assumed that $\mu = 1$). Of course, this estimate of T_c, like the estimate of ρ_c made above, is extremely crude. However, as we will see later, more valid stellar models, formulated without the assumption of the polytropic relationship between pressure and density, lead to results of the same order of magnitude. /491

3. Gravitational energy of the star. A very simple formula defining the gravitational energy, can be derived for a star in the form of a polytropic sphere. Let us denote the gravitational energy of a star by E. This quantity is negative and is numerically equal to the work which must be expended to remove all the layers of the star to infinity, i.e.,

$$E = -G \int \frac{M_r}{r} dM_r, \tag{35.29}$$

where the integration extends over the entire star.

Equation (35.29) can be rewritten in the form

$$E = -\frac{G}{2} \int \frac{dM_r^2}{r} = -\frac{GM^2}{2R} - \frac{G}{2} \int M_r^2 \frac{dr}{r^2}. \tag{35.30}$$

On the basis of Eqs. (35.4) and (35.7), we obtain

$$G \int M_r^2 \frac{dr}{r^2} = -\int \frac{M_r}{\rho} dP = -\frac{Ck}{k-1} \int M_r \, d\rho^{k-1}. \tag{35.31}$$

Integrating by parts and using Eqs. (35.3) and (35.6), we find

$$G \int M_r^2 \frac{dr}{r^2} = -4\pi \frac{Ck}{k-1} \int \rho^{k} r^2 \, dr = 4\pi \frac{k}{k-1} \int P r^2 \, dr. \tag{35.32}$$

Substitution of (35.32) into (35.30) gives

$$E = -\frac{GM^2}{2R} - 2\pi \frac{k}{k-1} \int Pr^2\, dr. \tag{35.33}$$

On the other hand, Eq. (35.29) can be transformed thus:

$$E = \int \frac{r}{\rho} \frac{dP}{dr} dM_r = 4\pi \int r^3 dP = -12\pi \int Pr^2\, dr. \tag{35.34}$$

From (35.33) and (35.34) it follows that

$$E = -\frac{GM^2}{2R} + \frac{k}{6(k-1)} E, \tag{35.35}$$

from which we have

$$E = -\frac{3}{5-n} \frac{GM^2}{R}. \tag{35.36}$$

The gravitational energy of a star with polytropic index n is defined by this formula. /492

As seen from Eq. (35.36), the quantity n cannot be greater than 5. The same result is obtained in the analysis of the Emden equation.

As already indicated, the energy, equal to -E, must be expended to disperse the star into space. Conversely, this energy must be released if a nebula is compressed to the stellar condition.

At first it was assumed that stars originate from nebulae and the radiation of a star arises because of the gravitational energy released during the contraction. Then, however, it was ascertained that the gravitational energy is insufficient for this.

Let us consider the Sun as an example. Assuming n = 3, from Eq. (35.36) we find that the gravitational energy of the Sun is equal to $E = -6 \cdot 10^{48}$ ergs. The luminosity of the Sun amounts to $4 \cdot 10^{33}$ ergs/sec. Therefore the gravitational energy will allow the Sun to radiate at a constant luminosity for no more than $5 \cdot 10^7$ years. According to geological data, however, the Earth has existed for at least $2 \cdot 10^9$ years, with the solar brightness not having changed significantly during that time. Consequently, the Sun possesses much more powerful energy sources than that represented by its gravitational energy.

For some stars, however, the gravitational energy released during contraction can play a significant role in stellar evolution. White dwarfs are such stars. The masses of white dwarfs are known to be equal, in order of magnitude, to the mass of the Sun, and their radii amount to some hundredths of a solar radius. Therefore the gravitational energy of a white dwarf will be about 10^{50} ergs. The luminosity of white dwarfs, however, is about a hundred times less than the luminosity of the Sun, i.e., it is about 10^{32} ergs/sec. From a comparison of these numbers it follows that in the case of the contraction of a white dwarf an energy should be released which can assure its radiation over a very long period of time. This, of course, does not answer the question of the actual energy sources of white dwarfs.

4. Equation of energy equilibrium. One of the fundamental equations of the theory of internal stellar structure—the equation of mechanical equilibrium (35.5)—was derived above. Now we will write down the second fundamental equation of this theory—the equation of energy equilibrium of a star. It must express the condition that the amount of energy produced in any volume element of the star is equal to the amount of energy which leaves this volume element.

Let ε be the amount of energy produced by one gram of stellar matter, and L_r—the amount of energy produced within a sphere of radius r. We have /493

$$L_r = 4\pi \int_0^r \varepsilon \rho r^2 \, dr. \tag{35.37}$$

Let us denote by H_r the energy flux in a radial direction at a distance r from the center of the star. On the basis of the condition cited, we obtain

$$4\pi r^2 H_r = L_r. \tag{35.38}$$

The expression for the quantity H_r is determined by the energy transfer mechanism within a star. Investigations have shown that radiation is the basis of these mechanisms (although convection and thermal conductivity must be taken into consideration in some cases).

If it is assumed that energy within a star is transferred only by radiation, then from the radiative transfer equation we find

$$\frac{dP_R}{dr} = -\frac{\varkappa \rho}{c} H_r, \tag{35.39}$$

where P_R is the radiation pressure, $\varkappa$ is the absorption coefficient calculated for unit mass, and c is the velocity of light.

From Eq. (35.38) and (35.39) it follows that

$$\frac{dP_R}{dr} = -\frac{\varkappa\rho}{c}\frac{L_r}{4\pi r^2}. \tag{35.40}$$

Substituting (35.37) into (35.40), we have

$$\frac{1}{r^2}\frac{d}{dr}\left(\frac{r^2}{\varkappa\rho}\frac{dP_R}{dr}\right) = -\frac{\varepsilon}{c}\rho. \tag{35.41}$$

This is the desired energy equilibrium equation of a star.

In deriving the mechanical equilibrium equation we designated the gas pressure by P. Below, P will denote the sum of the gas and radiation pressures. In other words, we will assume

$$P = P_G + P_R, \tag{35.42}$$

where

$$P_G = \frac{R_*}{\mu}\rho T \tag{35.43}$$

and

$$P_R = \frac{1}{3}aT^4. \tag{35.44}$$

If the expressions that have been presented for the pressures are substituted into Eqs. (35.5) and (35.41), then we obtain a system of two equations for determining two unknown functions of r: the density ρ and temperature T. The quantities ε, $\varkappa$ and μ entering into these equations should be considered unknown functions of ρ and T. /494

5. Standard stellar model. Before the discovery of nuclear reactions as the source of stellar energy, the quantity ε was not known. Therefore, in the theory of the internal stellar structure, different assumptions had to be made with respect to this quantity, so that different stellar models were obtained. The model, proposed by Eddington, played an important role in the theory. It is usually called the standard stellar model.

Let us take Eqs. (35.4) and (35.40) as the mechanical and energy equilibrium equations of a star. Dividing the second of these equations into the first, we obtain

$$\frac{dP_R}{dP} = \frac{\varkappa L_r}{4\pi c G M_r}. \tag{35.45}$$

Let us introduce the definition

$$\frac{L_r}{M_r} = \eta \frac{L}{M}. \tag{35.46}$$

Substituting (35.46) into (35.45), we have

$$\frac{dP_R}{dP} = \frac{\varkappa\eta}{4\pi cG} \frac{L}{M}. \tag{35.47}$$

Eddington made the assumption that within a star

$$\varkappa\eta = \text{const.} \tag{35.48}$$

Under this assumption the entire right side of Eq. (35.47) will be a constant. Therefore, after defining

$$\frac{\varkappa\eta}{4\pi cG} \frac{L}{M} = 1 - \beta, \tag{35.49}$$

from (35.47) we find

$$P_R = (1 - \beta)P, \tag{35.50}$$

and this means

$$P_G = \beta P. \tag{35.51}$$

We see that when the assumption (35.48) is satisfied, the ratio of the gas pressure to the radiation pressure does not vary in the star.

From Eqs. (35.43), (35.44), (35.50) and (35.51) it follows that

$$(1 - \beta)P = \frac{1}{3} aT^4, \qquad \beta P = \frac{R_*}{\mu} \rho T. \tag{35.52}$$

Eliminating T from these relations, we obtain

$$P = C\rho^{4/3}, \tag{35.53}$$

where /495

$$C = \left[\frac{3(1 - \beta)R_*^4}{a\beta^4\mu^4} \right]^{1/3}. \tag{35.54}$$

If it is assumed that the average molecular weight μ is constant in the star, then the quantity C will also be a constant. Therefore Eq. (35.53) will represent

a polytropic relationship between P and ρ for k = 4/3. In other words, the standard stellar model proves to be a polytropic sphere with n = 3. Consequently, the distribution of density, pressure and temperature in the standard model is given by the formulas that have been presented above, based on the solution of the Emden equation. In particular, the estimates of the density and temperature at the center of the Sun for n = 3, that were made above, correspond to the standard model.

Earlier, the constant C was defined for a polytropic sphere by Eq. (35.24) as a function of M, R and n. Now, using this formula, we can find the quantity β within a star. Equating the expressions for C, given by Eq. (35.24) for n = 3 and by Eq. (35.54), we find that the quantity β is defined by the equation

$$1 - \beta = C_1 \mu^4 M^2 \beta^4, \tag{35.55}$$

where

$$C_1 = \frac{\pi G^3 a}{48 R_*^4 [x_1^2 y'(x_1)]^2}. \tag{35.56}$$

From Eq. (35.55) it is seen that the light pressure fraction $(1 - \beta)$ increases along with the mass of the star ($\beta = 1$ when M = 0, and $\beta = 0$ when M = ∞).

The results of calculations of some characteristics for three stars, derived under the assumption that the stellar structure is that of the standard model, are listed in Table 56, taken from Chandrasekhar [3]. In the calculations it was assumed that $\mu = 1$.

TABLE 56. CHARACTERISTICS OF STARS ACCORDING TO THE "STANDARD MODEL"

Star	$\frac{M}{M_\odot}$	$\frac{R}{R_\odot}$	$\frac{L}{L_\odot}$	$1-\beta$	ρ_c	T_c
Sun	1,00	1,00	1,00	0,003	76,5	$20 \cdot 10^6$
Sirius A	2,34	1,78	38,9	0,016	31,7	$26 \cdot 10^6$
Capella A	4,18	15,9	120	0,045	0,080	$5 \cdot 10^6$

Commas represent decimal points.

Eddington, based on the stellar model itself, concluded that a relationship existed between the masses and luminosities of stars. His reasoning (in a somewhat altered form) was as follows. Let us consider Eqs. (35.49) and (35.55). Eliminating the quantity β from them, we arrive at a relationship between the quantities, M, L, $\varkappa\eta$ and μ. We will assume that the quantities $\varkappa\eta$ and μ are the same for all stars. Then the relationship between M and L is obtained. In this situation, for small M (i.e., for values of β close to 1) Eqs. (35.49) and (35.55) give

$$L \sim M^3, \tag{35.57}$$

and for large M (i.e., for small β values) from (35.49) it follows that

$$L \sim M. \tag{35.58}$$

Eddington compared his theoretical conclusions with observational data on stellar masses and luminosities and obtained agreement between them. It is, of course, impossible to consider this agreement as confirmation of the theory being considered since a number of unjustified assumptions were made during its development (the principal one of which is the assumption that $\varkappa\eta$ is a constant inside a star). Of interest, however, is the fact that in these investigations Eddington was the first to obtain a relationship between stellar masses and luminosities from observational data. This dependence is one of the fundamental relationships of stellar astronomy. /496

36. Physical Processes Inside Stars

1. Equation of state of stellar matter. In the previous section the physical conditions in stellar interiors were explained in their general aspects (i.e., values of density, temperature and pressure were estimated). Now let us return to a consideration of the physical processes occurring under these conditions. This will allow us, in particular, to derive expressions for these parameters which enter into the fundamental equations of the theory of internal stellar structure.

From the results that have been presented above, it follows that a considerable temperature increase occurs with depth into the star. The intense ionization of atoms inside the star is caused by this. As is known (see Section 13), the ratio of the number of ionized atoms n^+ to the number of neutral atoms n_1 is given by the following formula:

$$n_e \frac{n^+}{n_1} = \frac{g^+}{g_1} \cdot \frac{2(2\pi mkT)^{3/2}}{h^3} e^{-\frac{\chi_1}{kT}}, \tag{36.1}$$

where χ_1 is the ionization energy from the ground state. The ratio of the number of s-times ionized atoms to the number of (s - 1)-times ionized atoms is defined by a similar formula. From Eq. (36.1) it is seen that the degree of ionization is an intrinsic function of the ratio χ_1/kT and, roughly speaking, atoms jump into the subsequent stage of ionization when this ratio becomes of the order of unity. /497 Therefore light atoms, having low ionization potentials (in particular, hydrogen and helium), are already completely ionized in the surface layers of the star. And, as one goes deeper into the star, more and more electrons are removed from heavy atoms.

Thus, the gas within a star (which represents a high-temperature plasma) consists of a large number of free electrons, "bare" nuclei of light atoms and heavy atoms stripped of an appreciable portion of their electronic shells. Such a gas composition inside the star should be taken into consideration in writing down the equation of state of the gas and, in particular, in determining its mean molecular weight.

In the discussion of stellar atmospheres, we took the equation of state of a standard ideal gas as the equation of state of the material. One can assume that the state of the gas does not change as one goes deeper into the star (with the exception of special cases which will be discussed below). Therefore we will write the equation of state of the gas inside a star in the form

$$P = nkT, \tag{36.2}$$

where n is the number of particles in 1 cm^3. Converting, here, from the concentration n to the density ρ with the aid of the relation

$$n = \frac{\rho}{\mu m_H}, \tag{36.3}$$

where μ is the average molecular weight and m_H is the mass of a hydrogen atom, instead of (36.2) we obtain

$$P = \frac{k}{\mu m_H} \rho T, \tag{36.4}$$

i.e., an equation that is identical to the previously used Eq. (35.26) (since $R_* = k/m_H$).

The quantity μ, entering into the equation of state (36.4), has an importa... significance for the internal stellar structure theory. Let us find this quantity, using Eq. (36.3) and bearing in mind that the density ρ is determined primarily by atoms, and the concentration n—both by atoms and by free electrons. As a first approximation all atoms inside the star will be assumed to be completely ionized.

We will first assume that the star is composed of one element with atomic number Z and atomic weight A (as compared to the weight of a hydrogen atom). Since for total ionization there must be Z free electrons for each atom, then we have

$$n = \frac{\rho}{A m_H} (1 + Z). \tag{36.5}$$

Therefore for the quantity μ we obtain /498

$$\mu = \frac{A}{1 + Z}. \tag{36.6}$$

For hydrogen Eq. (36.6) gives $\mu = 1/2$, for helium $\mu = 4/3$, for other elements $\mu \approx 2$. Thus, the average molecular weight inside a star lies within relatively narrow limits. However, even small differences in the quantity μ are extremely significant. This is explained by the fact that the temperature is proportional to μ, and the amount of energy, released during nuclear reactions, depends very heavily on the temperature.

In reality a star is composed of a mixture of different elements. To derive a formula for μ in this case, let us denote by x_Z the weight fraction of an element with atomic number Z (i.e., we will assume that in a gram of stellar matter, x_Z grams must be atoms of the given element). For the quantity n we now find

$$n = \sum \frac{x_Z \rho}{A m_H} (1 + Z), \tag{36.7}$$

where the summation is done over all elements. Substitution of (36.7) into (36.3) yields

$$\mu = \frac{1}{\sum \frac{x_Z}{A} (1 + Z)}. \tag{36.8}$$

Let X be the weight fraction of hydrogen, Y—the weight fraction of helium and (1-X-Y)—the weight fraction of the other elements. Then instead of (36.8) we obtain

$$\mu = \frac{1}{2X + \frac{3}{4} Y + \frac{1}{2}(1 - X - Y)}, \tag{36.9}$$

or

$$\mu = \frac{4}{6X + Y + 2}. \tag{36.10}$$

As already indicated, Eq. (36.10) is valid only for complete ionization of the atoms at a given point of the star. If the ionization cannot be considered complete, then the number of electrons stripped from the atom must be written in (36.8) instead of Z. This number can be determined with the aid of the ionization formula (36.1).

2. Gas degeneracy. As one goes deeper into a star the density also increases along with the temperature. The density increase is especially great in stars with a high gravitational acceleration force at the surface (in particular, in /499 white dwarfs). In these cases, regions in which the gas is degenerate, i.e., not subject to the laws resulting from classical statistics, can exist inside stars. Therefore together with the equation of state (36.4) we must also have the equation of state of a degenerate gas.

Let us consider a gas comprising free electrons. Such a gas is known to be subject to Fermi-Dirac statistics, valid for particles possessing two properties: 1) the particles are indistinguishable, 2) no more than two particles can be present in each cell of phase space. According to these statistics the number of

free electrons with momentums from p to p + dp is given by the formula

$$dn_e = \frac{8\pi p^2 dp}{h^3} \frac{1}{De^{\frac{p^2}{2mkT}} + 1}, \tag{36.11}$$

in which the quantity D is determined from the condition that the total number of free electrons in a unit volume is given, i.e.,

$$n_e = \frac{8\pi}{h^3} \int_0^\infty \frac{p^2 dp}{De^{\frac{p^2}{2mkT}} + 1}. \tag{36.12}$$

In order to derive the equation of state of the electron gas, an expression for the pressure must be written down. If the particle velocities are small compared to the velocity of light, then we have

$$P_e = \frac{2}{3} \int \frac{p^2}{2m} dn_e, \tag{36.13}$$

or, on the basis of (36.11),

$$P_e = \frac{8\pi}{3mh^3} \int_0^\infty \frac{p^4 dp}{De^{\frac{p^2}{2mkT}} + 1}. \tag{36.14}$$

By elimanating the quantity D, from Eqs. (36.12) and (36.14) one can obtain a relationship between P_e, n_e and T, i.e., the desired equation of state of the gas.

Let us first assume that $D \gg 1$. Then from Eqs. (36.12) and (36.14) we obtain

$$n_e = \frac{2(2\pi mkT)^{3/2}}{h^3 D} \left(1 - \frac{1}{2^{3/2} D} + \ldots\right), \tag{36.15}$$

$$P_e = \frac{2(2\pi mkT)^{3/2}}{h^3 D} kT \left(1 - \frac{1}{2^{3/2} D} + \ldots\right). \tag{36.16}$$

From this it follows, approximately, that /500

$$P_e = n_e kT \left(1 + \frac{1}{2^{3/2} D} + \ldots\right) \tag{36.17}$$

and

$$D = \frac{2(2\pi mkT)^{3/2}}{h^3 n_e}. \tag{36.18}$$

We see that the equation of state (36.17) differs little from the equation of state of the standard ideal gas. Consequently, in the case being considered the gas is slightly degenerate. If the quantity D is very large, then degeneracy can be ignored. This corresponds to neglecting the ones in the denominator of Eq. (36.11) and represents a changeover from quantum statistics to classical.

With the aid of Eq. (36.18) for the quantity D we find that the condition of gas degeneracy (or, more precisely, of weak degeneracy) is the satisfaction of the inequality

$$\frac{2(2\pi mkT)^{3/2}}{h^3 n_e} \gg 1. \tag{36.19}$$

If, however, the reverse inequality is satisfied, then the gas will be highly degenerate. The degeneracy will be greater, the lower the temperature and the higher the density.

The equation of state of a highly degenerate electron gas can also be derived from Eqs. (36.12) and (36.14). Let us assume that T = 0. In this case according to classical statistics all particles are in the phase space element with momentum p = 0 and, consequently, the gas pressure is zero. In reality, however, electrons are subject to the Pauli principle, which forbids the presence of more than two particles in each element. Therefore when T = 0 the electrons occupy all elements with momentums from p = 0 to some p_{max}, and the gas pressure is nonzero.

In the given case, instead of (36.11) we have

$$dn_e = \frac{8\pi p^2 dp}{h^3} \tag{36.20}$$

and from Eqs. (36.12) and (36.14) we find

$$n_e = \frac{8\pi}{h^3}\int_0^{p_{max}} p^2 dp = \frac{8\pi}{3h^3} p_{max}^3, \tag{36.21}$$

$$P_e = \frac{8\pi}{3mh^3}\int_0^{p_{max}} p^4 dp = \frac{8\pi}{15mh^3} p_{max}^5. \tag{36.22}$$

Substitution of p_{max} from (36.21) into (36.22) gives /501

$$P_e = \frac{1}{20}\left(\frac{3}{\pi}\right)^{2/3} \frac{h^2}{m} n_e^{5/3}. \tag{36.23}$$

We have derived the equation of state of a completely degenerate electron gas. If the temperature is not equal to zero, then a corrective term, depending on n_e and T, must be added to the right side of this equation; however, it is small in the case of high degeneracy.

In the derivation of Eq. (36.23), Eq. (36.13), which is valid only for particle velocities that are small compared with the velocity of light, was used. This means that Eq. (36.23) applies to a nonrelativistic gas. However, the velocities of free electrons inside a star can be close to the velocity of light. Therefore we must derive an equation of state for the electron gas which would apply for this case.

If the particles can have velocities close to the velocity of light, then instead of Eq. (36.13) we must write

$$P_e = \frac{1}{3m} \int \frac{p^2}{\sqrt{1 + \frac{p^2}{m^2c^2}}} dn_e. \tag{36.24}$$

Substituting Eq. (36.20) here, we obtain

$$P_e = \frac{8\pi}{3mh^3} \int_0^{p_{max}} \frac{p^4}{\sqrt{1 + \frac{p^2}{m^2c^2}}} dp, \tag{36.25}$$

or, after integration,

$$P_e = \frac{\pi m^4 c^5}{3h^3} [x(2x^2 - 3)\sqrt{1 + x^2} + 3\operatorname{arcsh} x], \tag{36.26}$$

where $x = p_{max}/mc$.

We can now rewrite Eq. (36.21) in the form

$$n_e = \frac{8\pi m^3 c^3}{3h^3} x^3. \tag{36.27}$$

Equations (36.26) and (36.27) are the equation of state of a completely degenerate electron gas in parametric form. This equation is valid for an electron velocities.

If $x \ll 1$, then the previously derived Eq. (36.23) for a nonrelativistic gas results from Eqs. (36.26) and (36.27). If, however, $x \gg 1$, then from these /502

relations it follows that

$$P_e = \frac{1}{8}\left(\frac{3}{\pi}\right)^{1/3} ch\, n_e^{4/3}. \tag{36.28}$$

This is the equation of state of a relativistic completely degenerate electron gas.

3. Energy transfer inside a star. It has already been noted above that radiation plays the principal role in energy transfer inside a star. Therefore it is necessary to ascertain through what processes the absorption of radiant energy occurs inside a star. Just as in photospheres, the following processes are the basic ones: 1) the transitions of electrons from bound states to free, i.e., the photoionization of atoms; 2) the transitions of electrons from free states to free; 3) the scattering of radiation by free electrons.

Because of the very high temperatures inside a star, light atoms (in particular, hydrogen and helium) are completely ionized. Therefore the absorption of the radiation, associated with the photoionization of atoms, can be caused by heavy atoms only. Since the heavy atoms are also stripped of an appreciable portion of their electrons, they can be considered to be approximately hydrogen-like. The absorption coefficient, caused by the photoionization of hydrogen atoms, is given by Eq. (5.8) of Chapter I. The absorption coefficient, caused by the photoionization of hydrogen-like atoms, is written in a similar fashion:

$$\alpha_\nu' = n_e n^+ \frac{2^4 \pi e^6}{3\sqrt{3}\, ch\, m} \frac{Z_1^2}{(2\pi mkT)^{1/2}} \frac{\chi_1}{kT} \frac{1}{\nu^3} \sum_{i=i_0}^{\infty} \frac{g_{i\nu}}{i^3} e^{-\frac{\chi_i}{kT}}, \tag{36.29}$$

where Z_1 is the effective charge of the ion.

Free-free electron transitions occur primarily in the field of the hydrogen and helium nuclei. The absorption coefficient, caused by these transitions, is equal to

$$\alpha_\nu'' = n_e n^+ \frac{2^3 \pi e^6 Z_1^2}{3\sqrt{3}\, ch\, m (2\pi mkT)^{1/2}} \frac{g_\nu}{\nu^3}. \tag{36.30}$$

For $Z_1 = 1$, i.e., for hydrogen, Eq. (5.10) of Chapter I is obtained from this formula.

The scattering coefficient by free electrons, as is known, is given by the formula

$$\sigma_e = n_e \sigma_0 = n_e \frac{8\pi}{3}\left(\frac{e^2}{mc^2}\right)^2. \tag{36.31}$$

The mean absorption $\varkappa$, calculated per unit mass, enters into Eq. (35.41), expressing the energy equilibrium of a star. Therefore the expressions that have

been presented above for the volume absorption coefficients must be averaged over the frequency and the relationship $\bar{\alpha} = \varkappa\rho$ must be used. /503

The average absorption coefficient for hydrogen atoms has already been determined in Chapter I and is given by Eq. (5.34). This formula is also applicable to hydrogen-like atoms. Based on it, the following expression can be derived for the absorption coefficients caused by photoionizations and free-free transitions, respectively:

$$\varkappa' = 2{,}4\frac{\chi_1}{kT}\frac{n_e n^+}{\rho}\frac{80e^6h^2Z_1^2}{\pi^2\sqrt{3}\,c\,(2\pi m)^{3/2}}\frac{\bar{g}}{(kT)^{7/2}} \tag{36.32}$$

and

$$\varkappa'' = \frac{n_e n^+}{\rho}\frac{80e^6h^2Z_1^2}{\pi^2\sqrt{3}\,c\,(2\pi m)^{3/2}}\frac{\bar{g}}{(kT)^{7/2}}. \tag{36.33}$$

Here, the average value of the Gaunt factor is denoted by $\bar{g}$.

The quantities n_e and n^+, entering into Eqs. (36.32) and (36.33), depend on the density and chemical composition. Just as before, let X be the weight fraction of hydrogen and Y—the weight fraction of helium. The number of free electrons in 1 cm^3, originating through the ionization of hydrogen and helium, is equal to $X\rho/m_H$ and $Y\rho/2m_H$, respectively. One can assume that the ionization of the heavy elements gives $1/2A(1-X-Y)\rho/Am_H$ free electrons in 1 cm^3. Therefore the total density of free electrons will be equal to

$$n_e = \frac{1}{2}(1+X)\frac{\rho}{m_H}. \tag{36.34}$$

The quantity n^+, entering into Eq. (36.32), is the concentration of atoms of a given element in the ionization state beyond that in which the absorbing atoms exist. It is clear that at each point of the star absorption is caused primarily by atoms in one specific ionization state. As already mentioned, for this ionization state the quantity χ_1/kT must be of the order of unity. The quantity n^+ can be assumed to be approximately equal to the density of all atoms of the element being considered, i.e., equal to the weight fraction of this element, multiplied by ρ/Am_H. Summing the quantities $n^+Z_1^2$ for all the heavy atoms and assuming some average value for Z_1^2/A, we obtain the quantity $(1-X-Y)\rho Z_1^2/$ $/m_HA$. This analysis, of course, is quite crude.

The quantity n^+, entering into Eq. (36.33), is the density of ionized hydrogen or helium atoms. For hydrogen the quantity $n^+Z_1^2$ is equal to $X\rho/m_H$, and for helium $Y\rho/m_H$. The sum of these quantities is equal to $(X+Y)\rho/m_H$. /504

Taking into consideration what has been said, instead of Eqs. (36.32) and (36.33) we obtain

$$\varkappa' = C'g(1+X)(1-X-Y)\frac{\rho}{T^{7/2}} \tag{36.35}$$

and

$$\varkappa'' = C''g(1+X)(X+Y)\frac{\rho}{T^{7/2}}, \tag{36.36}$$

where C' and C'' are some constants.

Equations (36.35) and (36.36) are obtained by averaging the absorption coefficients over the frequency with a weighting function representing the Planckian intensity. Usually, however, the average absorption coefficient is found from Rosseland's formula. In this case, nevertheless, formulas similar to Eqs. (36.35) and (36.36) are obtained. Some difference between them is involved with the numerical coefficients only. For example, the following expressions are presented in M. Schwarzschild's book [4] for Rosseland's averages:

$$\varkappa' = 4.3\cdot 10^{25}\frac{g}{t}(1+X)(1-X-Y)\frac{\rho}{T^{7/2}}, \tag{36.37}$$

$$\varkappa'' = 3.7\cdot 10^{22}g(1+X)(X+Y)\frac{\rho}{T^{7/2}}. \tag{36.38}$$

Here t is the guillotine factor (of the order of unity).

The scattering coefficient by free electrons, defined by Eq. (36.31), is independent of the frequency. Assuming $\sigma_e = \varkappa_e\rho$ and using Eq. (36.34), we obtain

$$\varkappa_e = \frac{\sigma_0}{2m_H}(1+X) = 0.2(1+X). \tag{36.39}$$

The average absorption coefficients as a function of chemical composition, density and temperature are defined by Eqs. (36.37)-(36.39). From these formulas one can conclude that photoionization plays the biggest role in the absorption of radiant energy inside stars. Free-free transitions provide an appreciable contribution to absorption only when the relative amounts of hydrogen and helium /505 are large. Light scattering by free electrons has significance at low densities and high temperatures.

Besides radiation, thermal conductivity plays some role in the energy transfer inside stars. The amount of thermal energy inside a star even exceeds the amount of radiative energy. Radiation, nevertheless, plays a greater role than thermal conductivity since the velocity and mean free path length of photons is much greater than for electrons. Thermal energy is converted into radiant and

vice versa at each point of the star (through the absorption and emission of photons) and energy transfer occurs primarily when it is in the form of radiant energy. In some cases, however, the transfer of energy by electronic thermal conductivity must be taken into consideration. The relative role of electronic thermal conductivity increases with an increase in density. This role is especially large in the case of white dwarfs because of the degeneracy of the electron gas in them. This is explained by the fact that in a degenerate gas all the lower states are filled and the mean free path of an electron is very long.

When we studied the solar photosphere, one other energy transfer mechaism—convection—was considered (in Section 15). Convective energy transfer can play a significant role in the surface layers of stars. The use of the criterion (15.10) of Chapter III has shown that in some regions inside a star the radiative equilibrium can be unstable and convection should appear. If the power of the energy sources increases considerably with approach to the center of the star, then a convective nucleus must exist in the star. In this case Eq. (35.41), expressing the energy equilibrium condition of the star, must be altered in an appropriate manner.

4. Nuclear reactions as a source of stellar energy. In searches for stellar energy sources the idea was expressed some time ago that large amounts of energy can be released in the course of nuclear reactions. We will assume that in some reaction a nucleus is formed whose mass is ΔM less than the sum of the masses of the nuclei entering into the reaction. Then on the basis of Einstein's principle of the equivalence of mass and energy, the energy

$$\Delta E = c^2 \Delta M, \tag{36.40}$$

is released during such a reaction, where c is the velocity of light.

Nuclear reactions, transforming hydrogen into helium, play the major role in the release of energy inside stars. As is known, the atomic weight of hydrogen is 1.008, and the atomic weight of helium is 4.003 (in oxygen units). Therefore an energy corresponding to approximately 0.7% of the mass is released in the formation of one helium atom from four hydrogen atoms. Consequently, a star, composed initially of hydrogen, must release an energy equal to /506

$$\Delta E \approx 6 \cdot 10^{18} M, \tag{36.41}$$

where M is the stellar mass, when the hydrogen is converted into helium. In particular, for the Sun we obtain $\Delta E \approx 10^{52}$ ergs. This energy can provide for the solar radiation for 10^{11} years at its present brightness, i.e., for a sufficient time from the point of view of current concepts of the lifetimes of stars in the Galaxy.

The conversion of hydrogen into helium inside stars occurs by means of two reaction cycles: proton-proton and carbon.

The proton-proton cycle consists of three reactions:

$$
\begin{aligned}
&1)\ H^1 + H^1 \rightarrow H^2 + e^+ + \nu,\\
&2)\ H^1 + H^2 \rightarrow He^3 + \gamma,\\
&3)\ He^3 + He^3 \rightarrow He^4 + H^1 + H^1.
\end{aligned}
$$

We see that at first a deuteron (the nucleus of heavy hydrogen), a positron and a neutrino are formed when two protons meet. The positron, however, immdeiately combines with any electron and they disappear, emitting two γ rays. The neutrino escapes from the star unhindered, carrying away some portion of the energy being released. Then the deuteron that has been formed combines with some proton, forming the He^3 nucleus and emitting a γ ray. Finally, upon the collision of two He^3 particles the helium He^4 nucleus is formed (an α particle) and two protons. It should be noted that the last reaction of this cycle can occur by other means which we are not going to mention here.

The carbon cycle (also called the "Bethe cycle") is more complex. It consists of six reactions:

$$
\begin{aligned}
&1)\ C^{12} + H^1 \rightarrow N^{13} + \gamma,\\
&2)\ N^{13} \rightarrow C^{13} + e^+ + \nu,\\
&3)\ C^{13} + H^1 \rightarrow N^{14} + \gamma,\\
&4)\ N^{14} + H \rightarrow O^{15} + \gamma,\\
&5)\ O^{15} \rightarrow N^{15} + e^+ + \nu,\\
&6)\ N^{15} + H^1 \rightarrow C^{12} + He^4.
\end{aligned}
$$

In this cycle carbon emerges as the catalyst.

The amount of energy released in the formation of one helium nucleus in the first of these cycles amounts to $4.2 \cdot 10^{-5}$ erg, and in the second—$4.0 \cdot 10^{-5}$ erg. The difference between these numbers is explained by the fact that the energy /50
carried away by the neutrino is greater in the second cycle than in the first.

To determine the amount of energy generated by one gram of material in one second (this quantity was denoted by ε above), it is necessary to know the effective cross sections for the reactions being considered. These cross sections have been determined theoretically and experimentally (see, for example, [4] and [5]). Finally, it was established that for the proton-proton cycle

$$\varepsilon = 2.5 \cdot 10^6 \rho X^2 \left(\frac{10^6}{T}\right)^{2/3} e^{-33.8\left(\frac{10^6}{T}\right)^{1/3}}, \tag{36.42}$$

and for the carbon cycle

$$\varepsilon = 9.5 \cdot 10^{28} \rho X X_{CN} \left(\frac{10^6}{T}\right)^{2/3} e^{-152.3\left(\frac{10^6}{T}\right)^{1/3}}. \tag{36.43}$$

Here ρ is the density of the matter, T is the temperature, X is the hydrogen weight fraction, X_{CN} is the carbon and nitrogen weight fraction.

From the formulas that have been presented it is seen that the quantity ε for the carbon cycle increases more rapidly with temperature than for the proton-proton reaction. At temperatures of about 15-20 million degrees both formulas for ε yield approximately the same results. At lower temperatures the proton-proton reaction plays the major role in the release of energy, at the higher temperatures—the carbon cycle.

Besides the nuclear reactions considered above, whereby hydrogen is converted into helium, other reactions can also occur inside stars. At temperatures of the order of 10^8 degrees reactions that convert helium into heavier elements are most important.

Nuclear reactions are the obvious and, probably, the chief source of stellar energy. This, however, does not exclude the fact that other energy sources can exist in stars.

37. Structure and Evolution of Stars

1. Basic equations. The basic equations of the theory of internal stellar structure—Eqs. (35.5) and (35.41)—were written down in Section 35. The first of these expresses the mechanical equilibrium condition for a star, the second—the energy equilibrium condition. Further, it was explained how the parameters entering into these equations depend on the physical conditions inside the star. This makes it possible to obtain solutions to these equations without any of the additional assumptions characteristic of the first stage of the structure theory.

The basic equations of the internal stellar structure theory can be written in the form of the following system of equations: /508

$$\frac{dP}{dr} = -\frac{GM_r}{r^2}\rho, \tag{37.1}$$

$$\frac{dM_r}{dr} = 4\pi r^2\rho, \tag{37.2}$$

$$\frac{dT}{dr} = -\frac{3}{4ac}\frac{\varkappa\rho}{T^3}\frac{L_r}{4\pi r^2}, \tag{37.3}$$

$$\frac{dL_r}{dr} = 4\pi r^2\varepsilon\rho. \tag{37.4}$$

The substitution of (37.2) into (37.1) obviously gives Eq. (35.5), and the substitution of (37.4) into (37.3)—Eq. (35.41).

The pressure P entering into Eq. (37.1) is the sum of the gas and radiation pressures. The pressure P is expressed in terms of the temperature T, density ρ and average molecular weight μ by means of the equation of state of the gas and the Stefan-Boltzmann law. In turn, the quantity μ is determined by the specification of the chemical composition. It is expressed in terms of the hydrogen weight fraction X and helium weight fraction Y by Eq. (36.10).

The average absorption coefficient $\varkappa$ and the amount of energy ε produced are also expressed in terms of ρ, T, X and Y. The corresponding formulas were given in the previous section.

Thus, the system of four equations (37.1)-(37.4), presented above, serve to define the four unknown functions: M_r, L_r, ρ and T. The quantities X and Y, entering into this system, are assumed to be given.

Boundary conditions must still be added to this system of equations. At the center of the star we obviously have

$$M_r = 0, \; L_r = 0 \quad \text{for} \quad r = 0, \tag{37.5}$$

and at the boundary of the star

$$\rho = 0, \quad T = 0 \quad \text{for} \quad r = R. \tag{37.6}$$

It must, however, be kept in mind that some formulas, valid for the inner layers of the star (in particular, expressions for $\varkappa$ and μ), are not applicable to the surface layers. This is explained by the fact that in the derivation of these formulas intense gas ionization was assumed, whereas the degree of ionization is low in the surface layers. Therefore the use of the equations presented above, together with the boundary conditions (37.6), throughout the entire star can lead to unreliable results. A more correct way to solve the problem consists of determining the structure of the surface layers on the basis of photosphere theory /509
and of solving the equations presented for the "boundary conditions" resulting from data on photosphere structure.

The system of equations (37.1)—(37.4) completely defines the stellar structure for these boundary conditions and for specified values of X and Y. Values of the quantities M_r and L_r for r = R, i.e., the stellar mass M and luminosity L, are also found as a result of the solution of this system. In reality, the values of M and L are specified for each star. Therefore the problem of determining the stellar structure consists not only of solving this system of equations, but also in selecting suitable values of X and Y.

Large differences in chemical composition and, in turn, in the values of X and Y can, however, exist inside a star. Because of this the problem of determining the stellar structure is not defined. From a physical point of view the difference in chemical composition is caused by a change in the rate of the nuclear reactions from one point of the star to another: this rate is higher, the larger ρ and T. Therefore, inside stars, regions can exist in which the hydrogen

is completely or partially "burned out". Such considerations are taken into account in constructing theoretical models of stars. Consequently, the theory of internal stellar structure is closely associated with the problem of the evolution of stars.

It should be noted that before the discovery of the nuclear reactions occurring in stars the fundamental equations of internal stellar structure theory were solved for various assumptions with respect to the quantity ε (for a uniform distribution of energy sources, for a point source at the center, etc.). Certain general theorems were demonstrated in this work, concerning the equilibrium configurations of stars (see [3]). Questions of the stability of stellar configurations have also been considered in a number of papers. These questions were studied especially thoroughly by A. B. Severnyy [6].

2. Structure of main sequence stars. The vast complexity of the fundamental equations of internal stellar structure theory requires that they be solved by numerical methods. The equations are integrated either from the center of the star or from the surface. Sometimes the integration is done both from the center and from the surface, and then the solutions obtained are joined together. Electronic computers are now widely used for solving these equations.

We will not describe here the various means that have been selected for simplifying the computations. A description of these methods can be found in M. Schwarzschild's book [4]. We will only present some of the results taken from this book.

The results of a stellar model calculation of the upper portion of the main sequence are given in Table 57. In the calculations it was assumed that the chemical composition does not change inside the star. The same relative amounts of /510
hydrogen and helium (X = 0.90, Y = 0.09) were also assumed for all stars. Calculations were made for stars with masses equal to 10, 5 and 2.5 solar masses. The luminosity L, radius R and effective temperature T_e were determined for each star, as well as the density ρ_c and temperature T_c at the center.

TABLE 57. CHARACTERISTICS OF STARS OF THE UPPER PORTION OF THE MAIN SEQUENCE

$\frac{M}{M_\odot}$	$\lg \frac{L}{L_\odot}$	$\lg \frac{R}{R_\odot}$	$\lg T_e$	Spectrum	T_c	ρ_c
10	3,477	0,559	4.350	B1	$2,76 \cdot 10^7$	7,80
5	2.463	0,376	4.188	B5	$2,36 \cdot 10^7$	19,5
2,5	1,327	0.202	3.991	A2	$1,98 \cdot 10^7$	48,3

Commas represent decimal points.

For a comparison of the theory with observations, the results of the calculations were plotted on mass-luminosity and spectrum-luminosity diagrams. It

was found that the points corresponding to the calculated stellar models lie very close to the average curves plotted on the basis of the observational data. This can be considered as a confirmation of the correctness of the theory.

Of the stars on the lower portion of the main sequence, the Sun has been investigated most of all. Solar models have been formulated both with a homogeneous with an inhomogeneous chemical composition. The results of a calculation with one of the models are listed in Table 58, which contains values of the fundamental physical quantities as a function of the distance r from the center of the Sun

TABLE 58. MODEL OF THE SUN IN ITS PRESENT STATE

$\frac{r}{R}$	$\frac{M_r}{M}$	$\frac{L_r}{L}$	X	$\lg P$	$\lg T$	$\lg \rho$
0	0	0	0,494	17,351	7,165	+2,128
0,1	0,073	0,396	0,611	17,135	7,102	+1,93[illegible]
0,2	0,337	0,909	0,723	16,667	6,971	+1,5[illegible]
0,3	0,626	0,994	0,744	16,072	6,823	+1,109
0,4	0,818	1,000	0,744	15,432	6,676	+0,616
0,5	0,919	1,000	0,744	14,788	6,535	+0,113
0,6	0,967	1,000	0,744	14,144	6,397	−0,393
0,7	0,988	1,000	0,744	13,489	6,256	−0,907
0,8	0,996	1,000	0,744	12,792	6,103	−1,451
0,9	0,999	1,000	0,744	11,898	5,782	−2,204
1,0	1,000	1,000	0,744	—	—	—

Commas represent decimal points.

From the table it is seen that the value of X decreases as one approaches the center of the Sun. This corresponds to the assumption made concerning the depletion of the hydrogen in the central portions of a star in the course of evolution.

The formulation of a given stellar model is associated with an indeterminacy caused by a certain arbitrariness in the choice of chemical composition. Therefore in model calculations the probable evolutionary path of the star is taken into consideration. In this it is usually assumed that the star, in its initial state, has a homogeneous chemical composition with a large hydrogen content, and then the amount of hydrogen is reduced through the nuclear reactions. In general form, the reduction in the quantity X with time can be expressed thus: /511

$$\frac{\partial X}{\partial t} = f(\rho, T, X). \tag{37.7}$$

With a decrease in the quantity X, the quantities μ, $\varkappa$ and ε also change. This leads to a change in the structure of the star. After the establishment of a model for the initial state of a star with an assumed value of X (for time t = 0), the stellar model for time t_1 can be calculated with the values of X obtained for each

point of the star from Eq. (37.7). Analogously, the stellar model can be computed for a subsequent time t_2, etc. The evolutionary sequence of stellar models is thereby determined.

In these calculations the stellar mass is considered to be constant, and the luminosity and radius are computed. The data on stars of different spectral classes, presented in Table 57, refer to the initial state of these stars. The data for the Sun (Table 58), however, characterize its present state. For the Sun both the past and the future variation of the luminosity and radius were determined. It is, of course, impossible to place complete confidence in these calculations, but they are of some interest.

The method discussed for stellar model calculations is based on the assumption that at any instant of time the star is stationary. In other words, stellar evolution is considered to be a succession of equilibrium states. This method, however, must be considered to be only approximate. In reality, the equation of stellar evolution, describing its change with time, should be considered /512
instead of equations of equilibrium for the star for any instant of time. In the stellar evolution equations all the unknown quantities are functions of the distance r from the center of the star and the time t, and these are partial differential equations.

Calculations show that mechanical equilibrium of the star is established much more rapidly than energy equilibrium. Therefore Eqs. (37.1) and (37.2), expressing the conditions of mechanical equilibrium, can be left unchanged (after, however, replacing the ordinary differentials by partial). To derive, however, the equations that replace the energy equilibrium equation, the sum

$$\varepsilon - \frac{\partial}{\partial t}\left(\frac{R_*}{\mu}T\right) - P\frac{\partial V}{\partial t},$$

must be written instead of the quantity ε in Eq. (37.4), where V is the specific volume. The second term of this sum represents the decrease in the energy, evolved by a unit mass, because of heating, and the third term is the increase due to gravitational contraction. Since $V = 1/\rho$, the last term of the sum can be written in the form $(P/\rho)\,\partial\rho/\partial t$. Therefore instead of Eq. (37.4) we have

$$\frac{1}{4\pi r^2\rho}\frac{\partial L_r}{\partial r} = \varepsilon - \frac{\partial}{\partial t}\left(\frac{R_*}{\mu}T\right) + \frac{P}{\rho^2}\frac{\partial\rho}{\partial t}. \qquad (37.8)$$

Thus, we obtain Eqs. (37.1)—(37.3) (in which d/dr is replaced by $\partial/\partial r$) as the equations of stellar evolution, as well as Eq. (37.8).

A question arises with respect to when the stellar evolution equations can be replaced by the equilibrium equations and when they cannot. It is clear that in answering this question it is quite important to determine the average time during which the energy produced within the star escapes outward. If this time is small compared with the time during which the power of the energy sources is altered noticeably, then the substitution mentioned above is possible, in the opposite case—it is not.

To determine the average time required for the energy to escape from the star, we must divide the energy, inside the star, by the amount of energy leaving the star per unit time, i.e., by the stellar luminosity. On the basis of the virial theorem, the energy inside the star (thermal and radiant) is equal in order of magnitude to the absolute value of the gravitational energy. For crude calculations we can assume the star is a polytropic sphere and use Eq. (35.36) for its gravitational energy. In this case a determination of the average time for the energy to escape from the star leads to the following results: /513

$$\begin{aligned} \text{for the Sun} \quad & \bar{t} = 2\cdot 10^7 \text{ years}, \\ \text{for a BO star} \quad & \bar{t} = 10^5 \text{ years}, \\ \text{for an AO star} \quad & \bar{t} = 10^6 \text{ years}, \\ \text{for a KO star} \quad & \bar{t} = 5\cdot 10^7 \text{ years}, \\ \text{for an MO star} \quad & \bar{t} = 2\cdot 10^8 \text{ years}. \end{aligned}$$

A detailed study of the radiation diffusion process inside a star (see [7]) also allows one to determine the average time required for the energy produced at any point of the star, i.e., $\bar{t}(r)$, to escape. In particular, the average time required for energy produced at the center of the Sun to escape is equal to $\bar{t}(0) = 6\cdot 10^7$ years.

We see that very long times are required for the energy to escape from a star. But significant changes in the power of the energy sources within a star also occur very slowly. Therefore the assumption that stellar evolution can be represented as a succession of equilibrium states is valid to some degree. If, however, a rapid change from one energy source to another occurs inside a star, then the stellar evolution equations must be used. This must be done in studying the early stages of stellar evolution. In this case the condition of mechanical equilibrium assumed above must also be discarded.

3. Structure of white dwarfs. White dwarfs, as is known, lie in the lower left corner of the spectrum-luminosity diagram, i.e., they have very low luminosities and high surface temperatures. It follows immediately from this that the white dwarfs have very small radii (of the order of hundredth of a solar radius). Some white dwarfs are in binary systems, making it possible in principle to determine their masses. The masses for three white dwarfs have been determined and were found to be close to the solar mass. On the basis of these data one can conclude that white dwarfs are exceedingly dense: their average density is about 10^6 g/cm^3 and their average concentration is about 10^{30} cm^{-3}

Such high densities for white dwarfs suggest the possibility that the gas in them is degenerate. Let us apply the inequality (36.19), the condition for a nondegenerate gas, to white dwarfs. For electrons (for $n_e \approx 10^{30}$ and $T \approx 10^7$) the left side of this inequality is about 10^{-3}, and for protons—about 10^2 (it is still greater for other atomic nuclei). Consequently, the electron gas inside white dwarfs is degenerate, and the gas of nuclei is not degenerate.

The gas pressure inside a star is a combination of the pressure of free electrons and the pressure of atomic nuclei, i.e., $P_G = P_e + P_a$. But the pressure of the degenerate electron gas is considerably greater than the pressure of the nondegenerate nuclear gas, i.e., $P_e \gg P_a$ (this is one of the intrinsic effects of degeneracy). It is also easy to show that under white dwarf conditions the gas pressure is much greater than the radiation pressure. Therefore the total pressure P inside white dwarfs can be assumed to be equal to the pressure of the degenerate electron gas. /514

We have seen above that only the pressure and density enter into the equation of state of a highly degenerate electron gas; the temperature does not enter. This means that the pressure and density distributions inside a white dwarf can be found on the basis of the equation of state and the equation of mechanical equilibrium only. The equation of energy equilibrium need not be taken into consideration. Consequently the structure of a white dwarf is determined much more simply and reliably than the structure of other stars.

Let us first take Eq. (36.23) for P, i.e., we will assume that the degenerate electron gas is nonrelativistic. The equation of state (36.23), assuming $n_e = \rho/\mu_e m_H$, can be rewritten in the form

$$P = C\rho^{5/3}, \tag{37.9}$$

where

$$C = \frac{1}{20}\left(\frac{3}{\pi}\right)^{2/3} \frac{h^2}{m(\mu_e m_H)^{5/3}}, \tag{37.10}$$

and the quantity μ_e, on the basis of (36.34), is equal to

$$\mu_e = \frac{2}{1 + X}. \tag{37.11}$$

Equation (37.9) is the polytropic relationship between P and ρ. Therefore the white dwarfs being considered are polytropic spheres for which k = 5/3 and, in turn, n = 3/2. The distribution of P and ρ inside the star in this case is found on the basis of the Emden theory discussed above.

An inherent feature of white dwarfs must, however, be noted. In the Emden theory the constant C is assumed beforehand to be unknown and only later is it expressed in terms of M, R and n by Eq. (35.24). In the white dwarf case, however, the quantity C is given by Eq. (37.10). Since these expressions for C should be equal to each other, we come to the conclusion that the mass and radius of a white dwarf are interrelated. Namely from (35.24) (for n = 3/2) and (37.10) we find

$$MR^3 = \text{const.} \tag{37.12}$$

As already mentioned, the equation of state (37.9) is valid only for electrons whose velocities are low compared with the velocity of light. This means that the results presented apply only to white dwarfs with relatively low densities (since on the basis of Eq. (36.27) the density is proportional to the cube of the maximum momentum p_{max}). A more general theory of white dwarfs has been given by Chandrasekhar (see [3]), using relations (36.26) and (36.27) as the equation of state of the degenerate electron gas. /515

We can write these relations in the form

$$P = Af(x), \quad \rho = Bx^3, \tag{37.13}$$

where

$$A = \frac{\pi m^4 c^5}{3h^3}, \quad B = \frac{8\pi\mu_e m_H m^3 c^3}{3h^3} \tag{37.14}$$

and

$$f(x) = x(2x^3-3)\sqrt{1+x^2} + 3 \operatorname{arc\,sh} x. \tag{37.15}$$

Substituting Eqs. (37.13) into the equation of mechanical equilibrium (35.5), we obtain the following equation for determining the parameter x:

$$\frac{A}{B}\frac{1}{r^2}\frac{d}{dr}\left(\frac{r^2}{x^3}\frac{df(x)}{dr}\right) = -4\pi GBx^3. \tag{37.16}$$

It is easy to establish that

$$\frac{1}{x^3}\frac{df(x)}{dr} = 8\frac{d\sqrt{x^2+1}}{dr}. \tag{37.17}$$

Therefore, setting $\sqrt{x^2+1} = y$, instead of Eq. (37.16) we have

$$\frac{1}{r^2}\frac{d}{dr}\left(r^2\frac{dy}{dr}\right) = -\frac{\pi GB^2}{2A}(y^2-1)^{3/2}. \tag{37.18}$$

Obviously, the following boundary conditions must be attached to Eq. (37.18):

$$\frac{dy}{dr} = 0 \quad \text{for } r = 0, \tag{37.19}$$

$$y = 1, \quad \frac{1}{\rho}\frac{dP}{dr} = -\frac{GM}{R^2} \quad \text{for } r = R. \tag{37.20}$$

Thus, the solution of the second order differential equation under consideration must satisfy three boundary conditions. Therefore some relationship must exist between the parameters, entering into the equation and the boundary conditions. This leads to the relationship between the mass and radius of a white dwarf. /516

Chandrasekhar obtained this relationship in the form of Table 59, containing values of the mass, radius and mean density of the star. The table has been compiled for $\mu_e = 1$. If the quantity μ_e differs from unity, then the M values must be multiplied by μ_e^{-2}, the R values by μ_e^{-1}, and the $\bar{\rho}$ values by μ_e.

TABLE 59. RELATIONSHIP BETWEEN MASS AND RADIUS FOR WHITE DWARFS

$\frac{M}{M_\odot}$	R in cm	$\bar{\rho}$ in g/cm^3	$\frac{M}{M_\odot}$	R in cm	$\bar{\rho}$ in g/cm^3
5,75	0	∞	2,95	$1,51\cdot10^9$	$4,04\cdot10^5$
5,51	$4,13\cdot10^8$	$3,70\cdot10^7$	2,45	$1,72\cdot10^9$	$2,29\cdot10^5$
5,32	$5,44\cdot10^8$	$1,57\cdot10^7$	2,02	$1,93\cdot10^9$	$1,34\cdot10^5$
4,87	$7,69\cdot10^8$	$5,08\cdot10^6$	1,62	$2,15\cdot10^9$	$7,70\cdot10^4$
4,33	$9.92\cdot10^8$	$2,10\cdot10^6$	0,88	$2,79\cdot10^9$	$1,92\cdot10^4$
3,54	$1,29\cdot10^9$	$7,90\cdot10^5$	0	∞	0

Commas represent decimal points.

The quantity y and, in turn, the quantities ρ and P were also obtained, in the form of functions of r for different M values, by solving Eq. (37.18). Thus, for each mass there is a specific radius and a specific stellar structure.

For small masses the relationship between M and R, given by Table 59, passes over to Eq. (37.12). As M increases, this relationship deviates from Eq. (37.12). The stellar mass, consisting of the degenerate gas, cannot, however, be made as large as desired. This important statement is easy to prove. When the mean density of the star increases, the equation of state of the gas passes over to Eq. (36.28), which can be written in the form

$$P = C\rho^{4/3}, \tag{36.21}$$

where

$$C = \frac{1}{8}\left(\frac{3}{\pi}\right)^{1/3}\frac{ch}{(\mu_e m_H)^{4/3}}. \tag{36.22}$$

Consequently, the white dwarf approaches, in its structure, a polytropic sphere for which n = 3. A determination of the quantity C from Eq. (35.24) shows that this quantity depends only on M, and is independent of R. After equating the expressions for C, given by Eqs. (35.24) and (37.22), we obtain a value of $5.75\mu_e^{-2}M_\odot$

for the mass. This mass value obviously corresponds to the case when $\bar{\rho} \to \infty$ and $R \to 0$.

In reality, for very high gas densities, certain effects, ignored above, begin to play a role. One of these effects is the deviation of the gravitational field from Newtonian gravitational field. The problem of the equilibrium configurations of a degenerate gas in an Einsteinian gravitational field was examined by S. A. Kaplan [8]. He obtained, as limiting values, a finite configuration radius, a finite density at the center and a mass value somewhat different from the value given above.

The most important result of the theory of white dwarfs is the relationship between masses and radii derived for them. A comparison of theory with observations is of considerable interest; however, unfortunately, observational data are very scarce. At the present time the masses of only three white dwarfs are /517 known: 0.98 $M_\odot$ for Sirius B, 0.65 $M_\odot$ for Procyon B and 0.45 $M_\odot$ for 40 Eridani B. All these stars are in binary systems, and their masses are determined on the basis of Kepler's laws. The radius of a star, as is known, is found from its absolute magnitude and surface temperature, determined from the nature of the spectrum. Unfortunately, it is difficult to find the radius of the companion of Sirius because of the marked effect produced on its spectrum by the emission from Sirius itself. The radii of the companions of Procyon and 40 Eridani B were found to be equal to 0.010 $R_\odot$ and 0.016 $R_\odot$, respectively. A comparison of the observational data with the analytical results presented in Table 59 shows that in general the theory agrees with the observations. It can even be noted that the radii of the white dwarfs being considered are greater, the smaller the mass, just as theory predicts. However, detailed comparisons are premature now because of the uncertainty of the observational data. Moreover, the quantity μ_e, which, strictly speaking, is unknown (although, as we will see below, the quantity X for white dwarfs is probably very small and, consequently, the value of μ_e is very close to 2), still enters into the theoretical relationship between M and R.

It should be mentioned again that the quantity M/R can be determined directly from observations of white dwarfs. This determination is based on measuring the red shift of the spectral lines when the radiation leaves the gravitational field of the star. The magnitude of the "red shift", as is known, is given by the formula

$$\Delta\lambda = \lambda \frac{GM}{c^2 R} \tag{37.23}$$

and, expressed in velocity, can amount to about 100 km/sec for white dwarfs. It is, of course, impossible to distinguish the "red shift" from the Doppler shift, /518 caused by the movement of the star, for single stars; but it can be done for binary stars. The determinations of the quantity M/R, made for some white dwarfs, provide additional data for checking the theory.

In the theory that has been presented for white dwarfs, it was assumed that the electron gas is degenerate throughout the entire star. In reality, the electron gas is certainly not degenerate in the surface layers of the star. However, the envelope of nondegenerate gas has a relatively small mass and it can be neglected

in the internal stellar structure theory. This is explained by the fact that the gravitational acceleration in the surface layers of a white dwarf is very high, so that the temperature and density increase rapidly with depth (on the basis of Eqs. (4.48) and (4.49) of Chapter I the temperature gradient is proportional to g and $\rho \sim T^3$. Therefore the electron gas becomes degenerate even at short distances from the surface of the star. Calculations show that degeneracy begins in layers with a temperature of the order of a few million degrees. Practically no further temperature rise occurs because of the extremely high thermal conductivity of the degenerate electron gas. Thus, a white dwarf can be considered to be composed of an isothermal degenerate core, surrounded by a thin envelope of nondegenerate gas.

Knowing the density and temperature distribution inside a white dwarf, we can calculate its luminosity. Equation (36.42), defining the amount of energy released in the proton-proton reaction (this is the reaction, as we know, that plays the primary role in energy production at not very high temperatures), must be used for this. The hydrogen weight fraction X must again be specified for calculations with this formula. We will proceed differently: we will attempt to estimate the value of X from the observed stellar luminosity. Since the quantity $\bar{\varepsilon} = L/M$ is small for white dwarfs (about 10^{-2}) and the average density $\bar{\rho}$ is very high (about 10^6), then at a temperature of about $5 \cdot 10^6$ degrees Eq. (36.42) gives a very small value for the quantity X: $X \approx 10^{-3}$. Consequently, the relative abundance of hydrogen inside white dwarfs is much lower than in other stars. If we were to take a value of the order of unity for X, the calculated luminosity of the white dwarf would be about a million times greater than the observed luminosity.

The very low abundance of hydrogen found for white dwarfs does not, of course, refer to their surface layers, in which the temperature is low and practically no nuclear reactions occur. However, with increasing depth into the star the intensity of the nuclear reactions increases and the relative hydrogen content is reduced. The amount of hydrogen within a white dwarf may be negligibly /519 small, and the nuclear reactions that provide for the luminosity of the star will occur in the deeper layers of the envelope.

Besides the emission due to the nuclear reactions, white dwarfs can also radiate because of the energy released during gravitational contraction (as was explained in Section 35). However, contraction is possible only in the case of an incompletely degenerate gas since for complete degeneracy a given stellar mass corresponds to a specific radius. Because of the very low luminosities of white dwarfs, they can emit for a long time (remaining as white dwarfs) simply because of the thermal energy they contain, i.e., by slowly cooling.

A detailed discussion of the theory of white dwarfs can be found in E. Schatzman's monograph [9].

4. Problem of stellar evolution. Closely related to the internal stellar structure theory is one of the most important problems of astronomy—the problem of stellar evolution. At the present time the solution of this problem is based on the idea that nuclear reactions play a definite role in stellar evolution.

Therefore advances in nuclear physics have been of significant value to the development of the current opinions on stellar evolution. These opinions are discussed in many books (see, for example, [4] and [5]). We will consider them here very briefly.

Most researchers assume that stars originate from diffuse matter. Initially a contraction of a cloud of diffuse matter occurs, down to the dimensions of a star, due to the effect of the inherent gravitational attraction. A star, originating in this fashion, is heated because of the conversion of gravitational energy into thermal energy. Then, as the temperature rises, nuclear reactions begin in the star, converting hydrogen into helium. At this time the star has a homogeneous chemical composition and is composed, to an appreciable degree, of hydrogen. It is on the main sequence on the spectrum-luminosity diagram.

The subsequent fate of a star depends primarily on its mass. The greater the mass, the more rapidly the nuclear reactions occur within the star. As the hydrogen is burned up, the average molecular weight increases so that the temperature increases. This leads to an increase in the luminosity of the star, and on the spectrum-luminosity diagram it departs from the main sequence to the upper right. This, according to calculations, is the course of evolution of a star with a large mass. The Sun can remain on the main sequence for about 10 million years. Stars of the late spectral classes, i.e., with small masses, could not leave the main sequence during the life of the Galaxy.

Thus, an ensemble of stars of the same age should occupy a quite definite location on the spectrum-luminosity diagram: stars of the late classes should be /520 located on the main sequence, and early class stars should be displaced to the upper right. The break in the main sequence should shift toward the late classes as the ensemble of stars grows older. This theoretical conclusion can be checked against observational data. To do this, star clusters must be used since they, apparently, consist of stars of approximately the same age. It was found that the spectrum-luminosity diagrams, plotted for clusters from the data of observations, are quite similar to the theoretical diagrams. This makes it possible to distinguish young and old star clusters and to make a general statement about the age of the clusters. The excellent agreement between the theoretical and observed spectrum-luminosity diagrams for star clusters is considered to be one of the strongest arguments in favor of the current theory of stellar evolution.

The evolutionary paths of stars, after the major mass of hydrogen in them has been burned up, are extremely complicated. When the hydrogen in the center portion of the star is almost completely burned up, this region, stripped of energy sources, starts to contract rapidly. As a result of this, dense cores, in which the electron gas is degenerate, are formed inside stars. If the mass of the star is large, then contraction leads to such high temperatures that intense reactions are initiated in the cores, converting helium into heavier elements. This process may be terminated by an explosion of the star, which is observed in the form of a supernova outburst. For stars with less mass, after the hydrogen in the central portion is burned up, the hydrogen in the outer portion is burned up. Because of the rise in the temperature of the outer layers of the star, an unstable extended atmosphere is formed. A star in such a condition can evidently lose a large amount of matter. These stars are probably observed

as the red giants. As observations show, an ejection of material from the red giants does actually occur. The gradual dispersion of the atmosphere leads to the formation of a hot star in the form of a white dwarf. After the remnants of nuclear energy have been expended, the white dwarf still emits through cooling. Thus, white dwarfs are the final stage of stellar evolution.

Many difficult problems are encountered in developing a theory for stellar evolution. One of these involves the need to ascertain whether a mixing of the material inside a star occurs. The evolutionary path of a star, described above, is based on the assumption that mixing does not occur. In the opposite case, i.e., when hydrogen is continually entering the center region from the outer layers, /521 evolution proceeds more rapidly and the path of a star on the spectrum-luminosity diagram looks different. However, the agreement between the theoretical and observed spectrum-luminosity diagrams for clusters can be considered to be a confirmation of the assumption that stellar evolution occurs without a mixing of the material.

Another important problem concerns the role of the ejection of material from a star in the stellar evolution process. As already stated, in the stage preceding the formation of a white dwarf the star apparently loses a great deal of its mass. Also expressed has been the opinion [10, 11] that stellar evolution is accompanied by a significant decrease in mass in the earlier stages also. Observations do in fact show that a very intense ejection of matter occurs from certain stars (for example, from Wolf-Rayet and Be type stars). In many respects, however, these stars are exceptional. The masses of normal stars (for example, the Sun) change relatively little during the lifetime of the star. Moreover, the theory gives no indications whatsoever about the necessity for a decrease in the mass of the star. Therefore, in the current theories of stellar evolution the masses of the stars are usually assumed to be constant.

The study of the evolution of stars that enter into close binary systems also represents considerable difficulty for the theory. The effect of the companion certainly facilitates the ejection of matter from a star. Observational data indicate this quite definitely. In some cases the presence of the companion may cause severe instability and even lead to stellar outbursts. In this regard it should be noted that many of the novae (and maybe even all of them) are members of close pairs.

There is no doubt that the current theory of stellar evolution, which considers the evolution of a star to be the result of the nuclear reactions occurring in it, has achieved great success. There is, however, another direction in cosmogony—the striving to obtain information on the origin and evolution of stars by an analysis of observational data—that is of great interest. The most prominent achievement in this area is the discovery and investigation of stellar associations by V. A. Ambartsumyan and his colleagues [12].

As is known, a stellar association is a group of stars which, in terms of a number of characteristics, can be considered to have formed relatively recently (about a million years ago). The very fact that associations exist leads to two important conclusions: 1) stars are created in groups and 2) the process of star formation is continuing even up to the present time. V. A. Ambartsumyan

predicted the expansion of associations with velocities of about 5 km/sec, which was subsequently observed. He also hypothesized the formation of stars in the form of associations from denser prestellar bodies. Associations are very unstable formations (their energy is positive). They quickly disintegrate, and the stars composed of them intermingle with other stars formed earlier. One can attempt to establish the subsequent evolution of a star by investigating the spatial and kinematic characteristics of stars, as well as other observable features of them (see [12] and [13]). /522

V. A. Ambartsumyan's assumption that stars are formed from denser prestellar bodies has not been confirmed by direct observations, i. e., such bodies have not been observed. The possibility of the existence of superdense cosmic bodies has, however, been shown theoretically [14]. For this a calculation was made of equilibrium configurations consisting of a degenerate baryon gas (i. e., a gas of protons, neutrons and hyperons). As a result, configurations were found with masses of the order of the mass of the Sun and with radii of the order of a few kilometers. As already stated, such bodies have not actually been observed; it should be stressed, however, that they cannot be observed. Even if the surface temperature of these bodies were about a million degrees, they would still emit such a small amount of energy (because of their small size) in the visible spectrum, that it would be impossible to detect them from terrestrial observatories.

The fact that in the portion of the Universe, which we have been able to observe, the evolution of matter goes primarily from denser states to less dense can be advanced as an argument in favor of the hypothesis that stars originate from a dense prestellar material. As we know, observations show that the galaxies are flying apart with tremendous velocities, stellar clusters and multiple stars are breaking up, material is being ejected from stars. This argument can certainly not be considered to be particularly convincing. Only further development of astrophysics will make it possible to ascertain the nature of the material from which stars are formed.

REFERENCES

1. Emden, R. Gas spheres, 1907.
2. Eddington, A. Internal constitution of the stars, 1926.
3. Chandrasekhar, S. An introduction to the study of stellar structure, 1939. (Russ. translation: S. Chandrasekhar, An introduction to the study of stellar structure, Izd-vo inostr. lit., 1950).
4. Schwarzschild, M. Structure and evolution of the stars, 1958. (Russ. translation: M. Schwarzschild, Structure and evolution of the stars, Izd-vo inostr. lit., 1961).
5. Frank-Kamenetskiy, D. A. The physical processes inside stars, Fizmatgiz, 1959.
6. Severnyy, A. B. The stability and pulsations of gaseous spheres and stars, Izv. Krymskoy astrofiz. obs., v. 1, pt. 2, 1948.
7. Sobolev, V. V. Theory of stellar evolution, Astron. Zh. 37, No. 3, 1960. /523
8. Kaplan, S. A. Extremely dense stars, Uchen. zap. L'vovskogo un-ta, v. XV, 1949.

9. Schatzman, E. White dwarfs, 1958.
10. Fesenkov, V. G. A statement of the cosmogony problem in modern astronomy, Astron. Zh., 26, No. 2, 1949.
11. Masevich, A. G. Stellar evolution, accompanied by corpuscular radiation, from the viewpoint of the internal stellar structure, Astron Zh., 26, No. 4, 1949.
12. Ambartsumyan, V. A. Scientific proceedings, v. II, Erevan, 1960.
13. Kukarkin, B. V. Study of the structure and development of stellar systems on the basis of the radiation of variable stars, Gostekhizdat, 1949.
14. Ambartsumyan, V. A. and G. S. Saakyan. Current status of the theory of extremely dense celectial bodies, Cosmogony problems, No. IX, Izd-vo AN SSSR, 1963.

TABLES OF FUNDAMENTAL PHYSICAL AND ASTRONOMICAL CONSTANTS

Physical Constants

Velocity of light	$c = 2,99791 \cdot 10^{10}$ cm/sec
Constant of gravitation	$G = 6,668 \cdot 10^{-8}$ dynes-cm^2/g^2
Planck's constant	$h = 6,624 \cdot 10^{-27}$ erg-sec
Electronic charge	$e = 4,802 \cdot 10^{-10}$ esu
Electron mass	$m = 9,107 \cdot 10^{-28}$ g
Mass of hydrogen atom	$m_H = 1,673 \cdot 10^{-24}$ g
Boltzmann's constant	$k = 1,380 \cdot 10^{-16}$ erg/deg
Stefan's constant	$a = 7,568 \cdot 10^{-15}$ erg/cm^3-deg
Gas constant	$R = 8,314 \cdot 10^{7}$ erg/deg-g
Radius of first Bohr orbit	$a_0 = 0,529 \cdot 10^{-8}$ cm
Ionization frequency of hydrogen	$v_0 = 3,290 \cdot 10^{15}$ sec^{-1}
Electron volt in ergs	1 eV $= 1,602 \cdot 10^{-12}$ erg

Astronomical Constants

Astronomical unit	$1,496 \cdot 10^{13}$ cm
Parsec	$3,086 \cdot 10^{18}$ cm
Light year	$9,460 \cdot 10^{17}$ cm
Mass of Sun	$1,991 \cdot 10^{33}$ g
Luminosity of Sun	$3,86 \cdot 10^{33}$ erg/sec
Radius of Sun	$6,960 \cdot 10^{10}$ cm
Mean density of Sun	$1,41$ g/cm^3
Gravitational acceleration at surface of Sun	$2,740 \cdot 10^{4}$ cm/sec^2
Number of seconds in a year	$3,156 \cdot 10^{7}$ sec

Commas represent decimal points.

More detailed tables are contained in the book: C. W. Allen, Astrophysical Quantities, 1955 (Russ. translation: C. W. Allen, Astrophysical Quantities, Izd-vo inostr. lit., 1960).

SUBJECT INDEX

Abel's integral equation 190

Absorption
in continuous spectrum 45
at radio frequencies 204
by hydrogen atoms 47
by negative hydrogen ions 50
in a spectral line, 80
pressure effects 88
Stark effect 91
inside a star 459
coefficient 4, 217
lines
at radio frequencies 436
in presence of
coherent scattering 104
fluorescence 112
local thermodynamic equilibrium 95
noncoherent scattering 120
in spectra of
variable stars 357, 365
planets 242
lines,
central intensities 126
equivalent widths 97, 130
stellar 95-130
variation over the solar disk 129

Albedo of
particle 219, 407
planet, plane 228
planet, spherical 230

Ambartsumyan function 29, 118, 220

Atmosphere of
Earth 238
Mars 236
planet,
light scattering 216
optical properties 231
structure 245
temperature 245
upper layers 252
Sun (see Corona, Chromosphere) 165

Atmosphere of
  Venus 231
  star,
    chemical composition 138
    density of free electrons 144
    excitation and ionization of atoms 141
    magnetic fields 151
    turbulence 146
    theoretical model 249

Balmer
  decrement in the spectra of
    nebulae 286
    variable stars 347, 367
  discontinuity in the spectra of
    stars 63, 68
    nebulae 306, 313
    variable stars 350

Barometric formula 179, 196

Bethe cycle 463

Be type stars 340, 349

Binary stars 72, 77, 339, 357, 376, 476

Blanketing effect 71

Boltzmann's equation 46, 142

Brightness
  coefficient of planetary atmosphere 220, 233, 238, 241
  temperature of radio emission 203, 247, 248, 430

Carbon cycle 463

Central intensities of absorption lines 126

Chemical composition of
  planetary nebulae 302
  stellar atmospheres 140, 304

Chromosphere
  of the Sun 174
  172, 202, 212

Chromosphere,
distribution of atoms with depth 179
excitation of atoms 181
line intensities 174, 175
outbursts 172, 202, 212

Collisions of atoms with particles 88, 288, 295

Color excess 414

Cometary nebulae 359

Continuous emission spectrum 305, 310, 392

Continuous spectra of
Be type stars 350
cometary nebulae 359
gaseous nebulae 304
stars 57

Continuous spectrum of the
Crab nebula 186
solar corona 186

Convection 168, 462

Cosmic rays 397

Crab nebula 394

Curve of growth for
a nova 366
Eddington model 135
Schwarzschild-Schuster model 132

Curve of growth, plotted from observational
data 137

Degenerate gas 455

Density of matter
in gaseous nebulae 289
in solar corona 196
in stellar photospheres 40, 68, 166
within a star 445, 453, 466, 469

Diffuse nebulae (see Gaseous nebulae,
Dust nebulae)

Diffuse reflection of light 219, 223

Dilution factor of radiation 259, 274, 347, 420

Dissociation
energy of molecules 160
of molecules 159

Distribution of
atoms with depth in chromosphere 179
brightness over stellar disk 19, 58
brightness over disk of dust nebula 410
energy in spectrum of star 57

Doppler effect 84, 121, 327, 341, 346, 362, 435

Dust nebulae,
luminosity 406
nature of particles 412
relationship to stars 400

Eclipsing variables 20, 58, 76

Eddington method 14

Effective stellar temperature 36

Einstein transition coefficients 80
for forbidden lines 194, 292
for hydrogen atom 82

Ejection of stellar matter 385

Emden's equation 444

Emission coefficient 5, 218

Emission lines 194
in coronal spectrum 257, 292
in nebular spectra 339, 349, 347, 356,
in stellar spectra 360, 389

Emission lines,
intensities 286, 297, 345, 374
profiles 340, 341, 375

Energy balance of free electrons 277, 426

Energy,
evolved during nova outburst 377

Energy,
evolved during nuclear reactions 464

Energy transfer within a star 459

Envelopes of novae 362, 369, 377

Equation of
energy equilibrium of a star 449
mechanical equilibrium 64, 442
radiative equilibrium 6, 104, 122, 218, 316, 322, 329
radiative transfer 4
in a plane-parallel space 8, 105, 217, 316
in a spherically symmetrical space 8, 69, 407
in presence of Doppler effect 329
state of degenerate gas 456
state of ideal gas 40, 454
internal stellar structure theory 465
photosphere theory 64

Equilibrium equations of a star 442

Equivalent width of spectral line 97, 130

Evolution of stars 474

Excitation of atoms in
gaseous nebulae 283
interstellar space 422
stellar atmospheres 141
the chromosphere 181
the solar corona 198

Excitation of atoms by
collisions 288, 295
photoionizations and recombinations 283

Extended photospheres of stars 69

Faculae 172

Fluctuations of Milky Way brightness 402

Fluorescence 112, 258

Forbidden lines in
the coronal spectrum 193
galactic spectra 438

Forbidden lines in
nebular spectra 292
nova spectra 368

Free-free transitions 46, 48, 50, 56, 204, 304, 459

Galaxy,
magnetic fields 415, 436
radio emission 431, 433
structure 436

Gaseous nebulae,
chemical composition 302
densities 289, 300
distances 291
excitation of atoms 283
ionization of atoms 270
masses 289
radiation pressure 332
spectra 257, 292, 304
temperature 282, 300
of exciting stars 262, 268, 282

Gas pressure in
photosphere of Sun 164
photospheres of white dwarfs 68
photospheres of stars 40, 63

Gas pressure inside stars 446

Granulation 171

Gravitational energy of stars 447

Holtsmark function 92

Hydrostatic equilibrium 40, 442

Illuminance 2
of planets 246

Index of refraction of radio waves 210

Integral equation of radiation scattering 16, 116, 123, 220, 222, 319, 324, 408

Intensities of emission lines in
spectra of nebulae 286, 297
spectra of variable stars 345, 374

Internal structure of
stars of the main sequence 466
the Sun 467
white dwarfs 469

Interplanetary space 214

Interstellar hydrogen 415, 429, 433, 436

Interstellar gas,
density 426, 435
ionization 415, 418
motion 427
temperature 426, 430, 434

Interstellar
absorption lines 422
dust 400-415
dust,
density 413
luminosity 406
particle sizes 413

Invariance principle 220

Ionization energy of atoms 143

Ionization
temperature of stars 155
of atoms
in gaseous nebulae 270
in interstellar space 415
in stellar atmospheres 142
in the solar corona 195, 198
inside stars 453, 459
by collisions 198, 278
by radiation 46, 273

Kinetic temperature of
corona 195
interstellar gas 426, 433

Kirchhoff's law 33

L α line in spectrum of
nebula 321, 327
sun 184

Local sources of solar radio emission 212

Local thermodynamic equilibrium 34, 95

Long-period variables 356

Luminosity curve of
Hercules nova 372
a nova 360, 384
Venus 235

Magnetic
field of Galaxy 415, 436
fields of stars 151
fields of sunspots 172
stars 151

"Mass-luminosity" correlation 451

Masses of
diffuse nebulae 290
nova envelopes 370, 375
planetary nebulae 289

Maxwell's equation 272

Mean absorption coefficient 52

Mestastable state of an atom 194, 293, 353

Milne's integral equation 16

Models of
planetary atmospheres 249
stars 450, 466
stellar atmospheres 104, 109
stellar photospheres 63, 65, 66, 67
the solar chromosphere 181
the solar photosphere 166
the Sun 467

Molecules in
interstellar space 427
planetary atmospheres 236, 242
stellar atmospheres 159

Monochromatic radio emission of the Galaxy 433

Motion of
atoms, thermal 84, 146
envelopes of variable stars 385, 387
interstellar gas 427

"Nebular" lines 257, 268, 278, 368

Negative
absorption 48, 81
for radio frequencies 204
hydrogen ion 50

Neutrino 441, 463

Noncoherent scattering of light 120

Nonthermal radio emission 212, 248, 431

Novae,
energy, evolved during outburst 377
envelope expansion 362, 385
first stage of outburst 365
nebular phase 368
observational data 359

Nova Herculis 371

Nova-like variables 361

Nucleus
of planetary nebulae 258, 266, 269, 282

Nuclear reactions 462

Optical
depth 10, 217
for radio frequencies in solar corona 205
thickness of solar
corona 193
chromosphere 178
thicknesses of dust nebulae 412
thicknesses of planetary atmospheres 236, 237, 239

Origin of
planetary nebulae 335
stars 475

Oscillator strength 82, 132

Outflow of matter from stars 349, 352

Photoionization 46, 268, 270, 277, 283, 417

Photosphere of the Sun 166

Photospheres of
- cold stars 66
- stars, radiation absorption 45
- stars, structure 40, 69
- hot stars 60, 65
- stars 1
- stars, fundamental equations 8, 34, 40, 64
- white dwarfs 67

Planetary nebulae, see Gaseous nebulae

Planck's formula 33, 259

Polarization of
- coronal radiation 187, 191
- Crab nebula radiation 395
- dust nebulae radiation 413
- radio emission of sources on Sun 212
- stellar radiation 414
- Venus radiation 236

Pressure, see Gas pressure, Radiation pressure

Prestellar matter 476

Probabilities of atomic transitions 80, 292, 308

Profile of
- absorption line 98, 109, 112, 119, 125
- emission line 340, 341

Prominences 172

Propagation of radio waves in solar corona 210

Proton-proton cycle 463

Quasars 439

Radiation
  damping 84
  density 1
  field 1
  flux 2
  intensity 1
  pressure 42
    in gaseous nebulae 332
    in solar chromosphere 180
    in stellar photosphere 43
    inside stars 450, 470

Radiative equilibrium 6

Radio emission of
  Crab nebula 390, 394
  discrete sources in Galaxy 390
  interstellar gas 429, 431, 433
  the Metagalaxy 437
  planets 247
  the Sun 202
  the Sun,
    distribution over the disk 207
    quiet Sun 204
    sporadic Sun 212

Rayleigh scattering indicatrix 219

Reciprocity principle 225

Recombination coefficient 272

Recombinations 270, 273, 283, 304, 309, 316, 322, 345, 421

Reflecting nebulae 406

Reflection of light by surface of planet 235

Repeating novae 361

Resolvent of the integral equation of radiation scattering 20, 24

Rosseland theorem 260

Rotation of stars 147, 163

Saha's formula 47, 142

Scattering
coefficient 217
indicatrix 217
in dust nebulae 412
in planetary atmospheres 236, 239
of light
by free electrons 51, 75, 187, 459
in dust nebula 406
in gaseous nebula 315
in planetary atmosphere 216
in stellar atmosphere 104, 120
with frequency redistribution 120, 184, 321, 327
of radiation 315

Schwarzschild-Schuster method 11

Self-absorption in lines 175

Shock waves in
interstellar gas 428
stellar atmospheres 358

Solar activity 172

Solar corona,
electron density 190
excitation and ionization of atoms 198
propagation of radio waves 210
spectrum 186, 193
temperature 195

Solar wind 198, 214

Sources of stellar energy 447, 462

Space radio emission 429

Spectral classification 152

Spectral classification, effect of
gravitational acceleration 155

Spectral line emission 95, 104, 122

Spectrophotometric temperature of
nebulae 306
stars 62, 351, 356
Stark effect 91, 156, 163

Stars
of the main sequence 65, 466
with bright spectral lines 339

Stefan-Boltzmann law 33

Stellar associations 358, 476

Stratification of radiation in nebulae 277

Sun,
chromosphere 174
corona 186
internal structure 453, 467
photosphere 166
radio emission 202

Sunspots 171

Supercorona of Sun 213

Supernovae,
envelope masses 396, 397
observational data 389
radio emission of envelopes 390, 391

Synchrotron radiation 212, 248, 391, 432, 438

Temperature,
brightness 203
effective 36
excitation 131
spectrophotometric 62, 306
surface 36

Temperature inside a star 446, 467

Thermal conductivity 1, 462

Thermodynamic equilibrium, 32
deviations 103
local 34

Thomson's formula 51

True absorption coefficient 217

T Tauri stars 358

Turbulence
in stellar atmospheres 146
of interstellar gas 427

Two-photon emission 308

Ultraviolet spectrum of
the corona 201
stars 65
nuclei of planetary nebulae 266
the sun 182

Variable stars (see Novae, Supernovae, etc.) 338

White dwarfs,
atmospheres 160
internal structure 469
photospheres 67

Wien's displacement law 246

Wolf-Rayet type stars 339, 352

X-radiation of Sun 201

Z Andromedae stars 356

Zanstra's methods for determination of
stellar temperatures 262, 268

Zeeman effect 151, 172, 436

NATIONAL AERONAUTICS AND SPACE ADMINISTRATION
WASHINGTON, D. C. 20546

OFFICIAL BUSINESS

FIRST CLASS MAIL

POSTAGE AND FEES PAID
NATIONAL AERONAUTICS AND
SPACE ADMINISTRATION

050 001 55 51 3US 69328 00903
AIR FORCE WEAPONS LABORATORY/WLIL/
KIRTLAND AIR FORCE BASE, NEW MEXICO 87117

ATT E. LOU BOWMAN, CHIEF,TECH. LIBRARY

POSTMASTER: If Undeliverable (Section 158 Postal Manual) Do Not Return

"The aeronautical and space activities of the United States shall be conducted so as to contribute . . . to the expansion of human knowledge of phenomena in the atmosphere and space. The Administration shall provide for the widest practicable and appropriate dissemination of information concerning its activities and the results thereof."

—NATIONAL AERONAUTICS AND SPACE ACT OF 1958

NASA SCIENTIFIC AND TECHNICAL PUBLICATIONS

TECHNICAL REPORTS: Scientific and technical information considered important, complete, and a lasting contribution to existing knowledge.

TECHNICAL NOTES: Information less broad in scope but nevertheless of importance as a contribution to existing knowledge.

TECHNICAL MEMORANDUMS: Information receiving limited distribution because of preliminary data, security classification, or other reasons.

CONTRACTOR REPORTS: Scientific and technical information generated under a NASA contract or grant and considered an important contribution to existing knowledge.

TECHNICAL TRANSLATIONS: Information published in a foreign language considered to merit NASA distribution in English.

SPECIAL PUBLICATIONS: Information derived from or of value to NASA activities. Publications include conference proceedings, monographs, data compilations, handbooks, sourcebooks, and special bibliographies.

TECHNOLOGY UTILIZATION PUBLICATIONS: Information on technology used by NASA that may be of particular interest in commercial and other non-aerospace applications. Publications include Tech Briefs, Technology Utilization Reports and Technology Surveys.

Details on the availability of these publications may be obtained from:

SCIENTIFIC AND TECHNICAL INFORMATION DIVISION

NATIONAL AERONAUTICS AND SPACE ADMINISTRATION

Washington, D.C. 20546